

1999

Classification of plants the interpretation of CTFM sonar data

Neil Lindsay Harper
University of Wollongong

Follow this and additional works at: <https://ro.uow.edu.au/theses>

University of Wollongong

Copyright Warning

You may print or download ONE copy of this document for the purpose of your own research or study. The University does not authorise you to copy, communicate or otherwise make available electronically to any other person any copyright material contained on this site.

You are reminded of the following: This work is copyright. Apart from any use permitted under the Copyright Act 1968, no part of this work may be reproduced by any process, nor may any other exclusive right be exercised, without the permission of the author. Copyright owners are entitled to take legal action against persons who infringe their copyright. A reproduction of material that is protected by copyright may be a copyright infringement. A court may impose penalties and award damages in relation to offences and infringements relating to copyright material.

Higher penalties may apply, and higher damages may be awarded, for offences and infringements involving the conversion of material into digital or electronic form.

Unless otherwise indicated, the views expressed in this thesis are those of the author and do not necessarily represent the views of the University of Wollongong.

Recommended Citation

Harper, Neil Lindsay, Classification of plants the interpretation of CTFM sonar data, Doctor of Philosophy thesis, School of Information Technology and Computer Science, University of Wollongong, 1999.
<https://ro.uow.edu.au/theses/2006>

Research Online is the open access institutional repository for the University of Wollongong. For further information contact the UOW Library: research-pubs@uow.edu.au

CLASSIFICATION OF PLANTS BY THE INTERPRETATION OF CTFM SONAR DATA

A thesis submitted in fulfilment of the requirements for the award of the degree of

DOCTOR OF PHILOSOPHY

(Computer Science)

from

UNIVERSITY OF WOLLONGONG

by

Neil Lindsay Harper, BMath W'Gong, MCompSci W'Gong

School of Information Technology and Computer Science

1999

Acknowledgments

Throughout the process of this research, many have provided both intellectual and moral support and I would like to thank those who have helped me along the way. The most significant contributors are my supervisor at the University of Wollongong, Associate Professor Phillip M^cKerrow and Janice Sendt from Thomson-Marconi Sonar.

Phillip provided direction, support, and a research environment in which to complete this work at the Intelligent Robotics Laboratory (IRL) at the University of Wollongong. He also provided invaluable feedback during all stages of the work. Janice Sendt, the Acoustics Manager at Thomson-Marconi Sonar, supported this project through an Australian Research Council APIA scholarship, for which I am particularly grateful. Janice provided a large amount of her own time throughout this research and helped me both technically, and to set goals for the focus of the work. Over the time of this research, both Phillip and Janice have been inspirations for me, as well as personal friends.

I would also like to thank my colleagues in the IRL who provided an opportunity to present ideas and provided valuable feedback. Professor David Griffiths from the Applied Statistics department reviewed the draft and detailed areas for improvement in both the statistical and scientific sense. I would also like to thank Dr Alex Zelinsky who talked through some of the ideas with me early on in the process. Thanks to CISRA for the facilities to print and copy the final version of this thesis.

I would like to thank both my Dad, who reviewed this thesis several times throughout its evolution, and Mum, who has always encouraged me over the years. My earliest memories are of my father spending time in his study pouring through data on the way to his PhD, and my mother wondering when he was going to finish. History has a way of repeating itself.

Last but certainly not least, I would like to thank my wife Tracey, who provided support during all stages of this project from making the decision to take on the project;

leaving full time employment; and pushing towards the final goal. Over the last 12 months in particular, I would like to express my gratitude to her. Tracey has provided encouragement and motivation for me to complete this piece of work. I could not finish without also mentioning Jerry, who lay snoring under my feet or on his beanbag nearby day and night throughout most of this project.

List of Publications from this thesis

Harper, N., McKerrow, P., 1994, *Perception of Object Characteristics by the Interpretation of Ultrasonic Range Data*, Proceedings of the 7th Australian joint Conference on Artificial Intelligence, World Scientific, pp 418-426.

Harper, N., McKerrow, P., 1995, *Classification of Plant Species from CTFM Ultrasonic Range data using a Neural Network*, The 1995 IEEE International Conference on Neural Networks, Causal Productions, pp 2348-2352.

Harper, N., McKerrow, P., 1995, *Discrimination Between Plants with CTFM Range Information Using a Backpropagation Learning Algorithm*, The 1995 Australian Artificial Intelligence conference, World Scientific, pp 227-234.¹

Harper, N., McKerrow, P., 1997, *Recognition of Plants with CTFM Ultrasonic Range Data using a Neural Network.*, The 1997 IEEE International Conference on Robotics and Automation

Abstract

Environment sensing and perception is an active area of study because advances in automation depend on them. In addition, new transducers and increased processing power coupled with theoretical advances make new and better perception systems possible. These systems can bring improvements in both safety and productivity in the work place as well as the home. This thesis is the necessary pre-work for the implementation of a new machine perception system with potential application in mobile robotics.

A sonar system ensonifies the surrounding environment and from the scattered returns, provides information about the surfaces within the field of audition of the sensor. This thesis develops a model using the output of a Continuous Transmission Frequency Modulated (CTFM) sonar in the form of an acoustic density profile. The sensor measures the scattered returns at discrete ranges which are proportional to the size, orientation and texture of all of the surfaces at that particular range. The sum of the acoustic density profile is the “acoustic area” of the entire scene.

The acoustic sensor system is based on a commercial ultrasonic mobility aid for blind people [Kay, 1966]. The system consists of three transducers mounted in a sensing head, a set of earpieces and associated signal conditioning electronics. It ensonifies the surrounding medium (a sector of 60 degrees) with a CTFM signal and converts the return echo into audible tones. The pitch of the tone is determined by the range of the object. The user of the device receives rich information about the environment from the stereo tones which are produced through the earpieces. Blind people have shown that they can use a CTFM based mobility aid to navigate successfully and can detect and recognise objects. They can easily recognise and distinguish plants based on their physical structure so this study has focussed on plants.

Plants have been shown to produce recognisable characteristic outputs using this sensor system so have potential as natural landmarks for mobile robot navigation. The information from the sensor can be interpreted directly to provide information about the physical structure of the plant.

This thesis reviews the capabilities and limitations of the acoustic system and discusses some of the parameters which determine the performance of the device. It also includes techniques for interpreting the signal. This is unique, as current systems present a signal to a user who is responsible for interpreting the output. This thesis describes the information that is contained in the signal which is the information about the structure of the plant and techniques for a machine to interpret that data for complex decision making by a mobile robot.

A proof of concept is used to show that there is enough information in the signal to differentiate four different plant specimens to a reasonable accuracy and also provide benchmarks for comparison against more intelligent techniques. Data were collected from a large number of plants (>100) and results analysed. Correlation is a similarity measure and is used in this thesis to show how the plants change depending on the direction from which they are ensonified.

The echo received by the sensor varies depending on the angle from which the plant is ensonified as it is dependant on the structure and orientation of individual leaves. There is, however information in the signal which is relatively invariant through a change in orientation and this characterises the structure of the plant. This information has been captured by 19 features which are calculated directly from the echo in the frequency domain. These calculated features are analysed and their advantage over the raw signal is highlighted. They can be interpreted directly to provide information about the physical structure of different plants.

Classification methods demonstrate how well the plants can be separated from the others in the set based on how well an echo can be allocated to a set of pre-defined classes. All of the implementation issues for this sensor are then drawn together.

This thesis covers the following items :

1. A detailed study of CTFM ultrasonic sensing and its applicability to mobile robot natural landmark sensing;
2. A model which maps the frequency spectra to an acoustic density profile where the individual range lines represent the normal acoustic area of all of the surfaces at that particular range. This model allows robust interpretation of the information in the signal;
3. An algorithm to track echoes from surfaces in the returned signal over adjacent orientations or at multiple time periods in the case of moving plants;
4. A large database of CTFM sonar data which can be analysed further and used as a benchmark for further study;
5. A set of features which are shown to characterise the acoustic density profile from plants and are relatively consistent through orientation;
6. A transformation between the features (and hence the acoustic density profile) and the physical structure of the plant; and
7. A set of algorithms for implementation on a mobile robot platform which use plants as natural landmarks.

Table of Contents

1. Introduction	1-1
1.1 Background	1-1
1.2 The problem : Plant recognition from a mobile robot platform	1-2
1.3 Approach taken	1-5
1.4 Contributions made by this thesis	1-5
1.5 Thesis layout	1-6
1.6 Summary of thesis results	1-9
1.6.1 Static environment, known path, robot senses regularly	1-10
1.6.2 Static environment, known path, robot senses irregularly	1-10
1.6.3 Non-static environment and possible unknown path	1-10
1.6.4 Classified as an unknown plant	1-11
1.6.5 Moving leaves	1-11
1.6.6 Agriculture industry applications	1-11
1.7 Summary	1-11
2. Mobile Robot Sensing Requirements	2-1
2.1 Environment perception in robotics	2-1
2.1.1 Vision	2-2
2.1.2 Dead reckoning	2-2
2.1.3 Tactile sensing	2-3
2.1.4 Proximity sensing	2-3
2.1.5 Range sensing	2-3
2.1.6 Current state of sensing	2-4
2.2 Machine perception of plants	2-5
2.2.1 Introduction	2-5
2.2.2 Agricultural applications	2-5
2.2.3 Navigation among live plants using ultrasonic sensing	2-6

2.2.4 Classification of plant species	2-6
2.2.5 Plant feature location and grading	2-7
2.2.6 Summary of plant sensing applications	2-8
2.3 Ultrasonic sensing	2-9
2.4 Human perception and the ultrasonic mobility aid	2-11
2.4.1 Human auditory perception	2-11
2.4.2 Auditory perception and KASPA	2-12
2.5 Perception test by an inexperienced user	2-15
2.6 The place for a plant classifying sensor	2-16
2.7 Conclusion	2-16
2.8 Summary	2-17
 3. CTFM Sensor	 3-1
3.1 Introduction	3-1
3.2 Principles of CTFM sensing	3-1
3.3 Hardware and software	3-3
3.4 Technical data	3-5
3.5 Physical sensor properties for this application	3-7
3.5.1 Repeatability	3-8
3.5.2 Variation with environmental conditions	3-11
3.5.3 Amplitude variation with range	3-15
3.6 Analysis of system outputs	3-16
3.6.1 A tour of the lab wearing the blind aid	3-16
3.7 The acoustic density profile model	3-18
3.8 Data characteristics	3-20
3.8.1 CTFM sensor output from ensonifying simple objects	3-24
3.9 Acoustic density profile content from plants	3-29
3.9.1 Basic content of the acoustic density profile	3-29
3.9.2 Plant insonification	3-30

3.9.3 Freedman's theory of scattering and its relationship to plants	3-34
3.9.4 Acoustic shadowing	3-34
3.9.5 Increasing cell resolution	3-37
3.9.6 Area of interest	3-37
3.10 Scene prediction	3-38
3.11 Summary	3-39
 4. Classification of Plants using data from the Acoustic Density Profile	 4-1
4.1 Introduction	4-1
4.2 Experimental design	4-4
4.3 Neural network classifier	4-6
4.3.1 Introduction	4-6
4.3.2 Network architecture	4-9
4.4 Data preprocessing	4-11
4.5 Network training and results	4-13
4.5.1 Experiment 1 - differentiate a plant from plants of different species	4-13
4.5.2 Experiment 2 - testing different specimens of the same species	4-15
4.5.3 Experiment 3 - recognising plants at different ranges	4-16
4.5.4 Experiment 4 - differentiate plants of the same species	4-17
4.5.5 Experiment 5 - the effect of removing the leaves	4-18
4.6 Conclusion	4-19
4.7 Summary	4-20
 5. Plant Database	 5-1
5.1 Introduction	5-1
5.2 Database structure	5-1

5.2.1 Plant characteristics	5-1
5.2.2 Sensed data	5-4
5.3 Data collection	5-5
5.3.1 Equipment setup	5-5
5.4 File management	5-7
5.5 Tabulated results	5-7
5.6 Referencing the data to a standard range of 400 mm	5-10
5.7 Summary	5-11
 6. Ensonifying the Plant from a Limited Aspect	 6-1
6.1 Introduction	6-1
6.2 Background	6-1
6.3 Correlation calculation	6-2
6.4 Correlation between returns at adjacent orientations - Local correlation	6-5
6.5 Echo tracking	6-11
6.6 Conclusion	6-21
6.7 Summary	6-22
 7. Ensonifying the plant from any aspect	 7-1
7.1 Introduction	7-1
7.2 Correlation between non-adjacent acoustic density profiles - Global Correlation	7-1
7.2.1 Plant changes through rotation	7-2
7.3 Conclusion	7-9
7.4 Summary	7-9
 8. Feature Analysis	 8-1
8.1 Introduction	8-1
8.2 Feature extraction in order to characterise plants	8-1

8.2.1 Calculation of the features	8-4
8.2.2 Data preprocessing	8-8
8.3 Preliminary analysis of features	8-11
8.4 Qualities of the feature data	8-17
8.4.1 Feature filtering	8-18
8.5 Local correlation using features	8-28
8.6 Global Correlation using features	8-31
8.7 Global correlation using a template - Template Correlation	8-35
8.8 Properties of the features through rotation	8-38
8.9 Correlation between different plants	8-38
8.10 Conclusion	8-41
8.11 Summary	8-41
9. Mapping of Signal Features to Plant Physical Structure	9-1
9.1 Introduction	9-1
9.2 Background	9-1
9.3 Length of the acoustic density profile	9-4
9.4 Number of lines in the acoustic density profile above a fixed threshold	9-13
9.4.2 Transformation of number_above_threshold	9-41
9.5 The number of major peaks in the acoustic density profile	9-45
9.6 Sum of the acoustic density profile	9-50
9.7 Conclusion	9-54
9.8 Summary	9-54
10. Plant Classification	10-1
10.1 Introduction	10-1
10.2 Pattern recognition techniques	10-2
10.3 Input to the pattern recognition system	10-3
10.4 Data partitioning	10-6

10.5 Performance estimation	10-8
10.6 Template matching	10-10
10.7 Feature selection	10-11
10.8 The Wrapper Method of feature selection	10-13
10.9 Classification of plants using the statistical classifier	10-17
10.10 Pairwise classification results	10-20
10.11 Discriminant analysis techniques	10-28
10.12 Plants which are inconsistent through viewing angle	10-28
10.12.1 Non-linearly separable classes	10-30
10.13 Classifying plants using both raw data and features using several different classifier types	10-30
10.14 Plant grouping	10-32
10.15 Conclusion	10-32
10.16 Summary	10-33
 11. Implementation issues for mobile robot navigation	 11-1
11.1 Process timing	11-2
11.1.1 Theoretical timing	11-2
11.1.2 Empirical timing	11-4
11.2 Fundamental plant sensing	11-5
11.2.1 The effect of range to the plant	11-5
11.2.2 Positioning of the plant within the beam	11-7
11.2.3 When the platform moves past a plant	11-7
11.3 The effect of a moving sensor	11-10
11.3.1 Change in position of sense / receive point	11-11
11.3.2 The effect of the change in wavelength with motion (Doppler shift)	11-11
11.4 Multiple objects in the field of audition	11-15
11.4.1 Separating man made indoor surfaces	11-15

11.4.2 Distinguishing multiple plants	11-16
11.5 Some specific mobile sensing scenarios	11-17
11.5.1 Static environment, known path, robot senses regularly	11-17
11.5.2 Using the acoustic symmetry of plants for localisation	11-20
11.5.3 Static environment, known path, robot senses irregularly	11-21
11.5.4 Non-static environment and possible unknown path	11-22
11.5.5 Classified as an unknown plant	11-22
11.6 Improving sensor resolution	11-22
11.7 Summary	11-24
 12. Conclusion	 12-1
12.1 A basis for the interpretation of CTFM sensor data	12-1
12.2 Acoustic density profile	12-2
12.3 Sensor facilities	12-2
12.4 Data interpretation	12-4
12.4.1 Effects of plant foliage	12-5
12.4.2 Correlation	12-7
12.4.3 Features	12-8
12.4.4 Mapping of features to plant structure	12-8
12.4.5 Classification	12-9
12.4.6 Clustering	12-10
12.4.7 Implementation issues	12-10
12.4.8 Summary	12-10
12.5 Fitness for purpose	12-11
12.5 Future work	12-12
12.6 Conclusion	12-13
 A. Appendix A - Sample Plant Portfolios	 A-1

B. Appendix B - Echo tracking source code	B-1
B.1 Calculate echo range possibility	B-1
B.2 Echo tracking	B-2
 C. Appendix C - code segments	 C-1
C.1 Background	C-1
C.2 Array class	C-1
C.3 CTFM class	C-4
C.4 Feature class	C-6
C.5 Reference the spectra to a standard range	C-9
C.6 Calculate the number of range lines above threshold	C-11
C.7 Calculate the number of major peaks	C-11
C.8 Calculate the sum of the acoustic density profile	C-12
C.9 Calculate the front to peak distance	C-12
 D. Appendix D - Plant Grouping	 D-1
D.1 Taxonomy	D-1
D.2 Introduction to cluster analysis	D-2
D.2.1 A Simple clustering example	D-2
D.3 Common clustering techniques	D-7
D.4 Plant clustering using range data	D-11
D.5 Analysis of generated clusters	D-18
D.6 A set of plant groupings	D-21
D.7 Conclusion	D-22
 E. Appendix E - Sample plant returns	 E-1
E.1 Background	E-1
E.2 Eucalyptus maculata	E-1
E.3 Leptospermum laevigatum	E-6

F. Appendix F - Glossary and Acronyms	F-1
G. Appendix G - Bibliography	G-1
H. Appendix H - Movie of Ultrasonic Mobility Aid Sounds	H-1

1. Introduction

This chapter provides the background information about the problem under consideration, outlines the context of the problem, and documents approach taken to this research. A summary of the results of this thesis is also outlined.

1.1 Background

Professor Leslie Kay developed an ultrasonic mobility aid to help blind people to perceive their environment [Kay, 1966]. The mobility aid insonifies the environment with ultrasound, detects the echoes and converts them into audible stereo tones. The pitch of the tone is linearly proportional to the distance to the object, and the direction of the object is determined binaurally by the human auditory system [Kay, 1974]. The ultrasonic mobility aid is currently marketed under the name of KASPA (Kay's Advanced Spatial Perception Aid).

KASPA uses electrostatic transducers to detect the echoes from objects and then signal conditioning electronics convert them into tones that are audible to the listener. The audible representation of the echoes sound like squeals, chirps, tweets, warbles, swishes, and musical notes. These sounds may be single or multi-toned notes. The more complex the object, the more complex the tonal pattern as multiple surfaces produce their own echoes. The richness of the information in the tone enables a blind person to distinguish between objects with ease [Kay, 1974].

With KASPA, an experienced user can not only detect whether there is something in the way, but can extract a large amount of information from the signal. For example, The nature of the object is perceived from the tonal pattern, the height of the object is discovered by vertical scanning, and the width is detected by horizontal scanning. A smooth flat surface produces a hard, clear tone at a single pitch. In contrast, a textured surface produces a decrease in the intensity and the tone will contain adjacent frequencies. The closer the object, the lower the pitch of the tone. Multiple surfaces within the field of the sensor will result in a tone produced for each of the surfaces with the intensity of the

tone dependant of the texture, size and orientation of the surface. When the object is moving, the tone rises or falls in pitch depending on whether the object is moving away from or toward the listener.

Complex objects or groups of objects produce highly complex tonal patterns [Gissoni, 1966]. The human brain converts this information into a spatial pattern of the environment. People have successfully used Continuous Transmission Frequency Modulated (CTFM) based systems in several application areas. Not only have they been used by blind people as mobility aids [Kay, 1962], but also by underwater divers in areas of reduced visibility [de Roos, 1983]; by doctors as echocardiophones to detect spatial movement of the heart [Kay, 1977b]; by fisherman to detect and recognise different fish shoals [Kay, 1977] and by scientists to detect objects on the seafloor [de Roos *et al*, 1988].

1.2 The problem : Plant recognition from a mobile robot platform

In order for a machine to perceive the environment with this system, the signal is captured in a computer with specialised hardware including FFT (Fast Fourier Transform) hardware which transfers the audio signal into the frequency domain. After many months of practice, people can easily distinguish between the signals audibly but it is much more difficult to visually compare the outputs in the frequency domain on a display because of the complexity of the signal. In order to use the technology on a mobile robot, a machine perception system is required.

Blind users are easily able to distinguish between different broad classes of plants through their characteristic tones [Gissoni, 1966]. Experience with KASPA shows differences in the auditory signal when listening to the tones produced by different plants and the difference between plants which appear to be physically similar can also be detected.

As a proof of concept, a classifier, in this case an Artificial Neural Network (ANN), was trained to recognise four individual plants (each of different species) to a

high degree of accuracy. The ANN perception system showed good results for recognising these different plant specimens. Also, the recognition is independent of the orientation of the plant, the size of the plant (height and width) and the distance to the plant.

A pattern classification system which is developed by learning sample data alone is only satisfactory when the classifier will be operating in a fixed domain. For this system to be suitable for situations such as mobile robot navigation, a more flexible system is required; it must cope with changes to the environment, such as the presence of new plant specimens, or growth of an existing specimen. It is important to represent the information from the signal(s) in a way that allows robust reasoning.

For simple objects, the amplitude and frequencies of the audible tones heard through the headphones can be predicted after a small amount of training. When the object of interest however, contains multiple surfaces at different orientations (as is the case for plants), then the received signal becomes a function of the size, orientation and location of the leaves of the plant relative to the sensor. It is shown in this thesis that the signal is a function of the area, the orientation, the texture and the acoustic shadowing of the plant foliage.

Accordingly, the recognition task must consider the issue of a highly variable frequency spectrum as any individual plant is rotated (even by a small amount). This is due to the reflective properties of the leaves. When the leaf surfaces (or parts of a leaf surface) are orthogonally oriented to the insonifying/receiving system then they act as specular (mirror like) reflectors and produce a high amplitude (or high volume in the case of the audio signal). When the plant is rotated slightly, these same leaves may now reflect most of the acoustic energy away, only returning a small amount to the receiver due to the highly directional nature of the specular scatterers.

At ultrasonic frequencies, flat surfaces act like mirrors, so the majority of the transmitted acoustic energy is reflected away from the receiver unless there are parts of the surface orthogonal to the sensor. A leaf however, can generally be modelled as a bent body and unlike plane plates and straight cylinders which reflect waves over a narrow

solid angle, reflect waves over a wide solid angle [Shenderov, 1998]. This physical fact allows the same reflection characteristics to be measured at a range of different angles.

The frequency spectra can be modelled as an acoustic density profile where each range line represents the acoustic area at that particular range. The concept of acoustic area is outlined in detail in Chapter 3. When a plant is the only object in the field of audition of the sensor, the sum of the acoustic density profile is the acoustic area of the entire plant.

This thesis shows that some information in the spectrum remains relatively stable with rotation. It is also demonstrated that some plants are more reliable to use than others, based on their acoustic symmetry. As plants can look symmetrical to our eyes, they also exhibit symmetry at ultrasonic frequencies. This fact can be exploited by any system developed for use in the real world. It is fundamentally easier to recognise that a sample belongs to a particular class if that sample is representative of the training data.

This thesis describes the process of identifying the features of the signal which are important for differentiating between plants and are also consistent when viewing the plant from other orientations. A set of features of the spectrum which are specific to plant geometry have been defined. The features were extracted in order to capture all of the distinguishing information in the signal, for example the amplitude and shape of the spectra, and remove redundant or unnecessary information such as the absolute range to the plant. These calculated features capture information about the structure of the plant and are more robust than the information from the raw signal as they are less affected by the orientation of the plant.

It is difficult to separate individual species from the entire set of plants when they are all very similar. In the case when a plant cannot be identified with any confidence, then the features can be interpreted directly and/or grouped using statistical cluster analysis into one of the groups of similar plants. These groups can also be differentiated using physical features of the individual plants. Often, similar plants exhibit a physical feature (or features) which are also present in the other plants in that cluster.

Robot navigation can be decomposed into several tasks and environment sensing using natural landmarks is of particular significance. In order to implement this system, algorithms are developed with emphasis of using plants as natural landmarks.

1.3 Approach taken

In this thesis, the approach taken is to investigate the area of mobile robot sensing requirements, to verify the applicability of the sensor and then implement a proof of concept. The returned signal is then modelled as an acoustic density profile so that it can be interpreted accurately.

Once the concept was verified, a database of plants were collected and signals were verified in relation to the change of the viewing angle of the sensor. A set of features which characterise the plant through rotation and were defined and analysed in terms of how representative they are of plant structure. These features can also be interpreted directly to reveal different properties of a plant's structure.

A classifier was developed; this can reliably classify a plant based on the reflected signal. Cluster analysis was also used to group plants of similar physical structure.

The thesis is concluded by relating this information back to the mobile robot sensing requirements and a discussion of the best way to apply this sensor to different applications.

1.4 Contributions made by this thesis

This thesis further develops the field of object recognition using sonar by developing a model of information content of the frequency spectra produced by a CTFM system. The major outcomes of the thesis are :

1. A detailed study of CTFM ultrasonic sensing and its applicability to mobile robot natural landmark sensing;
2. A model which maps the frequency spectra to an acoustic density profile where the individual range lines represent the normal acoustic area of all of the surfaces at that

particular range. This model allows robust interpretation of the information in the signal;

3. An algorithm to track echoes from surfaces in the returned signal over adjacent orientations or at multiple time periods in the case of moving plants;
4. A large database of CTFM sonar data which can be analysed further and used as a benchmark for further study;
5. A set of features which are shown to characterise the acoustic density profile from plants and are relatively consistent through orientation;
6. A transformation between the features (and hence the acoustic density profile) and the physical structure of the plant; and
7. A set of algorithms for implementation on a mobile robot platform which use plants as natural landmarks.

1.5 Thesis layout

The layout of the thesis is shown in Figure 1.1. References to chapters are noted by the number on the top left of the ellipse.

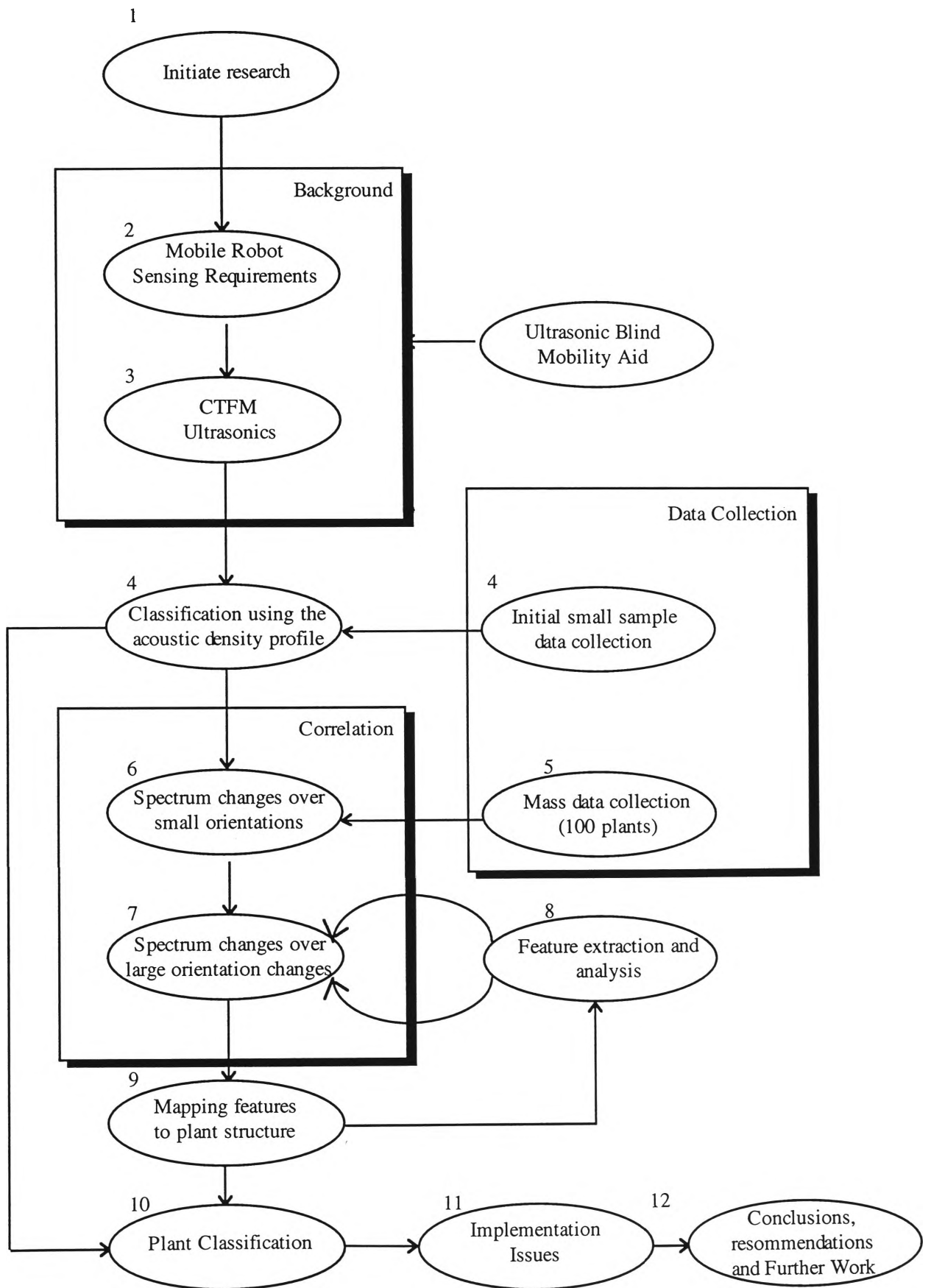


Figure 1.1 Thesis structure. Chapter numbers are shown adjacent to thesis components

Chapter 1 introduces this research. In Chapter 2, the current sensing systems for mobile robots are reviewed and the requirements for a new sensor are established. Existing plant perception systems are analysed, most of these are in the field of automating agricultural processes.

Ultrasonic sensing is reviewed and Continuous Transmission Frequency Modulated (CTFM) Ultrasonics is analysed in detail in Chapter 3. Background technical data are tabled, and system parameters are established. The hardware and software is outlined and sensor characteristics are established for this application. The sensor characteristics are analysed in terms of repeatability, effects of environmental conditions, amplitude variation and range variation. An introduction to use of the ultrasonic mobility aid is provided along with a rudimentary analysis of plant spectral content. The model of the acoustic density profile is developed and justified. The movie in Appendix H demonstrates the sounds that are produced from different types of objects and should be viewed in conjunction with this chapter.

Chapter 4 describes the proof of concept in order to test the sensor's for the intended application of plant classification. It describes a series of experiments which were carried out in order to prove that it is possible to use this sensor to differentiate a small number of plants from any orientation. It describes the application of an Artificial Neural Network (ANN) using a group of four plant specimens. This establishes a set of benchmark levels which are used as a comparison against more advanced techniques in Chapter 10.

Chapter 5 discusses the collection of a large database of echoes for 100 plants of different species. Information about the experimental setup and the data collection techniques is provided as well as details of the range normalisation algorithm.

Chapter 6 addresses the problem of navigation in a known environment with a known path. Plants act as navigation landmarks and are positioned in known locations. This chapter discusses the method of tracking plants from one view of the plant to the next using local correlation and a method of echo tracking is developed which significantly improves the reliability of the local correlation. It also provides the basis of a

record of how acoustically similar the echoes are from one orientation to the next which is a measure of the local acoustic symmetry of the plants.

Chapter 7 reports the issue of correlating an echo from a plant with an echo from a completely different orientation of the plant. This is useful in a non-static environment (ie. an environment which may change) since a plant needs to be identified from a single reading and may not always be viewed from the same orientation. Chapter 7 highlights the limitations of using this technique with the raw spectrum. A significant improvement can be made by characterising the spectrum by features and this is discussed in Chapter 8.

In Chapter 8, these features are developed and analysed with respect to both local and global correlation. The concept of template correlation is introduced; this gives good results for comparing a single insonification of a plant with signals from many different orientations of the plant.

Chapter 9 provides a basis for inferring the physical structure of the plant directly from the calculated features (and hence the raw spectrum). Features provide information about the plant including leaf density, the size of the reflective surfaces and the overall depth of the plant.

Chapter 10 uses statistical and neural classification techniques to classify any given echo as one of n plants. Good results are shown for classifying the signal reflected any orientation as one of ten plants but reduces dramatically as more plants are added to the population. However, if a plant is unknown (or is new to the classifier) then the plant can be grouped using a pre-defined cluster mapping and information about similar plants can provide clues about the new specimen. Furthermore, the features can be interpreted directly as outlined in Chapter 8.

Chapter 11 addresses implementation issues including processing chains and processor loads and Chapter 12 presents a summary of the thesis and the conclusions.

1.6 Summary of thesis results

The contributions made by this thesis were listed in Section 1.4. This thesis develops a model of the frequency spectra which allows direct interpretation of the spectra

in order to determine the structure of the plant under consideration. This is underpinned with the theory behind the technology, a proof of concept and an analysis of the practical characteristics of the sensor. The techniques used though out the thesis can be used as a basis for the implementation of this sensor in either an agricultural application or in mobile robot navigation.

Listed below are five situations and the recommendations about how the sensor outputs could be processed by a mobile robot navigation system. This is presented in more detail in Chapter 11.

1.6.1 Static environment, known path, robot senses regularly

In the situation where the environment is fixed, the path is known, and the robot is able to sense regularly (that is, the case where it is not moving at high speed), the most efficient method of navigation using plants as landmarks is to use local correlation of the features. Echo tracking would also be of benefit as the robot moves around the plant. These techniques are outlined in Chapter 6. This method is fast as it requires very little processing.

1.6.2 Static environment, known path, robot senses irregularly

When the robot is sensing irregularly (or if it is moving at high speed so there is a large displacement between sensing points), two signals from completely different orientations of a plant need to be compared. Local correlation is not sufficient for this as plants may look significantly different from different orientations (see Chapter 8). Instead, a more sophisticated method is required. Global correlation is not effective unless the plant is centred in the same place on the spectra, so features are calculated from the raw spectrum and these features correlated (see Chapter 9).

1.6.3 Non-static environment and possible unknown path

When the plants are not in fixed locations in the environment, or in the case of an unknown path, a single orientation of a plant is processed with a classifier in order to recognise the plant (see Chapter 10).

1.6.4 Classified as an unknown plant

In a case where a plant is classified as an unknown plant, or classified with low confidence, then the features can be interpreted directly to provide information about the physical structure of the plant (see Chapter 9). The plant can also be classified as one of a group of plants using cluster analysis in order to determine the plant type.

1.6.5 Moving leaves

If the leaves are moving in response to vibrations or wind then echo tracking of multiple signals can be performed in order to temporally correlate the signals.

1.6.6 Agriculture industry applications

In Chapter 2, agricultural applications of machine perception are discussed. Many recent systems work in a limited domain and have had limited success. When used in the form of a classifier, this perception system could have success in many areas including greenhouse automation and outdoor selective crop spraying

1.7 Summary

1. Environment sensing is an expanding area of research.
2. The ultrasonic mobility aid has potential application in the area of mobile robotics.
3. Plants are complex objects which produce characteristic tones and can be used as natural landmarks for mobile robot navigation.
4. Although the spectra changes significantly depending on the orientation from which the plant is viewed, there is a range of angles over which the reflective energy is constant due to their bent shape. The actual range of angles varies between species. A set of calculated features capture the information in the signal which is relatively invariant through rotation.
5. The frequency spectra produced by the system can be modelled as an acoustic density profile which allows a transformation between the characteristics of the

acoustic density profile to the physical structure of the plant.

6. This thesis covers methods for interpreting the data and could be used in the implementation of this acoustic sensing system.
7. Typical sensing scenarios are addressed and implementation techniques recommended.

2. Mobile Robot Sensing Requirements

This chapter introduces environment sensing in robotics with particular emphasis on ultrasonic sensing. Several applications of ultrasonic sensing in the robotics field are discussed. Machine perception of plants is also introduced and a detailed overview of current applications of plant recognition is outlined. Kay's Auditory Spatial Perception Aid (KASPA) is then profiled. As this mobility aid replaces a humans sense of sight with a series of auditory signals, a brief discussion of how the auditory system perceives sounds is included. The place for this CTFM sensor in mobile robotics is then outlined.

2.1 Environment perception in robotics

A robot's ability to sense the environment in which it operates and change its actions accordingly is what makes it both interesting for research, and a useful tool to have. Sensors provide information for the robot to make decisions in order to perform set tasks such as recognising object, avoiding collisions and following walls. Sensors allow the robots to work in all types of environments, including those which may be unsafe or monotonous for humans.

Often, the environment in which a robot needs to work is unstructured, so the need for sensing is paramount. Consider the application of collision avoidance. The system must deal with the position and orientation of obstacles, movement of obstacles and also the overall goal of reaching a given destination.

Researchers have found it easier to work with visual systems than ultrasonics because we are more experienced (as humans) in working with and understanding vision. There is a large amount of literature devoted to visual sensors and this has meant that there is much less work being carried out to apply other kinds of sensing to mobile robotics. Many of these other techniques are cheaper, require less processing and provide different

and complementary information to that provided by visual sensors. A comprehensive review of current sensing technology is available in Everett [1996]. A very brief summary of the major sensors follows.

2.1.1 Vision

Vision systems collect the light reflected from objects and form it into an image which can then be processed [McKerrow, 1991]. The image is an array of pixels which may either be binary, grey scale or colour. The resolution of the image is specified as the number of pixels per unit area of the image. Vision has been a popular sensing method for robotics researchers and has been used extensively in robotic applications.

Since vision systems work by gathering reflected light, the most important design consideration is how the lighting will be controlled. Backlit scenes can appear significantly different to those where the light source is behind the camera. However, decades of research in machine vision have resulted in a deep understanding of how to manage these issues and produce good results [Horn, 1985].

2.1.2 Dead reckoning

Dead reckoning is the process of estimating the current position of a robot from knowledge of its previous position and current velocity information (speed and direction). The velocity and direction of the robot can be determined by odometry, doppler shift or by using inertial navigation.

Odometry provides information about distance travelled by measuring the rotation of a wheel usually with either resolvers or optical encoders. Odometry is inaccurate as it is subject to problems caused by slippage, tread wear and tyre inflation pressures. Some schemes used to develop more accurate odometry systems have been successful [Kleeman, 1997]. Odometry errors can also be reduced by fusing the data with that of other sensors [McKerrow, 1996].

Doppler navigation systems provide information about the robot's speed with respect to the ground; these systems are of low cost and are accurate systems [Milner, 1990].

Inertial navigation involves sensing involves calculating position based on changes in acceleration over time. Barshan & Durrant-Whyte [1993] found that highly accurate systems can prove to be expensive.

2.1.3 Tactile sensing

Tactile sensors involve direct physical contact with an object and are commonly implemented in the form of bumpers. Many more sophisticated tactile sensors are available and can provide information about :

1. the presence of a force;
2. the size of a force; and
3. even the direction of a force

An overview of the major types of tactile sensors and their applications can be found in Harmon [1983].

2.1.4 Proximity sensing

Proximity sensors indicate whether there is an object in the immediate vicinity without making physical contact. This can be done with either magnetic, optical, inductive, capacitive, microwave or ultrasonic sensors. These kinds of sensors are usually simple and very reliable and are hence well suited to harsh environments [Peale, 1992].

2.1.5 Range sensing

There are many options available to provide information about the range to objects in the environment. Some of these are noted below.

Triangulation involves separating two sensors by a known distance and orienting them towards the object of interest. The distance of the object can then be calculated based on the distance between the sensors and the angle of the object of interest from the axis of both of the sensors. The sensors may be for example video cameras, lasers or solid state

imaging arrays. This situation is illustrated in Figure 2.1, where the two sensors, S_1 and S_2 , are separated by a distance A . The angles θ and α are dependant on the angle which the object is offset from the axis of the respective sensors and the distances B and C are then calculated using fundamental trigonometric rules. Triangulation ranging is also used extensively in the area of optical 3D digitising [Petrov *et al*, 1998].

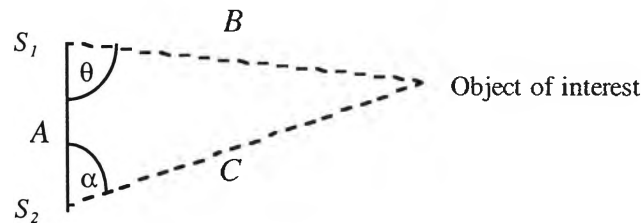


Figure 2.1 Triangulation ranging

Time of flight systems measure the time for a pulse of energy to travel to an object and reflect back to the receiver. The advantage of these systems is that the range is available without the need for complicated analysis. Energy sources are typically ultrasonic, radio frequency or optical.

Phase-shift measurement involves continuous wave transmission and provides information about the range as well as the direction and velocity of a moving target, from the doppler shift. A beam of amplitude modulated (AM) energy is transmitted, the phase of the return signal is measured and compared to the reference, and the phase shift is used to calculate the round trip distance. Frequency modulated continuous wave (FMCW) radar systems can also provide accurate range information.

Other ranging techniques include interferometry, range from focus, and the return signal intensity method.

2.1.6 Current state of sensing

Robot arms are currently being used in many areas but there are very few commercial applications of mobile robots. This lack of implementation is due to several reasons, one of which is that sensing is not sufficiently advanced. Improved sensors will allow us to program autonomous robots to handle a greater variety of situations and as a

result, they will gain wider acceptance. This CTFM sonar system will add to the sensors available for use on mobile robots and can provide information about the surfaces in the area to aid in scene analysis.

2.2 Machine perception of plants

2.2.1 Introduction

Plant recognition has not been exploited in the field of remote sensing for autonomous robotics. There are however some agricultural applications of live plant classification, all with limited success. Reasons for this include the large variation in plants characteristics with orientation and the considerable computation cost and illumination problems which occur when using vision systems. Vision is the technique which has been predominantly used to address the plant recognition problem but has only been applied under significant constraints.

2.2.2 Agricultural applications

Researchers have been automating agricultural processes for some time. An example of a highly automated system is the processing of fruits in packing houses [Reece & Taylor, 1996]. The most important steps in the process are of grading and sorting; these are still predominantly manual procedures. Significant benefits can be obtained by automating these steps. There is literature describing many of these studies. Some examples are in the areas of cut roses [Steinmetz *et al*, 1994], fish product [Hu *et al*, 1995], tobacco leaves [MacCormac, 1993] and tomatoes [Gunawardera *et al*, 1991].

Most of the work done with growing plants has been in the area of greenhouse automation. Plants have been used as navigation aids. Both live plants and cuttings have been studied directly in order to grade them. Some work has been published on classifying live plants.

Up until now, plant classification has not been attempted with ultrasonics due to the lack of an appropriate sensing device. Vision has some problems when classifying plants particularly in the area of consistency of lighting. Most of the plant identification

projects consider a small number of classes and are for the purpose of applying chemicals to the plants. Some of the plant identification and classification studies are reported below.

2.2.3 Navigation among live plants using ultrasonic sensing

The AURORA robot [Mandow, *et al* 1996] is an autonomous platform which uses plants as a navigational aid using time of flight ultrasonic sensing. AURORA sprays chemical products on plants within a greenhouse and ultrasonic sensing has proved to be suitable for navigating along plant rows under harsh environmental conditions. Mandow *et al* [1996] found that the high computation costs associated with vision sensing along with inherent illumination requirements rendered it inappropriate for their task. Their system can navigate in a changing environment where there is very little room for manouvering using the natural structures to guide itself along rows and from one row to the next. Its main reported advantage is that it is ideally suited to night time operation without any modification as it can operate irrespective of the lighting conditions.

2.2.4 Classification of plant species

Guyer *et al* [1993] researched the identification of plants based on the shape of their leaves. Their research was limited as they looked at leaves in isolation against a uniform background of soil. Individual leaves of plants at various growth stages were carefully placed on the soil so that they were all at the same distance from the camera and orthogonal to it. They achieved poor results of 68% recognition to separate a leaf from seven other species on a test set which only contained 16 samples. They found that the errors in classification were due to poor images, poor segmentation, and natural scene variation. They reported that the major problem for vision systems in agricultural applications is biological variability within plant species.

Classification of plant cuttings has been implemented by Singh & Montemerlo [1997] where three different Cultivars of *geraniums* have been graded as either small, medium, or large to high accuracy (90%) using computer vision. A single two dimensional image is input and carefully selected features allow for accurate determination

of the grade of the cutting. They found that the appearance of the cutting is changed significantly by the change in viewing angle of the sample but good feature calculation can reduce the effects of this. Humphries & Simonton [1993] have also studied *geranium* cuttings but have concentrated on identifying plant features based on the colours in the captured image.

2.2.5 Plant feature location and grading

Sites & Delwiche [1988] have developed a system which can locate fruit on a tree to high accuracy and found that lighting variations during the day caused most of the problems. Problems included direct light from behind the plant, reflectance of direct sunlight and natural lighting variations caused by cloud cover. They solved the problem by using artificial lighting during daytime operation.

In order to determine the effects of different treatments on ornamental plants, Sistler [1990] attempted to grade plant growth consistent with the Horticulturalist's scale of 0 (dead plant) to 10 (best grade). Experienced graders classify the plants based on size, form, dry mass and growth index and different graders achieve a high correlation to each other in the resulting grade on any particular specimen. They took images from two orthogonal orientations under very specific lighting conditions and calculated features. Results revealed a low correlation between the value calculated from the image and that made by the horticulturalist. It was found to be very difficult to develop a system which could duplicate graders. Unfortunately, Sistler was unable to draw a conclusion about the accuracy of his system and no details about the experiments are presented.

Nabout *et al* [1994] investigated the automatic identification of plant species to separate weeds from crop in order to apply herbicides. They found that there are many different kinds of plants with complex forms and they cannot be described using simple geometric models. They report that they could recognise 17 different weed species to 82% accuracy. Unfortunately, the paper lacks detail.

Seedlings were classified as one of two classes "acceptable" or "cull" by a vision system which captured a silhouette of the seedling in order to measure several physical

properties of the seedlings [Rigney & Kranzler, 1988]. The system is extremely fast and has a low classification error.

Acquisition of geometrical structure of artificial corn plants was performed by Chapron *et al* [1993] with some success. Images from two cameras are matched and contour images are generated. They obtained the best results when information about the specific plant crop is used to build the model. They found that the reconstructions were then quite good.

A vision system which can differentiate between broadleaf and grassy plants in real time has been proposed by Runtz [1991] and has achieved some success. It has the added advantage that a plant does not need to be viewed in isolation in order to be classified.

A model of natural plants was used by Ashok *et al* [1994] to accurately capture the prominent features of trees and plants. The model is an L-system fractal and the authors argue that the model can be used to aid in the recognition of plants. The results show that a classifier can classify images very well. Unfortunately the images were generated by a computer and consisted of plant branches only. The authors recognise that the branches in natural plants are difficult to extract from an image in general but their results could be used in future research.

Other research includes inspection of leaves of tobacco plants which are graded using a vision system in Zimbabwe under controlled lighting conditions based on a series of calculated features [MacCormac, 1993]. Rough hardwood lumber is also graded using a vision system which detects a limited number of defect types [Cho *et al*, 1990]. Huang *et al* [1992] looked at identifying plant roots under the ground as being distinct from the background soil. Seginer *et al* [1992] monitored the tips of the leaves of tomato plants to detect wilt.

2.2.6 Summary of plant sensing applications

In summary, researchers have found that vision is a reasonable tool for analysing plants but have not used it for recognising different plants in an indoor environment. Some plant grading systems give very good results with a small number of different

plants but the analysis is not performed for a large number of samples. Most of the research is limited as the researchers control the environment in order to make it easier for the plant to be analysed. Examples include placing all of the samples at a known distance, against certain backgrounds, very specific lighting conditions, and even placing leaves to be recognised in certain positions within the frame. This is acceptable for some applications but is not a general solution.

Some of the problems encountered with vision systems can be addressed with ultrasonic sensors. This thesis focuses on ultrasonic sensing but a further project could combine vision and ultrasonic sensing resulting in a more robust system.

2.3 Ultrasonic sensing

Ultrasonic sensing is a well established method of remote sensing and is based on the transmission and reception of sound at frequencies above that of human hearing. The basic principle is to transmit a sound wave (at an ultrasonic frequency) and that signal is then reflected from a nearby object (or objects). The echo is received (and captured) by an ultrasonic transducer. The time that the sound takes for the return trip indicates the distance to the object (and back). The amplitude can be used to give properties of the reflecting surface.

Ultrasonic sensing has attracted attention in the robotics community because of its simplicity in construction and low cost [Barshan & Kuc, 1992]. It provides accurate information about the range of objects without the need for complex calculations as is the case with visual sensors [Cai & Retigen, 1993]. Compared to vision, ultrasonic systems are faster and more accurate over medium distances [Kuc & Siegel, 1987]. They do not need any special lighting conditions and use less power, an important consideration for mobile robotics. They are also useful where objects are optically transparent (for example, in a glass factory), where background objects confuse the optical processor, or where the lighting cannot be controlled [Lach & Ermert, 1991]. Ultrasonics can provide highly accurate information about range and bearing of targets and amplitude information can also provide information about the surface.

Some successful applications of ultrasonics in robotics include a system for object localisation [Barshan & Kuc, 1992]; a system to recognise different shaped objects [Cai & Regtien, 1993]; target localisation and classification [Kleeman, 1994]; and fusion of binaural sensor data for object recognition [Kuc, 1996]. They are also used in commercial areas such as BMW's Park Distance Control system [Siuru, 1994]. [Saito, 1994] used wavelet feature extraction for various applications.

Ultrasonic sensing works by generating high frequency pressure waves with a vibrating transducer. The pressure waves propagate through the air and reflect from interfaces between regions of different density. These reflections are then detected by the receiver. The most fundamental information in an ultrasonic signal is the range of the surface.

At present, most common ultrasonic systems are based on pulse technology. A tone is pulsed (the tone is usually 8 to 32 wavelengths long) and the time delay (for the round trip) is measured between the transmission of the pulse and the detection of the echo. This time delay, t , can be used to calculate the range, r , to the target as shown.

$$r = \frac{t.c}{2} \quad 2.1$$

where c is the speed of sound.

The speed of sound, c , is given by Equation 2.2, where *temperature* is measured in degrees Celsius (Note that the effects of humidity, altitude and attenuation due to air particles are small, so are ignored). This equates to approximately 343.5 ms^{-1} at a temperature of 20 degrees C.

$$c = 331.6 \sqrt{1 + \frac{\text{temperature}}{273.15}} \quad 2.2$$

In general, the intensity of the sound pulse decreases in proportion to the square of the distance from the transmitter. However, it also decreases with attenuation of the

signal, where attenuation is caused by factors such as particles in the air or absorption at the surface of the object.

There is also a variation in the intensity of the signal with respect to the angle of the transducer due to destructive interference. There is a very characteristic beam pattern which consists of a strong central lobe and a series of side lobes at much lower intensities [Kinsler *et al*, 1982].

When an object is insonified with ultrasonic energy, the scattering of the signal depends on the size, shape, orientation and texture of the surface. Most of the echo that returns is a result of specular reflection (reflected directly from the surface of the object). In the case of complex objects (objects with multiple surfaces), there may be multiple echoes returning to the receiver. These echoes may also consist of energy that has been diffracted.

In the case of a single coincident transmitter/receiver, very smooth flat surfaces are not detected until the normal from the surface of the object lies within the field of audition of the transducer. Depending on the geometry of the object, it may reflect more energy in some directions than others as it will reflect different amounts of acoustic energy.

For texture to be a significant contributor to the return echo, the roughness must exceed the wavelength by many orders of magnitude. For the KASPA frequencies, the wavelength are in the order of 5 mm, thus roughness only becomes important above 1 cm.

The strength of the echo is also dependent on the shape of the object. A concave object will focus the echo increasing its intensity. In contrast, a convex object such as the corner of a desk will spread the echo, reducing its intensity.

2.4 Human perception and the ultrasonic mobility aid

2.4.1 Human auditory perception

Recognising and classifying environmental sounds is very important. Perception involves receiving information from the environment, as well as the coding, transmission and processing of that information. The ear and its constituent parts reduce sound to its

individual frequencies and pass that information to the brain. The auditory cortex is then responsible for processing the signal. The auditory cortex contains some neurons which respond to certain frequencies and neurons which respond to more abstract features such as changes in frequency [Sekuler and Blake, 1994]. The human auditory perception system can single out complex tones from complex backgrounds such as for example, voices at a party or particular instruments in a musical piece. The ability to discriminate tones based on frequency is one which improves with practice. For example, musical instrument tuners become better with practice.

The brain contains approximately 10^{10} neurons, each of them being connected to about 10^4 others. The neuron is the basic unit of the brain and can be considered as a stand-alone analogue logical processing unit.

A given type of musical instrument will produce its own pattern of harmonics which gives it a characteristic sound, or timbre. Differentiating two different instruments playing the same note, is based on timbre.

2.4.2 Auditory perception and KASPA

CTFM technology has been implemented in a mobility aid for blind people (KASPA) [Kay, 1961]. Both adults and children have successfully used the aid to navigate in complex environments. It was previously sold commercially under the name Sonicguide. Testing of KASPA in several countries has shown that 90 percent of the users can interpret the spatial information provided [Kay & Strelow, 1977].

The mobility aid helps the unsighted to perceive the environment using stereo audio tones. The user develops a completely new perceptual ability. The geometric structure of the environment is perceived directly from stereo sound. In this situation, brain perceives the environment by sound instead of vision.

This reconstruction of the environment from sound has a novel corollary with a very rare condition known as Synesthesia which affects humans. Synesthesia has been known and documented for over two centuries [Cytowic, 1989]. The sensory channels are mixed by the brain and the world is perceived differently from the majority of us.

Some have the ability to see sounds or taste shapes. This leads to added senses which can be rich in information. KASPA can also be looked upon as an added sense.

Gissoni [1966] who is completely blind, taught himself to use the mobility aid. He states that he hears notes singularly and in combination, and that they can be as meaningful and informative as words spoken to him in his native tongue. The sensor can not only detect the presence or absence of objects but can give accurate range indications to within ten millimetres when the unit is set on short range. Object movement is detected by rising or falling pitch: If an object is moving away, the pitch will increase.

As an example, different types of plants produce different signals depending on their leaf or needle structure. Tree trunks are distinguished from poles by the texture of the tree trunk reflecting the acoustic energy differently. Other everyday objects such as doormats and picket fences have their own special signals. Scanning along a picket fence produces tones that sound like ducks quacking. A flight of steps produces a series of tones, each increasing in pitch as the aid is scanned up the steps.

In familiar territory the aid is useful for detecting land marks. Gissoni also refers to a signal bank that he has built up in his mind over eight months of using the device. He uses this knowledge to navigate in unfamiliar territory and detect unfamiliar objects. He describes an experience where he was presented with an object that sounded like a rock wall with foliage growing through it. Upon examination by touch, he found that it was exactly that. He had detected both rock walls and foliage individually in the past and was able to link that experience to what he was detecting now.

He achieved increased independence using the system. For example, he can locate the position of elevator signal buttons. He can then detect the opening doors and assess whether people are moving in and out so that he can judge his own entry. Gissoni claims that with the mobility aid he can thread his way through heavy pedestrian traffic, smoothly and gracefully, without collision; find an empty seat on a bus; an empty desk in a classroom; or a table in a restaurant.

Gissoni emphasises the high information content in the tones and stresses the intense practice required to be able to use this information effectively.

Thornton [1975] had used the aid effectively for a period of four years. He has walked more than 8000 kilometres without a companion using the aid under widely different conditions, often over unfamiliar terrain. He believes that the aid allows him to be more aware of the environment and has a more relaxed attitude to mobility.

Farmer [1975], describes the use of the mobility aid by several trainees in adverse weather. The trainees were taught to navigate by using landmarks such as trees, hedges, telephone boxes, fences, driveways, mail boxes and signs. They can detect moving pedestrians and then follow them down the street. Farmer notes that there are problems with the aid during heavy rain and snow. Also, the trainees were able to detect low hanging, snow covered branches to enable them to avoid getting snow in their faces or down their backs. He notes that the trainees were able to determine the distance, size and direction of objects.

The aid has also been used successfully to improve the mobility and independence of young children [Strelow *et al*, 1978]. Newcomer [1977] reports on children who have gained independence using the aid. The children were surprised when they could detect previously unknown objects that exist in the environment. Roy, a high school student uses the aid to navigate along congested footpaths and train platforms without contacting people with his cane. Roy can detect the position of queues standing to buy train tickets, make his way through turnstiles and detect the position of train doors once the train arrives at the platform.

CTFM has also been used underwater using different transducers. A system is available to assist divers to navigate underwater in areas of low visibility such as murky water or in the absence of light [de Roos *et al*, 1981]. The transducers are mounted on a helmet that is worn on the diver's head. The system can be used to locate objects on the sea floor; determine the position of fixtures around oil rigs; or can be used to determine the extent of marine growth on submerged structures. Different shapes and surfaces give characteristic audio outputs which allow the diver to detect the range, direction and type of object.

The mobility aid allows the user to easily discriminate between stationary and moving objects [Kay, 1977]. An Echocardiograph was developed to take advantage of this feature and allows the user to monitor the movement of cardiac structures [Kay *et al*, 1977]. It is used to monitor positional change of the four valves of the heart and the sound patterns can be used to distinguish a normal mitral valve compared to the motion of a severely stenotic one.

Kay [1977b] tested a fishing sonar which can detect fish at a distance up to 135 metres. Multiple shoals of fish can be differentiated in terms of their relative position. Also, different species of fish can be distinguished by their own distinctive tonal patterns.

Porto[1989] has used CTFM sonar to detect spheres underwater at varying distances. His neural network classifier identifies the presence or absence of large metal objects which are submerged in the ocean.

The success of these applications inspired this research in the area of CTFM ultrasonics. This investigation focuses on exactly what is in the signal that allows objects to be recognised by the human perceptual system.

2.5 Perception test by an inexperienced user

The inexperienced user is bombarded with a multitude of information when starting to use the ultrasonic mobility aid. Consequently, it is very difficult to differentiate different types of complex objects based on the tonal patterns. All of the sounds tend to be the same for the inexperienced user.

This situation occurs in other areas of sound perception. How many times have you heard a fed up parent say to one of their children “Will you turn that heavy metal music off please? It all sounds the same”. Or, similarly, a child may ask “Will you turn off that classical music please? It all sounds the same”. There are many reasons for this; one is that the individual has not developed an appreciation for the particular combination of sounds and the fine differences in tone which makes one piece different from another.

The user of the mobility aid quickly learns the difference between simple objects, but those which are characterised by smaller differences take longer to separate.

For example, the inexperienced user can clearly hear the difference between plants when they are placed in close proximity and the aid is moved from one plant to another. It is harder however, to remember the differences between one plant and the other when the user listens to them separated by some time period.

2.6 The place for a plant classifying sensor

Plants are useful natural landmarks which exist in many office and home environments so are good candidates for use in mobile robot localisation. There are many sensors for mobile robots commercially available but none of them have proved to be an outstanding success on its own. The application of plant classification in the field of agriculture has only had limited success.

A CTFM sensor is well suited to the application of plant classification and this is investigated further in this thesis.

2.7 Conclusion

This chapter introduced environment sensing in robotics and specifically sensing using CTFM ultrasonics. Currently there are very few commercial applications of mobile robots and one of the reasons is that sensing is not sufficiently advanced. CTFM sensing will add to the current sensing capability for mobile robotics.

A review of plant sensing applications shows that some work being undertaken with applications in the areas of greenhouse automation and agricultural grading. These systems are mostly based on vision sensors and results are generally weak. They are however, successful when the environment is carefully controlled.

Many blind people have successfully used the CTFM based ultrasonic mobility aid and experience shows that the device is practical and accurate. This thesis shows that the device can be applied to the mobile robotics area as a machine can interpret the complex signals which are generated.

2.8 Summary

1. In order for a mobile robot to interact with its environment, it needs sensors.
2. There are many sensing techniques available for mobile robots but there are very few commercial autonomous robots in use.
3. There are several agricultural applications of plant sensing including greenhouse automation and grading. In order to be successful, the applications need to control their environmental conditions carefully.
4. Many blind people have used the ultrasonic blind mobility aid called KASPA with great success. They can navigate successfully in unfamiliar environments.
5. Ultrasonic range data can provide information which can be interpreted in isolation or in combination with other sensors.
6. Human auditory perception is a complex process which is very good at analysing the frequencies of tones.
7. There is potential for application of this sensor in mobile robotics.

3. CTFM Sensor

3.1 Introduction

This chapter introduces Continuous Transmission Frequency Modulated (CTFM) ultrasonics and provides references to other publications for comprehensive information about the electronics and the signal processing. The hardware and software used is outlined in detail. Certain parameters are configured to determine the limits in range and also the resolution of the system and these are described. The physical properties of the sensor are then established for this application. This is done in terms of repeatability, environmental effects, amplitude variation and range variation.

The model of the acoustic density profile is developed in order to interpret the information in the echo reflected from the plant. The frequency spectra of the received echo is then interpreted based on this acoustic density profile model. The frequency lines are interpreted as range lines where the amplitude at each range line is directly proportional to the normal area of all of the surfaces at that range. That is, each range cell is a measure of the acoustic area. The entire density profile becomes the acoustic area of the entire scene.

In order to provide an understanding of the signal, the output of the system is analysed with reference to simple objects. Plant sensing is then discussed in terms of range cells.

3.2 Principles of CTFM sensing

CTFM was originally modelled on the same principles used by bats by Professor L. Kay [Kay, 1961]. Bats have shown that they make good use of ultrasonic waves and can recognise their prey against a complex background [Kay, 1964].

Currently, pulse (or time of flight) systems dominate research into ultrasonic sensing technology because [de Roos, 1986] :

1. Significant advancements were made in pulse radars in the 1950's and many of the techniques used were being applied to sonar resulting in a great deal of knowledge of these systems being developed; and
2. Current electronics (in the 1950's) favoured pulse systems. Time domain systems require accurate gating and timing mechanisms which were available at the time. Frequency domain systems require linear frequency modulators and precise spectrum analysers.

Now that the technology has caught up with the theory, the CTFM sonar output is accurate. The advantages of using CTFM include low susceptibility to noise and greater information in the return signal. CTFM has also found application in radar [Neininger, 1977]. A comprehensive comparison of short pulse sonar, chirped linear FM pulse sonar and CTFM sonar can be found in de Roos [1986].

Unlike conventional ultrasonic systems which were discussed in Section 2.3, a CTFM system transmits a sine wave signal that is repeatedly frequency swept over a one octave range (typically 100 to 50 kHz with a sweep period of 102.4 ms). The return echo is a replica of the original, offset in time. When the echo is received, the transmit signal is used to demodulate it and the resulting frequency is proportional to the range of the target. The demodulation process produces audible tones in the range of 0 to 5 kHz. In the audio signals, the pitch is directly proportional to the distance to the object. A model of the signal in the frequency domain is shown in Figure 3.1. The demodulated signal is shown at the bottom of the diagram; this indicates the frequencies of the tones which are heard in the audio frequency range. With a CTFM system, echoes are resolved based on their frequency (pitch) instead of their elapsed time, as is the case with conventional ultrasonic systems.

The electronics and signal processing techniques have been detailed in the following publications. For information about the transducers see Rowell [1970] and Martin [1969]; for the details of the signal processing see Hayes [1989] pp 58 - 79, de Roos [1986], or Kay [1984].

Note that the current system uses a Fast Fourier Transform (FFT) to transform the signal to the frequency domain as in Hayes [1989]; this is compared to de Roos [1986] who chose to use contiguous bandpass filters. With improvements in technology, the speed of FFT hardware has increased and it is now practical to use the method in real time applications.

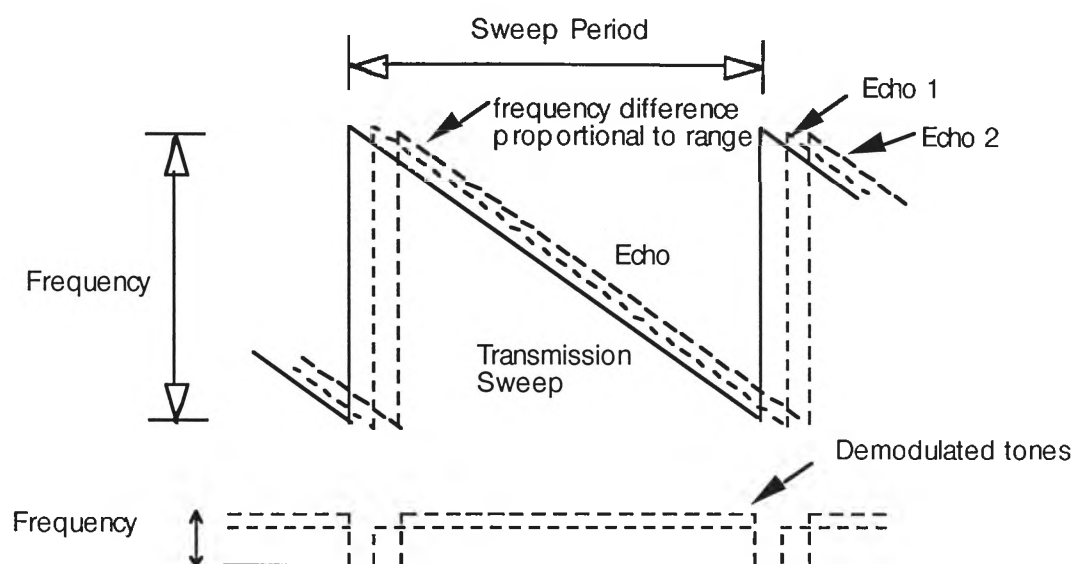


Figure 3.1 The model of the CTFM system

The analysis of the output of a CTFM signal is fundamentally different to that for pulse sonars in that it is analysed in the frequency domain instead of the time domain [de Roos *et al*, 1988]. The CTFM signal can be represented more simply in terms of the frequencies that it contains.

3.3 Hardware and software

Bay Advanced Technologies produce the ultrasonic mobility aids. An experimental system was purchased for this research. It consists of a binaural sensor connected to a microcomputer through a spectrum analyser with appropriate transmit/receive electronics (Figure 3.2). Frequency domain signals are available for analysis on the computer.

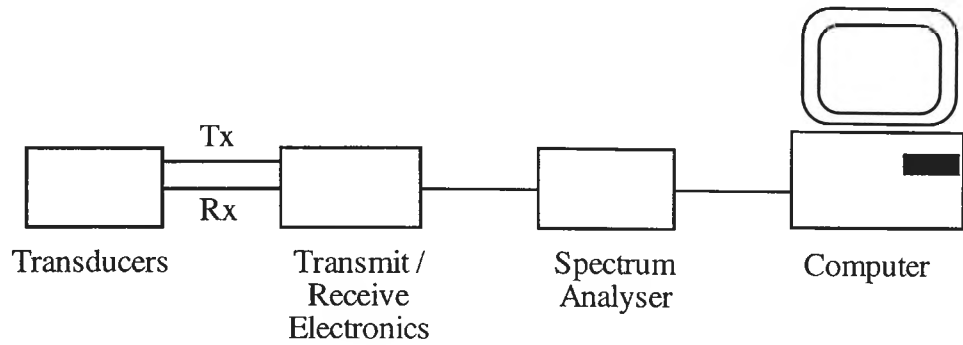


Figure 3.2 Schematic of the experimental system

The sensor head consists of three transducers (Figure 3.3), with the centre one transmitting continuously and the left and right sensors receiving the echoes from the environment.

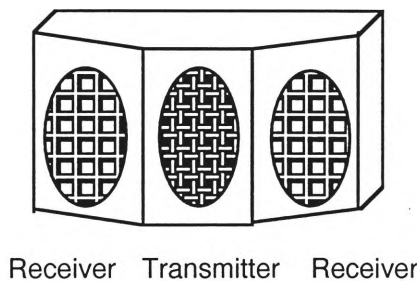


Figure 3.3 A representation of the sensor head

The FFT transforms the time domain signal to the frequency domain where it can be analysed in the form of a spectrogram. The 1024 point FFT produces positive amplitude values for 512, 9.77 Hz frequency bands over the range of 0 to 5 kHz. Just as a human perceives range from the pitch of the audible tone, the frequency on the spectra at which an amplitude threshold is exceeded corresponds to the range to the surface. This threshold highlights objects as distinct from background noise. The amplitude of the spectral line is proportional to the intensity of the echo and hence to the area of the reflecting surface normal to the receiver.

The sensing system is run on an IBM compatible personal computer with a 386 processor. The transducers are connected directly to transmit/receive electronics which are contained inside a small box. Specifications for the transmit/receive electronics can be found in Kay [1974]. The frequency sweep is generated by a custom designed digital sweep card which is housed in the personal computer. The received signal is processed

by the transmit/receive electronics and the analogue audio signal is fed to the analogue to digital converter and FFT hardware then converts it into the frequency domain which is available to an application program.

The software to run the system and produce a rudimentary display was provided by Bay Advanced Technology (BAT system) and is written in the C programming language.

3.4 Technical data

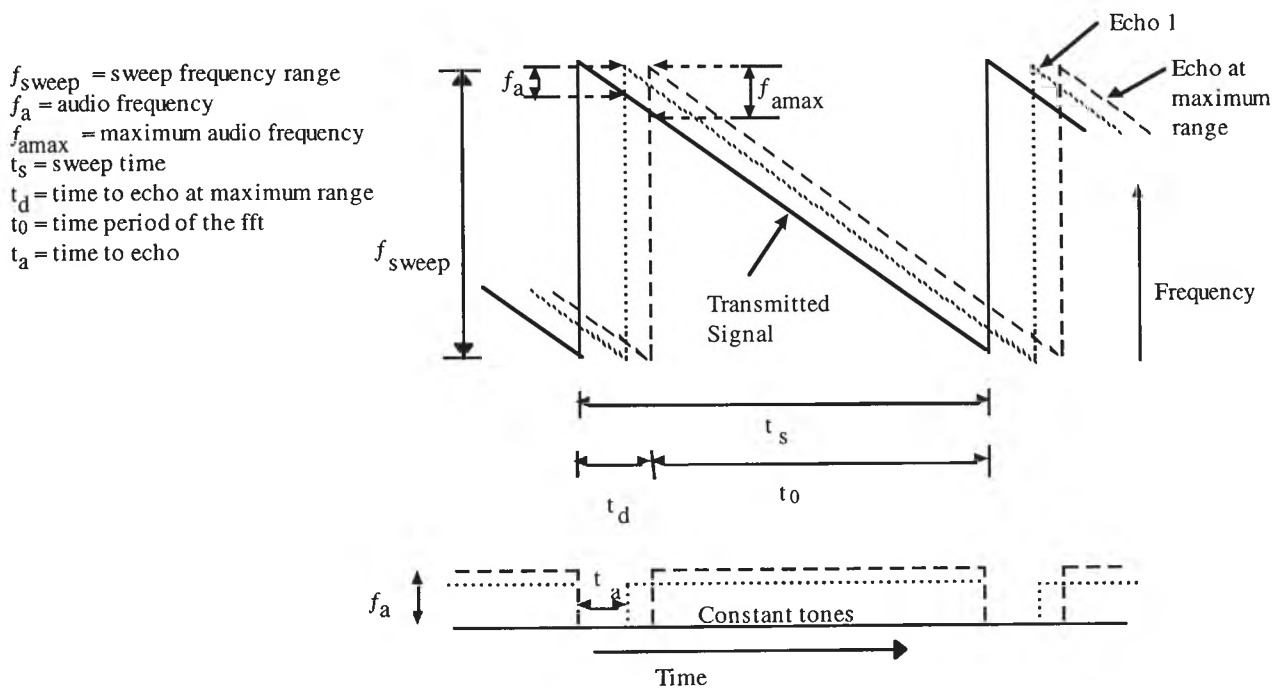


Figure 3.4 CTFM signal (in frequency domain) with demodulated signal below

The maximum range of an ultrasonic sensing system is determined by the transmitted power, the speed and absorption of sound in air, and the receiver sensitivity. A CTFM system has a maximum operating range which is controlled by selecting a maximum audio frequency ($f_{a\max}$) and a sweep time for the transmitted signal (t_s). The audio frequency (f_a in Figure 3.4) is the difference between the echo frequency and the transmitted frequency at any instant in time. The range is proportional to an audio frequency and the maximum range can be increased by increasing the sweep time (t_s). The

scaling factor (s_f) from audio frequency to range is the ratio of the maximum range (range at the maximum audio frequency) to the frequency at the maximum operating range.

$$r_a = \frac{t_a \cdot c}{2} = f_a \cdot s_f \quad 3.1$$

where $s_f = r_m / f_{amax}$

r_m = max operating range = $c \cdot t_s / 2 \cdot f_{sweep}$

r_a = range at frequency a

c = speed of sound = 343.5 ms^{-1} at 20°C

When choosing a sweep time, the designer has to consider the requirements of the FFT. The minimum sweep time is the time for the signal to travel to and from an object at the maximum range (t_d) plus the length of signal required to perform an adequate FFT (t_0). This ensures that the signal presented to the FFT will consist of a set of continuous tones, eliminating errors caused by discontinuities at the start and end of the tones. The minimum sweep time, t_{smin} , is given by Equation 3.2. The FFT sampling interval, t_i , is given by Equation 3.3. The FFT sampling frequency, f_{samp} , is given by Equation 3.4.

$$t_{smin} = t_d + t_0 \quad 3.2$$

$$t_i = \frac{t_0}{N} \quad 3.3$$

where N is the number of points in the FFT.

$$f_{samp} = \frac{1}{t_i} \quad 3.4$$

This sampling frequency must be greater than twice the maximum audio frequency to satisfy the Nyquist criterion for sampling [Strum & Kirk, 1989]. The range resolution

of the system is determined by the frequency spacing (δf) of the spectral lines in the FFT and is given by Equation 3.6.

$$\delta f = \frac{f_{a\max}}{N} \quad 3.5$$

$$range_resolution = \delta f \cdot s_f \quad 3.6$$

The system used in the experiments has been set to sweep from 100 kHz to 50 kHz. A practical sweep period was chosen to be 102.4 milliseconds.

When testing the blind aid device, operators found that 5 kHz was the maximum frequency that most of the users of the device could perceive. The maximum frequency was configured as part of the device. This reduces the maximum range of the sonar for a given sweep time but has no effect on the resolution of the device.

A 1024 point FFT is used and 512 useful spectral lines are available with a frequency spacing of 9.77 Hz. This gives a resulting range resolution of 3.44 mm between frequency bins. This resolution can be improved by interpolation between the bins using a sinc function.

The radial resolution of the system is the distance by which two objects need to be separated before they are identified as two. A criterion proposed by Rayleigh is often used to define the separation of objects in the frequency domain. It is based on a drop in signal intensity between two peaks in the frequency domain and has shown to be twice the wavelength [Kay, 1985]. For a frequency of 75 kHz (the average frequency), this is 10.32 mm.

3.5 Physical sensor properties for this application

This section analyses the way the physical characteristics of the system determine suitability for mobile robotics. This data analysis establishes confidence by analysing repeatability, effects of environmental conditions and the variation with range. All of the tests were run in a sealed room in order to minimise environmental disturbances

3.5.1 Repeatability

It is important to know the statistical properties of the signal when the system is operated in air. A signal which is not repeatable is of limited use.

This section outlines the conditions of the experiment and the results are given in both graphical and tabular form. Table 3.1 shows the conditions under which the experiment was run.

Table 3.1 Repeatability Experimental Conditions

date	23/10/95
temperature	24.9 degrees C
humidity	41.8 %
surface	white laminex board
distance	465 mm (measured)
no. of samples	400

An example of the frequency spectra of a typical return is shown in Figure 3.5. An expanded graph of Figure 3.5 is shown in Figure 3.6. The Frequencies on the x axis represent the spectral lines 120 to 150.

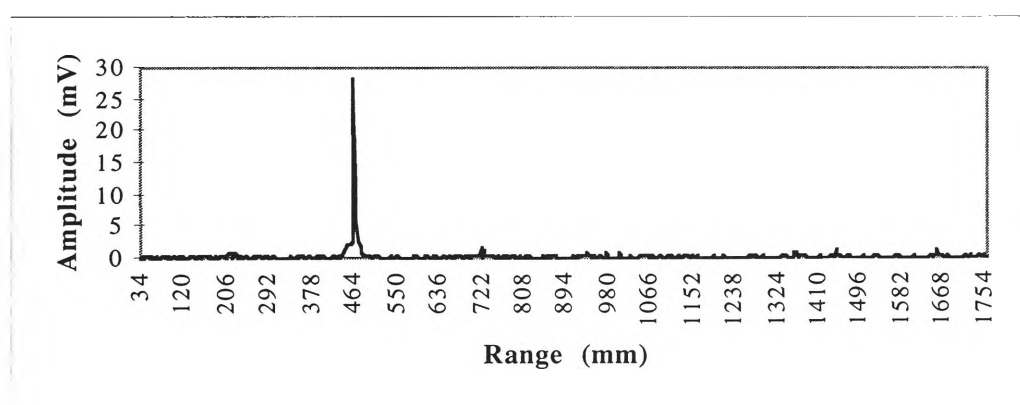


Figure 3.5 The frequency spectra when a small laminex board at a range of 464 mm is ensonified

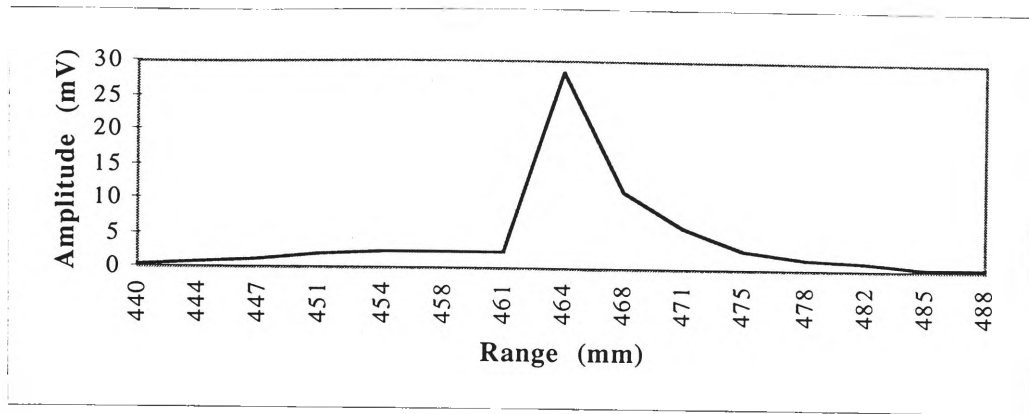


Figure 3.6 An expanded view of the point of interest from Figure 3.5

The spectral line with the maximum amplitude is used as the representative frequency and the means, standard deviations and coefficients of variation were then computed. The results are shown in Table 3.2.

Table 3.2 An analysis of Frequency Line 135 which corresponds to a range of 464mm for the laminex board ensonified in Figure 3.5

fft line	135 (range 464 mm)
mean (mV)	27.3
stdev	1.03
variance	26.68
coeff. var.	0.038
Randomness	0.0014
No.Obs	400

The coefficient of variation is 3.8% which is extremely low. This indicates that the information from the binaural system is very repeatable (coefficient of variation = stdev / mean).

The randomness factor is calculated using Equation 3.7. Figure 3.7 is a frequency polygon of the variation of frequency line 135, also shown on the histogram are the Gaussian (Equation 3.8) and Rician (Equation 3.9) fit of the amplitudes for the frequency line. A Rician model is often used in a system with a dominant scatterer [Nielsen, 1991].

$$R = \frac{\text{variance}}{\text{mean}^2 + \text{variance}}$$

3.7

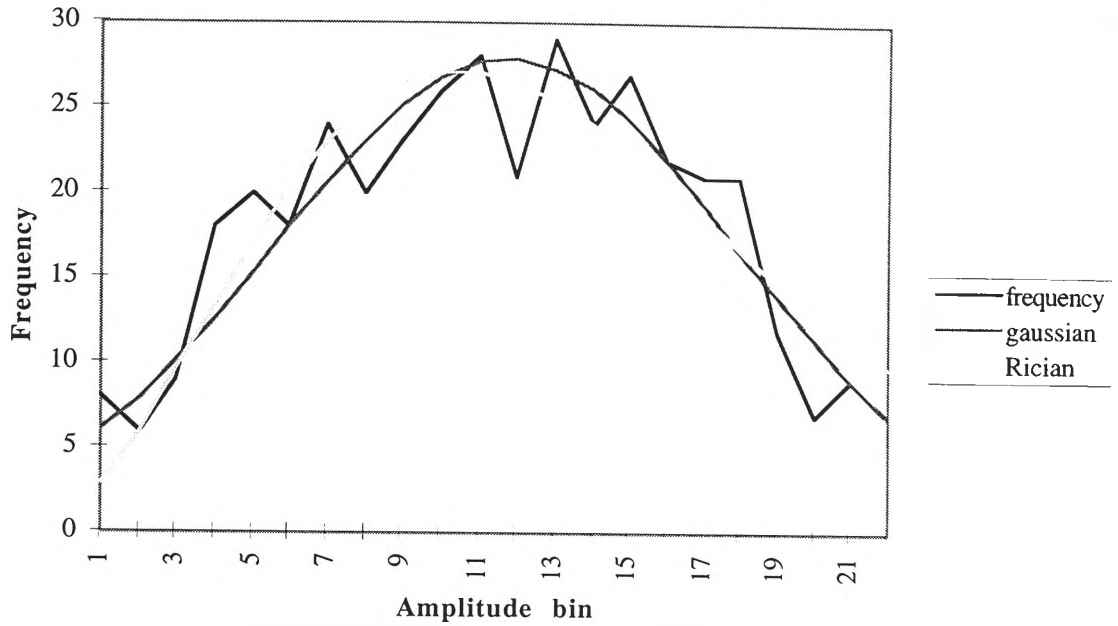


Figure 3.7 A frequency polygon of the amplitudes of FFT line 135 (corresponding to range 464 mm) also shown is the Gaussian and Rician fit

The Gaussian equation used is :

$$b(n) = \frac{1}{\sqrt{2 \cdot \pi \cdot \sigma}} \cdot \exp \left[-\frac{(n - \mu)^2}{2 \cdot \sigma^2} \right] \quad 3.8$$

The Rician equation used is :

$$p(x) := \frac{1+s}{\mu} \cdot \exp \left(-s - \frac{x(1+s)}{\mu} \right) \cdot I_0 \left[2 \cdot \sqrt{\left(\frac{x}{\mu} \cdot s(1+s) \right)} \right] \quad 3.9$$

where I_0 is the Modified bessel function of 0 order [Skolnik, 1980]. The error of each of the distributions against the actual values are:

Gaussian 50.6; and

Rician 63.0.

In summary, the data items in the acoustic density profile fit a Gaussian distribution and have a very low coefficient of variation. This means that the signal is very consistent and can be said to be reliable.

3.5.2 Variation with environmental conditions

The previous section dealt with the variation in the signal with samples which are taken consecutively over a short time period. When a large number of samples are taken consecutively over a long period of time however, environmental conditions (specifically temperature and humidity) may change. The effect of humidity on a signal is negligible but a temperature change can affect the result as it affects the transmission of sound in air [Kinsler *et al*, 1982]. It is also useful to know whether the performance of the overall system remains constant over a period of time. For example, if the sensor degrades over a period of time, care may have to be taken when taking measurements.

An experiment was set up to take readings every 15 minutes. The sensor head was pointed at a very specular object (a plain wall) at a distance of exactly 600 mm. Care was taken to ensure that the sensor was orthogonal to the wall. Every 15 minutes, 20 readings of the frequency spectrum were taken. At the same time, the environmental probe was sampled to record the current values of temperature and humidity.

The apparatus was located in the back room of the lab which has large north facing windows which meant that the temperature in the room could rise significantly over the period of a day. This temperature increase affects the speed of sound and the object in view “appears” closer than it actually is as the temperature rises. In other words, the wall seems to move towards the sensor as the temperature rises.

When the experiment started, the temperature was 21 degrees C, the speed of sound at this temperature is 344 ms^{-1} , which results in a frequency of 1703 Hz, and energy appears in FFT bin number 174. When the experiment finished though, the temperature was 26 degrees C, the speed of sound at this temperature is 347 ms^{-1} , which results in a frequency of 1686 Hz, which will put the energy into FFT bin number 173. This is a completely different frequency bin! In other words, the wall will appear to be

3.4 mm closer to the head of the sensor. In a practical system which requires very precise range information, this change in temperature will need to be considered.

The change in the spectra with time is shown in Figure 3.8. The corresponding graph of temperature is shown in Figure 3.9. It can be seen that the spike in the graph moves forward slowly over the period of the day.

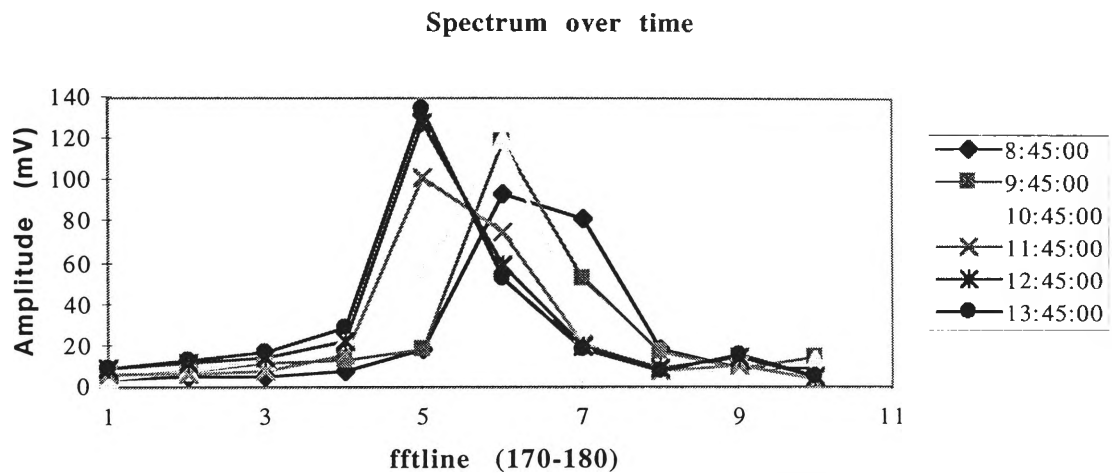


Figure 3.8 The average spectrum as it changed over the day

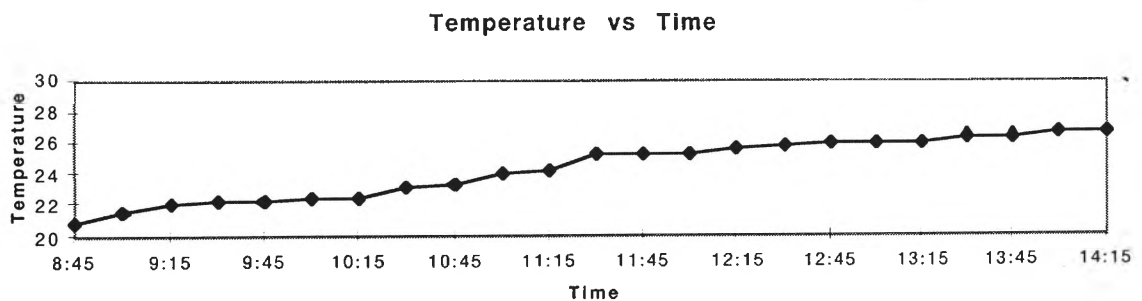


Figure 3.9 Temperature change throughout the day

The change can also be observed by viewing a single frequency line over a period of time as shown in Figure 3.10. It can be seen that the temperature increased steadily throughout the day and the humidity decreased. There comes a time just after 10:45 when the temperature had risen enough for the energy which was previously in the prior spectral bin to step forward into this bin which causes the amplitude of the graph to rise significantly.

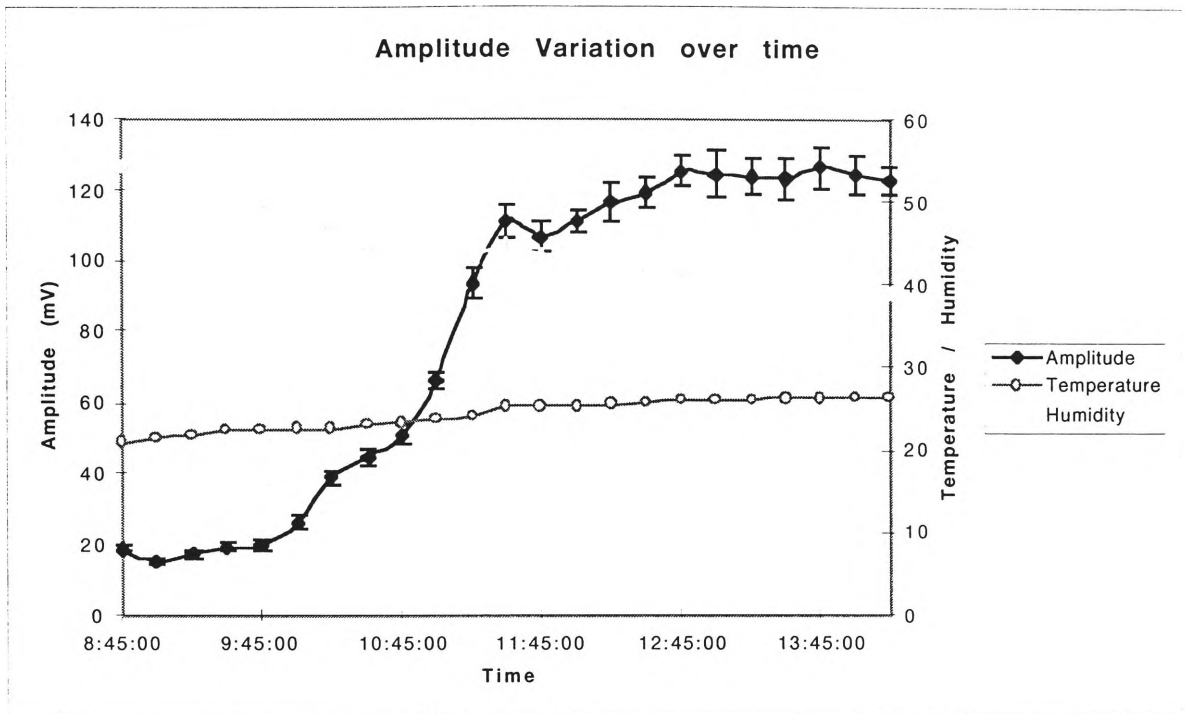


Figure 3.10 The amplitude variation over time for FFT bin 175 (1709 Hz corresponding to a range of 602 mm)

Temperature affects the position of the echo in the frequency domain. It will also affect the total amplitude but that will be in proportion to the absolute temperature. This is shown in 3.11 with the error bars showing a single standard deviation on each side of the sum of the amplitudes. The graph shows the sum of FFT lines 170-180 at each of the time periods. It can be seen that the amplitude rises in proportion to the rise in temperature and the statistical correlation between the variables is calculated as 0.89 which means that the two distributions are highly correlated. Figure 3.11 shows the same information on a single chart, with a straight line shown fitted using the method of least squares. The line passes well within a standard deviation each side of the measurements so shows that the relationship between temperature and the sum of the amplitudes is linear.

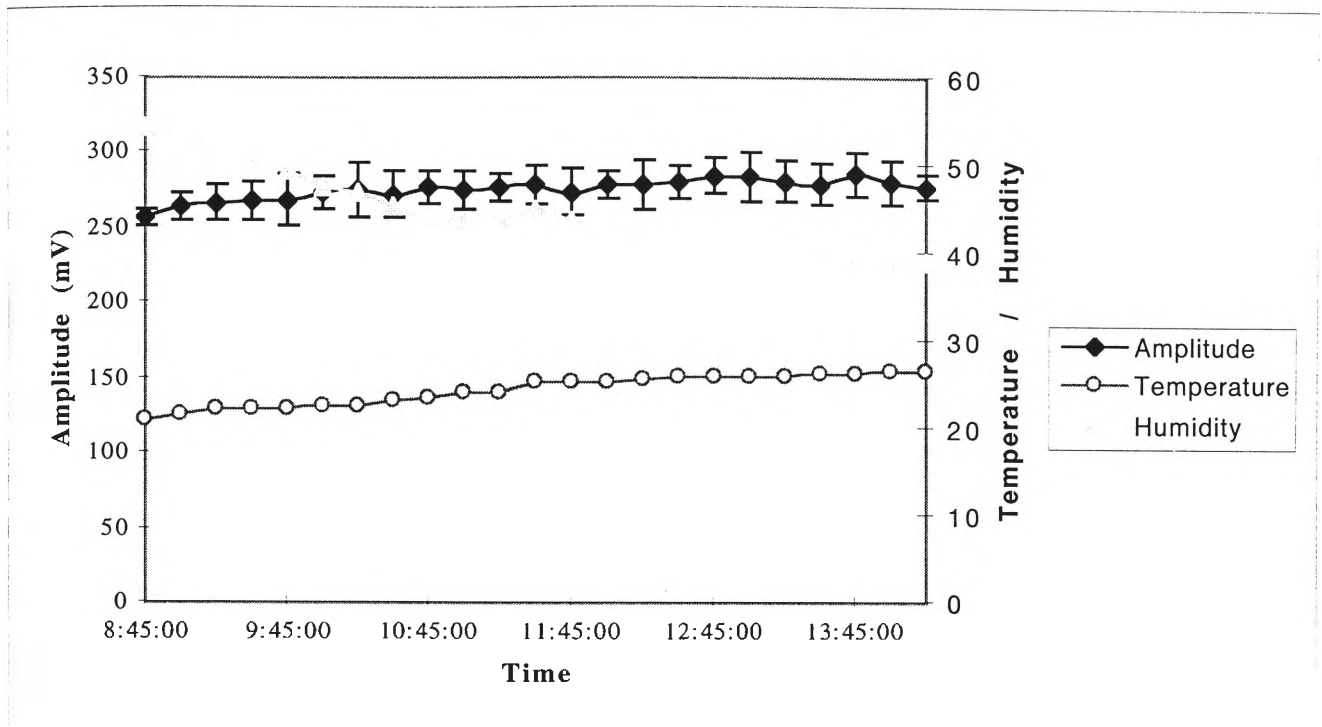


Figure 3.11 The sum of FFT bins 170-180 over the day. Error bars are one standard deviation

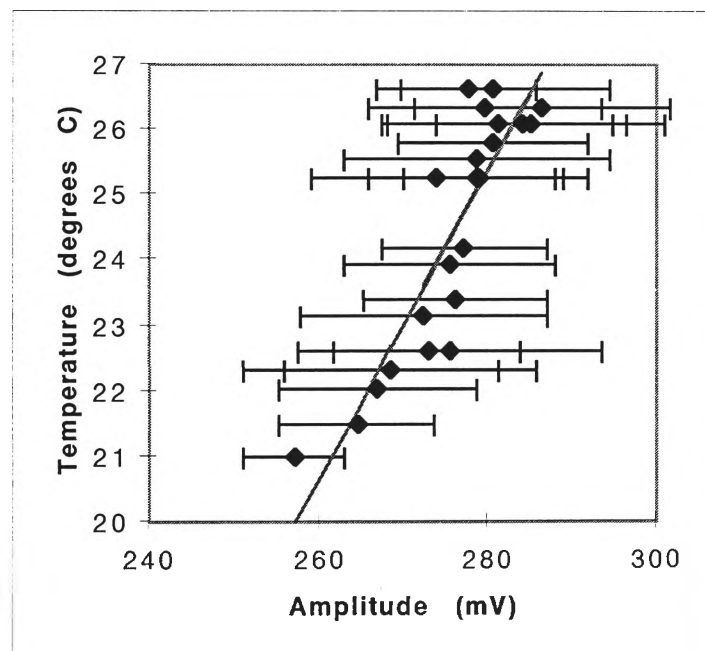


Figure 3.12 Temperature against the sum of the amplitude. Error bars are one standard deviation

3.5.3 Amplitude variation with range

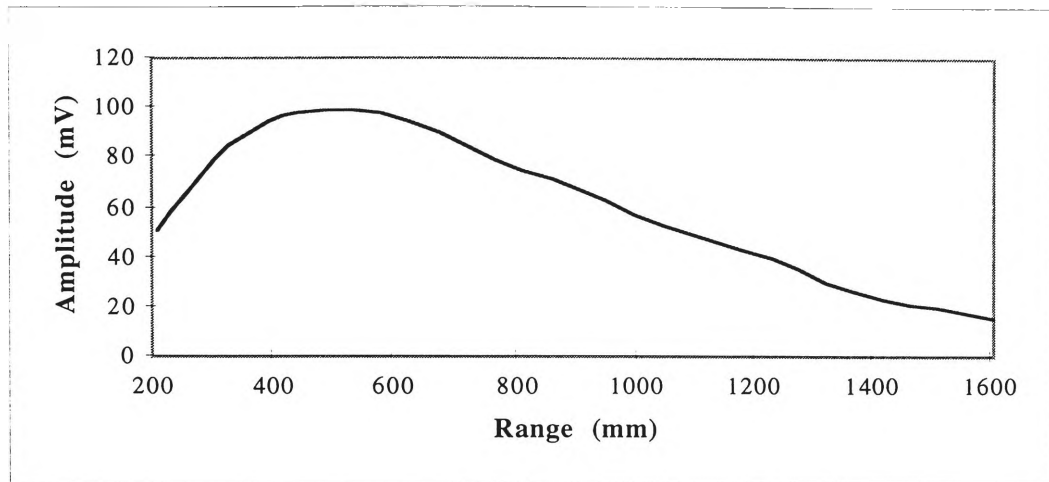


Figure 3.13 Change in amplitude with range

Figure 3.13 shows the change in amplitude of the received signal with range. A specular object (a large flat laminated board) was set up orthogonal to the sensor head and measurements were taken at 17 different distances from it. Measurements closer than 200 mm were discarded as there was too many multiple path reflections between the board and the sensor head which obscured the data. The temperature was 19.4 degrees C and the humidity was 48.3%. There is some conditioning of the signal within the mobility aid electronics which processes the audio signal by frequency shaping to correct for loss of propagation with distance, earphone frequency response and also the users audio frequency response. These combine to give the change in amplitude with range shown in Figure 3.13.

The graph shows a gradual increase in amplitude as the object moves out to a distance of 400 mm from the sensor and a similar decrease once the range goes past 600 mm. This datum can be used in a practical system to scale the received information. From the absolute range of the object, all of the frequencies can be scaled so that they are comparable to an object at some standard range of, for example, 500 mm.

3.6 Analysis of system outputs

3.6.1 A tour of the lab wearing the blind aid

We do not have a commercial version of the Ultrasonic Blind Aid in our lab but there is an experimental version of the system which can be either connected to a spectrum analyser or a pair of headphones. It involves a sensor head on the end of a rod connected to a processing box. The rod holding the sensor head is held in the user's hand and can be waved around to inspect different objects.

The richness of the tones heard through the ears is immediately obvious. If the sensor happens to be pointing at a wall, a very clear note is perceived in both ears. Other specular objects also produce similar single tones. An inexperienced user can very quickly focus on the basics of the audio signal while examining simple scenes with the device. Some of the basics are described below.

The pitch of the tone depends on the distance to the object, and the volume depends on the amount of echo which is received by the transducer. So the volume depends on the distance to the object (Figure 3.11) and also the fine surface texture of the object. As you move away from a specular object (once you get past 500 mm from it), the pitch increases and the volume decreases. Two objects with different textures on their surfaces at the same distance will produce a tone of the same pitch (since they are both at the same distance) but of a different volume. The volume will be different due to the different amount of scattering caused by the surfaces (a smoother surface will reflect more of the acoustic energy directly back to the sensor than one which is rougher - the rougher surface will scatter the acoustic energy more). Note that the volume will also be affected by the range variation as shown in Section 3.5.3.

The audio signal from a specular reflector can be analysed based on the pitch and volume of the tone. A sensor pointing at a smooth wall at a distance of one metre will produce a tone of a similar pitch as when pointing at a cloth covered wall at the same distance. The difference will be a minor tonal difference and a significant volume decrease. An inexperienced user can quickly learn to estimate the distance to single objects

based on the pitch of the tone. This is because they have a relatively small number of variables to estimate.

More careful analysis is required when multiple objects are in view or more complex everyday objects are introduced, that is just about every situation you will have when using KASPA. More complex surfaces (or multiple objects) are commonly encountered when using the device indoors. An example is with office furniture or other laboratory equipment where there may potentially be many reflective surfaces within any one scene. When the difference in distance from the sensor between any two surfaces in the scene is greater than the smallest perceivable distance then more than one pitch (depending on the number of surfaces at different ranges) will be heard. The smallest perceivable difference will depend on the hearing sensitivity of the individual user. Each surface (at a different range) will produce a single frequency so when there are multiple surfaces, a combination (a possibly complex combination) of frequencies will be heard together.

From experience gained over many months of training, the user can interpret the signal and describe the structure of the scene in great detail. For the inexperienced user however, it becomes very difficult to interpret the audio signal. Note that even though the mobility aid requires months of practice, the training period for a blind person is less than that required for the long cane.

Difficulty arises when the user is trying to resolve all of the components of a sound produced by multiple surfaces. Each individual surface will produce a frequency which is proportional to its range and the volume at that frequency will depend on the range and the texture of the surface. The user now has many variables to estimate. Figure 3.14 illustrates that the user would have to estimate the pitch and volume for every frequency within the field of audition.

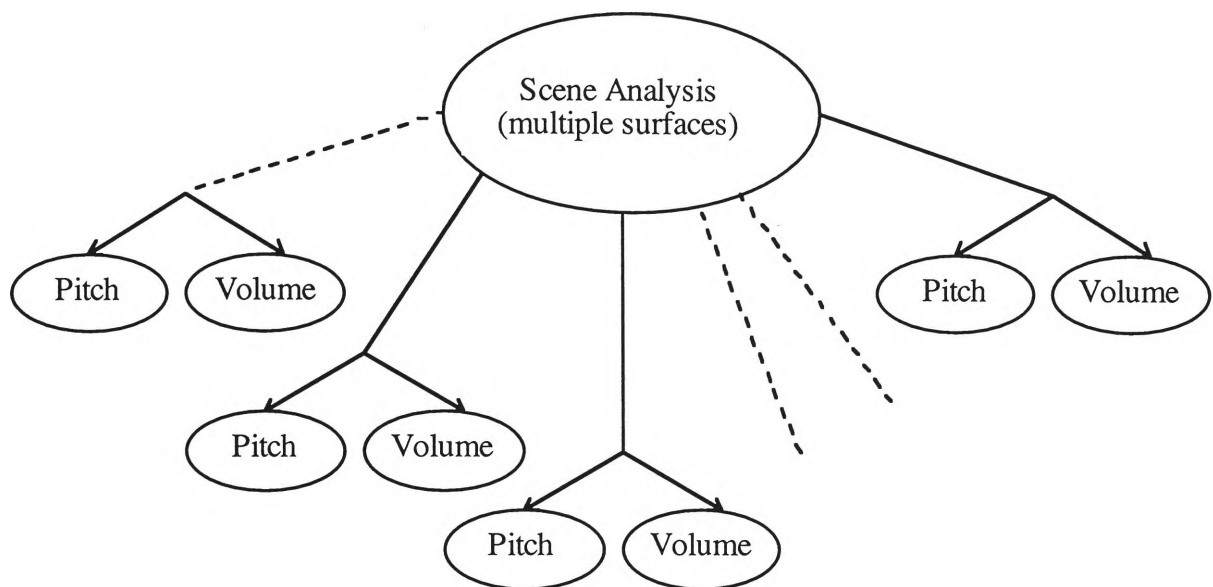


Figure 3.14 The analysis required for a scene with multiple surfaces

It is not clear whether blind users resolve the signal into its individual components or build up a memory of the patterns and relate that to a particular kind of object or scene. It is not even clear to the users themselves. It is like asking someone how their brain processes visual images, it just does!

A walk around the lab quickly reveals that different scenes give very different signals. It is most interesting to listen to the tones produced by different kinds of books on the shelves. Large thick books produce a very different sound to a row of narrow journals. It is obvious that different kinds of objects produce their own characteristic tones and that it may take some time to learn how to use the device effectively.

3.7 The acoustic density profile model

The information in the frequency of the signal is a range measurement to every near normal surface that is in the insonified region. A small amount of the signal is a result of multiple reflections and interference. The information gives an indication of the structure of the object(s) in the field of audition.

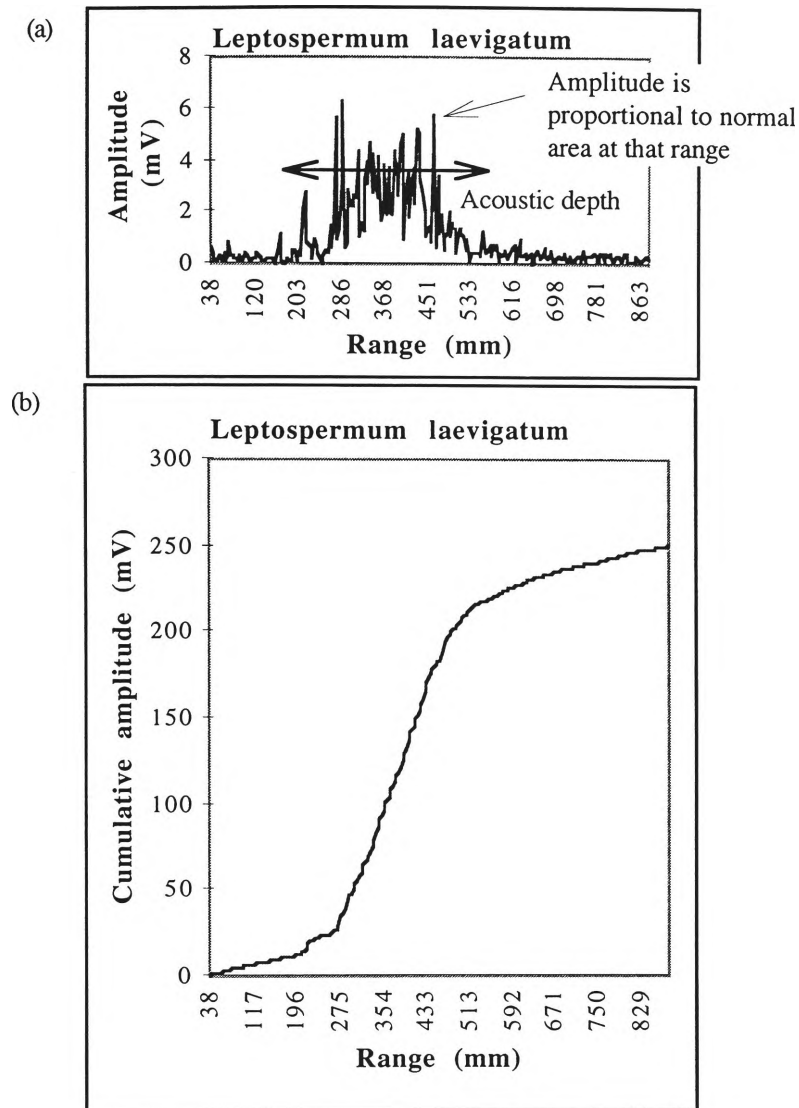


Figure 3.15 The acoustic density profile model

The frequency spectrum provides information about the range, size and orientation of surfaces within the field of view so can be modelled directly as an acoustic density profile. The sensor then measures the acoustic area at each range and the sum of all of the ranges gives the acoustic area of the plant. The acoustic density profile model (Figure 3.15) shows (a) the acoustic density profile for a specimen of *Leptospermum laevigatum* and (b) the cumulative density profile of the same specimen. The cumulative density profile is the accumulated value of each of the range cells from the acoustic density profile shown in part (a) and is a measure of the acoustic area of the plant.

The acoustic density profile is a measure of the acoustic density at each particular range from the sensor. Figure 3.15 (a) shows a significant acoustic density between the ranges of 200 mm and 540 mm and this corresponds to the position of the plant in space.

The amplitude of the individual range lines are a function of the properties of the surfaces at that range and are a function of:

1. the area of the leaf;
2. the orientation of the leaf; and
3. the amount of occlusion that affects the leaf.

Part (b) of the figure shows that a significant change in the slope of the cumulative amplitude function indicates the start and end of the plant. The frequency spectra will be referred to as the acoustic density profile from this point on.

The acoustic density profile model is developed in order to interpret the information in the echo reflected from the plant. The frequency spectra of the received echo is then interpreted based on this acoustic density profile model. The entire density profile becomes the acoustic area of the entire scene.

3.8 Data characteristics

When viewed from one orientation, specular surfaces have a narrow band signal which often consist of a very large magnitude at a single range and this can be seen in Figure 3.16. Diffuse scatterers result in much smaller magnitudes. Complex objects (objects which have multiple surfaces) result in echoes being generated from each of these multiple surfaces and hence the resulting acoustic density profile contains information about all of the surfaces at different ranges from the sensor. Figure 3.16 shows how the signal varies between the two broad classes of objects, simple and complex. Classes of objects within these categories are then characterised by more subtle differences in the tonal patterns.

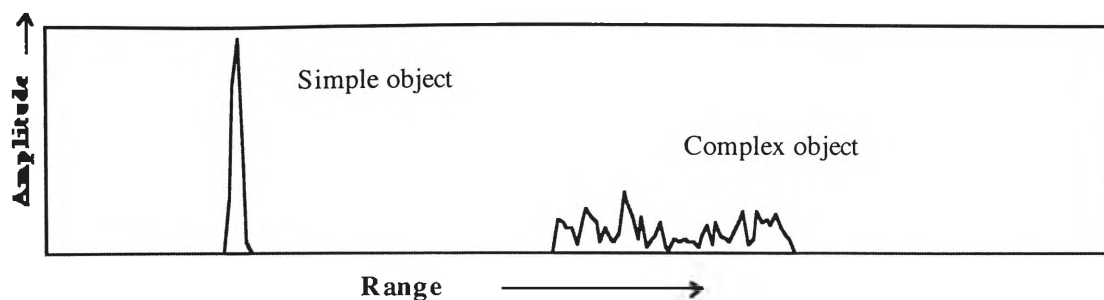


Figure 3.16 Range distributions of different types of objects

The graph in Figure 3.17 is the acoustic density profile resulting from a flat wall. There is a very large amplitude (almost 100 mV) at a range of 602 mm (corresponding to a frequency of 1.7 kHz). It is the only object in the field of audition so is the only significant amplitude in the spectrum.

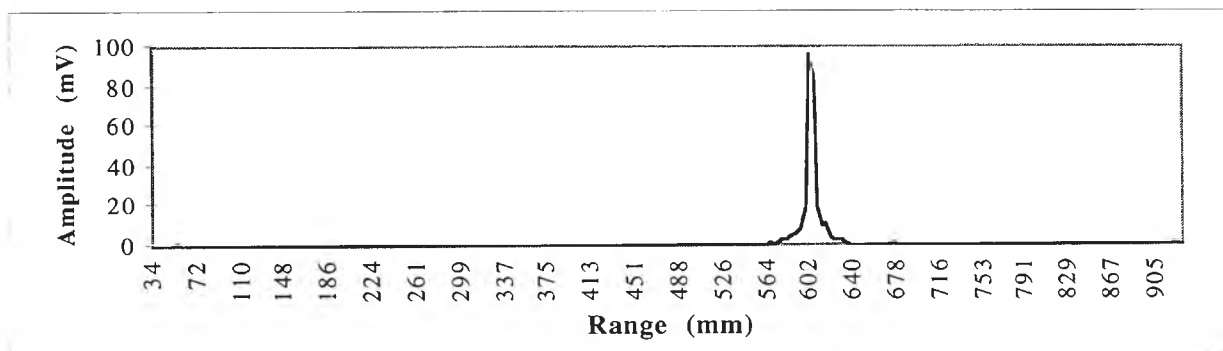


Figure 3.17 The CTFM output when a flat wall at a range of 602 mm from the transmitter is ensonified

The graph in Figure 3.18 is the acoustic density profile resulting from a flat wall with a metal rod placed 60 mm in front of it. The wall is still in the same position and has the same amplitude as Figure 3.17. There is an additional echo at a range which corresponds to the position of the rod. Note that the rod has a significantly lower amplitude as it reflects less of the acoustic energy back to the receiver due to its much smaller orthogonal. Note that the rod would return an even lower amplitude if it were at the same range as the board as the signal has travelled a greater distance so will be of a lower amplitude. This is consistent with the range profile shown in Figure 3.13.

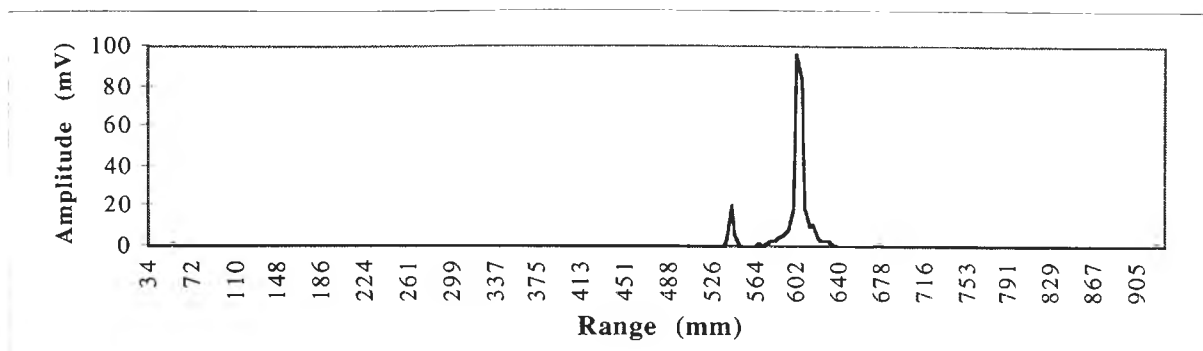


Figure 3.18 The CTFM output when a flat wall at a range of 602 mm from the transmitter is ensonified. There is also a rod 60 mm in front of the wall

A change in the range to the plant will result in a slight decrease in the arrival angle at the plant. For those leaves which this change results in their reflections remaining within the “solid angle” the reflection coefficient will remain unchanged although the amplitude of the return signals will be reduced due to geometric spreading. Other leaves which are on the limit of the “solid angle” will return a diffuse scattering response as the distance is increased and will cease to be a major contributor to the signal.

The amplitude of any particular range line is determined by several things:

1. the physical characteristics of the surface (specifically its reflectivity of ultrasound);
2. the distance of the surface from the sensor;
3. the area of the surface; and
4. the orientation of the surface of the object.

The information in a single range line is summarised in Figure 3.19.

The information in a range line	
<i>Range :</i>	gives the absolute range to the surface.
<i>Amplitude:</i>	gives the size, specularity or orientation of a surface.

Figure 3.19 The information in each range line

Figure 3.20 shows the acoustic density profile and visual image for a specimen plant of the species *Diploglottis campbelli*. Since there are many reflective surfaces, the return signal is much more complex than Figure 3.17. You will also notice that the

maximum amplitude (5 mV) is significantly smaller than for the wall (100 mV) or the metal rod (20 mV) shown in Figure 3.18.

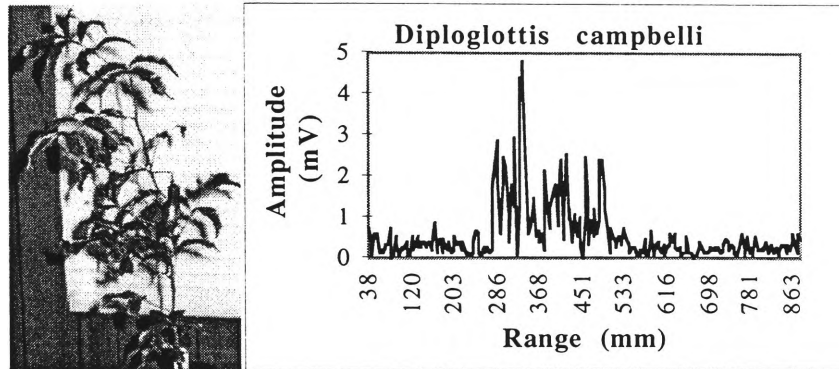


Figure 3.20 *Diploglottis campbelli* with a sample spectrum

As the range of the object is changed, the absolute amplitudes of the range lines are changed due to geometric spreading but the relative amplitudes are still in the same ratio. By normalising the amplitude data, the variations due to the distance of the plant from the sensor are removed. Then, the amplitudes of the range lines will only contain information about the surface properties of the object, that is area, texture of surfaces and distance between surfaces. This also means that the size of the plant does not affect the acoustic density profile. This normalisation is outlined in Chapter 5.

The raw amplitude data was normalised to account for the electrical filtering as described in Chapter 5 prior to further processing. Thus, a recognition system can be developed and will be almost completely independent of:

1. the distance to the plant;
2. the height of the plant; and
3. the width of the plant

provided that enough of the plant is in the field of audition.

The bearing of an object is given by the amount that the peaks are offset between range cells and the amplitudes of the left and right channels [Stanley & McKerrow, 97]. An object is resolved as one when the difference in ranges between left and right is within some limit. This limit changes with the displacement between the receiving transducers.

When more than one object or feature is in the range of the sensors, they appear as distinct sets of lines in the acoustic density profile. Objects at the same range may be distinguished binaurally, although ambiguities can occur.

3.8.1 CTFM sensor output from ensonifying simple objects

In this section, the most simple scene possible is used (one which contains no objects) and built on by adding simple objects one at a time. A simple scene is one which contains zero or more simple surfaces (objects) within the field of view of the sensor. The maximum range of the system is 1.8 m (determined by system settings).

When there is no object within the range of the sensor, the acoustic density profile consists of noise. This is illustrated in Figure 3.21. This determines the noise floor below which it is difficult to detect objects. The FFT has already achieved considerable integration of the echo to increase the signal to noise ratio of the spectrum.

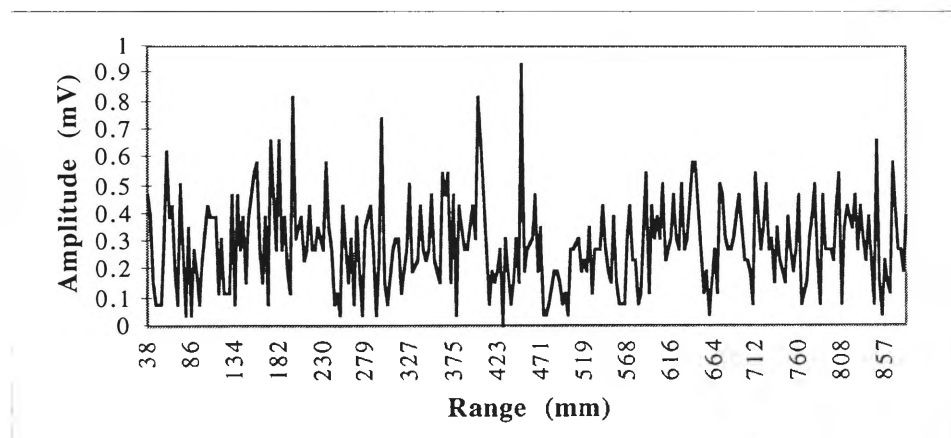


Figure 3.21 The acoustic density profile showing the background noise only

When there is a single large specular object within the field of audition, the result is a very large amplitude at the frequency corresponding to the distance to the object. Note that the resolution of the FFT is 3.4 mm. If the specular object lines up with the centre of the “bin” then the result is a very clean acoustic density profile as shown on the upper graph of Figure 3.22. The bin leakage problem could also result in an acoustic density profile such as that in the lower graph of Figure 3.22. Bin leakage occurs when the range to the surface is not aligned to one of the range bins, and “spills over” into neighbouring bins.

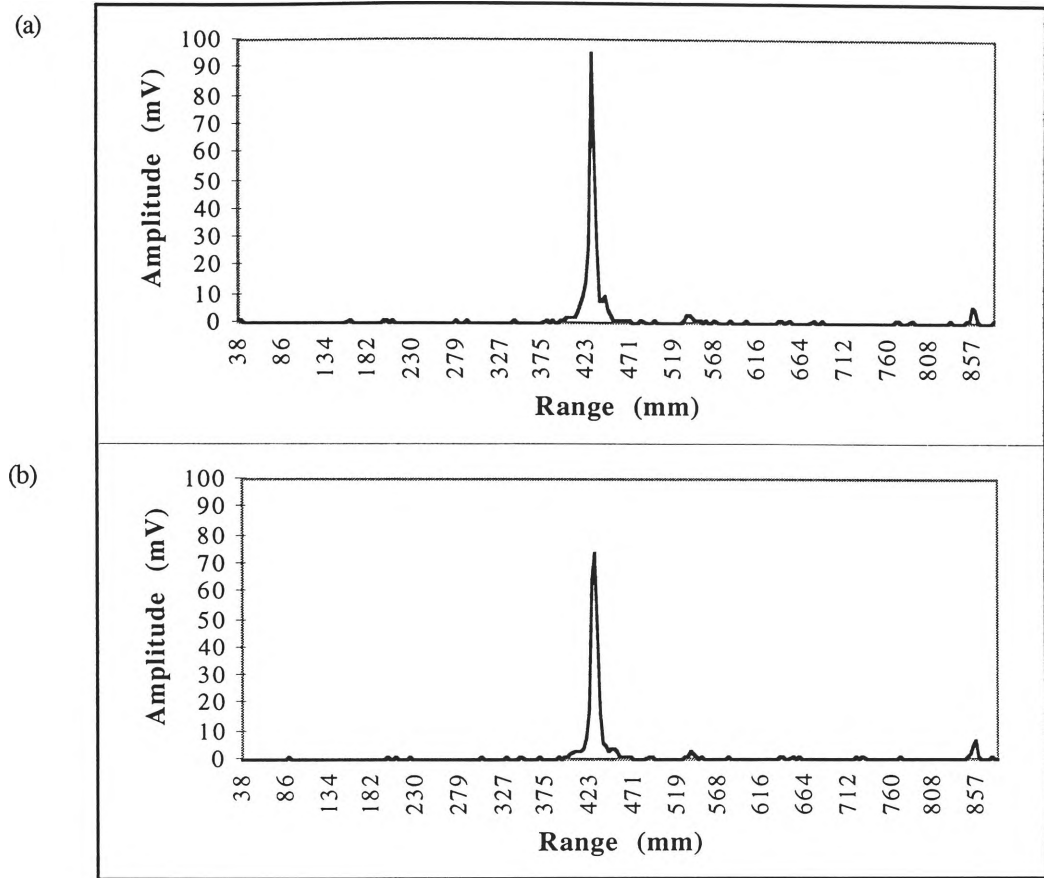


Figure 3.22 A single specular object (a) without bin leakage and (b) with bin leakage

When the range is changed, the acoustic density profile changes slightly. As the sensor moves closer to the object, the amplitude increases because less of the transmitted signal is absorbed in the atmosphere.

When an object is placed in front of the specular object in Figure 3.22, the resulting acoustic density profile depends on the size of the object placed in the foreground. If the object in the foreground occludes the object in the background, then that will be the only object present in the acoustic density profile. Otherwise, the object will show up in the foreground as in Figure 3.23. Note that if the object is within 3.44 mm of the original object then the objects are not separated enough in range and will appear as one.

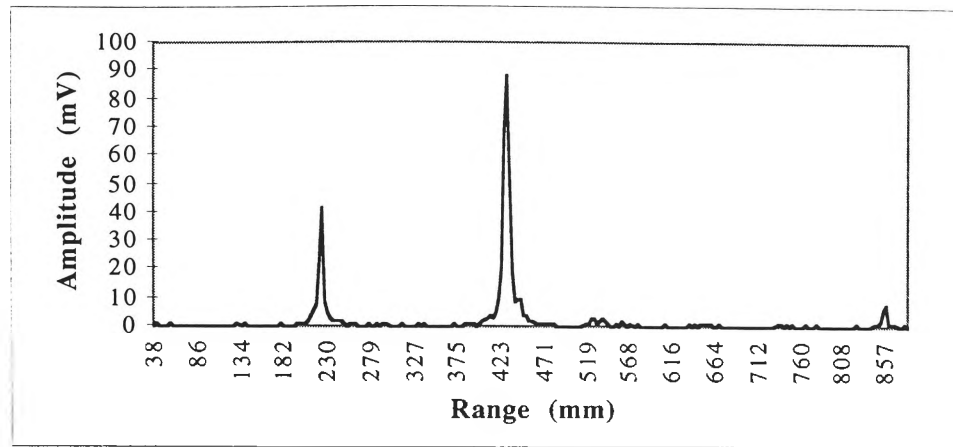


Figure 3.23 Acoustic density profile of two specular objects

When two cylindrical rods are mounted on a rotating stage, a change in the acoustic density profile can be observed as the stage is rotated. The configuration of the apparatus is shown in Figure 3.24.

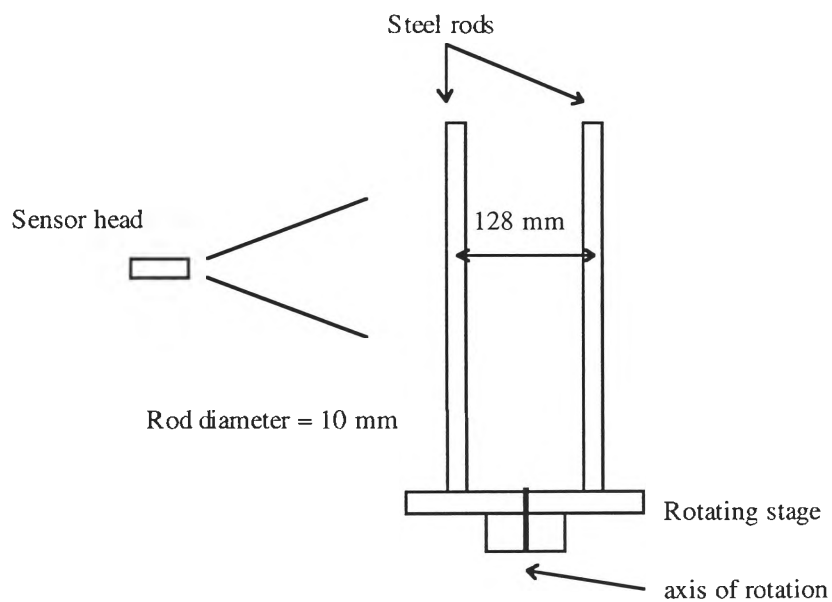


Figure 3.24 Experimental setup

When both rods are at the same distance from the sensor, they are not resolved as two separate objects as shown in Figure 3.25 and appear at the same range in the acoustic density profile.

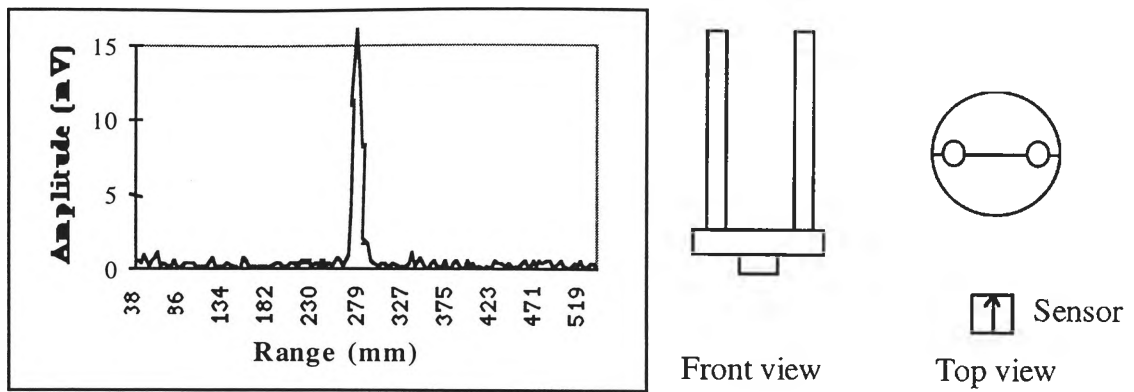


Figure 3.25 Both rods are at the same distance from the sensor

When the stage is rotated through 45 degrees, the two rods are resolved separately in the acoustic density profile (Figure 3.26). They are separated in the acoustic density profile by the distance between the rods from the point of view of the sensor.

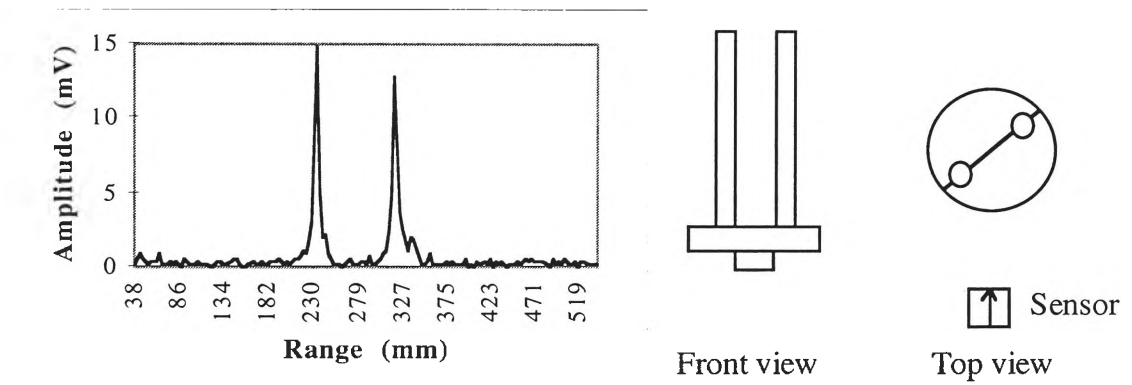


Figure 3.26 The stage is rotated through 45 degrees

When the stage is rotated through 90 degrees (Figure 3.27), the occluded rod is still present in the acoustic density profile due to diffraction of the transmitted acoustic energy. The acoustic energy is diffracted around the first rod and is reflected back to the transmitter in the same fashion.

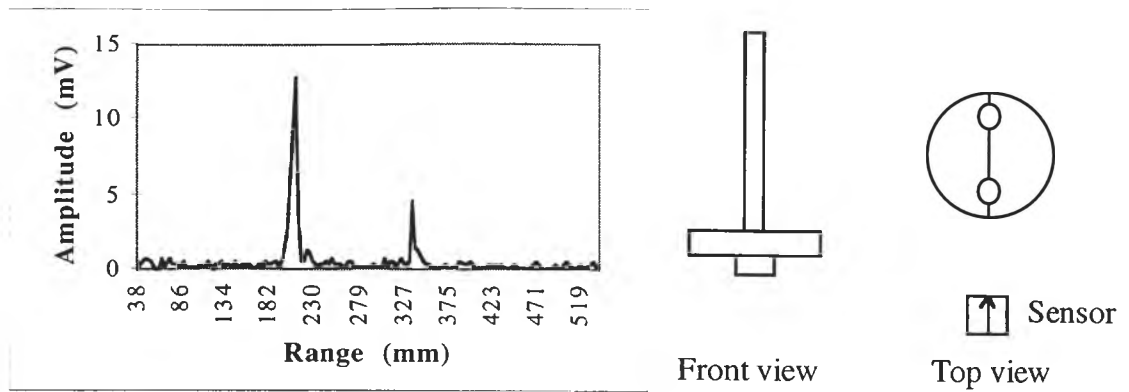


Figure 3.27 The stage is rotated through 90 degrees

When three rods are mounted on the stage (the extra one is mounted between the two already on the stage), the results are similar to those when there are two rods, except that there is an extra spike present in the acoustic density profile. When two rods are occluded, they are still present in the acoustic density profile but they are at very low amplitudes.

For this example, we know the positions of the two rods on the stage as this is fixed. From any acoustic density profile, it is possible to calculate the orientation of the stage through 0 to 180 degrees. Consider the acoustic density profile in Figure 3.28. Each of the rods are 65 mm apart on the rotating stage (fixed for the experiment). From the acoustic density profile we can see that the first rod appears at 232 mm, the second rod appears at 277 mm and the third rod appears at 322 mm, so in this acoustic density profile, they are separated by a distance of 45 mm. Thus, the stage is oriented at

$\theta = \sin^{-1}(45 / 65) * 180/\pi = 44$ degrees. The physical position of the rods was approximately 45 (plus or minus two) degrees so this is within limits of the measurements.

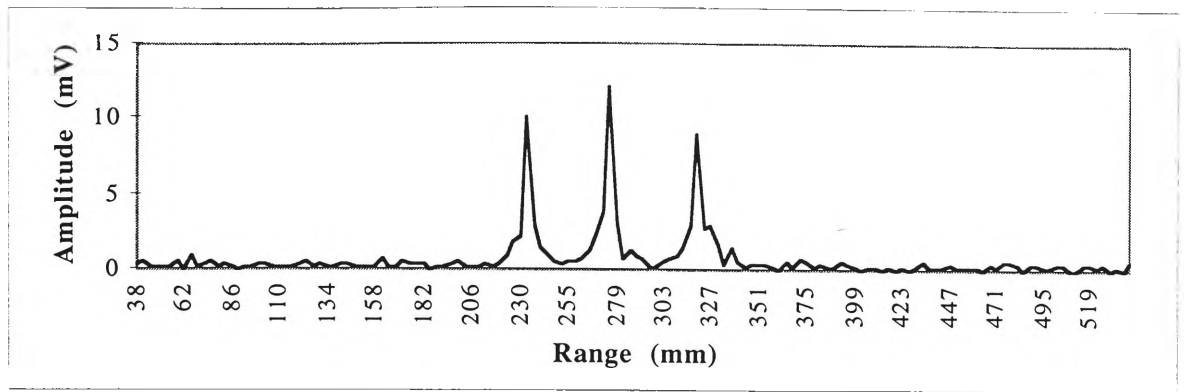


Figure 3.28 The acoustic density profile produced by three rods at 45°

When a specular spherical (or cylindrical) surface is considered you get narrow band return similar to a flat surface (although lower in amplitude). When you look at a sphere with a slightly textured surface, some diffraction of the acoustic energy occurs and the sensor gets a small amount of energy off the surface of the sphere at ranges slightly offset from the major peak. Figure 3.29 is an example of the return from a polystyrene sphere with a radius of 100 mm.

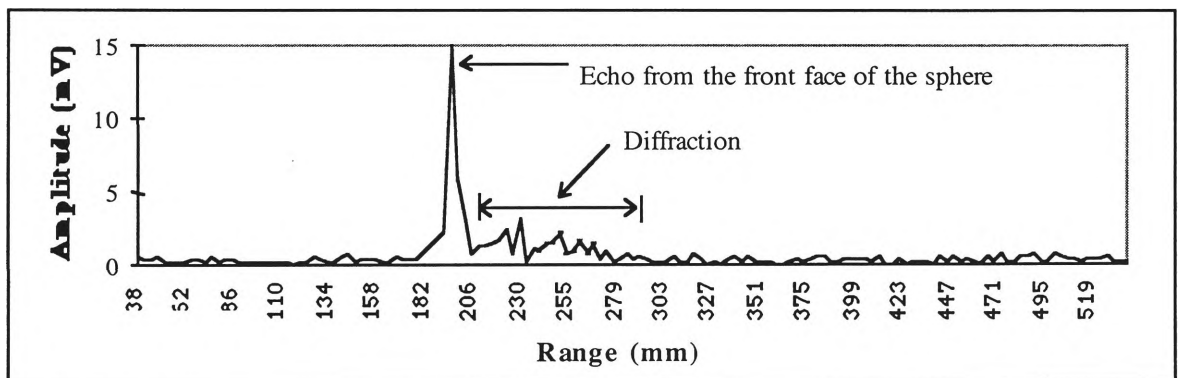


Figure 3.29 The acoustic density profile produced by a polystyrene sphere

3.9 Acoustic density profile content from plants

3.9.1 Basic content of the acoustic density profile

The acoustic density profile contains information about the range to surfaces within the field of audition of the sensor. The signal is affected by the following properties of the plants :

1. Size, orientation and number of leaves;

2. The spatial positioning of leaves within the plant;
3. The orientation of the plant.

3.9.1.1 Size, orientation and number of leaves

Depending on the orientation and curvature of the leaf surface, the larger the leaf, the more acoustic energy will be reflected so a higher amplitude will be received. Leaves which do not have any part of their surface normal to the sensor will reflect some (if not all) of the acoustic energy away from the receiver.

The surface of the leaf will also have an effect on the amount of acoustic energy returned - smooth flat surfaces will reflect more back to the receiver than textured surfaces. In general, the more leaves that are on a plant, the larger the percentage of acoustic energy that will be reflected.

3.9.1.2 Positioning of leaves within a plant

This will determine the distribution of reflections throughout the acoustic density profile. Leaves spread throughout the plant will reflect the energy and the acoustic density profile will show these leaves spread through several range cells. Peaks in the acoustic density profile can indicate groups of leaves at that particular range. However, leaves may occlude those behind them so not all of the leaves will be detected at any one time.

3.9.1.3 The orientation of the Plant

Small changes in the orientation of the plant can result in large changes in the acoustic density profile due to the specular nature of leaves. Many leaves however, are not flat and will return acoustic energy from several different orientations.

3.9.2 Plant insonification

For each aspect (orientation) of the plant, the received acoustic energy represents the properties of the scatterers at a set of different ranges. Figure 3.30 shows the process of plant insonification. Waves are transmitted by the transmitter T_x and propagate through the air. In Figure 3.30, the boundary of the plant is represented by the circle and leaves

are represented as filled ellipses. The waves reflect from the surfaces of the scatterers (in this case the leaves of the plant) and these reflected waves are detected by the receiver R_x . In the case of CTFM, the received acoustic energy is demodulated against a copy of the transmitted signal and the resulting acoustic density profile gives information about the scatterers in particular range cells. For the case of a transmitter and a single receiver, each range cell is bounded by a spherical surface through the plant as is illustrated in Figure 3.30. The surfaces are illustrated in the diagram as arcs as they are viewed from above.

A typical acoustic density profile for a plant is shown in Figure 3.31. Each range cell is 3.4 mm wide due to the signal processing (the FFT which converts the tones into the frequency domain). Figure 3.31 shows that a specimen of *Sarcomelicope simplifolia* is a relatively deep plant with a large number of range lines containing scatterers. Even though the figure shows the situation in two dimensions, it is indeed a three dimensional signal and has similar properties in the vertical plane although the beam is slightly narrower in the vertical direction (Section 3.4), due to the overall shape of the transducers.

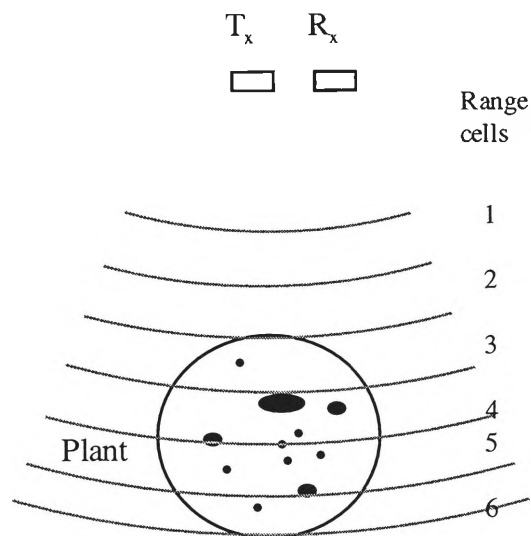


Figure 3.30 Schematic of plant insonification

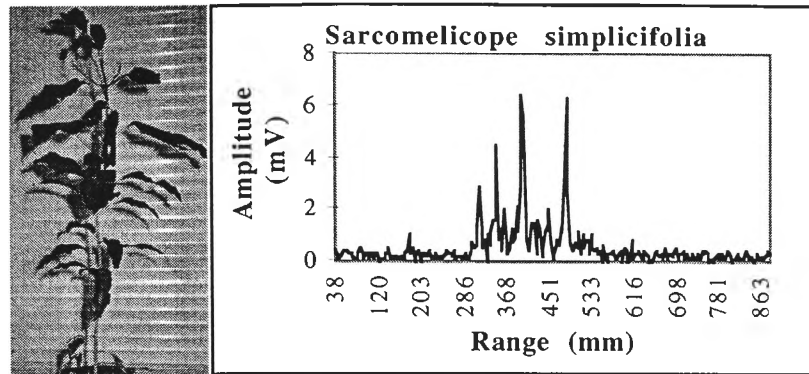


Figure 3.31 The image and acoustic density profile for a specimen of *Sarcomelicope simplicifolia*

To examine the information in each of the range cells, consider the situation in Figure 3.32, where two plants are insonified. The two different scenarios are illustrated as follows :

- (a) $d_1 + d_2 \neq d_3 + d_4$; and
- (b) $d_1 + d_2 = d_3 + d_4$.

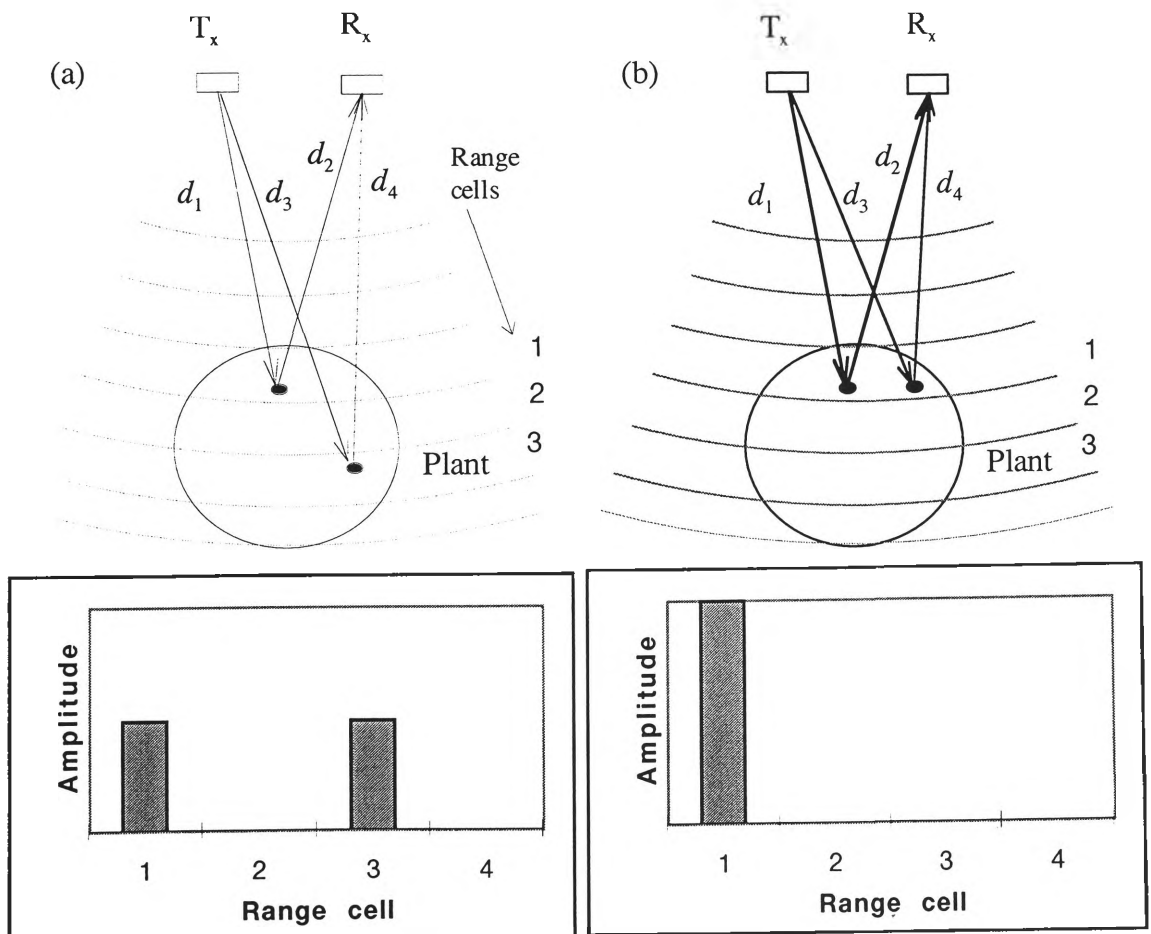


Figure 3.32 The two different situations for reflections from multiple scatterers

For the situation in Figure 3.32(a), there are two leaves present and the reflections are received from them in different range cells. This results in an amplitude being registered for each of those range cells. This is illustrated by the graph in Figure 3.32 where a reflection is present in both range cells one and three. The amplitude of the reflection will depend on the size and the orientation of the leaf.

When reflections are received from scatterers in the same range cell as is the case for Figure 3.32(b), they combine to give a result which is larger than if there was a single scatterer only. This is illustrated in the figure.

In the case of plants, their volume is made up of a series of scatterers. The scatterers in any range cell may be either :

1. specular reflectors;
2. diffuse reflectors; or
3. completely absent.

Whether a leaf produces a specular or diffuse reflection depends on its orientation. In general, diffuse scatterers produce an amplitude which is approximately 10 dB down on a specular reflector (measured). So, for any given range cell size (determined by the bin width of the FFT), the received amplitude a , can be calculated using Equation 3.10.

$$a = \sum \text{power of the specular and diffuse scatterers} \quad \mathbf{3.10}$$

When there is less than 100 diffuse scatterers, this equation approximates to the sum of the specular scatterers. Alternatively, when there are no specular scatterers in the range cell then the result is reduced to the sum of the diffuse scatterers.

In summary, the range cells (or the FFT bins) contain information about all of the surfaces of the plant at a particular range. This however assumes that all of the surfaces are visible to the sensor combination. Many of the leaves from plants (particularly from dense plants) will be obscured from the sensor by other leaves. This situation can be used to our advantage as properties of the plant can be postulated based on the result of this acoustic shadowing.

3.9.3 Freedman's theory of scattering and its relationship to plants

Freedman [1962a], developed a model of scattering for a non dissipative medium using a point source radiator and receiver. The model shows that the echoes generated by the scattering body are created by the step discontinuities in the derivatives with respect to range, of the solid angle subtended at the transducer by the scatterer.

In other words, as the normal cross-section area is increased, the amount of signal which returns to the receiver is increased, and hence a higher amplitude in the range cell which corresponds to that physical range. Also reflections occur at discontinuities in the cross sectional area and any of its derivatives. Thus, each spectral line represents an increase in the reflecting area. This model has recently been validated in air [Tsakiris & McKerrow, 1998]. The discussion in Sections 3.8 and 3.9 of this chapter, are consistent with the model.

3.9.4 Acoustic shadowing

Acoustic shadowing occurs when the ultrasonic wave either does not reach a reflector or is reflected but does not reach the receiver due to another reflector being in the way. Acoustic shadowing is the acoustic equivalent of the optical term occlusion. Consider Figure 3.30, where the entire plant is split into range cells - in Section 3.9, it was shown that each range cell is the sum of all of the scatterers within the cell. This however, fails to consider the fact that some of the scatterers may be shadowed by other scatterers between it and either the transmitter or receiver.

Figure 3.33 shows some acoustic shadowing on the bottom right hand corner. The large leaf prevents the bulk of the acoustic energy from penetrating into the range cells behind it. Some refraction may occur in this situation. Refraction allows a small amount of the acoustic energy to penetrate but this will result in a very small contribution to the amplitude in the range cell.

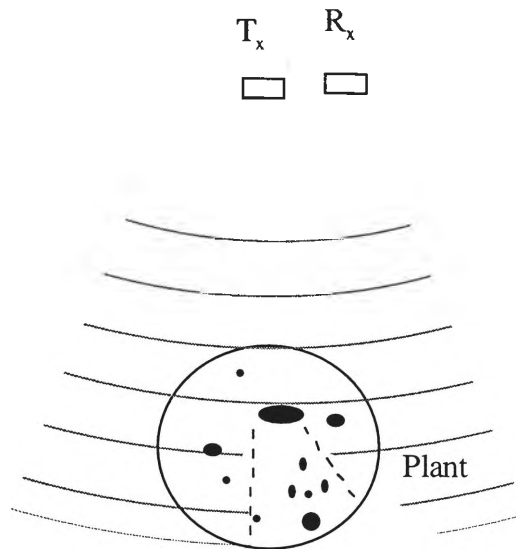


Figure 3.33 Schematic of plant insonification showing some shadowing

The discussion in the previous section can be qualified by saying that the range cell contains information about all of the scatterers in that cell *except* when they are in an acoustic shadow.

Plants which are very dense will result in more shadowing and less of the resulting acoustic density profile will be a measure of the leaves beyond the front surface of the plant. On the other hand, sparse plants or plants with smaller leaves will result in more of the plant being audible (lack of shadowing) and the foliage at the back of the plant will be represented in the acoustic density profile. This can be exploited by a system which is trying to differentiate plants based on their acoustic density profile.

Eucalyptus maculata and *Polyscias murrayi* are plants of similar depth - their images and acoustic density profiles are shown in Figure 3.34. *Polyscias murrayi* is much more dense than *Eucalyptus maculata* and this is indicated in the acoustic density profile having a large peak early in the acoustic density profile followed by low amplitude peaks. Leaves in the background are shadowed so they are not present in the acoustic density profile. This contrasts with *Eucalyptus maculata* where echoes from the leaves in the background are present in the acoustic density profile. Note that the background shown in the image is not present when the acoustic density profile is measured.

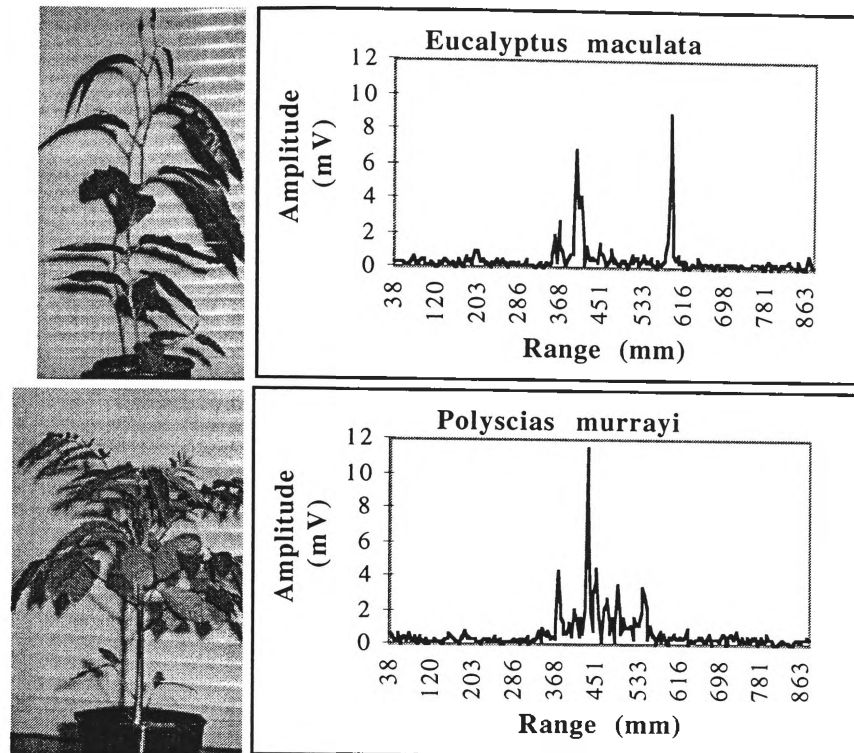


Figure 3.34 Images and acoustic density profiles of (a) *Eucalyptus maculata* and (b) *Polyscias murrayi*.

Polyscias murrayi has a large number of reflectors at the distance indicated by the large amplitude (of 12 mV) in the figure. Its acoustic density profile shows that very little acoustic energy penetrates this layer of foliage and that which does return is at a significantly lower amplitude. This part of the acoustic density profile is made up of two separate components :

1. acoustic energy which has penetrated the front layer of foliage and managed to reflect directly to the receiver; and
2. acoustic energy which has travelled an indirect path back to the receiver - multiple reflection paths.

In general, dense plants have a significantly large amplitude which corresponds to the front of the plant. More sparse plants have a much lower amplitude in general but they reveal more about the structure of the plant as acoustic energy penetrates more deeply into them.

3.9.5 Increasing cell resolution

In Section 3.9.1, a single transmitter / receiver pair was considered. More information however, can be extracted by considering a more complex receiver arrangement. Instead of the plant being split into range cells, it can be broken up into a grid of much smaller range cells called voxels. The acoustic density profile can now be considered as a three dimensional grid. Each of the cells in the grid is assigned a value based on the amplitude in the two acoustic density profiles. This will provide more information about the properties of the plants and would be more robust, but requires an array of receivers and also results in increased processing requirements.

3.9.6 Area of interest

Figure 3.35 shows the acoustic density profile of a *Eucalyptus leucoxylon*. The area which contains the plant signature is enclosed by dashed lines. The remainder of the acoustic density profile is noise. For the purpose of this research, a simple algorithm is implemented to extract the part of the acoustic density profile which contains the plant. From the maximum amplitude, move either up or down the acoustic density profile (depending on whether you are finding the start or the end of the acoustic density profile) until 10 consecutive frequencies are less than the noise threshold. Using 10 consecutive frequencies ensures that components of the plant signature are not interpreted as noise when there may be diffuse scatterers present whose strength are below the noise level.

In general, the level of noise within the plant signature is insignificant compared to frequency lines where range information is present, so, it can be ignored.

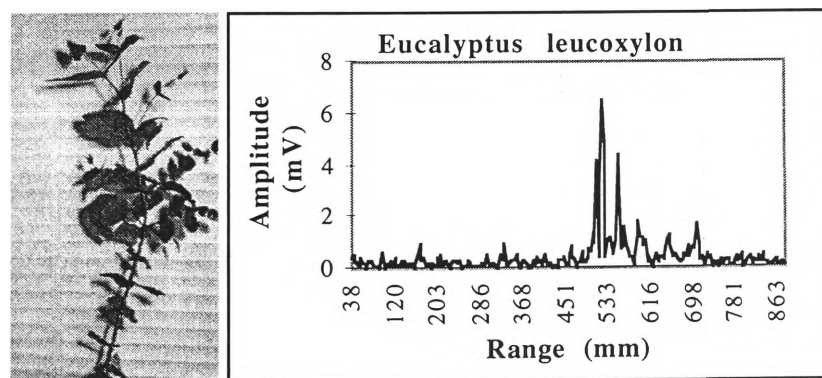


Figure 3.35 Acoustic density profile of *Eucalyptus leucoxylon* with area of interest highlighted

3.10 Scene prediction

It is relatively easy to determine the acoustic density profile which results from insonifying simple objects (Section 3.8.1). Complex objects however produce more complex signals. These signals are difficult to analyse visually when the differences between two plants are subtle. However, the tonal differences can be quite noticeable to the ears.

With a simple scene, the resulting acoustic density profile can be estimated based on the geometric structure of the surfaces. If the characterisation of a plant was simple in a similar sense, the process of recognition would be easy. This concept is illustrated in Figure 3.36. Significant differences between plants such as described in Section 3.9.4, allow differentiation plants into broad classes. Even after a large amount of practice, however, inexperienced users found that it was difficult to separate plants which have subtle physical differences by visual inspection of the acoustic density profile.

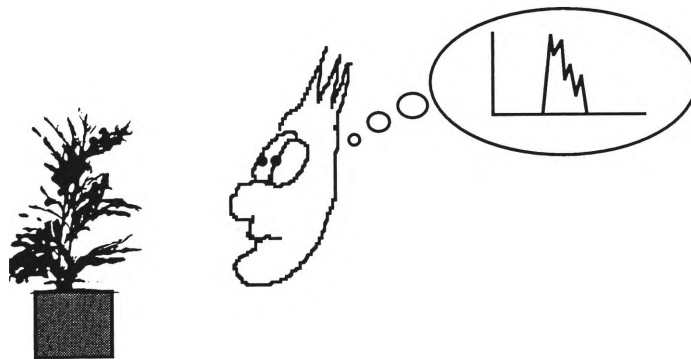


Figure 3.36 **Visualisation of the acoustic density profile from a plant**

Visualisation of the acoustic density profile did provide information about the way that the signals vary between plants and even within plants as they are rotated. This background enabled formulation of a set of calculated features which characterise the individual plants. Playing the audio signals through ear pieces provides much more information but the inexperienced user does not have a life time of using this kind of sensory information in order to distinguish plants.

3.11 Summary

1. CTFM is modelled on the way that bats use ultrasonic signals.
2. The experimental system uses a frequency sweep from 100 kHz down to 50 kHz with a sweep period of 102.4 ms^{-1} .
3. The range resolution is determined by the resolution of the FFT and is 3.4 mm.
4. The signal is very repeatable over successive readings which means that it is suitable for application on a mobile robot.
5. The signal varies with changes in the environmental conditions and a system which needs highly absolute range information would need to take this into account.
6. The frequency spectrum can be modelled as an acoustic density profile and is much easier to interpret.
7. Tones are resolved based on both their frequency and amplitude.
8. It is very easy to predict the signal given a simple scene.
9. Complex objects produce their own characteristic tones.
10. It is difficult to predict the signal given a complex object as it can vary considerably with orientation.

4. Classification of Plants using data from the Acoustic Density Profile

4.1 Introduction

In previous chapters, the operating parameters of the system were analysed, other implementations of the technology were outlined and the information content of the signal discussed. In this chapter, a series of experiments are described which serve to establish the suitability of this sensor for classifying plants. A proof of concept is described which tests the properties of the data produced by the sensor from four plant samples.

The experiments described in this chapter use data collected by ensonifying four small plants from different orientations equally spaced around the plant. A benchmark is established by finding the capabilities of a simple classifier which is trained and tested using the sample data. In subsequent chapters, the signal is analysed to a greater depth in order to extract fundamental information about the plant specimen. Also, it is shown that when input data is processed more intelligently, a classifier recognises individual returns to a higher accuracy and at greater speed.

In this chapter, an Artificial Neural Network (ANN) is used as a classifier. The ANN was chosen over other methods as it is a black box method. If a network is capable of differentiating plants using “raw” sensor data then there is a good case to pursue the system further and study the data using more intelligent classifiers. Five experiments are described which show that a classifier can differentiate four plants of different species, recognise plants at different ranges and can also differentiate plants of the same species if that is what the network is trained to do. The final experiment involved removing all of

the leaves from the plant in order to confirm that the leaves are the part of the plant which is important for classification.

Four plants of approximately the same size were chosen for the experiments. The following common indoor plants were chosen :

1. *Azalea indica*;
2. *Schefflera arboricola*;
3. *Hypoestes*; and
4. *Chamaedorea elegans*.

Figure 4.1 shows images of the four plants along with the acoustic density profile from several different orientations of the plant. The acoustic density profiles shown were taken from points approximately 90 degrees apart, around the plant.

The acoustic density profiles show that changes in orientation of the plant can affect the signal considerably as the leaf structure and arrangement can be different from one orientation to the next. Overall however, this chapter shows that the signal contains the same basic information through orientation change as any given signal can be classified as a particular plant to a reasonable accuracy. Appendix E graphically shows how the acoustic density profiles change over one degree increments through a rotation of 50° for two different plants.

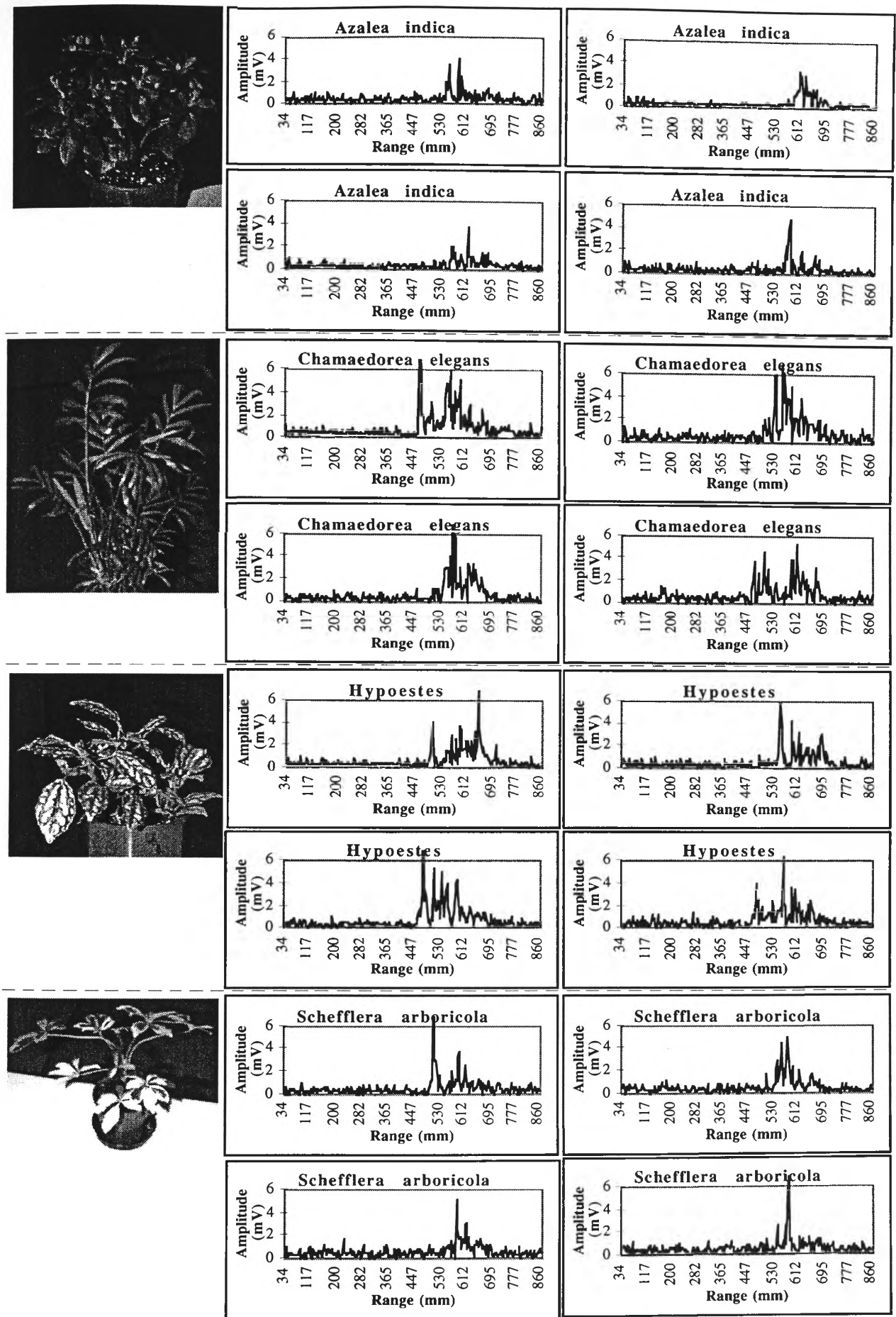


Figure 4.1 Images of the specimens with selected acoustic density profiles

4.2 Experimental design

Measurements of plants were taken at two distances from the sensor. In order to quantify the part of the plant the signal was coming from, readings were also taken with the plant's leaves removed. All measurements were taken at approximately the same temperature and humidity to minimise the effect of these on the transmission of sound in air.

During the experiments, the plants were attached to the rotating stage of a precision positioner. The positioner locates the plants accurately in two dimensional space (this can be seen in Figure 5.1) and can also rotate objects about their z axis. Readings were taken from the stationary plants as they were rotated through three hundred and sixty degrees in three degree increments. Thus, 120 samples were collected for each plant. Collecting data from many different orientations ensures that the network once trained should be able to recognise the plant at any orientation.

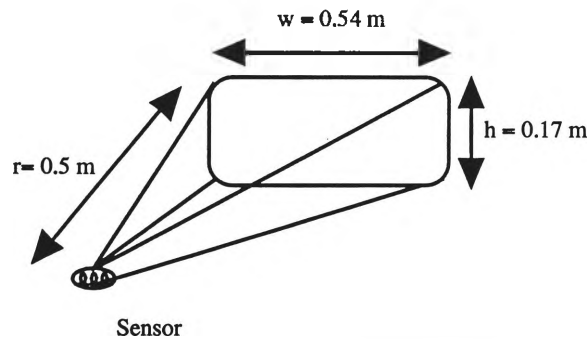


Figure 4.2 Sensor field of insonification

The centre of the area ensonified by the sensor was approximately one third from the top of the plant. The edges of the region of insonification (Figure 4.2) of the sensor were verified with a solid object before the plant was moved into position. This was done to ensure that the plant was being scanned instead of other objects in the environment such as the stand or the pot. Care was taken to ensure that the entire width of the plant was in the region of insonification of the sensor.

To obtain the data required to determine the ability of the system to classify and discriminate between objects, 5 experiments were conducted :

Experiment 1 was conducted to verify that a plant could be differentiated from a group of four similar sized plants of different species. One plant specimen from each of the different species was involved in this experiment. Two thirds the data were used for training the network (320 records) and the remaining third was used for testing (160 records). The records used for testing were chosen randomly from the entire set by a pre-processing module.

Experiment 2 was designed to determine if a network trained with 4 different species can differentiate between other plants of the same species (not the ones that the system was trained on). Thus the network was trained in the first experiment and then tested with other plants of the same species (480 records).

Experiment 3 focussed on verifying that a network trained with information at a certain range could recognise plants at a different range. Data for plants of the same species measured at a different (smaller) range was used as input to the network trained in Experiment 1 to see if it could classify the plants correctly.

Experiment 4 was conducted to determine if a network could be trained to differentiate between three plants of the same species. As in Experiment 1, seventy-five percent of the data were used to train the network and the other twenty-five percent was used for testing.

Experiment 5 was conducted to determine whether an altered version of the original plant could still be recognised. The question that we wanted to answer is whether the returned signal depends on the entire plant structure including the leaves or whether the structure of the foliage holds the key.

4.3 Neural network classifier

4.3.1 Introduction

Research into Artificial Neural Systems dates back to the 1800's [Simpson, 1990] and had a resurgence in the late 1980's. Research in the area has increased considerably and Artificial Neural Networks have been used in a wide range of applications [Wasserman, 1993]. There are many different algorithms, each with its own specific purposes and they are used for both supervised and unsupervised learning. They have many advantages over traditional statistical models including robustness, adaption, and the fact that they are non-parametric [Lippman, 1987]. Also, it has been shown that they can learn underlying relationships which are difficult to find, can generalise, and can handle noisy or incomplete data [Hammerstrom, 1993a].

ANN's are all essentially vector mappers, where a set of inputs is transformed into a set of outputs. The network is usually represented as a set of *processing elements* (nodes) and the *weights* between the elements (arcs). A simple model of a processing element adapted from Beale & Jackson [1990] is shown in Figure 4.3. The processing element multiplies all of the inputs by their corresponding weights and sums the result. The result is then thresholded and the output of the processing element is assigned the result.

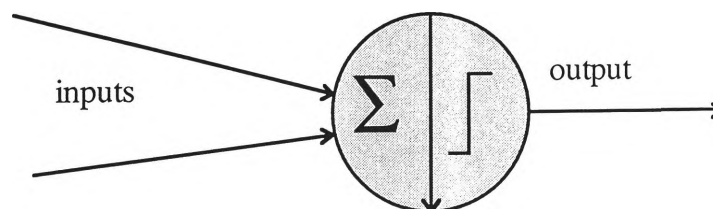


Figure 4.3 Outline of the basic model of a Processing Element

A diagram of a network of these processing elements is shown in Figure 4.4. The numbers on connections between processing elements are weights. A pattern is presented to the input vector and a result is produced on the output vector.

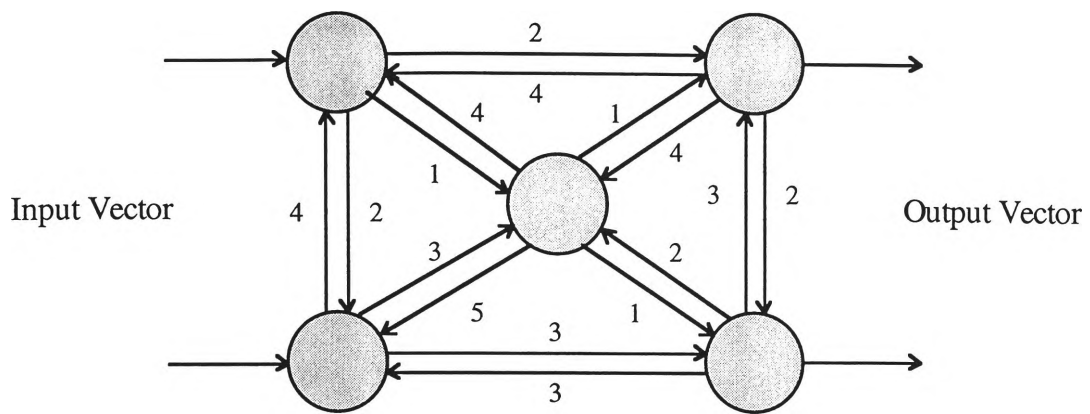


Figure 4.4 Outline of a Neural Network shown with weights

When networks are used for supervised learning, the weights are adapted during training to improve the performance. Unsupervised techniques result in different output vectors being activated based on the input pattern. Networks differ by the way that their nodes are connected, the way their processing elements operate and the mathematical operations which control the network processing as a whole.

The Backpropagation algorithm was used to show that plants could be differentiated based on their CTFM acoustic density profile. Other techniques were used subsequently to identify the specific parts of the signals which make one plant different to another.

The Backpropagation learning algorithm [Rumelhart & McClelland, 1986] was chosen for several reasons :

- The training data collected suited supervised learning since it was going to be taken from known objects;
- None of the outputs of the network were to be fed back to the inputs so a feed forward network was applicable;
- A commercial software package was available on our hardware [NeuralWare, 90];
- The paradigm had been used successfully before (in fact it has been used in over 85% of published applications [Wasserman, 1993]); and
- There are many examples of neural networks being successful in the acoustics

field. They have been used to recognise underwater objects [Moore *et al*, 1991], [Gorman & Sejnowski, 1988], and recognising objects in air [Watanabe & Masahide, 1992] and classifying textures based on side-scan sonar images [Shang & Brown, 1992].

The Backpropagation training algorithm uses a fully connected network. This means that all nodes in one layer are connected to all nodes in the next layer. They are arranged in at least 3 layers: an input layer; a hidden layer; and an output layer. The input pattern is presented to the input layer, and the output is computed and given on the output layer. The hidden layer has no connections to the input or the output but this intermediate layer allows the networks to model complex functions. A model is shown in Figure 4.5.

During training, the pattern is presented and propagated through the network and the output is computed. This output is then compared with the desired output and the difference is propagated back through the network and the weights are adapted. Once the network is trained, the test patterns are presented to the network and the output indicates the class to which the pattern belongs.

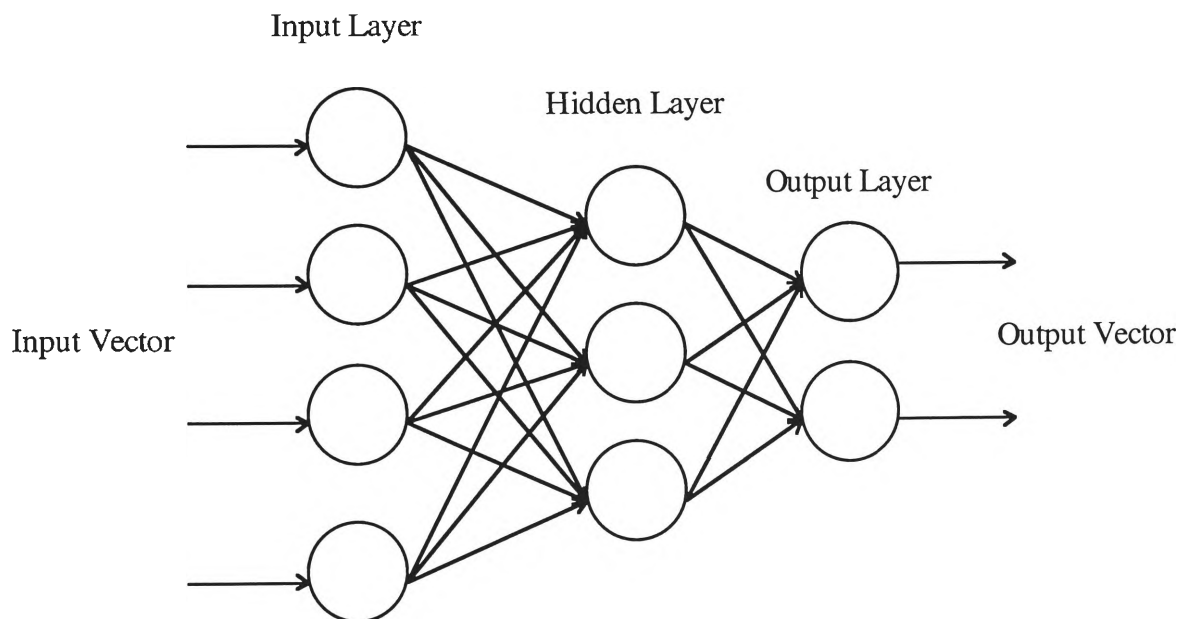


Figure 4.5 The model of a multi-layer Perceptron

4.3.2 Network architecture

The Backpropagation algorithm was simulated with the Neural Works Professional II/Plus application from Neural Ware. A simple hierarchy with one hidden layer was chosen since it has been shown that it is sufficient to distinguish arbitrarily complex shapes [Hornik *et al*, 1989]. It has also been proven that networks with more than one hidden layer are prone to fall into bad local minima. They are harder to train and initial weight choices affect the end result more [de Villiers & Barnard, 1989].

In the training phase, the classifier is trained with data that is representative of the scanned objects together with the associated output vectors which define the class. A multiple class model was used for the output nodes where each class of plant has a separate output node. During the testing phase, previously unseen data was presented to the network and the output vectors were assigned based on the values of the output nodes. The winner-takes-all method was used to determine which output to choose ie. the output with the highest activation designates the class.

It is extremely difficult to specify an effective architecture given a particular problem and the best way to find one is through experimentation [Masters, 1993]. The number of inputs was chosen by analysing the raw signal and was set at one hundred. The envelope of the signal for all of the plants scanned fell within a range of one hundred spectral lines. This relates to the depth of the plant.

The Cascade-correlation technique [Fahlman, 1990] can be used to determine the optimal network topology but was not possible due to the lack of processing power available on our computer. This meant choosing the number of hidden nodes by empirical methods and the minimum number of nodes was selected which produced reasonable performance. When selecting the topology, the goal was to create a network large enough to learn but small enough to generalise well. The amount of training was also determined empirically so that the network did not over train and learn irrelevant details of the individual training vectors.

Four output nodes were used in Experiments 1, 2, 3 and 5 since they are classifying into 4 classes. Experiment 4 only classifies into 3 classes so the number of

output nodes is 3. A representation of the network is shown in Figure 4.6. There are connections from all units in one layer to all units in the next layer.

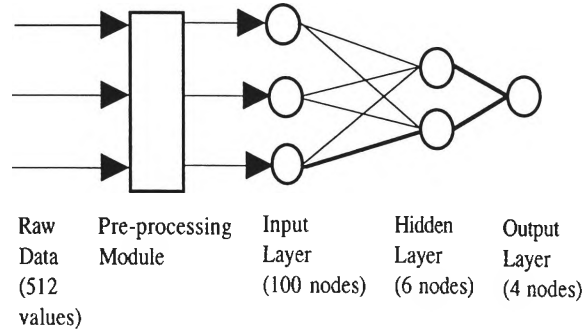


Figure 4.6 Network schematic

The ANN is essentially a function (Equation 4.1) which maps a given input set to a selected output set. Each node has 0 to n-1 inputs from each of the nodes in the previous layer. There are also weights on each of the connections between the nodes. An assumed input called a bias also exists, which is set to 1.0. The output of each node is calculated with :

$$output = f\left(\sum_{i=0}^{n-1} x_i w_i + w_n\right) \quad 4.1$$

where x_i is the value of input i and w_i is the weight. The bias is denoted by w_n . The function f is the transfer function. The choice of transfer function is not critical as long as it is not linear and bounds the output [Wasserman, 1993]. I chose to use the 'tanh' activation function (Equation 4.2) for all of the processing elements in the network. The choice of transfer function makes little difference when the network is trained but it has been shown that the tanh function has the best overall properties in training a layered feed forward network [Kahlman & Kwansky, 1992]. The tanh function requires the inputs to be scaled between values of -1.0 and +1.0 before presentation to the network.

$$\tanh(x) = \frac{e^x - e^{-x}}{e^x + e^{-x}} \quad 4.2$$

Before the network was trained, the weights were initialised to small random numbers between -0.1 and +0.1. Training samples were presented to the network and a measure of the error on the output nodes was calculated. The weights were then updated

in such a way that the error was reduced. The error function being used is the mean squared error divided by two.

$$E_p = \frac{1}{2} \sum_j (t_{pj} - o_{pj})^2 \quad 4.3$$

where E_p is the error function for pattern p ;

t_{pj} is the target output for pattern p on node j ; and

o_{pj} is the actual output on that node.

The minimisation of this error is done only during the training phase. A learning rule is used to adapt the weights between the processing elements during this phase. The process of changing these weights to achieve the desired result is called adaption. The learning rule chosen was the Normalised-cumulative Delta-rule. This rule accumulates the weight changes over several epochs and makes the changes all at once. Its advantage is that the network is much less sensitive to the order of the training set. This rule automatically adjusts the learning coefficients as training progresses.

In summary, an input vector is presented and the output is computed; the error is computed as the difference between what was expected and what was produced; and the weights are then modified in order to minimise the error.

The momentum parameter is important in improving the speed of convergence when training the network. It was modified until the best results were achieved with the test set and was set to 0.3.

4.4 Data preprocessing

Data pre-processing is required to make it easier for the network to learn. Because of the large number of outputs from the spectrum analyser (512), it is necessary to extract only the information relevant to the object of interest. This is done by selecting the area of the acoustic density profile where the range information is grouped. The range information can be decomposed into :

1. absolute range to the plant; and
2. relative range between parts of the plant.

Relative range information is the information used for classifying individual plant specimens. Each signal is represented by a single vector that attempts to capture the features of the object. Several algorithms were trialed for calculating the position of the envelope of data from the acoustic density profile. The most successful is the algorithm given in Algorithm 4.1.

Algorithm 4.1 Finding the position of the object in the acoustic density profile

1. Find the frequency with maximum amplitude in the acoustic density profile;
2. Define this point as the centre of the object ;
3. The start and end of the object are selected as being 50 spectral lines each side of the central point.

This processing ensures that the peak of the acoustic density profile is always in the same position within the envelope. As a result, sets of data are aligned and the network can learn the information more easily. Figure 4.7 shows the section of the acoustic density profile which is extracted using this algorithm.

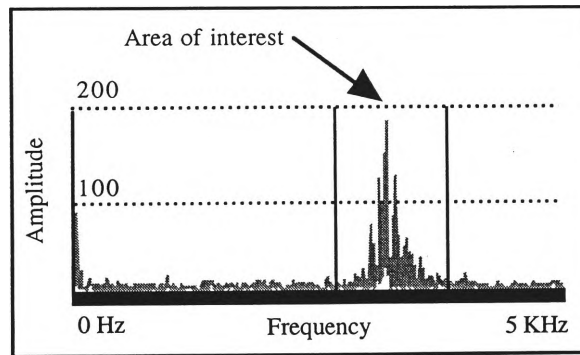


Figure 4.7 Data extracted from the acoustic density profile for presentation to the network

The resulting data are then scaled [Wasserman, 1993] to be in the range 0 to +1. This flattens the shape of the input data and zeroes the low signal values. The data is then scaled to lie between -1 and +1. The normalisation and scaling process will make the data easier for the network to learn by removing extreme values and ensures that it is within limits for the tanh activation function. Training data are presented to the network in a random order.

4.5 Network training and results

For all of the experiments, the network was trained for set numbers of iterations and the test performance logged. The weights within the network are initialised to small random numbers so can affect the results. For this reason, multiple run throughs were performed (twenty) and results averaged.

4.5.1 Experiment 1 - differentiate a plant from plants of different species

The results of *Experiment 1* are shown in Table 4.1. It shows the classification error percentage of the test data for networks with a given number of hidden units (in this case six hidden units). The classification error is the percentage of the test data that is not classified correctly by the network.

Tests were run for networks with varied numbers of hidden nodes. The number of hidden nodes is shown in column 1. Column 2 represents the number of presentations of individual training vectors. The number of presentations was not selected by any particular method other than being round numbers over a wide range. The number of epochs can be calculated by dividing the number of presentations by the number of training records. Column 3 shows the average classification error (as a percentage) for 20 separate runs of the test data. Column 4 shows the standard deviation of the error percentage.

Table 4.1 Results of Experiment 1

<i>Experiment 1</i> - 4 different species of plant 320 training records, 160 testing records (average of 20 runs)			
Hidden Units	Number of Presentations	Classification Error (percentage)	Standard Deviation (percentage)
6	4000	5.66	2.28
	5000	5.09	1.09
	6000	5.19	1.14
	7000	4.96	1.16
	8000	5.03	1.07
	10000	5.31	1.14
	15000	5.53	0.73

The table shows that up to a certain point, the error percentage improves as the network is trained for a higher number of training record presentations. Once the network is trained for too long, however, it over fits the training data and hence performs poorly on the unseen test set.

The optimal amount of training is the point which gives the best classification for the unseen test data, and for this particular network occurs at 7000 presentations (or 19 epochs) and is 4.96%. This may initially seem to be a high error percentage but the acoustic density profile of a plant specimen can change quite significantly between orientations, as described in Chapter 3 and also shown graphically in Appendix E. This is also highlighted in

Figure 4.1 where the acoustic density profiles from different views of the four plants are somewhat different. This classifier could be improved significantly by using multiple views of the plant.

This error percentage of 4.96% indicates a high chance of recognising a plant at an arbitrary angle once the network is trained but does not give any indication of the generalisation qualities of the network. Table 4.2 shows the classification matrix for one (of the 20) networks which was trained with 7000 presentations. There are only seven records which were classified incorrectly. The table shows the following misclassification:

two records from *Azalea indica* were classified as *Schefflera arboricola*;

three records from *Schefflera arboricola* were classified as *Azalea indica*, and one was classified as *Hypoestes*; and

one record from *Hypoestes* was classified as *Azalea indica*; and

None of the records from *Chamaedorea elegans* were classified incorrectly.

The classification matrix highlights the fact that *Azalea indica* and *Schefflera arboricola* are the two plants which are most likely to be misclassified as each other.

Table 4.2 Classification matrix for a network trained with 7000 presentations

Classification Matrix - Experiment 1				
Actual	Classified Plant 1	Classified Plant 2	Classified Plant 3	Classified Plant 4
Plant 1	36	2	0	0
Plant 2	3	38	1	0
Plant 3	1	0	39	0
Plant 4	0	0	0	40
Number of records misclassified = 7				
Classification Error Rate = 4.37%				

4.5.2 Experiment 2 - testing different specimens of the same species

Table 4.3 shows the results of Experiment 2. In this experiment, data from different plant specimens of the same species were used with the network that was trained in Experiment 1 (that is, four new plants all of the same species as those that the network was trained on in Experiment 1). The plants were a similar physical size and positioned at approximately the same range as those which were used to train the network.

Table 4.3 Results of Experiment 2

Experiment 2- 4 different species of plant 320 training records, 480 testing records (each test file) (average of 20 runs)			
Hidden Units	Number of Presentations	Classification Error (percentage)	Standard Deviation (percentage)
6	5000	6.89	0.88
	6000	6.68	1.12
	7000	7.32	0.90
	8000	7.17	0.88
	9000	7.32	0.81
	10000	7.52	1.54

These results show that a network trained with 4 different species can classify new unseen plants of the same species to an accuracy not significantly different to those which were used to train the network (6.68% error, or 1.72% higher than Experiment 1). This experiment used a significantly larger amount of test data (three times as much) than the first and proved that it could still classify well. The lowest error percentage was

6.68%. This means that there is enough information in the data to classify with new plants of the same species correctly.

Table 4.4 Classification matrix for a network trained with 6000 presentations

Classification Matrix - Experiment 2				
Actual	Classified Plant 1	Classified Plant 2	Classified Plant 3	Classified Plant 4
Plant 1	112	3	2	0
Plant 2	5	104	1	0
Plant 3	2	13	118	3
Plant 4	1	0	0	117
Number of records misclassified = 30				
Classification Error Rate = 6.24%				

4.5.3 Experiment 3 - recognising plants at different ranges

Experiment 3 used the same network trained for Experiments 1 and 2, but involved testing the network with data scanned at different distances. All of the scans reported so far used data from plants scanned at a range of approximately 550 mm. The results shown in Table 4.5 show classification errors for the test set which is the acoustic density profile for plants at a distance of 290 mm from the sensor head.

Table 4.5 Results of Experiment 3

Experiment 3- Plants at different ranges 320 training records, 480 testing records (average of 20 runs)			
Hidden Units	Number of Presentations	Classification Error (percentage)	Standard Deviation (percentage)
6	5000	12.81	0.98
	6000	13.02	1.05
	7000	13.64	0.94
	8000	13.47	1.34
	9000	13.34	0.86
	10000	14.53	0.95

As can be seen from these results, the recognition system is not as good at recognising these new plants at different ranges (12.81% error for 5000 presentations) as it is at recognising them at the same range as the network was trained (6.89% error). This experiment shows the absolute differences between the signals but could be significantly improved by normalising the raw data for range (see Chapter 5).

Table 4.6 Classification matrix for a network trained with 5000 presentations

Classification Matrix - Experiment 3				
Actual	Classified Plant 1	Classified Plant 2	Classified Plant 3	Classified Plant 4
Plant 1	105	7	16	2
Plant 2	15	106	8	2
Plant 3	1	6	92	0
Plant 4	1	1	3	116
Number of records misclassified = 62				
Classification Error Rate = 12.89%				

4.5.4 Experiment 4 - differentiate plants of the same species

Experiment 4 involved differentiating between different plants of the same species. Ultrasonic images from three plants of the same species were used (*Azalea indica*). As in Experiment 1, seventy-five percent of the data was used to train the network and the other twenty-five percent was used for testing. Results are shown in Table 4.7.

Table 4.7 Results of Experiment 4

Experiment 4 - 3 samples of same species 360 training records, 120 testing records (average of 20 runs)			
Hidden Units	Number of Presentations	Classification Error (percentage)	Standard Deviation (percentage)
6	1000	10.11	10.61
	2000	5.09	5.55
	3000	3.12	1.44
	4000	2.74	0.99
	5000	3.01	1.47
	10000	3.23	1.13

The results shown indicate the ability of the network to differentiate between individual plants within a species. This fine discrimination means that this perception system could be very useful. In its present form however, it would only be of use in an application with a limited domain. Training data would have to be collected in that domain and the network would be able to perform accurate recognition within that domain. An example of this may be recognition of items on a conveyor belt.

Table 4.8 Classification matrix for a network trained with 4000 presentations

Classification Matrix - Experiment 4			
Actual	Classified Plant 1	Classified Plant 2	Classified Plant 3
Plant 1	39	2	0
Plant 2	1	38	0
Plant 3	0	0	40
Number of records misclassified = 3			
Classification Error Rate = 2.5%			

4.5.5 Experiment 5 - the effect of removing the leaves

Experiment 5 involved testing the network that was trained in Experiment 1 with the data from the plants that had their leaves trimmed off. Great care was taken to remove only the leaves of the plants using a pair of pruners. Measurements were then taken from this plant before the minor stems were removed. This left the plants with one or two major trunks. The results are shown in Table 4.9.

Table 4.9 Results of Experiment 5

Experiment 5- 4 samples of same species with leaves removed 360 training records, 480 testing records (average of 20 runs)			
Hidden Units	Number of Presentations	Classification Error (percentage)	Standard Deviation (percentage)
6	5000	49.97	3.08
	6000	49.11	2.80
	7000	50.04	3.02
	8000	50.41	3.98
	9000	51.91	3.52
	10000	51.21	3.01

The network is unable to recognise the plants once their leaves have been removed. This shows that the envelope of frequencies in the sensor data is highly dependant on the leaf structure of the plant and is not significantly affected by the branches of the plant.

Table 4.10 Classification matrix for a network trained with 6000 presentations

Classification Matrix - Experiment 5				
Actual	Classified Plant 1	Classified Plant 2	Classified Plant 3	Classified Plant 4
Plant 1	28	9	0	0
Plant 2	61	76	18	27
Plant 3	24	17	43	2
Plant 4	9	18	61	92
Number of records misclassified = 246				
Classification Error Rate = 50.72%				

Visual inspection of the acoustic density profiles from the plants once the leaves are removed (Figure 4.8) reveals that very little of the original signal is reflected back to the receiver so it is impossible to characterise the plants based on the structure of their stems. This is because the stems are round, so the echoes are spread over a wide angle and hence the receiver detects a very low amplitude.

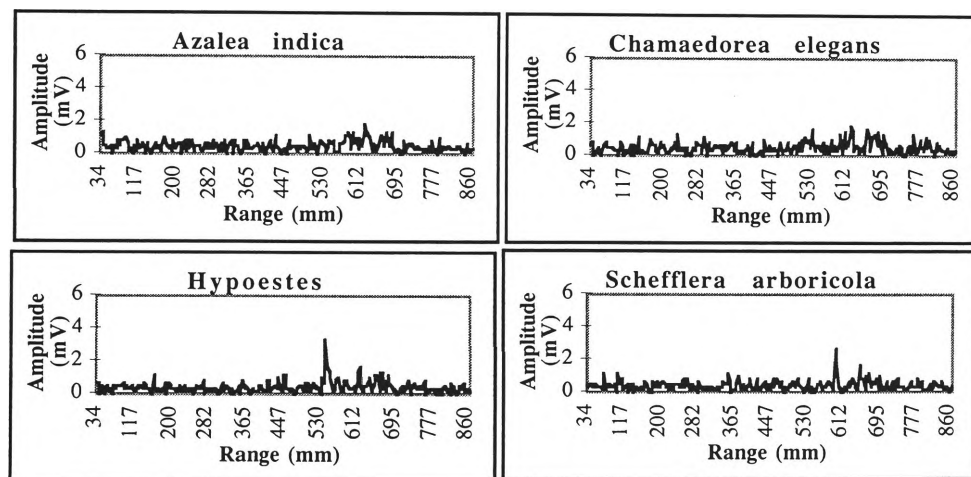


Figure 4.8 Acoustic density profiles from the four plant specimens with their leaves removed

4.6 Conclusion

A feed forward Artificial Neural Network has been trained to recognise plant specimens of different species. Plants of a certain species can be used to train the network and then another plant of the same species can be recognised using the trained network. There is an extremely high chance of recognising the plants that were used in training, there is a good chance of recognising another plant of the same species and it is also possible to recognise plants of the same species at different distances from the sensor

head. Also, we found that there is sufficient information in the signal to enable discrimination between plants of the same species.

In summary, this is a perception system which is independent of the size of the plant and the distance to the plant. It is also highly sensitive to the external structure of the object, that is to the leaf structure.

While an ANN may be trained to recognise objects, there is currently no good way of extracting information from the weights. The network acts as a “black box” and provides no way of interpreting the knowledge in the data. As is often the case with statistics [Elder, 1995], there is more value in a model structure which will allow the extraction of meaning. This is discussed in Chapters 9 and 10. The network can however, give an indication of whether there is enough information in the signal to use the set-up for object recognition.

The experiments described in this chapter using a simple neural network architecture have shown that there is sufficient information in the signal to develop a recognition system that is independent of the height of the plant and the width of the plant. There is a slightly higher error rate when plants are at varying distances from the sensor and this shows that the system is almost independent of range. The echo contains information about the geometric structure of the plant : leaf size, leaf shape, leaf orientation and leaf density. Hence, by analysing of the echo, a plant classification system can be developed.

4.7 Summary

1. ANN's have been an active area of study and are good at classifying data.
2. As a proof of concept, an ANN can classify a small number of plants based on their acoustic density profile.
3. It is difficult to extract information from the weights but there is enough information in the signal to differentiate between complex objects.

5. Plant Database

5.1 Introduction

In order to analyse the signals comprehensively, a large database of information is required. The research up to this point focused on small indoor plants as they tend not to change as rapidly as outdoor plants. The problem is obtaining a large sample of indoor plants for the experiments. One hundred is a reasonable number of plants and is a good starting point for experimentation. The staff at the local botanic gardens provided 100 plants for the experiments. Their specialty is outdoor native Australian plants but they were all young, compact plants which suited the criteria.

Plants were provided in family groups so analysis could be made of the way that plants change within and between families. Chapter 8 shows however, that plants of the same family are not necessarily similar in terms of their acoustic density profile. The acoustic density profile is more dependant on the size, shape, orientation and overall positioning of the leaves. There is different information in the acoustic density profiles than botanists use to group plants into families.

Once the records are collected, the problem becomes one of analysing the data and this is pursued in subsequent chapters.

5.2 Database structure

5.2.1 Plant characteristics

For each plant, a portfolio was established which contains data about the plant and a photograph so that an association can be made between the plant's name and its physical characteristics. In the portfolio, each plant is characterised by the following pieces of information:

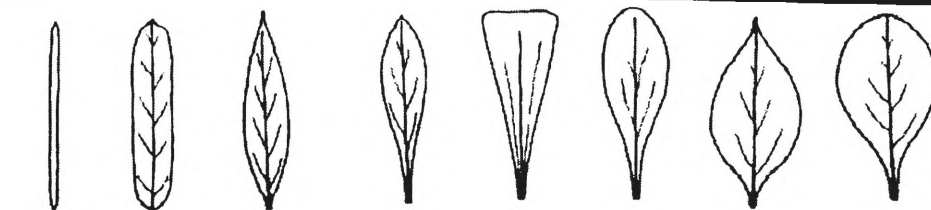
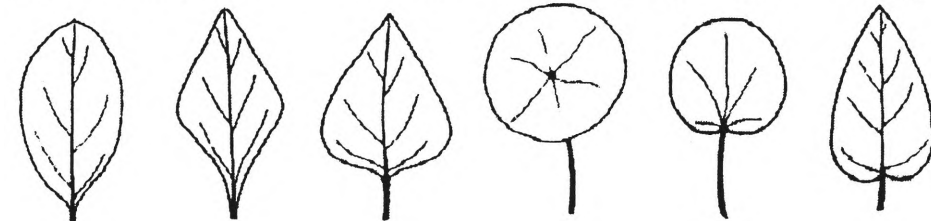
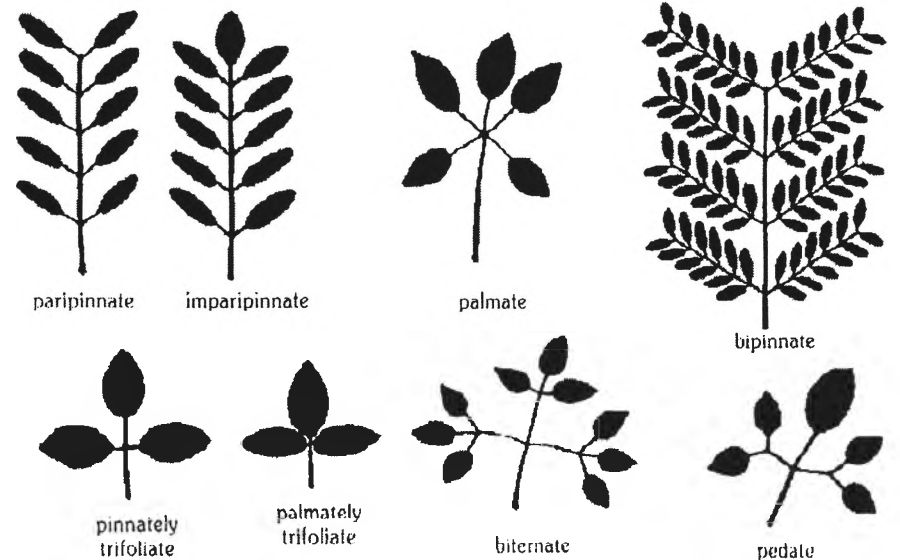
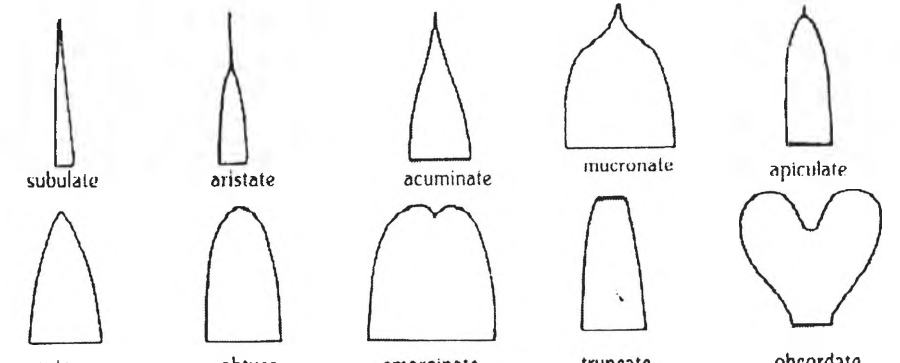
1. Scientific name;
2. Common name;


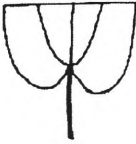


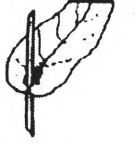




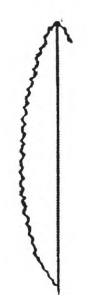





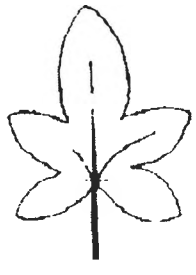
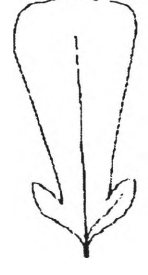

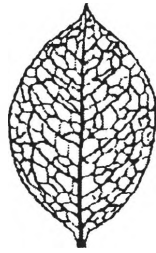

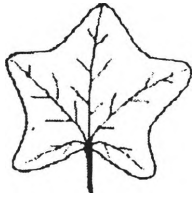
3. Height;
4. Approximate width;
5. Leaf shape;
6. Approximate leaf size;
7. A photo of the plant;
8. The conditions under which the plant was processed ie. date, time, temperature and humidity; and
9. A sample acoustic density profile for the plant.

A selection of sample plant portfolios are listed in Appendix A. The complete document is located in the Intelligent Robotics Laboratory at the University of Wollongong. As well as the observed characteristics above, there is basic structural information documented about each of the species, the fields of which are listed in Table 5.1.

Table 5.1 Characteristics of plant species

Plant name	This is the scientific name of the plant species.
Common name	The assigned common name.
Family	The family of plant to which this species belongs.
Height	The total height of the specimen from the soil to the top of the highest point measured in millimetres.
Width	The total width of the plant at its widest point measured in millimetres.
Leaf Length	The average leaf length from the base to the tip of the leaf. Since the plants were on loan, it was not possible to remove all of the leaves and measure them, instead a good estimate was made by measuring several leaves which were judged to be of an average length. This measurement was made in millimetres.
Leaf Width	This was the average width of the leaves at their widest point. Measured in millimetres.
Number of Leaves	A count of the total number of leaves on this specimen
Leaf density	This was an estimate at how dense the plant is on a coarse scale of high, medium or low. The plants with high density have a large leaf area in relation to the volume which they occupy.
Leaf Shape	This is an indication of the leaf shape of a typical plant of this species. Details of the leaf shapes from Roger & Carolin [1990] are shown below.

	 <p>linear oblong lanceolate oblanceolate cuneate spathulate ovate obovate</p>  <p>elliptical rhomboid deltoid orbicular (also pellate) reniform cordate</p>
Leaf Arrangement	This is the arrangement of the leaves in relation to each other and the plant stems.
Compound leaves	<p>If the leaves of the plant are composed of several parts then they are said to be compound. Compound leaves can be arranged in several different configurations and they are noted in this column. Details from Roger & Carolin [1990] are shown below.</p>  <p>paripinnate imparipinnate palmate bipinnate</p> <p>pinnately trifoliate palmately trifoliate biternate pedate</p>
Leaf Apices	<p>The shape of the leaf at its apex. Details from Roger & Carolin [1990] are shown below.</p>  <p>subulate aristate acuminate mucronate apiculate</p> <p>acute obtuse emarginate truncate oboordate</p>
Leaf Bases	The shape of the leaf at its base. Details from Roger & Carolin [1990] are shown below.

	      oblique cordate sagittate hastate stem-clasping decurrent
Leaf Margin	<p>This is the pattern of the leaf around its outer edge. Details from Roger & Carolin [1990] are shown below.</p>       serrate serrulate dentate denticulate crenate sinuate
	     lobed pinnatifid pinnatisect palmatifid lyrate
Venation Patterns	<p>The manner in which the veins of leaves are arranged. Details from Roger & Carolin [1990] are shown below.</p>     parallel reticulate penniveined palmate
Leaf Indumentum	The hairy or scaly surface of the leaf
Comments	Some notes taken about the physical characteristics of the plants

5.2.2 Sensed data

For each orientation of the plant, the acoustic density profile is stored. All 512 data items are saved as consecutive records in a file which is named using the scientific name of the plants.

5.3 Data collection

5.3.1 Equipment setup

The individual plants were mounted on the rotating stage of a precision positioner. The positioner is shown in Figure 5.1 with a plant on the rotating stage. The beam pattern of the signal is three dimensional but is shown in two dimensions. The sensing head is located on one of the ends of the positioner and is linked to the microcomputer.

The positioner is interfaced to a personal computer via the serial port and commands are generated in software to control it. The positioner itself is controlled by Slo-Syn enhanced programmable indexers which are attached to stepper motors. The indexers allow the user to position the centre stage accurately at a set distance from the sensor and the stage can also be rotated precisely. The command structure for the indexers is based on industry standard RS274-D.

Plants are rotated through 360 degrees and a reading is taken at each orientation (of the 360). After each movement of one degree, a pause of 10 seconds ensures that the leaves on the plant had completed their motion and had returned to a stationary position. The experiment was controlled through software so that it was a simple matter of positioning the plant in the centre of the rotating stage and initiating the program. The software also writes the acoustic density profile to a specified file. Care was taken to eliminate other disturbances such as air movements or shaking of the floor by positioning the equipment in a room separate from the rest of the laboratory.

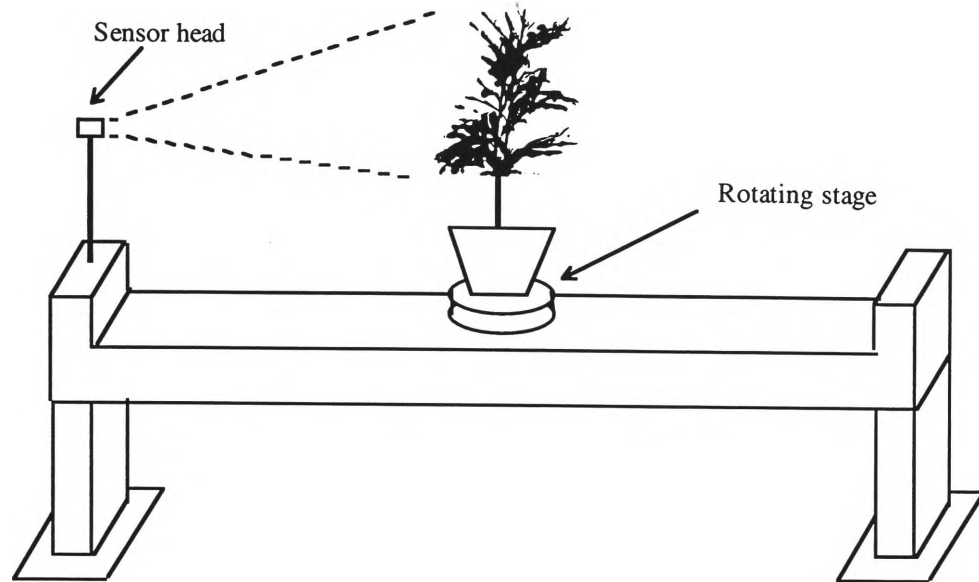


Figure 5.1 A Precision Positioner with the sensor head mounted

The environmental conditions under which the experiment was run were recorded so that the data could be adjusted at a later date if required. Once the plant is placed on the stage, a file name is entered, the software then pauses for 30 seconds for researchers to leave the room and close the door to establish the experimental conditions. The angle of the left and right sensor can be adjusted so that they point out to the side as they are for blind users. Care was taken to make sure that the sensors were aligned in a straight line with the central transmitter (Figure 5.2).

The experiments resulted in a database of 360 records for each of 100 plants (36000 records in total). Each of the records is the raw acoustic density profile consisting of 512 data values. The process took approximately one hour per plant and the data were collected over a period of several weeks.

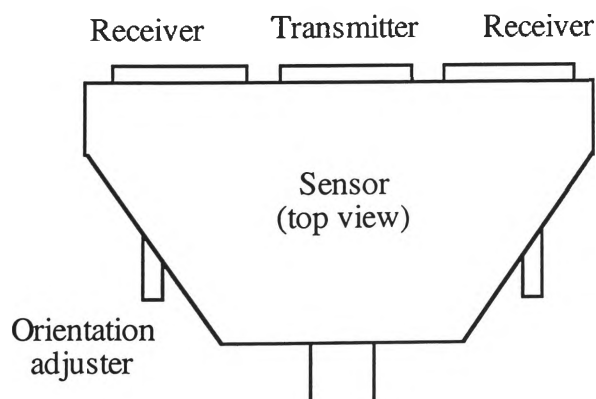


Figure 5.2 Top View of the sensor head

5.4 File management

The software supplied with the system was modified to control the positioner and also to save the acoustic density profile to a file for later processing. The data for each plant is saved in a separate text file. The file has 360 records, each with 512 fields.

5.5 Tabulated results

Table 5.2 shows the information collected about each of the plants. An explanation of each field was given in Table 5.1.

Table 5.2 Details of plants 1 to 49 (plants 50 to 100 are shown in Table 5.3)

ID	Plant	Family	Common name	Hgt cm	Wth cm	Leaf length	Leaf width	No. of leaves	Leaves density	Leaves orient.	Leaf Shape	Leaf Arrang.	Compound Leaves	Leaf Apices	Leaf Bases	Leaf Margins	Venation Patterns	Leaf Cross Section	Indumentum Upper Surface	Comments
1	<i>Acacia binervata</i>	Mimosaceae	2-veined hickory	55	30	8	4	66	high	45 elliptic-lanceolate	alternate		acute		asymmetric	entire	longitudinal	flat		medium size leaves prominent veins
2	<i>Acacia cultriformis</i>	Mimosaceae	Knife-leaf wattle	40	4	2	1	52	low	obliquely triangular to obliquely obovate	alternate		acute		asymmetric	entire	reticulate			single central stem with small leaves
3	<i>Acacia falcata</i>	Mimosaceae		60	25	8	3	31	low	horizontal	lanceolate		obtuse to subacute				lateral			1 or 2 side branches
4	<i>Acacia howittii</i>	Mimosaceae		40	30	1.2	0.4	450	high	various	oval?		acute to subacute							small roundish leaves along branches, bent over
5	<i>Acacia irrorata</i>	Mimosaceae	Green wattle	35	38	10	5	18	medium	horizontal	linear to oblong		bipinnate							typical wattle type leaves bipinnate
6	<i>Acacia longifolia</i>	Mimosaceae	Syd Golden wattle	35	35	10	1	340	high	various	oblong to narrow elliptic						longitudinal			many long thin leaves
7	<i>Acacia measmii</i>	Mimosaceae	Black wattle	38	25	10	6	9	low	horizontal	linear oblong		bipinnate						minutely pubescent	typical wattle leaves similar to <i>irrorata</i> smaller specimen
8	<i>Acacia melanoxylon</i>	Mimosaceae	Blackwood	43	15	8	1	20	low	various	sublanceolate		bipinnate	acute to obtuse						2 different kinds of leaves long thin and wattle type
9	<i>Acacia podalyrifolia</i>	Mimosaceae	Old Silver wattle	30	15	4	3	56	medium	horizontal	sublanceolate			acute to obtuse	symmetric				glabrous	main stem with one side branch same as one out front
10	<i>Acacia stricta</i>	Mimosaceae		30	20	8	0.7	64	medium	vertical	narrow-oblong to elliptic			obtuse						symmetrical looking all leaves pointing up
11	<i>Acronychia laevis</i>	Rutaceae	Glossy Acronychia	48	40	4	2	168	high	various										very specular medium sized waxy leaves
12	<i>Agapanthus praecox dwarf</i>	Agavaceae	Dwarf Agapanthus	15	15	12	1	7	medium	vertical		basal								leaves sprouting up from the base
13	<i>Agapanthus praecox</i>	Agavaceae	Agapanthus	33	44	32	3	12	medium	vertical		basal								large leaves sprouting from the base
14	<i>Alyxia ruscifolia</i>	Annonaceae	Prickly Alyxia	55	6	2	0.8	77	low	horizontal	narrow lanceolate to broad ovate	whorled		acute			recurved		glabrous	tall spindly plant with a single stem, very few leaves
15	<i>Archontophoenix cunninghamiana</i>	Arecaceae	Bangalow Palm	35	40	20	15	5	medium	45 segments linear		basal	pinnate			sheathing				very large pinnately divided leaves, only about 6
16	<i>Avicaria distylis</i>	?	Twin-leaf Cogera	40	18	6	2	28	medium	horizontal										wobbly edge leaves mostly oriented in one direction
17	<i>Azalea alba magnifica</i>	Ericaceae	Azalea	50	40	2	0.8	140	medium	45										spindly large azalea with several large sub-branches
18	<i>Azalea cultivar splenda</i>	Ericaceae	Azalea	44	40	3	1	250	medium	45										bushy but not symmetric about 9 minor vertical branches
19	<i>Banksia ericifolia</i>	Proteaceae	Heath Banksia	40	6	1.5	0.3	67	low	horizontal	linear	alternate		truncate (with notches)	attenuate		entire	flat		1 main stem with very small leaves around it
20	<i>Banksia integrifolia</i>	Proteaceae	Coast Banksia	60	30	10	2	212	high	various	narrow obovate to narrow elliptic	whorled					entire	lateral	tomtense	bushy plant, most of the leaves on one angled branch
21	<i>Carpentaria acuminata</i>	Arecaceae	Carpentaria Palm	50	30	20	10	4	low	various	2 elliptic or narrowly lanceolate lobes	basal	lobed							large pinnately divided leaves but not many of them
22	<i>Casuarina glauca</i>	Casuarinaceae	Swamp Oak	65	35	8	0.1	300	medium	45 elliptic			sessile						glabrous	needle like leaved, relatively bushy for a casuarina
23	<i>Casuarina stricta</i>	Casuarinaceae	Drooping Sheoak	60	50	15	0.1	160	medium	45 elliptic			sessile							very long needles mainly off the central stem
24	<i>Casuarina torulosa</i>	Casuarinaceae	Forest Sheoak	40	33	6	0.1	400	high	30 elliptic		whorled	sessile							dense shapely kind of symmetrical
25	<i>Cinnamom oliveri</i>	Lauraceae	Oliver's Sassafras	48	10	6	1.5	7	low	horizontal	lanceolate to narrow elliptic	opposite		acuminate			reticulate			a stick with about 6 leaves near the top
26	<i>Citriobatus paucifloris</i>	Pittosporaceae	Orange Thorn	15	15	0.5	0.5	300	high	various	ovate to obicular or obovate to broad-cuneate	alternate				entire				a very compact plant with many small leaves
27	<i>Cordyline australis</i>	Agavaceae		35	60	40	0.6	450	medium	45		basal								very long thin leaves from the base
28	<i>Correa alba</i>	Rutaceae	White Correa	30	20	3	2	88	medium	45 ovate to circular or obovate			rounded		rounded to cuneate				hairy	cupped leaves from 3 main branches, top sided
29	<i>Crinum mauritianum</i>	Amaryllidaceae		60	30	60	2	6	medium	vertical		basal								long leaves from base from each side of the plant
30	<i>Crinum pedunculatum</i>	Amaryllidaceae	Swamp Lily	30	15	50	3	6	low	vertical	narrow-oblong	basal		bluntly acuminate			undulate			short stem with long leaves radiating upwards
31	<i>Cryptocarya bidwillii</i>	Lauraceae	Yellow Laurel	23	12	8	2	15	low	horizontal	narrow elliptic			acuminate						small plant with only a few leaves
32	<i>Cryptocarya laevigatum</i>	Lauraceae	Red-fruited Laurel	39	20	6	3	56	medium	30 ovate-elliptic to narrow-elliptic				acuminate					glabrous	glossy leaves, 2 minor branches leaves angled down
33	<i>Cryptocarya williwilliana</i>	Lauraceae	Small-leaved Laurel	24	15	1.5	1	80	low	horizontal	ovate to broad-elliptic						areolate			small leaves many branches from trunk with leaves
34	<i>Cupaniopsis anacardioides</i>	Sapindaceae	Tuckeroo	28	14	8	3	22	low	horizontal	obovate or oblong elliptic	alternate	paripinnate	obtuse to retuse	obtuse to cuneate	entire			glabrous	leaves on branches off main trunk sparse
35	<i>Cupaniopsis parvifolia</i>	Sapindaceae		31	12	6	2	17	low	horizontal	narrow-obovate to oblong-elliptic	alternate	paripinnate	obtuse or retuse	cuneate	entire			glabrous	leaves on branches off main trunk sparse
36	<i>Diptelotaxis australis</i>	Sapindaceae	Native Tamarind	15	20	12	6	5	low	horizontal	oblong to elliptic-oblong	alternate	paripinnate	rounded	asymmetric	entire			glabrous	small plant with large leaves
37	<i>Diptelotaxis campbellii</i>	Sapindaceae		60	30	6	1.5	77	high	horizontal	elliptic-oblong to ovate	alternate	paripinnate	acute	asymmetric	entire			glabrous	quite a few leaves spread well throughout the branches
38	<i>Dodonaea triquetra</i>	Sapindaceae	Hopbush	39	31	15	6	30	high	horizontal	elliptic			acute to acuminate	narrow cuneate to attenuate	entire or sinuate			glabrous	large leaves of main stem and 2 small branches
39	<i>Dodonaea viscosa</i>	Sapindaceae		39	30	10	1	140	high	30 linear to obovate				obtuse to acuminate	attenuate to cuneate	entire to toothed			glabrous	bushy plant with long leaves from several branches
40	<i>Doranthus paucifloris</i>	Agavaceae	Spear Lily	60	60	60	6	8	medium	vertical	sword-shaped	basal								large sword shaped leaves radiating from base
41	<i>Endiandra intorsa</i>	Lauraceae	Dorridge Plum	35	18	8	2	47	medium	30 narrow-elliptic to oblong elliptic		alternate		bluntly acuminate			undulate	obscured	glabrous	many large leaves from stems
42	<i>Endiandra pubens</i>	Lauraceae	Hairy Walnut	29	30	8	2.5	41	medium	30 elliptic		alternate		rounded or bluntly acuminate			areolate		glabrous	small with large leaves compact and dense
43	<i>Eriostemon myrsinoides</i>	Rutaceae	Native Daphne	23	12	6	0.8	34	medium	vertical	oblong to narrow-elliptic	alternate	simple				entire		glabrous	single main stem slightly on and angle
44	<i>Eucalyptus botryoides</i>	Myrtaceae	Southern Mahogany	25	15	1	6	37	medium	horizontal	broad-lanceolate to ovate	opposite					penniveined			random leaves on many small stems from main trunk
45	<i>Eucalyptus leucocorylon</i>	Myrtaceae	Rosea	60	24	6	5	52	low	30 ovate to broad-lanceolate		opposite								large roundish leaves off a single main stem
46	<i>Eucalyptus maculata</i>	Myrtaceae	Spotted Gum	48	32	20	4	18	medium	30 elliptic to ovate							lateral			very large leaves on small stalks from central stem
47	<i>Ficus rubiginosa</i>	Moraceae	Port Jackson Fig	42	20	8	3	26	high	down	obovate to ovate or elliptic					entire			glabrous	a "ball" of leaves on a central stem
48	<i>Goodia lotifolia</i>	Fabaceae		44	12	1	0.8	80	low	down	obovate to obovate-cuneate	3-foliate				entire			glabrous	climber type leave stem looks about half way up
49	<i>Grevillea balfouriana</i>	Proteaceae		25	22	15	15	8	medium	30 lobes oblong			lobes							large leaves with lobes coming from central stem

Table 5.3 Details of plants 50 to 100 (plants 1 to 49 are shown in Table 5.2)

id	Plant	Family	Common name	Hgt cm	Wth cm	Leaf lgth	Leaf wth	No Leaves	Leaves density	Leaves orient.	Leaf Shape	Leaf Arrang.	Compound Leaves	Leaf Apices	Leaf Bases	Leaf Margins	Venation Patterns	Leaf Cross Section	Indumentum Upper Surface	Comments
50	Grevillea hillebrandii	Proteaceae	White Silky Oak	38	35	22	2	11	medium	horizontal	lobes linear to lanceolate		lobes			recurved				long thin alternate leaves with many thin lobes
51	Grevillea marmalade	Proteaceae	Orange Marmalade	40	40	10	1.5	36	medium	vertical										central stem with 1 large branch angled alternate leaves
52	Goiaa semigauca	Sapindaceae		37	15	4	1.5	28	low	horizontal	obovate to narrow-elliptic		alternate pinnate	obuse		entire			glabrous	leaves grouped on small stems from main trunk
53	Hakea salicifolia	Proteaceae	Willow-leaf Hakea	46	34	6	2	48	medium		45 narrow-lanceolate to lanceolate			acute			lateral			central stem with 1 large angled branch
54	Howea forsteriana	Arecaceae	Kenia Palm	50	50	30	30	4	medium		45 lanceolate		pinnate							spindly palm
55	Hymenosporum flavum	Pittosporaceae	Native Frangipani	22	8	4	1	10	low	horizontal	obovate to oblanceolate		whorled	acuminate or apiculate					glabrous	small plant with few leaves alternate folded
56	Indigofera australis	Fabaceae	Australian Indigo	29	13	12	3	11	medium	down	obovate to oblong		alternate pinnate	obuse						branches with many leaves grouped like wattle but bigger
57	Jacaranda mimosifolia	Bignoniaceae	Jacaranda	40	27	1.5	0.5	500	medium	horizontal										jacaranda
58	Laccospadix australasica	Araceae	Atherton Palm	34	38	20	8	5	low	vertical	linear to lanceolate		pinnate							small spindly palm
59	Leptospermum laevigatum	Myrtaceae	Coast Tea Tree	30	28	2	0.7	900	high	various	obovate to narrow-elliptic		alternate	obuse			reticulate	flat or recurved		bushy plant with many branches covered in leaves
60	Leptospermum morrissonii	Myrtaceae	Tea Tree	31	16	6	2	110	medium		45 narrow-elliptic to oblanceolate			acute			flat or recurved			symmetric plant with leaves on branches
61	Leptospermum petersonii	Myrtaceae	Lemon Sc. Tea T.	50	20	0.7	0.1	520	high	various	narrow-elliptic to lanceolate			retuse			flat or recurved	glabrous		lots of leaves and many small branches
62	Licuala ramsayi	Arecaceae	Hessian Hair Fan Palm	46	48	20	20	5	medium	vertical	lanceolate		alternate				parallel			large hand like leaves about 6
63	Litsea reticulata	Lauraceae	Bolly Gum	60	15	6	1.5	16	low	horizontal	obovate to elliptic			rounded obtuse			reticulate			a few leaves on a stem and end of an angled branch
64	Livistona sp. 'Carnarvon'	Arecaceae	Cabbage Palm	35	15	20	5	5	low	vertical	oblong-elliptic?		basal palmate							a couple of very large leaves oriented vertically
65	Melaleuca decora	Myrtaceae		50	16	1	0.2	280	medium	various	linear to narrow-elliptic		alternate	acute			flat		glabrous	tiny leaves along trunk and several branches
66	Melaleuca erubescens	Myrtaceae		15	6	1	0.1	170	low	various	narrow-linear		alternate	apiculate					glabrous	tiny leaves along tiny branches and trunk
67	Melaleuca quinquenervia	Myrtaceae	Broad-leaved Paper	53	15	5	0.8	184	medium		45 lanceolate-elliptic		alternate	obuse			longitudinal		hairy	leaves along symmetrical branches upright plant
68	Melaleuca stypheloides	Myrtaceae	Prickly-leaved Tea T.	40	6	3	0.5	64	low	horizontal	lanceolate to ovate-acuminate		alternate	pungent			longitudinal		glabrous	single central stem with small leaves
69	Microcotrus australis	Rutaceae	Bush Lime	35	15	1	0.2	206	medium	horizontal	obovate to elliptic or rhombic		alternate	notched	cuneate	crenate			glabrous	crazy plant with strange zig zag branches with leaves
70	Ficus obliqua	Moraceae	Small-leaved Fig	50	24	6	2	29	medium		30 oblong-lanceolate to elliptic						lateral			plant with 2 major stems but with a big lean on it
71	Mishocarpus australis	Sapindaceae		28	18	13	4	15	medium	horizontal	elliptic-oblong to ovate-oblong		opposite paripinnate	acuminate to acute	acute to obtuse	entire undulate	reticulate		glabrous	small plant with large leaves on stalks from trunk
72	Omalanthus populifolius	Euphorbiaceae	Bleeding Heart	15	8	5	4	5	medium	down	broad-ovate to acuminate		spiral				penninerved		glabrous	tiny bleeding heart
73	Phyllanthus albidiflorus	Euphorbiaceae		38	22	1.2	0.8	350	medium		30									leaves along stems opposite several minor stems
74	Pittosporum crassifolium	Pittosporaceae	Karo	38	30	5	4	100	high		45									waxy leaves round numerous
75	Pittosporum james	Pittosporaceae		55	30	1.1	0.8	160	low	various										many long branches with small leaves scattered
76	Pittosporum revolutum	Pittosporaceae	Brisbane Laurel	55	22	8	4	33	medium	down	ovate to oblong-elliptic		clustered	shortly acuminate			entire	revolute		groups of leaves on the end of 3 branches
77	Pittosporum rhombilolium	Pittosporaceae		30	16	4	2	30	medium	horizontal	ovate to rhombic		alternate				toothed		glabrous	several minor branches from trunk with leaves on all
78	Pittosporum undulatum	Pittosporaceae		30	12	8	2	12	medium		45 narrow-ovate to elliptic or ovate oblong		alternate	acute to acuminate			undulate		glabrous	medium size leaves on main stem
79	Polyscias australiana	Araliaceae		50	50	8	5	40	medium	horizontal			opposite imparipinnate					pinnate		fairly symmetric with 5 or 6 minor branches w/leaves
80	Polyscias elegans	Araliaceae	Celery Wood	50	25	7	3	40	medium	down	ovate to elliptic		opposite bipinnate	acuminate			entire			leaves on small branches. a bit lop sided
81	Polyscias murrayi	Araliaceae	Pencil Cedar	30	30	7	2.5	54	high	horizontal	oblong-elliptic		opposite pinnate	acute to acuminate	truncate		minutely toothed			leaves on small branches symmetric
82	Radermachia tenecis	Bignoniaceae	China Doll	31	40	2	0.9	400	high		30		opposite							china doll, numerous leaves
83	Rhododendron bryophyllum	Ericaceae		32	18	5	1	150	medium	horizontal			whorled							odd shaped rhodo one large off centre branch plus others
84	Rhododendron chlorinda	Ericaceae		40	25	8	3	40	medium		30 oblong to lanceolate									large folded waxy leaves around end of trunk & main branch
85	Rhopalostylis baneri	Arecaceae	Norfolk Palm	25	25	20	10	4	medium	vertical	linear to lanceolate		basal pinnate				longitudinal			another palm
86	Rhopalostylis sapida	Arecaceae	Nikau Palm	55	40	25	15	3	medium	vertical	linear to lanceolate		basal pinnate				longitudinal			scrappy palm with large leaves
87	Sarcobothria heterophylla	Sapindaceae		40	40	15	3	38	medium		30									large leaves on branches off main trunk
88	Sarcocaulis simplicifolia	Rutaceae		70	25	11	5	22	medium		30 ovate-elliptic or obovate		opposite							large leaves on stalks off main trunk
89	Solanum aviculare	Solanaceae	Kangaroo Apple	15	20	20	8	7	medium	down	lobes lanceolate to narrow-elliptic		pinnate lobed				entire		glabrous	large lobed leaves on a very small plant
90	Solanum brownii	Solanaceae	Devil's Needles	60	35	15	8	15	medium		30 narrow-ovate to elliptic		broad-deltoid				entire or sinuate			large leaves with spikes on stalks from main trunk angled
91	Solanum lacinatum	Solanaceae	Lrg Flower, Kang. Appl	40	12	10	1.5	6	low	horizontal	lobes broad ovate		lobed				entire			a few leaves on the end of main trunk
92	Solanum vesum	Solanaceae		30	40	20	10	11	medium	various	lobes broad ovate		lobed				entire		glabrous	large lobed leaves in various orientations
93	Stenocarpus sinuatus	Proteaceae	Firewheel Tree	40	40	20	30	8	medium	horizontal	oblong lanceolate		alternate irregularly lobed	obuse			entire	longitudinal		huge lobed leaves on stalks from trunk
94	Streblis brunianus	Moraceae	Whalebone Tree	40	10	7	3	16	medium	down	elliptic to ovate or lanceolate		alternate	acuminate			regularly toothed		scabrous	leaves hanging down from small stalks from trunk
95	Syzygium leuhamni	Myrtaceae	Riberry	40	25	2	1	208	high	various	ovate to lanceolate		opposite	long acuminate						a dense kind of plant kind of like a fig
96	Syzygium paniculatum	Myrtaceae		45	16	5	2	94	medium	various	lanceolate to obovate		opposite	acuminate	cuneate		lateral		glabrous	leaves off stem and also angled branch
97	Tabebuia chrysaliricha	Bignoniaceae		30	29	5	5	43	medium	horizontal	elliptic-circular?		opposite pinnately trifoliate			crenate?	pinnate			furry leaves in groups of 3 at end of stems, serrated
98	Tristanopsis collina	Myrtaceae	Mount Water Gum	35	10	5	1.5	27	low	horizontal	narrow elliptic		alternate	acuminate					glabrous	leaves from central trunk
99	Westringia fruticosa	Lamiaceae	Rosemary	15	7	1	0.2	60	low		45									rosemary - leaves from central stem
100	Ziera collina	Rutaceae		50	25	1.5	0.2	146	medium	various										many small leaves along trunk and branches angled

5.6 Referencing the data to a standard range of 400 mm

The raw data are referenced to a standard range by using the calibration curve of range change by amplitude given in Section 3.5.3. This is valid due to the basic physics of the system. In Chapter 3, the range resolution was shown to be 3.44 mm for the configuration used. This resolution is constant through the entire range of the sensor, ie two surfaces which are separated by three range cells when at a distance of 500 mm from the sensor, will still be separated by three range cells when they are a distance of 1200 mm from the sensor. So, if the same plant is at two different ranges, the relative range information is constant. Plants at greater ranges however, will result in less of the echo returning to the sensor due to beam spread and attenuation over the greater distance. This means that some information about surfaces within the plant may be lost if the surfaces are small and are not distinct from background noise.

This calibration curve was established recording the amplitude of the acoustic density profile for a standard object at different ranges as shown in Chapter 3. All of the ranges in between the measurements are interpolated. The start of the plant is moved to the element corresponding to the required standardised distance and it is scaled so that it has the equivalent amplitude that it would have had at that distance, the rest of the elements of the plants signature are moved to the elements proceeding the start of the plant and are scaled appropriately for their range changes.

To do this, the start and end position of the plant's signature is determined within the acoustic density profile. For each of the elements of the plant, move it to the position indicated by the standardised distance and scale it by multiplying the amplitude by (the calibration curve value at the current plant position) / (calibration curve value at the new element position). The pseudo code for this function is outlined in Algorithm 5.1. The code for this is given in Appendix C. Figure 5.3 shows the acoustic density profile of *Indigofera australis* at a range of 800 mm from the sensor, and the same acoustic density profile referenced to a range of 400 mm.

Algorithm 5.1 Algorithm for range referencing function

```

REFERENCE THE RAW ACOUSTIC DENSITY PROFILE TO A STANDARD RANGE
This function is passed an array with a raw acoustic density
profile and the range to which the function should reference the
data to. The start and end of the plant is found and each element
is moved to the standardised distance and scaled by the following
function :
    the calibration curve at the new position /
    the calibration curve at the current position
This function assumes the existence of the following constant :
    float  calibration_array[512]      this is the
                                         calibration array

Parameters :
    profile      this is an array which contains the acoustic
                  density profile
    ref_range_mm this is the range that the data should
                  be scaled to start from in millimetres

Returns
    ref_profile  this is the acoustic density profile scaled
                  to the new distance.

BEGIN
    Call the function to calculate the start position of the plant.
    Call the function to calculate the end of the plant.
    Convert the passed ref_range_mm to a range cell number.

    Process all of the elements in the acoustic density profile
    BEGIN
        Calculate the scale factor as calibration[norm_range]
        divided by calibration[plant_range]
        Element in new acoustic density profile at new range =
            the element in the acoustic density profile * scale
    END
END

```

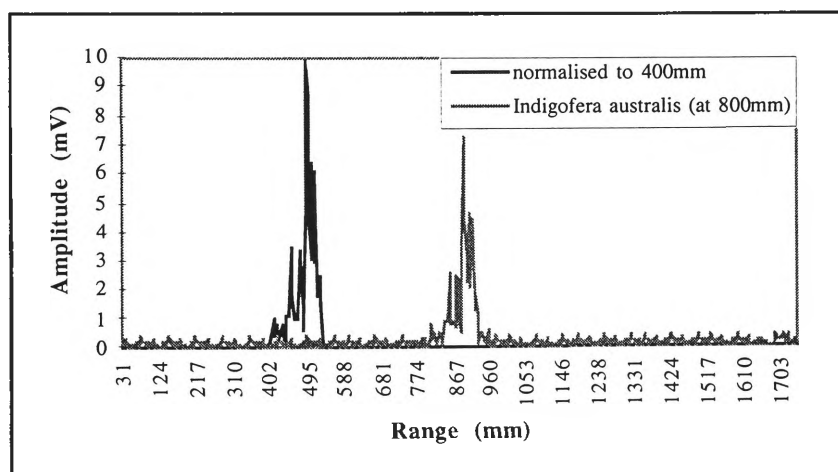


Figure 5.3 The acoustic density profile of *Indigofera australis* with the same profile referenced to a range of 400 mm

5.7 Summary

1. A large database of data was required so that valid experiments could be run.

2. Plants were mounted on the precision positioner and data were taken for all orientations of the plant (rotating from 0 to 360 degrees in 1 degree increments).
3. Detailed information about the plants was recorded to facilitate cross referencing.

6. Ensonifying the Plant from a Limited Aspect

6.1 Introduction

This chapter analyses the changes in the acoustic density profile from one orientation and its adjacent orientation (separated only by one degree). This provides a benchmark for comparison with other techniques. A technique is developed for tracking echoes between orientations which improves the comparison between adjacent orientations. The adjacent acoustic density profiles are compared by calculating the correlation between them.

This comparison between adjacent acoustic density profiles is useful for mobile robotics in a fixed environment with a known path when the robot is able to sense regularly. In this case, the plants would be used as landmarks and as the robot moves around the plant, the acoustic density profile would be correlated with a previous acoustic density profile and a confidence measure is assigned about whether it is sensing the same plant and hence, is on the correct path.

6.2 Background

When developing a system which will work in an environment such as an office or a laboratory, it is important that the classifying technique can cope with sensing the plants from different orientations. This is a difficult requirement when considering the sensing system used.

When considering two echoes of the plant from slightly different orientations, the information about the different sensing locations can be used to geometrically adjust for the change in orientation and track echoes with a change in the sensing location.

However, even with this echo tracking, the correlation of the acoustic density profiles from different plant orientations is not good. Generally, the variation between

two echoes increases with angle. A method of quantifying this variation is cross correlation. The method is developed in this chapter.

The correlations also provide information about the types of plants which are being analysed. For example, plants with a thick outer layer of foliage have acoustic density profiles which are more consistent through rotation, as all of the reflections come from a concentrated area at the outside of the plant. Those with a wide spread of leaves vary substantially between adjacent orientations but can often produce similar acoustic density profiles from opposing orientations (ie. opposite sides of the plant). In this chapter, the use of correlation to quantify this variation is developed.

6.3 Correlation calculation

As a plant is insonified from different orientations, the changes in the acoustic density profile are due to:

1. the change in orientation of the reflectors within the plant;
2. shadowing; and
3. the change in the relative difference between the transmitter / reflector / receiver for a given reflector orientation

The similarity of these signals from different orientations can be measured using correlation. The correlation (Pearson's product moment correlation) between two signals X and Y is the result of dividing the covariance between the signals by the product of the standard deviations and is given by Equation 6.1.

$$r_{x,y} = \left| \frac{Cov(X,Y)}{s_x \cdot s_y} \right| \quad 6.1$$

$$\text{where } Cov(X,Y) = \frac{1}{n} \sum_{i=1}^n (x_i - \bar{x}_x)(y_i - \bar{y}_y);$$

s = variance; and

n = number of samples.

Correlation is a number which lies between 0 and 1 and indicates the level of similarity between the signals. The correlation is close to 1 when the values in vector X are similar to those in the corresponding position in vector Y .

When correlating the raw data, it is possible to achieve a high correlation which is based on noise. This situation arises where the plant is sparsely foliated or where there are diffuse reflectors which provide signal return near the noise floor of the system (Figure 6.1).

This can be visualised by plotting 2 vectors against each other. Data which form a straight line which originates at the origin and projects to the top right hand corner of the graph is perfectly correlated [Spatz, 1993]. If all data points line on a straight line, correlation is “perfect” and is 1 for a line of positive slope and -1 for a line of negative slope.

Figure 6.1 shows 2 acoustic density profiles from *Polyscias australis* plotted with different scales. The line from the origin to the top right hand corner of the plot is the line along which perfectly correlated data lies. The circle in the bottom left hand corner of the figure with a logarithmic axis shows the points in the data which are noise, that is there are no detectable surfaces at the range which they represent. When this plot is displayed on a linear scale (as shown on the left of Figure 6.1), these points are closer to the line of perfect correlation than most of the actual data so the result is a correlation value which is higher than should be the case.

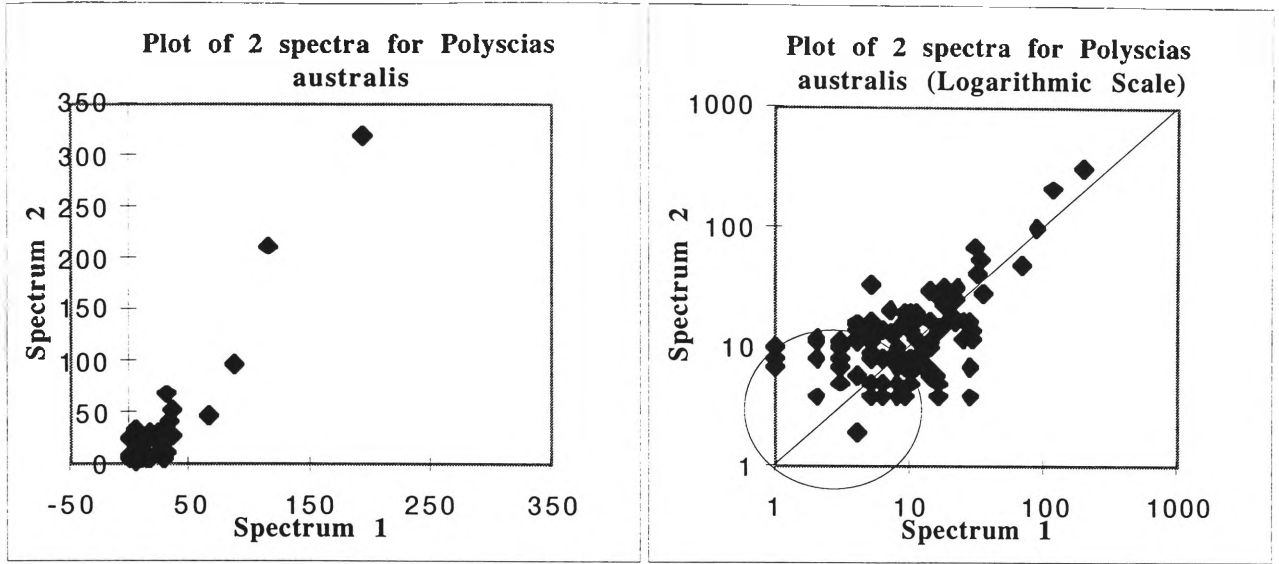


Figure 6.1 Plot of 2 acoustic density profiles of *Polyscias australis*

A more suitable measure of correlation is one which is adapted from the field of signal processing [Strum & Kirk, 1989] as it is a better measure of the similarity between the two signals. The correlation between two vectors is found by summing the products of the individual elements. It is then scaled to a range between 0 and 1 by dividing through by the vector with the greatest 'autocorrelation'. This is shown in Equation 6.2.

$$r_{x,y} = \frac{\sum_{i=1}^n x_i y_i}{Scale} \quad 6.2$$

$$\text{where } Scale = Maximum_of\left(\sum_{i=1}^n x_i x_i, \sum_{i=1}^n y_i y_i\right)$$

This correlation value is the sum of the products and will bias the result towards signal rather than noise.

As a plant is rotated, the correlation is calculated to measure the similarity between two signals. One approach is to select a reference orientation and compare the signals from other orientations to it. A different approach is to consider the reference point as the previous orientation of the plant $a_{current-1}$ in which case the acoustic density profiles are relatively stable through small rotations and the correlations are relatively high. The second technique is investigated in this chapter, and the first in the next chapter.

6.4 Correlation between returns at adjacent orientations - Local Correlation

Two acoustic density profiles of an *Acacia binervata* taken at adjacent orientations are shown in Figure 6.2. The acoustic density profiles are visually similar and the correlation between these 2 records is accordingly high, calculated as 0.94 using Equation 6.2.

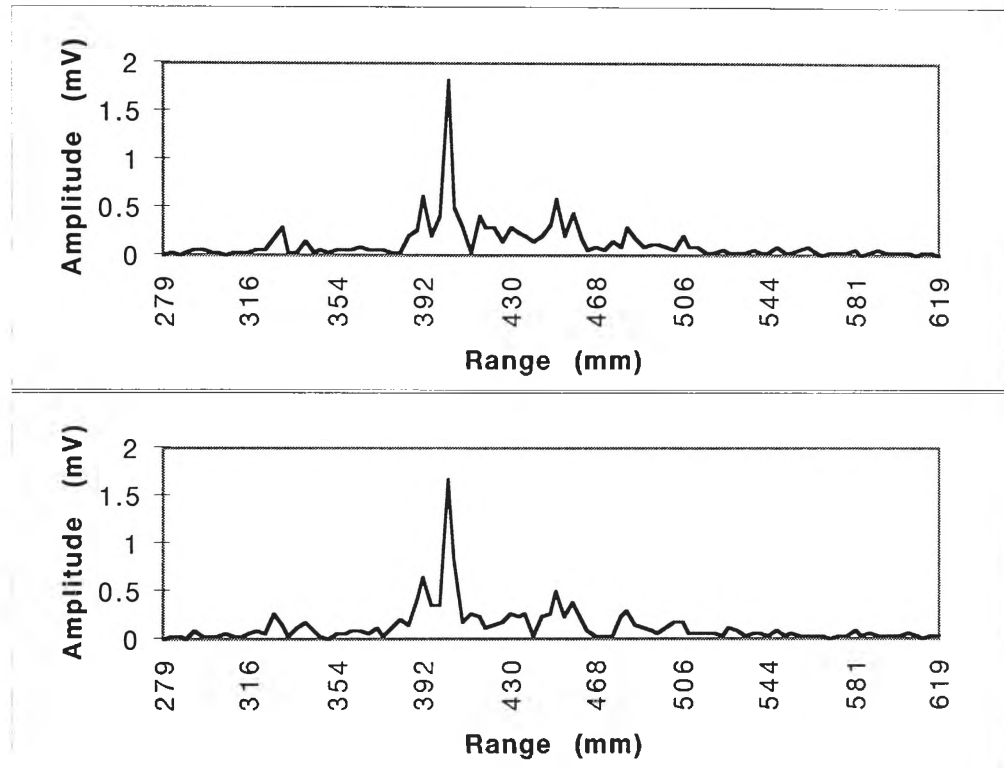


Figure 6.2 The acoustic density profiles of adjacent orientations of *Acacia binervata* ($r_{x,y} = 0.94$)

Stepping through the entire file and calculating the correlation between 360 adjacent records for this plant gives an average correlation coefficient of 0.81, with a maximum of 0.98, a minimum of 0.57 and a standard deviation of 0.07. Correlating records from adjacent orientations of the plant will be called local correlation in this thesis.

Local correlation for this plant is quite good as it exceeds the generally accepted threshold of positive correlation of 0.7. The fact that there are two adjacent orientations which are only correlated to a level of 0.57 indicates a significant change in the acoustic density profile.

The two records which show this low correlation coefficient are shown in Figure 6.3. The significant differences between these 2 records and also those shown in Figure 6.2 are in the narrowband component of the signal. The narrowband threshold is indicated in Figure 6.3 with dashed lines and is a consequence of the specular reflections (reflections directly from surfaces). The signals can be considered without the narrowband components by averaging these components with their adjacent broadband returns. This results in an improvement in the correlation which goes from 0.57 (with the narrowband) to 0.77 (without the narrowband). Similarly, the correlation between the top graphs from both figures is 0.33 and once the narrowband components are removed, the correlation becomes 0.58 which is a considerable improvement. Removing the narrowband can improve the correlation but it contains important information about the characteristics of the surfaces so it is not practical to remove this component. It does illustrate however, that the correlation can be affected considerably by the presence of a small number of narrowband components in the signal.

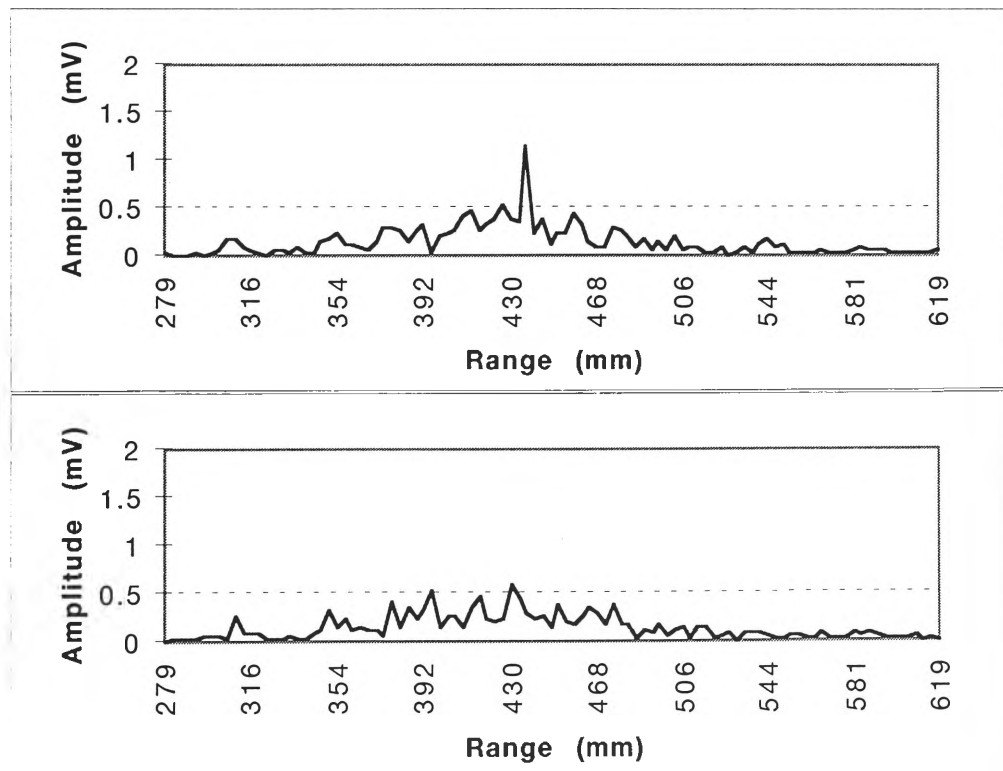


Figure 6.3 The acoustic density profiles of adjacent orientations for *Acacia binervata* ($\rho_{x,y} = 0.57$)

The average correlation between adjacent orientations was calculated for each plant in the database of 100 plants and the values are shown in Table 6.1 in order of decreasing average correlation. The average of the correlations is 0.80, with a maximum average of 0.9 and a minimum average of 0.74. This shows that there is a considerable range of these correlations. The local correlation with respect to rotation is graphed for eight plants in Figure 6.4 (highlighted in Table 6.1).

The plants with the highest correlations are closest to the top of the table and are those with very few leaves. These plants are the ones which either don't have a narrowband component of their signal (the plants with small leaves), or have only a few leaves in the entire revolution which have a narrowband component (that is, the plants with 1 or 2 large leaves, for example, the palms).

The plants with the lowest local correlations are those which have a large number of narrow band specular reflectors where the leaf approximates a flat surface. This is because the set of specular reflectors change in the acoustic density profile on subsequent orientations, causing the signal to change significantly from one orientation to the next. The positions of the specular reflectors also change slightly in the acoustic density profile as their absolute range changes through rotation which results in a lower correlation.

Table 6.1 Local Correlation (average and standard deviation) ordered by correlation value

Plant Name	Avg	Std			
<i>Carpentaria acuminata</i>	0.90	0.06	<i>Guioa semiglauca</i>	0.80	0.10
<i>Melaleuca styphelioides</i>	0.89	0.07	<i>Tabebula chrystricha</i>	0.80	0.09
<i>Crinum mauritianum</i>	0.88	0.08	<i>Correa alba</i>	0.80	0.07
<i>Crinum pedunculatum</i>	0.87	0.08	<i>Szygium paniculatum</i>	0.80	0.08
<i>Livistona sp 'Carnarvon'</i>	0.86	0.09	<i>Agapanthus praecox</i>	0.80	0.10
<i>Acacia cultriformis</i>	0.85	0.09	<i>Leptospermum morrisonii</i>	0.80	0.08
<i>Agapanthus praecox dwarf</i>	0.85	0.08	<i>Rhopalostylis baneri</i>	0.80	0.09
<i>Archontophoenix cunninghamiana</i>	0.85	0.09	<i>Diploglottis campbelli</i>	0.80	0.08
<i>Polyscias australiana</i>	0.85	0.09	<i>Sarcotoechia heterophylla</i>	0.80	0.07
<i>Banksia ericifolia</i>	0.85	0.08	<i>Solanum brownii</i>	0.80	0.09
<i>Goodia lotifolia</i>	0.84	0.08	<i>Rhododendron bryophyllum</i>	0.79	0.08
<i>Melaleuca quinquenervia</i>	0.83	0.07	<i>Grevillea marmalade</i>	0.79	0.09
<i>Stenocarpus sinuatus</i>	0.83	0.10	<i>Dodonaea triquetra</i>	0.79	0.09
<i>Melaleuca erubescens</i>	0.83	0.08	<i>Cryptocarya williwilliana</i>	0.79	0.08
<i>Tristaniopsis collina</i>	0.83	0.08	<i>Polyscias murrayi</i>	0.79	0.07
<i>Doryanthes palmeri</i>	0.83	0.11	<i>Acacia longifolia</i>	0.79	0.10
<i>Streblis brunonianus</i>	0.83	0.10	<i>Melaleuca decora</i>	0.79	0.09
<i>Cinnamom oliveri</i>	0.83	0.09	<i>Diploglottis australis</i>	0.79	0.08
<i>Laccospadix australasica</i>	0.83	0.09	<i>Eucalyptus leucoxylon</i>	0.79	0.08
<i>Microcitrus australis</i>	0.83	0.07	<i>Acacia podalyrifolia</i>	0.79	0.10
<i>Cryptocarya bidwilli</i>	0.83	0.08	<i>Banksia integrifolia</i>	0.79	0.09
<i>Cupaniopsis anacardioides</i>	0.82	0.08	<i>Ficus rubiginosa</i>	0.79	0.09
<i>Sarcomelicope simplifolia</i>	0.82	0.09	<i>Pittosporum crassifolium</i>	0.79	0.07
<i>Eucalyptus maculata</i>	0.82	0.09	<i>Acacia mearnsii</i>	0.79	0.08
<i>Eucalyptus botryoides</i>	0.82	0.08	<i>Casuarina glauca</i>	0.79	0.08
<i>Rhododendron clorinda</i>	0.82	0.07	<i>Szygium leuhmanni</i>	0.79	0.08
<i>Pittosporum revolutum</i>	0.82	0.08	<i>Grevillea baileyana</i>	0.78	0.09
<i>Polyscias elegans</i>	0.82	0.08	<i>Pittosporum james</i>	0.78	0.08
<i>Pittosporum undulatum</i>	0.82	0.08	<i>Pittosporum rhombifolium</i>	0.78	0.09
<i>Westringa fruticosa</i>	0.82	0.08	<i>Howea forsteriana</i>	0.78	0.08
<i>Omalanthus populifolius</i>	0.82	0.08	<i>Acrornychia laevis</i>	0.78	0.07
<i>Citriobatus paucifloris</i>	0.82	0.08	<i>Rhopalostylis sapida</i>	0.78	0.09
<i>Grevillea hilliana</i>	0.82	0.11	<i>Ficus obliqua</i>	0.78	0.09
<i>Litsea reticulata</i>	0.82	0.09	<i>Solanum vescum</i>	0.78	0.09
<i>Azalea alba magnifica</i>	0.82	0.09	<i>Casuarina torulosa</i>	0.78	0.10
<i>Cordyline australis</i>	0.81	0.11	<i>Indigofera australis</i>	0.77	0.10
<i>Acacia binervata</i>	0.81	0.07	<i>Acacia irrorata</i>	0.77	0.08
<i>Endiandra introrsa</i>	0.81	0.08	<i>Acacia stricta</i>	0.77	0.11
<i>Cryptocarya laevigatum</i>	0.81	0.08	<i>Leptospermum petersonii</i>	0.77	0.07
<i>Azalea cultivar splenda</i>	0.81	0.07	<i>Phyllanthus albiflorus</i>	0.76	0.08
<i>Cupaniopsis parvifolia</i>	0.81	0.07	<i>Solanum laciniatum</i>	0.76	0.10
<i>Alyxia ruscifolia</i>	0.81	0.09	<i>Leptospermum laevigatum</i>	0.76	0.07
<i>Endiandra pubens</i>	0.81	0.06	<i>Solanum aviculare</i>	0.76	0.08
<i>Hymenosporum flavum</i>	0.81	0.10	<i>Radermacheria fenecis</i>	0.76	0.08
<i>Hakea salicifolia</i>	0.81	0.08	<i>Ziera collina</i>	0.76	0.07
<i>Acacia melanoxylon</i>	0.80	0.09	<i>Acacia falcata</i>	0.76	0.13
<i>Casuarina stricta</i>	0.80	0.09	<i>Dodonaea viscosa</i>	0.76	0.08
<i>Ayrtera distylis</i>	0.80	0.09	<i>Licuala ramsayi</i>	0.75	0.08
<i>Eriostemon myoporoides</i>	0.80	0.10	<i>Jacaranda mimosifolia</i>	0.75	0.08
<i>Mishocarpus australis</i>	0.80	0.09	<i>Acacia howittii</i>	0.74	0.08

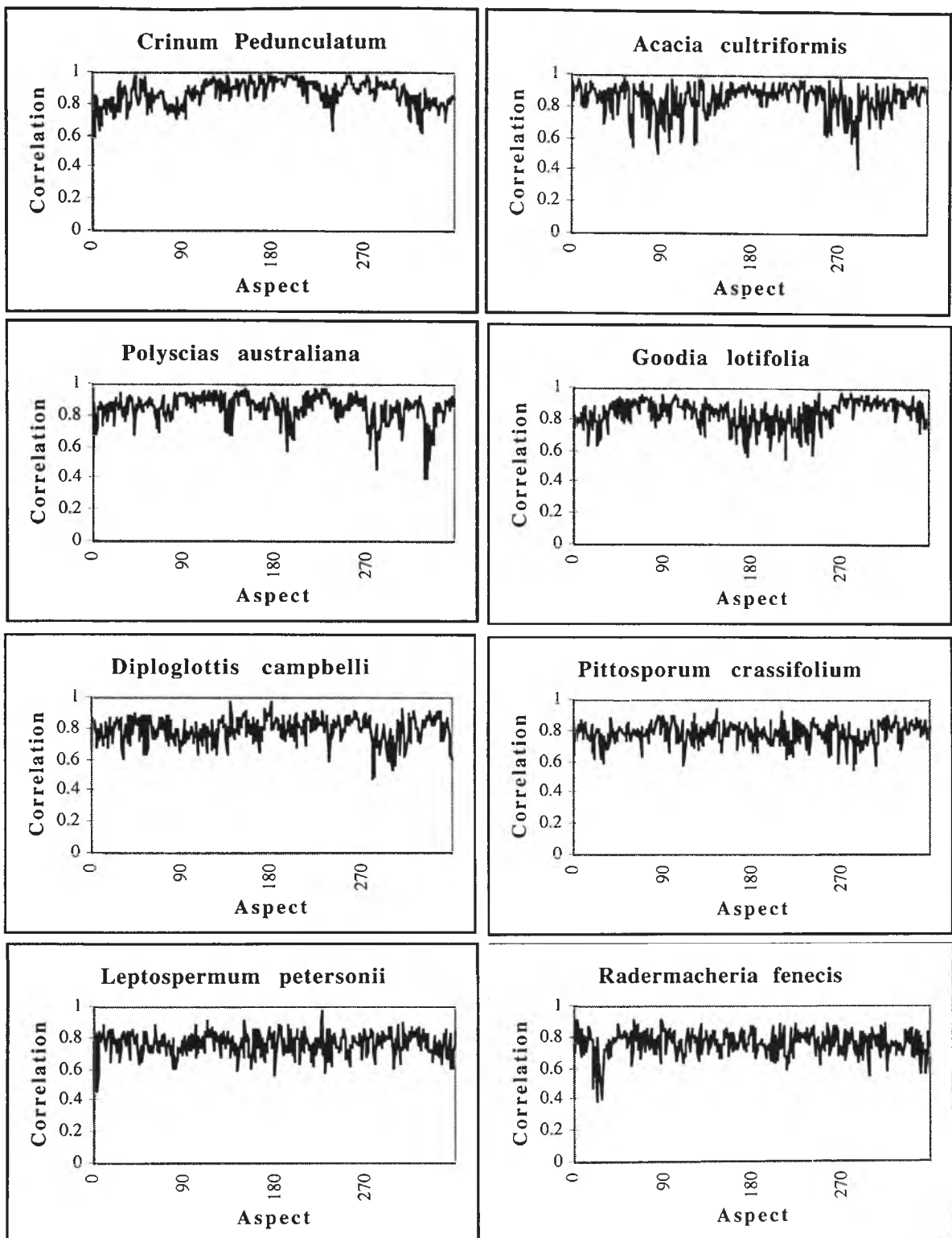


Figure 6.4 Local correlation by angle for eight selected plants

Figure 6.4 shows the local correlation as the plant is rotated through an entire revolution for eight selected plants. The examples graphed were chosen because of their basic physical structure (Figure 6.5) and are also spaced throughout the range from high correlation (*Crinum pedunculatum*) to low correlation (*Radermacheria fenecis*) as highlighted in Table 6.1. The graphs show how much the raw acoustic density profile

changes in respect to the previous orientation as analysis proceeds around the plant. A low value for the correlation indicates a significant change between one orientation and the next as the plant is rotated. A sequence of low correlations indicates that the acoustic density profile is continuing to change substantially with subsequent orientations.

The graphs show that the data is quite well correlated for a high proportion of the orientations. There are however, some groups of adjacent orientations with low correlations. This is most significant in the correlation graph of *Radermacheria fenecis*. There is a group of 15 orientations where the acoustic density profile is continuing to change significantly for each orientation (these orientations are between 18 and 32 degrees from the point where data collection commenced). This is a result of a branch which is protruding out toward the sensor. The branch is going out of the field of audition of the sensor and as the plant is rotated, echoes from less and less of that particular branch are received.

This branch information may be used to our advantage in a practical system where particular plants may be characterised by the fact that branches are protruding.

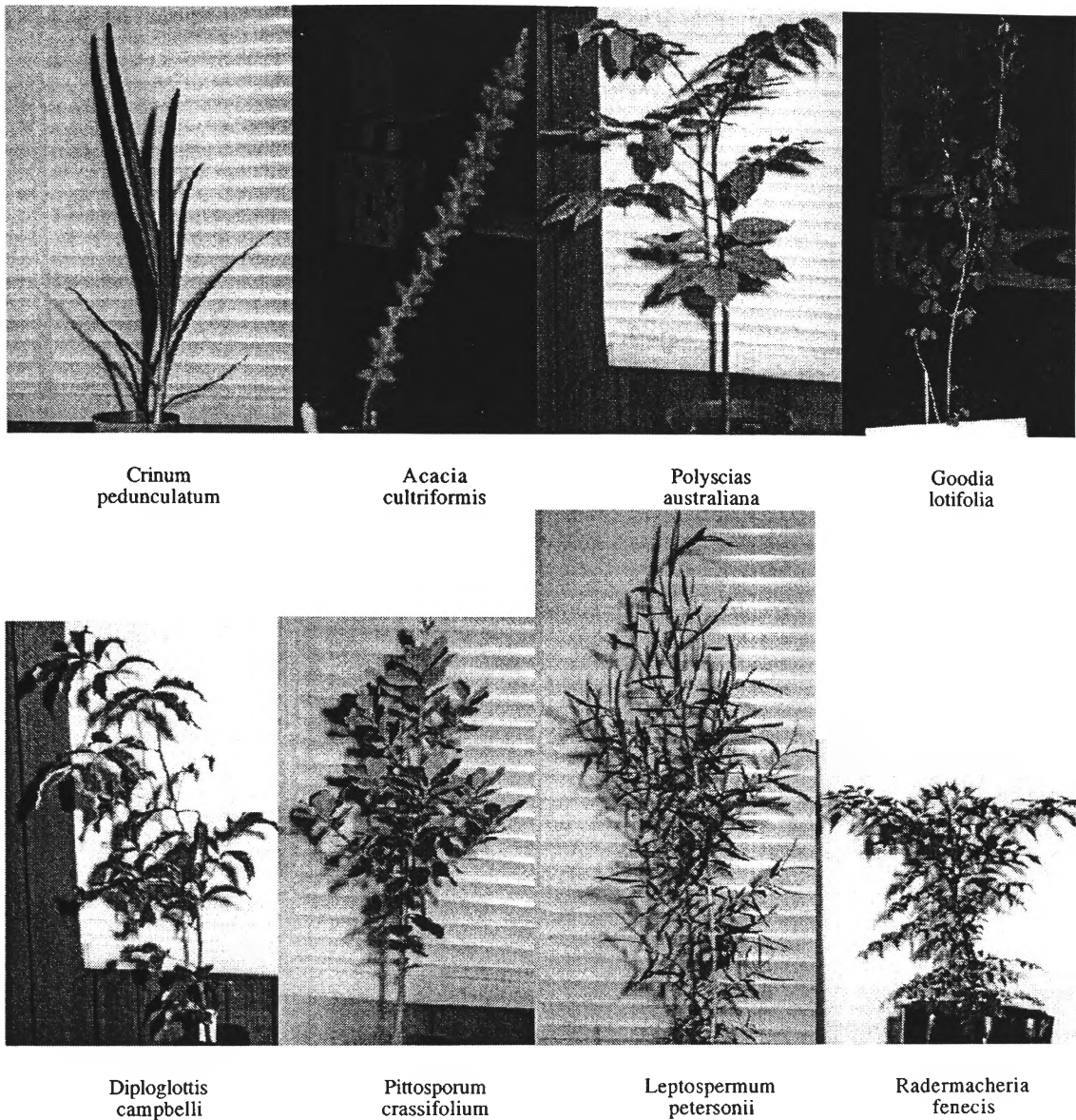


Figure 6.5 Images of eight plants

In summary, most of the plants are well correlated in terms of local correlation. There are groups of adjacent orientations however, where the acoustic density profile changes significantly from one orientation to the next as a sudden change in foliage structure is present - this however, is in contrast to the rest of the orientations where there are only small changes from one orientation to the next.

The results show that plants which have smaller, sparse foliage are more correlated through rotation for single steps.

6.5 Echo tracking

When adjacent acoustic density profiles are being analysed, two slices of the plant from different orientations are considered. When the change in orientation is small, the

geometric structure of the system can be used to track echoes between the acoustic density profiles. In this section, a method of echo tracking is developed and its effect on local correlation is evaluated.

For example, if there is a strong reflection from a leaf from an orientation but at the next orientation, the echo is no longer present at the same range, then there a high probability that the echo is in a nearby range cell (a different FFT line) due to a change in distance to that particular leaf. Note, leaves are not flat so may return acoustic energy to the receiver across a range of different orientations. The configuration can be analysed geometrically and the possible positions of that echo calculated. Echoes can then be matched across adjacent acoustic density profiles.

Consider Figure 6.6, which is a view of the sensing geometry from above. The axis of rotation of the plant is at distance R from sensing point P_1 . Acoustic energy is transmitted with beam angle θ and a surface s is detected at range r . The plant is then rotated by angle β and the sensor is now at sensing point P_2 . The echo tracking issue is to determine the possible range at which surface s could appear (if at all) from point P_2 ?

When the initial beam is transmitted from P_1 , s is at range r but can be anywhere along the arc a , so when the sensor is moved to point P_2 , the surface will be somewhere between r_{min} and r_{max} from point P_2 . If a surface is detected within that range then there is a high probability that it is an echo from the same surface. This means that echoes can be matched between one reading and the next by correcting for the difference in position. The distance between the two sensing points is given by :

$$d^2 = R^2 + R^2 - 2RR\cos\beta \quad (\text{from the cos rule})$$

$$d = \sqrt{2R^2(1 - \cos\beta)} \quad 6.3$$

We can then calculate the length of r_{min} using the Cosine rule (see, for example, Thomas [1962]) :

$$r_{\min}^2 = d^2 + r^2 - 2dr\cos\alpha \quad 6.4$$

where $\alpha = \gamma - (\frac{\theta}{2})$ (from simple geometry); and

where $\gamma = (\frac{180 - \beta}{2})$ (from simple geometry).

now, Equation 6.4 can be manipulated further to become :

$$r_{\min} = \sqrt{2R^2(1 - \cos 1^\circ) + r^2 - 2\sqrt{2R^2(1 - \cos 1^\circ)}r\cos(\frac{180 - \beta}{2} - \frac{\theta}{2})} \quad 6.5$$

Similarly, r_{\max} is given by :

$$r_{\max} = \sqrt{2R^2(1 - \cos 1^\circ) + r^2 - 2\sqrt{2R^2(1 - \cos 1^\circ)}r\cos(\frac{180 - \beta}{2} + \frac{\theta}{2})} \quad 6.6$$

where all angles are given in degrees.

The entire beam angle of the sensor (θ) is 54.17° (note that θ has been used to refer to the entire beam angle of the sensor from the first side lobe on one side to the first one on the other side, and not just the angle from the central axis to the side lobe). For the database of data described in chapter 6, the central axis of each plant was at a range(R) of 0.442 metres.

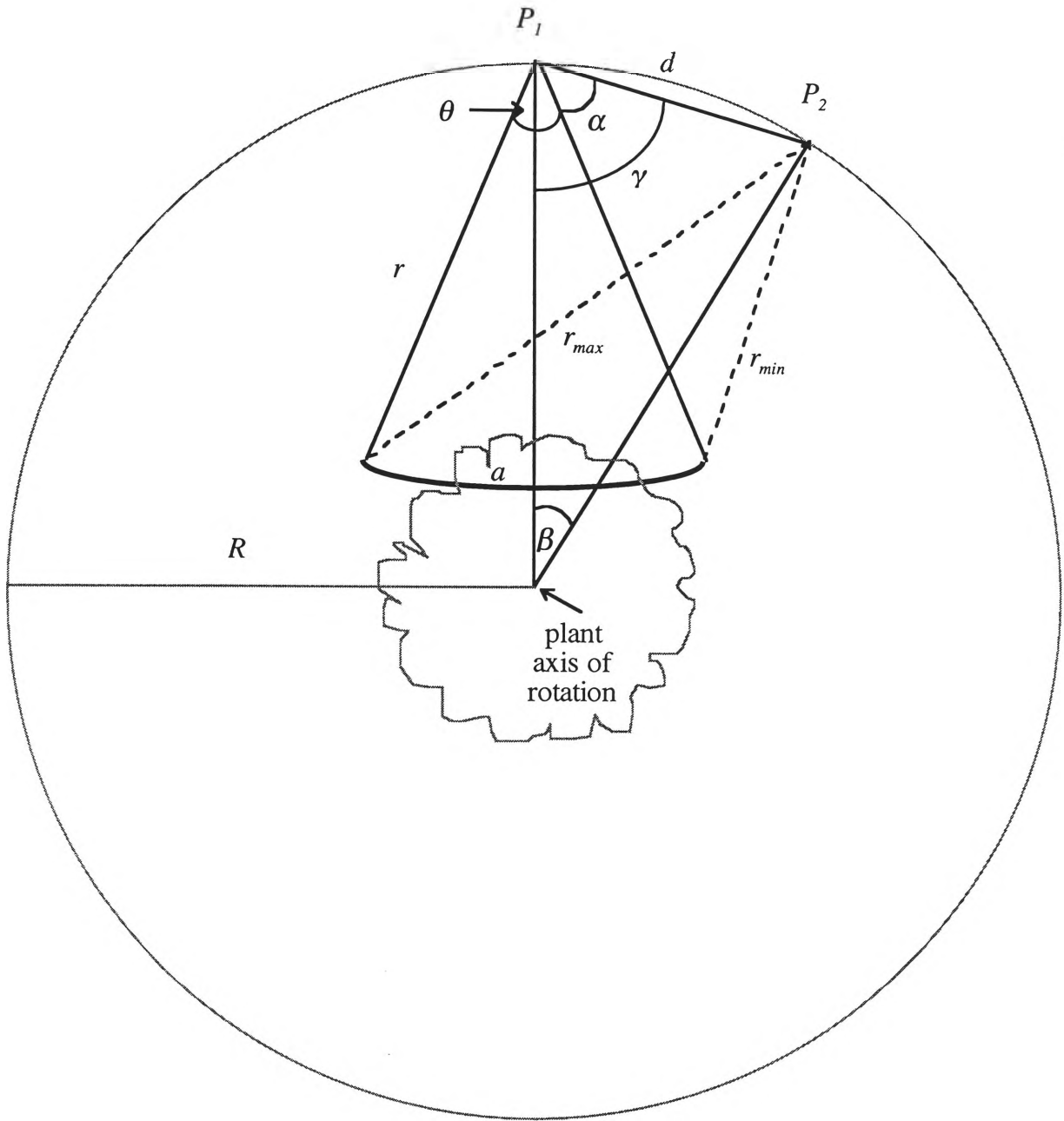


Figure 6.6 The geometry of the system for tracking echoes through rotation

In the case of CTFM ultrasonics, there is not a single range value but an acoustic density profile which indicates the range to all of the visible surfaces. At point P_1 , the scene is insonified and the ranges to all of the surfaces is stored. Once the scene is insonified from point P_2 , we have a second range profile from a slightly different orientation. The acoustic density profiles can then be matched and echoes from the same surface moved so that they line up with the corresponding element in the other acoustic density profile. For each of the cells in P_2 , a group of cells from P_1 can be associated with

it based on Equation 6.5 and Equation 6.6. These new “corrected” acoustic density profiles can be correlated to develop a more accurate correlation picture. This echo tracking could also be used in the situation where the leaves of the plants are moving.

An example of this range tracking is shown in Example 6.1.

$R = 1000$ mm (range to the plant axis)
 $r = 450$ mm (range to the surface s when insonified from P_1)

the plant is then insonified from point P_2

$r_{min} = 442.2$ mm (the minimum distance to surface s using Equation 6.5)
 $r_{max} = 458.1$ mm (the maximum distance to surface s using Equation 6.6)
 this range difference of 15.9 millimetres corresponds to a range of approximately 5 FFT lines (FFT range resolution is 3.44 mm).
 Consider the fragments of acoustic density profiles below insonified from point P_1 :

cell corresponding to $r = 450$ mm

↓

0.0	0.1	0.2	10	0.1	0.2	0.8
-----	-----	-----	----	-----	-----	-----

insonified from point P_2 :

cell corresponding to $r = 450$ mm

↓

0.0	9	0.2	0.1	0.1	0.2	0.8
-----	---	-----	-----	-----	-----	-----

In the acoustic density profile from point P_1 , there is a surface which returns an echo of 10 mV in the cell corresponding to a range of 450 mm. In the acoustic density profile generated at point P_2 , there is an echo of similar amplitude which is closer to the sensor but within the window of 5 FFT cells so it is likely to be the same surface. We can adjust the new the acoustic density profile so that the echoes correspond to the first acoustic density profile and hence correlate better with the original signal. The second the acoustic density profile becomes:

cell corresponding to $r = 450$ mm

↓

0.0	0.1	0.2	9	0.1	0.2	0.8
-----	-----	-----	---	-----	-----	-----

Example 6.1 Echo tracking with orientation change

The calculation of the possible range is implemented as a C function and is shown in Appendix B. The pseudo code is shown below :

CALCULATE ECHO RANGE POSSIBILITY

This function calculates the threshold for determining the range over which a surface could be visible from one orientation to the next. The object is rotated around its axis (or the sensing point is moved around the object). This function is specific to the following two situations :

1. In the case of the object being rotated. The range to the axis of rotation is fixed and the object is moved through a fixed angle OR
2. In the case of the sensing point being moved. The range to the axis of the object is held constant and moved through some angle.

The acoustic density profile is captured at a set orientation. The object is sensed using a sensor with a fixed beam angle (passed to this

Table 6.2 Range possibilities for different surface ranges for plant axis = 0.442 metres, orientation change = 1 degree and beam angle = 54.17 degrees

Surface Range	Possible ranges (mm)	Possible ranges (FFT lines)	0.377400	0.702207	2.065315	0.496400	0.702230	2.065381
			0.380800	0.702208	2.065319	0.499800	0.702230	2.065382
			0.384200	0.702209	2.065322	0.503200	0.702230	2.065383
			0.387600	0.702210	2.065325	0.506600	0.702231	2.065384
0.272000	0.702143	2.065126	0.391000	0.702211	2.065327	0.510000	0.702231	2.065385
0.275400	0.702146	2.065137	0.394400	0.702212	2.065330	0.513400	0.702231	2.065386
0.278800	0.702150	2.065147	0.397800	0.702213	2.065333	0.516800	0.702231	2.065387
0.282200	0.702153	2.065156	0.401200	0.702214	2.065335	0.520200	0.702232	2.065387
0.285600	0.702156	2.065166	0.404600	0.702215	2.065338	0.523600	0.702232	2.065388
0.289000	0.702159	2.065175	0.408000	0.702216	2.065340	0.527000	0.702232	2.065389
0.292400	0.702162	2.065183	0.411400	0.702216	2.065343	0.530400	0.702233	2.065390
0.295800	0.702165	2.065191	0.414800	0.702217	2.065345	0.533800	0.702233	2.065390
0.299200	0.702168	2.065199	0.418200	0.702218	2.065347	0.537200	0.702233	2.065391
0.302600	0.702170	2.065207	0.421600	0.702219	2.065349	0.540600	0.702233	2.065392
0.306000	0.702173	2.065214	0.425000	0.702219	2.065351	0.544000	0.702233	2.065392
0.309400	0.702175	2.065221	0.428400	0.702220	2.065353	0.547400	0.702234	2.065393
0.312800	0.702177	2.065227	0.431800	0.702221	2.065355	0.550800	0.702234	2.065394
0.316200	0.702179	2.065234	0.435200	0.702221	2.065357	0.554200	0.702234	2.065394
0.319600	0.702182	2.065240	0.438600	0.702222	2.065359	0.557600	0.702234	2.065395
0.323000	0.702184	2.065246	0.442000	0.702222	2.065360	0.561000	0.702234	2.065395
0.326400	0.702185	2.065251	0.445400	0.702223	2.065362	0.564400	0.702235	2.065396
0.329800	0.702187	2.065257	0.448800	0.702224	2.065363	0.567800	0.702235	2.065396
0.333200	0.702189	2.065262	0.452200	0.702224	2.065365	0.571200	0.702235	2.065397
0.336600	0.702191	2.065267	0.455600	0.702225	2.065367	0.574600	0.702235	2.065397
0.340000	0.702193	2.065272	0.459000	0.702225	2.065368	0.578000	0.702235	2.065398
0.343400	0.702194	2.065277	0.462400	0.702226	2.065369	0.581400	0.702235	2.065398
0.346800	0.702196	2.065281	0.465800	0.702226	2.065371	0.584800	0.702236	2.065399
0.350200	0.702197	2.065286	0.469200	0.702226	2.065372	0.588200	0.702236	2.065399
0.353600	0.702199	2.065290	0.472600	0.702227	2.065373	0.591600	0.702236	2.065400
0.357000	0.702200	2.065294	0.476000	0.702227	2.065375	0.595000	0.702236	2.065400
0.360400	0.702201	2.065298	0.479400	0.702228	2.065376	0.598400	0.702236	2.065400
0.363800	0.702203	2.065302	0.482800	0.702228	2.065377	0.601800	0.702236	2.065401
0.367200	0.702204	2.065305	0.486200	0.702229	2.065378	0.605200	0.702236	2.065401
0.370600	0.702205	2.065309	0.489600	0.702229	2.065379	0.608600	0.702236	2.065401
0.374000	0.702206	2.065312	0.493000	0.702229	2.065380			

The aim of the echo tracking algorithm is to align the corresponding echoes from the two sensing points P_1 and P_2 . They are passed as arrays to the echo tracking algorithm implemented below. The echoes from sensing point P_2 (array2) are aligned so that they match the corresponding echoes received from sensing point P_1 (array1). These two sensing arrays can then be correlated. The pseudo code for this function is shown below and the C code for this function is in Appendix A.

ECHO TRACKING

This function tracks signal returns between one orientation and the next by adjusting for the geometry of the system. The sensor is in a fixed position with the plant at a certain distance. The acoustic density profile is captured before the plant is rotated by a fixed angle. Once the plant is at the new orientation, the surfaces which produced reflections at the previous orientations may still be present in the acoustic density profile but offset by 1 or a number of range cells. This amount by which they are offset can be passed as a fixed value (movement threshold) or can be calculated using CALCULATE ECHO RANGE POSSIBILITY.

Parameters :

base_range	the range to the first range cell in the arrays
axis_range	the range to the axis of the plant
orientation_change	than angle in degrees through which the plant has been rotated between array1 and array2
beam_angle	the beam angle of the sensor
fft_range_resolution	the resolution of an individual range cell
*array1	the data from the first orientation.
*array2	the data from the second orientation.

```

        array_length      the length of the arrays of data.
        movement_threshold the amount of range cells which the
                           features can move or 0 in which
                           case function Calc_movement_threshold
                           will be called to calculate the
                           threshold.

BEGIN

    Create a new array of indexes into array1 which indexes array1 in descending
    order (descending_indexes).
    WHILE not all elements of descending_indexes array processed
    BEGIN
        IF movement_threshold = 0 THEN
            possible_range = CALCULATE ECHO RANGE POSSIBILITY
            movement_threshold = (possible_range / range cell resolution) / 2
        END
        element =
        Find the position of the maximum item in array2 which:
            1. is within movement_threshold array elements of the
               position of the element in array1; and
            2. hasn't already been moved.
        Swap the element in array2 at the position corresponding to that in
        array1 with the element at array2 which is the maximum.
    END
END

```

The average correlation for adjacent orientations was calculated for the entire database of 100 plants with echo tracking and is shown in Table 6.3. The average of all of the average correlations is 0.84 with a maximum correlation of 0.91 and a minimum average of 0.79. The maximum correlation is only slightly up on correlating the raw data without echo tracking (0.91 cf 0.9) but the average is higher (0.84 cf 0.80) and the minimum is considerable higher (0.79 cf 0.74). The plants in the second half of the table are the ones which have been affected more by the echo tracking. This is due to the fact that these plants have many more surfaces returning acoustic energy so the correlation is affected much more by a slight change in the positioning of the echoes within the acoustic density profile.

It is also evident that *Acacia cultriformis* has dropped down the table as its average has not increased as much as the other plants around it. This is due to the nature of the specimen as even though it is compact with good reflective leaves, its central trunk has quite a lean (Figure 6.5). This means that not only are the echoes changing due to the change in leaves but the overall position of the plant is changing and this is outside the range calculated by the Calc_echo_range_possibility function.

Table 6.3 Correlations adjacent records WITH echo tracking (average and standard deviation)

<i>Carpentaria acuminata</i>	0.91	0.06	<i>Polyscias murrayi</i>	0.84	0.07
<i>Melaleuca styphelioides</i>	0.91	0.07	<i>Diploglottis australis</i>	0.84	0.07
<i>Crinum pedunculatum</i>	0.89	0.06	<i>Szygium paniculatum</i>	0.84	0.07
<i>Crinum mauritianum</i>	0.89	0.08	<i>Acacia melanoxylon</i>	0.84	0.08
<i>Agapanthus praecox dwarf</i>	0.88	0.06	<i>Grevillea marmalade</i>	0.84	0.08
<i>Livistona sp 'Carnarvon'</i>	0.88	0.08	<i>Agapanthus praecox</i>	0.84	0.09
<i>Polyscias australiana</i>	0.88	0.09	<i>Eucalyptus leucoxydon</i>	0.84	0.08
<i>Goodia lotifolia</i>	0.88	0.07	<i>Casuarina stricta</i>	0.84	0.09
<i>Pittosporum revolutum</i>	0.87	0.07	<i>Mishocarpus australis</i>	0.84	0.08
<i>Archontophoenix cunninghamiana</i>	0.87	0.09	<i>Acronychia laevis</i>	0.84	0.06
<i>Acacia cultriformis</i>	0.87	0.09	<i>Solanum brownii</i>	0.84	0.08
<i>Stenocarpus sinuatus</i>	0.87	0.09	<i>Leptospermum morrisonii</i>	0.84	0.08
<i>Banksia ericifolia</i>	0.87	0.08	<i>Szygium leuhmanni</i>	0.84	0.07
<i>Melaleuca quinquenervia</i>	0.87	0.06	<i>Banksia integrifolia</i>	0.84	0.08
<i>Eucalyptus maculata</i>	0.87	0.08	<i>Howea forsteriana</i>	0.84	0.07
<i>Eucalyptus botryoides</i>	0.87	0.07	<i>Hymenosporum flavum</i>	0.84	0.09
<i>Rhododendron clorinda</i>	0.87	0.07	<i>Dodonaea triquetra</i>	0.84	0.09
<i>Melaleuca erubescens</i>	0.86	0.07	<i>Melaleuca decora</i>	0.84	0.08
<i>Cinnamom oliveri</i>	0.86	0.08	<i>Rhopalostylis baneri</i>	0.84	0.08
<i>Tristania collina</i>	0.86	0.07	<i>Guioa semiglauc</i>	0.84	0.09
<i>Sarcomelicope simplifolia</i>	0.86	0.09	<i>Cryptocarya williwilliana</i>	0.84	0.08
<i>Microcitrus australis</i>	0.86	0.07	<i>Pittosporum james</i>	0.84	0.07
<i>Cupaniopsis anacardioides</i>	0.86	0.07	<i>Acacia mearnsii</i>	0.84	0.07
<i>Azalea cultivar splenda</i>	0.86	0.06	<i>Rhopalostylis sapida</i>	0.84	0.08
<i>Azalea alba magnifica</i>	0.86	0.08	<i>Ficus obliqua</i>	0.84	0.08
<i>Endiandra pubens</i>	0.86	0.06	<i>Casuarina glauca</i>	0.84	0.08
<i>Cryptocarya bidwilli</i>	0.86	0.08	<i>Eriostemon myoporoides</i>	0.84	0.09
<i>Streblis brunonianus</i>	0.86	0.09	<i>Grevillea baileyana</i>	0.83	0.08
<i>Citriobatus paucifloris</i>	0.86	0.07	<i>Leptospermum laevigatum</i>	0.83	0.06
<i>Polyscias elegans</i>	0.86	0.07	<i>Solanum aviculare</i>	0.83	0.07
<i>Acacia binervata</i>	0.86	0.06	<i>Acacia podalyrifolia</i>	0.83	0.09
<i>Laccospadix australasica</i>	0.86	0.08	<i>Acacia irrorata</i>	0.83	0.08
<i>Endiandra introrsa</i>	0.86	0.07	<i>Solanum vescum</i>	0.83	0.08
<i>Cryptocarya laevigatum</i>	0.86	0.07	<i>Pittosporum rhombifolium</i>	0.83	0.08
<i>Pittosporum undulatum</i>	0.85	0.07	<i>Ficus rubiginosa</i>	0.83	0.08
<i>Doryanthes palmeri</i>	0.85	0.10	<i>Leptospermum petersonii</i>	0.83	0.07
<i>Correa alba</i>	0.85	0.06	<i>Phyllanthus albiflorus</i>	0.83	0.08
<i>Hakea salicifolia</i>	0.85	0.07	<i>Acacia longifolia</i>	0.83	0.10
<i>Omalthus populifolius</i>	0.85	0.08	<i>Ziera collina</i>	0.83	0.07
<i>Litsea reticulata</i>	0.85	0.08	<i>Dodonaea viscosa</i>	0.83	0.07
<i>Sarcotoechia heterophylla</i>	0.85	0.06	<i>Indigofera australis</i>	0.82	0.09
<i>Westringa fruticosa</i>	0.85	0.08	<i>Radermacheria fenecis</i>	0.82	0.08
<i>Cupaniopsis parvifolia</i>	0.85	0.07	<i>Licuala ramsayi</i>	0.82	0.07
<i>Tabebuia chrystricha</i>	0.85	0.08	<i>Solanum laciniatum</i>	0.82	0.09
<i>Grevillea hilliana</i>	0.85	0.10	<i>Casuarina torulosa</i>	0.82	0.10
<i>Diploglottis campbelli</i>	0.85	0.07	<i>Jacaranda mimosifolia</i>	0.82	0.08
<i>Rhododendron bryophyllum</i>	0.85	0.07	<i>Acacia howittii</i>	0.82	0.08
<i>Ayrtera distylis</i>	0.85	0.08	<i>Acacia stricta</i>	0.81	0.11
<i>Alyxia ruscifolia</i>	0.85	0.08	<i>Acacia falcata</i>	0.79	0.12
<i>Pittosporum crassifolium</i>	0.85	0.06			
<i>Cordyline australis</i>	0.85	0.10			

Table 6.4 Comparison of signals from 8 individual plants with and without echo tracking

	raw signals		raw signals <u>with</u> echo tracking	
	average	standard deviation	average	standard deviation
<i>Crinum pedunculatum</i>	0.87	0.08	0.89	0.06
<i>Acacia cultriformis</i>	0.85	0.09	0.87	0.09
<i>Polyscias australiana</i>	0.85	0.09	0.88	0.09
<i>Goodia lotifolia</i>	0.84	0.08	0.88	0.07
<i>Diploglottis campbelli</i>	0.8	0.08	0.85	0.07
<i>Pittosporum crassifolium</i>	0.79	0.07	0.85	0.06
<i>Leptospermum petersonii</i>	0.77	0.07	0.83	0.07
<i>Radermacheria fenecis</i>	0.76	0.08	0.82	0.08

The average correlation of all of the selected plants is improved by using echo tracking. The comparison of the selected eight plants (Table 6.4) are consistent with the overall trend where the plants which have more reflective surfaces have their correlation improved more than those plants which have less reflective surfaces. In general, echo tracking improves both the average correlation and the standard deviation of the correlation. The graphs of correlation with angle for these plants are shown in Figure 6.7. In general, correlations are slightly higher than shown in Figure 6.4.

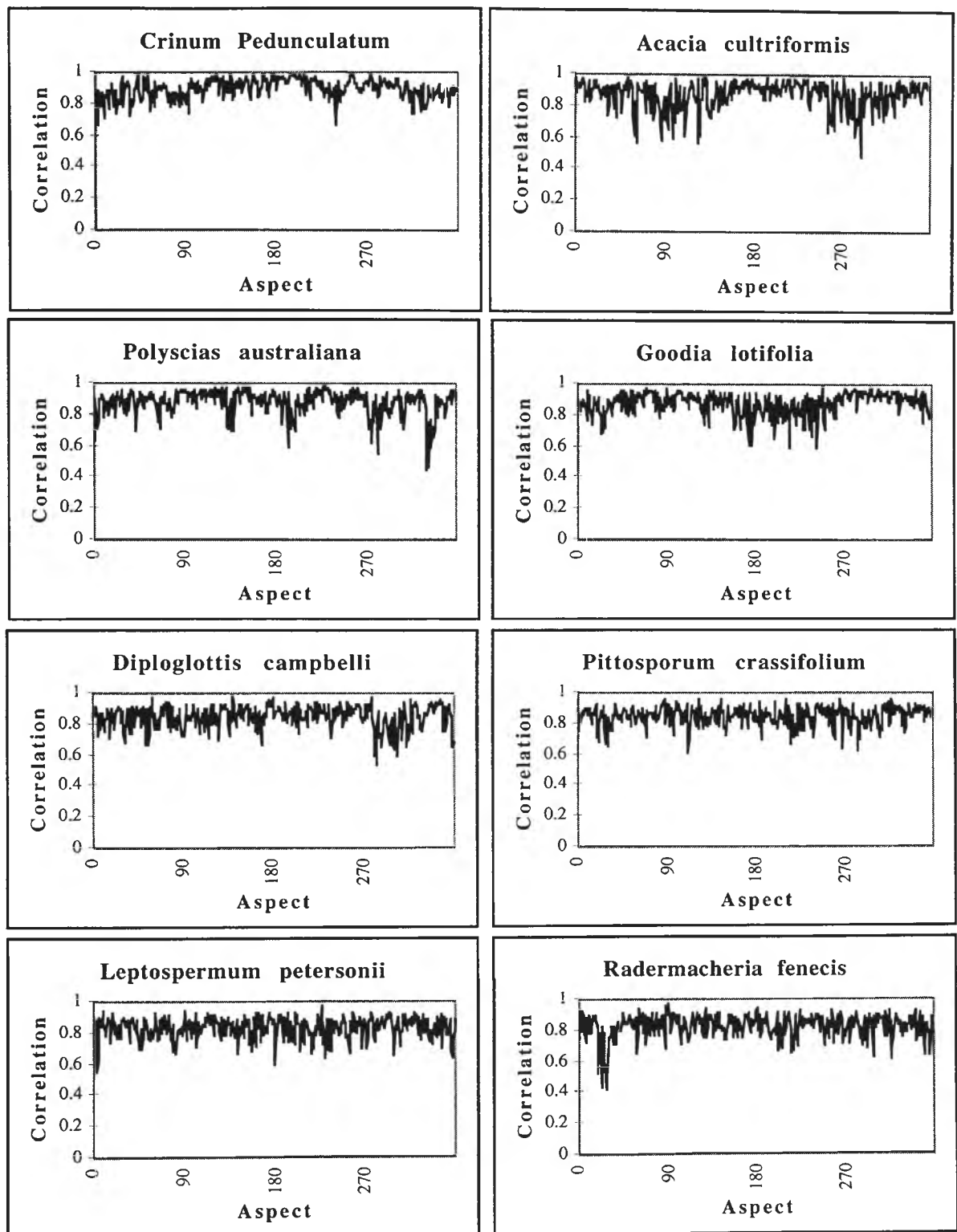


Figure 6.7 Correlation between adjacent orientations by angle for eight different plants WITH echo tracking

6.6 Conclusion

Correlation can provide information about how plants change locally with orientation. Local correlation gives us an indication of how the acoustic density profile changes with small changes in orientation and whether a plant is locally acoustically

symmetric (or consistent) but does not tell us whether the plant is globally acoustically symmetric. Consequently, a plant which displays high local symmetry is a very good landmark as the sensor may be a few degrees from the expected orientation and still get good correlation and hence recognition. Partial symmetry is acceptable for mobile robot navigation since the robot will only sense a sector of the plant (usually less than 180° of it).

Echo tracking also enhances the ability of the system to work in an outdoor environment or any environment which may cause some movement of the leaves. The algorithm which calculates the range over which the leaves may have moved could be configured for this situation by determining some kind of movement threshold. This would result in a significantly higher performance of the overall sensing system.

Local correlation provides information about the local consistency of the signal but provides no information of how well the acoustic density profile correlates with other orientations which may not be adjacent such as 90° around the plant or even the view from the other side of the plant (global correlation). This is considered in Chapter 7.

6.7 Summary

1. Correlation can be used to analyse the way that plants change through rotation.
2. Plants with more reflective surfaces produce echoes that are less consistent through local orientation change.
3. Echoes can be tracked between adjacent orientations to improve correlation
4. Local correlation provides no information about how the plant changes globally, that is between orientations that are not adjacent.

7. Ensonifying the plant from any aspect

7.1 Introduction

This Chapter expands the concepts developed in Chapter 6 where local correlation of the raw acoustic density profile was examined. In this chapter, global correlation is investigated. This provides information about the overall acoustic symmetry of the plant as global changes of similarity are examined.

When a mobile robot is sensing irregularly or is moving at high speed in a static, known environment, plants can be used as natural landmarks for localisation. In Chapter 6, echoes from plants over a small orientation change were correlated. Also, an algorithm was developed to track individual echoes over subsequent orientations with good results. In this chapter, it is shown that global correlation of the raw acoustic density profile is generally weak. The plants with a high number of reflective surfaces are worse than those with smaller reflective surfaces. This is however considerably improved by using features which characterise the acoustic density profile as a small number of calculated measures of the acoustic density profile, and this is outlined in Chapter 8.

7.2 Correlation between non-adjacent acoustic density profiles - Global Correlation

In the previous chapter, the case of correlating signals from adjacent orientations of the plant was considered (local correlation). In this section, the case of correlating signals which are from completely different orientations is considered. One orientation is selected as the reference, and all of the other orientations in the revolution can be correlated against that orientation. This will provide a measure of:

global symmetry;

partial symmetry; and
rate of change of symmetry.

Figure 7.1 shows the graphs of the correlation of the eight plants studied in Chapter 6 correlated against a reference point selected arbitrarily as an orientation of 256 degrees - the reference point is marked with a dashed line.

The x axis shows the orientation of the plant from 1 to 360 degrees (an entire revolution). All of the graphs have one thing in common - several of the records on each side of the reference point are highly correlated to it, but drop off significantly with angular rotation. This is in contrast to the local correlation in Chapter 6 where records were highly correlated throughout an entire revolution. This high correlation is due to the fact that the acoustic density profile changes gradually as the plant orientation is changed so the overall change is not observed. The global correlation measures provide more information about the way that the plant changes through rotation.

Each of the plants show slightly different properties through rotation and these properties are consistent with the physical properties of the plant. The graphs can be considered in combination with Figure 7.2 where orientation 100 was chosen randomly as the reference point. The change in correlation reveals information about the physical properties of the plants. For comparison, the raw acoustic density profiles are shown in Figure 7.3. An explanation of the shape of the graphs is provided below

7.2.1 Plant changes through rotation

In this section, the global correlations for each of the plants studied in Chapter 6 is analysed.

7.2.1.1 *Crinum pedunculatum*

Crinum pedunculatum has smooth leaves which are very long and thin with the tips oriented vertically. The cross section of the leaf is rounded evenly which means that the leaves will reflect at multiple orientations. In general, the leaves do not protrude horizontally from the central stem so they allow little opportunity for the acoustic energy to penetrate and reflect from other surfaces within the plant except at certain orientations.

The acoustic density profile does change through rotation due to the changing orientations of leaves and leaf edges which cause different amounts of acoustic energy to be reflected. There are three primary leaves, two of which are opposite each other with the third leaf being orthogonal. This means that for any particular signal return, there is a good chance that there will be two other signal returns from different orientation which are very similar as they will be insonifying similar foliage. This is shown in the figure with several orientations being highly correlated to the reference even though they are acoustic density profiles from completely different orientations, for example, orientations 180 and 256 are highly correlated even though they are 76° apart.

7.2.1.2 *Acacia cultriformis*

Acacia cultriformis is a very compact plant with flat leaves which form a regular pattern around the central trunk. Similarly to *Crinum pedunculatum*, once the orientation changes by a small amount, the correlation between the signals is very low. The flat surface of the leaf is orthogonal to the sensor which results in a larger signal received at the sensor. In the case of the orientation 100 being used as a reference, a group of orientations around 330 degrees from the initial orientation, are shown to be similar to that of the reference. Both of the peaks are relatively symmetric which mean that the returns are becoming more similar to the reference up to a certain point. after which they slowly become more dissimilar. Most of the other orientations within the plant produce very different signals so the correlation is low. This can be partially attributed to the lean on the specimen tested since the correlation only considers the raw acoustic density profile.

7.2.1.3 *Polyscias australiana*

Polyscias australiana has evenly spread medium size leaves which are oriented in the horizontal plane to catch light compared to acoustic energy projected from the side of the plant. This means that there is often very little surface area for the acoustic energy to return from, but those which do reflect acoustic energy are distributed throughout the entire plant. Both of the reference orientations have the correlation reduced significantly as

the plant is rotated. There are also other orientations which are highly correlated with the set reference point which are on the opposite side of the plant.

7.2.1.4 Goodia lotifolia

Goodia lotifolia has very small leaves which are spread from the central trunk on small stems. As you move away from the reference points, the correlation becomes gradually smaller. There are no other orientations which are highly correlated with the chosen reference points but the correlation does not drop down as low as the first plants.

7.2.1.5 Diploglottis campbelli

Diploglottis campbelli is more of a bushy plant with many leaves distributed throughout. The acoustic density profile of the plant in Figure 7.3 shows that signals are received from many of the surfaces within the plant from range differences of over 200 millimetres. The correlation charts show that the correlation reduces relatively consistently with the distance from the reference orientation.

7.2.1.6 Pittosporum crassifolium

Pittosporum crassifolium is a plant with very dense foliage so acoustic energy will be returned primarily from the front and the sides of the plant. The foliage is relatively consistent as the plant is rotated and this is reflected by the correlation graphs. Beside the notable peak at the point where the reference is correlated with itself, the graphs are relatively consistent with the correlation hovering around the 0.5 mark for the entire revolution. The other point of note is the large dip in correlations at orientation 144. This is a result of an area of inconsistency in the foliage.

7.2.1.7 Leptospermum petersonii

Leptospermum petersonii is a plant with many small leaves spread throughout the entire volume of the plant. More of the acoustic energy penetrates the outer layer of foliage than does with *Pittosporum crassifolium* and the resulting correlations are correspondingly different. There is a more distinct peak in the correlations which means that the records close to the reference record are more similar to it and the correlations drop away further through rotations of larger angles

7.2.1.8 *Radermacheria fenecis*

Radermacheria fenecis is a compact plant with many small leaves. The leaves shadow those behind in a similar fashion to the *Pittosporum crassifolium* resulting in a narrow peak where the reference point is correlated with itself and sharply drops off on either side of the reference. The rest of the orientations are all relatively consistently correlated with all of the other records around the 0.5 mark.

The plants with small reflective areas are more consistent when the signals are correlated with adjacent signals (local correlation) as there are less surfaces overall to be correlated. This is in contrast to correlating against fixed orientations - the plants with small reflective areas are far less consistent. When there are many leaves within a plants volume, the shadowing of a leaf or if a leaf reflects all of the signal away from the sensor then there is a good chance that another leaf will return some acoustic energy to the receiver in its place.

Even though there is a high correlation between adjacent orientations of the plant, the results are extremely poor when some fixed orientation of the plant is chosen. This indicates that viewing the plant from more than a few degrees each side of the original sensing point will produce a significantly different return. It is therefore necessary to characterise the signal using some data which is more stable through rotation of the plant.

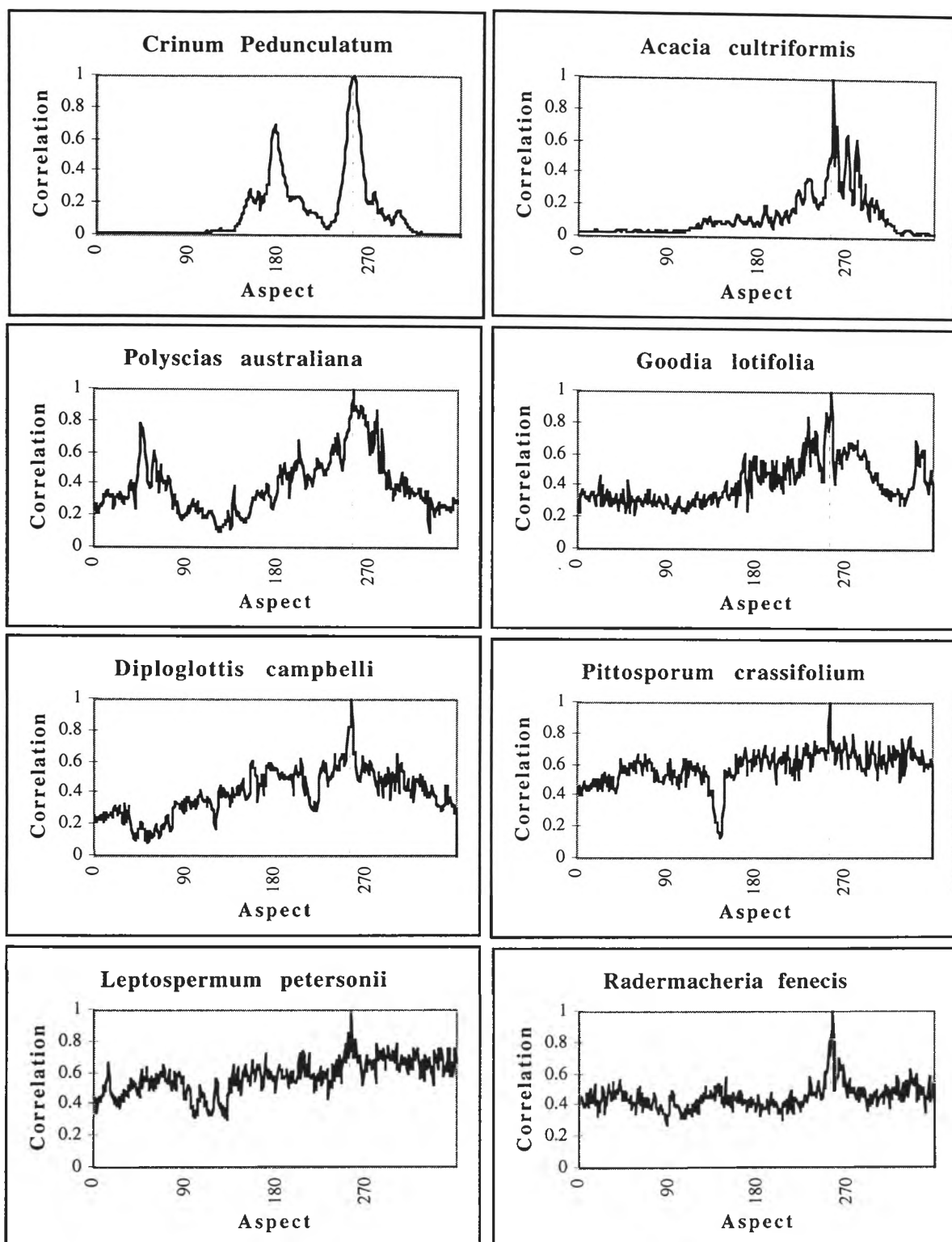


Figure 7.1 Eight plants correlated against the orientation at 256 degrees

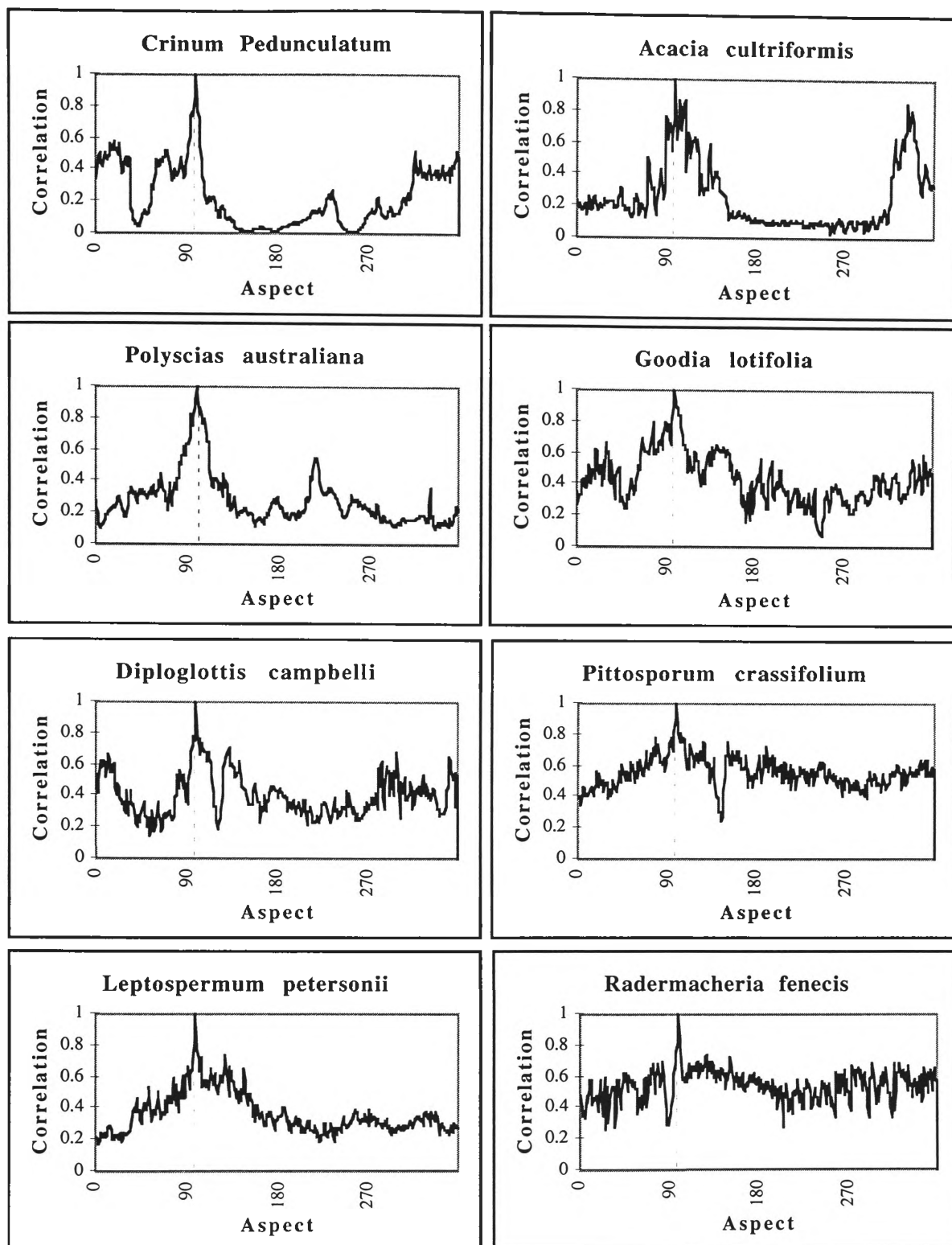


Figure 7.2 Eight plants correlated against the orientation at 100 degrees

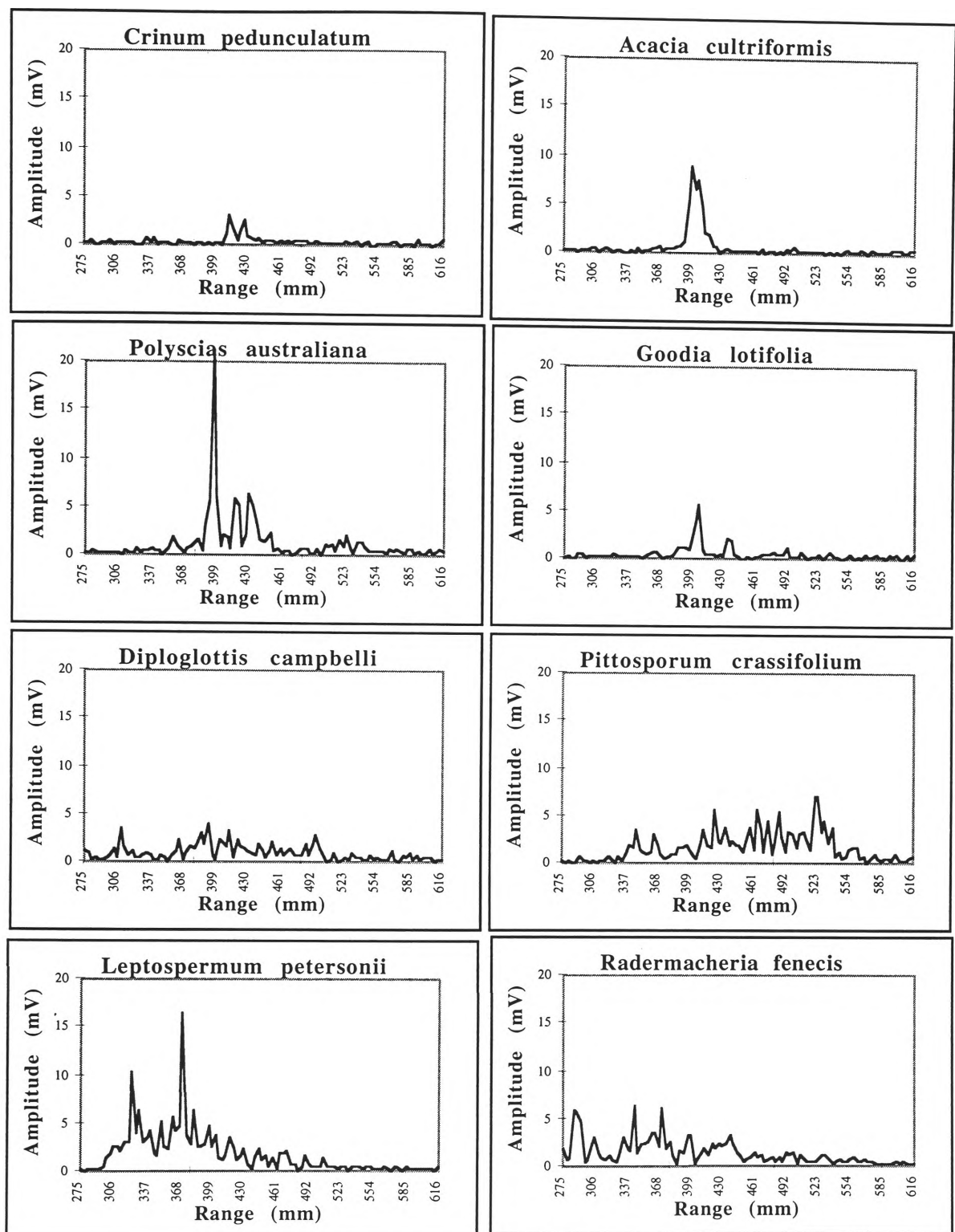


Figure 7.3 Part of the acoustic density profiles for all eight plants for orientation 100

For the correlations outlined in this section, the reference points were chosen randomly. This was done to show how quickly the signal changes with respect to the angle from which the plant is viewed. For improved results, a more advanced way of selecting the reference point may be required such as choosing the point based on the orientation which shows the best local correlation over a wide angle.

7.3 Conclusion

Global correlation provides a measure of how the whole plant varies through rotation ie. it provides a measure of the change of echo throughout an entire revolution of the plant. Most plants produce poor results when all orientations of the plant are correlated against a selected orientation. This is because a small change in range places the echoes in different range cells so acoustic density profiles' will be poorly correlated once an angle more than several degrees from the reference is used. The information in the acoustic density profile can be more reliably interpreted by considering the pattern of the foliage. This is done by capturing the characteristics of the density profile and is detailed in Chapter 8.

7.4 Summary

1. Global correlation provides a measure of how the signal changes through larger rotations of the plant.
2. Many of the plants are highly correlated with orientations close to the reference orientation.
3. Once more than several degrees from the reference orientation are used, the correlation is low.

8. Feature Analysis

8.1 Introduction

Correlation between the acoustic density profiles from adjacent orientations of plants gives good results as shown in Chapter 6. Chapter 7 however, shows that results are poor when the acoustic density profile from orientations of the plant more than several degrees from a reference orientation are correlated. In order to improve the correlation, more orientation independent information about the plants needs to be extracted. This will also facilitate plant recognition in general as the plant can be characterised by a smaller amount of data. More orientation independent information can be obtained by calculating different measures of the acoustic density profile which characterise the patterns. Once measures (or features) are calculated, they are analysed in terms of their rotation invariance and their ability to differentiate plants from all orientations.

Once the best features are selected, they are used to correlate plants using a single orientation as the reference (global correlation) and a significant improvement is achieved over correlation of the raw acoustic density profile as was shown in Chapter 7. In Chapter 9, the features are related to the physical structure of the plant.

8.2 Feature extraction in order to characterise plants

Feature extraction is a transformation which concentrates discriminatory information from an input into relatively few features [Qiang, 1995]. Its purpose is to reduce data by measuring certain features (or properties) that distinguish between the input patterns. Classification systems which have fewer parameters are more tractable and have better generalisation. It can also be advantageous to sacrifice some information to keep the system parameters to a minimum [Etemad *et al*, 1995]. When the number of features is high, it is hard to get good estimates for the decision rule(s) as the search space is too large. If the observations are reduced to a smaller number of features the decision rule will become more reliable [Therrien, 1989].

The goal of a feature extraction module is to reduce the number of data items in the input vector, while capturing its important properties. This is done by calculating the new features directly from an input pattern. Consider the plants shown with their acoustic density profiles in Figure 8.1. It is visually obvious from the acoustic density profile that the *Melaleuca quinquenervia* has a much higher peak than the *Casuarina stricta*, so a feature which would distinguish these two particular acoustic density profiles is the maximum amplitude of the acoustic density profile. This feature is 5.3 mV for the *Casuarina stricta*, and 9.9 mV for the *Melaleuca quinquenervia*. If this feature is consistent through rotation then this is a good feature to distinguish these two particular plants.

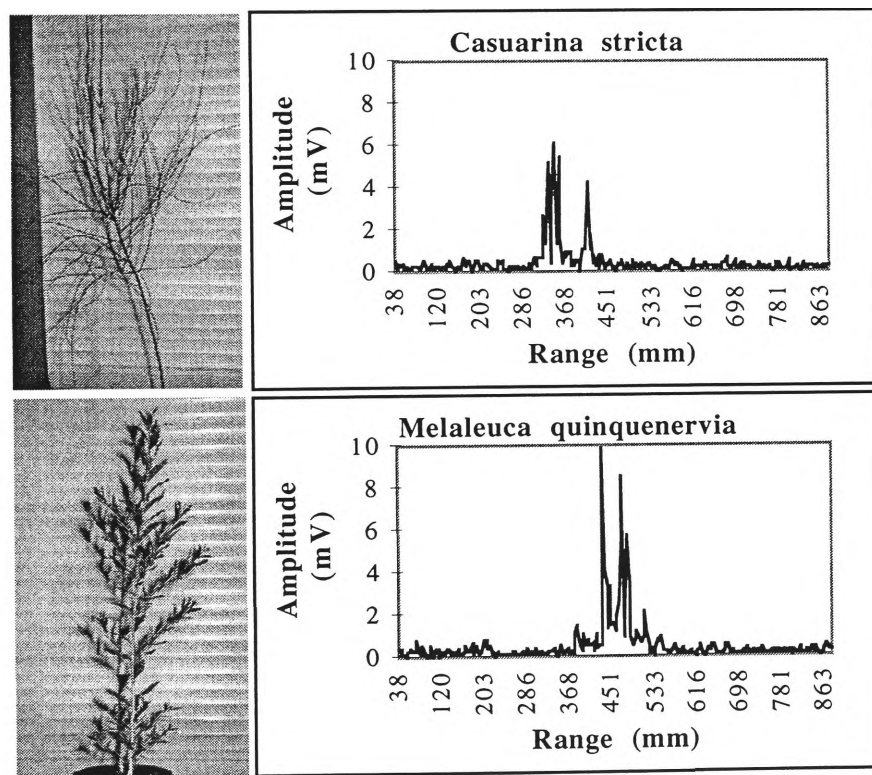


Figure 8.1 Images and acoustic density profiles for two plants

There are several ways to establish the candidates for the feature vector. The major ones are summarised by [Famili, 97, *et al*] as :

Data Driven : where data analysis is used to focus on the interrelationship between parameters in the data set and the new features are derived based on existing ones;

Knowledge Driven : where a system expert applies knowledge to construct the new representation space; and

Hypothesis Driven : where the system incrementally transforms the representation space by analysing the results in one iteration and applies deduced results to the next iteration.

The approach used in this work was to study the acoustic density profile of different objects and define measures to characterise the shape of the patterns. This is a *Knowledge Driven* approach to feature selection and has also been used by others when dealing with acoustic information. It has been used in the field of non-destructive evaluation [Chan *et al*, 1982] for the identification of different types of aeroplanes [Scott *et al*, 1993], and for the identification of different types of transport noise (heavy vehicle, aeroplanes and a mixture of traffic) [Mohajeri *et al*, 1996]. Knowledge driven feature extraction is commonly used in other fields such as machine vision [Parker, 1997].

The major advantage of this approach is that the calculated features can be interpreted more easily by a human looking at the output of a classifier. For example, it may be seen that the differences between two different plants is given by the length of the acoustic density profile - this can then be related to the physical depth of the plant.

In Chapter 3 the basic information in the signal was discussed, in particular the area of acoustic density profile differences between plants. This background information has been combined with the results of correlating the raw acoustic density profiles to develop a set of 67 features. The acoustic density profile has the potential to change substantially from one view to another when significant orientation changes occur. If the patterns can be represented in more basic terms, then the plant's acoustic density profiles will be represented more robustly. The entire feature set was developed using the physical plant geometry as a basis and this is detailed in Section 8.2.1. Once the feature set was developed, it was reduced down to a manageable set using mathematical techniques developed from visualisation of the distributions. This reduces the feature set from 67 down to 19 and is detailed in Section 8.4.1.

8.2.1 Calculation of the features

This section lists a comprehensive set of features and the physical properties of the plant that they are trying to capture. The features were developed based on the reflected acoustic density profiles by considering the analysis in Chapter 3. They are postulated based on the shapes and spread of the acoustic density profile patterns. The purpose is to consider many different measures of the pattern and then look at how well each of them characterise the plants. They are listed in no particular order. Each of the features are listed with some brief notes on what they are trying to measure (Table 8.1). Once the feature set is reduced, further analysis of the important features is given in Section 8.4.1.

This contrasts to [Kao *et al*, 1996] who calculates the autocorrelation of the signal and then used the resulting autocorrelation as an input vector to their classification process. Calculating features based on the raw acoustic density profiles directly makes it simpler to relate the results back to the acoustic density profiles and hence gain an understanding of the way that the signal reflects from different plant structures. Also, the autocorrelation applies well when they are attempting to interpret scenes from man made objects such as steps and cars.

Some of the features given in Table 8.1 are measured relative to a standard calibration measure in order to make them independent of minor variations in the particular transducers that are being used for the experiments. The calibration measure, m , was selected as the amplitude detected at the transducer when a large specular surface is insonified at a range of 0.500 metres and the constant 10000 is a scaling factor. This calibration value was established when the plant database was collected in Chapter 5 and was found to be 100 mV.

Table 8.1 The full set of features

Feat No	Name	Notes
1-10	no_above_threshold1 no_above_threshold2 no_above_threshold3 no_above_threshold4 no_above_threshold5 no_above_threshold6 no_above_threshold7 no_above_threshold8 no_above_threshold9 no_above_threshold10	Thresholds. These 10 features are the number of lines in the acoustic density profile above a set threshold t mV where $t = 59 * m / 10000, 78 * m / 10000, 98 * m / 10000, 117 * m / 10000, 156 * m / 10000, 195 * m / 10000, 295 * m / 10000, 300 * m / 10000, 490 * m / 10000$ and

		<p>$580 * m / 10000$ mV where m is the calibration measure = 100mV for the sensors used in this research. These thresholds were chosen based on approximately equal intervals. Full details of the function used to reference the acoustic density profile for range is given in Chapter 5.</p> <p>These features give an indication of the specularity of the surfaces, the number of surfaces, the orientation of the surfaces, the size of the individual surfaces and the depth of the plant. Different threshold levels serve to differentiate plants with different spreads of those properties.</p> <p>For example, compare a plant with many small leaves to one with several large leaves. The acoustic density profile for the plant with the small leaves will have much lower amplitudes than that for the plant with large leaves. Also, depending on the spread of the leaves through the plant, the signals may be spread through the acoustic density profile to reflect the depth of the plant.</p> <p>Consider two plants with the same depth, one with small leaves and one with large leaves. Both plants will have similar values for low thresholds as this is a function of the number of reflecting surfaces. As the threshold is increased however, the value of the feature will reduce far more quickly for the plant with small leaves as it has fewer leaves which produce large amplitudes.</p>
11	no_of_major_peaks1	<p>The number of major peaks.</p> <p>An amplitude is defined as a major peak if it is greater than $195 * m / 10000$ mV (where m is the calibration measure = 100 mV for the sensors used in this research) and five of the range cells on each side of it (17 mm each side) are less than it.</p> <p>If the acoustic density profile of a plant contains more than one major peak, the number of peaks is an indication of the layers of foliage. A layer of foliage may occur when there is a group of coincident leaves which reflect the signal back to the receiver.</p>
12	sum_of_density_profile	<p>Sum all of the amplitudes.</p> <p>This feature is the size of the “area under the curve” and is the sum of all of the reflectors in the field of audition. This is a function of leaf size, orientation, surface texture and the occlusion generated by the structure of the plant. This is proportional to the sum of all of the visible surfaces and is known as the acoustic area.</p>
13	maximum_amplitude	<p>The maximum value of the acoustic density profile.</p> <p>This indicates the amplitude of the greatest audible surface within the field of audition. It is a function of the specularity, size and orientation of the surface at the corresponding range.</p>
14-20	percentage_within_thresh1 percentage_within_thresh2 percentage_within_thresh3 percentage_within_thresh4 percentage_within_thresh5 percentage_within_thresh6 percentage_within_thresh7	<p>Thresholds for signal spread</p> <p>Accumulate the amplitude values within n range cells each side of the centre and calculate the result to be the percentage of this sum to the sum of the total acoustic density profile. $n = 10, 15, 20, 25, 30, 35, 40$. The number of points chosen was based on the approximate depth of the plants. $n = 10$ represents a depth of 6.88cm (one range line represents 3.44 mm), and $n = 40$ represents a depth of 27.52 cm.</p>

		<p>These features give an indication of how spread the acoustic density profile is about the centre; this provides information about the density of the physical plant. It is a measure of the wide band content of the echo. The range line of the end of the plant minus the range line of the start of the plant. This is the acoustic depth of the plant.</p> <p>This gives an indication of the depth of the plant. Note that this would only be for plants which are relatively sparse. Plants with a large number of leaves will prevent acoustic energy from penetrating to the back of the plant.</p> <p>The distance between the maximum value and the start of the plant in the acoustic density profile.</p> <p>This will give a measure of how compact the plant is and also the depth of the plant (see Feature 21)</p> <p>The length of the acoustic density profile divided by the number of major peaks.</p> <p>This will give a measure of the distance between the layers in the foliage.</p> <p>Returns the height of the acoustic density profile which contains this percentage of the data mass. Percentages = 80, 70, 60, 50, 40, 30. For example, when the percentage is 80, the result will be the amplitude at which 80% of the sum of the data falls below.</p> <p>This gives an indication of the specularity, orientation and size of the leaves as well as the number of leaves</p> <p>The average amplitude of the acoustic density profile between the start and of the plant.</p> <p>This gives information about the size, orientation, specularity and spread of the leaves.</p> <p>The median amplitude</p> <p>This measure is similar to feature 30 and gives information about the size, orientation, specularity and spread of the leaves.</p> <p>The standard deviation of the amplitudes.</p> <p>This gives information about how much the acoustic density profile varies</p> <p>The variance of the amplitude</p> <p>The coefficient of variation of the amplitudes</p> <p>The mean absolute deviation of the amplitudes</p> <p>The skew of the amplitudes</p> <p>The average position from the start of the plant to the narrowband lines.</p> <p>This gives an indication of the position of the specular reflectors within the acoustic density profile.</p> <p>The average range. This is half way between the start and end of the acoustic density profile.</p> <p>The median range.</p> <p>The standard deviation of the ranges in the acoustic density profile</p> <p>The variance of the ranges in the acoustic density profile</p> <p>The coefficient of variation of the ranges in the acoustic density profile</p> <p>The mean absolute deviation of the ranges in the acoustic</p>
21	length_of_density_profile	
22	front_to_peak_dist	
23	repetition_of_layers	
24-29	threshold_data_mass1 threshold_data_mass2 threshold_data_mass3 threshold_data_mass4 threshold_data_mass5 threshold_data_mass6	
30	average_amplitude	
31	median_amplitude	
32	stdev_amplitude	
33	variance_amplitude	
34	coeff_of_var_amplitude	
35	mean_abs_dev_amplitude	
36	skew_amplitude	
37	avg_posn_narrowband	
38	average_range	
39	median_range	
40	stdev_range	
41	variance_range	
42	coeff_of_var_range	
43	mean_abs_dev_range	

		density profile
44	skew_range	The skew of the ranges in the acoustic density profile
45-47	count_quarter_height count_half_height count_3quarter_height	Count the number of lines in the acoustic density profile which are above: one quarter of the height of the maximum amplitude; half of the height of the maximum amplitude; and three quarters of the height of the maximum amplitude respectively.
48	ratio_max_amp_len	The ratio of the maximum amplitude of the acoustic density profile to the length of the acoustic density profile
49	ratio_avg_amp_len	The ratio of the average amplitude of the acoustic density profile to the length of the acoustic density profile
50	ratio_max_amp_avg	The ratio of the maximum amplitude of the acoustic density profile to the average amplitude.
51	ratio_max_amp_sum_profile	The ratio of the maximum amplitude of the acoustic density profile to the sum of the acoustic density profile
52	ratio_avg_amp_sum_profile	The ratio of the average amplitude to the sum of the acoustic density profile
53	ratio_length_sum_profile	The ratio of the length of the acoustic density profile to the sum of the acoustic density profile
54	ratio_range_stdev_sum_profile	The ratio of standard deviation of the ranges in the acoustic density profile to the sum of the acoustic density profile
55	ratio_range_stdev_max_amp	The ratio of the standard deviation of the ranges in the acoustic density profile to the maximum amplitude
56	ratio_range_stdev_avg_amp	The ratio of the standard deviation of the ranges in the acoustic density profile to the average amplitude
57	ratio_range_stdev_length	The ratio of the standard deviation of the ranges in the acoustic density profile to the length of the acoustic density profile
58-60	slope_25_peak slope_50_peak slope_75_peak	The rise slope between the range cell at 25% of the maximum and the maximum; 50% if the maximum; and 75% of the maximum respectively. This gives an indication of the slope of the acoustic density profile from various points and hence the density of the plant.
61-63	slope_25_peakA slope_50_peakA slope_75_peakA	The rise slope between the range cell at 25% of the maximum and the maximum (note that in this case the maximum is actually the average of five points around the average).
64-66	range_25_acoustic_area range_50_acoustic_area range_75_acoustic_area	The range cell from the start at which 25% of the total area is observed; that where 50% of the area is observed; and that where 75% of the area is observed.
67	no_of_major_peaks2	The number of major peaks. An amplitude is defined as a major peak if it is greater than $156/m$ mV (where m is the calibration measure = 100 mV for the sensors used in this research) and five of the range cells on each side of it (17 mm each side) are less than it.

8.2.2 Data preprocessing

Raw data from the sensor is generally in the range of 0 to 100 mV (100 mV is the signal echoed from a flat wall at a distance of 0.5 m from the sensor). Once the features are calculated, each of the individual features has its own range of values with its own units. For example, `no_above_threshold1` is a count; `sum_of_density_profile` is a value in Volts; and `percentage_within_thresh1` is a percentage. In order to make decisions about the data, all of the features need to be in the same scale. It is very difficult to compare a count, to a value in mV, to a percentage so all of the features are normalised to the same scale. I have chosen to scale the data so that most of the values lie between 0 and 100 for this group of 100 plants. The specific scaling algorithm is outlined in Table 8.2.

The intent of the scaling outlined in Item 3 of Table 8.2 is based on scaling with respect to the mean and standard deviation of the range of values. When the transformation is applied using the maximum value for the feature as the scaling factor, the result is affected very badly by outliers. That is, if there is one record with a very large value, all of the other records will be accordingly reduced so that they lie over a very small scale. Using the mean and the standard deviation eliminates the problem of an outlier being used as a scaling factor and it is more likely that the data will be relatively evenly spread throughout the range of 0 to 100. This algorithm does however mean that some extreme raw values will be scaled to numbers over 100.

In the implementation described in this chapter, Steps one and two of the algorithm were performed in advance of processing each of the plants individually. Sensed data for all 100 plants is read, features are calculated for all records of all plants and the mean and standard deviation of all 36000 records are calculated. A file is then written which contains $\bar{x} + (2 * s)$ for each of the 67 features, these scaling factors are shown in Table 8.3. The algorithm to scale the data using the scaling factors is shown in Algorithm 8.1.

A block diagram of the entire pre-processing is shown in Figure 8.2. Sensor data is the input to the process, with an example of *Indigofera australis* shown adjacent. It is

referenced to the standardised range of 400 mm and the features are calculated. Most of the features are not visible because the scale of the graph is very large due to some large features. The scaling data shown in Table 8.3 is used to scale each of the features into the range of 0 to 100 before further processing.

Note that an alternative and more conventional statistical approach would be to use Equation 8.1 to standardise the features to have a mean of zero and a standard deviation of one. In order to make most of the data fall between zero and 100, it would be multiplied by 25 (to result in a standard deviation of 25) and then 50 would be added to it (so the average is 50 instead of 0).

$$z = \frac{x_{ij} + \bar{x}_i}{s_i} \quad 8.1$$

where \bar{x}_i is the mean of all of the data for feature i ; and

s_i is the standard deviation

Table 8.2 The algorithm for scaling the data

	Step	Data
1	Establish a data set with all of the data under consideration.	Each row will contain the features calculated from the raw sensor reading. $x_n = \{x_{1n}, x_{2n}, \dots, x_{67n}\}$ where n is the number of records in the dataset.
2	Calculate the average and standard deviation for each feature in the dataset (each column).	This results in two rows : one has the averages for the entire dataset $\mathbf{x} = \{\bar{x}_1, \bar{x}_2, \dots, \bar{x}_{67}\}$; and the other has the standard deviations for the entire dataset $\mathbf{s} = \{s_1, s_2, \dots, s_{67}\}$.
3	Scale the original dataset so that most of the values lie between 0 and 100 using the formula below. $x'_{ij} = \frac{x_{ij} * 100}{\bar{x}_i + (2 * s_i)}$ where i is the number of features; j is the number of records in the dataset; \bar{x}_i is the average of feature i ; and s_i is the standard deviation of feature i .	All of the features end up in the required range.

Table 8.3 All 67 features and their $\bar{x} + (2 * s)$

Feature name	$\bar{x} + (2*s)$	ude	
no_above_threshold1	72.965	mean_abs_dev_amplitude	66.966
no_above_threshold2	63.651	skew_amplitude	11.472
no_above_threshold3	54.314	avg_posn_narrowband	44.976
no_above_threshold4	47.363	average_range	150.977
no_above_threshold5	36.735	median_range	149.933
no_above_threshold6	29.133	stdev_range	24.654
no_above_threshold7	17.771	variance_range	551.621
no_above_threshold8	11.712	coeff_of_var_range	0.206
no_above_threshold9	8.183	mean_abs_dev_range	20.564
no_above_threshold10	6.004	skew_range	3.497
no_of_major_peaks1	6.484	count_quarter_height	33.642
sum_of_density_profile	4484.800	count_half_height	12.401
maximum_amplitude	508.572	count_3quarter_height	4.926
percentage_within_thresh1	124.803	ratio_max_amp_len	17.820
percentage_within_thresh2	151.302	ratio_avg_amp_len	3.959
percentage_within_thresh3	173.764	ratio_max_amp_avg	9.269
percentage_within_thresh4	194.641	ratio_max_amp_sum_profile	0.275
percentage_within_thresh5	216.295	ratio_avg_amp_sum_profile	0.077
percentage_within_thresh6	237.042	ratio_length_sum_profile	0.047
percentage_within_thresh7	258.565	ratio_range_stdev_sum_pro	0.013
length_of_density_profile	100.371	file	
front_to_peak_dist	49.934	ratio_range_stdev_max_amp	0.184
repetition_of_layers	36.885	ratio_range_stdev_avg_amp	0.819
threshold_data_mass1	202.748	ratio_range_stdev_length	0.305
threshold_data_mass2	141.534	slope_25_peak	239.893
threshold_data_mass3	99.160	slope_50_peak	318.073
threshold_data_mass4	69.031	slope_75_peak	339.739
threshold_data_mass5	47.161	slope_25_peakA	51.231
threshold_data_mass6	30.929	slope_50_peakA	79.101
average_amplitude	79.441	slope_75_peakA	91.012
median_amplitude	50.684	range_25_acoustic_area	30.451
stdev_amplitude	104.290	range_50_acoustic_area	46.200
variance_amplitude	16519.100	range_75_acoustic_area	63.745
coefficient_of_var_amplit	1.574	no_of_major_peaks2	7.340

Algorithm 8.1 Outline of the function to calculate the scaled feature records**CALCULATE SCALED FEATURES FROM ACOUSTIC DENSITY PROFILE**

This function is passed an acoustic density profile consisting of 512 amplitude values. It calls a function to reference the acoustic density profile so that the plant is at a standard range (see Chapter 5), then calls a function to calculate the features and then scales the features so that most of them lie between 0 and 100. The scaling factors are then applied - a scaling factor for each feature (see Table 8.3) and the range referenced scaled features are returned

profile the name of a file which contains the
acoustic density profile

Outputs

an array of scaled features calculated from the
range referenced acoustic density profile

BEGIN

Call REFERENCE THE RAW ACOUSTIC DENSITY PROFILE TO A STANDARD
RANGE (Ch 5)

Call a function to calculate features from the range referenced
acoustic density profile.

FOR each feature calculated.

BEGIN

new feature value = feature value / scaling factor * 100.

END

Return the new feature array. **END**

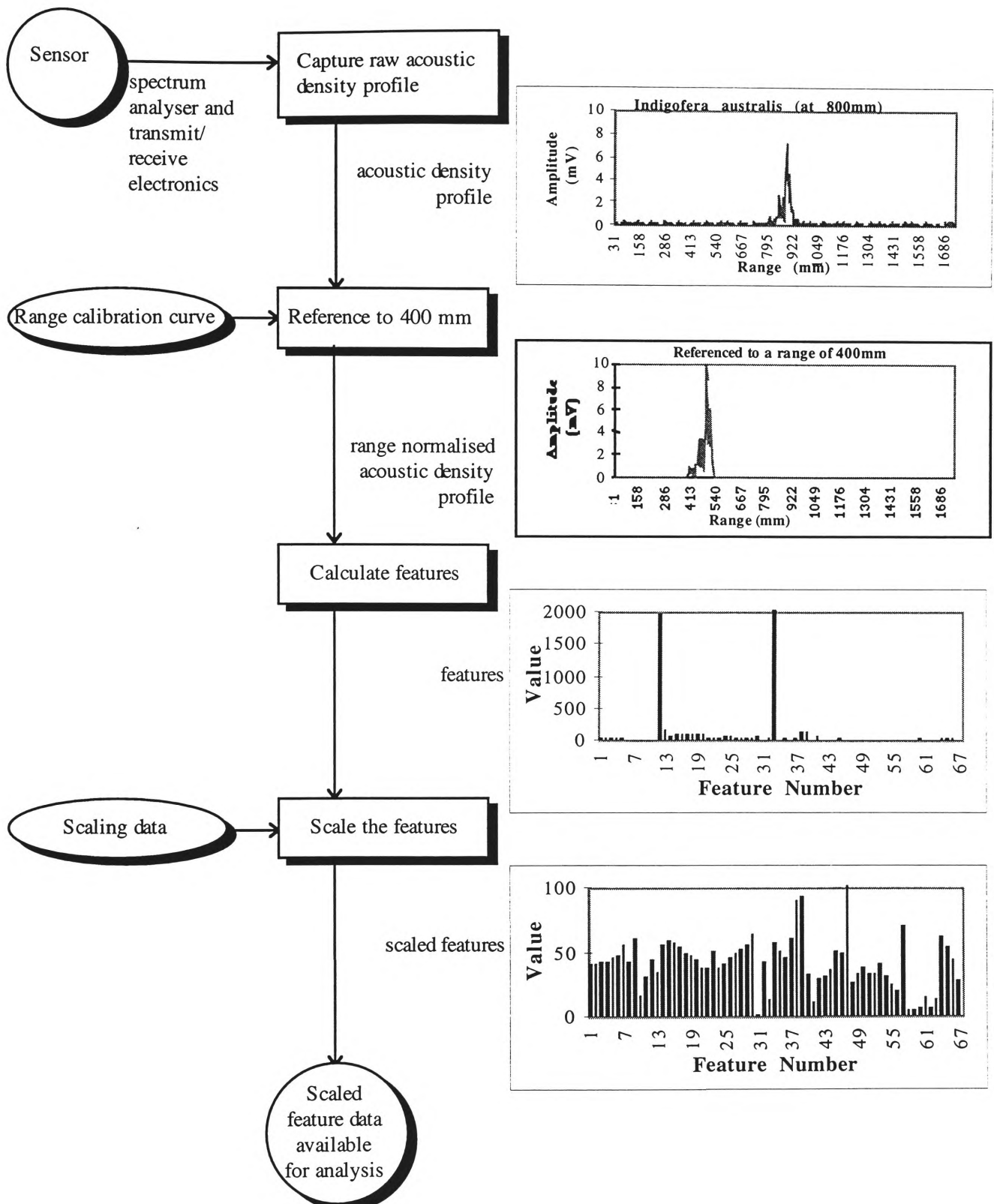


Figure 8.2 Schematic of the data pre-processing with an example for *Indigofera australis* shown on the right hand side

8.3 Preliminary analysis of features

The scaled features were calculated for the data in the plant database described in the previous chapter. Features were calculated for each of the 36000 records and the

results analysed in several different ways. It is very difficult to visualise large numbers of variables, so often a good place to start is with the distribution of a single variable [Cohen, 95]. This section introduces a visualisation of data from four plants (out of the total of 100) to show how plants can be separated using the features calculated in a small number of dimensions. More advanced techniques are required when a larger number of plants need to be differentiated as more features are required to distinguish them. Analysis will be expanded to deal with all 100 plants in a subsequent section.

Four plants were selected for the initial analysis :

1. *Cryptocarya williwilliana* (Small-leaved Laurel);
2. *Leptospermum laevigatum* (Coast Tea-tree);
3. *Szygium leuhmanni*; and
4. *Westringa fruticosa* (Rosemary).

Images of the plants are shown in Figure 8.3.

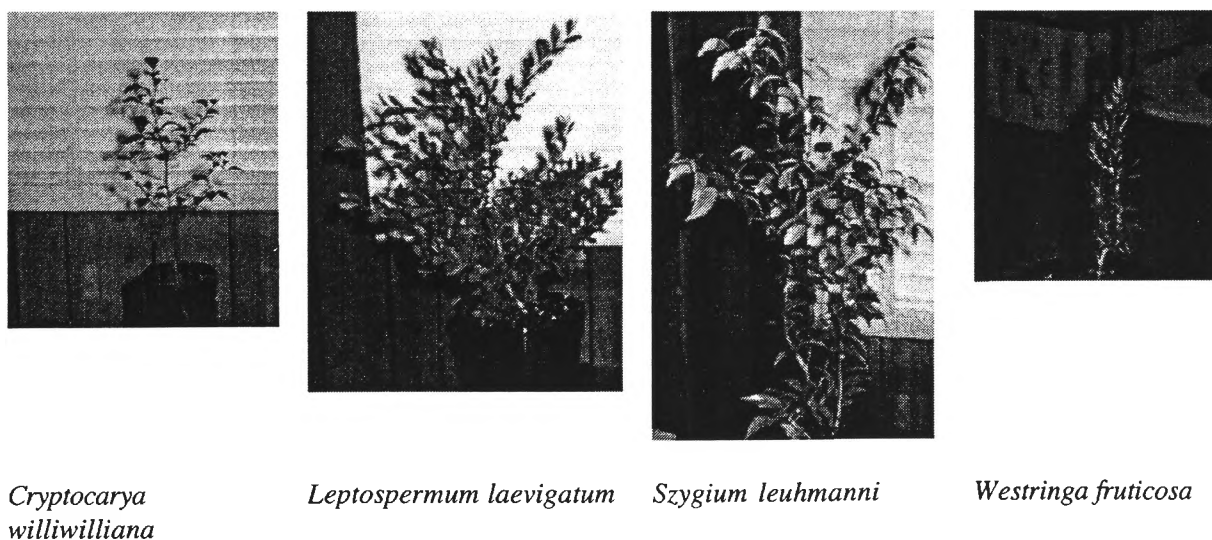


Figure 8.3 Images of the plants under consideration

A frequency histogram allows the number of occurrences of different values within a distribution to be illustrated on a graph. Initially, all the data was scaled using the algorithm in Section 8.2.2. Figure 8.4 shows the histogram for all 360 records of the four plants for feature 1 (`no_above_threshold1`). The x-axis represents the value of

no_above_threshold1 and shows values in the range of 0 to 105. The frequency bins are five wide and each is a count of the number of records in the dataset which fall within that particular range of values. The bins are labelled with the upper limit of the bin, for example the first bin is labelled five and any value within the range of 0 to 5 will fall in that bin. That is, the bin labelled five accumulates one unit for every value of no_above_threshold1 between 0 and 5. All 360 records for each plant are included with different plants shown in different colours.

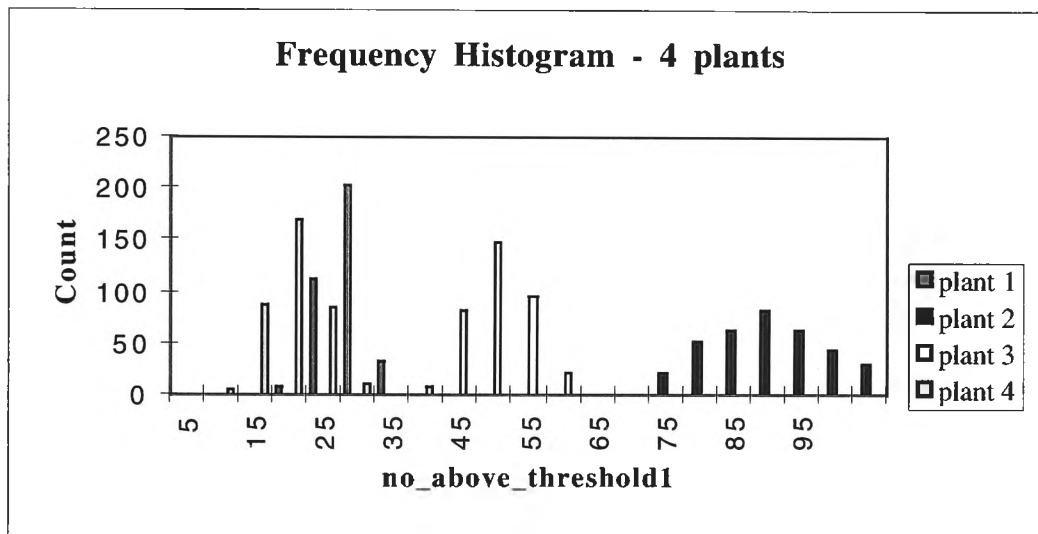


Figure 8.4 Frequency distribution of feature 1 (no_above_threshold1)

Gaps in the distribution are usually suggestive of features in the data [Cohen, 95] and the data in the figure appears to fall into three distinct groups. Analysis of the individual plants shows that two of the plants fall in their own separate positions in the histogram (*Leptospermum laevigatum* and *Syzygium leuhmanni*). The other two plants (*Cryptocarya williwilliana* and *Westringa fruticosa*) overlap ie. for bins 15, 25, 30 and 35 there are some records from *Cryptocarya williwilliana* and *Westringa fruticosa* which have those values. So if we have an acoustic density profile which we calculate as having no_above_threshold1 = 25, then we know that it is one of the two plants, but we can not say which one it is using this feature only. This is clearly illustrated in Figure 8.5 which shows each of the plants on separate graphs. In summary :

Leptospermum laevigatum is characterised by high values of this feature (around 90);

Syzygium leuhmanni is characterised by medium values of this feature (around 50);

and

Both of the remaining plants are characterised by lower values of this feature (around 20).

Based on this single feature (`no_above_threshold1`) two of the plants can be identified (*Leptospermum laevigatum* and *Syzygium leuhmanni*) as different and also as different from the other two plants. However, it is not possible to differentiate between *Cryptocarya williwilliana* and *Westringa fruticosa* as they both produce similar values for this particular feature. In order to separate them, another feature needs to be considered.

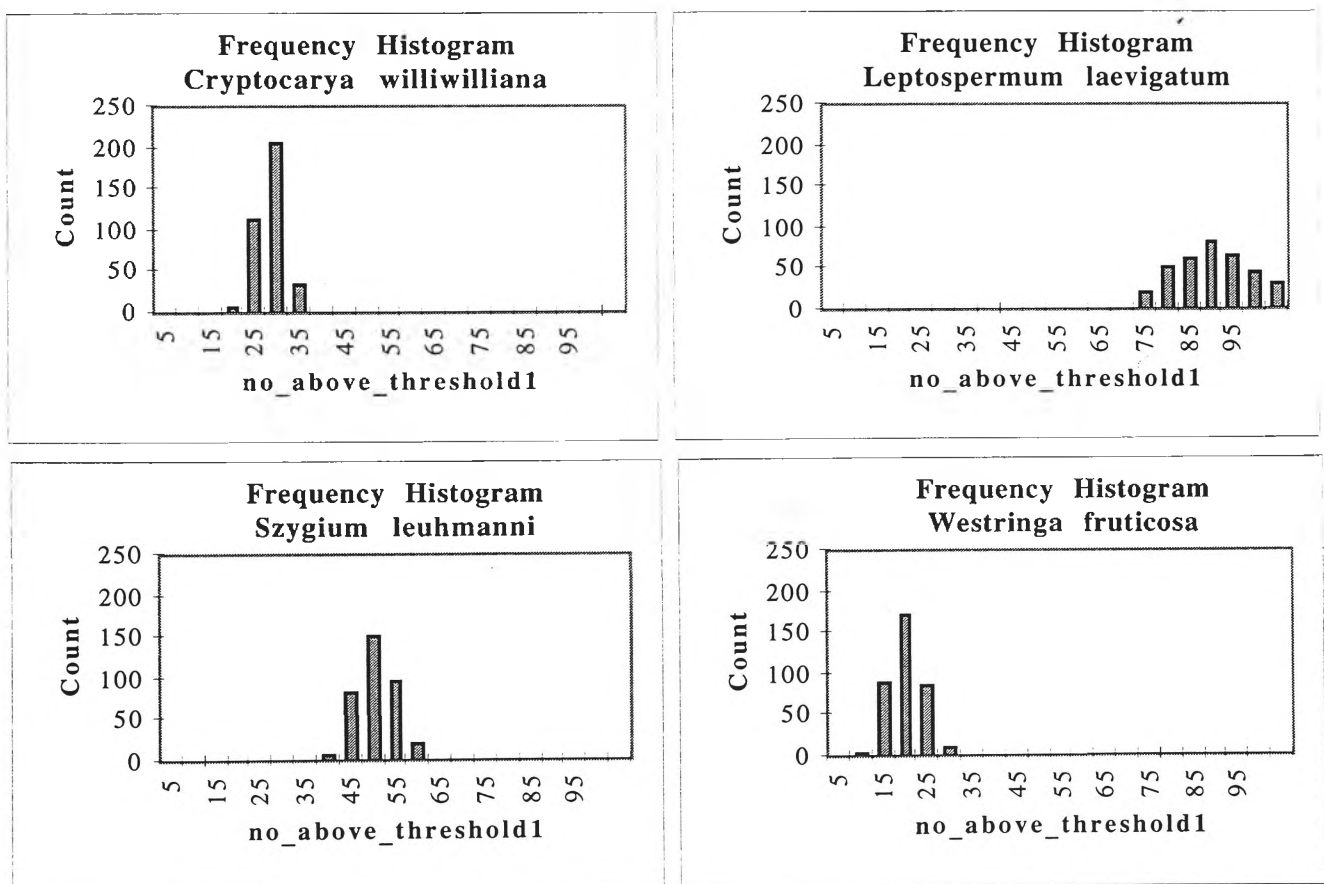


Figure 8.5 Frequency Histograms for each of the individual plants for Feature 1 (`no_above_threshold1`)

The data for each of the plants can be represented concisely using statistical measures and these are shown in Table 8.4.

**Table 8.4 Summary Statistics for four plants for feature 1
(no_above_threshold1)**

Summary Statistic	<i>Cryptocarya williwilliana</i>	<i>Leptospermum laevigatum</i>	<i>Szygium leuhmanni</i>	<i>Westringa fruticosa</i>
Mean	26.55	87.57	48.47	17.85
Standard Deviation	2.81	8.39	4.42	3.78
Minimum	17.88	65.55	37.74	7.95
Maximum	33.77	108.26	67.54	28.80
Count	360	360	360	360

In order to separate the remaining plants, another feature is added to the analysis (no_above_threshold2). The plot of the two features are shown in Figure 8.6. This graph shows that there is still an overlap between the two plants in the lower left hand corner of the figure so either another feature should be added or a different feature added. Note that I have not attempted to select features based on any criterion (for example, orthogonal features could have been selected) but have simply selected consecutive features in the dataset in order to demonstrate the process of higher dimension visualisation. Selection of the best feature for any particular classes of plants depends on the physical properties of the plants which you are trying to separate. This is discussed further in Chapter 10. Heuristic techniques for selecting features based on their discriminating power are also discussed there.

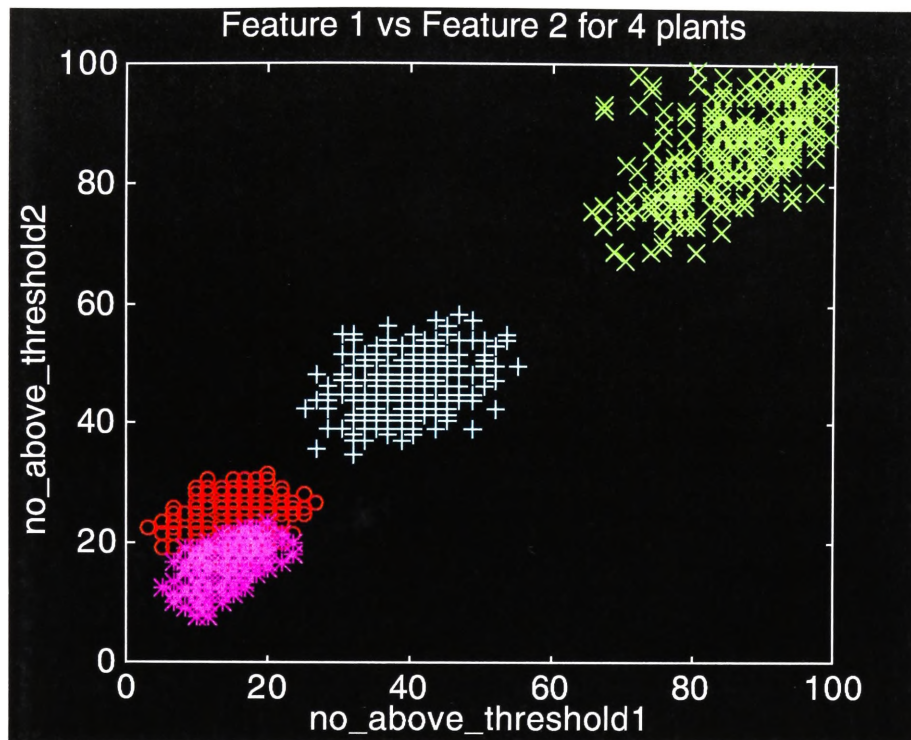


Figure 8.6 Feature 1 vs Feature 2 for the four plants

Adding another feature gives the result shown in Figure 8.7. There is still a some overlap between the groups so another feature still needs to be added.

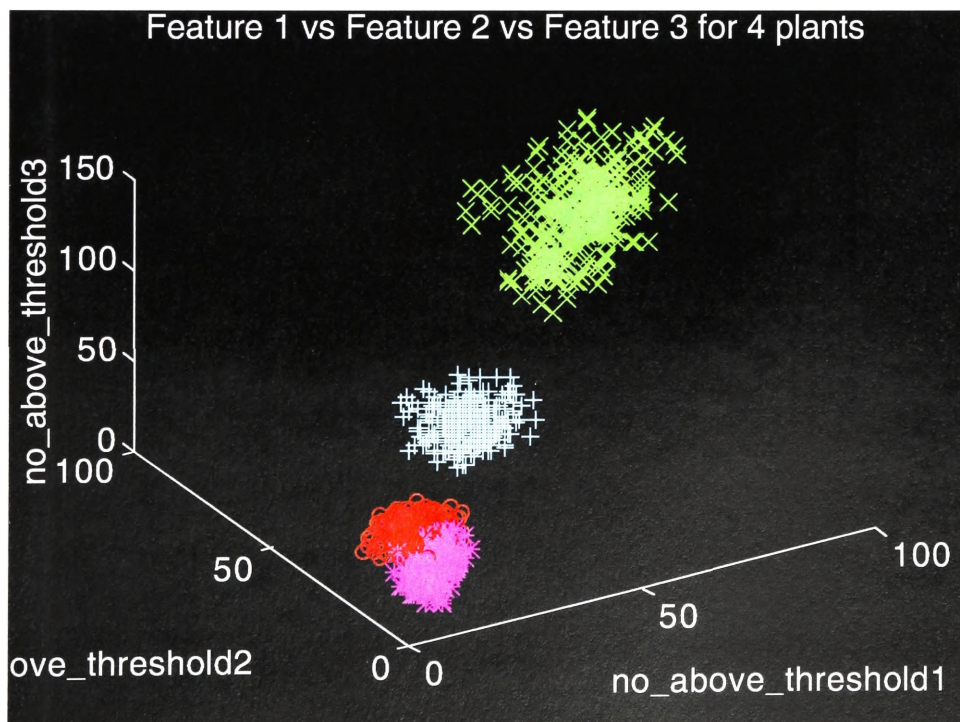


Figure 8.7 Feature 1 vs Feature 2 vs Feature 3 for the four plants

This simplified example shows that the powerful tool of data visualisation can be used to isolate individual plants based on the features calculated from their raw acoustic

density profile. This technique is satisfactory when working with a small number of plants and with features which discriminate well. When a large number of plants and/or variables are available, more sophisticated methods are required.

Features should be selected based primarily on their discriminatory power rather than simply selecting the first feature, and then adding them one by one as I have done in the above example.

At times, data will separate nicely on a graph allowing a straight line to separate groups in one dimension, two dimensions, or n dimensions. These are examples of classes which are linearly separable and classification can be performed using a simple linear classifier. The more common situation is where the groups are intertwined in such a way that they can not be separated by a straight line [Wasserman, 89]. In this case more complex classifiers (such as multi-layer neural networks) are required to perform the classification.

A good measure of the discrimination between classes (plants) is based on the discriminating ability of a pattern classification system. and this is considered in detail in Chapter 10.

8.4 Qualities of the feature data

Since plants may be insonified at any angle it is important for features to remain constant or change in a known way independently of the orientation of the plant. Features can be either invariant throughout an entire revolution of the plant or a partial revolution. When plants are being used as landmarks for navigation, they will only be sensed through a certain angle, as illustrated in Figure 8.8.

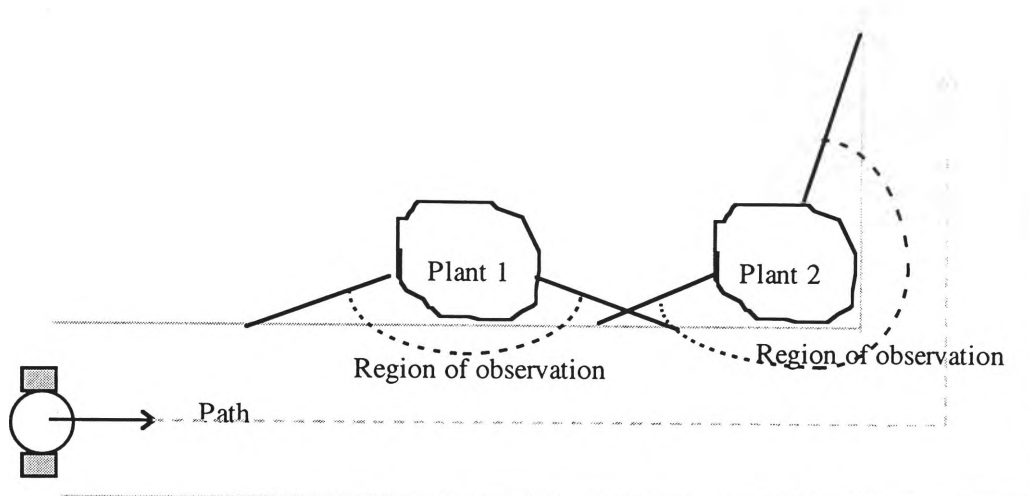


Figure 8.8 Mobile robot with planned path and region of observation for plants shown.

The design goal is to develop a feature reduction technique which optimises the feature list in favour of features which are invariant throughout an entire revolution. Details about practical implementation are provided in Chapter 11.

8.4.1 Feature filtering

The Feature Filtering method of reducing features is independent of any pattern classification technique and is one of the earliest approaches to feature selection [Langley, 1994]. This section describes a feature filtering technique to reduce the total number of features from 67 to 19.

In general, the choice of features is complex because even though an individual feature may appear to be non-discriminatory, when it is combined with other features, it may assist in classifying an echo as being from a particular plant or group of plants. If a feature is poor enough however, there is a good chance that it will not contribute in any meaningful way to the classification process. Consideration of all possible combinations of variables can be a time consuming process when there is a large number of them. So a first pass reduction of the features becomes a necessity and is described in this section.

One way of reducing the number of features is to use only features which will provide discrimination within the population and are representative of the particular plant, that is, features which allow separation of a plant or group of plants from the rest of the plants and features which are relatively constant through rotation. All 67 features were

calculated for each plant and the results collated. In this section, features are analysed independently and the ones which are shown to be poor performers are discarded.

Figure 8.9 shows a graph of the average and standard deviation of feature 1 (`no_above_threshold1`) for all 100 plants. The plants are shown on the x-axis and are arranged in increasing order of the average value of the feature. The error bars on the chart show one standard deviation each side of the average. Plant names are shown on the axis as numbers and the cross reference table is shown on the left hand side. Note that the data have been referenced for range and scaled (Section 8.2.2).

It is evident that over the entire population of 100 plants, the entire range of values is represented (they are spread throughout the range) and the standard deviations are relatively small. If you wish to distinguish two plants, say *Banksia ericifolia* and *Leptospermum laevigatum* then they can be separated quite well using this feature alone (*Banksia ericifolia* is the plant with the lowest value and *Leptospermum laevigatum* is the one with the highest value). If plants are far enough apart then a good classification can be made with that feature. A second feature could then be used for confirmation. If the plants are close then additional features are needed to separate them.

This feature (Figure 8.9) is in stark contrast to some other features such as feature 47 (`count_3quarter_height`) which has virtually no ability to discriminate plants (Figure 8.10).

Figure 8.9 Feature 1 (no_above_threshold1) for all 100 plants

No	Name	No	Name
19	<i>Banksia ericifolia</i>	8	<i>Acacia melanoxylon</i>
66	<i>Melaleuca erubescens</i>	67	<i>Melaleuca quinquenervia</i>
30	<i>Crinum pedunculatum</i>	26	<i>Citriobatus paucifloris</i>
68	<i>Melaleuca styphelioides</i>	77	<i>Pittosporum rhombifolium</i>
36	<i>Diploglottis australis</i>	70	<i>Ficus obliqua</i>
21	<i>Carpentaria acuminata</i>	85	<i>Rhopalostylis baneri</i>
25	<i>Cinnamom oliveri</i>	76	<i>Pittosporum revolutum</i>
2	<i>Acacia cultriformis</i>	93	<i>Stenocarpus sinuatus</i>
12	<i>Agapanthus praecox dwarf</i>	71	<i>Mishocarpus australis</i>
98	<i>Tristaniopsis collina</i>	9	<i>Acacia podalyrifolia</i>
99	<i>Westringia fruticosa</i>	41	<i>Endiandra introrsa</i>
72	<i>Omalanthus populifolius</i>	17	<i>Azalea alba magnifica</i>
91	<i>Solanum laciniatum</i>	24	<i>Casuarina torulosa</i>
29	<i>Crinum mauritianum</i>	45	<i>Eucalyptus leucoxydon</i>
13	<i>Agapanthus praecox</i>	73	<i>Phyllanthus albidiflorus</i>
64	<i>Livistona sp 'Carnarvon'</i>	6	<i>Acacia longifolia</i>
35	<i>Cupaniopsis parvifolia</i>	88	<i>Sarcomelicope simplifolia</i>
27	<i>Cordyline australis</i>	92	<i>Solanum vescum</i>
48	<i>Goodia lotifolia</i>	96	<i>Syzygium paniculatum</i>
16	<i>Ayrtia distylis</i>	75	<i>Pittosporum james</i>
55	<i>Hymenosporum flavum</i>	79	<i>Polyscias australiana</i>
52	<i>Guioa semiglauc</i>	49	<i>Grevillea baileyana</i>
31	<i>Cryptocarya bidwilli</i>	86	<i>Rhopalostylis sapida</i>
15	<i>Archontophoenix cunninghamiana</i>	22	<i>Casuarina glauca</i>
44	<i>Eucalyptus botryoides</i>	28	<i>Correa alba</i>
50	<i>Grevillea hilliana</i>	95	<i>Syzygium leuhmanni</i>
84	<i>Rhododendron clorinda</i>	53	<i>Hakea salicifolia</i>
78	<i>Pittosporum undulatum</i>	80	<i>Polyscias elegans</i>
33	<i>Cryptocarya williwilliana</i>	38	<i>Dodonaea triquetra</i>
43	<i>Eriostemon myoporoides</i>	47	<i>Ficus rubiginosa</i>
23	<i>Casuarina stricta</i>	100	<i>Ziera collina</i>
63	<i>Litsea reticulata</i>	32	<i>Cryptocarya laevigatum</i>
14	<i>Alyxia ruscifolia</i>	61	<i>Leptospermum petersonii</i>
51	<i>Grevillea marmalade</i>	1	<i>Acacia binervata</i>
40	<i>Doryanthes palmeri</i>	39	<i>Dodonaea viscosa</i>
34	<i>Cupaniopsis anacardioides</i>	74	<i>Pittosporum crassifolium</i>
89	<i>Solanum aviculare</i>	4	<i>Acacia howittii</i>
58	<i>Laccospadix australasica</i>	37	<i>Diploglottis campbelli</i>
60	<i>Leptospermum morrisonii</i>	97	<i>Tabebuia chrystricha</i>
83	<i>Rhododendron bryophyllum</i>	20	<i>Banksia integrifolia</i>
94	<i>Sireblis brunonianus</i>	42	<i>Endiandra pubens</i>
54	<i>Howea forsteriana</i>	5	<i>Acacia irrorata</i>
65	<i>Melaleuca decora</i>	57	<i>Jacaranda mimosifolia</i>
3	<i>Acacia falcata</i>	11	<i>Acroneychia laevis</i>
56	<i>Indigofera australis</i>	81	<i>Polyscias murrayi</i>
69	<i>Microcitrus australis</i>	87	<i>Sarcotoechia heterophylla</i>
7	<i>Acacia mearnsii</i>	82	<i>Radermacheria fenecis</i>
90	<i>Solanum brownii</i>	18	<i>Azalea cultivar splenda</i>
10	<i>Acacia stricta</i>	62	<i>Licuala ramsayi</i>
46	<i>Eucalyptus maculata</i>	59	<i>Leptospermum laevigatum</i>

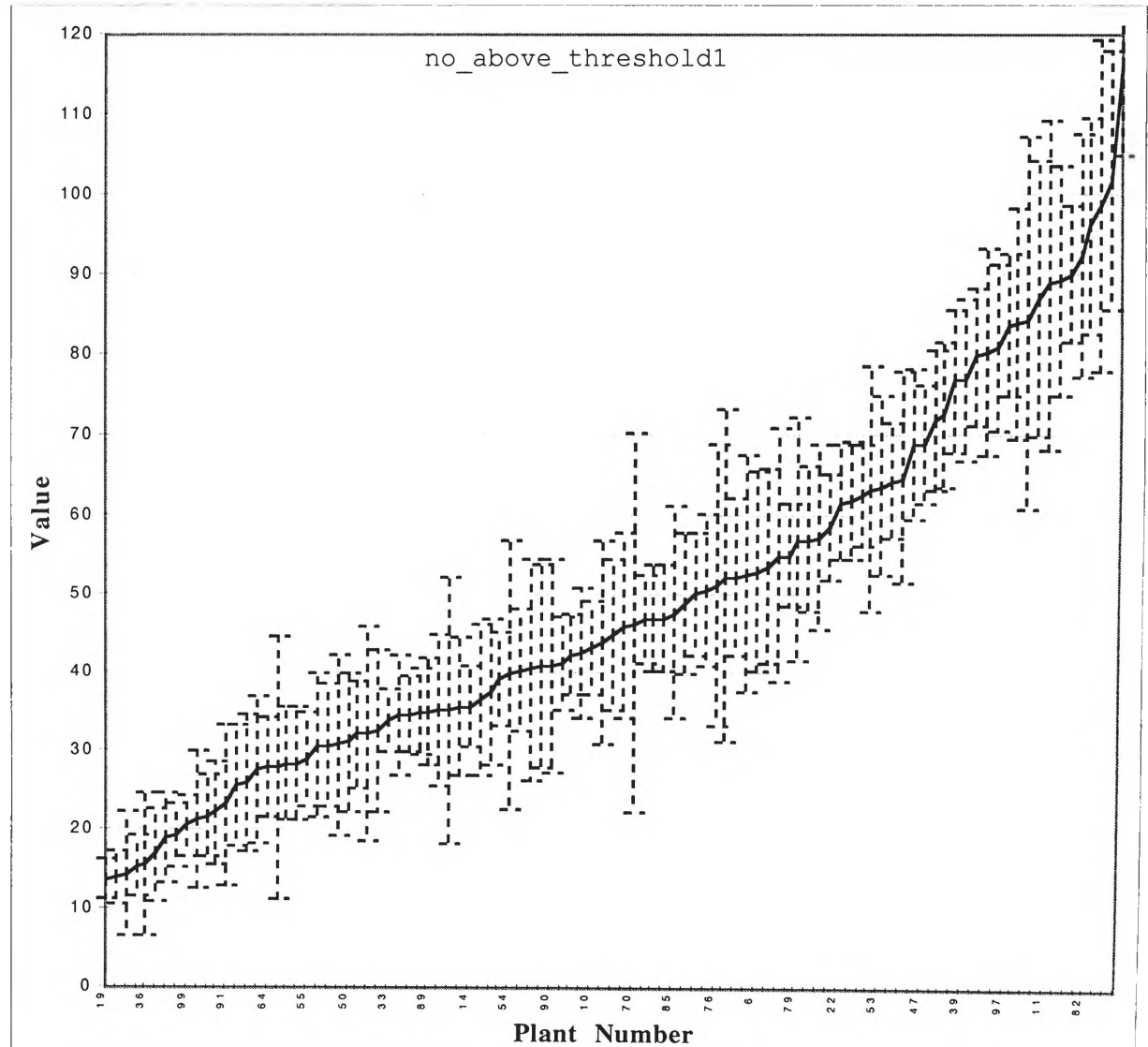
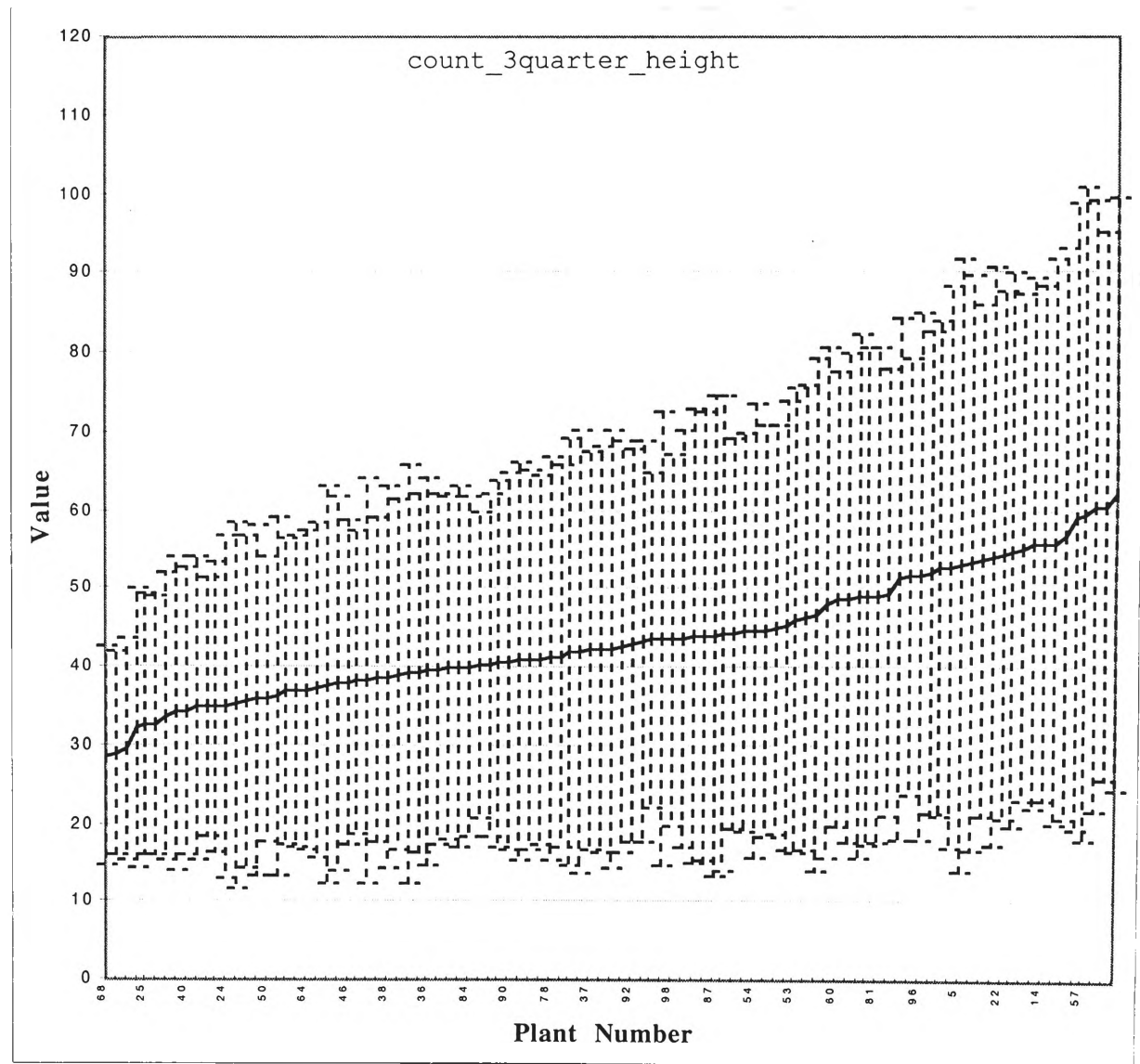


Figure 8.10 Feature 47 (count_3quarter_height) for all 100 plants

No	Name	No	Name
21	<i>Carpentaria acuminata</i>	97	<i>Tabebuia chrystricha</i>
68	<i>Melaleuca styphelioides</i>	43	<i>Eriostemon myoporoides</i>
29	<i>Crinum mauritianum</i>	92	<i>Solanum vescum</i>
79	<i>Polyscias australiana</i>	9	<i>Acacia podalyrifolia</i>
25	<i>Cinnamom oliveri</i>	17	<i>Azalea alba magnifica</i>
30	<i>Crinum pedunculatum</i>	99	<i>Westringia fruticosa</i>
13	<i>Agapanthus praecox</i>	67	<i>Melaleuca quinquenervia</i>
48	<i>Goodia lotifolia</i>	98	<i>Tristaniaopsis collina</i>
76	<i>Pittosporum revolutum</i>	35	<i>Cupaniopsis parvifolia</i>
40	<i>Doryanthes palmeri</i>	47	<i>Ficus rubiginosa</i>
51	<i>Grevillea marmalade</i>	83	<i>Rhododendron bryophyllum</i>
27	<i>Cordyline australis</i>	87	<i>Sarcotoechia heterophylla</i>
2	<i>Acacia cultriformis</i>	91	<i>Solanum laciniatum</i>
24	<i>Casuarina torulosa</i>	54	<i>Howea forsteriana</i>
41	<i>Endiandra introrsa</i>	49	<i>Grevillea baileyana</i>
44	<i>Eucalyptus botryoides</i>	71	<i>Mishocarpus australis</i>
50	<i>Grevillea hilliana</i>	55	<i>Hymenosporum flavum</i>
34	<i>Cupaniopsis anacardioides</i>	77	<i>Pittosporum rhombifolium</i>
6	<i>Acacia longifolia</i>	53	<i>Hakea salicifolia</i>
12	<i>Agapanthus praecox dwarf</i>	75	<i>Pittosporum james</i>
64	<i>Livistona</i> sp. 'Carnarvon'	82	<i>Radermacheria fenecis</i>
3	<i>Acacia falcata</i>	32	<i>Cryptocarya laevigatum</i>
46	<i>Eucalyptus maculata</i>	60	<i>Leptospermum morrisonii</i>
88	<i>Sarcomelicope simplifolia</i>	89	<i>Solanum aviculare</i>
72	<i>Omalanthus populifolius</i>	85	<i>Rhopalostylis baneri</i>
94	<i>Streblis brunonianus</i>	7	<i>Acacia mearnsii</i>
15	<i>Archontophoenix cunninghamiana</i>	81	<i>Polyscias murrayi</i>
69	<i>Microcirtus australis</i>	65	<i>Melaleuca decora</i>
38	<i>Dodonaea triquetra</i>	86	<i>Rhopalostylis sapida</i>
70	<i>Ficus obliqua</i>	56	<i>Indigofera australis</i>
93	<i>Stenocarpus sinuatus</i>	96	<i>Syzygium paniculatum</i>
45	<i>Eucalyptus leucoxydon</i>	26	<i>Citriobatus paucifloris</i>
84	<i>Rhododendron clorinda</i>	11	<i>Acrornychia laevis</i>
23	<i>Casuarina stricta</i>	39	<i>Dodonaea viscosa</i>
36	<i>Diploglottis australis</i>	42	<i>Endiandra pubens</i>
58	<i>Laccospadix australasica</i>	5	<i>Acacia irrorata</i>
31	<i>Cryptocarya bidwilli</i>	33	<i>Cryptocarya williwilliana</i>
19	<i>Banksia ericifolia</i>	61	<i>Leptospermum petersonii</i>
52	<i>Guioa semiglaucula</i>	22	<i>Casuarina glauca</i>
10	<i>Acacia stricta</i>	28	<i>Correa alba</i>
16	<i>Ayrtia distylis</i>	62	<i>Licuala ramsayi</i>
90	<i>Solanum brownii</i>	95	<i>Syzygium leuhmanni</i>
20	<i>Banksia integrifolia</i>	14	<i>Alyxia ruscifolia</i>
66	<i>Melaleuca erubescens</i>	4	<i>Acacia howittii</i>
78	<i>Pittosporum undulatum</i>	74	<i>Pittosporum crassifolium</i>
1	<i>Acacia binervata</i>	73	<i>Phyllanthus albidiflorus</i>
63	<i>Litsea reticulata</i>	57	<i>Jacaranda mimosifolia</i>
80	<i>Polyscias elegans</i>	59	<i>Leptospermum laevigatum</i>
8	<i>Acacia melanoxylon</i>	18	<i>Azalea cultivar splenda</i>
37	<i>Diploglottis campbelli</i>	100	<i>Ziera collina</i>



In Figure 8.10, the entire population of plants have almost the same value with them all overlapping and between 15 and 100. They also have an extremely large range of values within each plant as illustrated by the large standard deviations. This shows that the feature is not consistent through rotation of the plant. Using this feature, none of the 100 plants can be distinguished from any other plant. This feature is so poor that it is unlikely that it would be of any use in combination with the other features so would be a good candidate for removal before wasting time processing it with a classifier.

shows a selection of other features (of the 67) to illustrate the distributions. As you move from the graph in the top left of the figure to the one in the bottom right, the features become progressively worse at separating individual plants.

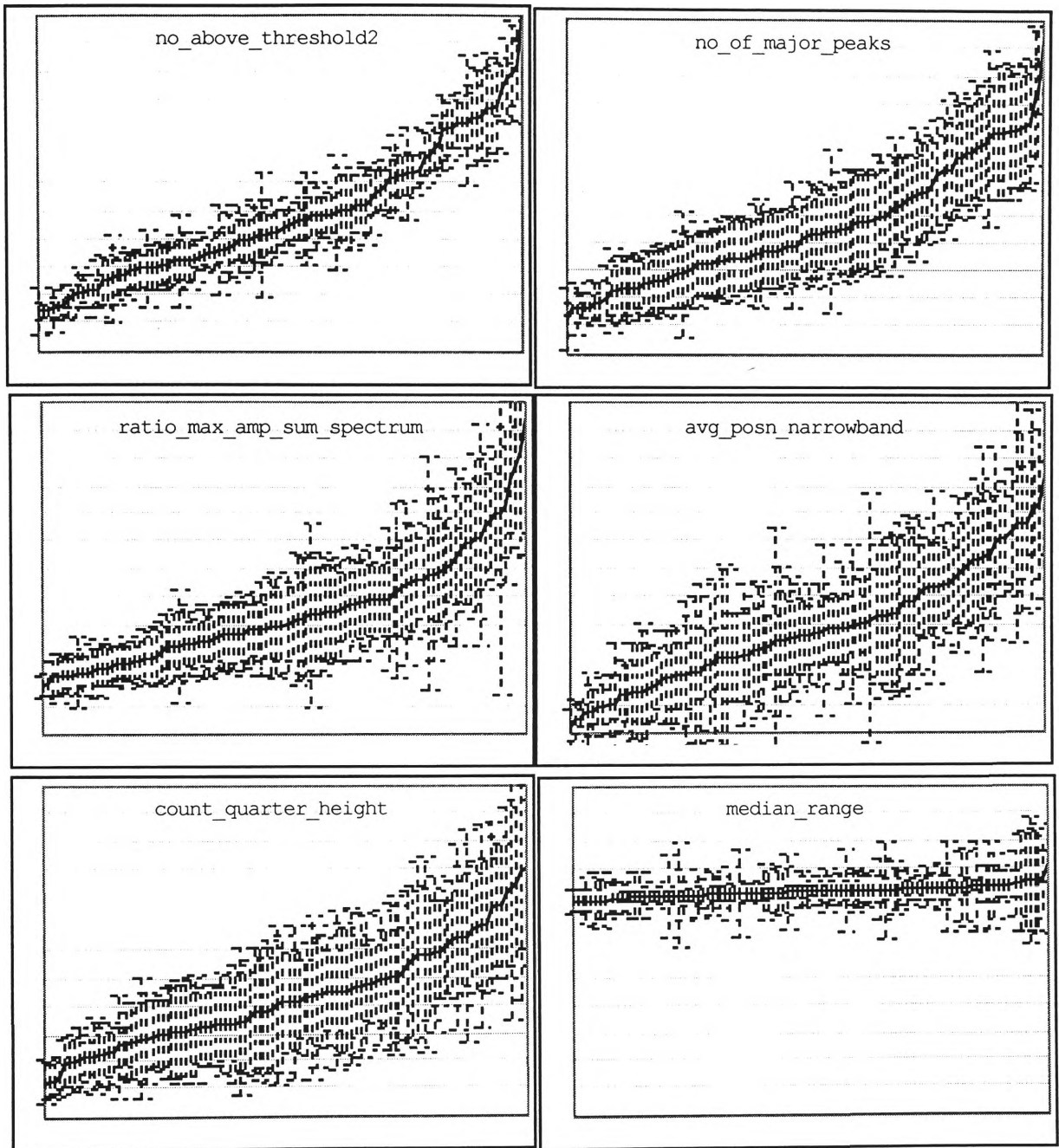


Figure 8.11 Distributions of some values for some different features

When considering features for removal, it is important to consider not only the range of values which different plants have for the feature but also the standard deviations of the plants. In, `count_quarter_height` has a good slope but a bad standard deviation so all of the plant overlap. The converse situation exists for `median_range` where the standard deviations are small but the slope of flat so the plants can not be distinguished. Both of these features are poor but for different reasons, and a measure is required based on these two properties of the distributions to select the best features. The features are considered based on :

- 1 how much they change through rotation - measured by standard deviation;
and
- 2 how well they separate different plants - measured by slope of line.

In order to select the features which are candidates for removal, a separability criterion was developed which considers the slope of the graph and the overlap of the standard deviations.

The plant averages for a particular feature are given by the vector \mathbf{a} :

$$\mathbf{a} = \{a_1, a_2, \dots, a_n\} \text{ where } n \text{ is the number of plants.}$$

Note that for all $a_i, a_i < a_{i+1}$ (ie. the averages are sorted into ascending order).

The standard deviation of the feature for a particular plant is given by the vector \mathbf{s} :

$$\mathbf{s} = \{s_1, s_2, \dots, s_n\} \text{ where } n \text{ is the number of plants}$$

Since the values are ordered, a simple measure would be to compare the difference between the first and last average :

$$d = a_{100} - a_1$$

This does not however, consider the spread of the values (the standard deviation) for that feature over all of the plants. An initial improvement would be to consider the amount of crossover which is obtained when the standard deviation of the first plant is added to its average and the standard deviation of the last plant is subtracted from its average. This is illustrated by

$$d = (a_{100} - s_{100}) - (a_1 + s_1)$$

This is reasonable except for the fact that the plants at either end of the scale are usually so extreme that they could be considered to be outliers. To reduce the effects of the outliers, the standard deviations used can be averaged across the highest 20 plants and the lowest 20 plants. This is illustrated in Equation 8.2.

$$\begin{aligned} \text{separability criterion} &= (\text{avg}(a_{81}, a_{82}, \dots, a_{100}) - \text{avg}(s_{81}, s_{82}, \dots, s_{100})) - \\ &\quad (\text{avg}(a_1, a_2, \dots, a_{20}) - \text{avg}(s_1, s_2, \dots, s_{20})) \end{aligned} \quad \mathbf{8.2}$$

The results can be plotted and thresholds established at the points where the separability drops sharply. Table 8.5 shows the separability criterion for all 67 features

ordered from the highest separability to the lowest (ie. the best feature to the worst according to this criterion).

Table 8.5 Separability criterion for all 67 features

Ran	Sep	Feature Name	No				
k	Crit						
1	45.32	no_above_threshold3	3	46	6.80	count_quarter_height	45
2	45.16	no_above_threshold4	4	47	6.76	variance_amplitude	33
3	44.86	no_above_threshold2	2	48	6.05	percentage_within_thresh7	20
4	43.72	no_above_threshold5	5	49	5.59	ratio_range_stdev_max_amp	55
5	43.29	no_above_threshold1	1	50	2.78	maximum_amplitude	13
6	42.04	no_above_threshold6	6	51	1.80	ratio_range_stdev_length	57
7	39.38	sum_of_density_profile	12	52	-2.38	coefficient_of_var_amplit	34
8	37.76	variance_range	41	53	-8.37	ratio_max_amp_avg	50
9	35.59	no_above_threshold7	7	54	-9.19	average_range	38
10	32.96	front_to_peak_dist	22	55	-9.76	skew_amplitude	36
11	32.83	length_of_density_profile	21	56	-9.76	median_range	39
12	32.52	stdev_range	40	57	-12.26	slope_25_peakA	61
13	32.20	mean_abs_dev_range	43	58	-13.10	count_half_height	46
14	29.47	coeff_of_var_range	42	59	-15.12	skew_range	44
15	28.36	range_75_acoustic_area	66	60	-16.56	repetition_of_layers	23
16	28.27	no_above_threshold8	8	61	-17.96	slope_75_peak	60
17	27.64	no_of_major_peaks2	67	62	-20.36	slope_50_peakA	62
18	26.35	no_of_major_peaks1	11	63	-21.41	slope_25_peak	58
19	22.47	no_above_threshold9	9	64	-22.01	slope_50_peak	59
20	20.77	range_50_acoustic_area	65	65	-23.93	median_amplitude	31
21	19.51	percentage_within_thresh1	14	66	-24.00	slope_75_peakA	63
22	19.47	ratio_range_stdev_avg_amp	56	67	-31.12	count_3quarter_height	47
23	18.49	percentage_within_thresh2	15				
24	18.22	ratio_avg_amp_sum_profile	52				
25	16.88	ratio_range_stdev_sum_pro	54				
26	16.80	mean_abs_dev_amplitude	35				
27	16.63	no_above_threshold10	10				
28	15.44	threshold_data_mass5	28				
29	15.36	percentage_within_thresh3	16				
30	15.24	threshold_data_mass6	29				
31	15.14	threshold_data_mass4	27				
32	15.13	ratio_max_amp_sum_profile	51				
33	15.03	ratio_avg_amp_len	49				
34	15.01	average_amplitude	30				
35	13.99	threshold_data_mass3	26				
36	13.86	ratio_length_sum_profile	53				
37	12.72	range_25_acoustic_area	64				
38	12.62	ratio_max_amp_len	49				
39	12.53	avg_posn_narrowband	37				
40	12.14	percentage_within_thresh4	17				
41	12.01	threshold_data_mass2	25				
42	11.14	stdev_amplitude	32				
43	9.45	percentage_within_thresh5	18				
44	8.81	threshold_data_mass1	24				
45	7.47	percentage_within_thresh6	19				

The measure of separability of features can be used as a guide to the quality of the features. It is not a measure of the absolute quality of the feature as it does not consider relationships which may exist in higher dimensions but it can indicate the features which are poor and need not be considered. Figure 8.12 is a graph of the separability criterion by feature in the same order as the table above. The quality of the features reduce from left to right and sudden drops in the separability criterion indicate places where features after the drop are significantly less useful than the features immediately preceding the drop. Some of these drops are highlighted on the graph with vertical dashed lines. These drops highlighted with vertical dashed lines indicate the best places for differentiating between good and poor features using this separability criterion.

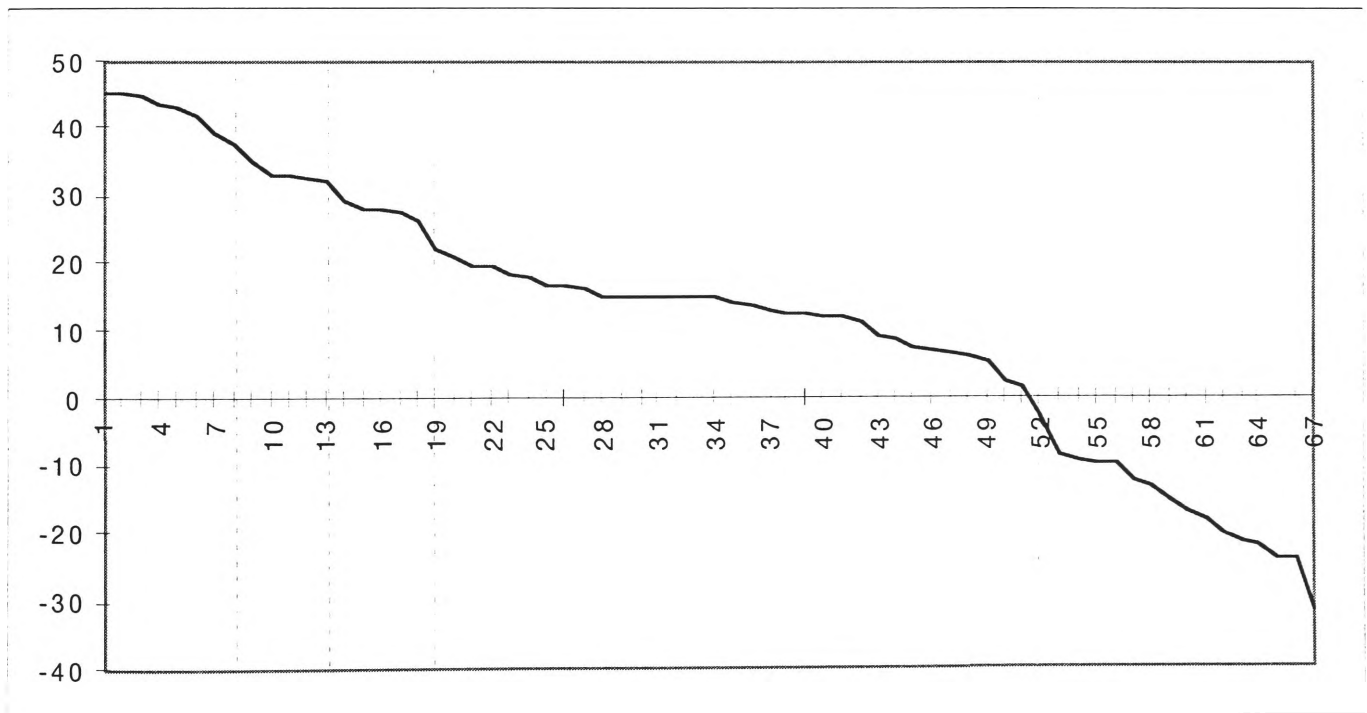


Figure 8.12 Separability criterion by feature

There are several potential points for choosing features indicated by the dashed lines. I chose the point at around feature 19 to be the cut off line to be a trade off between too many features and losing too much discriminatory information. Since this feature reduction technique simply identifies poor features and does not consider higher dimension relationships between the variables, good information could be discarded by

keeping too few features. Similarly, to keep too many features would result in significant computations and possible over fitting of the data to the training sets.

These first 19 features are the ones which will be considered for further analysis and are shown in Table 8.6.

Table 8.6 The features which characterise plant acoustic density profiles

Feature	Description
no_above_threshold1 - 9	These features are counts of the number of range cells in the acoustic density profile at a specified threshold t , where $t = 59 * m / 10000, 78 * m / 10000, 98 * m / 10000, 117 * m / 10000, 156 * m / 10000, 195 * m / 10000, 295 * m / 10000, 300 * m / 10000, 490 * m / 10000$ and $580 * m / 10000$ mV (where m is the calibration measure). These features give an indication of the magnitude of the reflections at different ranges. This is related to the size and specularity of the leaves, the number of leaves, and the orientation of the leaves.
sum_of_density_profile	This is the sum of all of the range cells in the acoustic density profile and indicates the properties over the entire plant. This is equal to the acoustic normal area.
variance_range, stdev_range, mean_abs_dev_range, coeff of var range	These features measure the variation of the detected reflections from the central point of the acoustic density profile. It is an indicator of the spread of ranges over which a signal is received.
front_to_peak_dist	This is the distance from the first detectable surface to the surface with the highest amplitude. This indicates the rate at which the foliage builds up over subsequent range cells. This shows how quickly the leaves become dense.
length_of_density_profile	This is a measure of the range over which reflections are detected. In the case of sparse plants, it gives the depth of the plant. The acoustic depth.
range_75_acoustic_area	The range cell from the first detected reflecting surface where 75% of the sum of the acoustic density profile is accumulated. This is a measure of the compactness of the plant.
no_of_major_peaks1, no_of_major_peaks2	A range line is a major peak if its amplitude is greater than $195 / m$ mV and five of the range lines (17.2 mm) on each side of it are less than it. It is a count of range cells which have reflections significantly stronger than those around it and is a measure of the grouping of leaves. Note that no_of_major_peaks2 is the same except that the amplitude has to be greater than $156 * m / 10000$ mV to be counted.

The features tabled, measure different properties of the pattern (acoustic density profile). The following features measure the reflective surfaces within the field of audition. They contain information about the size, number and orientation of the visible surfaces :

```
no_above_threshold1 - 9;
sum_of_density_profile; and
```

no_of_major_peaks1 - 2.

The following features are a measure of how the surfaces are distributed within the acoustic density profile:

variance_range;
stdev_range;
mean_abs_dev_range;
coeff_of_var_range;
front_to_peak_dist;
length_of_density_profile; and
range_75_acoustic_area.

The feature filtering has removed all of the features which are either poor discriminators or change significantly depending on the orientation from which the plant is insonified. Feature which are kept are those which may be useful for plant classification. In the following sections, the performance of the features will be analysed using local and global correlation.

8.5 Local correlation using features

In Chapters 6 and 7, correlation was used to show how the acoustic density profile changes through a change in orientation of the plant specimen. In this section, the 19 scaled features are analysed using local correlation (Table 8.7). The average correlation is 0.88 with a standard deviation of 0.04, a maximum of 0.97 and a minimum of 0.72. This is significantly better than the raw data which was detailed in Chapter 6 (average 0.80, or average 0.84 with echo tracking). The standard deviation is also significantly lower within each of the plants than with the raw data. Unlike the correlation using the raw acoustic density profile, large and small leaf plants; sparse and dense plants are distributed throughout the range of values because the features characterise all types of plants well. The correlation of features provides a better picture of how consistent the plants reflect the signal through changes of orientation.

Table 8.7 Correlations adjacent feature vectors - average and standard deviation

<i>Azalea cultivar splenda</i>	0.93	0.08	<i>Archontophoenix</i>	0.88	0.12
<i>Leptospermum laevigatum</i>	0.93	0.08	<i>cunninghamiana</i>		
<i>Endiandra pubens</i>	0.93	0.08	<i>Polyscias australiana</i>	0.88	0.12
<i>Pittosporum crassifolium</i>	0.93	0.08	<i>Crinum mauritianum</i>	0.88	0.14
<i>Acacia binervata</i>	0.93	0.07	<i>Acacia falcata</i>	0.88	0.14
<i>Tabebula chrystricha</i>	0.93	0.08	<i>Acacia mearnsii</i>	0.88	0.10
<i>Acacia irrorata</i>	0.93	0.08	<i>Rhododendron bryophyllum</i>	0.88	0.11
<i>Diploglottis campbelli</i>	0.92	0.08	<i>Azalea alba magnifica</i>	0.88	0.15
<i>Radermacheria fenecis</i>	0.92	0.08	<i>Livistona sp 'Carnarvon'</i>	0.88	0.14
<i>Cryptocarya laevigatum</i>	0.92	0.08	<i>Guioa semiglauc</i>	0.87	0.10
<i>Correa alba</i>	0.92	0.08	<i>Litsea reticulata</i>	0.87	0.13
<i>Acronychia laevis</i>	0.92	0.08	<i>Cupaniopsis anacardioides</i>	0.87	0.12
<i>Jacaranda mimosifolia</i>	0.92	0.08	<i>Pittosporum undulatum</i>	0.86	0.12
<i>Acacia howittii</i>	0.92	0.08	<i>Laccospadix australasica</i>	0.86	0.12
<i>Ficus rubiginosa</i>	0.92	0.09	<i>Pittosporum revolutum</i>	0.86	0.16
<i>Sarcotoechia heterophylla</i>	0.92	0.09	<i>Acacia cultriformis</i>	0.86	0.11
<i>Casuarina glauca</i>	0.92	0.08	<i>Cordyline australis</i>	0.86	0.12
<i>Polyscias murrayi</i>	0.91	0.09	<i>Rhopalostylis baneri</i>	0.86	0.15
<i>Melaleuca quinquenervia</i>	0.91	0.09	<i>Solanum brownii</i>	0.86	0.12
<i>Leptospermum petersonii</i>	0.91	0.08	<i>Solanum vescum</i>	0.86	0.12
<i>Hakea salicifolia</i>	0.91	0.09	<i>Eucalyptus leucoxylon</i>	0.86	0.17
<i>Banksia integrifolia</i>	0.91	0.10	<i>Hymenosporum flavum</i>	0.86	0.11
<i>Licuala ramsayi</i>	0.91	0.09	<i>Goodia lotifolia</i>	0.86	0.12
<i>Acacia podalyrifolia</i>	0.91	0.09	<i>Eucalyptus maculata</i>	0.85	0.18
<i>Polyscias elegans</i>	0.91	0.09	<i>Solanum aviculare</i>	0.85	0.11
<i>Dodonaea viscosa</i>	0.91	0.09	<i>Grevillea hilliana</i>	0.85	0.12
<i>Phyllanthus albiflorus</i>	0.91	0.09	<i>Banksia ericifolia</i>	0.85	0.12
<i>Acacia melanoxylon</i>	0.91	0.09	<i>Acacia longifolia</i>	0.85	0.14
<i>Ziera collina</i>	0.91	0.09	<i>Ficus obliqua</i>	0.85	0.14
<i>Endiandra introrsa</i>	0.90	0.09	<i>Agapanthus praecox</i>	0.85	0.13
<i>Szygium paniculatum</i>	0.90	0.09	<i>Tristaniopsis collina</i>	0.85	0.11
<i>Pittosporum james</i>	0.90	0.09	<i>Cupaniopsis parvifolia</i>	0.84	0.13
<i>Citriobatus paucifloris</i>	0.90	0.09	<i>Microcitrus australis</i>	0.84	0.14
<i>Szygium leuhmanni</i>	0.90	0.09	<i>Eucalyptus botryoides</i>	0.84	0.14
<i>Casuarina torulosa</i>	0.90	0.09	<i>Stenocarpus sinuatus</i>	0.83	0.14
<i>Casuarina stricta</i>	0.90	0.09	<i>Cryptocarya bidwilli</i>	0.83	0.13
<i>Doryanthes palmeri</i>	0.90	0.09	<i>Omalanthus populifolius</i>	0.82	0.16
<i>Grevillea baileyana</i>	0.90	0.09	<i>Howea forsteriana</i>	0.81	0.22
<i>Indigofera australis</i>	0.90	0.09	<i>Melaleuca styphelioides</i>	0.81	0.14
<i>Dodonaea triquetra</i>	0.90	0.10	<i>Westringa fruticosa</i>	0.81	0.14
<i>Streblis brunonianus</i>	0.89	0.09	<i>Solanum laciniatum</i>	0.80	0.17
<i>Sarcomelicope simplifolia</i>	0.89	0.10	<i>Ayrtera distylis</i>	0.80	0.16
<i>Acacia stricta</i>	0.89	0.09	<i>Carpentaria acuminata</i>	0.80	0.18
<i>Melaleuca decora</i>	0.89	0.09	<i>Melaleuca erubescens</i>	0.80	0.15
<i>Alyxia ruscifolia</i>	0.89	0.09	<i>Agapanthus praecox dwarf</i>	0.80	0.20
<i>Mishocarpus australis</i>	0.89	0.09	<i>Cinnamom oliveri</i>	0.79	0.16
<i>Pittosporum rhombifolium</i>	0.89	0.10	<i>Rhododendron clorinda</i>	0.79	0.23
<i>Eriostemon myoporoides</i>	0.89	0.09	<i>Crinum pedunculatum</i>	0.78	0.21
<i>Cryptocarya williwilliana</i>	0.88	0.10	<i>Grevillea marmalade</i>	0.78	0.25
<i>Leptospermum morrisonii</i>	0.88	0.09	<i>Diploglottis australis</i>	0.72	0.26
<i>Rhopalostylis sapida</i>	0.88	0.14			

Local correlation can be graphed to get a picture of how the correlations change through rotation and this is shown in Figure 8.13 for the selected eight plants. Figure 8.14 shows the same information with the local correlation of the raw acoustic density profile from Figure 6.4. The figure shows that the local correlation is better using features than it is with the raw acoustic density profile as input.

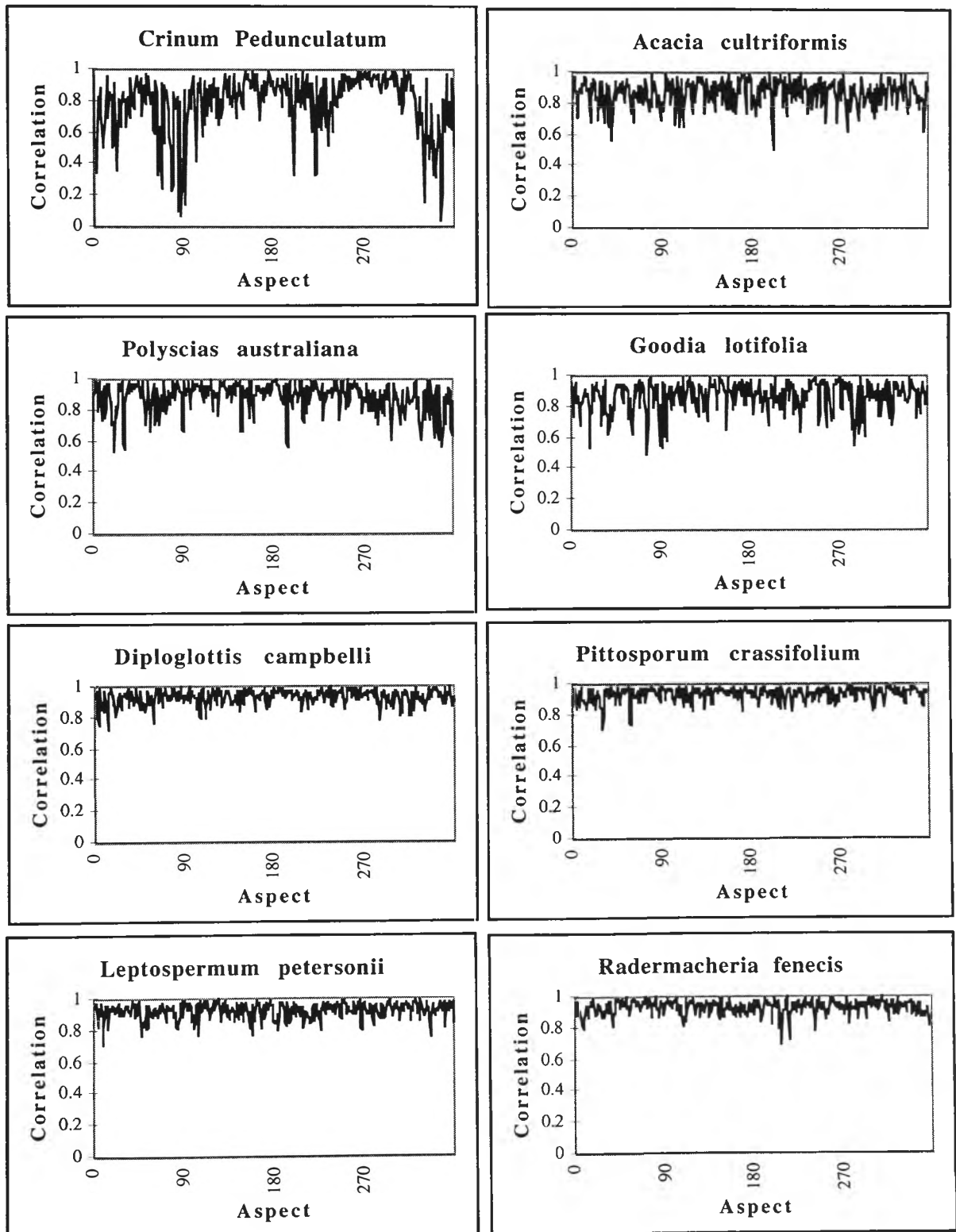


Figure 8.13 Local correlation for the eight plants using all 19 features

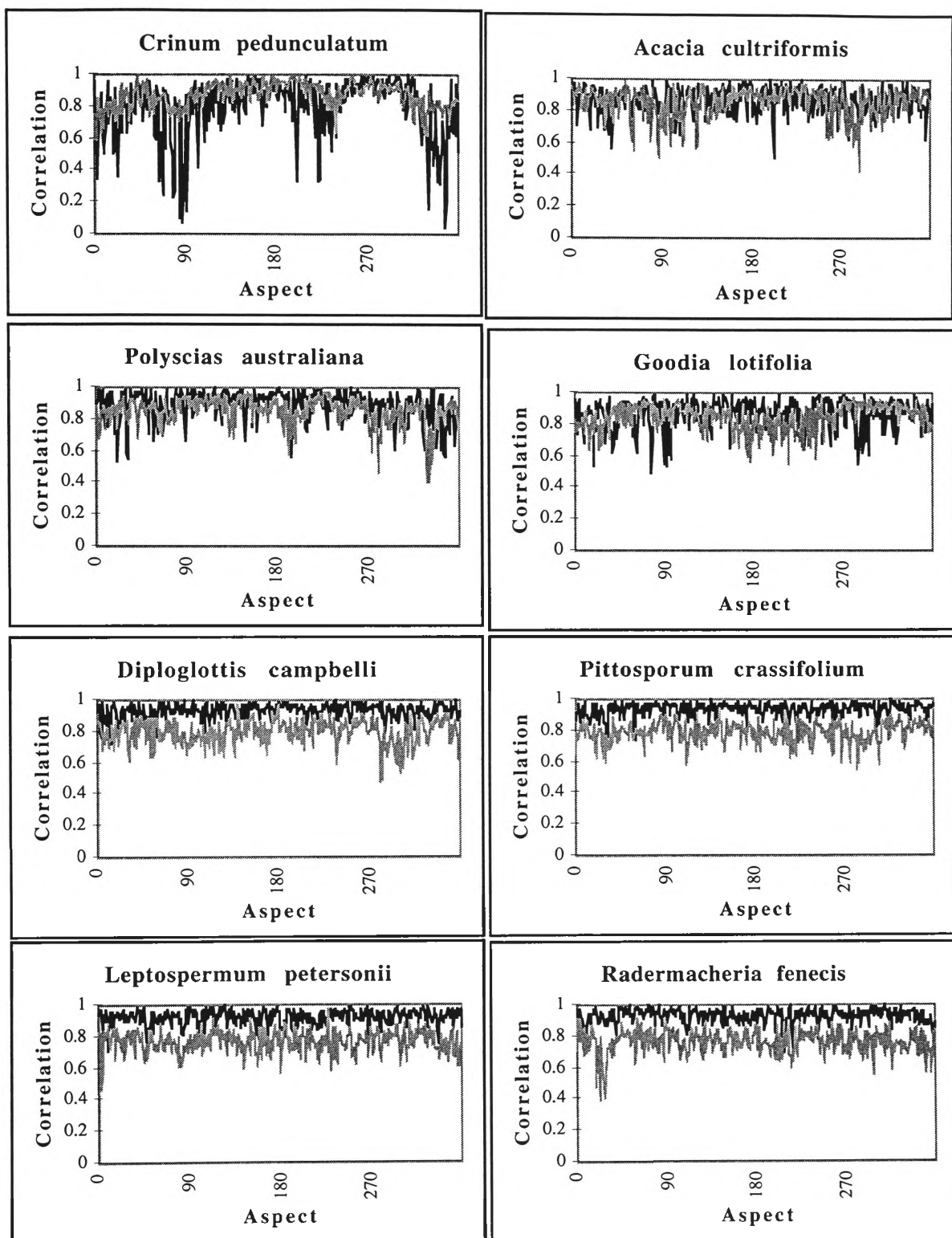


Figure 8.14 Local correlation for the eight plants using 19 features (black) and the raw acoustic density profile (grey) from Figure 6.4

8.6 Global Correlation using features

Global correlation can also be calculated for the features. The same eight plants with orientation 256 as the reference point are shown in Figure 8.15. The most important characteristic of the graph is that there is not a gradual reduction in the correlation with

increasing reference point separation as there was for global correlation with the raw acoustic density profile in Chapter 7. The correlation is more consistent throughout the entire revolution.

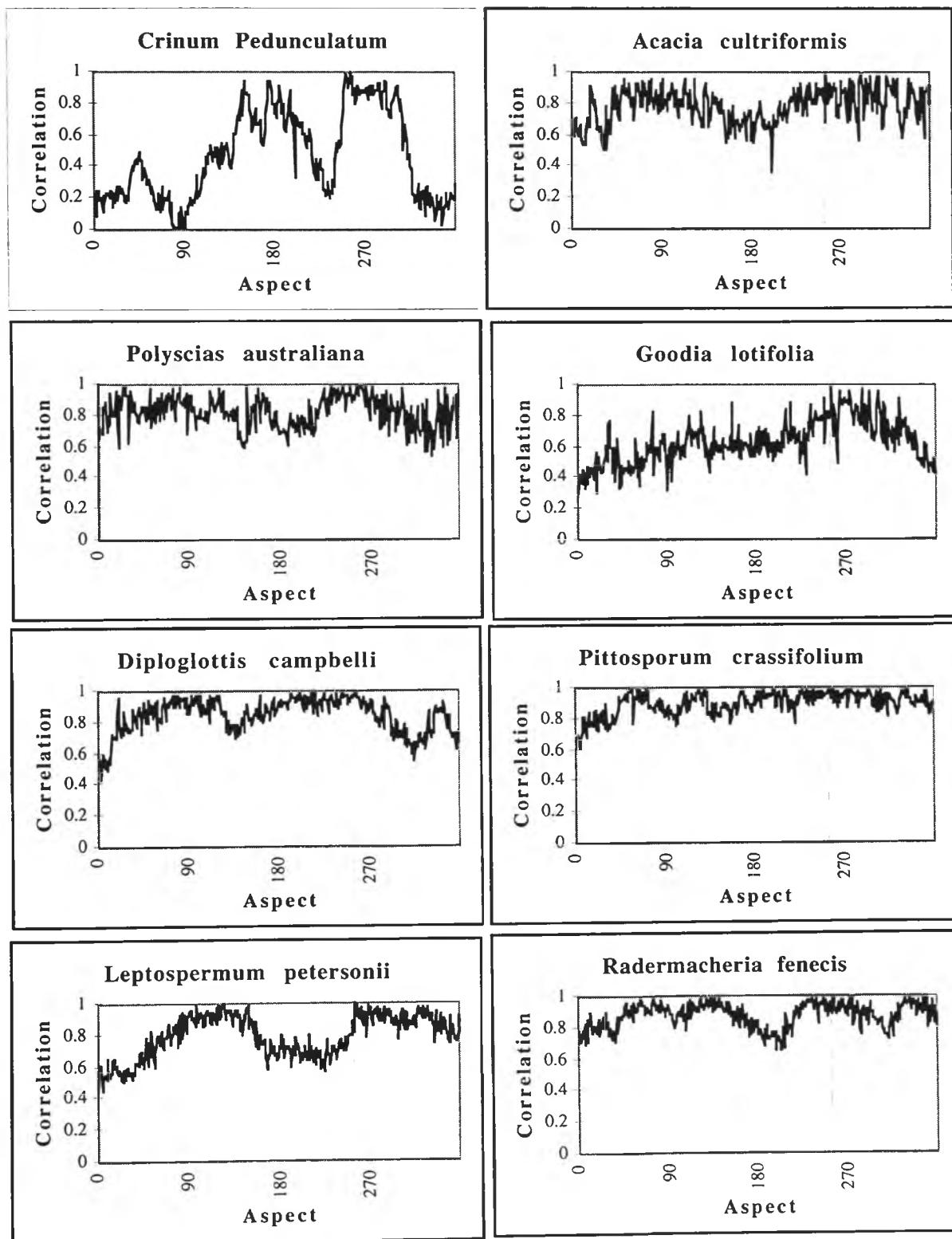


Figure 8.15 Correlations for eight plants using orientation 256 as the reference

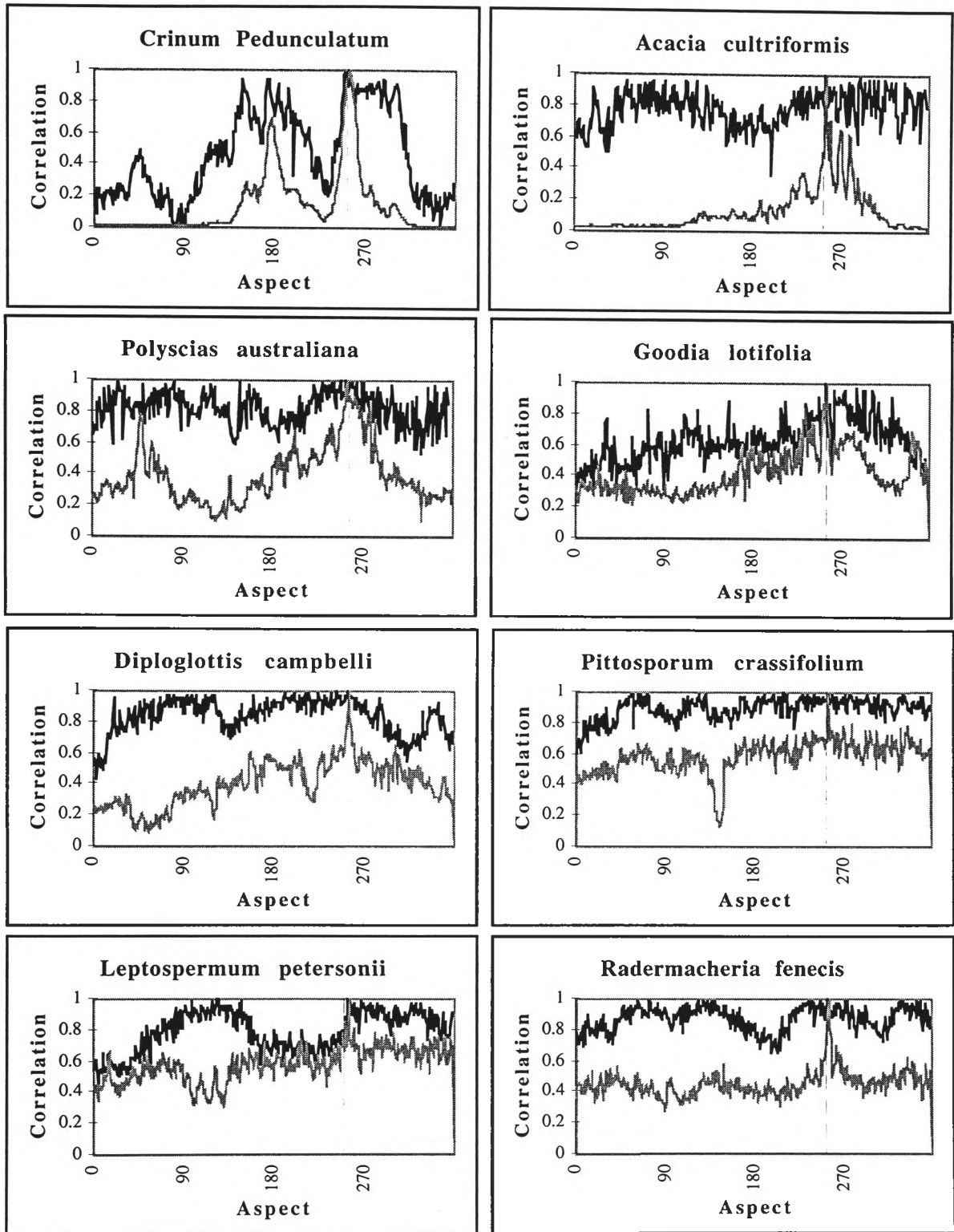


Figure 8.16 Correlation for eight plants using orientation 256 as the reference - black is the feature data and grey is the raw acoustic density profile (Figure 7.1)

Figure 8.16 shows the global correlation using orientation 256 as the reference for both the raw acoustic density profile and the calculated features. The features are significantly better than the raw acoustic density profile which means that they capture more rotation invariant information from the acoustic density profile.

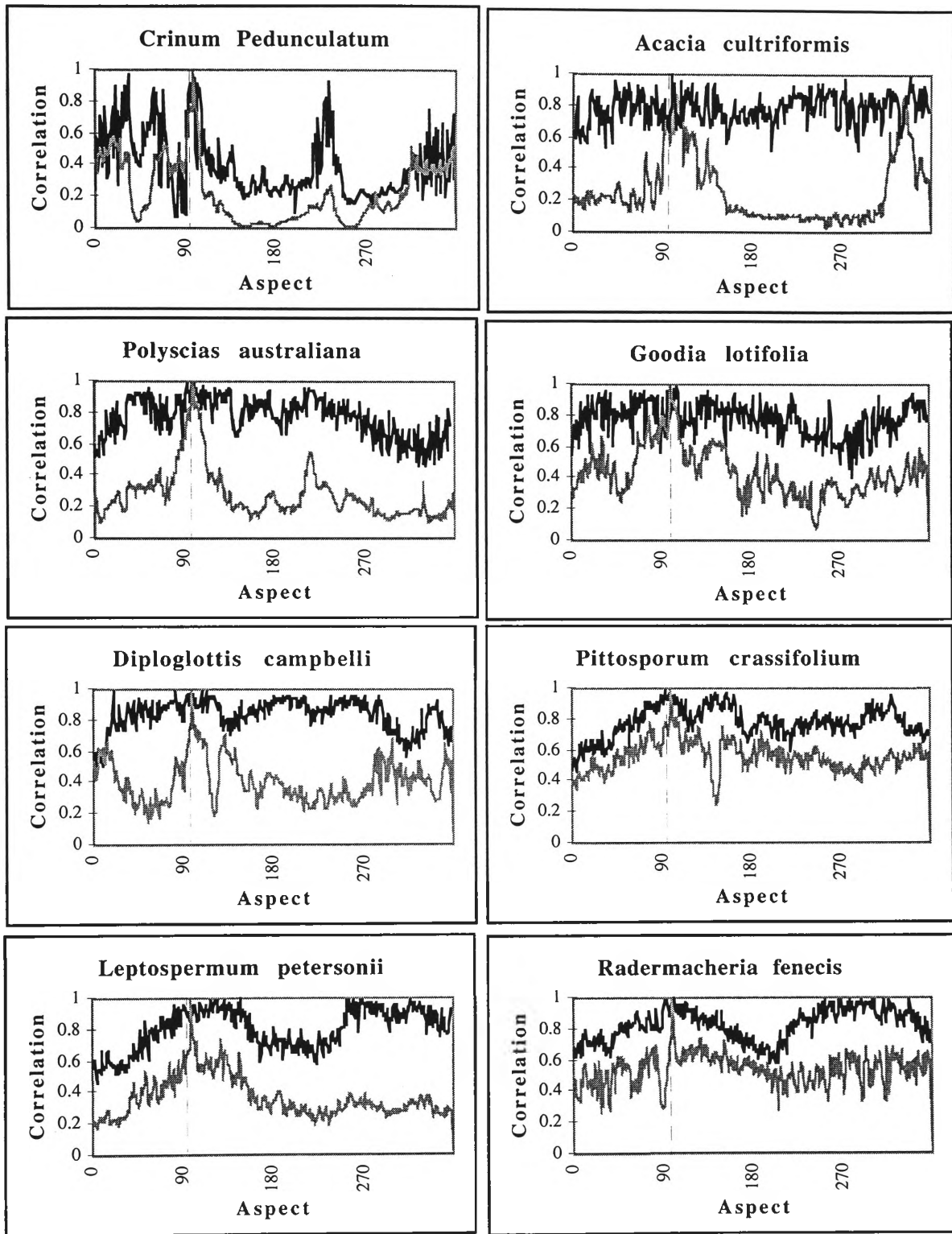


Figure 8.17 Correlation for the eight plants using orientation 100 as the reference - black is the feature data and grey is the raw acoustic density profile

8.7 Global correlation using a template - Template Correlation

Instead of selecting a particular orientation as the reference point, a template can be built which attempts to represent the features through rotation. The template is simply the average of all of the features for a particular plant for all 360 orientations. The template characterises the features and is used as the reference orientation. Each of the 360 orientations are then correlated against this template.

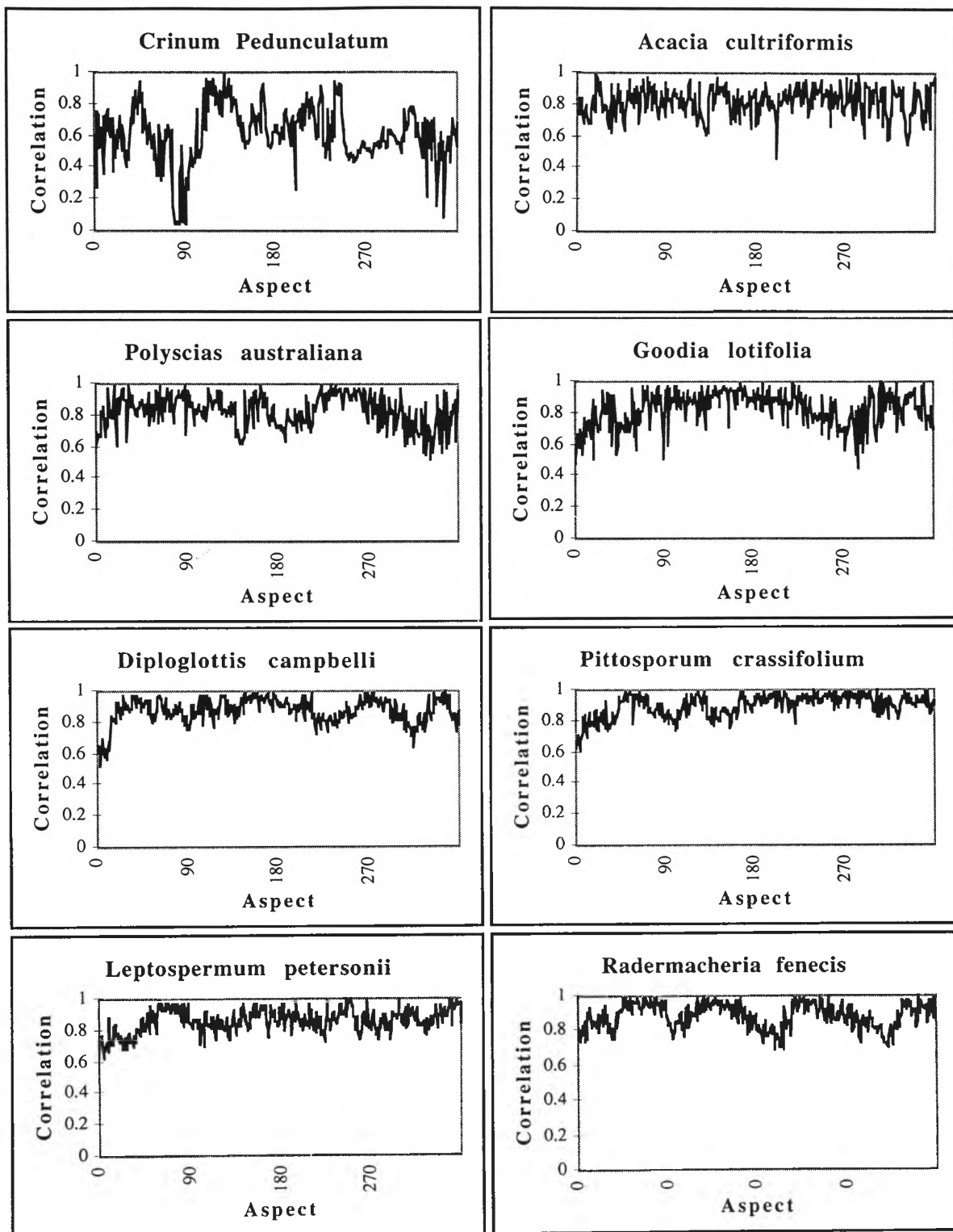


Figure 8.18 Correlation for eight plants using the template as the reference

All of the plants can be correlated against their templates as outlined above and the results are shown in Table 8.8. This is a more realistic measure of how the plants change through rotation because the template represents the features over all orientations. The plants at the top of the list are the ones which return consistent signals through rotation and the ones lower down in the table are less consistent.

The plants at the top of the table have a large number of leaves and no minor branches. There are plenty of surfaces to reflect signals. Plants with less leaves have a smaller amount of signal to return which means that some orientations return strong signals from leaves, while at other orientations, they produce no signal at all. Some sparse plants can however be consistent through rotation provided that there are no branches protruding from their trunk.

Table 8.8 Correlation against templates - average and standard deviation

<i>Leptospermum laevigatum</i>	0.92	0.08	<i>Rhododendron bryophyllum</i>	0.85	0.11
<i>Szygium leuhmanni</i>	0.92	0.09	<i>Pittosporum james</i>	0.85	0.11
<i>Tabebuia chrystricha</i>	0.91	0.09	<i>Indigofera australis</i>	0.84	0.11
<i>Jacaranda mimosifolia</i>	0.90	0.09	<i>Polyscias elegans</i>	0.84	0.11
<i>Cryptocarya laevigatum</i>	0.90	0.09	<i>Casuarina torulosa</i>	0.84	0.10
<i>Acacia howittii</i>	0.90	0.09	<i>Hymenosporum flavum</i>	0.84	0.11
<i>Cryptocarya williwilliana</i>	0.90	0.09	<i>Acacia irrorata</i>	0.84	0.11
<i>Correa alba</i>	0.90	0.09	<i>Litsea reticulata</i>	0.83	0.12
<i>Pittosporum crassifolium</i>	0.89	0.10	<i>Acacia podalyrifolia</i>	0.83	0.11
<i>Ziera collina</i>	0.89	0.09	<i>Streblis brunonianus</i>	0.83	0.12
<i>Melaleuca quinquenervia</i>	0.89	0.10	<i>Banksia ericifolia</i>	0.83	0.11
<i>Acacia binervata</i>	0.88	0.08	<i>Endiandra pubens</i>	0.83	0.11
<i>Dodonaea triquetra</i>	0.88	0.10	<i>Polyscias australiana</i>	0.83	0.12
<i>Endiandra introrsa</i>	0.88	0.10	<i>Acacia melanoxylon</i>	0.83	0.11
<i>Radermacheria fenecis</i>	0.88	0.10	<i>Pittosporum undulatum</i>	0.83	0.12
<i>Grevillea baileyana</i>	0.88	0.09	<i>Stenocarpus sinuatus</i>	0.82	0.13
<i>Sarcotoechia heterophylla</i>	0.88	0.10	<i>Cordyline australis</i>	0.82	0.12
<i>Casuarina glauca</i>	0.88	0.09	<i>Goodia lotifolia</i>	0.82	0.13
<i>Melaleuca decora</i>	0.88	0.10	<i>Cupaniopsis anacardioides</i>	0.82	0.12
<i>Licuala ramsayi</i>	0.88	0.10	<i>Melaleuca styphelioides</i>	0.82	0.13
<i>Ficus rubiginosa</i>	0.87	0.10	<i>Acacia cultriformis</i>	0.81	0.11
<i>Casuarina stricta</i>	0.87	0.09	<i>Acacia longifolia</i>	0.81	0.13
<i>Diploglottis campbelli</i>	0.87	0.10	<i>Omalanthus populifolius</i>	0.81	0.14
<i>Alyxia ruscifolia</i>	0.87	0.10	<i>Pittosporum revolutum</i>	0.81	0.13
<i>Dodonaea viscosa</i>	0.87	0.10	<i>Guioa semiglauca</i>	0.81	0.11
<i>Phyllanthus albiflorus</i>	0.87	0.09	<i>Tristaniopsis collina</i>	0.81	0.12
<i>Citriobatus paucifloris</i>	0.87	0.10	<i>Acrornychia laevis</i>	0.80	0.10
<i>Polyscias murrayi</i>	0.86	0.10	<i>Melaleuca erubescens</i>	0.80	0.13
<i>Solanum aviculare</i>	0.86	0.10	<i>Eucalyptus botryoides</i>	0.79	0.13
<i>Pittosporum rhombifolium</i>	0.86	0.10	<i>Laccospadix australasica</i>	0.79	0.12
<i>Azalea cultivar splenda</i>	0.86	0.11	<i>Westringa fruticosa</i>	0.79	0.12
<i>Sarcomelicope simplifolia</i>	0.86	0.11	<i>Azalea alba magnifica</i>	0.79	0.15
<i>Szygium paniculatum</i>	0.86	0.10	<i>Eucalyptus maculata</i>	0.78	0.16
<i>Leptospermum morrisonii</i>	0.86	0.10	<i>Grevillea hilliana</i>	0.78	0.13
<i>Mishocarpus australis</i>	0.86	0.10	<i>Cupaniopsis parvifolia</i>	0.78	0.13
<i>Acacia mearnsii</i>	0.86	0.10	<i>Cinnamom oliveri</i>	0.78	0.14
<i>Eriostemon myoporoides</i>	0.86	0.10	<i>Livistona sp 'Carnarvon'</i>	0.78	0.19
<i>Leptospermum petersonii</i>	0.86	0.10	<i>Doryanthes palmeri</i>	0.78	0.14
<i>Acacia stricta</i>	0.85	0.10	<i>Rhopalostylis sapida</i>	0.78	0.15
<i>Hakea salicifolia</i>	0.85	0.10	<i>Microcitrus australis</i>	0.78	0.15

<i>Rhopalostylis baneri</i>	0.77	0.15	<i>Crinum mauritianum</i>	0.72	0.19
<i>Cryptocarya bidwilli</i>	0.77	0.14	<i>Carpentaria acuminata</i>	0.70	0.14
<i>Archontophoenix cunninghamiana</i>	0.77	0.14	<i>Rhododendron clorinda</i>	0.70	0.18
<i>Solanum vescum</i>	0.77	0.13	<i>Diploglottis australis</i>	0.70	0.22
<i>Banksia integrifolia</i>	0.77	0.14	<i>Agapanthus praecox dwarf</i>	0.69	0.18
<i>Acacia falcata</i>	0.77	0.17	<i>Solanum laciniatum</i>	0.68	0.19
<i>Eucalyptus leucoxylon</i>	0.76	0.19	<i>Ficus obliqua</i>	0.67	0.20
<i>Solanum brownii</i>	0.74	0.14	<i>Ayrtera distylis</i>	0.67	0.20
<i>Howea forsteriana</i>	0.74	0.22	<i>Grevillea marmalade</i>	0.66	0.20
<i>Agapanthus praecox</i>	0.73	0.14	<i>Crinum pedunculatum</i>	0.61	0.18

8.8 Properties of the features through rotation

The feature data captures the properties of the acoustic density profile which are relatively rotation invariant. The features are measures of different properties of the raw acoustic density profile and do not vary considerably with a change in orientation like the raw data. The graphs show that the correlation of signals from adjacent orientations are high compared to the raw acoustic density profile and the correlation values calculated using the features do not reduce significantly with rotation. This means that it is considerably easier to use them to identify plants from any orientation.

8.9 Correlation between different plants

It was shown in Section 8.5 that features are much more consistent through rotation of the plant than the raw acoustic density profile. The other important piece of information about the features is how they correlate with different plants. That is, for features to be good discriminators, not only do they have to be highly correlated for different orientations of the same plant but they must also have a low correlation with echoes from other plants.

A template was created for each plant (as in Section 8.5) and this was correlated against all of the records for the 99 other plants in the database and the average correlation was calculated. The results are shown in Table 8.9. The rows represent the templates which are created for each plant and the columns are the data set of 360 orientations. So for example, the value in the cell at the intersection of row number 19 (*Banksia ericifolia*) and column number four (*Acacia howitti*) gives the average correlation of correlating the template of *Banksia ericifolia* with all of the records of *Acacia howitti*. The value in row

number four and column number 19 is the result of correlating the template of *Acacia howitti* with all of the records from *Banksia ericifolia*. The way that the data in the table were calculated is illustrated in Figure 8.19.

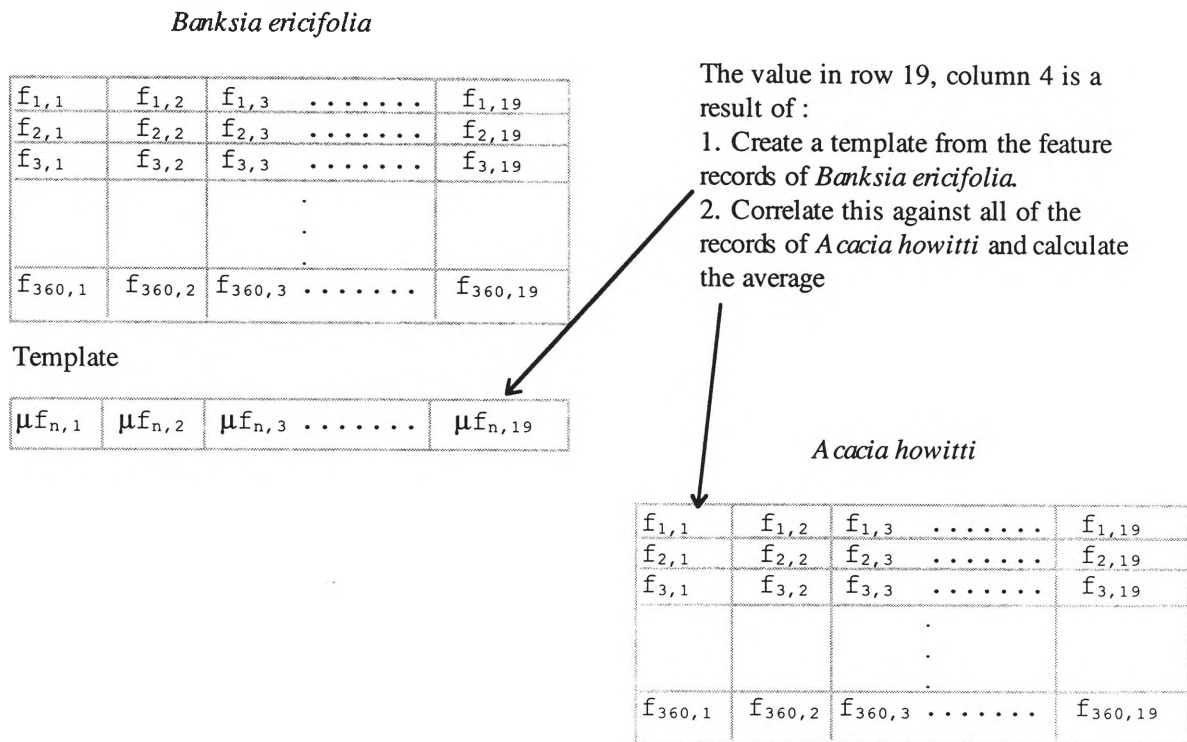
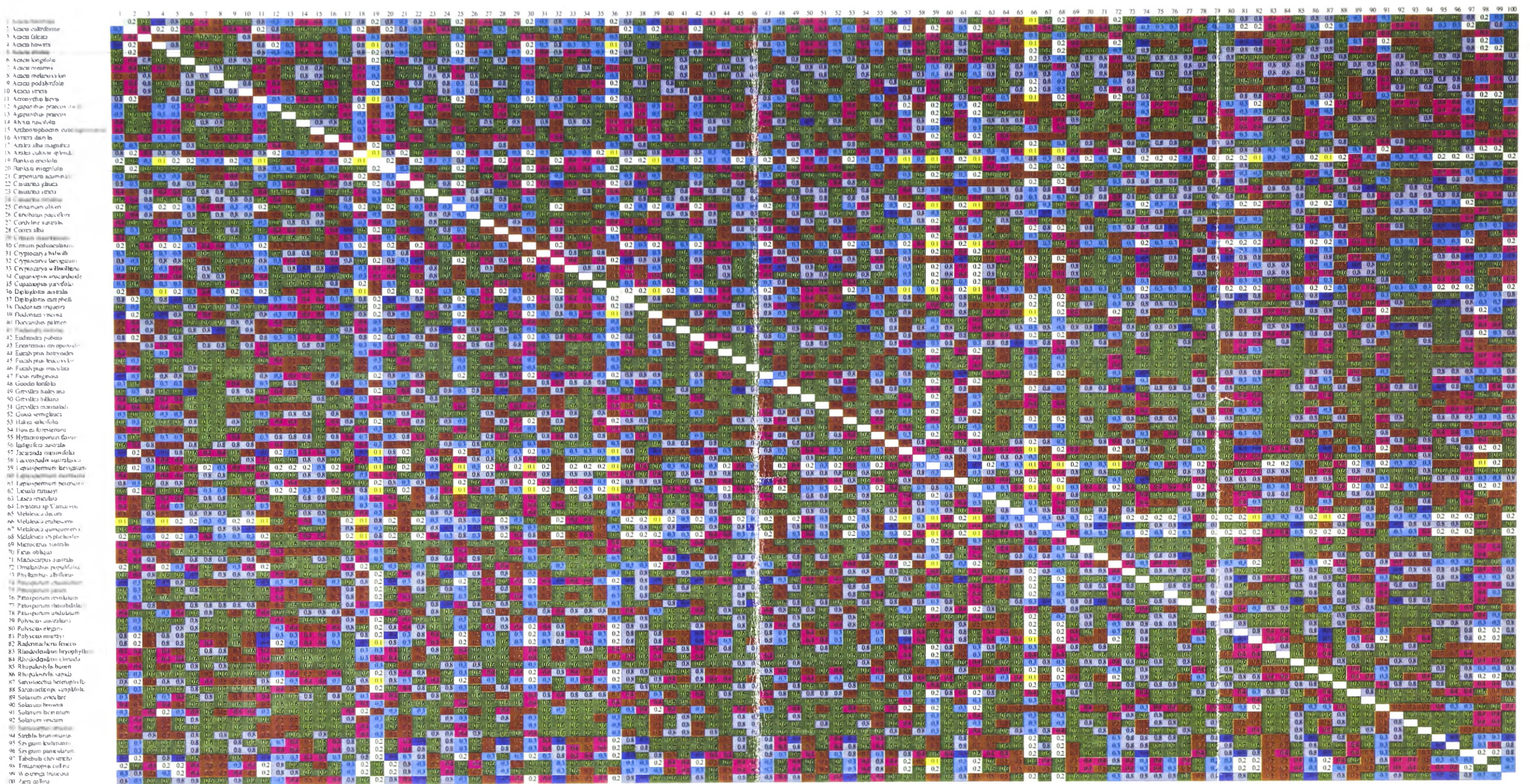


Figure 8.19 The interpretation of Table 8.9

The most favourable result is the lowest result as this means that it is unlikely that a record from one plant will be mis-interpreted as one from another plant. The low result (0.1 for these two plants when both *Banksia ericifolia* and *Acacia howitti* are used as the template) is aided by the fact that these two plants are extremely well correlated over successive orientations ie. *Banksia ericifolia* is correlated at 0.83 and *Acacia howitti* is correlated at 0.9 over all orientations (Table 8.8), that is, both of the plants are rotationally invariant.

In Table, the correlations greater than 0.7 are highlighted. This shows that the feature data produced for these plants are similar to each other, so the plants appear similar to the sensor based on these calculated features.

Table 8.9 Correlation between the templates of all 100 plants



8.10 Conclusion

In this chapter, feature extraction was discussed and 67 features were calculated from the acoustic density profile. The aim of the features is to characterise the pattern of the range information so that it is immune to minor perturbations such as small range and amplitude variations between adjacent samples. The features were analysed and reduced to a group of 19 features which will be considered for further analysis. Local correlation, global correlation and template correlation were performed on the thesis and results tabulated.

The features are more representative of the plants than the raw acoustic density profile and will be analysed further in Chapter 9. In Chapter 10, classification of different plants is performed before the applications of this thesis are summarised in Chapter 11.

8.11 Summary

1. Features can simply characterise complex patterns.
2. Feature reduction techniques can limit the search space by eliminating poor features.
3. Features characterise the plants well through orientation changes.

CLASSIFICATION OF PLANTS BY THE INTERPRETATION OF CTFM SONAR DATA

A thesis submitted in fulfilment of the requirements for the award of the degree of

DOCTOR OF PHILOSOPHY

(Computer Science)

from

UNIVERSITY OF WOLLONGONG

by

Neil Lindsay Harper, BMath W'Gong, MCompSci W'Gong

School of Information Technology and Computer Science

1999

9. Mapping of Signal Features to Plant Physical Structure

9.1 Introduction

In previous chapters, a transformation from the physical plant structure to the acoustic density profile was developed based on the acoustic density profile model. This can be considered a forward transformation from plant structure, to echo, to acoustic density profile. However, the inverse transformation is required to relate the physical structure of a plant to its echo. In this chapter, the inverse transformation is established, that is, a transformation from acoustic density profile to plant physical structure is defined. This allows the sensing system to quantify the significant features of an unknown plant that is within the sensors field of audition.

9.2 Background

The frequency spectra of the echo was discussed in Chapter 3 in terms of representing the acoustic density profile. A relationship between the plants physical structure and the echo was developed into a model shown in Figure 9.1.

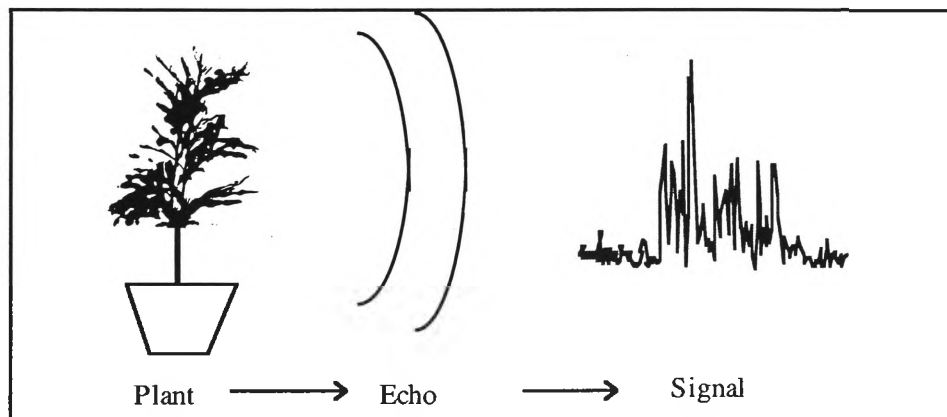


Figure 9.1 The forward transform starts with a plant, an echo is reflected, and that echo is converted into a signal as outlined in Chapter 3

In Chapter 8, a set of 19 features were developed. These are calculated from the acoustic density profile and thus can be called signal features. The inverse transformation can then be decomposed into two separate transformations :

1. Signal features to acoustic features; and
2. Acoustic features to plant physical features.

The difficulty with many inverse transforms is that they do not result in a one to one mapping and therefore the result is not unique. If such a transformation can be achieved however, at least in concept, then we are well along the way to understanding echolocation and a scientific basis for plant discrimination.

The height of a range line in the acoustic density profile is the most fundamental signal feature. Examination of the signal processing (FFT) shows that the height of the range line is directly proportional to the energy in the reflected signal. From the model of an acoustic density profile (Chapter 3), we can say that it is a transformation of the acoustic area of the plant at that range. Thus the first transform is simple and is from signal amplitude to acoustic area. That is, a transformation from signal feature to acoustic feature (1) above.

The second transform is more complex. The acoustic area is composed of the sections of leaves that reflect the acoustic energy which sums to give an echo at that range (that is, the acoustic area at that range). The acoustic area is a function of the geometric area of the leaves of the plant, but not a simple function.

For a section of a leaf to reflect toward the receiver it must be oriented near normal to the axis of the receiver as the surface is specular. In air, surface texture of the leaf has the effect of spreading the echo over a greater angle resulting in a lower signal level. The echo strength is also reduced by the curvature of the specular surfaces due to the reduced surface area. The transformation function is further complicated by acoustic shadowing (energy not reaching leaves) and multiple echo paths (energy reflecting off several leaves before reaching the receiver).

Thus, for this simple measure (the height of a range line), we have a one to one transform from signal feature (amplitude of the range line) to acoustic feature (acoustic

area). We then have a complex mapping from acoustic feature to physical plant feature (near normal area, diffraction, leaf curvature, acoustic shadowing, and multiple echoes). When more than one range line is considered however, we can use the relative information in the range lines to develop a model of the overall physical structure of the plant as detailed below.

An initial analysis of the features developed in Chapter 8 showed that they are representative of the plants that were insonified. This chapter shows that the features provide useful information directly, for example, `length_of_density_profile` gives the acoustic depth of the plant (which is less than or equal to the actual plant depth), while other features such as the threshold features give an indication of several different properties of the plant's physical structure, the density of the surfaces within the plant and the size of the reflective surfaces.

The acoustic density profile of the plant provides information about surfaces within the field of audition of the sensor. This can be related directly to Freedman's model [Freedman, 1962b] which states that as the normal cross-sectional area is increased, the amount of acoustic energy which returns to the receiver is increased, and hence a higher amplitude in the range cell which corresponds to that physical range. Also reflections occur at discontinuities in the cross sectional area and any of its derivatives. Thus, each range line represents an increase in the reflecting area.

In this Chapter, several features (from the 19) are analysed with their relationship to plant physical structure. These particular features are selected because there is a direct link between them and a physical property of the plant. Many of the overall set of features measure similar properties of the plant but measure them in slightly different ways so are difficult to interpret directly. However when these features are combined with the entire set, they allow for very fine discrimination of plants by a classifier and this is shown in Chapter 10. The following features calculated from the acoustic density profile are analysed in this chapter :

```
length_of_density_profile  
no_above_threshold1 - 9
```

no_of_major_peaks1 - 2

sum_of_density_profile

The result of this chapter is a mapping from signal to plant structure (Figure 9.2). The mapping does not provide a complete description of the physical plant as that is not within the capability of the sensor, but does provide information about the structure of the plant which can be used by a practical system.

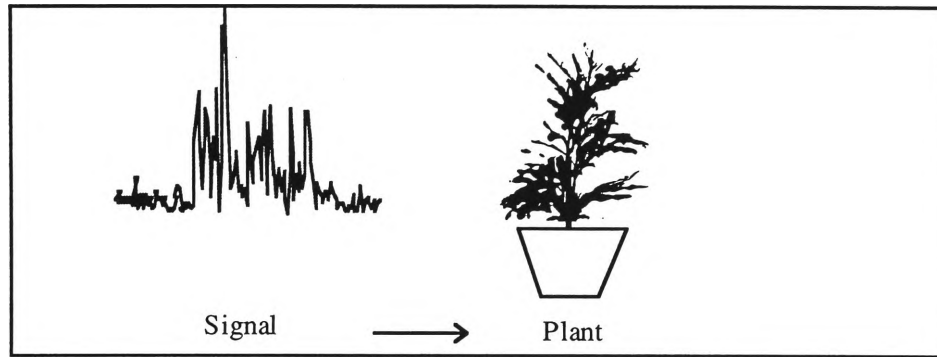


Figure 9.2 The inverse transform from signal to the physical structure of the plant. This chapter outlines a method for determining information about the structure of the plant from the signal

9.3 Length of the acoustic density profile

The length of the acoustic density profile is calculated as the distance between the first and the last range line and hence is, the acoustic depth of the plant. If there are surfaces which reflect acoustic energy at both extremities of the plant, then it is a measure of the depth of the plant. In practice however, it gives the distance between the first and last detectable surface so is an indication of the *minimum* depth (or lower bound depth) of the plant.

Figure 9.3 shows a graph of the average of this feature (length_of_density_profile) for each of the plants in the database with the standard deviation of this minimum depth shown as error bars. The data used to produce the graph are also shown in Table 9.1. The figure shows that most of the plants are relatively consistent through rotation as they all have small standard deviations. The plant depth which has been calculated from the acoustic density profile ranges between 42 millimetres and 351 millimetres with most of the plants being evenly spread between the two extremes. Figure 9.5 shows the variation of this feature with rotation for one specimen of

Pittosporum crassifolium. It shows that the feature is close to 250 mm for most orientations but varies between 200 and 300 mm.

For plants which have a very thick outer layer of leaves, less acoustic energy penetrates through the plant, so the acoustic density profile mostly contains information about the external structure of the plant. The echo reflected from the plant will consist of direct reflections from the surfaces which are directly visible from the sensor and some diffraction from the back of the plant. Most of the energy in the echo will be from direct reflection from the front of the plant and leaves which protrude from the side of the plant. This was shown in Section 3.9.

Plants which have a more sparse leaf structure allow more of the acoustic energy to penetrate into its internal structure and acoustic energy can then reflect directly from leaves within and at the back of the plant. Since these plants are sparse however, there are not always surfaces (leaves) which can reflect the acoustic energy back to the sensor at either the front of the plant, or the back of the plant (or both) so the length calculated from the acoustic density profile is indeed less than that measured by a ruler and can cause a significant variation of the value for this feature depending on the orientation of the plant. At some orientations the plant appears deep, and at others it appears narrow.

The calculated values are compared against to plant depth as measured (Figure 9.4). This figure shows the measured plant depth on the horizontal axis and the average minimum plant depth (acoustic depth) calculated from the acoustic density profile on the vertical axis. Error bars on the x axis represent the estimated error for measurement with a ruler, and error bars on the y axis are the standard deviation of the feature for the plant through an entire revolution of the plant.

In order to interpret the results and to justify the size of the error bars, the following discussion defines the measurement techniques used. It is not possible to get an average plant depth measure using a ruler as it is not practical to measure all orientations of the plant accurately. Instead, the physical measurements of plant depth are based on the maximum depth of the plant, that is, the plant depth was measured from above at the orientation which produced the maximum value. There may be many other orientations of

the plant whose measured depth are less than this value so it is expected that the average value calculated from the acoustic density profile will be less than this value unless the plant is perfectly symmetric (that is, the same measure is produced from all orientations of the plant).

The images of some of the outlying plants are shown in Figure 9.4 and will be discussed further below. The dashed line shown indicates the line on which plants would be positioned if the value calculated from the acoustic density profile is equal to the plant depth measured with the ruler. In practice, the plants do not all lie along that line as the `length_of_density_profile` indicates the average acoustic depth of the plant. This acoustic plant depth may not be equal to the measured plant depth so most of the sample points lie on the lower right hand side of that line. It can be seen on the graph that many of the points lie close to the line but the majority of the points lie below it.

The plants which lie close to the line are the ones which are more consistent through rotation and tend to have a greater number of larger leaves than the rest of the samples. This can be seen by the images shown on the graph. The plants which lie to the extreme lower right hand corner have few reflective surfaces to return good acoustic energy to the receiver, resulting in leaves only occasionally being detected at the extremities of the plant. All of the plants shown in that corner of the graph have large leaves which are on an angle to the horizontal which reflects most of the acoustic energy either down towards the ground or up into the air instead of back to the receiver. There are also gaps between the protruding leaves, so there are orientations where little (if any) acoustic energy is reflected towards the receiver.

The plants which lie above the line (that is, their measured plant depth is less than that calculated from the acoustic density profile) are plants which were difficult to measure accurately with a ruler and were actually deeper than that measured. However, these measurements are within the error limits as shown by the error bars.

In summary, this feature provides an indication of the minimum possible depth of the plant. The plant may be deeper than this value indicates but it is not less than the value of `length_of_density_profile`. In addition to this, plants which are away from the

central line, particularly those in the bottom right hand corner of the graph would not be good plants to use in an application which requires reasoning about the properties of the plant as the signal does not provide a true indication of the structure of the plant.

As discussed earlier, plants which have sparse foliage are likely to be more inconsistent for this feature through orientation from which the plant is insonified as reflective surfaces from the extremities of the plant (particularly the front and rear) appear and disappear in the acoustic density profile. This means that the plants which are sparse will have a high standard deviation relative to their average. This is also called the coefficient of variation. Those plants with a low coefficient of variation are dense plants. This is shown in Table 9.2. Sparse plants are at the top of the table (high coefficient of variation) and plants with more dense foliage are at the bottom. Even though this measure gives a simple measure of the foliage density, it is not particularly useful for a practical system as the average and standard deviation have been calculated using echoes from all 360 orientations of each plant. If it is possible for the sensing system to sense the plant over a group of orientations, then it is feasible that an estimate of the average and standard deviation for the plant can be established and the system could reason about the density of the foliage. Another measure of the foliage density can be calculated from the threshold features in the next section and can be calculated from a single insonification of the plant.

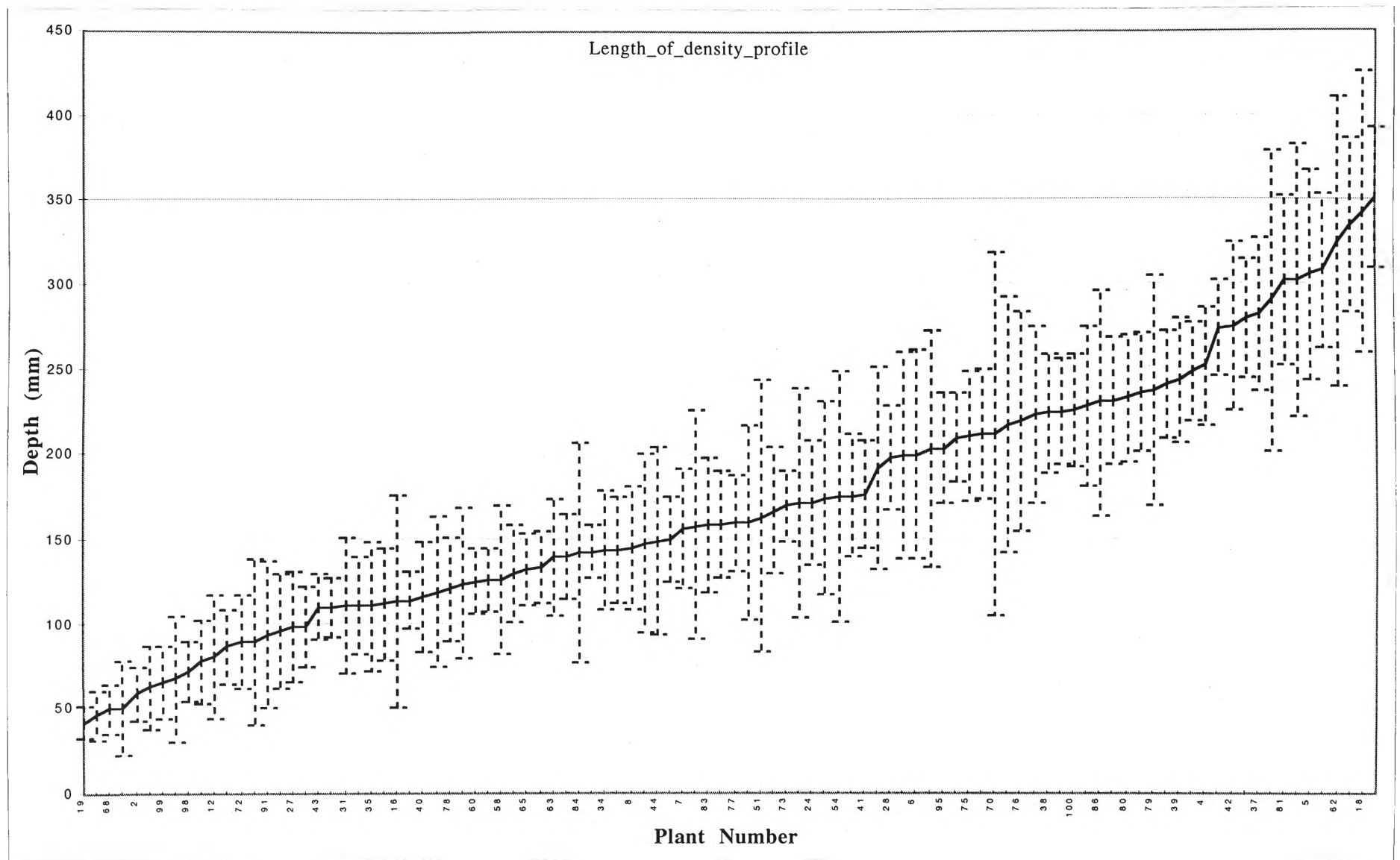


Figure 9.3 The average *minimum* plant depth for all 100 plants (error bars are standard deviation)

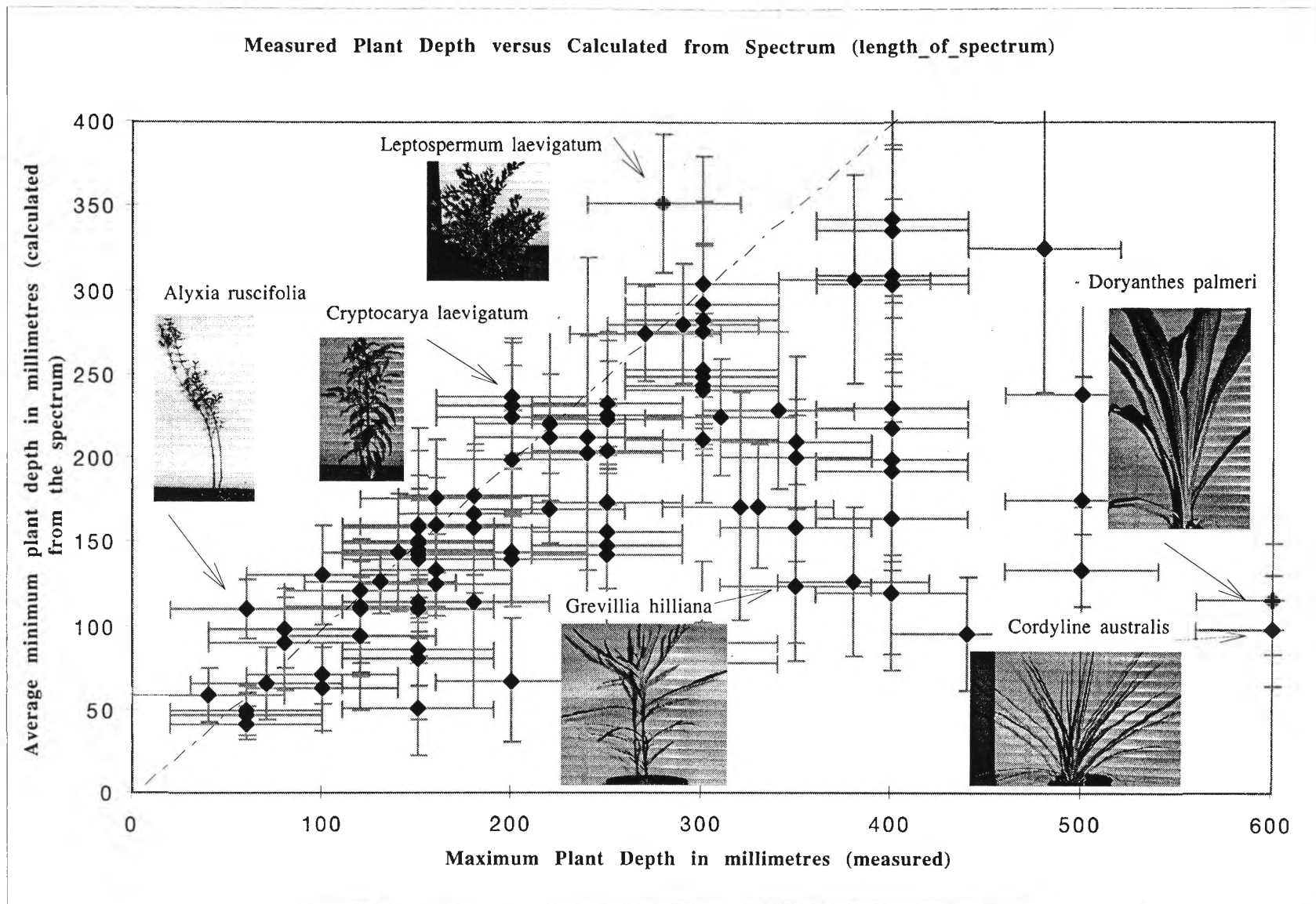


Figure 9.4 Measured plant depth versus depth calculated from the acoustic density profile with images of outlying plants. Error bars on the x-axis represent the estimated error for measurement and the error bars on the y-axis are the standard deviation of the calculated feature throughout a revolution of the plant.

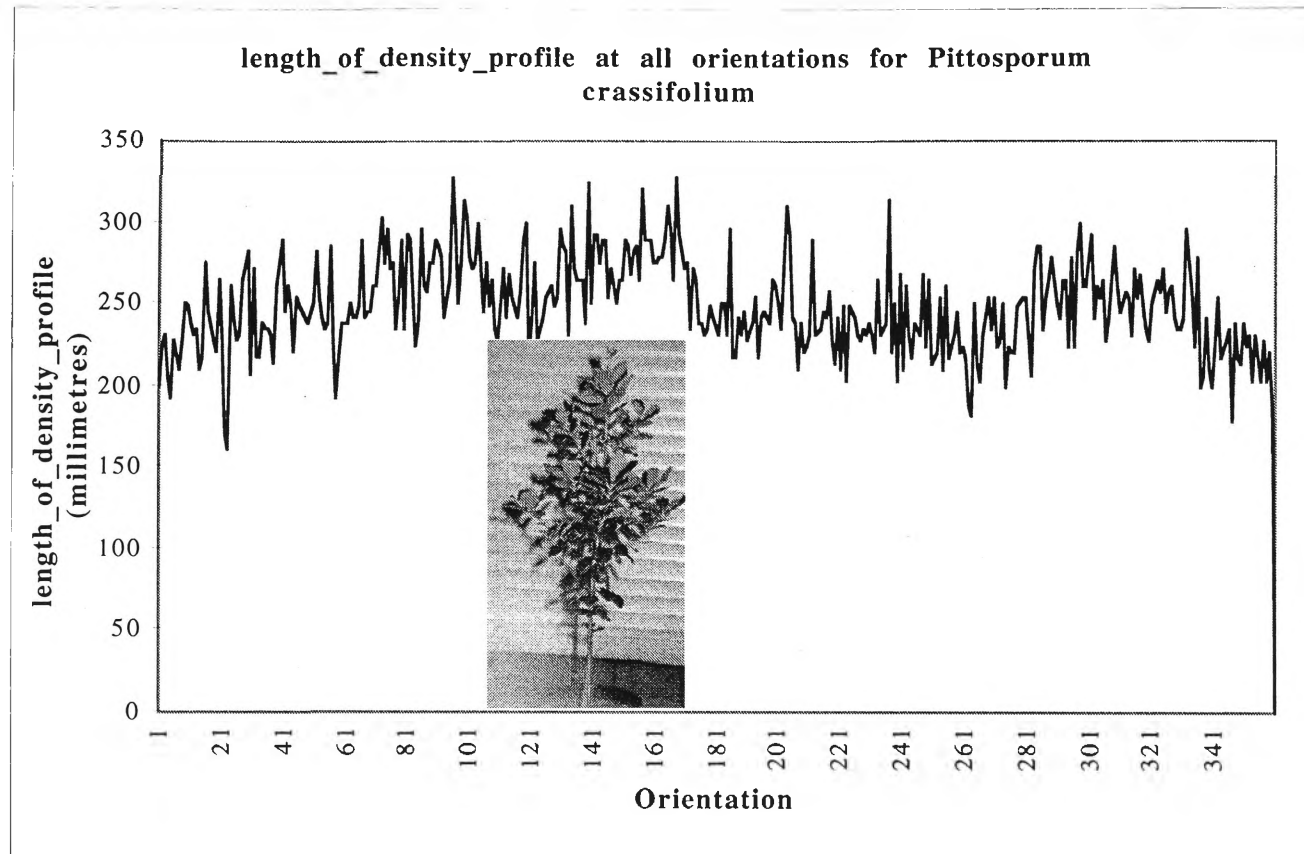


Figure 9.5 length_of_density_profile for all orientations of *Pittosporum crassifolium* with plant image

**Table 9.1 Average *acoustic* plant depth for 100 plants
(length_of_density_profile) with measured plant depth**

Plant Name	Avg	Stdev	Mea			
<i>Acacia podalyrifolia</i>	158.9	31.0	150			
<i>Banksia ericifolia</i>	42.2	9.5	60	<i>Pittosporum rhombifolium</i>	159.6	28.5 160
<i>Melaleuca erubescens</i>	46.5	14.4	60	<i>Microcitrus australis</i>	159.8	57.5 150
<i>Melaleuca styphelioides</i>	49.9	14.5	60	<i>Grevillea marmalade</i>	163.1	80.3 400
<i>Crinum pedunculatum</i>	50.4	27.9	150	<i>Mishocarpus australis</i>	167	36.7 180
<i>Acacia cultriformis</i>	58.7	16.1	40	<i>Phyllanthus albiflorus</i>	169.6	20.4 220
<i>Cinnamom oliveri</i>	62.7	24.5	100	<i>Eucalyptus maculata</i>	170.8	67.7 320
<i>Westringa fruticosa</i>	65.5	21.8	70	<i>Casuarina torulosa</i>	171.1	36.4 330
<i>Diploglottis australis</i>	67.5	36.9	200	<i>Rhopalostylis baneri</i>	173.6	56.9 250
<i>Tristaniopsis collina</i>	71.8	18.0	100	<i>Howea forsteriana</i>	174.7	74.0 500
<i>Crinum mauritianum</i>	78.0	24.6	300	<i>Szygium paniculatum</i>	175.7	35.7 160
<i>Agapanthus praecox dwarf</i>	80.5	36.2	150	<i>Endiandra introrsa</i>	176.6	31.8 180
<i>Livistona sp 'Carnarvon'</i>	86.4	22.2	150	<i>Solanum vescum</i>	191.8	59.1 400
<i>Omalanthus populifolius</i>	89.3	27.7	80	<i>Correa alba</i>	198.2	30.5 200
<i>Carpentaria acuminata</i>	89.7	48.9	300	<i>Stenocarpus sinuatus</i>	198.9	60.2 400
<i>Solanum laciniatum</i>	93.8	43.8	120	<i>Acacia longifolia</i>	199.6	60.7 350
<i>Agapanthus praecox</i>	95.7	33.6	440	<i>Eucalyptus leucoxylon</i>	202.7	69.7 240
<i>Cordyline australis</i>	97.9	32.8	600	<i>Szygium leuhmanni</i>	203.5	31.7 250
<i>Hymenosporum flavum</i>	98.2	23.5	80	<i>Casuarina glauca</i>	209.7	25.5 350
<i>Eriostemon myoporoides</i>	109.8	19.7	120	<i>Pittosporum james</i>	210.4	37.6 300
<i>Alyxia ruscifolia</i>	110.1	17.7	60	<i>Grevillea baileyana</i>	211.8	37.5 220
<i>Cryptocarya bidwilli</i>	110.7	40.7	120	<i>Ficus obliqua</i>	212.1	106.9 240
<i>Guioa semiglauca</i>	110.7	29.2	150	<i>Azalea alba magnifica</i>	217.3	74.8 400
<i>Cupaniopsis parvifolia</i>	110.7	38.4	120	<i>Pittosporum revolutum</i>	219.5	64.0 220
<i>Goodia lotifolia</i>	111.7	33.8	120	<i>Sarcomelicope simplifolia</i>	223.4	52.0 250
<i>Ayrtera distylis</i>	113.5	62.6	180	<i>Dodonaea triquetra</i>	224.2	34.8 310
<i>Cryptocarya williwilliana</i>	113.9	16.7	150	<i>Leptospermum petersonii</i>	224.8	30.9 200
<i>Doryanthes palmeri</i>	115.6	32.9	600	<i>Ziera collina</i>	225.4	32.5 250
<i>Archontophoenix cunninghamiana</i>	118.9	45.1	400	<i>Hakea salicifolia</i>	228.4	46.9 340
<i>Pittosporum undulatum</i>	120.7	31.1	120	<i>Rhopalostylis sapida</i>	230.2	66.6 400
<i>Grevillea hilliana</i>	124.1	45.1	350	<i>Ficus rubiginosa</i>	230.7	37.2 200
<i>Leptospermum morrisonii</i>	125.1	19.7	160	<i>Polyscias elegans</i>	232.7	37.2 250
<i>Indigofera australis</i>	125.8	18.9	130	<i>Cryptocarya laevigatum</i>	236.2	34.8 200
<i>Laccospadix australasica</i>	126.0	44.1	380	<i>Polyscias australiana</i>	237.6	66.9 500
<i>Streblis brunonianus</i>	129.7	29.4	100	<i>Acacia binervata</i>	240.3	31.6 300
<i>Melaleuca decora</i>	132.8	21.3	160	<i>Dodonaea viscosa</i>	243	37.0 300
<i>Casuarina stricta</i>	133.2	21.3	500	<i>Pittosporum crassifolium</i>	248.2	28.5 300
<i>Litsea reticulata</i>	139.4	34.6	150	<i>Acacia howittii</i>	251.9	34.5 300
<i>Acacia stricta</i>	140.1	25.4	200	<i>Jacaranda mimosifolia</i>	273.9	28.6 270
<i>Rhododendron clorinda</i>	141.9	64.6	250	<i>Endiandra pubens</i>	275.4	50.3 300
<i>Melaleuca quinquenervia</i>	142.6	15.7	150	<i>Tabebula chrystricha</i>	279.8	35.7 290
<i>Cupaniopsis anacardioides</i>	143.5	35.1	140	<i>Diploglottis campbelli</i>	282.1	45.5 300
<i>Solanum aviculare</i>	143.6	32.0	200	<i>Banksia integrifolia</i>	290.8	88.9 300
<i>Acacia melanoxylon</i>	144.8	37.0	150	<i>Acronychia laevis</i>	302.7	80.9 400
<i>Acacia falcata</i>	147.4	53.4	250	<i>Polyscias murrayi</i>	302.7	50.1 300
<i>Eucalyptus botryoides</i>	148.7	55.5	150	<i>Acacia irrorata</i>	306.2	62.4 380
<i>Citriobatus paucifloris</i>	150.0	25.2	150	<i>Radermacheria fenecis</i>	308.3	46.4 400
<i>Acacia mearnsii</i>	156.3	34.7	250	<i>Licuala ramsayi</i>	325.3	85.9 480
<i>Solanum brownii</i>	158.1	67.7	350	<i>Sarcotoechia heterophylla</i>	334.9	51.7 400
<i>Rhododendron bryophyllum</i>	158.5	39.6	180	<i>Azalea cultivar splenda</i>	342.9	83.4 400
				<i>Leptospermum laevigatum</i>	351.4	41.7 280

Table 9.2 Plants length_of_density_profile ordered by coefficient of variation

Plant Name	Avg	Std	Coeff				
<i>Crinum pedunculatum</i>	50.4	27.9	0.5536	<i>Cupaniopsis anacardioides</i>	143.5	35.1	0.2446
<i>Ayrtera distylis</i>	113.5	62.6	0.5515	<i>Azalea cultivar splenda</i>	342.9	83.4	0.2432
<i>Diploglottis australis</i>	67.5	36.9	0.5467	<i>Hymenosporum flavum</i>	98.2	23.5	0.2393
<i>Carpentaria acuminata</i>	89.8	48.9	0.5445	<i>Sarcomelicope simplifolia</i>	223.3	52.0	0.2329
<i>Ficus obliqua</i>	212.1	106.9	0.5040	<i>Streblis brunonianus</i>	129.8	29.5	0.2273
<i>Grevillea marmalade</i>	163.1	80.3	0.4923	<i>Banksia ericifolia</i>	42.2	9.5	0.2251
<i>Solanum laciniatum</i>	93.8	43.8	0.4670	<i>Solanum aviculare</i>	143.6	32.0	0.2228
<i>Rhododendron clorinda</i>	141.9	64.6	0.4553	<i>Acacia mearnsii</i>	156.3	34.7	0.2220
<i>Agapanthus praecox dwarf</i>	80.5	36.2	0.4497	<i>Mishocarpus australis</i>	167.0	36.7	0.2198
<i>Solanum brownii</i>	158.1	67.7	0.4282	<i>Casuarina torulosa</i>	171.1	36.4	0.2127
<i>Howea forsteriana</i>	174.7	74.0	0.4236	<i>Hakea salicifolia</i>	228.4	46.9	0.2053
<i>Eucalyptus maculata</i>	170.8	67.7	0.3964	<i>Acacia irrorata</i>	306.2	62.4	0.2038
<i>Cinnamom oliveri</i>	62.7	24.5	0.3907	<i>Szygium paniculatum</i>	175.7	35.7	0.2032
<i>Archontophoenix cunninghamiana</i>	118.9	45.1	0.3793	<i>Acacia podalyrifolia</i>	158.9	31.0	0.1951
<i>Eucalyptus botryoides</i>	148.7	55.5	0.3732	<i>Endiandra pubens</i>	275.4	50.3	0.1826
<i>Cryptocarya bidwilli</i>	110.7	40.7	0.3677	<i>Acacia stricta</i>	140.1	25.4	0.1813
<i>Grevillea hilliana</i>	124.1	45.1	0.3634	<i>Endiandra introrsa</i>	176.6	31.7	0.1795
<i>Acacia falcata</i>	147.4	53.4	0.3623	<i>Eriostemon myoporoides</i>	109.9	19.7	0.1793
<i>Microcitrus australis</i>	159.7	57.5	0.3601	<i>Pittosporum james</i>	210.4	37.6	0.1787
<i>Agapanthus praecox</i>	95.7	33.6	0.3511	<i>Pittosporum rhombifolium</i>	159.7	28.5	0.1785
<i>Laccospadix australasica</i>	126.0	44.1	0.3500	<i>Grevillea baileyana</i>	211.8	37.5	0.1771
<i>Cupaniopsis parvifolia</i>	110.7	38.4	0.3469	<i>Citriobatus paucifloris</i>	150.0	25.2	0.1680
<i>Azalea alba magnifica</i>	217.2	74.8	0.3444	<i>Polyscias murrayi</i>	302.7	50.1	0.1655
<i>Eucalyptus leucoxydon</i>	202.7	69.7	0.3439	<i>Diploglottis campbelli</i>	282.1	45.5	0.1613
<i>Cordyline australis</i>	97.9	32.8	0.3350	<i>Ficus rubiginosa</i>	230.7	37.2	0.1612
<i>Westringia fruticosa</i>	65.5	21.9	0.3344	<i>Alyxia ruscifolia</i>	110.1	17.7	0.1608
<i>Rhopalostylis baneri</i>	173.6	56.8	0.3272	<i>Melaleuca decora</i>	132.8	21.3	0.1604
<i>Crinum mauritianum</i>	78.0	24.6	0.3154	<i>Casuarina stricta</i>	133.2	21.3	0.1599
<i>Omalanthus populifolius</i>	89.3	27.7	0.3102	<i>Polyscias elegans</i>	232.7	37.2	0.1599
<i>Melaleuca erubescens</i>	46.5	14.4	0.3097	<i>Leptospermum morrisonii</i>	125.1	19.7	0.1575
<i>Solanum vescum</i>	191.8	59.1	0.3081	<i>Szygium leuhmanni</i>	203.5	31.7	0.1558
<i>Banksia integrifolia</i>	290.8	88.9	0.3057	<i>Dodonaea triquetra</i>	224.2	34.8	0.1552
<i>Acacia longifolia</i>	199.6	60.7	0.3041	<i>Sarcotoechia heterophylla</i>	334.9	51.7	0.1544
<i>Stenocarpus sinuatus</i>	198.9	60.3	0.3032	<i>Correa alba</i>	198.2	30.5	0.1539
<i>Goodia lotifolia</i>	111.7	33.8	0.3026	<i>Dodonaea viscosa</i>	243.0	36.9	0.1519
<i>Pittosporum revolutum</i>	219.5	64.0	0.2916	<i>Radermacheria fenecis</i>	308.3	46.4	0.1505
<i>Melaleuca styphelioides</i>	49.9	14.5	0.2906	<i>Indigofera australis</i>	125.9	18.9	0.1501
<i>Rhopalostylis sapida</i>	230.2	66.5	0.2889	<i>Cryptocarya laevigatum</i>	236.2	34.8	0.1473
<i>Doryanthes palmeri</i>	115.6	32.9	0.2846	<i>Cryptocarya williwilliana</i>	113.9	16.7	0.1466
<i>Polyscias australiana</i>	237.6	66.9	0.2816	<i>Ziera collina</i>	225.4	32.5	0.1442
<i>Acacia cultriformis</i>	58.7	16.1	0.2743	<i>Leptospermum petersonii</i>	224.8	31.0	0.1379
<i>Acronychia laevis</i>	302.7	80.9	0.2673	<i>Acacia howittii</i>	251.9	34.5	0.1370
<i>Licuala ramsayi</i>	325.4	85.9	0.2640	<i>Acacia binervata</i>	240.3	31.6	0.1315
<i>Guioa semiglauc</i>	110.7	29.1	0.2629	<i>Tabebula chrystricha</i>	279.8	35.7	0.1276
<i>Pittosporum undulatum</i>	120.7	31.1	0.2577	<i>Casuarina glauca</i>	209.7	25.5	0.1216
<i>Livistona sp 'Carnarvon'</i>	86.4	22.2	0.2569	<i>Phyllanthus albiflorus</i>	169.6	20.4	0.1203
<i>Acacia melanoxylon</i>	144.8	37.0	0.2555	<i>Leptospermum laevigatum</i>	351.4	41.7	0.1187
<i>Tristaniopsis collina</i>	71.8	18.0	0.2507	<i>Pittosporum crassifolium</i>	248.2	28.5	0.1148
<i>Rhododendron bryophyllum</i>	158.5	39.6	0.2498	<i>Melaleuca quinquenervia</i>	142.6	15.6	0.1094
<i>Litsea reticulata</i>	139.4	34.6	0.2482	<i>Jacaranda mimosifolia</i>	273.9	28.6	0.1044

9.4 Number of lines in the acoustic density profile above a fixed threshold

There are nine features (of the 19 under consideration) which are based on the number of range lines on an acoustic density profile which are above a set threshold. This process of calculating thresholds, discards relative range information and provides a succinct measure of the surfaces within the plant but does not use relative positioning information. These features are counts of the number of range lines where the acoustic area is greater than the given threshold and give an indication of:

1. the specularity of the surfaces;
2. the number of surfaces;
3. the orientation of the surfaces; and
4. the size of the surfaces

Each of the threshold constants are scaled by the calibration measure, m , as documented in Chapter 8, where m is the amplitude detected from a large specular surface 0.500 metres from the sensor. For the sensor used with this research, m was measured to be 100 mV. The features and the corresponding threshold values are shown in Table 9.3.

The pseudo code for the function to calculate one of these features is shown in Algorithm 9.1. The function which implements this algorithm is called several times, once for each of the thresholds that are passed to the function. Note that these thresholds have been developed from range data which have been referenced to the standard distance of 400 mm (the algorithm to reference the data to a standard range is discussed in Chapter 5). The code which implements the function is given in Appendix C.

Table 9.3 Threshold features and the threshold levels

Feature Name	Value in mV
no_above_threshold1	59 / <i>m</i>
no_above_threshold2	78 / <i>m</i>
no_above_threshold3	98 / <i>m</i>
no_above_threshold4	117 / <i>m</i>
no_above_threshold5	156 / <i>m</i>
no_above_threshold6	195 / <i>m</i>
no_above_threshold7	295 / <i>m</i>
no_above_threshold8	300 / <i>m</i>
no_above_threshold9	490 / <i>m</i>

Algorithm 9.1 Algorithm for calculating threshold features.

```

CALCULATE THRESHOLD FEATURE
    This function calculates the number of range lines in an acoustic
    density profile which are above a given threshold level. The
    count is only made for range lines which are between the start
    and end of the plant's echo.
    Parameters :
        profile      this is an array which contains the acoustic
                      density profile.
        threshold    this is the threshold above which lines are
                      counted.
        m            this is the calibration measure. It is the
                      amplitude received by the system when
                      pointing at a large specular
                      surface at a range of 0.5 metres.

    Returns :
        the count of the number of elements greater than threshold
        between the start and end of the plant.
BEGIN
    Initialise the count to 0.
    Call the function to calculate the position of the start of
        the plant.
    Call the function to calculate the position of the end of
        the plant.
    Process elements from start_index to end_index.
    BEGIN
        IF the element is greater than the threshold / m
        THEN
            Increment the count.
        END
    END
    return the count.
END

```

In Chapter 3, the content of the raw signal was discussed in detail with particular emphasis on the analysis of “range cells” which provide information about the properties of the surfaces corresponding to the physical range that is represented by each individual range cell. The amplitude of a line in the acoustic density profile represents the acoustic

area at a particular range. These threshold features are a count of the number of range cells which have amplitudes above a particular threshold and are hence a measure of all of the above properties of the surfaces within the particular range cell. This means that plants with several small leaves at a certain range could have a larger echo than one with a single large leaf at that range. This is because the normal area of the larger leaf may be smaller than the sum of the normal areas of the surfaces of the small leaves. So even though the large leaves have a larger overall surface area, they may be at an orientation which does not reflect a large amount of acoustic energy back to the sensor, that is, the two smaller leaves combined, have a larger acoustic area.

Different threshold levels serve to differentiate plants with different spreads of the properties outlined above. The general cases for different plant structures are modelled in Figure 9.6. The figure shows six general cases (a - f) with the graph on the left hand side representing the raw acoustic density profile and the graph on the right being an indication of the calculated threshold feature values which result from the given acoustic density profile. On this graph, the nine threshold features are spaced equally along the x axis (an example of these features for a real plant can be seen in Figure 9.13). On the right hand side of Figure 9.6 is a description of the physical plant characteristics that produce the given acoustic density profile.

In Figure 9.6 :

- (a) shows the acoustic density profile for a plant with small reflective surfaces spread evenly over all of the ranges cells. This results in a high count for low threshold values and a low count for higher thresholds. For this particular example, the features are constant until the threshold level reaches a critical value, at which point the value of the feature drops to zero;
- (b), the reflective surfaces are more sparse, so the count is much lower overall with a similar drop down to zero once the threshold reaches a critical value;

(c) shows a plant which has much larger reflective surfaces throughout the entire plant and hence returns more acoustic energy. For this plant, all of the features are high as the amplitudes are larger than the highest threshold;

(d) shows a specimen with large reflective surfaces which are sparse so overall has a much lower count.;

(e) is a mixture of small and large reflective surfaces. Initially, the value of the feature is high but as the threshold rises above that of the smaller reflective surfaces, there is a drop in the count so that only the range cells which contain larger reflective surfaces are included in the count; and

(f) shows a similar situation with more sparse reflective surfaces which means that the overall counts are lower.

This model shows the general cases only. In practice however, the range cells in the acoustic density profiles from a plant will not contain either large or small values but a continuum of amplitudes and these will fall at different places throughout the acoustic density profile. The acoustic density profile of most plants will be somewhere between one of the general cases given and will not align exactly with any of them. Plants can be viewed from all orientations and leaf surfaces are not orthogonal to the sensor from all orientations, so a plant which is composed entirely of large surfaces will often produce low amplitudes. A similar situation occurs for plants with small surfaces where a large number of them may be present in a range cell, resulting in a high amplitude. This means that instead of having sharp steps in the threshold feature counts as illustrated in the model, there is a gradual change between amplitude values and this is illustrated when the features are graphed for particular acoustic density profiles in Section 9.4.1.1. This effect is also amplified by the fact that there is no clear differentiation between “large” amplitudes and “small” amplitudes, but there is a continuous scale of amplitudes. A less abstract model is shown in Figure 9.8. This model is more realistic as it illustrates what happens when the amplitudes are not all of the same approximate height, that is, there is some variation. Data from actual plants have far more variation than shown in this less

abstract model but the same general classes can be extracted. A selection of plants are analysed in more detail in Section 9.4.1.1.

Figure 9.7 shows the relationship between the acoustic density profile (and hence the physical properties of the plants) and the calculated features for plants which are narrower than the ones modelled in Figure 9.6. The acoustic density profiles have similar properties to those shown in Figure 9.6, but all of the amplitudes are lower in direct proportion to the depth of the plant. It is important to note that plants of similar structure can have higher feature values calculated for them due to the overall depth of the plant. In order to normalise the plant depth from the analysis, the acoustic density profiles can be divided through by the feature `length_of_density_profile`. These new normalised features can then be compared directly to plants of similar physical properties but of different depths. This is investigated further in Section 9.4.1.2.

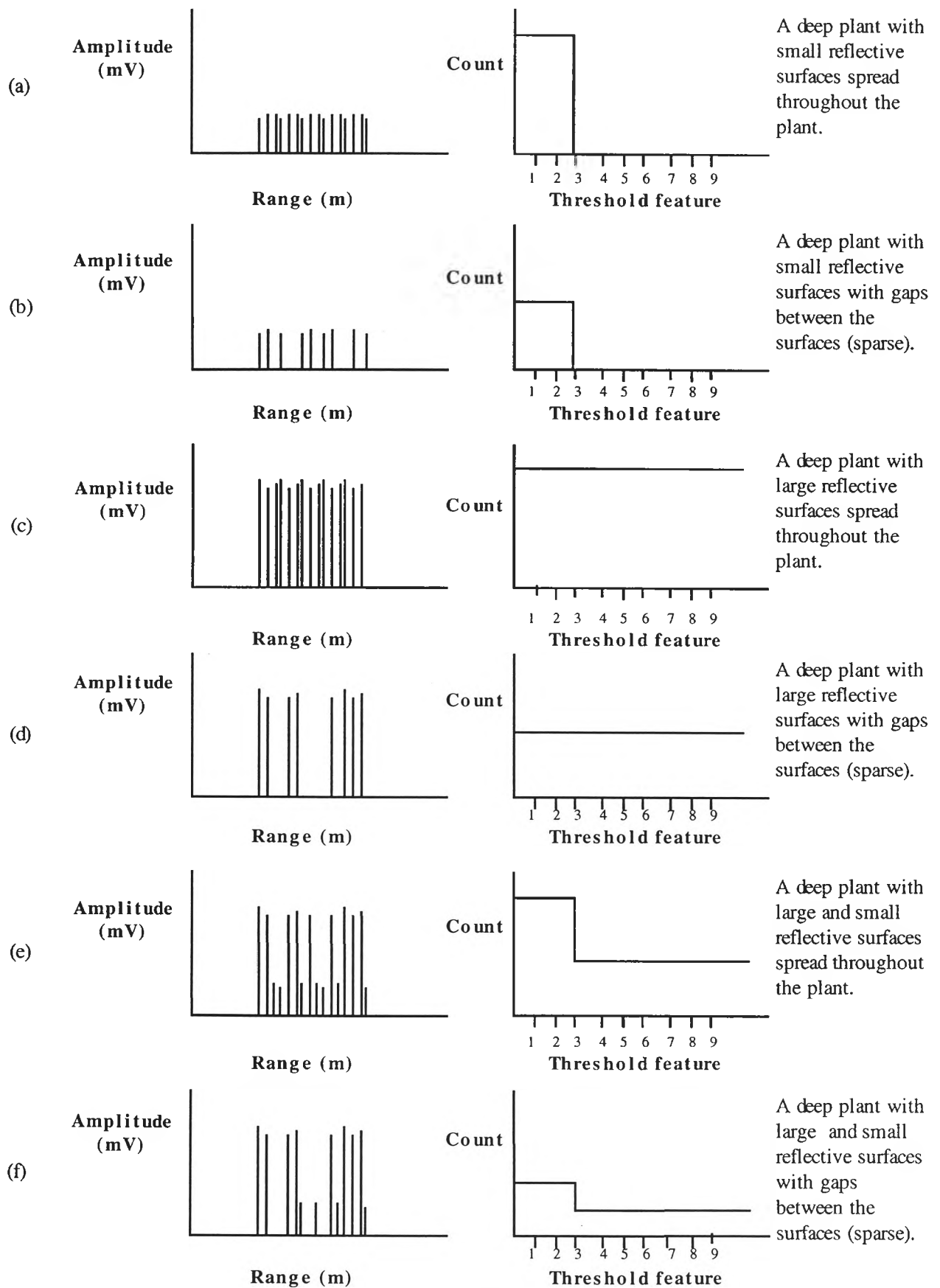


Figure 9.6 An abstract model of the relationship between plant type and the 9 threshold features for deep plants.

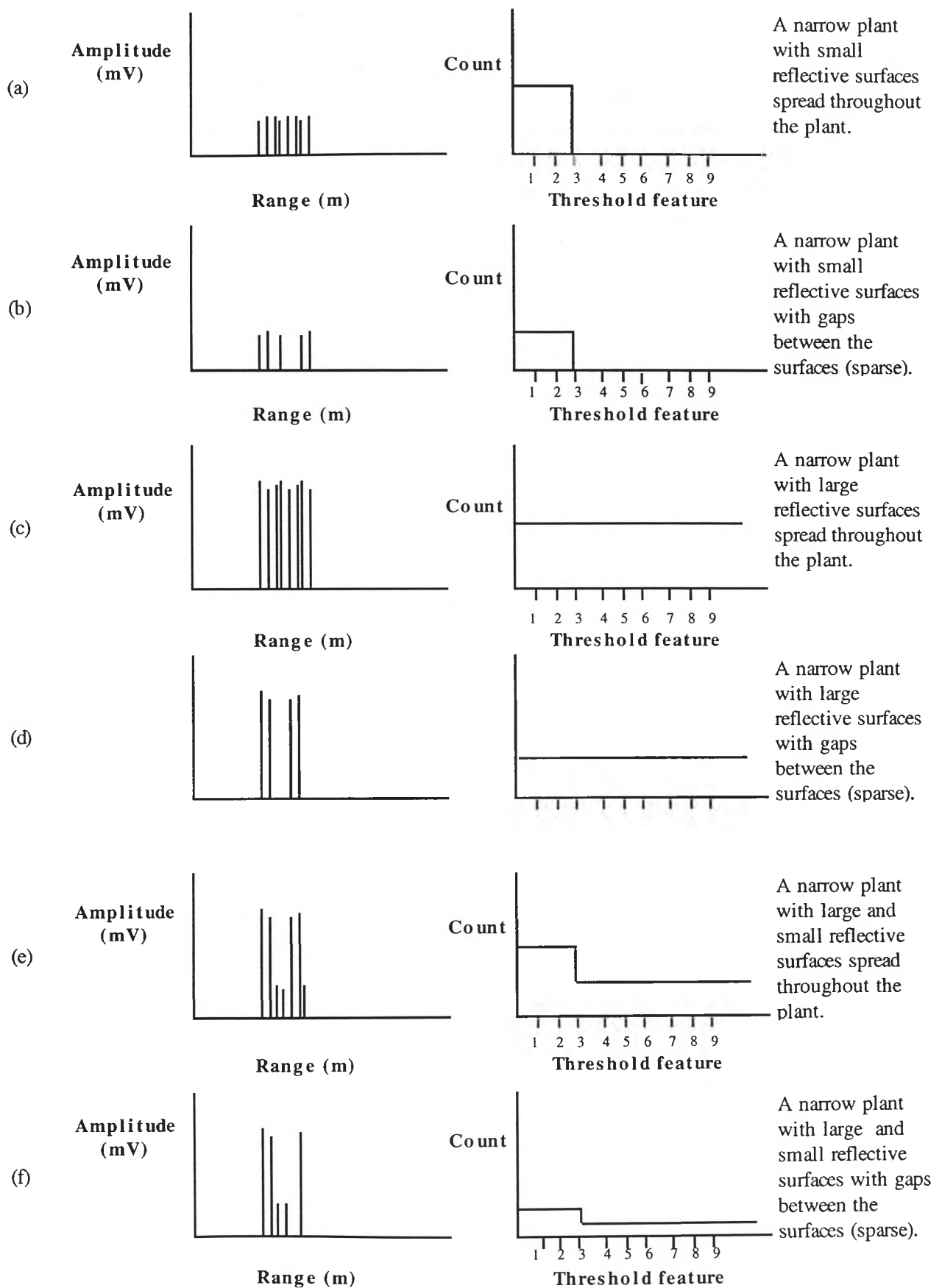


Figure 9.7 An abstract model of the relationship between plant type and the 9 threshold features for narrow plants.

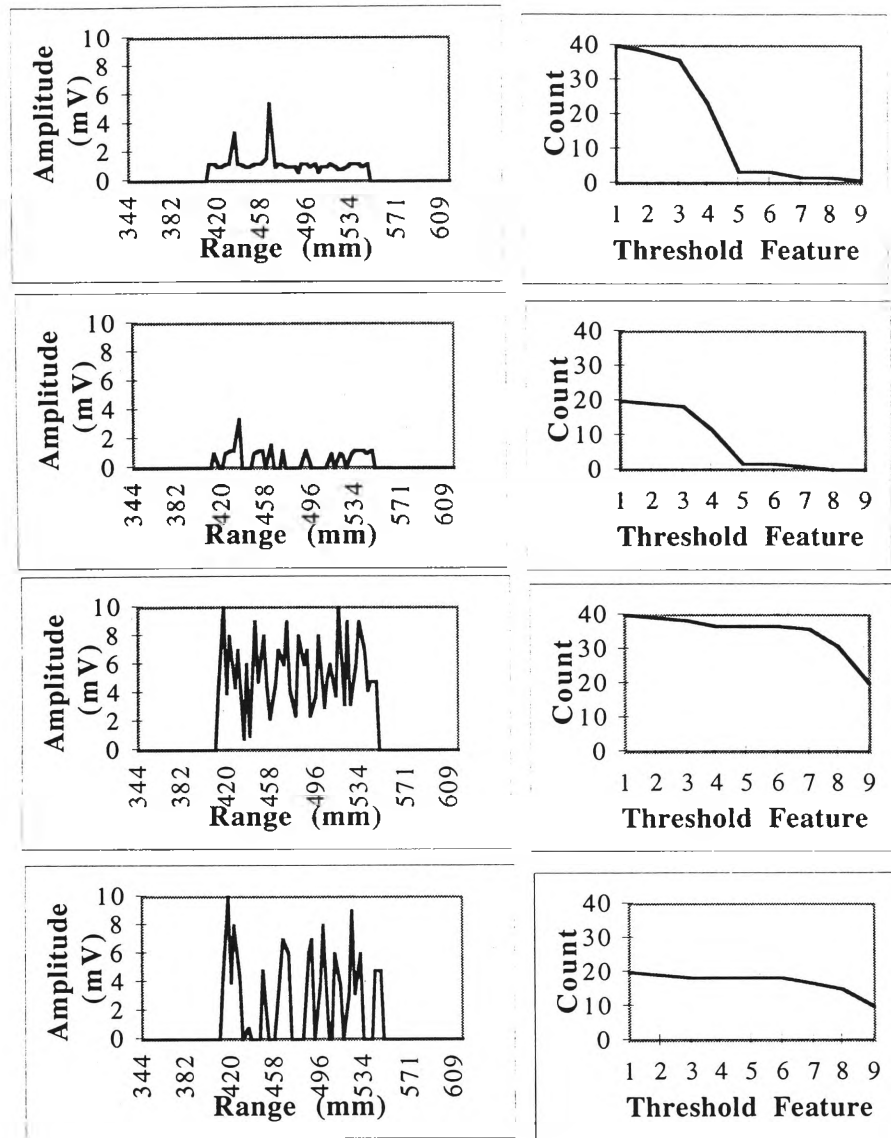


Figure 9.8 A less abstract model than that shown in Figure 9.6 for deep plants

In the following section, a selection of sample plants are analysed and the information in the threshold features discussed. It will be shown that plants with similar physical characteristics have similar acoustic density profiles and this can be made independent of the depth of the plant by normalising the threshold feature by the length of the acoustic density profile. In the process of analysing the features, six basic plant structures have been defined. They are listed in Table 9.4 along with identifiers which have been assigned to them.

Table 9.4 Six general plant structures

Reference from Figure 9.6	Reflectors	Spread	Assigned Name
a	small reflective surfaces	spread evenly	A
b	small reflective surfaces	gaps between the surfaces	B
c	large reflective surfaces	spread evenly	C
d	large reflective surfaces	gaps between the surfaces	D
e	small and large reflectors	spread evenly	E
f	small and large reflectors	gaps between the surfaces	F

A graph of all nine features for the 100 plants is shown in Figure 9.9. Because a graph of 100 plants is too cluttered, the features are shown for graphs of ten plants. The most significant point to note on the graphs are the first (`no_above_threshold1`) and the last features (`no_above_threshold9`), but there is also some important information in the remaining seven features as they provide information about how the acoustic density profile is changing between the two extremes. Figure 9.10 shows a different visualisation of the same information for a subset of the entire plant database. It can be seen more clearly on these graphs that the steps between adjacent features are not linear but map out a function which can provide more detail about the physical characteristics of the plant. Lines drawn are a linear mapping between the first and the last feature shown.

In Section 9.4.1.1, an analysis of deep plants is performed and related to the generalisations in Figure 9.6. In Section 9.4.1.2, a similar analysis of several shallow plants is performed and the characteristics can be related to Figure 9.7. The values of these thresholds however, can be normalised with respect to the depth of the plant (`length_of_density_profile`) and all of the plants can be compared on an equal basis i.e. the measures become independent of the depth of the plant. A set of depth independent rules emerge which can be used to classify plants as one of the general types in Algorithm 9.3.

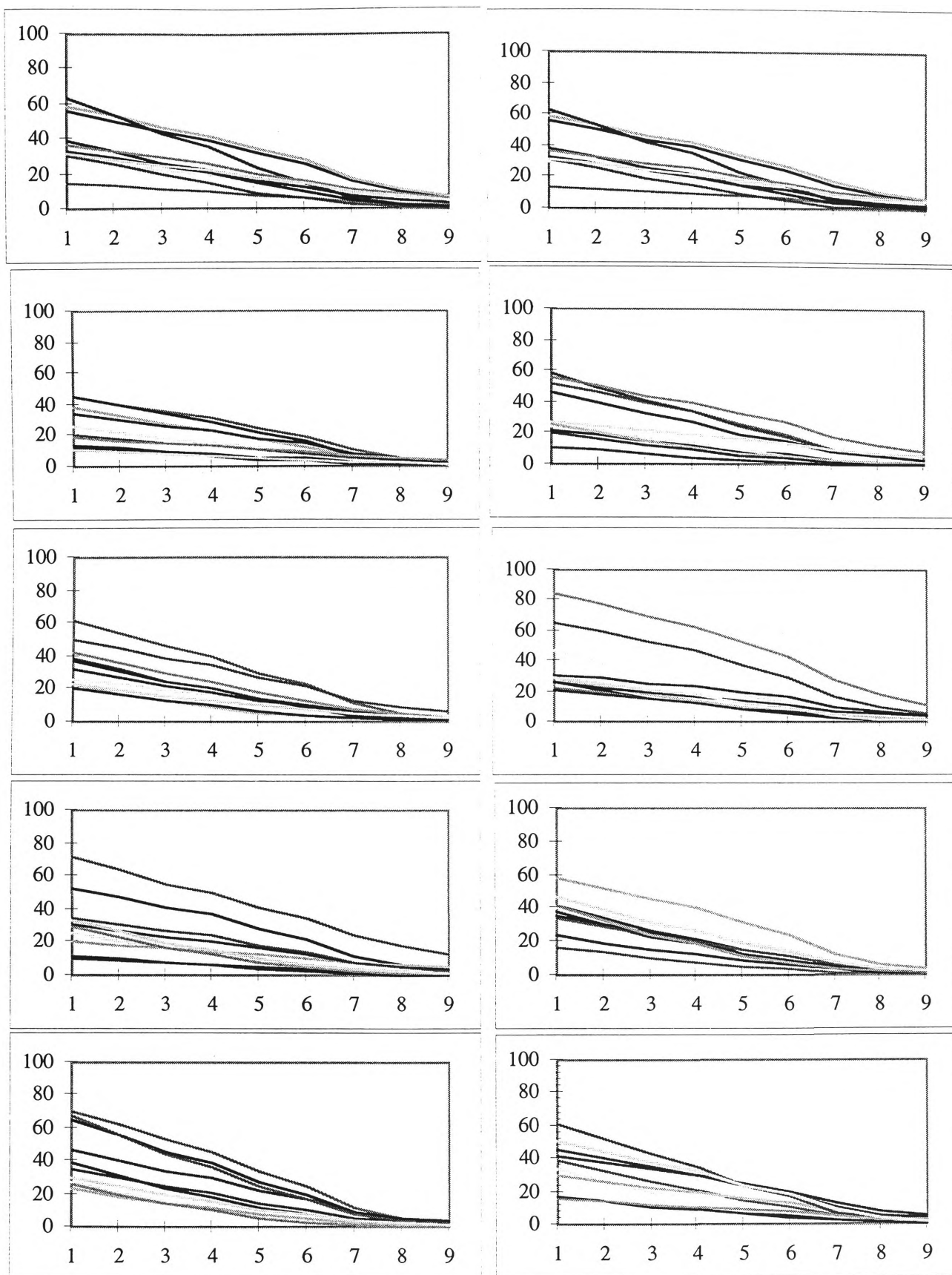


Figure 9.9 Graphs of the values of the threshold features `no_above_threshold1` - `no_above_threshold9` for all 100 plants, shown 10 plants per graph. x axis is the feature number, y axis is the count.

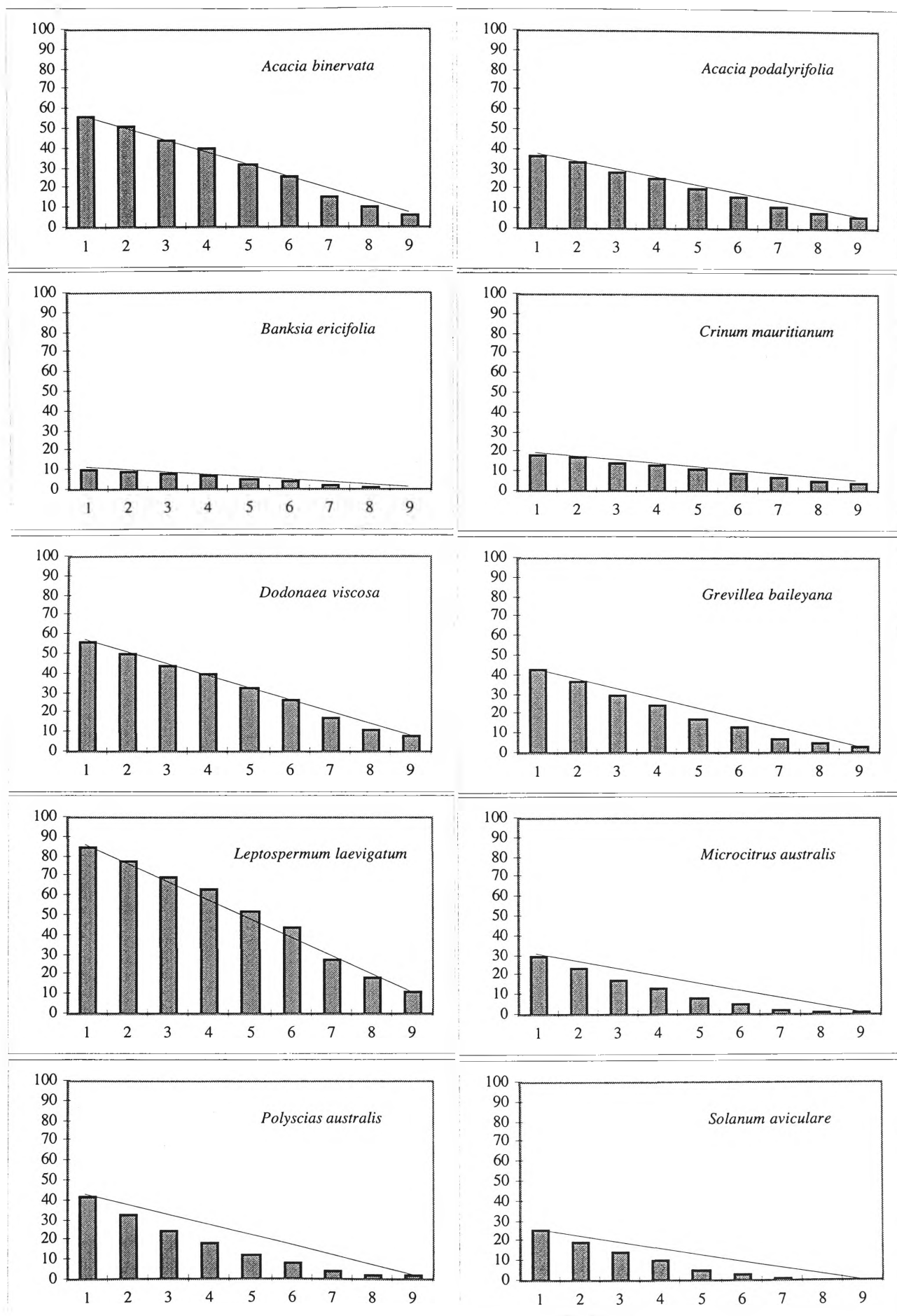


Figure 9.10 Bar graphs of the features for selected plants in order to show the relationship between the nine threshold features. y axis is the count and x axis is the features.

9.4.1.1 Analysis of a selection of deep sample plants

In this section, the threshold features calculated from a group of six deep plants is analysed. A deep plant has been chosen to be one which has an acoustic depth of at least 170 mm. Within the subset of deep plants, six of them were selected and are analysed below.

9.4.1.1.1 *Pittosporum* 'James Sterling' (type A)

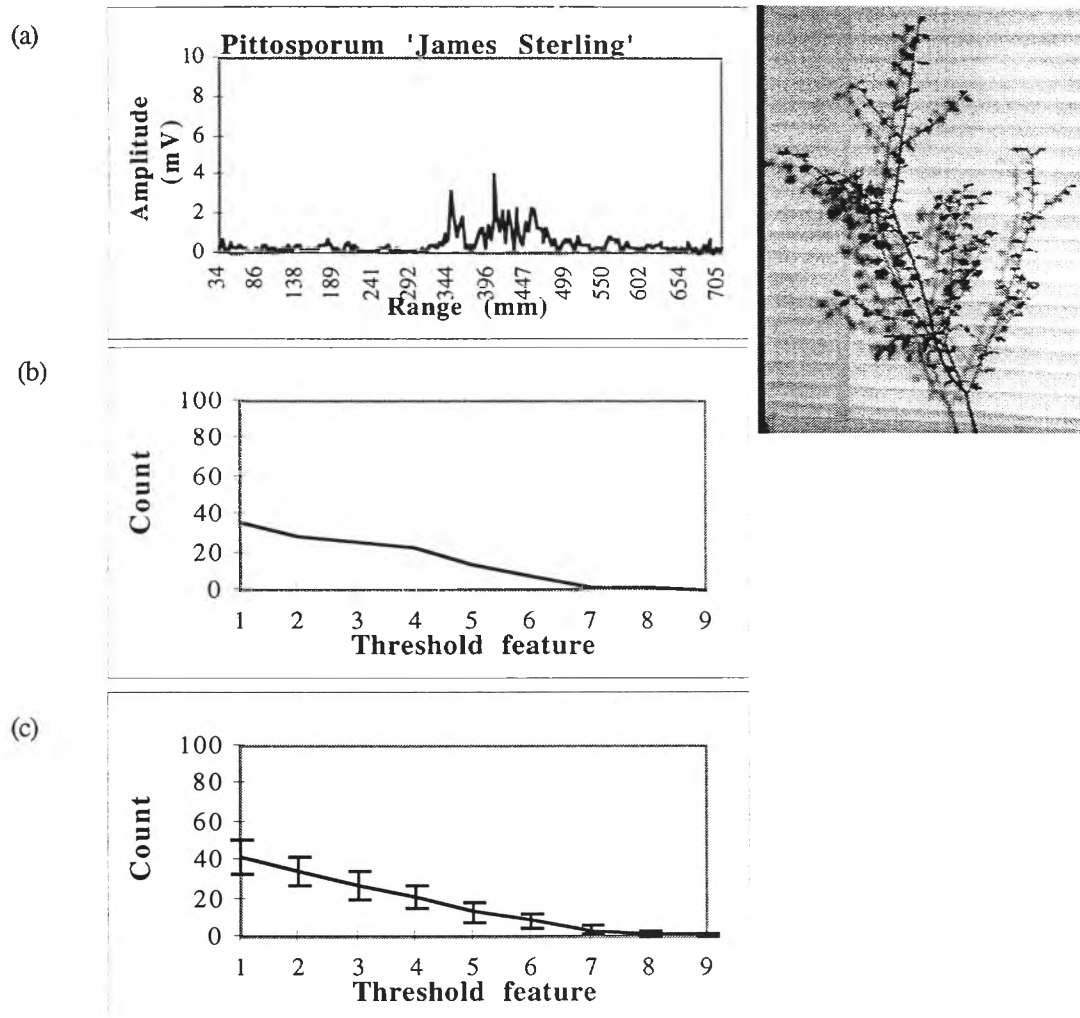


Figure 9.11 *Pittosporum* 'James Sterling' with (a) a sample of its acoustic density profile, (b) the nine threshold features calculated from that the acoustic density profile and (c) the averages of the nine features through an entire revolution of the plant with standard deviation shown as error bars.

An acoustic density profile from one orientation of *Pittosporum* 'James Sterling' is shown in Figure 9.11 (a) along with its image, features which are calculated for this the acoustic density profile (b), and the averages of these features for all orientations of the

plant (c). The image shows that the sample is a relatively deep plant with many small reflective surfaces.

The acoustic density profile shown in the figure shows that surfaces are detected over a large depth of approximately 65 range lines (or 223 mm).

When considering the acoustic density profile shown in Figure 9.11, most of the amplitudes are relatively low. The first feature (`no_above_threshold1`) is quite high as all of the range lines within the plant are above the base threshold of 0.59 mV. As the threshold is increased, the number of lines included in the count is less. Between the features `no_above_threshold4` (threshold 1.17 mV) and `no_above_threshold5` (1.56 mV), there is a significant drop in the count. This can be seen on the acoustic density profile where, many of the amplitudes are around 1.17 mV. Because the plant has only few, small reflecting areas in any particular range cell, there are few (if any) lines above the higher threshold features (`no_above_threshold7`, 8 and 9).

This plant specimen can be characterised by certain properties of the acoustic density profile and the properties of the acoustic density profile can provide information about the physical characteristics of the plant.

The acoustic density profile covers a wide group of ranges, so the plant is not narrow. `no_above_threshold1` is 36 which indicates that there is at least 124 mm between the first and last detectable surface at this particular orientation.

`no_above_threshold9` is small (it is zero in the example shown). This indicates that there are no range cells in the acoustic density profile where there are any surfaces with significant acoustic area. This indicates one of several possibilities :

- that the plant is sparse; or
- that the surfaces are small; or
- they are not oriented towards the receiver.

Table 9.5 (on page 9-34) shows all of the plants with their corresponding values of the features `no_above_threshold1` and `no_above_threshold9`. Each of the columns of plant names are ordered by the value of the feature for the particular plant. On the left hand side of the table, is a list of all 100 plants and their corresponding average value for

the feature `no_above_threshold1`. Plants at the top of the graph have low values for the feature and plants at the bottom of the table, have high values for the feature. The columns on the right hand side of the table show similar information for `no_above_threshold9`. The centre column consists of lines drawn between two cells of plants of the same name for fast reference. For example, the plant *Banksia ericifolia* is in the first row of the left hand side of the table as it has the smallest average for the feature `no_above_threshold1`. It is in row seven on the right hand side of the table and the line between the two cells shows how much the feature changes with respect to the other plants in the set. The values of the features can be considered relative to the other plants in the set as the values of `no_above_threshold9` are relatively small as they are unscaled. The sample plants are highlighted by the plant type and the lines between these sample plants are bold. The types for the deep plants are noted in upper case with the narrow plants in lower case.

The plant currently under consideration (*Pittosporum 'James Sterling'*) is in row 71 on the left hand side of the table and row 20 on the right hand side. So in relation to the other plants in the set, it has a high value for `no_above_threshold1` and has a relatively low value for `no_above_threshold9`. Referring back to Figure 9.6, we see that plants with large counts for small amplitudes and small counts for large amplitudes are of type A (as defined in Table 9.4). The description of plants of **type A**, is of small surfaces spread evenly though out the depth of the plant.

9.4.1.1.2 *Microcitrus australis* (type B)

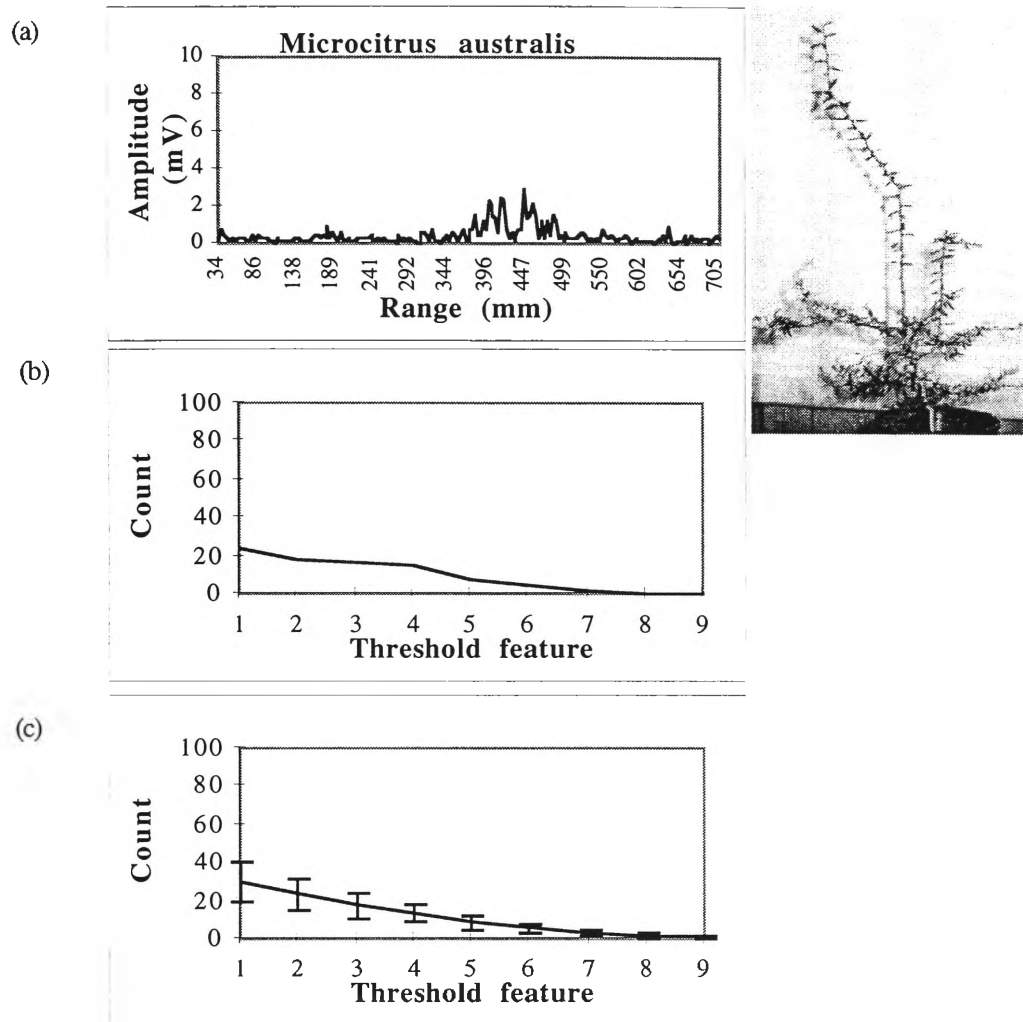


Figure 9.12 *Microcitrus australis* with (a) a sample of its acoustic density profile, (b) the features calculated from that acoustic density profile, and (c) the averages of the nine features through an entire revolution with standard deviation shown as error bars

As shown in Figure 9.12, leaves within *Microcitrus australis* are relatively sparse with small reflective surfaces which reflect only a small amount of the acoustic energy back to the receiver. There is acoustic energy reflected from over a relatively large depth but many of the returns are below the first threshold. Out of 33 range cells, only 24 of them are above the first threshold. All of the returns are of very low amplitude. For the acoustic density profile shown, the count starts from a very low level and quickly drops down to zero for threshold 8 and 9.

Table 9.5 lists the plants in order of the first and last threshold features and shows that this plant has a low value with respect to the others in the population (row 19) and

ends up with an extremely low value for `no_above_threshold9` (row 4). This acoustic density profile/feature pattern is shown to be **type B** in Figure 9.6.

9.4.1.1.3 *Leptospermum laevigatum* (type C)

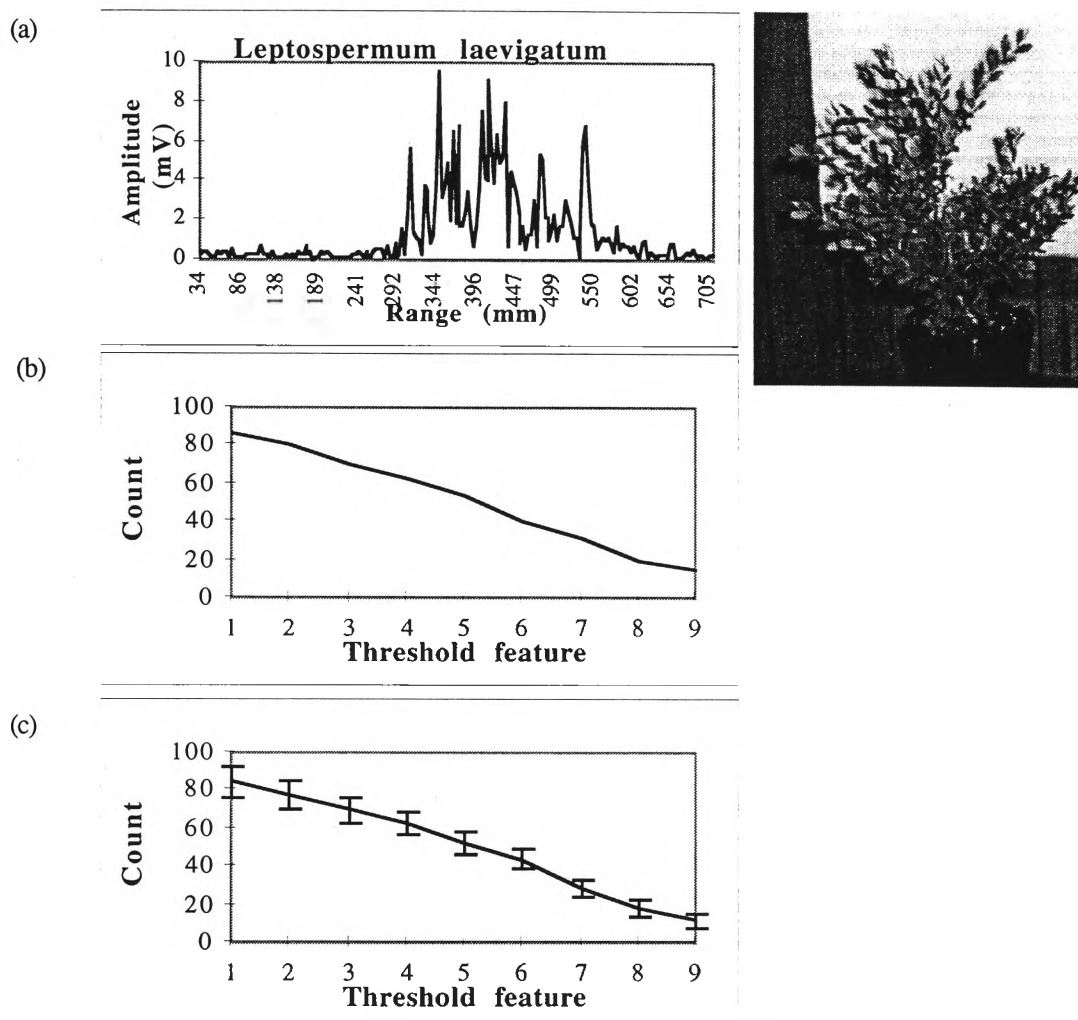


Figure 9.13 *Leptospermum laevigatum* with (a) a sample of its acoustic density profile, (b) the features calculated from that acoustic density profile and (c) the averages of the nine features through an entire revolution of the plant with standard deviation shown as error bars.

An acoustic density profile from one orientation of *Leptospermum laevigatum* is shown in Figure 9.13(a) along with its image, (b) the features which are calculated from this acoustic density profile and (c) the averages of these features for all orientations of the plant. The plant has many leaves which produce a significant echo over quite a depth. In general, when there is more than one surface at a particular range, then the echo received is proportional to the total surface which reflects acoustic energy and this explains why the amplitude is so high.

The first threshold feature (no_above_threshold1) is very high due to the fact that the plant is so deep and there are reflecting surfaces within the entire plant. There is a gradual decrease in the count of lines above different thresholds and the feature which measures the largest threshold (no_above_threshold9) is relatively high due to the strong echoes which are reflected from the plant.

When you look at this plant in Table 9.5, You will note that it has an extremely high value for both of the features shown. Referring again to Figure 9.6, the plant types which show large values for both of these features are **type C**. That is, dense plants with large reflecting surfaces at all ranges throughout the plant. Note that even though this plant has a small leaves, the large number of them at any particular range from the sensor contribute to make a large reflective surface.

9.4.1.1.4 *Rhopalostylis baneri* (type D)

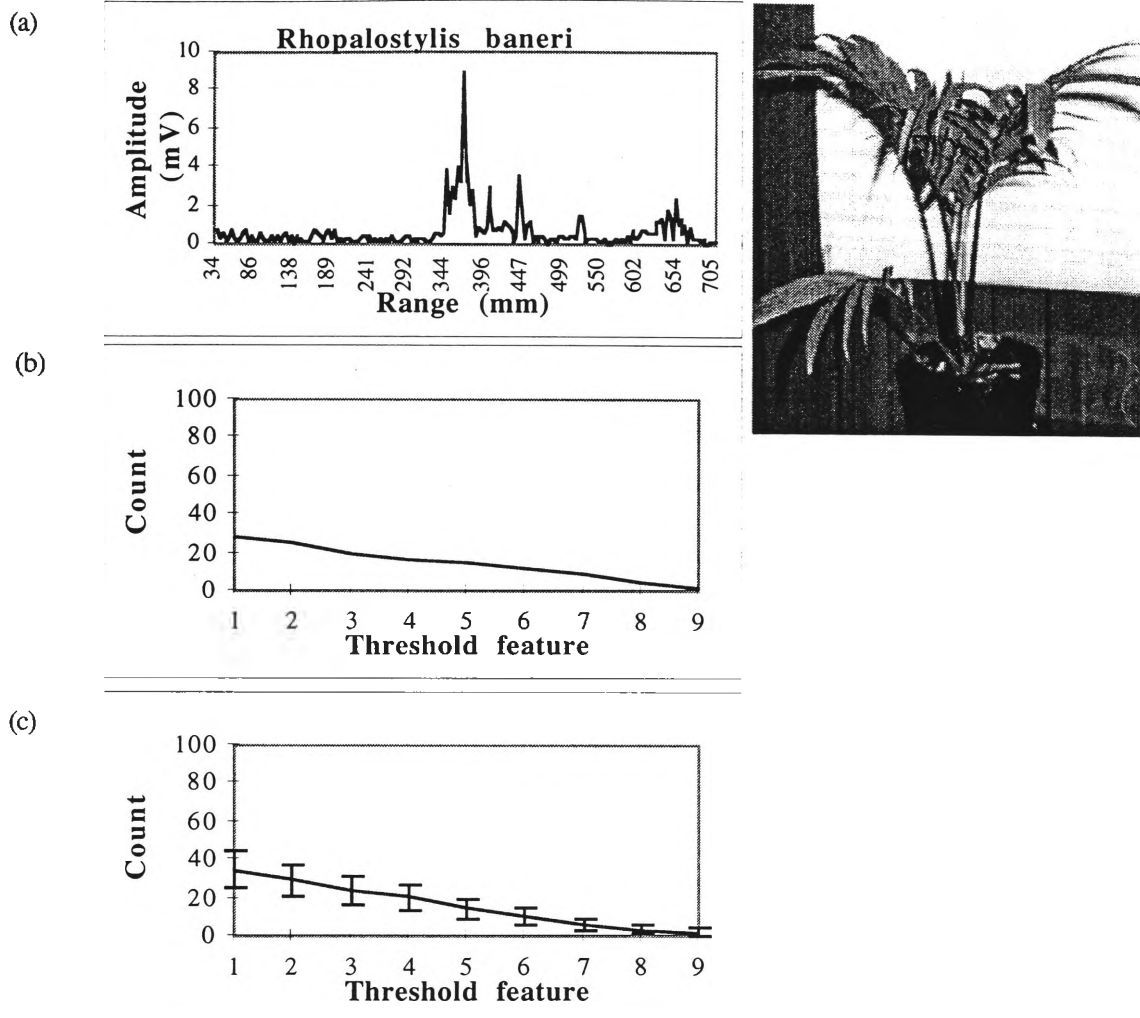


Figure 9.14 *Rhopalostylis baneri* with (a) a sample of its acoustic density profile, (b) the features calculated from that acoustic density profile and (c) the averages of the nine features through an entire revolution of the plant with standard deviation shown as error bars.

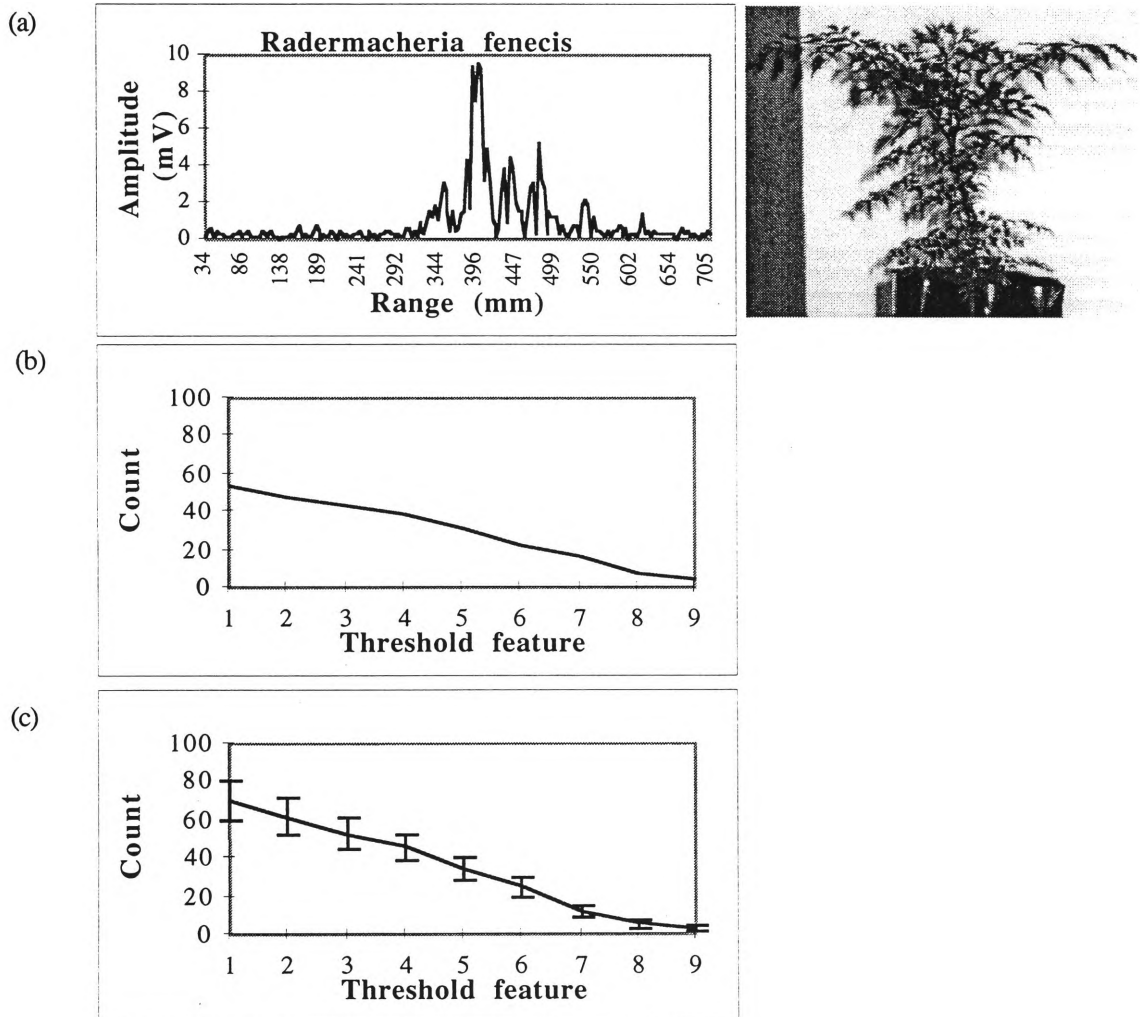
Rhopalostylis baneri is shown in Figure 9.14. The plant has some large leaves which produce a large echo. There are also open spaces between the leaves which do not reflect any acoustic energy back to the sensor. This is shown in the acoustic density profile (Figure 9.14(a)) where a leaf at approximately 380 mm from the sensor produces a significant amplitude (9 mV). This is followed by some smaller reflections and a region where there are no surfaces that reflect acoustic energy back to the sensor between 450 mm and 510 mm. Another small surface is detected at a range of 540 mm and a group of surfaces between 610 mm and 680 mm.

The first threshold feature (no_above_threshold1) is not particularly high due to the fact that there are areas in the acoustic density profile where there are no echoes. It can

be seen that the threshold features for this plant reduce more gradually for this plant than they do for other plants among the group of 100.

When you look at this plant in Table 9.5, It has medium value for both of the features shown. Referring again to Figure 9.6, the plant types which show medium values for both of these features are **type D**. A deep plant with large reflective surfaces with gaps between the surfaces.

9.4.1.1.5 *Radermacheria fenecis* (type E)



Radermacheria fenecis is a deep plant with many small reflective surfaces. The result is an acoustic density profile which contains a mixture of both high and small amplitudes. The value of the first feature is high due to the large number of reflective

surfaces. This is followed by a gradual reduction in the count as the threshold is increased.

Table 9.5 shows that this plant has a high ranking for the first threshold feature (ranked 97) and has a medium ranking for the last feature (ranked 73). This means that there are a considerable number of large returns even for high threshold values. Referring again to Figure 9.6, the plant types which show these characteristic features are **type E**, that is a deep plant with both large and small reflective surfaces.

9.4.1.1.6 *Solanum vescum* (type F)

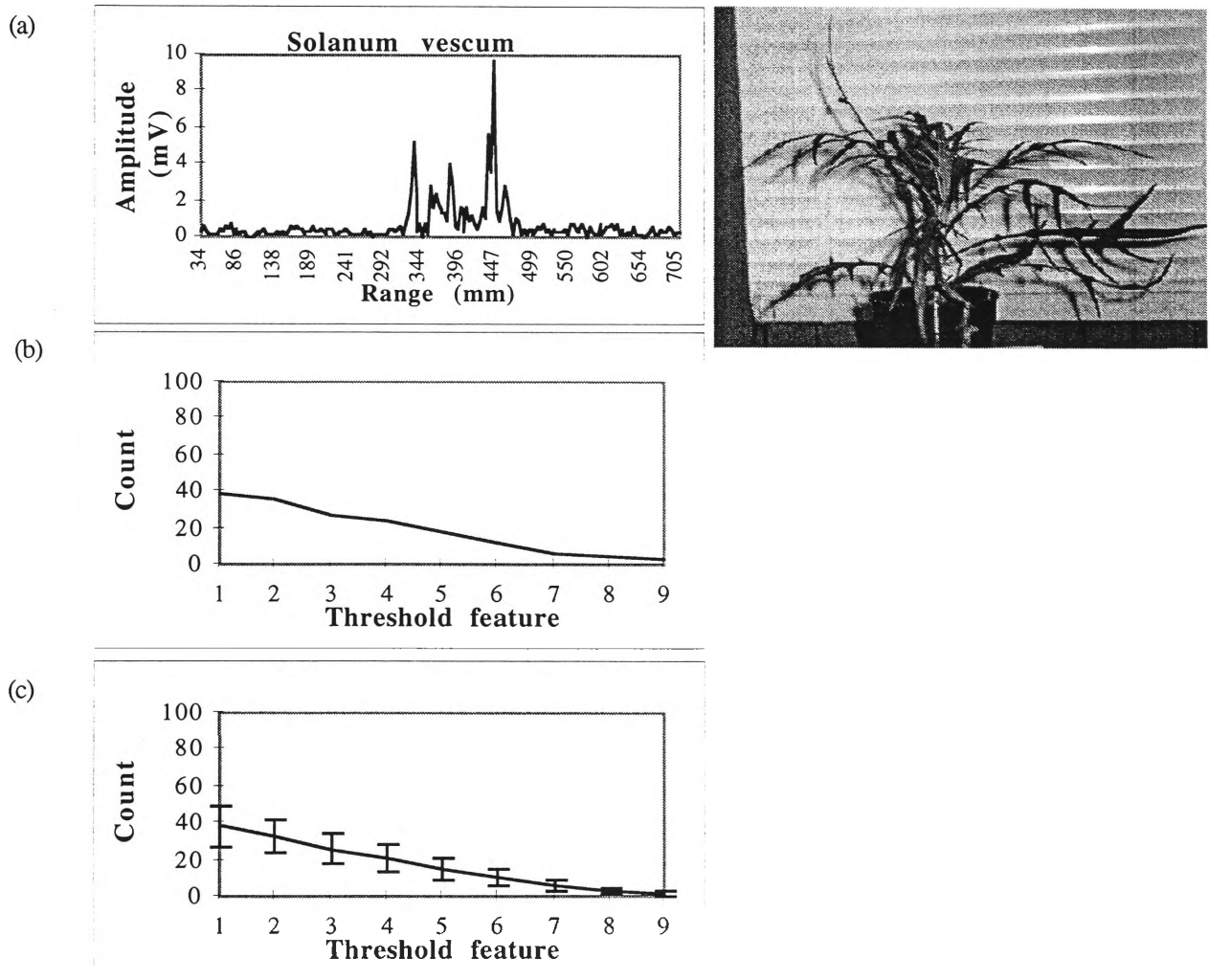


Figure 9.16 *Solanum vescum* with (a) a sample of its acoustic density profile, (b) the features calculated from that acoustic density profile and (c) the averages of the nine features through an entire revolution of the plant with standard deviation shown as error bars.

Solanum vescum is a deep plant with large horizontal leaves, with most of the plant surfaces not producing any echoes at all. The result is an acoustic density profile

which contains a small number of returns of both high and small amplitudes. The value of the first feature is medium due to a number of reflective surfaces. There is a gradual reduction in the count as the threshold is increased.

Table 9.5 shows that this plant has a medium ranking for the first threshold feature (ranked 64) and has a medium-low ranking for the last feature (ranked 40). This means that there are a number of large returns even for high threshold values. Referring again to Figure 9.6, the plant types which show these characteristic features are **type F**, that is a deep plant with large and small reflective surfaces with gaps between the surfaces.

Table 9.5 Plants listed by no_above_threshold1 and no_above_threshold9 with lines linking the same plants in different tables

no above threshold1	Avg	Std	no above threshold9	Avg	Std
Banksia ericifolia	10.1	1.9	Diploglottis australis	0.2	0.5
Melaleuca erubescens	10.2	2.5	Solanum aviculare	0.3	0.6
Crinum pedunculatum	10.6	5.8	Cryptocarya williwilliana	0.6	0.8
Melaleuca styphelioides	11.3	2.8	Cupaniopsis parvifolia	0.6	0.8
Diploglottis australis	11.5	6.5	Melaleuca erubescens	0.8	0.9
Cinnamom oliveri	12.4	4.2	Ayrtera distylis	0.8	0.9
Carpentaria acuminata	13.9	4.2	Banksia ericifolia	0.8	1.1
Acacia cultriformis	14.1	3.0	Acacia mearnsii	0.9	1.0
Westringia fruticosa	15.0	2.8	Solanum laciniatum	1.0	1.0
Agapanthus praecox dwarf	15.6	6.4	Rhododendron bryophyllum	1.0	1.4
Tristaniaopsis collina	15.8	3.8	Tristaniaopsis collina	1.0	1.3
Omalanthus populifolius	16.2	4.7	Omalanthus populifolius	1.1	1.1
Solanum laciniatum	17.0	7.4	Goodia lotifolia	1.1	1.1
Crinum mauritianum	18.7	5.6	Eucalyptus botryoides	1.2	0.9
Agapanthus praecox	19.0	6.4	Cinnamom oliveri	1.2	1.0
Cupaniopsis parvifolia	20.2	6.9	Cupaniopsis anacardioides	1.3	1.0
Livistona sp 'Carnarvon'	20.4	4.6	Cryptocarya bidwilli	1.3	1.2
Ayrtera distylis	20.4	12.1	Microcitrus australis	1.4	1.3
Goodia lotifolia	20.8	5.2	Stenocarpus sinuatus	1.5	1.2
Cordyline australis	20.8	5.3	Pittosporum james	1.7	0.8
Hymenosporum flavum	21.2	4.5	Leptospermum morrisonii	1.7	1.4
Cryptocarya bidwilli	22.4	6.7	Alyxia ruscifolia	1.7	1.6
Guioa semiglauc	22.5	5.8	Litsea reticulata	1.7	1.8
Eucalyptus botryoides	22.5	8.3	Hymenosporum flavum	1.9	1.4
Grevillea hilliana	22.8	6.4	Rhododendron clorinda	1.9	1.9
Pittosporum undulatum	23.5	4.9	Melaleuca styphelioides	1.9	1.9
Rhododendron clorinda	23.6	10.1	Pittosporum undulatum	2.0	1.7
Archontophoenix cunninghamiana	23.8	7.5	Ficus obligna	2.0	2.0
Cryptocarya williwilliana	24.9	2.9	Phyllanthus albiflorus	2.0	1.9
Litsea reticulata	25.3	5.6	Grevillea marmalade	2.0	1.5
Eriostemon myoporoides	25.3	3.6	Guioa semiglauc	2.2	1.5
Casuarina stricta	25.6	4.0	Acacia melanoxylon	2.2	2.7
Solanum aviculare	25.6	5.0	Acacia irrorata	2.2	1.2
Cupaniopsis anacardioides	25.7	7.1	Solanum brownii	2.2	1.9
Grevillea marmalade	25.8	12.4	Agapanthus praecox dwarf	2.3	2.0
Laccospadix australasica	26.0	6.4	Endiandra introrsa	2.3	1.0
Alyxia ruscifolia	26.1	3.6	Howea forsteriana	2.3	1.6
Doryanthes palmeri	26.8	7.1	Azalea alba magnifica	2.3	1.3
Rhododendron bryophyllum	27.5	6.8	Sarcomelicope simplifolia	2.5	1.5
Leptospermum morrisonii	28.7	4.4	Solanum vescum	2.5	1.8
Howea forsteriana	29.1	12.5	Carpentaria acuminata	2.5	2.1
Strebliis brunonianus	29.6	5.8	Mishocarpus australis	2.7	1.5
Microcitrus australis	29.6	10.3	Ziera collina	2.8	2.0
Acacia falcata	30.0	9.4	Pittosporum revolutum	2.9	2.1
Solanum brownii	30.0	10.0	Polyscias australiana	2.9	2.3
Melaleuca decora	30.2	4.5	Correa alba	2.9	1.9
Indigofera australis	31.0	3.7	Eucalyptus leucoxylon	3.0	1.9
Acacia mearnsii	31.1	6.1	Crinum pedunculatum	3.0	1.6
Acacia stricta	31.6	4.4	Casuarina stricta	3.0	1.6
Eucalyptus maculata	32.1	9.5	Hakea salicifolia	3.1	1.7
Acacia melanoxylon	32.9	7.1	Agapanthus praecox	3.2	1.9
Stenocarpus sinuatus	33.7	8.6	Rhopalostylis baneri	3.3	2.5
Ficus obligna	33.8	17.6	Westringia fruticosa	3.3	2.2
Melaleuca quinquenervia	34.3	4.1	Pittosporum rhombifolium	3.3	1.8
Pittosporum rhombifolium	34.3	5.0	Tabebuia chrystricha	3.5	1.8
Citriobatus paucifloris	34.4	5.1	Acronychia laevis	3.6	2.2
Rhopalostylis baneri	34.8	9.8	Acacia cultriformis	3.6	1.7
Mishocarpus australis	35.8	6.6	Casuarina torulosa	3.9	2.1
Endiandra introrsa	36.6	5.8	Grevillea hilliana	4.0	2.3
Acacia podalyrifolia	37.0	7.1	Sarcotoechia heterophylla	4.0	2.0
Pittosporum revolutum	37.4	13.0	Eucalyptus maculata	4.1	3.0
Eucalyptus leucoxylon	38.2	15.2	Polyscias murrayi	4.2	2.9
Casuarina torulosa	38.2	7.4	Melaleuca quinquenervia	4.2	3.7
Solanum vescum	38.5	11.0	Melaleuca decora	4.3	1.7
Acacia longifolia	38.7	9.2	Citriobatus paucifloris	4.3	2.5
Sarcomelicope simplifolia	39.2	9.0	Polyscias elegans	4.6	2.2
Azalea alba magnifica	40.2	11.6	Archontophoenix cunninghamiana	4.6	2.0
Phyllanthus albiflorus	40.2	4.8	Endiandra pubens	4.7	2.6
Polyscias australiana	41.6	11.3	Banksia integrifolia	4.7	2.3
Syzygium paniculatum	41.7	6.7	Cryptocarya laevigatum	4.8	2.0
Pittosporum james	41.8	8.5	Grevillea baileyana	4.8	2.5
Grevillea baileyana	42.7	4.9	Casuarina glauca	4.9	2.6
Casuarina glauca	45.1	5.2	Radermacheria fenecis	4.9	2.5
Correa alba	45.2	5.4	Acacia longifolia	5.0	2.2
Syzygium leuhmanni	45.8	4.6	Dodonaea triquetra	5.0	2.2
Rhopalostylis sapida	46.2	11.3	Cordyline australis	5.3	2.6
Hakea salicifolia	46.6	8.2	Eriostemon myoporoides	5.3	2.7
Dodonaea triquetra	47.0	5.3	Diploglottis campbelli	5.5	3.9
Polyscias elegans	47.3	9.6	Syzygium leuhmanni	5.5	3.0
Ziera collina	50.4	6.9	Rhopalostylis sapida	5.6	2.3
Ficus rubiginosa	50.4	5.4	Pittosporum crassifolium	5.7	2.5
Cryptocarya laevigatum	52.5	6.3	Strebliis brunonianus	5.7	2.6
Leptospermum petersonii	53.0	6.6	Leptospermum petersonii	5.7	3.3
Acacia binervata	56.1	6.4	Laccospadix australasica	5.1	2.9
Dodonaea viscosa	56.2	7.3	Azalea cultivar splenda	6.4	3.0
Pittosporum crassifolium	58.3	6.2	Indigofera australis	6.6	2.9
Diploglottis campbelli	58.7	9.4	Crinum mauritianum	8.6	3.3
Acacia howittii	59.1	7.4	Livistona sp 'Carnarvon'	8.7	3.3
Tabebuia chrystricha	61.1	8.5	Acacia stricta	8.8	2.9
Endiandra pubens	61.3	10.5	Acacia falcata	7.5	3.2
Banksia integrifolia	61.5	16.9	Syzygium paniculatum	7.5	3.4
Acacia irrorata	63.6	12.6	Jacaranda mimosifolia	7.8	2.8
Acronychia laevis	64.9	15.0	Ficus rubiginosa	8.0	3.1
Polyscias murrayi	65.3	10.5	Doryanthes palmeri	8.6	3.7
Jacaranda mimosifolia	65.7	6.2	Acacia podalyrifolia	9.3	3.6
Sarcotoechia heterophylla	67.4	11.1	Acacia binervata	10.0	4.1
Radermacheria fenecis	70.2	9.9	Acacia howittii	10.9	3.0
Licuala ramsayi	72.0	15.0	Dodonaea viscosa	11.7	3.8
Azalea cultivar splenda	74.2	11.8	Leptospermum laevigatum	17.9	5.3
Leptospermum laevigatum	84.9	8.2	Licuala ramsayi	18.0	4.3

9.4.1.2 Analysis of a selection of shallow sample plants

In this section, the threshold features calculated from some shallow plants is analysed. A shallow plant is one which has an acoustic depth of at most 170 mm.

9.4.1.2.1 *Cupaniopsis parvifolia* (type A)

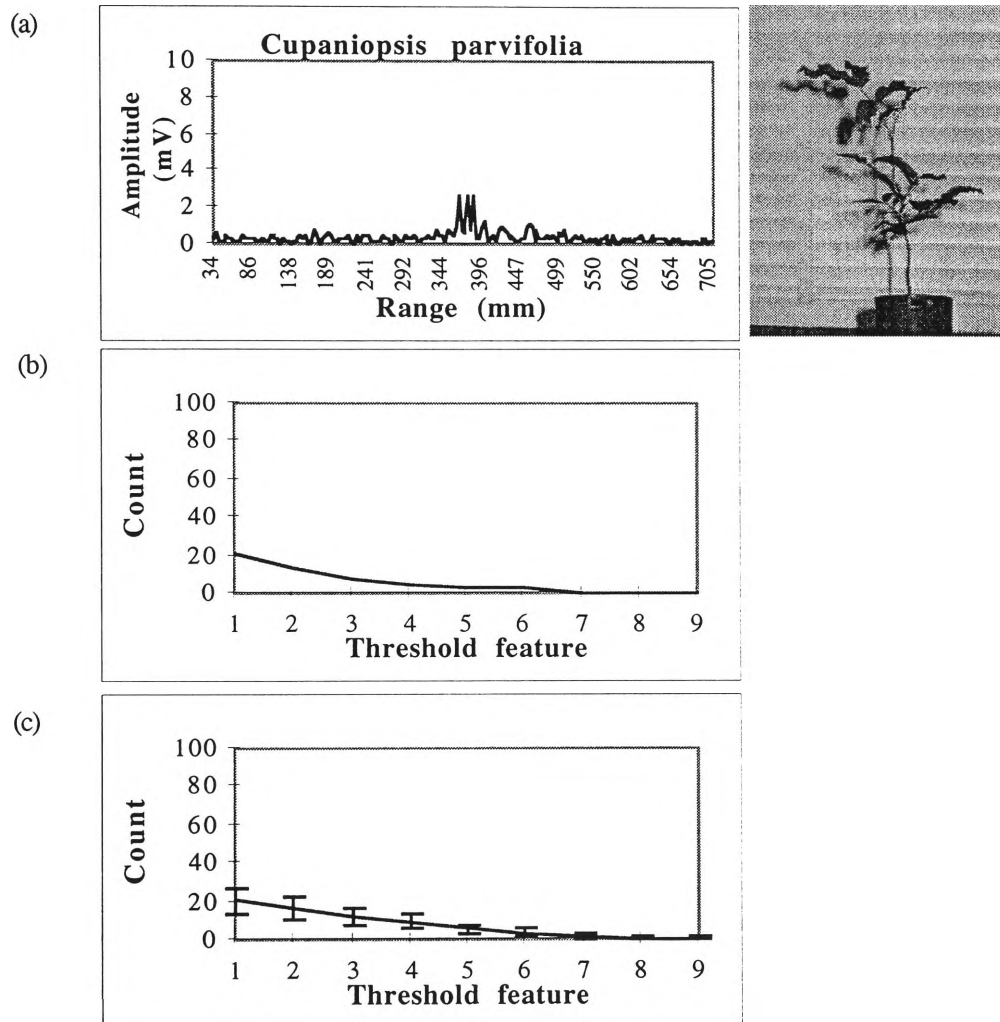


Figure 9.17 *Cupaniopsis parvifolia* with (a) a sample of its acoustic density profile, (b) the features calculated from that acoustic density profile, and (c) the averages of the nine features through an entire revolution with standard deviation shown as error bars

As shown in Figure 9.17, the plant is relatively compact with small reflective surfaces which return acoustic energy back to the sensor. This is because none of the leaves are orthogonal to the sensor. The reflected signal is all of very low amplitude. For the acoustic density profile shown, the count starts from a very low level and quickly drops down to a very low level (close to 0). Table 9.5 shows that this plant has a low

value with respect to the others in the population (row 19) and ends up with an extremely value for no_above_threshold9 (row 4). This acoustic density profile/feature pattern is shown to be **type A** in Figure 9.7.

9.4.1.2.2 *Citriobatus paucifloris* (type C)

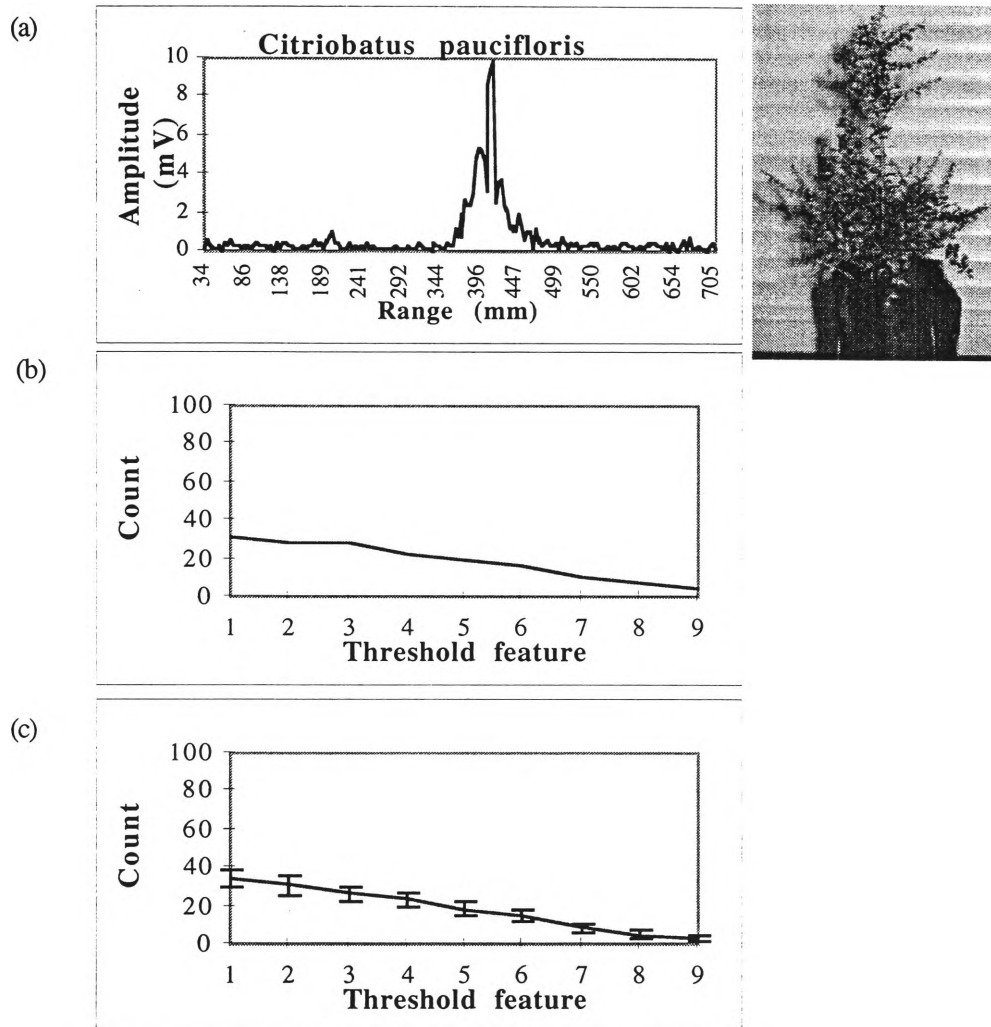


Figure 9.18 *Citriobatus paucifloris* with (a) a sample of its acoustic density profile, (b) the features calculated from that acoustic density profile, and (c) the averages of the nine features through an entire revolution with standard deviation shown as error bars.

Citriobatus paucifloris is a compact plant with many surfaces returning acoustic energy to the receiver. All of the returns are of a high amplitude because of the large number of surfaces at each range. It has a low number for the count of range lines for all of the features because it is so shallow. The count does not drop as significantly as other plants because many of the range cells contain high amplitudes. When this is compared against the models in Figure 9.7, this plant is of **type C**.

9.4.1.3 Discussion of Plant Depth

Detailed analysis of the models of plant types in Figure 9.6 and Figure 9.7 shows that there is not enough information in the threshold features alone to classify a plant as one of the major types. For example, a deep plant of type B, has the same threshold features as a narrow plant of type A. Similar situations occur for distinguishing narrow plants of type C from deep plants of type C. This is complicated further by the fact that true acoustic density profiles are often somewhere between one of the generalised models.

In order to eliminate the plant depth issue, the threshold features can be normalised by dividing by the acoustic depth of the plant (the feature `length_of_density_profile`). Table 9.6 shows similar information to Table 9.5 except that the threshold features have been divided through by `length_of_density_profile`. It is immediately obvious that the plants of similar type are now in a similar position in the table (they are much closer together) for both `no_above_threshold1` and `no_above_threshold9`. The type A plants are now situated together at the bottom of the acoustic density profile and the type C plants are at the top whether they are deep or shallow. This confirms that normalisation for depth can be useful for differentiating between plants.

The same information is also shown in Figure 9.19. Plants are labelled with their number (see Chapter 5 for a cross reference of plant identifiers). Plants with small reflective surfaces and sparse foliage are in the bottom left hand corner of the graph and the other plant types are labelled into their major groups. The lines shown on the graph represent the average value for the samples from each of the axes. These lines separate the major groups but in reality, there is a continuum of levels between large and small, and dense and sparse. The graph shows that of the data from the plant samples, those which are the smallest and most sparse are nearest to the origin, and similarly those with the most dense foliage and largest surfaces are those which are closest to the top right hand corner.

Table 9.6 Plants listed by no_above_threshold1 and no_above_threshold9, both divided by length_of_density_profile

	thresh1/length_density_profile	Avg		thresh9/length_density_profile	Avg	
Sparse Plants	Eucalyptus botryoides	0.5210		Solanum aviculare	0.0030	Small Reflective Surfaces
	Carpentaria acuminata	0.5320		Diploglottis australis	0.0050	
	Grevillea marmalade	0.5440		Cryptocarya williiwilliana	0.0067	
	Ficus obliva	0.5480		Cupaniopsis parvifolia	0.0082	
	Rhododendron clorinda	0.5720		Acacia mearnsii	0.0106	
	Howea foresteriana	0.5730		Ayrtia distylis	0.0119	
	Stenocarpus sinuatus	0.5820		Rhododendron bryophyllum	0.0125	
	Diploglottis australis	0.5860		Pittosporum james	0.0142	
	Pittosporum revolutum	0.5860		Stenocarpus sinuatus	0.0148	
	Rhododendron bryophyllum	0.5970		Acacia irrorata	0.0150	
	Polyscias australiana	0.6030		Eucalyptus botryoides	0.0170	
	Sarcomelicope simplifolia	0.6030		Microcitrus australis	0.0177	
	Solanum aviculare	0.6140		Cupaniopsis anacardioides	0.0193	
	Cupaniopsis anacardioides	0.6170		Solanum laciniatum	0.0193	
	Ayrtia distylis	0.6190		Ficus obliva	0.0202	
	Solanum laciniatum	0.6230		Goodia lotifolia	0.0217	
	Litsea reticulata	0.6250		Melaleuca erubescens	0.0220	
	Omalanthus populifolius	0.6250		Sarcomelicope simplifolia	0.0231	
	Cupaniopsis parvifolia	0.6280		Azalea alba magnifica	0.0235	
	Grevillea hilliana	0.6320		Acronychia laevis	0.0237	
	Azalea alba magnifica	0.6360		Omalanthus populifolius	0.0246	
	Microcitrus australis	0.6380		Tabebuia chrystricha	0.0248	
	Goodia lotifolia	0.6390		Cryptocarya bidwilli	0.0252	
	Eucalyptus maculata	0.6460		Leptospermum morrisonii	0.0253	
	Eucalyptus leucosylon	0.6480		Polyscias australiana	0.0257	
	Solanum brownii	0.6540		Phyllanthus albilorus	0.0261	
	Casuarina stricta	0.6600		Litsea reticulata	0.0263	
	Agapanthus praecox dwarf	0.6650		Sarcotoechia heterophylla	0.0263	
	Acacia longifolia	0.6670		Ziera collina	0.0269	
	Pittosporum undulatum	0.6690		Rhododendron clorinda	0.0271	
	Cinnamom oliveri	0.6790		Grevillea marmalade	0.0274	
	Agapanthus praecox	0.6820		Pittosporum revolutum	0.0276	
	Pittosporum james	0.6830		Endiandra introrsa	0.0278	
	Acacia mearnsii	0.6840		Tristaniopsis collina	0.0278	
	Archontophoenix cunninghamiana	0.6890		Howea foresteriana	0.0283	
	Rhopalostylis baneri	0.6900		Hakea salicifolia	0.0290	
	Solanum vescum	0.6900		Alyxia ruscifolia	0.0293	
	Rhopalostylis sapida	0.6910		Solanum brownii	0.0293	
	Sarcotoechia heterophylla	0.6920		Solanum vescum	0.0300	
	Grevillea baileyana	0.6940		Polyscias murrayi	0.0308	
	Cryptocarya bidwilli	0.6980		Correa alba	0.0309	
	Acacia falcata	0.6990		Eucalyptus leucosylon	0.0314	
	Guioa semiglauc	0.6990		Acacia melanoxylon	0.0316	
	Polyscias elegans	0.6990		Pittosporum undulatum	0.0347	
Dense Plants	Hakea salicifolia	0.7010		Radermacheria tenecis	0.0349	Size of Reflective Surfaces
	Laccospadix australasica	0.7110		Banksia integrifolia	0.0353	
	Endiandra introrsa	0.7140		Mishocarpus australis	0.0359	
	Acacia irrorata	0.7150		Banksia ericifolia	0.0367	
	Diploglottis campbelli	0.7160		Endiandra pubens	0.0368	
	Crinum pedunculatum	0.7210		Hymenosporum flavum	0.0381	
	Dodonaea triquetra	0.7210		Rhopalostylis baneri	0.0389	
	Banksia integrifolia	0.7270		Diploglottis campbelli	0.0396	
	Cordylina australis	0.7310		Guioa semiglauc	0.0410	
	Acronychia laevis	0.7370		Cinnamom oliveri	0.0412	
	Mishocarpus australis	0.7370		Azalea cultivar splenda	0.0418	
	Pittosporum rhombifolium	0.7390		Polyscias elegans	0.0420	
	Casuarina glauca	0.7400		Pittosporum rhombifolium	0.0432	
	Hymenosporum flavum	0.7420		Casuarina torulosa	0.0441	
	Polyscias murrayi	0.7420		Cryptocarya laevigatum	0.0443	
	Azalea cultivar splenda	0.7450		Pittosporum crassifolium	0.0483	
	Tabebuia chrystricha	0.7510		Dodonaea triquetra	0.0485	
	Ficus rubiginosa	0.7520		Casuarina stricta	0.0496	
	Cryptocarya williiwilliana	0.7530		Grevillea baileyana	0.0500	
	Melaleuca erubescens	0.7580		Casuarina glauca	0.0511	
	Tristaniopsis collina	0.7590		Rhopalostylis sapida	0.0514	
	Licuala ramsayi	0.7610		Eucalyptus maculata	0.0529	
	Cryptocarya laevigatum	0.7640		Acacia longifolia	0.0544	
	Endiandra pubens	0.7650		Szygium leuhmanni	0.0549	
	Casuarina torulosa	0.7670		Leptospermum petersonii	0.0567	
	Ziera collina	0.7690		Agapanthus praecox dwarf	0.0596	
	Szygium leuhmanni	0.7740		Grevillea hilliana	0.0642	
	Acacia stricta	0.7750		Citriobatus paucifloris	0.0650	
	Melaleuca styphelioides	0.7760		Carpentaria acuminata	0.0665	
	Acacia melanoxylon	0.7810		Jacaranda mimosifolia	0.0668	
	Melaleuca decora	0.7820		Melaleuca quinquenervia	0.0676	
	Radermacheria tenecis	0.7830		Agapanthus praecox	0.0695	
	Streblis brunonianus	0.7830		Melaleuca decora	0.0733	
	Correa alba	0.7840		Melaleuca styphelioides	0.0799	
	Westringia fruticosa	0.7860		Archontophoenix cunninghamiana	0.0824	
	Leptospermum morrisonii	0.7880		Ficus rubiginosa	0.0864	
	Citriobatus paucifloris	0.7890		Acacia binervata	0.0943	
	Eriostemon myoporoides	0.7940		Streblis brunonianus	0.0969	
	Dodonaea viscosa	0.7950		Acacia howittii	0.0971	
	Doryanthes palmeri	0.7960		Szygium paniculatum	0.1001	
	Acacia podalyrifolia	0.8020		Eriostemon myoporoides	0.1012	
	Acacia binervata	0.8030		Laccospadix australasica	0.1021	
	Acacia howittii	0.8070		Westringia fruticosa	0.1036	
	Pittosporum crassifolium	0.8090		Cordylina australis	0.1113	
	Leptospermum petersonii	0.8110		Leptospermum laevigatum	0.1116	
	Livistona sp 'Carnarvon'	0.8120		Dodonaea viscosa	0.1146	
	Alyxia ruscifolia	0.8140		Acacia falcata	0.1158	
	Phyllanthus albilorus	0.8150		Indigofera australis	0.1206	
	Szygium paniculatum	0.8160		Acacia stricta	0.1217	
	Banksia ericifolia	0.8210		Crinum pedunculatum	0.1266	
	Crinum mauritianum	0.8240		Acacia cultriformis	0.1269	
	Jacaranda mimosifolia	0.8260		Acacia podalyrifolia	0.1329	
	Melaleuca quinquenervia	0.8270		Licuala ramsayi	0.1370	
	Acacia cultriformis	0.8280		Doryanthes palmeri	0.1759	Large Reflective Surfaces
	Leptospermum laevigatum	0.8310		Livistona sp 'Carnarvon'	0.1929	
	Indigofera australis	0.8470		Crinum mauritianum	0.1949	

Foliage density Vs Size of reflective surface

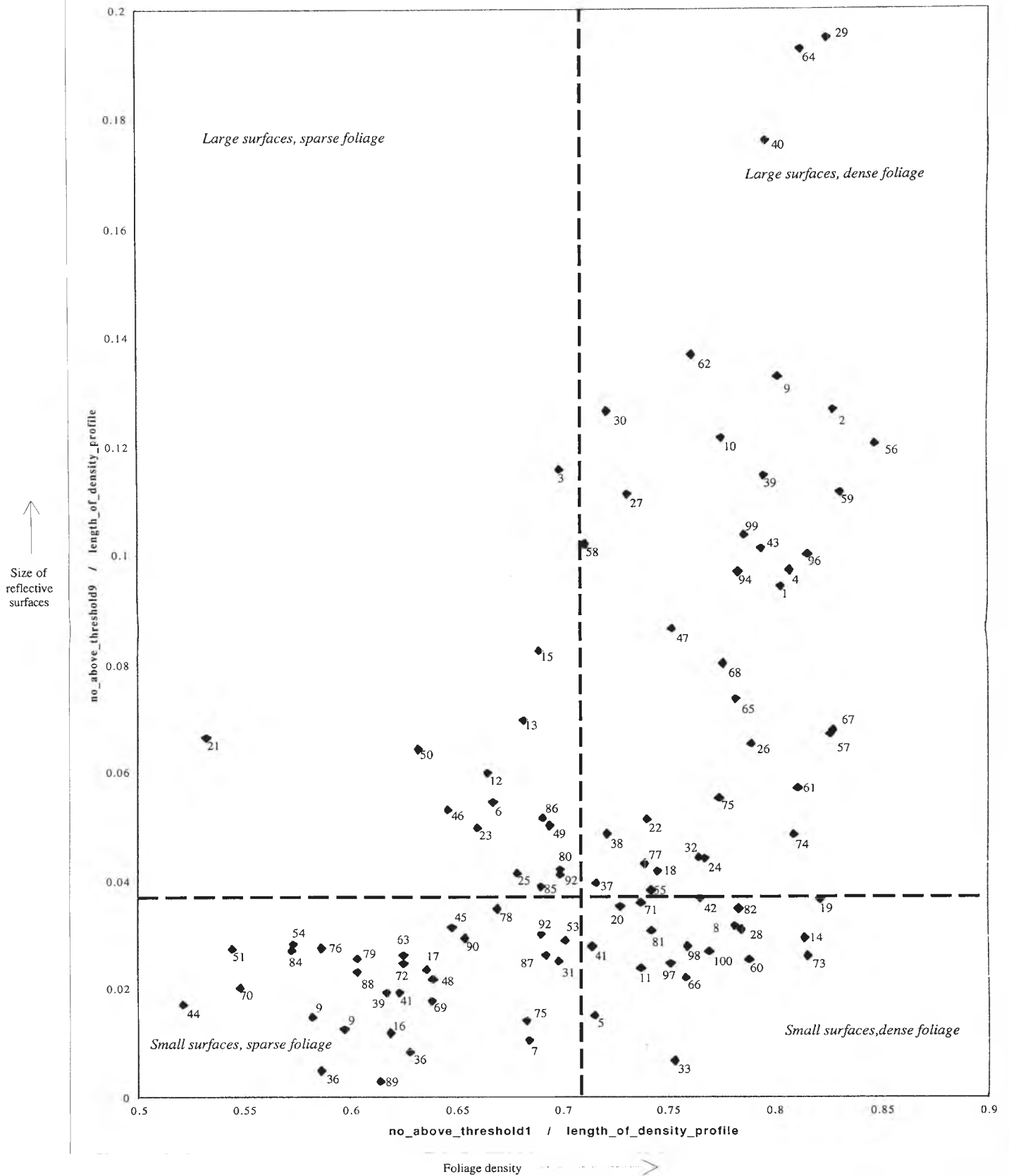


Figure 9.19 Foliage density vs Size of reflective surfaces

9.4.1.4 Interpretation of Results

Figure 9.6 can be used as the basis of interpreting the normalised data. Basic plant types can be identified using simple rules developed directly from the model and are given in Algorithm 9.2. The values for HIGH, MEDIUM and LOW can be calculated from the data for the particular feature. Cut off points of 33 and 66% of the range of the features classify 51% of the plants into one of these broad classes. A significant improvement can be made by adding rules to cater for the conditions not covered in this table. These rules could be implemented in many different ways, but a set of fuzzy rules would be particularly useful with results based on the fuzzy set membership of each plant.

Algorithm 9.2 Simple rules to interpret the threshold features

```
feature1 = no_above_threshold1/length_of_density_profile
feature2 = no_above_threshold9/length_of_density_profile

If feature1 is HIGH and feature2 is LOW
THEN
    type A
    the plant has small reflecting surfaces spread throughout the
plant
ELSE
    If feature1 is MEDIUM and feature2 is LOW
    THEN
        Type B
        the plant has small reflective surfaces and sparse
    ELSE
        If feature1 is HIGH and feature2 is HIGH
        THEN
            type C
            the plant has large reflective surfaces spread
evenly
        ELSE
            If feature1 is MEDIUM and feature2 is MEDIUM
            THEN
                type D
                the plant has large surfaces spread sparsely
            END
        END
    END
END
END
```

These rules developed from the model can be simplified into rules which independently provide information about the spread of the surfaces within the plant and the size of the reflective surfaces.

Algorithm 9.3 A simplified set of rules to determine the major plant types

```
IF feature1 is HIGH
THEN
    there are surfaces spread through out the plant
ELSE
    the surfaces are sparse
END
IF feature2 is HIGH or MEDIUM
THEN
    the surfaces are large
ELSE
    the surfaces are small
END
```

This can be related directly to Table 9.6. The higher the value of `no_above_threshold1/length_of_density_profile`, the more evenly spread are the surfaces within the plant. Similarly, the right hand side of the table gives an indication of the size of the reflective surfaces, that is, the higher the value of `no_above_threshold9/length_of_density_profile`, the larger the reflective surfaces.

Heuristic 9.1 Interpretation of threshold features

```
no_above_threshold1/length_of_density_profile is proportional to the density of
the leaves
no_above_threshold9/length_of_density_profile is proportional to the size of the
surfaces
```

9.4.2 Transformation of number_above_threshold

From the above analysis, we can define, in concept at least, the transform from signal feature to plant physical feature for a set of signal features called `number_above_threshold1 - 9`.

As stated earlier, the height of a range line is proportional to the acoustic area of the reflectors at that range. In Section 9.6, we see that the sum of the amplitudes of the lines is the total acoustic area of the plant. Thresholding the amplitude of the range lines gives a granular measure of the acoustic area of the plant. Thus, the number of lines above threshold n is the number of acoustic areas (one per range) in the plant that are larger than a certain size. Normalisation, by dividing the count by the depth, and

discarding information in all but the first threshold (`no_above_threshold1`) and the last threshold (`no_above_threshold9`) allows direct interpretation of the physical structure of the plant.

A high value for a threshold feature represents a large acoustic area and this is the transformation from signal feature to acoustic feature. The thresholds breaks up the acoustic area into nine levels. A large acoustic area can be due to a few large leaves or many small leaves with surfaces oriented towards the sensor.

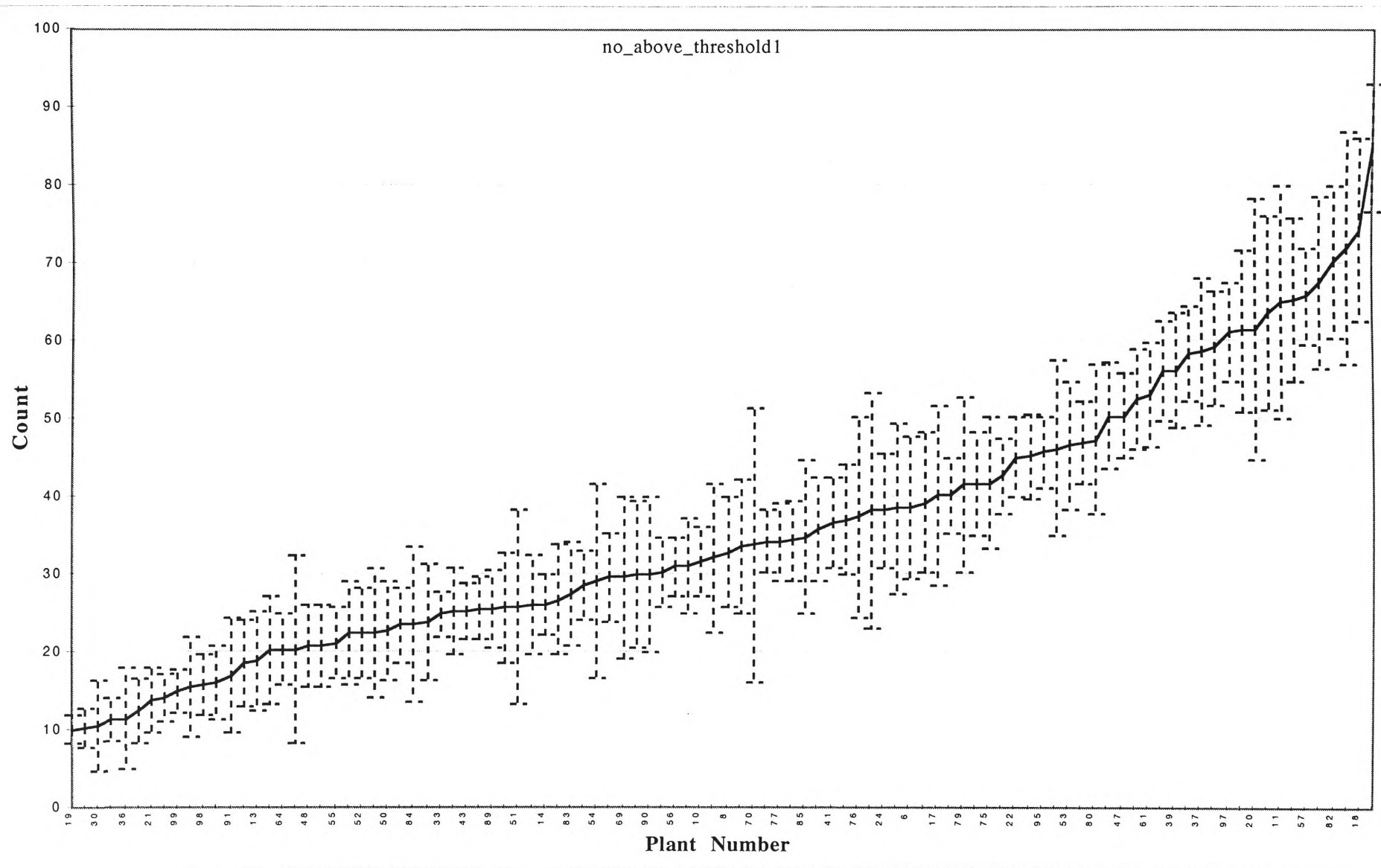


Figure 9.20 The average of no_above_threshold1 for all 100 plants (error bars are standard deviation)

Table 9.7 no_above_threshold1 for all 100 plants

Plant Name	Avg	Std			
			<i>Acacia melanoxylon</i>	32.9	7.1
<i>Banksia ericifolia</i>	10.1	1.9	<i>Stenocarpus sinuatus</i>	33.7	8.6
<i>Melaleuca erubescens</i>	10.2	2.5	<i>Ficus obliqua</i>	33.8	17.6
<i>Crinum pedunculatum</i>	10.6	5.8	<i>Melaleuca quinquenervia</i>	34.3	4.1
<i>Melaleuca styphelioides</i>	11.3	2.8	<i>Pittosporum rhombifolium</i>	34.3	5.0
<i>Diploglottis australis</i>	11.5	6.5	<i>Citriobatus paucifloris</i>	34.4	5.1
<i>Cinnamom oliveri</i>	12.4	4.2	<i>Rhopalostylis baneri</i>	34.8	9.8
<i>Carpentaria acuminata</i>	13.9	4.2	<i>Mishocarpus australis</i>	35.8	6.6
<i>Acacia cultriformis</i>	14.1	3.0	<i>Endiandra introrsa</i>	36.6	5.8
<i>Westringa fruticosa</i>	15.0	2.8	<i>Acacia podalyrifolia</i>	37.0	7.1
<i>Agapanthus praecox dwarf</i>	15.6	6.4	<i>Pittosporum revolutum</i>	37.4	13.0
<i>Tristaniopsis collina</i>	15.8	3.8	<i>Eucalyptus leucoxylon</i>	38.2	15.2
<i>Omalanthus populifolius</i>	16.2	4.7	<i>Casuarina torulosa</i>	38.2	7.4
<i>Solanum laciniatum</i>	17.0	7.4	<i>Solanum vescum</i>	38.5	11.0
<i>Crinum mauritianum</i>	18.7	5.6	<i>Acacia longifolia</i>	38.7	9.2
<i>Agapanthus praecox</i>	19.0	6.4	<i>Sarcomelicope simplifolia</i>	39.2	9.0
<i>Cupaniopsis parvifolia</i>	20.2	6.9	<i>Azalea alba magnifica</i>	40.2	11.6
<i>Livistona sp 'Carnarvon'</i>	20.4	4.6	<i>Phyllanthus albiflorus</i>	40.2	4.8
<i>Ayrtera distylis</i>	20.4	12.1	<i>Polyscias australiana</i>	41.6	11.3
<i>Goodia lotifolia</i>	20.8	5.2	<i>Szygium paniculatum</i>	41.7	6.7
<i>Cordyline australis</i>	20.8	5.3	<i>Pittosporum james</i>	41.8	8.5
<i>Hymenosporum flavum</i>	21.2	4.5	<i>Grevillea baileyana</i>	42.7	4.9
<i>Cryptocarya bidwilli</i>	22.4	6.7	<i>Casuarina glauca</i>	45.1	5.2
<i>Guioa semiglauca</i>	22.5	5.8	<i>Correa alba</i>	45.2	5.4
<i>Eucalyptus botryoides</i>	22.5	8.3	<i>Szygium leuhmanni</i>	45.8	4.6
<i>Grevillea hilliana</i>	22.8	6.4	<i>Rhopalostylis sapida</i>	46.2	11.3
<i>Pittosporum undulatum</i>	23.5	4.9	<i>Hakea salicifolia</i>	46.6	8.2
<i>Rhododendron clorinda</i>	23.6	10.1	<i>Dodonaea triquetra</i>	47.0	5.3
<i>Archontophoenix cunninghamiana</i>	23.8	7.5	<i>Polyscias elegans</i>	47.3	9.6
<i>Cryptocarya williwilliana</i>	24.9	2.9	<i>Ziera collina</i>	50.4	6.9
<i>Litsea reticulata</i>	25.3	5.6	<i>Ficus rubiginosa</i>	50.4	5.4
<i>Eriostemon myoporoides</i>	25.3	3.6	<i>Cryptocarya laevigatum</i>	52.5	6.3
<i>Casuarina stricta</i>	25.6	4.0	<i>Leptospermum petersonii</i>	53.0	6.6
<i>Solanum aviculare</i>	25.6	5.0	<i>Acacia binervata</i>	56.1	6.4
<i>Cupaniopsis anacardioides</i>	25.7	7.1	<i>Dodonaea viscosa</i>	56.2	7.3
<i>Grevillea marmalade</i>	25.8	12.4	<i>Pittosporum crassifolium</i>	58.3	6.2
<i>Laccospadix australasica</i>	26.0	6.4	<i>Diploglottis campbelli</i>	58.7	9.4
<i>Alyxia ruscifolia</i>	26.1	3.8	<i>Acacia howittii</i>	59.1	7.4
<i>Doryanthes palmeri</i>	26.8	7.1	<i>Tabebula chrystricha</i>	61.1	6.5
<i>Rhododendron bryophyllum</i>	27.5	6.8	<i>Endiandra pubens</i>	61.3	10.5
<i>Leptospermum morrisonii</i>	28.7	4.4	<i>Banksia integrifolia</i>	61.5	16.9
<i>Howea forsteriana</i>	29.1	12.5	<i>Acacia irrorata</i>	63.6	12.6
<i>Streblis brunonianus</i>	29.6	5.8	<i>Acronychia laevis</i>	64.9	15.0
<i>Microcitrus australis</i>	29.6	10.3	<i>Polyscias murrayi</i>	65.3	10.5
<i>Acacia falcata</i>	30.0	9.4	<i>Jacaranda mimosifolia</i>	65.7	6.2
<i>Solanum brownii</i>	30.0	10.0	<i>Sarcotoechia heterophylla</i>	67.4	11.1
<i>Melaleuca decora</i>	30.2	4.5	<i>Radermacheria fenecis</i>	70.2	9.9
<i>Indigofera australis</i>	31.0	3.7	<i>Licuala ramsayi</i>	72.0	15.0
<i>Acacia mearnsii</i>	31.1	6.1	<i>Azalea cultivar splenda</i>	74.2	11.8
<i>Acacia stricta</i>	31.6	4.4	<i>Leptospermum laevigatum</i>	84.9	8.2
<i>Eucalyptus maculata</i>	32.1	9.5			

9.5 The number of major peaks in the acoustic density profile

These two features (`no_of_major_peaks1` and `no_of_major_peaks2`) are a measure of the number of peaks in the acoustic density profile and this section shows that it gives information about the distribution of surfaces within the plant.

A major peak is defined as a range cell where the amplitude is greater than a set amplitude and is also greater than that of the five range cells on each side of it in the acoustic density profile. `no_of_major_peaks1` is incremented when the amplitude is greater than $195/m$ mV and for `no_of_major_peaks2` the threshold is $156/m$ mV (Note that m is the calibration measure defined in Chapter 8). The algorithm for calculating these features is given in Algorithm 9.4. To calculate these features, the function is called with the parameters of 195, 5 and 156, 5. The code for calculating these features is given in Appendix C.

Algorithm 9.4 Algorithm for calculating `no_of_major_peaks` features

```
CALCULATE NUMBER OF MAJOR PEAKS
  This function is passed a threshold level, a width value and an
  acoustic density profile. It calculates the number of major peaks
  in the acoustic density profile by looking for range cells which
  are greater than the threshold and width range cells either side
  are less than it. Note that this is done only range cells which
  are between the start and end of the plant.
  Parameters :
    profile      an array which contains the raw
                  acoustic density profile.
    threshold    value which the cell needs to be greater than.
    width        number of range cells the peak needs to be
                  greater than.
    m            the calibration measure which is the amplitude
                  received by the system when pointing at
                  a large specular surface
                  at a range of 0.005 metres.

  Returns :
    the count of the number of peaks in the acoustic
    density profile

BEGIN
  Initialise the count to 0.
  Call the function to calculate the position of the start of
    the plant.
  Call the function to calculate the position of the end of
    the plant.
  Process elements from start_index to end_index
  BEGIN
```



```

        IF the element is greater than the threshold / m
        THEN
            set major_peak_flag to TRUE
            Process elements from
                current-point - width TO current_point + width
            WHILE major_peak_flag is TRUE
            BEGIN
                if element > this peak
                THEN
                    set major_peak_flag to FALSE
                END
            END
            IF major_peak_flag is still TRUE
            THEN
                increment the count of major peaks
            END
        END
    END
END

```

The major peaks detected by this function are ones which are 17.2 mm (the equivalent of five range cells) away from any other acoustic areas of equal or greater size. This provides a measure of the distribution of the foliage in respect to the orientation from which the plant is insonified.

Table 9.8 shows the value of no_of_major_peaks1 calculated for each of the 100 plant specimens and this is also graphed in Figure 9.22.

Figure 9.21 shows a plant from above being insonified with areas of large reflective surfaces shown as grey filled areas and every five range cells shown as light grey lines. As the sensing system is moved around the plant (or the plant is rotated), the position of the leaves in the acoustic density profile changes depending of the place that the plant is insonified from.

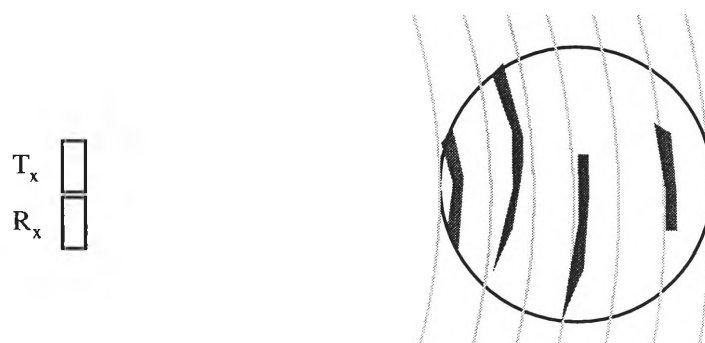


Figure 9.21 Insonification of a plant showing leaves from two different positions

Plants at the top of the table only have a small number of these peaks and are plants which are very narrow (for example, *Banksia ericifolia* 6 cm, *Melaleuca erubescens*

6 cm, and *Melaleuca styphelioides* 6 cm) or are deep but only have a few leaves (for example, *Crinum mauritianum* 30 cm, *Carpentaria acuminata* 30 cm, and *Cordyline australis* 60 cm). Plants with a high value of this feature are not necessarily the deepest (for example, *Leptospermum petersonii* 20 cm and *Ficus rubiginosa* 20 cm), but generally, those plants which are the deepest have their acoustic density profile spread over the greatest number of range lines and hence there is a greater chance that they will have a higher number of peaks.

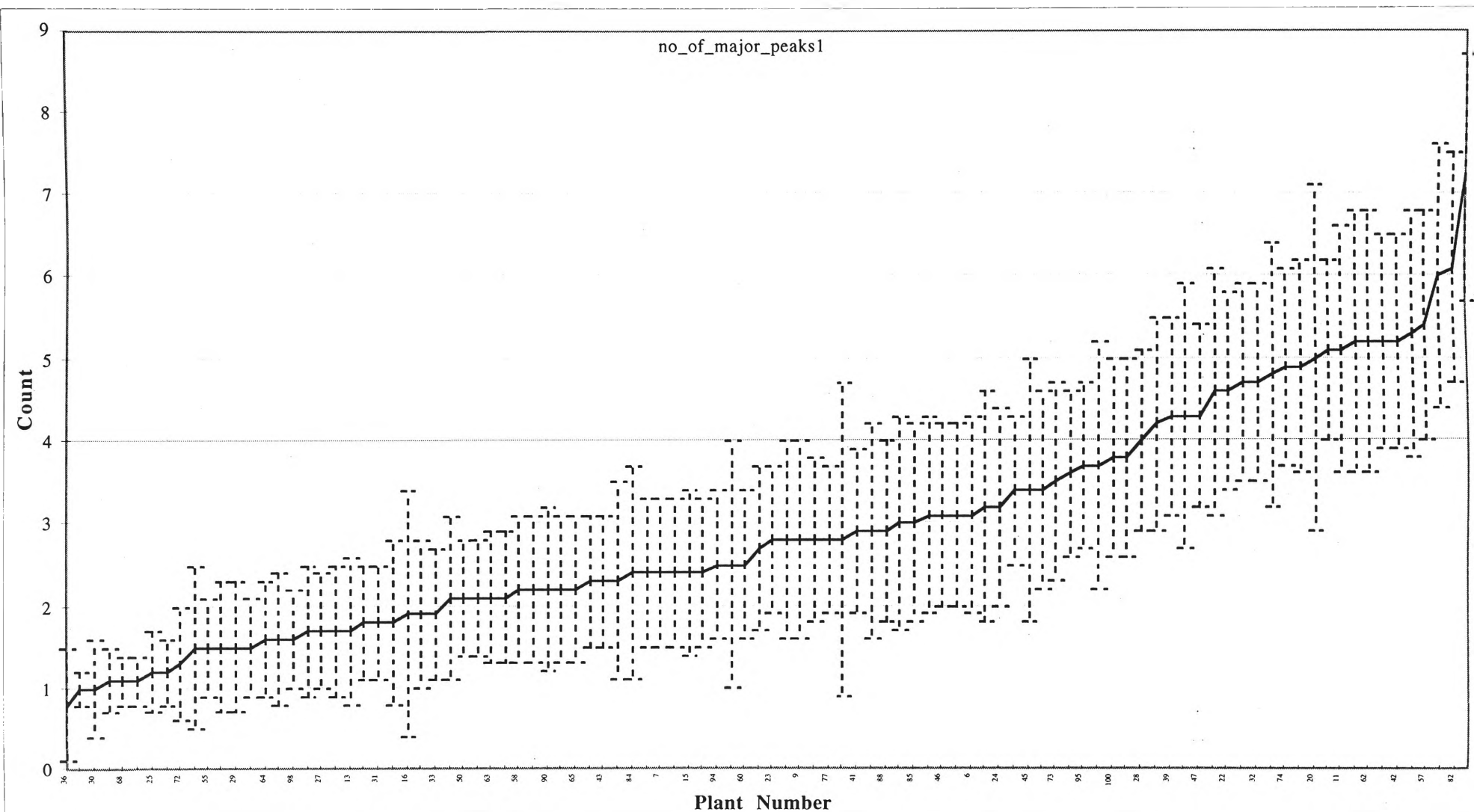


Figure 9.22 The average no_of_major_peaks1 for all 100 plants (error bars are standard deviation)

Table 9.8 Average no_of_major_peaks1 for all 100 plants

Plant Name	Avg	Std			
<i>Diploglottis australis</i>	0.8	0.7	<i>Casuarina stricta</i>	2.8	0.9
<i>Banksia ericifolia</i>	1.0	0.2	<i>Acacia falcata</i>	2.8	1.2
<i>Crinum pedunculatum</i>	1.0	0.6	<i>Acacia podalyrifolia</i>	2.8	1.2
<i>Melaleuca erubescens</i>	1.1	0.4	<i>Grevillea baileyana</i>	2.8	1.0
<i>Melaleuca styphelioides</i>	1.1	0.3	<i>Pittosporum rhombifolium</i>	2.8	0.9
<i>Westringa fruticosa</i>	1.1	0.3	<i>Ficus obliqua</i>	2.8	1.9
<i>Cinnamom oliveri</i>	1.2	0.5	<i>Endiandra introrsa</i>	2.9	1.0
<i>Acacia cultriformis</i>	1.2	0.4	<i>Solanum vescum</i>	2.9	1.3
<i>Omalanthus populifolius</i>	1.3	0.7	<i>Sarcomelicope simplifolia</i>	2.9	1.1
<i>Solanum laciniatum</i>	1.5	1.0	<i>Pittosporum james</i>	3.0	1.3
<i>Hymenosporum flavum</i>	1.5	0.6	<i>Rhopalostylis baneri</i>	3.0	1.2
<i>Agapanthus praecox dwarf</i>	1.5	0.8	<i>Azalea alba magnifica</i>	3.1	1.2
<i>Crinum mauritianum</i>	1.5	0.8	<i>Eucalyptus maculata</i>	3.1	1.1
<i>Carpentaria acuminata</i>	1.5	0.6	<i>Acacia melanoxylon</i>	3.1	1.1
<i>Livistona sp 'Carnarvon'</i>	1.6	0.7	<i>Acacia longifolia</i>	3.1	1.2
<i>Solanum aviculare</i>	1.6	0.8	<i>Polyscias australiana</i>	3.2	1.4
<i>Tristaniopsis collina</i>	1.6	0.6	<i>Casuarina torulosa</i>	3.2	1.2
<i>Guioa semiglauca</i>	1.7	0.8	<i>Melaleuca quinquenervia</i>	3.4	0.9
<i>Cordyline australis</i>	1.7	0.7	<i>Eucalyptus leucoxylon</i>	3.4	1.6
<i>Cupaniopsis parvifolia</i>	1.7	0.8	<i>Szygium paniculatum</i>	3.4	1.2
<i>Agapanthus praecox</i>	1.7	0.9	<i>Phyllanthus albiflorus</i>	3.5	1.2
<i>Goodia lotifolia</i>	1.8	0.7	<i>Dodonaea triquetra</i>	3.6	1.0
<i>Cryptocarya bidwilli</i>	1.8	0.7	<i>Szygium leuhmanni</i>	3.7	1.0
<i>Eucalyptus botryoides</i>	1.8	1.0	<i>Pittosporum revolutum</i>	3.7	1.5
<i>Ayrtera distylis</i>	1.9	1.5	<i>Ziera collina</i>	3.8	1.2
<i>Rhododendron bryophyllum</i>	1.9	0.9	<i>Hakea salicifolia</i>	3.8	1.2
<i>Cryptocarya williwilliana</i>	1.9	0.8	<i>Correa alba</i>	4.0	1.1
<i>Cupaniopsis anacardioides</i>	2.1	1.0	<i>Polyscias elegans</i>	4.2	1.3
<i>Grevillea hilliana</i>	2.1	0.7	<i>Dodonaea viscosa</i>	4.3	1.2
<i>Pittosporum undulatum</i>	2.1	0.7	<i>Rhopalostylis sapida</i>	4.3	1.6
<i>Litsea reticulata</i>	2.1	0.8	<i>Ficus rubiginosa</i>	4.3	1.1
<i>Doryanthes palmeri</i>	2.1	0.8	<i>Acacia howittii</i>	4.6	1.5
<i>Laccospadix australasica</i>	2.2	0.9	<i>Casuarina glauca</i>	4.6	1.2
<i>Microcitrus australis</i>	2.2	0.9	<i>Leptospermum petersonii</i>	4.7	1.2
<i>Solanum brownii</i>	2.2	1.0	<i>Cryptocarya laevigatum</i>	4.7	1.2
<i>Stenocarpus sinuatus</i>	2.2	0.9	<i>Acacia irrorata</i>	4.8	1.6
<i>Melaleuca decora</i>	2.2	0.9	<i>Pittosporum crassifolium</i>	4.9	1.2
<i>Alyxia ruscifolia</i>	2.3	0.8	<i>Acacia binervata</i>	4.9	1.3
<i>Eriostemon myoporoides</i>	2.3	0.8	<i>Banksia integrifolia</i>	5.0	2.1
<i>Howea forsteriana</i>	2.3	1.2	<i>Tabebula chrystricha</i>	5.1	1.1
<i>Rhododendron clorinda</i>	2.4	1.3	<i>Acronychia laevis</i>	5.1	1.5
<i>Citriobatus paucifloris</i>	2.4	0.9	<i>Sarcotoechia heterophylla</i>	5.2	1.6
<i>Acacia mearnsii</i>	2.4	0.9	<i>Licuala ramsayi</i>	5.2	1.6
<i>Acacia stricta</i>	2.4	0.9	<i>Diploglottis campbelli</i>	5.2	1.3
<i>Archontophoenix cunninghamiana</i>	2.4	1.0	<i>Endiandra pubens</i>	5.2	1.3
<i>Indigofera australis</i>	2.4	0.9	<i>Polyscias murrayi</i>	5.3	1.5
<i>Streblis brunonianus</i>	2.5	0.9	<i>Jacaranda mimosifolia</i>	5.4	1.4
<i>Grevillea marmalade</i>	2.5	1.5	<i>Azalea cultivar splenda</i>	6.0	1.6
<i>Leptospermum morrisonii</i>	2.5	0.9	<i>Radermacheria fenecis</i>	6.1	1.4
<i>Mishocarpus australis</i>	2.7	1.0	<i>Leptospermum laevigatum</i>	7.2	1.5

9.6 Sum of the acoustic density profile

This feature (`sum_of_density_profile`) is the sum of all of the range lines between the start and end of the plant. This feature is the sum of all of the reflective surfaces within the plant so is the acoustic area of the plant. It is an absolute measure of the reflective surfaces of the plant and is a direct measure of the acoustic area of the surfaces of the plant.

Plants with a small value for `sum_of_density_profile` are those with very few reflective surfaces. This means that there are few leaves which are rarely orthogonal to the transmitter.

The 5 plants with the smallest `sum_of_density_profile` are shown in Figure 9.23. The plants with the largest `sum_of_density_profile` are shown in Figure 9.24. The images show that the plants with very few reflective surfaces produce a small value for this feature and those with large leaves produce a very high value.

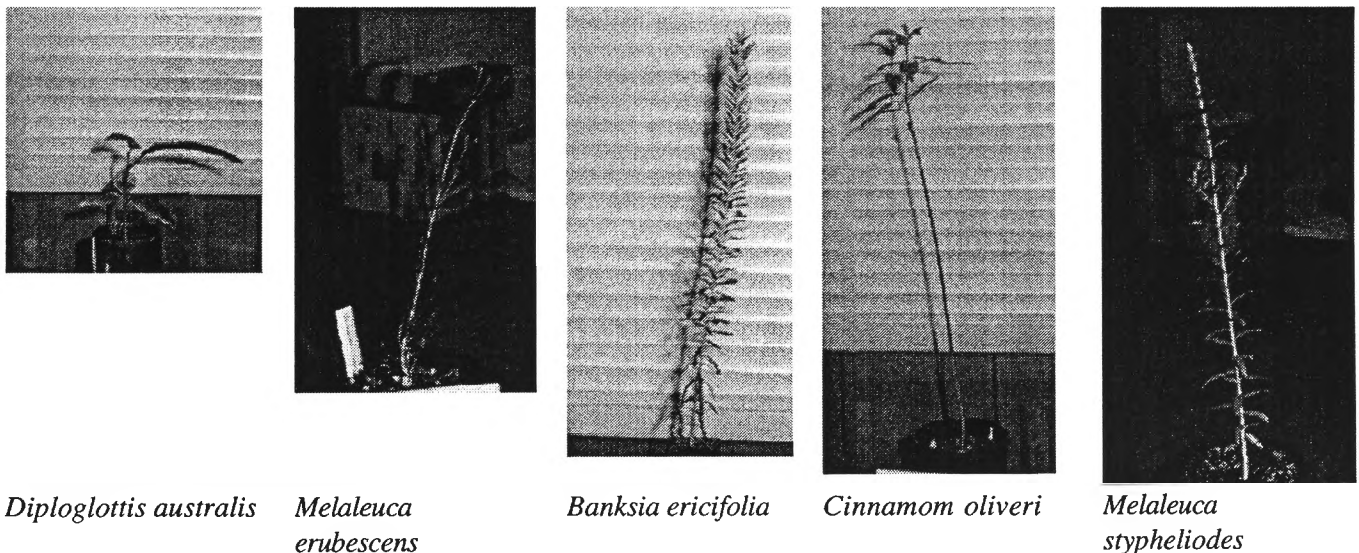


Figure 9.23 The plants with the lowest values for `sum_of_density_profile`



*Jacaranda
mimosifolia*



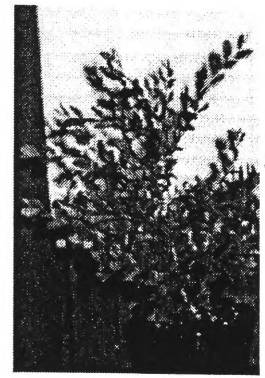
Acacia howittii



*Azalea cultivar
splenda*



Licuala ramsayi



*Leptospermum
laevigatum*

**Figure 9.24 The plants with the highest values for
sum_of_density_profile**

The amplitude of the acoustic density profile at each range is the acoustic energy that is reflected from surfaces at that range. As stated earlier, the quantity of energy is proportional to the acoustic area at that range. Thus, the sum of the amplitude of all of the range lines in the acoustic density profile of a plant is the total acoustic energy reflected from the plant to the receiver. Hence, the sum of the amplitudes is the total acoustic area of the plant.

If a plant is replaced with a large flat concave surface, with radius of curvature equal to the absolute range, then the maximum acoustic energy is reflected to the receiver. The energy reflected to the plant is a percentage of this maximum. The percentage of energy reflected is equal to the acoustic area divided by the acoustic area of the concave reflector.

Thus, the first transform is from the sum of the individual range lines of the acoustic density profile to the acoustic area of the plant. The second transform is from the acoustic area to the physical area from the percentage of energy reflected.

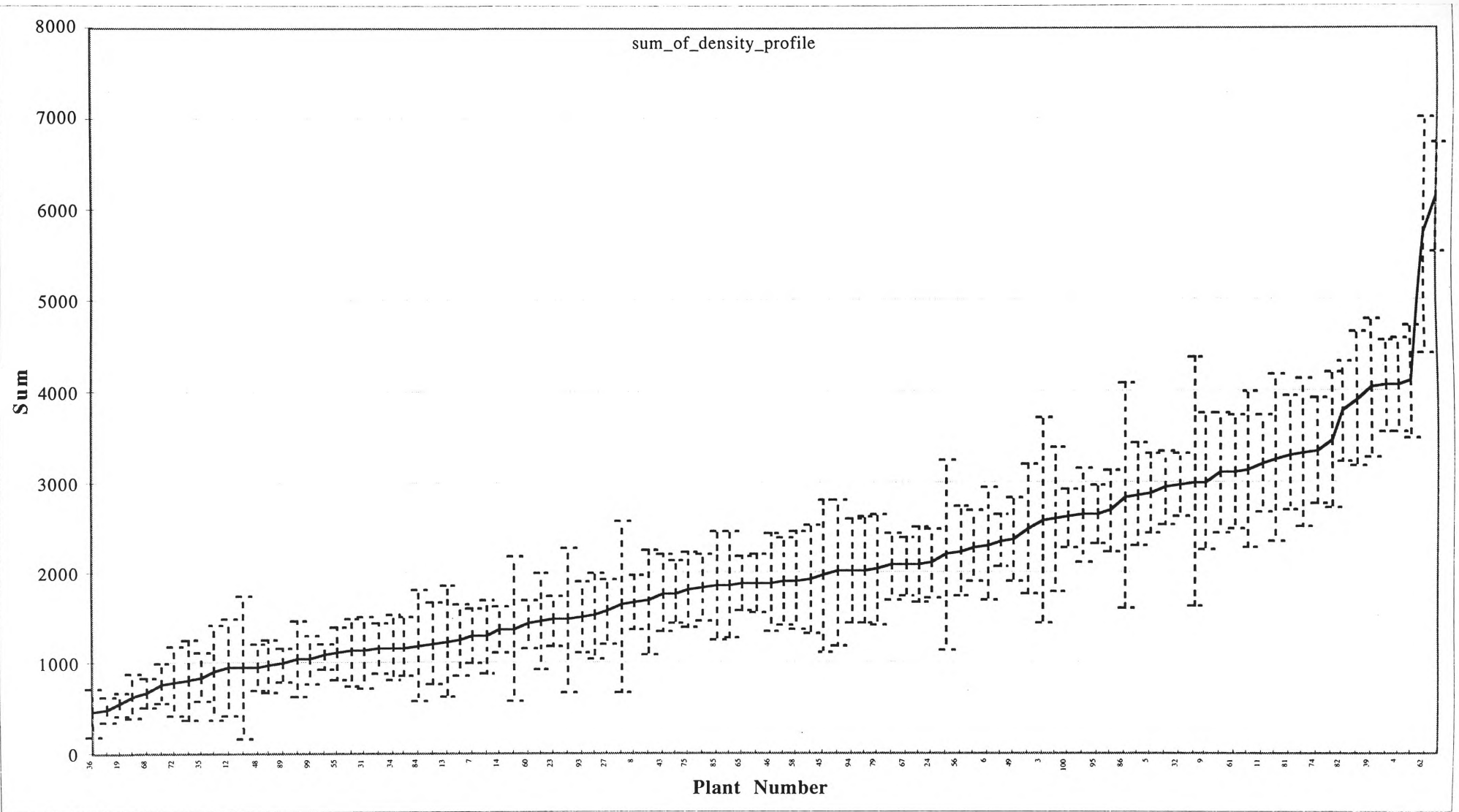


Figure 9.25 The average sum_of_density_profile for all 100 plants

Table 9.9 **sum_of_density_profile for all 100 plants**

Plant Name	Avg	Std			
			<i>Eucalyptus maculata</i>	1891.7	542.2
<i>Diploglottis australis</i>	459.2	268.2	<i>Sarcomelicope simplifolia</i>	1919.0	487.9
<i>Melaleuca erubescens</i>	492.4	134.1	<i>Laccospadix australasica</i>	1919.5	543.6
<i>Banksia ericifolia</i>	547.6	135.9	<i>Solanum vescum</i>	1929.4	596.9
<i>Cinnamom oliveri</i>	652.1	247.6	<i>Eucalyptus leucoxylon</i>	1971.1	858.4
<i>Melaleuca styphelioides</i>	678.6	171.8	<i>Livistona sp 'Carnarvon'</i>	2012.8	801.9
<i>Tristaniopsis collina</i>	773.2	224.2	<i>Streblis brunonianus</i>	2023.1	582.6
<i>Omalanthus populifolius</i>	810.0	388.8	<i>Azalea alba magnifica</i>	2029.8	588.9
<i>Solanum laciniatum</i>	820.3	440.9	<i>Polyscias australiana</i>	2040.6	613.5
<i>Cupaniopsis parvifolia</i>	851.2	270.0	<i>Phyllanthus albiflorus</i>	2080.9	364.2
<i>Ayrtera distylis</i>	902.3	515.8	<i>Melaleuca quinquenervia</i>	2084.5	318.9
<i>Agapanthus praecox dwarf</i>	945.8	534.1	<i>Citriobatus paucifloris</i>	2089.5	414.8
<i>Crinum pedunculatum</i>	963.3	793.8	<i>Casuarina torulosa</i>	2102.5	376.7
<i>Goodia lotifolia</i>	963.8	259.7	<i>Crinum mauritianum</i>	2198.4	1068.3
<i>Carpentaria acuminata</i>	978.6	294.2	<i>Indigofera australis</i>	2252.3	501.4
<i>Solanum aviculare</i>	992.0	195.5	<i>Hakea salicifolia</i>	2295.3	389.7
<i>Eucalyptus botryoides</i>	1043.2	429.2	<i>Acacia longifolia</i>	2318.6	632.8
<i>Westringa fruticosa</i>	1044.1	269.1	<i>Correa alba</i>	2357.2	298.2
<i>Cryptocarya williwilliana</i>	1079.9	138.1	<i>Grevillea baileyana</i>	2381.0	463.7
<i>Hymenosporum flavum</i>	1104.6	286.6	<i>Acacia stricta</i>	2484.1	705.0
<i>Acacia cultriformis</i>	1124.3	374.5	<i>Acacia falcata</i>	2573.8	1135.1
<i>Cryptocarya bidwilli</i>	1127.5	383.5	<i>Polyscias elegans</i>	2595.8	794.7
<i>Rhododendron bryophyllum</i>	1166.5	278.5	<i>Ziera collina</i>	2611.9	329.2
<i>Cupaniopsis anacardioides</i>	1176.4	349.8	<i>Dodonaea triquetra</i>	2633.9	529.7
<i>Guioa semiglauca</i>	1186.7	322.0	<i>Szygium leuhmanni</i>	2655.5	316.6
<i>Rhododendron clorinda</i>	1203.3	625.6	<i>Casuarina glauca</i>	2687.3	448.5
<i>Pittosporum undulatum</i>	1223.9	449.8	<i>Rhopalostylis sapida</i>	2838.9	1247.2
<i>Agapanthus praecox</i>	1244.5	629.7	<i>Szygium paniculatum</i>	2877.0	574.1
<i>Litsea reticulata</i>	1260.7	385.2	<i>Acacia irrorata</i>	2889.6	442.6
<i>Acacia mearnsii</i>	1300.1	302.3	<i>Tabebula chrystricha</i>	2947.4	406.8
<i>Microcitrus australis</i>	1302.8	405.9	<i>Cryptocarya laevigatum</i>	2974.3	361.9
<i>Alyxia ruscifolia</i>	1367.9	251.6	<i>Doryanthes palmeri</i>	2997.6	1376.8
<i>Grevillea marmalade</i>	1380.4	797.8	<i>Acacia podalyrifolia</i>	3003.9	745.4
<i>Leptospermum morrisonii</i>	1437.4	268.2	<i>Diploglottis campbelli</i>	3108.9	655.7
<i>Grevillea hilliana</i>	1465.2	530.6	<i>Leptospermum petersonii</i>	3116.0	628.3
<i>Casuarina stricta</i>	1481.8	271.8	<i>Banksia integrifolia</i>	3141.2	851.7
<i>Howea forsteriana</i>	1489.0	792.0	<i>Acronychia laevis</i>	3204.8	536.4
<i>Stenocarpus sinuatus</i>	1515.9	404.5	<i>Sarcotoechia heterophylla</i>	3269.9	908.6
<i>Solanum brownii</i>	1532.5	478.5	<i>Polyscias murrayi</i>	3321.0	630.1
<i>Cordyline australis</i>	1571.9	353.4	<i>Endiandra pubens</i>	3322.8	803.2
<i>Ficus obliqua</i>	1637.8	944.5	<i>Pittosporum crassifolium</i>	3357.8	583.0
<i>Acacia melanoxylon</i>	1673.3	302.7	<i>Ficus rubiginosa</i>	3459.6	739.5
<i>Archontophoenix cunninghamiana</i>	1678.7	584.8	<i>Radermacheria fenecis</i>	3767.2	547.6
<i>Eriostemon myoporoides</i>	1773.7	421.6	<i>Acacia binervata</i>	3915.7	731.0
<i>Endiandra introrsa</i>	1783.6	346.2	<i>Dodonaea viscosa</i>	4037.2	742.2
<i>Pittosporum james</i>	1822.6	428.7	<i>Jacaranda mimosifolia</i>	4057.0	509.5
<i>Pittosporum rhombifolium</i>	1843.7	373.1	<i>Acacia howittii</i>	4065.0	507.7
<i>Rhopalostylis baneri</i>	1866.6	590.2	<i>Azalea cultivar splenda</i>	4104.9	615.3
<i>Pittosporum revolutum</i>	1873.7	584.4	<i>Licuala ramsayi</i>	5730.2	1299.7
<i>Melaleuca decora</i>	1884.1	296.4	<i>Leptospermum laevigatum</i>	6124.0	599.6
<i>Mishocarpus australis</i>	1889.9	338.2			

9.7 Conclusion

This chapter outlines the information content of the features (and hence the acoustic density profile) for different kinds of plant structures. The features provide information which is useful for determining the basic structure of the plant. The features and the physical plant characteristics that they measure are :

<code>length_of_density_profile</code>	- acoustic depth of the plant
<code>no_above_threshold1 - 9</code>	- leaf density and size of reflective surfaces
<code>no_of_major_peaks1 - 2</code>	- layering of the foliage
<code>sum_of_density_profile</code>	- acoustic area of the plant

The features can be interpreted directly to provide information about the foliage structures of plants (Figure 9.2). This completes the inverse transformation from signal, to acoustic features plant physical structure and provides the basis for a direct interpretation of the acoustic density profile.

The acoustic density profile provides information about the structure of the plant and not the individual components such as the leaf size or branch configuration. In Chapter 10, plant classification methods are outlined and in Chapter 11, implementation issues for a mobile robot are discussed

9.8 Summary

1. `length_of_density_profile` provides information about the minimum depth of the plant;
2. The `no_above_threshold` features provide information about how sparse the foliage is within the plant and also the size of the reflective surfaces;
3. The `sum_of_density_profile` is the acoustic area of the plant and provides information about the overall amount of foliage on the plant; and
4. `no_of_major_peaks` provides information about the layering of the surfaces.

10. Plant Classification

10.1 Introduction

For a mobile robot to navigate in an environment which is unknown, a map can be built using echoes from different objects such as plants, door frames and furniture. Plants are useful natural landmarks for localisation because of their complex geometric structure. In this chapter, a classifier is described which is able to recognise a plant and this can be used to aid the mapping process. A plant classifier can also be useful in Agricultural applications such as greenhouse monitoring, selective spraying or plant growth monitoring. The advantage of this sensor in the area of greenhouse automation is that it needs no special lighting and so can be used in adverse weather conditions and/or during the night.

When there is a small number of plants, the classes are often linearly separable so individual plants are easily classified with a simple classifier. For larger numbers of plants or in the case where plants can not easily be represented by a single template (ie different portions of the plant reflect the acoustic energy differently) then a non-linear classifier such as an artificial neural network is required. In the case where the classifier can not identify a plant or when information about the structure of the plant is sufficient, the features calculated can be interpreted directly, as shown in Chapter 9.

In Chapter 8, a set of features were developed and analysed for their ability to discriminate the population of plants. In this chapter, pattern recognition techniques are used to show how well an individual sample can be differentiated from a population of plants, that is, using the features to classify individual plants. Plants can also be grouped into groups which have similar acoustic density profiles.

10.2 Pattern recognition techniques

In this Chapter, pattern recognition techniques are used to measure the success of allocating a record from a single orientation of a plant to one of a set of pre-defined classes of plants.

Pattern estimation and detection methods occur in numerous scientific and engineering problems so there is a large amount of previous work in the area [Weiss & Kulikowski, 1991]. The fundamental goal is to identify the class to which a given pattern belongs. There are examples of these techniques in diverse fields such as medical diagnosis [Marchand *et al*, 1983], speech recognition [Mammone *et al*, 1996], robotics [Kuc, 1996] and investment planning [Hammerstrom, 1983a]. Often the information used to classify these patterns is imprecise and multi-dimensional in nature, so the classifier needs to be robust.

There is a significant amount of literature describing the techniques of pattern recognition with several major areas of research known as Statistical Pattern Recognition, Neural Networks and Machine Learning Methods. All of the techniques have been thoroughly discussed in the literature and are well developed [Therrien, 1989], [Fukunaga, 1979], [Beale and Jackson, 1990], [Wasserman, 1993], [Michie, 1986], [Quinlan, 1993]. There are also many examples of comparisons between the different techniques [Atlas *et al*, 1990], [Fisher and McKusick, 1989] but the best technique is different for the specific problem. There are other techniques such as syntactic pattern recognition which can be used for pattern recognition problems but are not used in this thesis. Syntactic pattern recognition involves representing a pattern in pattern descriptive language [Chen, 1982]. Because of the variable nature of the data and the difficulty involved in making a structural description of the patterns being dealt with, the method has not been used. Knowledge based systems [Hopgood *et al*, 1989], fuzzy systems [Kummert, 1993] and Hybrid systems [Ghosh *et al*, 1992] are also commonly used.

When the characteristics of the data are not well known, it is impossible to say which of the techniques will work the best [Weiss and Kulikowski, 1991]. Several different techniques should be tried and results compared. This thesis however, is more

focussed towards discovering the information in the echoes (as in Chapter 9) and simple pattern recognition techniques such as linear statistical pattern recognition and non-linear neural networks produce good results.

Pattern recognition techniques are broadly divided into *supervised* and *unsupervised* methods and both learn directly from sample experience. In *supervised* techniques, the patterns are labelled with their true class and during training a decision rule is established based on the patterns in that class. *Unsupervised* techniques attempt to group patterns with similar mathematical properties and is used to group plants which have similar physical structure.

A supervised classifier is presented with a set of data, in this case is a set of features calculated from the acoustic density profile, and the associated plant. The classifier uses this input data to construct a decision model. The objective is to customise the classifier to the specific problem by finding a general way of relating the input acoustic density profile to one of the specified plant classes. Each input pattern is simply a set of observations and the corresponding correct class. The classifier must identify essential patterns in the data which are not overly specific to the sample data, otherwise it will perform poorly with new data.

Unsupervised learning involves grouping the sample data, resulting in similar patterns clustering together in pattern space. This process can be used to identify patterns which are similar and dissimilar and is important in many areas of research [Bouguettaya, 1996]. Cluster Analysis has been used to group similar plants into like groups. Clustering of plants is outlined in this chapter with detail provided in Appendix D.

10.3 Input to the pattern recognition system

The pattern is given in pattern space by the vector \mathbf{x} :

$$\mathbf{x} = \{x_1, x_2, \dots, x_n\}$$

10.1

where n = length of pattern

Each element of the vector \mathbf{x} represents some physical measurement which in this case is the calculated features. The output class is denoted by ω_j where j is the class number. The observation vector \mathbf{x} is input to the classifier and the result is a classification into one of j classes of plants (or individual plants). This model is illustrated in Figure 10.1.

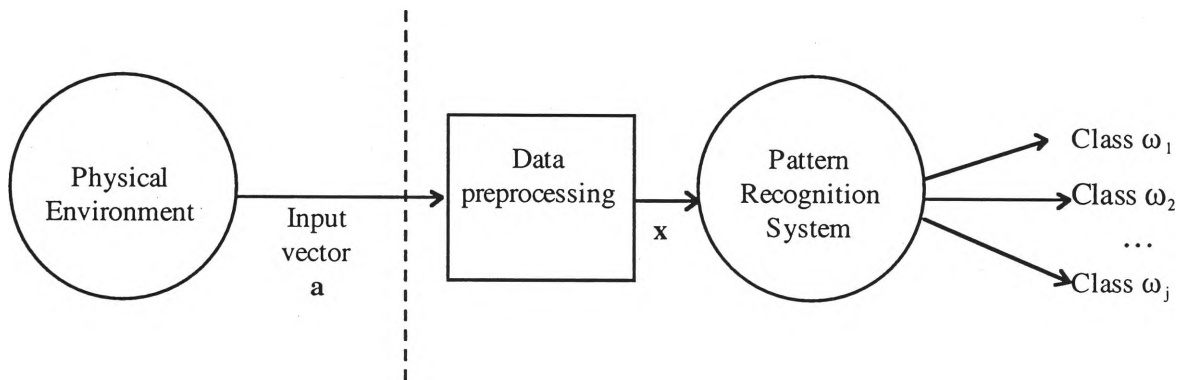
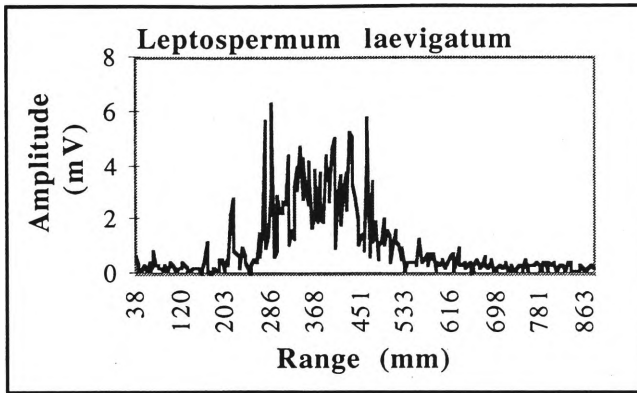


Figure 10.1 The model of a simple classification system

For the problem under consideration, the input vector \mathbf{a} consists of an acoustic density profile. In the data preprocessing stage, the acoustic density profile is referenced to a standard range, features are calculated and then scaled as discussed in Chapter 8. In this case, x_i represents each of the individual features. The input data to the pattern recognition system then consists of a vector of 19 elements, that is, $\mathbf{x} = \{x_1, x_2, \dots, x_{19}\}$. A sample acoustic profile of *Leptospermum laevigatum*, and the range referenced and scaled features calculated are shown in Figure 10.2. These features are used as input to the pattern recognition system.

Acoustic density profile :



Features :

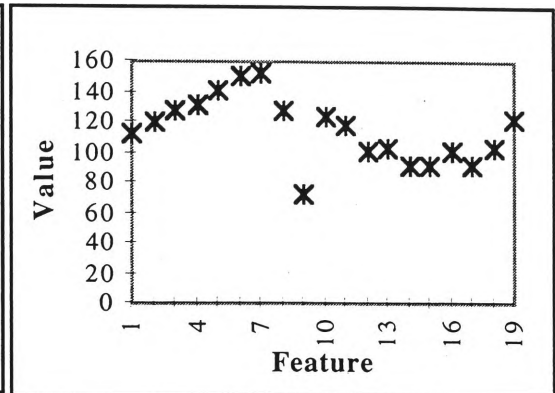


Figure 10.2 Acoustic density profile and range referenced, scaled features calculated from this profile for *Leptospermum laevigatum*

The quality of any classification system is dependant on the quality of the sample data used to train it and the predictive capability of that data. If the training set is too small, inaccurate, or fails to characterise the distribution of the data, then classes may overlap and ambiguities may be introduced that no classifier can possibly resolve. The task then becomes one of producing the best classification possible with the given data. Another may be that the original data can not discriminate the object to the level that is expected. The implicit assumption in this whole approach is that training and testing conditions are comparable [Mammone *et al*, 1996].

There are two techniques commonly used to reduce the size of the input set while maintaining the predictive capability of the raw data and these are given below.

1. *Feature Extraction* is used to create new features which are calculated directly from the input pattern, (this has been described in depth in Chapter 8).
2. *Feature Selection* reduces the input pattern by selecting the items of the input pattern which are the most discriminatory. For sample data such as that shown in Figure 10.2 this involves selecting the individual features which discriminate particular plants. Feature selection is usually preformed on features which have been calculated using feature extraction. Feature selection is outlined in Section 10.7.

In Chapter 8, a set of features was extracted to characterise the plants. When the characteristics of the acoustic density profiles are condensed using these features, differences between plants can be interpreted more easily as was shown in Chapter 9.

10.4 Data partitioning

A supervised learning system aims to recognise objects based on previous knowledge. There are usually three stages involved in building pattern recognition systems :

1. training;
2. testing; and
3. implementation.

During the training stage, a model is developed where the relationship between the features and the plant is established. The criterion to develop a good model is based on minimising the error between the model and the training data. The training data are occasionally split up into a training set, a test set to tune the decision rule and a cross-validation set to test the resulting classifier.

Various researchers choose different proportions of the data to allocate to their training set (up to 90%). I have chosen to use 50% (or 75% in the case of cross validation). Restriction of the training set will allow for a larger size testing set and hence a more reliable predictor of the performance of the classifier. In order to train the classifier with representative data, it is important that the records are randomly assigned into either the test set or the training set and this is performed using Algorithm 10.1. When a cross-validation set is being used, approximately 50% will go to training, 25% is allocated to the validation set and the remaining 25% is assigned to the test set.

Algorithm 10.1 Generation of data sets

GENERATE TRAIN TEST CROSS VALIDATION SET

This function is passed an array of features and the associated plant identifier. It is also passed a reference to 3 output files, the file which is to contain the training set, the file which is to contain the testing set and the file which is to contain the validations set. This function writes the record to one of the three files based on the weighting of 50%, 25%, 25% to the training, testing and validation set.

Parameters :

features an array containing the features and the associated plant.
train, test, valid references to the open files which are to contain the training, test and cross validation set.

Returns :

true if the record was written to one of the files successfully.
false if there was an error writing the record.

BEGIN

WHILE more records in the data set

BEGIN

 r = a random number between 0 and 1

 IF r < 0.5

 THEN

 write record to training set

 ELSE

 IF r < 0.75

 THEN

 write record to validation set

 ELSE

 write record to test set

 END

 END

END

END

Some researchers do not use a cross-validation set but it provides a better measure of the expected accuracy of the classifier as the data has not been used to tune the classifier. In this study, the cross-validation set has been implemented to facilitate feature selection. This ensures that the test set is kept aside until the classifier has been developed and a near optimal set of features have been selected. The test set is completely unseen by the classifier prior to the final testing phase. The task of testing involves running the model against data which it has not seen before, and noting success or failure.

10.5 Performance estimation

The objective of any classification system is to correctly identify the class given a set of input data so that some action can be taken. To get the true error rate of a classifier you need to test the classifier against all of the possible data that could arise for the particular class. Weiss and Kulikowski [91], define the true error rate as : ‘statistically defined as the error rate of the classifier on an asymptotically large number of new cases that converge in the limit to the actual population distribution’. This means that the true error rate is achieved when the test set represents all possible values.

In practice, the error rate must be estimated because only a finite amount of data are available. The general form of the error rate equation is given in Equation 10.2.

$$\text{error rate} = \text{number of errors} / \text{number of cases} \quad 10.2$$

An error occurs when the classifier calculates an incorrect class for a certain input vector, that is, it misclassifies a case.

During the testing phase, the classifier is presented with a feature vector along with its true class. The classifier then calculates the class based on the data and if it is different to the given class then it is noted as an error. At the completion of the entire test set, the errors are tallied and an error rate is calculated using Equation 10.2.

In Section 8.3, four plants (Figure 8.3) were compared (*Cryptocarya williwilliana*, *Leptospermum laevigatum*, *Szygium leuhmanni*, and *Westringa fruticosa*). A simple classifier can be established using template matching and the error rate provides a good measure of the linear separation of the classes. The frequency distribution for the first feature (`no_above_threshold1`) for 360 records for each of the plants was shown in Figure 8.4 and the statistics for the selected plants were shown in Table 8.3. As shown in Section 8.3, the plants can be partially distinguished by plotting the first three features on a graph (Figure 8.7).

A classifier can be run to classify the records based on this set of features. Details of the classifier are given subsequently (Section 10.6) but are not important in order to interpret the classification matrix shown. Initially, input to the classifier is feature 1

(no_above_threshold1) and the corresponding class to which the plant belongs. For this particular example, 50% of the data was used to train the network (approx 720 records), 25% was used as a validation set (approx 360 records) and the remaining 25% were used to test the classifier. Note that the number of records assigned to each group is only approximate as they are allocated based on the random allocation scheme shown in Algorithm 10.1.

The resulting classification matrix and the error rate for the four plants is shown in Table 10.1. The columns in the matrix represent the plant identifier which was calculated by the classifier for the particular sample while the rows represent the actual plant which the data came from. For example, column 1 row 4 represents the number of records which were classified as plant 1 but were actually samples from plant 4. In this particular case, 4 records were classified as plant 1, even though they were from plant 4.

Table 10.1 Classification Matrix for 4 plants with feature 1 (no_above_threshold1)

Classification Matrix				
Actual	Classified Plant 1	Classified Plant 2	Classified Plant 3	Classified Plant 4
Plant 1	82	0	0	10
Plant 2	0	112	0	0
Plant 3	0	0	91	0
Plant 4	4	0	0	89
Number of records misclassified = 14				
Classification Error Rate = 3.61%				

The classification matrix shows that there is a very low error rate of 3.61% which corresponds to only 14 of the records in the test data being misclassified. Previously, Section 8.3 showed that it was difficult to differentiate between *Cryptocarya williwilliana* (plant 1) and *Westringa fruticosa* (plant 4) using visualisation. This is also confirmed by the classification matrix. The matrix shows that 4 records which should have been classified as *Cryptocarya williwilliana* have actually been classified as *Westringa fruticosa*. Similarly, there are 10 records which have been classified as *Cryptocarya williwilliana* when they were from *Westringa fruticosa*.

It is also evident that there were no misclassifications at all for the other plants - the only confusion was between *Cryptocarya williwilliana* and *Westringa fruticosa*. The addition of the second feature (`no_above_threshold2`) produces the classification matrix shown in Table 10.2, which reduces the total misclassification by 4 plants.

Table 10.2 Classification Matrix for 4 plants with 2 features

Classification Matrix				
Actual	Classified Plant 1	Classified Plant 2	Classified Plant 3	Classified Plant 4
Plant 1	82	0	0	7
Plant 2	0	94	0	0
Plant 3	0	0	92	0
Plant 4	3	0	0	105
Number of records misclassified = 10				
Classification Error Rate = 2.61%				

The addition of the second feature (`no_above_threshold2`) and the third feature (`no_above_threshold3`) improves the classifier by lowering the error rate and this is shown in Table 10.3. In practice, the addition of features can add to the time that it takes to compute a result so only features which contribute positively to the performance of the classifier against the test set should be used. This is discussed further in section 10.7.

Table 10.3 Classification Matrix for 4 plants with 3 features

Classification Matrix				
Actual	Classified Plant 1	Classified Plant 2	Classified Plant 3	Classified Plant 4
Plant 1	88	0	0	6
Plant 2	0	87	0	0
Plant 3	0	0	106	0
Plant 4	1	0	0	80
Number of records misclassified = 7				
Classification Error Rate = 1.90%				

10.6 Template matching

This is the simplest type of statistical classifier. It is a linear classifier so is only effective when the classes are linearly separable. Templates are created based on the training data and when a new record is presented to the classifier, it is allocated to a class based on the template which it is most similar to.

The template created for each class is simply the average of each of the individual records in the training set for the class :

$t_i = \{\mu_1, \mu_2, \dots, \mu_n\}$ where i is the number of classes, and n is the number of features.

A new record is presented to the classifier as :

$$\mathbf{x} = \{x_1, x_2, \dots, x_n\}$$

the euclidean (or mean square) difference is calculated between it and each of the templates :

$$diff_i = (\mathbf{x} - t_i)^2$$

the resulting class is the one with the smallest *diff*. This result is then compared with the true class and if there is a difference then it is noted as an error. Since this classifier model does not weight the features in any way, the result can be affected by noisy, unrepresentative, or redundant features so the data needs to be prepared in some way. In order for the classifier to work effectively, the best features need to be selected and this is discussed in Section 10.7.

10.7 Feature selection

In practice features can be poor, noisy or redundant and the performance of any classifier can be improved if those features are removed before the data is presented to the classifier. The performance of all learning systems can be dramatically affected by the choice and specification of these features [Weiss & Kulikowski, 1991].

Selection of relevant features to discriminate different classes is a central problem in the pattern recognition field. Once features are calculated, those which are the most discriminatory for a particular combination of plants are selected to improve the reliability of the classifier.

A common technique used for feature minimisation is called principal component analysis. It allows reduction of the number of individual variables while retaining as much of the variation present in the original data as possible. The result is achieved by transforming the data into a new set of variables called principle components which have zero correlation [Duszak *et al*, 1994]. This technique was not pursued in this thesis but is an option for further work.

Some researchers have used brute force methods which test every combination of features for a particular classification problem such as characterising aircraft joints using ultrasonics[Hansch *et al* 1994]. This technique has the advantage of producing an optimal classifier but requires the testing of 2^n combinations (where n is the number of features) and can result in a vast amounts of computation when dealing with a large amount of data. For 19 features, this means testing 524288 combinations of features.

Other feature minimisation algorithms reduce the dimensionality by selecting only the best individual features to represent the data. These feature selection algorithms attempt to optimise the recognition rate achieved on the cross validation data for that particular combination of features. It is often impossible to examine every combination of features, so strategies have been developed to estimate the best combination of features. They may all produce different results given any particular data set.

One of the most commonly used feature selection algorithms is known as *stepwise forward selection*. This technique starts with the best single feature. At each step, it tests every one of the remaining features with the features already selected and adds the one which is the best. It continues until it reaches some specified minimum error rate, or until all of the items from the pattern space are exhausted. A comprehensive discussion of feature selection algorithms can be found in [Weiss & Kulikowski, 1991].

The result is not an optimal set of features but one which is based on the discrimination quality of the individual features. Similar stepwise techniques have been used in many other areas including fault diagnosis in integrated circuits [Lin & Meador, 1992], identifying airborne acoustic sources [Cabell & Fuller, 1989], in biomedical applications [Ciaccio *et al*, 1993].

In this thesis, a small optimisation has been made to this algorithm where features are added until all of the features have been added and the recognition percentage achieved using the cross validation set is recorded at each step (Algorithm 10.3). The result is then a set of features which result in the best recognition percentage of the cross validation set. This is an improvement over the recognised stepwise forward selection algorithm as the

chance of falling into a local minima are reduced but has the drawback of testing more feature combinations and hence increased processing time during training.

The stepwise techniques provide the strategy to guide the search but there still needs to be a way of evaluating alternative subsets of features. The earliest approaches to feature selection used the filter method [Langley, 94] which filter the features before the classification is performed. The filter approach [Almuallim & Dietterich, 94] is independent of the classifier and removes the irrelevant features based on the characteristics of the training dataset. This was demonstrated in Section 7.10.1 where the feature set was reduced from 67 to 19 features. The wrapper method is based on a different underlying philosophy as it runs the classifier on the candidate features and uses the resulting classification error to select the best combination, that is, the combination of candidate features which produce the lowest error.

10.8 The Wrapper Method of feature selection

In this section, a new algorithm is described which uses the wrapper method and combines both modified stepwise forward selection (Algorithm 10.3) and stepwise elimination (Algorithm 10.4) functions over multiple iterations in order to get a more reliable set of features for the particular combination of plants. The cross-validation method of generating test data outlined in Algorithm 10.1 is also used.

Input Data : there are 19 features as input to the classifier and a field to indicate the true class to which the data belongs, for example 1 = plant 1, 2 = plant 2, 3 = plant 3 and 4 = plant 4. The training set, the testing set, and the cross-validation set have approximately 50%, 25% and 25% of the data respectively (assigned with Algorithm 10.1) and are selected using Algorithm 10.2.

Algorithm 10.2 The enhanced algorithm for feature selection

ENHANCED FEATURE SELECTION

This function implements the new enhanced feature selection method to select a good set of features for input to a classifier. This function is passed a pointer to a piece of memory which contains a data structure which contains the entire training set, and another pointer to a data structure which contains the entire cross-validation set. It is also passes an array into which the resulting features are inserted and returns the number of features in this array.

Parameters :

train_set a pointer to a data structure with the training set.
valid_set a pointer to a data structure with the cross validation set.
features an array with the list of features selected.

Returns :

the number of features selected or 0 if an error is encountered.

BEGIN

 Initialise the candidate set as the complete feature set

 WHILE the recognition percentage continues to improve

 BEGIN

 The current feature set is run through the classifier and the results are displayed as both a classification matrix and as a percentage when tested against the cross validation set.

 IF it is the first time though

 THEN

 use the empty set as input to the stepwise feature selection only (leave complete set for elimination).

 ELSE

 Perform Stepwise forward feature selection (Algorithm 10.3)

 END

 Perform Stepwise feature elimination (Algorithm 10.4)

 If feature elimination produces better results

 THEN

 select that subset as the one to continue with

 ELSE

 select the subset resulting from the feature elimination

 END

 END

END

Stepping through Algorithm 10.2, the initial candidate features is a set of all possible features. A modified *stepwise forward feature selection* (Algorithm 10.3) is performed. This adds features one at a time based on how good they are at classifying the cross validation set in combination with the features already selected (Algorithm 10.3). The stepwise feature elimination algorithm is then executed (Algorithm 10.4) to try and

minimise the number of features selected. Whichever of the two feature sets produces the best result are used as input to the next iteration of the loop.

The process is terminated when the recognition percentage is not improved from one iteration to the next. The only exception is when the recognition stays the same and a feature is eliminated. Iteration continues because the classifier has the same predictive capability using less features which is desirable.

Algorithm 10.3 An improved algorithm for stepwise forward feature selection

```
STEPWISE FORWARD FEATURE SELECTION
    This function is passed the current set of features selected and
    adds features one at a time based on the feature which produces
    the best result when tested with the cross validation set. At
    each step the recognition percentage is stored. The process
    continues until all of the features are added. The result is the
    list of features which produce the best recognition result.
    Parameters :
        train_set    a pointer to a data structure with the
training set.
        valid_set    a pointer to a data structure with the cross
                    validation set.
        features     an array with the list of features selected.
    Returns :
        the number of features selected or 0 if an error
        is encountered.
BEGIN
    WHILE all features not selected
    BEGIN
        WHILE all features not tested
        BEGIN
            get the next feature
            run classifier using features already selected
            and this feature
            store the recognition percentage
        END
        add the feature with the best recognition percentages
        to the list of selected features
        store the recognition percentage
    END
    Select the feature with the highest recognition percentage
    as the last feature selected
    Set up the feature array and return the number of features
END
```

Stepwise feature elimination involves removing one feature at a time from the current feature set based on the one that results in the highest classification percentage. At each step, each feature is removed in turn and the resulting error percentage is calculated.

The feature which results in the lowest error percentage when removed is the one which is taken from the feature set. In the case of more than one feature giving the same result, then the winner is chosen randomly between those that give the same result. The general stepwise feature elimination algorithm terminates when the recognition percentage on the cross validation data set is not improved by removing a feature. In this implementation, the process continues until all features are eliminated. The result of each step are then compared, and the set with the highest recognition percentage on the cross validation set is used. The advantage of this is that it reduces the chances of falling into local minima but requires more processing to produce a result. The algorithm for feature elimination is shown in Algorithm 10.4.

Algorithm 10.4 The algorithm for Stepwise Feature Elimination

```

STEPWISE FEATURE ELIMINATION
    This function is passed the current set of features selected and
    removes features one at a time based on the feature which
    produces the best result when tested with the cross validation
    set. At each step the recognition percentage is stored. The
    process continues until all of the features are removed. The
    result is the list of features which produce the best recognition
    result.
    Parameters :
        train_set    a pointer to a data structure with the
training set.
        valid_set    a pointer to a data structure with the cross
validation set.
        features     an array with the list of features selected.
    Returns :
        the number of features selected or 0 if an error is
encountered
BEGIN
    WHILE all features not eliminated
    BEGIN
        WHILE all features not tested
        BEGIN
            get the next feature
            run classifier without features already
            removed and this feature
            store the recognition percentage
        END
        add the feature with the best recognition percentages
        to the list of eliminated features
        store the recognition percentage
    END
    Select the feature with the highest recognition percentage
    as the last feature eliminated
END

```

10.9 Classification of plants using the statistical classifier

A sample run for the four plants analysed in Section 8.3 is shown in Table 10.4. On completion of the entire feature selection cycle, the progressive recognition percentages are shown, that is, the features are listed with the percentage recognition against the training set after each feature is added. This allows the number of features to be balanced against the predictive qualities of the features. This is a trade off between the accuracy of the classifier and the amount of time that the classifier will take to make a decision on any input pattern.

Finally, the classifier is tested against the test data file. This test data is completely separate to the validation set which is used to tune the features.

Results in Table 10.4 demonstrate that the calculated features are very good at differentiating these 4 plants (correct classification percentage of 98.4% on the unseen test set). The only confusion arose where 3 records from plant 1 (*Cryptocarya williwilliana*) were classified as plant 4 (*Westringa fruticosa*) and 3 records from plant 4 were classified as plant 1. This is consistent with the overlapping of feature values between these 2 plants that was illustrated in Section 8.3

Table 10.4 also highlights the features which were the best for separating these 4 plants.

They are :

- 17. mean_abs_dev_range;
- 6. no_above_threshold6;
- 18. range_75_acoustic_area;
- 10. no_major_peaks;
- 16. coeff_of_var_range;
- 19. no_major_peaks2; and
- 8. no_above_threshold7.

Table 10.4 Run of feature selection with classifier for all 19 features

Classifier starting..
Start time = Wed Mar 11 15:40:03 1998

Number of inputs : 19
Number of outputs : 1

Iteration number : 1
Classification Matrix

Actual	Calculated			
	Class1	Class2	Class3	Class4
Class1	87	0	0	3
Class2	0	81	0	0
Class3	0	0	95	0
Class4	3	0	0	87

Correct Classification Percentage = 98.3146

Stepwise forward selected: 2 18 4 17 5
3 7 1
.. which gives a recognition
percentage of : 98.8764
Stepwise forward eliminated : 7 1 2 3
4 11 12 9 5 13 15 14
.. which gives a recognition
percentage of : 98.8764
Will eliminate those features
highlighted..

Iteration number : 2
Classification Matrix

Actual	Calculated			
	Class1	Class2	Class3	Class4
Class1	87	0	0	3
Class2	0	81	0	0
Class3	0	0	95	0
Class4	1	0	0	89

Step forward selected: 17 6 18 10 8 16
19
.. which gives a recognition
percentage of : 98.8764

Stepwise forward eliminated : 8
.. which gives a recognition
percentage of : 98.5955

Feature selection is complete, final
recognition = 98.8764

Algorithm Selected : 17 6 18 10 16 19
8
.. which gives a recognition
percentage of : 98.8764
The following features were used
17 6 18 10 16 19 8
Progressive recognition percentages
92.6966 17
96.3483 17 6
97.7528 17 6 18
98.5955 17 6 18 10
98.0337 17 6 18 10 16
98.5955 17 6 18 10 16 19
98.8764 17 6 18 10 16 19 8

Now testing against new test data

Classification Matrix 2

Actual	Calculated			
	Class1	Class2	Class3	Class4
Class1	94	0	0	3
Class2	0	102	0	0
Class3	0	0	87	0
Class4	3	0	0	81

Correct Classification Percentage = 98.3784

End time = Wed Mar 11 15:42:38 1998

The correlation matrix for these four plants against their template is shown in Chapter 8 and is reproduced in Table 10.5. It shows that they are all well correlated through orientation change so are good candidates for a system which needs to classify individual plant species to a high degree. Because the plants are relatively consistent through orientation (as shown by the high template correlation values), there is a good chance that an acoustic density profile from any particular orientation will be similar to the template stored for that plant, rather than being incorrectly classified as one of the other plants.

**Table 10.5 Template
correlation for four plants**

<i>Cryptocarya williwilliana</i>	0.90
<i>Leptospermum laevigatum</i>	0.92
<i>Szygium leuhmanni</i>	0.92
<i>Westringa fruticosa</i>	0.79

Table 10.6 shows the correlation between the template of each plant and all of the records for the plant indicated in the column. This is in the same format as the larger Table 8.8. The template of *Cryptocarya williwilliana* is the most highly correlated with the records from *Westringa fruticosa* with a correlation level of 0.6. Similarly, the template of *Westringa fruticosa* is correlated against all of the records of *Cryptocarya williwilliana* to a level of 0.6.

Note that even though correlations were calculated with all 19 features, they are still indicative of the performance of the classifier with these seven selected features in that the plants with the highest correlation are the ones likely to be misclassified and this is true for *Cryptocarya williwilliana* and *Westringa fruticosa*. This simple fact illustrates that there is a relationship between the correlation between plants and the results achieved by a classifier. So, when plants are highly correlated to each other then there is a good chance that it will be hard to differentiate between them.

**Table 10.6 Template correlation against the
other four plants**

		1	2	3	4
1	<i>Cryptocarya williwilliana</i>		0.2	0.5	0.6
2	<i>Leptospermum laevigatum</i>	0.2		0.5	0.2
3	<i>Szygium leuhmanni</i>	0.5	0.5		0.3
4	<i>Westringa fruticosa</i>	0.6	0.2	0.4	

Similar groups of four plants produce good results but once the number of plants becomes too high, the features overlap in linear space, so a non-linear classifier may be required to separate the plants.

10.10 Pairwise classification results

The statistical classifier was run on all pairs of plants in order to determine the plants which are the most similar to each other. It answers the following question : given any particular plant, what is the average classification against all of the 99 other plants using the Sonar data. Table 10.7 shows a grid where each cell is the result of running a statistical classifier which tries to differentiate between the two plants. The classifier design is similar to that outlined in Section 10.8 where 2 plants are used as input and the result is a percentage which gives the number of records which were classified correctly. The high level outline of the function used to generate the table is shown in Algorithm 10.5.

Algorithm 10.5 The algorithm to build the pairwise classification table

```
BUILD PAIRWISE CLASSIFICATION TABLE
  This function runs the classifier on all of the combinations of
  the 100 plants in order to produce a table of plant combinations
  and the corresponding classification percentages using the test
  set.
BEGIN
  FOR plant1 = 1 to 99
    FOR plant2 = plant1 to 100
      Establish train, validation and test sets for
        plant1 vs plant2
      Run the classifier using the feature
        selection algorithm
      Record the result of testing with the test set
    END
  END
END
END
```

Each location in the resulting table gives the classification percentage for the two plants. For example, the cell at the point which intersects row numbered 4 and the column number 2 is the classification resulting from the test set when the classifier is run for plants *Acacia howitti* and *Acacia cultriformis*. In this particular case, the result is 100 percent, that is, when the classifier is run using the data from those plants, 100% of the test set is classified correctly. The adjacent cell which is at the point in column 1 and row 4 indicates that when the classifier is run for *Acacia howitti* and *Acacia binervata*, the test set is only classified correctly at a rate of 61%, that is, 39% of the data is classified incorrectly. Plants which have a low classification percentage against the rest of the population (less than 75%) are highlighted by greying the cells.

Table 10.7 Classification of combinations of two plants against the corresponding test set

[illegible]

10-22

Table 10.8 shows a summary of the results of the testing of plant combinations.

Table 10.8 Recognition for plant combinations

maximum correct classification	100
minimum	50.57
average	90.5
standard deviation	9.6

Most of the combinations produce good results and many of the combinations classify 100% of the test set. There are also plant combinations which result in a small percentage of the plants being correctly classified. For example, the plant specimens *Ayrtera distylis* and *Cupaniopsis parvifolia* result in a correct classification of only 50.6%. This is a similar probability to a random guess ($1/2 = 50\%$) so it can be said that the two specimens cannot be distinguished from each other. This can indicate either :

1. The acoustic density profile changes so much through rotation that the plants are impossible to characterise; or
2. The plants are similar to each other.

Reviewing the table shows that both of these plants can be easily distinguished from other plants in the population. *Ayrtera distylis* can be classified up to 100% of the test set against other plants in the population, and similarly, *Cupaniopsis parvifolia* can also be classified up to 100% against certain plants, so this shows that it is possible to characterise the plants. This means that the acoustic density profile of these two plants are similar. These two plants are shown in Figure 10.3 with a sample of their acoustic density function and the average of the features calculated for all 100 samples of the plants.

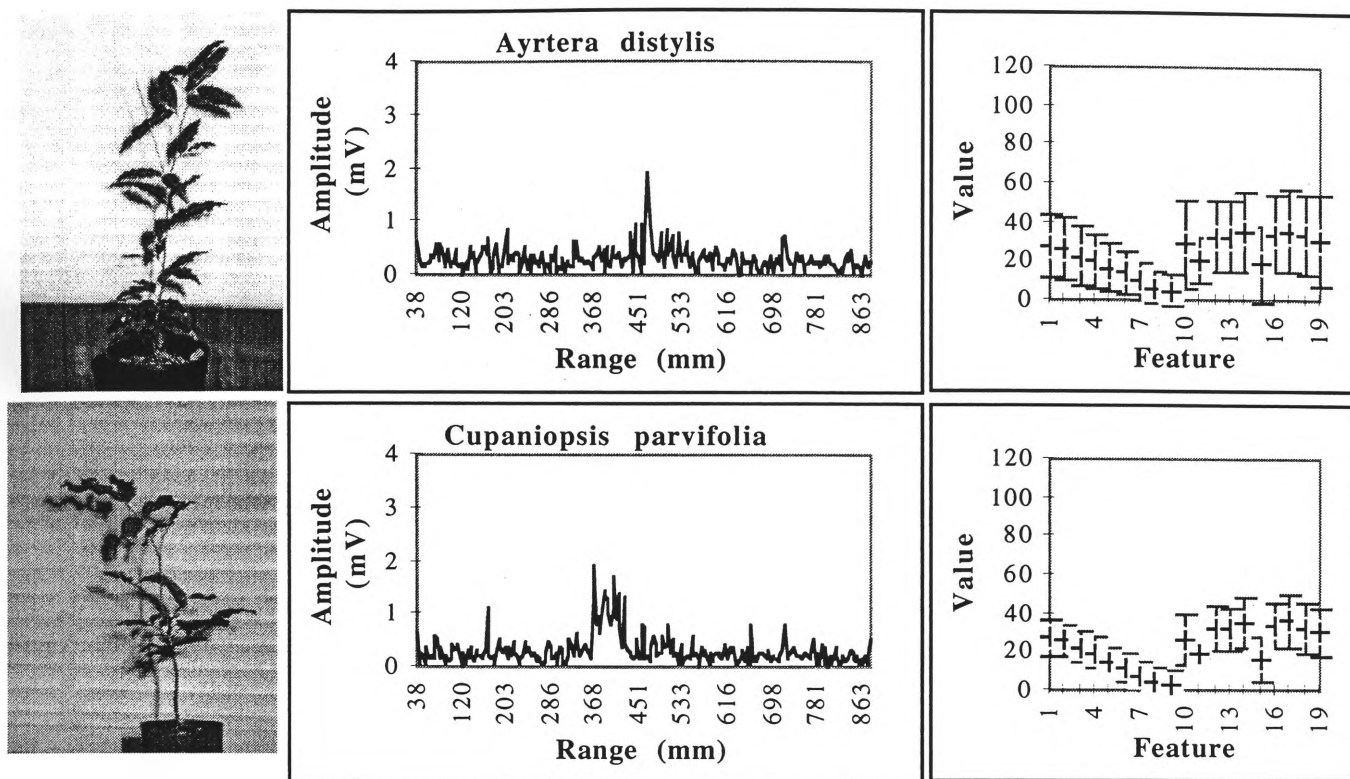


Figure 10.3 Images, a sample acoustic density profile and the average of all of the features (with standard deviation shown as error bars) for *Ayrtera distylis* and *Cupaniopsis parvifolia*

Both of the plants shown in Figure 10.3 have similar reflected acoustic density profiles due to their similar foliage structure. The figure shows that both plants reflect very little of the acoustic energy (both peak at approximately 3 mV) and their calculated features are almost identical. The plants both have medium to small sized leaves, most of which are horizontal, that is, end on to the sensor. The leaves are relatively spread through the plant so echoes return from a range of different surfaces.

When we consider how each of these individual plants are classified against the other 98 plants in the population (from Table 10.7) we see that there is a range of classification percentages which can be summarised as shown in Table 10.9. The percentages shown are the dual classification of the plant specimen given and all of the other plants, that is, it is the classification percentage for all of the test records of both the plant shown and each of the other plants in the data set of 100.

Table 10.9 The average classification of specimens against all other plants in the population

<i>Ayrtera distylis</i>	85.87 %
<i>Cupaniopsis parvifolia</i>	89.79 %

As a comparison, consider the samples of *Radermacheria fenecis* and *Archontophoenix cunninghamiana* which have a high classification percentage as a pair. Their classifications against all of the other plants in the test set is illustrated in Table 10.10.

Table 10.10 The average classification of specimens against all other plants in the population

<i>Radermacheria fenecis</i>	95.27 %
<i>Archontophoenix cunninghamiana</i>	85.90 %

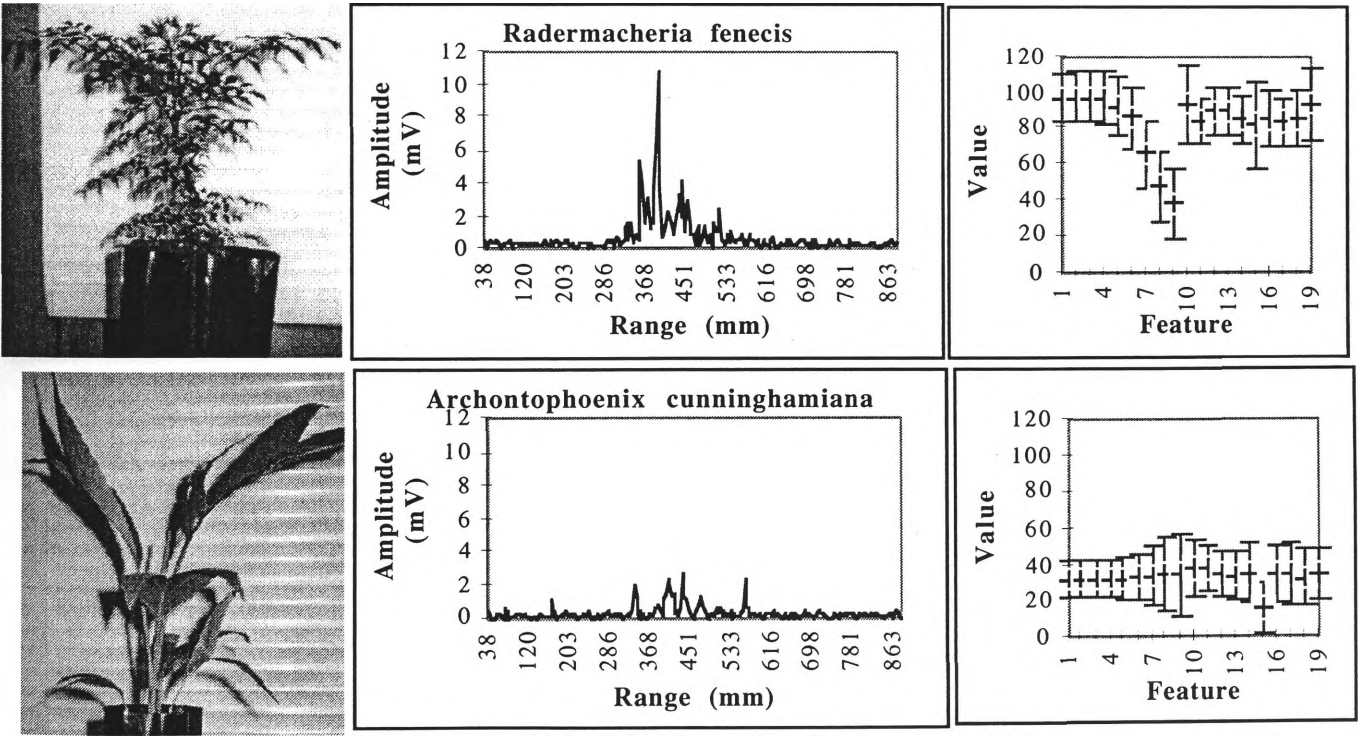


Figure 10.4 Image and acoustic density profiles, and features for *Radermacheria fenecis* and *Archontophoenix cunninghamiana*

These plants are very different both physically and in the acoustic energy which is reflected.

The average recognition percentage of each plant of the 100 plants against each other plant is shown in Table 10.11. It is in ascending order and highlights the plants which are the most different to all of the other plants in the population.

The plants which are near the top of the table are the most distinct plants compared to those which are further down the list whose acoustic density profiles are more similar to some others in the population. In a practical system, it would be beneficial to use plants which are different to all of the other plants which are present in the environment this would ensure that a mobile robot could recognise the different plants much more easily.

Table 10.11 Average percentage classification against all of the other plants in the population of 100 ordered by percentage

<i>Leptospermum laevigatum</i>	99.63	<i>Leptospermum petersonii</i>	92.17
<i>Licuala ramsayi</i>	97.18	<i>Solanum aviculare</i>	92.11
<i>Jacaranda mimosifolia</i>	96.88	<i>Acacia irrorata</i>	92.00
<i>Azalea cultivar splenda</i>	96.39	<i>Diploglottis campbelli</i>	91.95
<i>Acacia howittii</i>	96.15	<i>Correa alba</i>	91.77
<i>Dodonaea viscosa</i>	95.58	<i>Acacia podalyrifolia</i>	91.75
<i>Banksia ericifolia</i>	95.31	<i>Acacia stricta</i>	91.58
<i>Radermacheria fenecis</i>	95.27	<i>Endiandra pubens</i>	91.58
<i>Melaleuca erubescens</i>	95.05	<i>Doryanthes palmeri</i>	91.33
<i>Tabebula chrystricha</i>	94.57	<i>Citriobatus paucifloris</i>	91.29
<i>Westringa fruticosa</i>	94.43	<i>Dodonaea triquetra</i>	91.29
<i>Melaleuca styphelioides</i>	94.29	<i>Melaleuca decora</i>	91.20
<i>Acacia binervata</i>	94.23	<i>Grevillea baileyana</i>	90.83
<i>Pittosporum crassifolium</i>	94.13	<i>Cordyline australis</i>	90.78
<i>Indigofera australis</i>	93.85	<i>Acronychia laevis</i>	90.70
<i>Sarcotoechia heterophylla</i>	93.70	<i>Eriostemon myoporoides</i>	90.70
<i>Diploglottis australis</i>	93.62	<i>Rhododendron bryophyllum</i>	90.68
<i>Szygium paniculatum</i>	93.38	<i>Acacia mearnsii</i>	90.61
<i>Acacia cultriformis</i>	93.34	<i>Omalanthus populifolius</i>	90.61
<i>Crinum mauritianum</i>	93.27	<i>Leptospermum morrisonii</i>	90.39
<i>Szygium leuhmanni</i>	93.19	<i>Pittosporum james</i>	90.16
<i>Ficus rubiginosa</i>	93.17	<i>Hymenosporum flavum</i>	90.12
<i>Ziera collina</i>	93.00	<i>Sarcomelicope simplifolia</i>	89.87
<i>Crinum pedunculatum</i>	92.97	<i>Cupaniopsis parvifolia</i>	89.79
<i>Polyscias murrayi</i>	92.89	<i>Endiandra introrsa</i>	89.75
<i>Cryptocarya laevigatum</i>	92.79	<i>Pittosporum revolutum</i>	89.72
<i>Livistona sp 'Carnarvon'</i>	92.74	<i>Casuarina stricta</i>	89.71
<i>Cryptocarya williwilliana</i>	92.73	<i>Laccospadix australasica</i>	89.53
<i>Casuarina glauca</i>	92.63	<i>Eucalyptus botryoides</i>	89.52
<i>Melaleuca quinquenervia</i>	92.53	<i>Goodia lotifolia</i>	89.24
<i>Phyllanthus albiflorus</i>	92.37	<i>Polyscias elegans</i>	89.15
<i>Cinnamom oliveri</i>	92.32	<i>Hakea salicifolia</i>	89.02
<i>Alyxia ruscifolia</i>	92.22	<i>Acacia falcata</i>	88.97
<i>Tristaniaopsis collina</i>	92.22	<i>Stenocarpus sinuatus</i>	88.91
<i>Carpentaria acuminata</i>	92.18	<i>Streblis brunonianus</i>	88.65

<i>Agapanthus praecox dwarf</i>	88.64	<i>Microcitrus australis</i>	86.28
<i>Cupaniopsis anacardioides</i>	88.58	<i>Pittosporum undulatum</i>	86.25
<i>Acacia melanoxylon</i>	88.56	<i>Rhopalostylis sapida</i>	86.19
<i>Casuarina torulosa</i>	88.47	<i>Howea forsteriana</i>	86.07
<i>Polyscias australiana</i>	88.46	<i>Ficus obliqua</i>	85.93
<i>Guioa semiglauc</i>	88.03	<i>Archontophoenix</i>	85.90
<i>Solanum laciniatum</i>	87.90	<i>cunninghamiana</i>	
<i>Mishocarpus australis</i>	87.89	<i>Ayrtera distylis</i>	85.87
<i>Cryptocarya bidwilli</i>	87.72	<i>Rhododendron clorinda</i>	85.06
<i>Pittosporum rhombifolium</i>	87.61	<i>Rhopalostylis baneri</i>	84.99
<i>Grevillea hilliana</i>	87.58	<i>Eucalyptus leucoxylon</i>	84.91
<i>Agapanthus praecox</i>	87.50	<i>Eucalyptus maculata</i>	84.82
<i>Litsea reticulata</i>	87.18	<i>Grevillea marmalade</i>	84.32
<i>Banksia integrifolia</i>	87.15	<i>Solanum vescum</i>	83.86
<i>Acacia longifolia</i>	86.80	<i>Solanum brownii</i>	83.03
<i>Azalea alba magnifica</i>	86.51		

The plants which are at the top of the table are the ones which have characteristics which are not common in other plants in the population and are also very consistent through rotation. For example, the first plant in the table *Leptospermum laevigatum* is a very bushy plant with many reflective surfaces. This means that the specimen will be very consistent through rotation.

The image, sample acoustic density profile and the features with the standard deviations for *Leptospermum laevigatum* are shown in Figure 10.5. There is a large number of ranges which return echoes and they are all of relatively large amplitude. It can also be noted that all of the calculated features are very high as they are all around or above 100 which is the value that all of the features are scaled towards. Most of the features have small standard deviations (shown by small error bars) which means that these features are relatively consistent through a change in orientation. This contrasts with the features calculated for *Ayrtera distylis* (shown in Figure 10.3) which have large standard deviations.

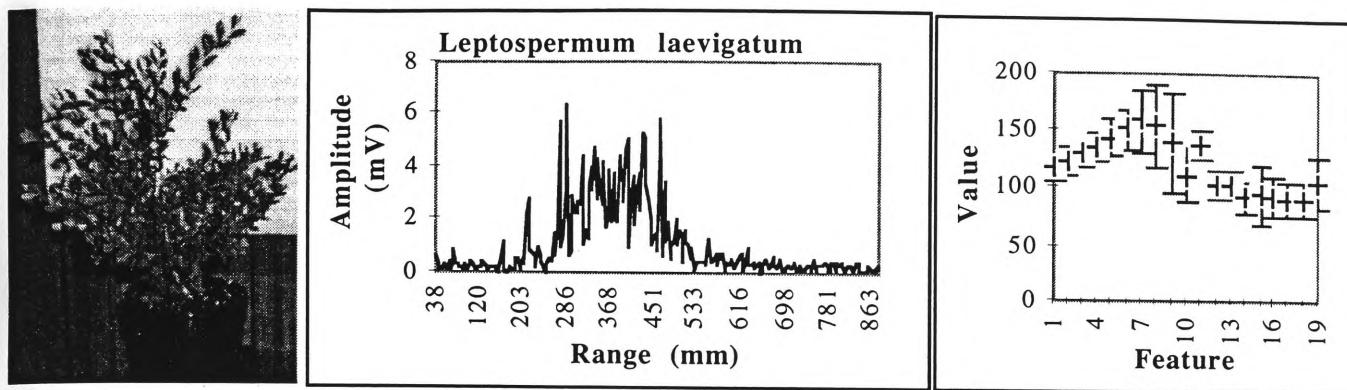


Figure 10.5 The image, a sample acoustic density profile, and the average of each feature shown with standard deviation as error bars for *Leptospermum laevigatum*

10.11 Discriminant analysis techniques

Discriminant analysis is a tool which is used to classify an individual sample into one of a finite number of groups of classes. Predictive discriminant analysis techniques can be used to develop a mathematical rule or discriminant function to estimate the class to which an individual sample belongs. The discriminant function consists of a linear combination of variables for each class which predicts membership of that class. When a new sample is presented, the discriminant function for each class is calculated and the class is assigned based on the predefined class which the sample is closest to. Discriminant analysis were used but produce similar results to that given for the template matcher in Table 10.12, so are not shown.

10.12 Plants which are inconsistent through viewing angle

Not all of the plants are consistent through change in viewing angle and this is what causes problems for a classifier. Figure 10.6 shows a model of two different plants, (a) represents a plant which produces an acoustic density profile which is relatively similar regardless of the angle from which it is insonified. Figure 10.6(b) however, represents a plant that is consistent across a range of orientations but once the plant is sensed from the positions separated by the rays in the figure, the leaves are arranged differently and produce significantly different acoustic density profiles.

In this particular case, a statistical classifier fails as the differences between each of the different sectors inherent in (b) are averaged in the template so none of the orientations will match this template. When test records are presented to the classifier for that particular plant, they are likely to match neither of the templates well, so will be allocated to that which is most similar.

In order for a classifier to correctly characterise the plant, four templates need to be built for this particular plant. This could be done manually, or the classifier could have the capability of automatically storing the different templates. In the case shown in the figure, the classifier will store one template for plant (a), and four templates for plant (b), so when a test record is received, it will be classified as being from the correct plant. In landmark recognition for mobile robots, the ability to classify a partially symmetric plant from different orientations provides additional information to the navigation system. It gives a coarse measure of the orientation of the plant which helps localise the robot relative to the plant.

The alternative is to use a classifier model which can inherently store information about multiple patterns for a single class. This can be done with a neural network and is pursued further in Section 10.13.

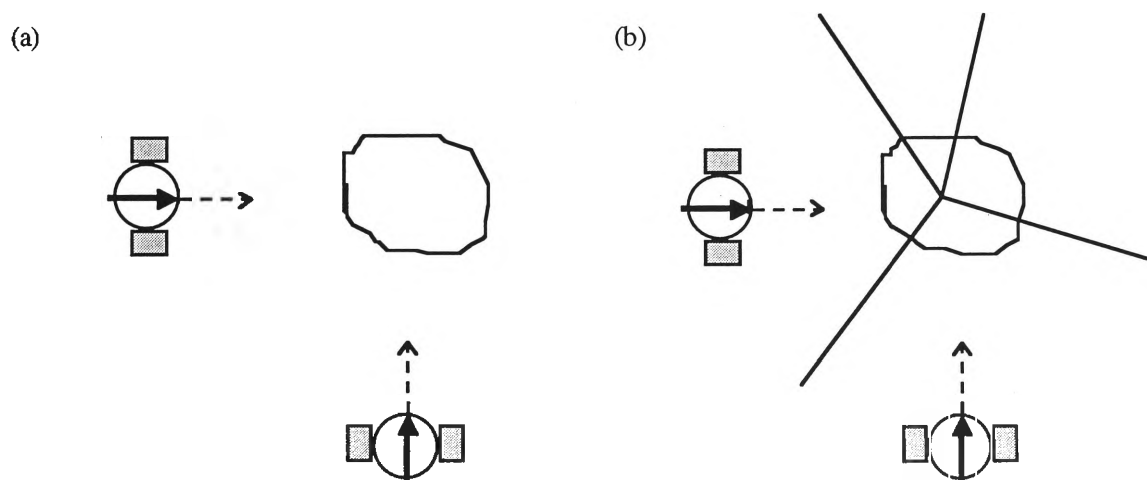


Figure 10.6 Two plants which have different characteristics depending on the position from which they are sensed (a) is consistent through orientation, where (b) has regions of similar return but is not consistent through an entire rotation

10.12.1 Non-linearly separable classes

Figure 10.7 shows 2 features plotted against each other in two dimensional space. In (a), the classes are linearly separable as the classes can be separated by a straight line and are easily classified as different plants by a linear classifier which does not weight individual features. A multi-layer feedforward network however, can separate classes which are not linearly separable as in (b). This means that plants which vary through orientation may be characterised better using a multi-layer feedforward network and that is pursued in Section 10.13.

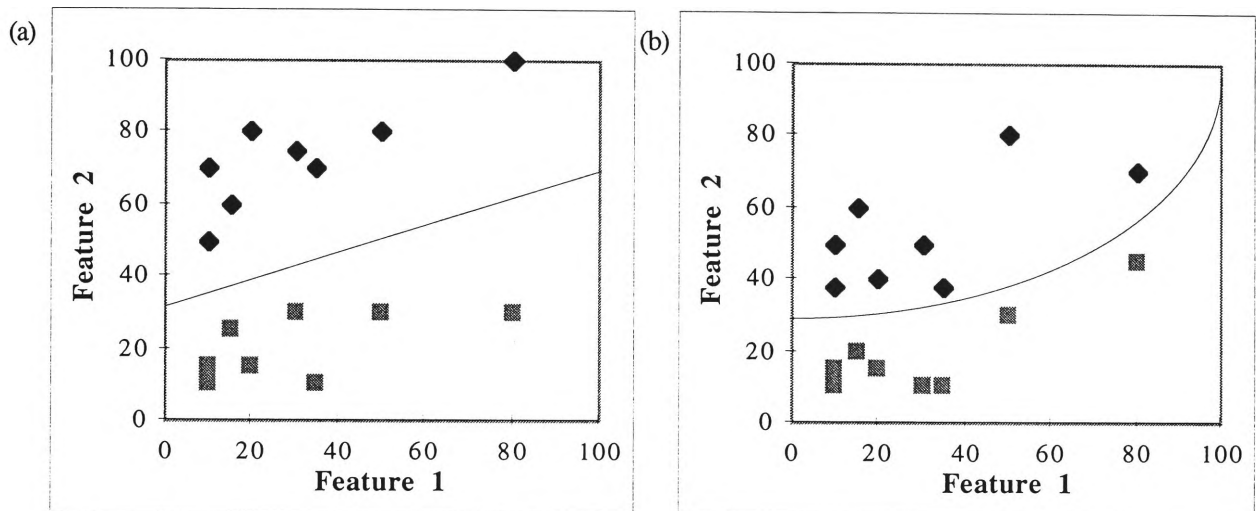


Figure 10.7 Two feature distributions (a) is linearly separable while (b) can only be separated with a curve

10.13 Classifying plants using both raw data and features using several different classifier types

In this Section, different classification schemes are tabulated for selected sets of plants with their corresponding results. In Chapter 4, A set of benchmarks was established which showed that plants can be classified using CTFM Sonar data, with a Neural Network. In Chapter 8, a set of 19 features were developed and shown to be superior to the raw acoustic density profile at capturing the discriminatory parts of the acoustic density profile. In this section, the classification of plants is tabulated using both features and the data from the raw acoustic density profile with both a simple statistical

classifier, a classifier which uses discriminant analysis (outlined in Section 10.11), and a non-linear neural network classifier.

The results are shown in Table 10.12. The first column has the names of the plants used to train and test the classifier, while the rest of the table provides the results of running each of the statistical classifier and the neural network with the different types of input data (the acoustic density profile or the neural network).

The table shows that the features provide better results in all cases. It can also be seen that there is widely varying results depending on the combination of plants which are being used by the classifier. As the number of plants become larger, the correct classification percentages generally become lower. The results of classifying a single return as one of 100 plants are low. When there is such a large number of plants, there is a high probability that some of them are similar acoustically and hence are classified incorrectly as each other.

When the classifiers are run using 100 inputs from the acoustic density profile, a large amount of processing time is required to build the classifier.

Table 10.12 Comparison of different input data and classifiers

Plant Combination	Acoustic Density Profile		Features	
	Template Matcher	Neural Network	Template Matcher	Neural Network
<i>Cryptocarya williwilliana</i> <i>Leptospermum laevigatum</i> <i>Szygium leuhmanni</i> <i>Westringa fruticosa</i>	94.96	91.42	98.38	99.73
<i>Ayrtera distylis</i> <i>Cupaniopsis parvifolia</i>	68.18	74.29	50.56	77.71
<i>Archontophoenix cunninghamiana</i> <i>Radermacheria fenecis</i>	96.98	98.18	100.00	100.00
<i>Acacia binervata</i> <i>Acacia cultriformis</i> <i>Azalea splenda</i> <i>Polyscias murrayi</i>	82.24	86.98	83.00	87.95
<i>Leptospermum laevigatum</i> <i>Jacaranda mimosifolia</i> <i>Agapanthus praecox</i> <i>Szygium leuhmanni</i>	89.24	87.02	98.67	98.55
<i>Acacia binervata</i> <i>Acacia cultriformis</i> <i>Acacia falcata</i> <i>Acacia howittii</i>	48.97	40.05	67.39	66.67

<i>Acacia irrorata</i>				
<i>Acacia longifolia</i>				
<i>Acacia mearnsii</i>				
<i>Acacia melanoxylon</i>				
<i>Acronychia laevis</i>				
<i>Agapanthus praecox</i>				
<i>Acacia binervata</i>	76.64	91.19	98.92	95.94
<i>Acacia cultriformis</i>				
<i>Alyxia ruscifolia</i>				
<i>Leptospermum laevigatum</i>				
<i>All 100 plants</i>	9.30	11.58	16.50	18.40

10.14 Plant grouping

Plants can be efficiently grouped as 1 of n similar plants using statistical clustering techniques. The plants with similar physical characteristics are grouped with other plants on the basis of templates calculated for each of the plants. Plants from different groups are then tested using the classifier and plants which are in the same cluster are hard to separate and plants which are from different clusters are easy to separate. This is because plants which cluster together have similar acoustic properties.

Appendix D provides the full details of the experiments and the results that were obtained. A simple system which only needs the acoustic group of the detected plant could exploit this technique instead of implementing a more processor intensive classifier.

10.15 Conclusion

Analysis of the acoustic density profiles of 100 different plants shows that they can be separated using pattern classification techniques when a small sample is are considered. This is achieved even with a very simple classifier. When a greater number of plants are added however, the chance of classifying a species correctly is reduced significantly.

The statistical classifier is a significant improvement over the ANN discussed in chapter 4 as it provides a list of features with inherent ordering of the most discriminatory. This provides important information about the differences between different combinations of plants.

10.16 Summary

1. Most plants can be discriminated well from other plants based on their acoustic density profile.
2. Some plants are too similar to each other so it is difficult for a classifier to discriminate between them reliably.
3. The features calculated from the acoustic density profile consistently produce lower classification error than when using the spectra as input to any type of classifier.

11. Implementation issues for mobile robot navigation

One of the areas of potential application for this sensor is in the area of mobile robot navigation. This sensor has not yet been implemented on a mobile robot, but this Chapter describes some of the implementation issues for this sensor.

Mobile robot navigation is the process of managing a robot on its course. This task usually has an overriding purpose such as reaching a specific goal or performing a pre-defined task. To achieve this, an interface to the outside world is required which is in the form of either passive or active sensors (or combinations of these). There has been considerable research effort in the area of navigation algorithms [Zelinsky, 1991]. McKerrow [1991], decomposes the process of navigation into three sub-tasks : mapping and modelling the environment; path planning and selection; and path traversal and collision avoidance.

This thesis describes a sensor which is used in the environment modelling sub-task of navigation and is capable of facilitating mobile robot navigation. There are several different ways of implementing the system depending on the level of sophistication or “intelligence” required. Many researchers are working towards sophisticated robots. The goal of these robots is to interact with their environment at a high level by reacting to new and changing situations which often occur in the “real world”. However, there are situations where the most simple solution is the best as it will be more robust and require the lowest processing load.

In this Chapter, the timing for different tasks is discussed, the fundamental sensing situations are considered, and the effect of sensing while in motion is outlined. This is followed by several different plant sensing scenarios and how the sensor could be used the most effectively in the environment.

11.1 Process timing

The physics of the sensor constrains the CTFM sensor system in terms of the rate at which information from the environment can be obtained and this is discussed in this section. The software operations are extremely fast compared to the time that it takes to sweep through the frequency range from 100 to 50 kHz. This means that the processor is available during the time that the sensor is collecting data to perform other tasks such as :

1. processing data from other CTFM sensors;
2. controlling other sensors such as visual sensors;
3. fusing sensor information; or
4. performing high level reasoning such as that required for navigation.

Section 11.1.1 shows the theoretical timing of the system and Section 11.1.2 is a summary of the empirical results.

11.1.1 Theoretical timing

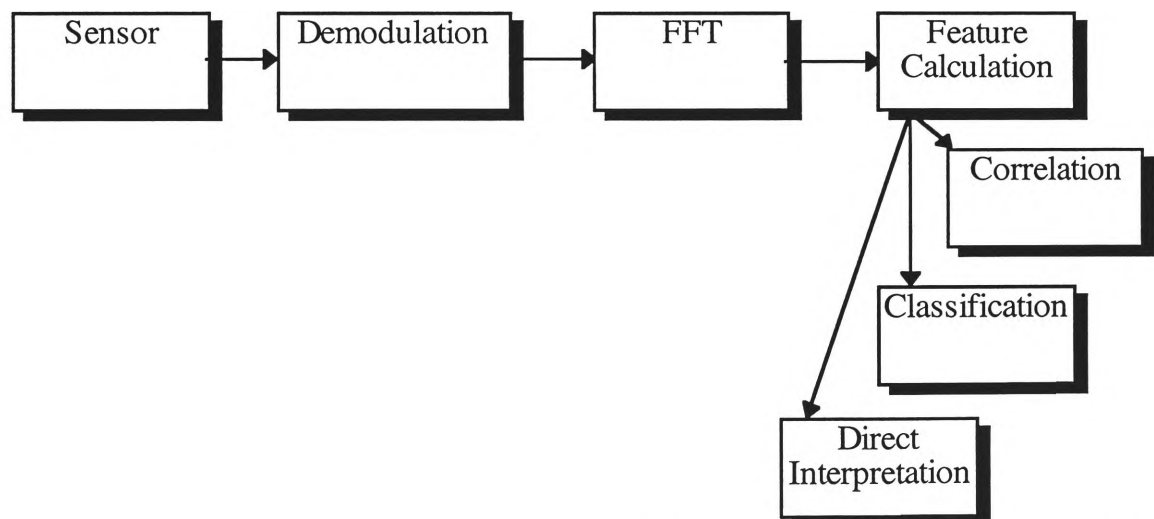


Figure 11.1 The processing chain of data from the sensor to result

Figure 11.1 shows the processes involved from capturing the signal to a result. The receiver detects the echo, it is demodulated against a copy of the transmitted signal and a FFT is performed to transform the result into the frequency domain. In the feature calculation process, the data is referenced to a standard range, individual features calculated and scaled. Depending on what the data is being used for, a correlation module

may be used to detect changes between two echo returns, the feature data may be used in a classifier, and / or the features could be interpreted directly.

The sensing, demodulation and FFT are handled by an embedded system in order to leave the general purpose processor to perform other tasks. Timing for these DSP processes can be found in references such as Embree [1995].

The processes that perform the other tasks shown in Figure 11.1, of referencing to a standard range, calculating and scaling features; correlation; and running a classifier are implemented in software for the purpose of this research. The exact number of instructions required to execute the processes depends on the target processor and the compiler used to build the code which runs on the processor so cannot be determined exactly. In Table 11.1, the timing of the operations are documented in terms of the order of the algorithm and in some cases d which is the depth of the plant as determined from the acoustic density profile. The timings illustrated provide a guideline for the implementation of the system which is not constrained to any particular hardware. Some empirical values for these algorithms implemented on particular hardware are given in Section 11.1.2.

Table 11.1 Empirical timing of the software processes

Correlation	<p>The correlation algorithm documented in Chapter 5 is from the signal processing field and performs three discrete correlation steps, one correlation between the two input patterns and then a correlation of each input pattern with itself (autocorrelation). These additional autocorrelations are performed in order to scale the result so that it lies between 0 and 1.</p> <p>An individual correlation consists of accumulating the sum of the products of the two input arrays, so depends on the size of the input array and is hence of order N. As stated above, the correlation algorithm used in this thesis consists of three steps, so is of order $3N$, where N is the size of the array that is being correlated. This array is of size 19 when the features are being correlated.</p>
Calculating the depth of the plant	<p>The amount of time that it takes to calculate the individual features from the acoustic density profile depends on the depth of the plant d as calculated from the individual acoustic density profile. This depth d was shown in Chapter 9 to be the minimum depth of the plant.</p> <p>In order to calculate the depth of the plant, for a scene which consists of a plant only, the range line</p>

	which contains the highest amplitude in the acoustic density profile is found. From this range line, step back until the start of the plant is detected. Similarly, start from the range line where the maximum amplitude occurs and work up until we meet the condition where the plant is detected. This process is of order N to find the maximum amplitude and is of order d to find the depth of the plant. So, the order of the algorithm to calculate the position of the start and end of the plant within the acoustic density profile of the plant is of order $N + d$
Referencing the plants to a standard range	This operation involves translating and scaling each of the range lines within the plant to a standardised distance. This involves performing a simple operation on each of the range lines within the plant, and is hence of order d .
Calculating the features	The 19 features documented in Chapter 8, are mostly of order d . The exception is the <code>length_of_density_profile</code> feature which is calculated directly as the end range line minus the start range line.
Scaling the features	This task involves multiplying the calculated features by the scaling values so is of order N , where N is the number of features calculated which is 19 for this thesis.
Assign a record to 1 of x classes	The template classifier documented in Chapter 10 calculates the mean squared difference of the individual record against each of the x templates stored by the classifier. The mean squared difference is calculated as the square of the difference between the individual elements of the two input arrays. This assignment process is of order xN where x is the number of plants, and N is the number of elements which are input to the classifier.

11.1.2 Empirical timing

In the current system, the sensing, capture, demodulation and FFT are run as an embedded system so it is difficult to get empirical timing for these processes. However, the software can be measured more easily. The software was measured as run on a 75 MHz, PowerPC 603e processor running the *MacOS* operating system and the results are summarised in Table 11.2. The processes outlined in the table were run for one million iterations and the total time taken was divided by one million to get a measure of the approximate time to perform each operation. The original implementation was performed for elegance (speed was not a particular consideration) so optimisation of the code will improve the results. Note that the times shown in the table are extremely small compared to the time that it takes to perform a frequency sweep (102.4 milli seconds).

Table 11.2 Approximate timing for processes

Process	Approximate time (ms)
Correlation of 100 items	0.108
Correlation of 100 items with echo tracking	4.39
Correlation of 19 items	0.012
Reference to a standard range and calculate 19 features	0.95317
Assign a record to 1 of 4 classes (template classifier)	0.563667

11.2 Fundamental plant sensing

In previous chapters, the situation of a plant located in the centre of the beam was considered. In this section, the application to a mobile robot is further analysed. The mobile platform will be sensing the environment as it moves so a plant detected by the sensor may not necessarily be positioned in the centre of the beam. In this section, the fundamental issues of plant sensing from a mobile platform are considered.

11.2.1 The effect of range to the plant

The resolution of the system is constant through range up to the range limit of the sensor (1.5 m for the settings used in the experimental system). This means that if a plant is within the range of the sensor, then the relative position of the surfaces are constant regardless of how far away the plant is. In terms of the echo strength however, there may be some information lost through the beam spread and through attenuation but this will only be a small amount. Scaling the plant acoustic density profile with respect to the range calibration curve (Chapter 5) will make the echo pattern independent of range. The only caveat is that at long range, the echo from small surfaces within the plant may be completely hidden due to background noise. In the case where recognition is required, a closer audition of the plant may be necessary.

Consider the situation shown in Figure 11.2. In (a), the robot is approaching the plant and in (b) the robot is leaving the plant. In both cases, the sensor is pointing directly at the plant (in the figure, the direction of the sensor is indicated by the heavy arrow). The plant is always in the centre of the beam which means that the plant will move along the acoustic density profile depending on the absolute range to the surfaces of the leaves within the plant. The normalisation of the acoustic density profile (Chapter 6), ensures

that the absolute range information can be removed from the profile, but relative range information is kept, this relative range information is also scaled, so the resulting range referenced and scaled acoustic density profile will hold reasonably constant.

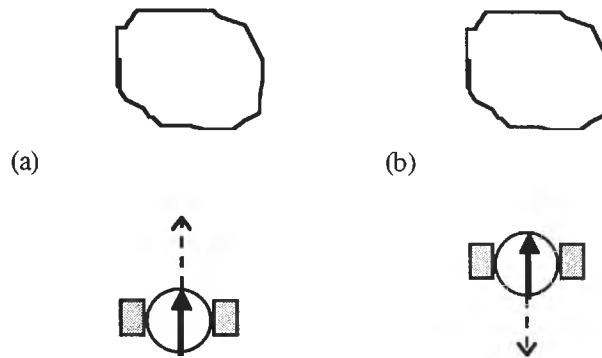


Figure 11.2 In (a), the robot is approaching the plant and in (b) the robot is leaving the plant. The direction of the sensor is indicated by the heavy arrow.

When the plant is large, or when the sensor is very close to the plant, it is possible that the entire plant will not be insonified by the beam and hence the entire plant will not contribute to the acoustic energy detected by the receiver. The minimum range at which the entire plant is in the sensor's field of audition depends on the size of the plant (Figure 11.3).

The sensor is swept through a frequency range and the width of the beam is directly affected by the frequency at which it is operating. The beamwidth of the sensor in the horizontal plane, varies from 30 degrees at the top of the sweep (100 kHz) to 80 degrees at the bottom of the sweep (50 kHz) that is, an average beamwidth of 55 degrees. Similarly, in the vertical plane, the beamwidth varies from 12 degrees at 100 kHz to 25 degrees at 50 kHz for an average beamwidth of 18.5 degrees in the vertical plane.

For a plant which is 300 mm wide at its widest point, the range to its axis calculated using the tangent rule (Figure 11.3) is 185 mm. Similarly, the minimum range in the vertical plane, is calculated as 448 mm.

For a larger plant, say 1 m wide, when the sensor is closer than 960 mm then the sensor will not insonify the whole plant, but rather a slice of the plant. The effect of this has not been determined empirically but it should not be a problem as the sensor will still

be able to detect the structure of the surfaces within the plant. This issue should be investigated further as the next stage of the research.

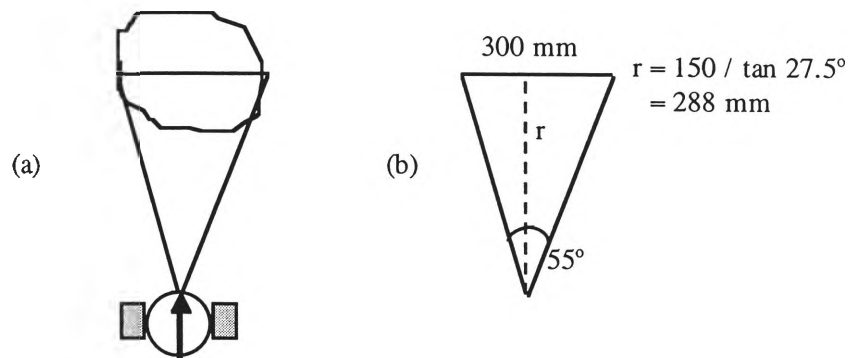


Figure 11.3 The minimum range at which the entire plant is in the field of audition of the sensor

11.2.2 Positioning of the plant within the beam

When the plant is not in the central lobe of the sensor beam, the result will be similar. Figure 11.4 shows a plant in different positions within the central lobe of the sensor. The range to surfaces within the plant will be similar so the resulting acoustic density profile is similar.

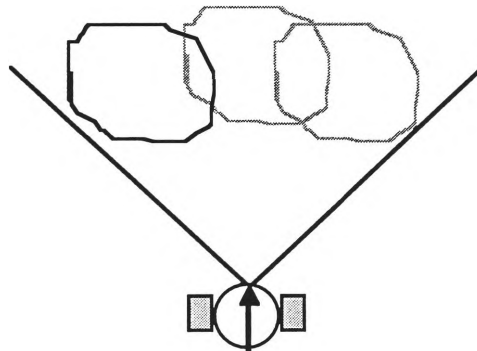


Figure 11.4 A plant in different positions within the field of audition

11.2.3 When the platform moves past a plant

Consider the situation shown in Figure 11.5. The initial position of the mobile robot is shown on the left and it is sensing orthogonally to the direction in which it is moving. Subsequent sensing positions of the mobile platform are shown in light grey and are numbered sequentially from 1 to 5. From the first sensing position, 1, nothing is

insonified by the sensor, at sensing point 2, a small amount of the edge of the plant is detected. At sensing point 3, the entire plant is within the field of audition of the sensor. Sensing point 4 detects a small amount of the plant similarly to sensing point 2. And finally, at sensing point 5, none of the plant is in the field of audition.

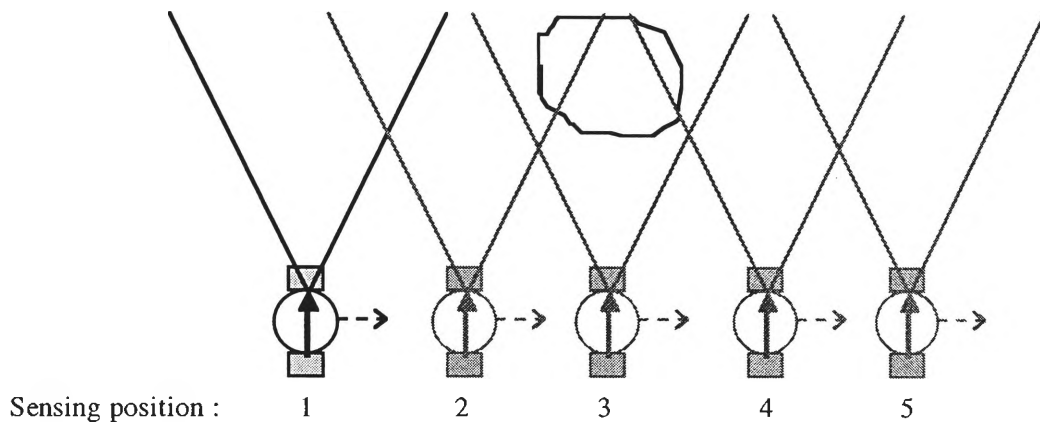
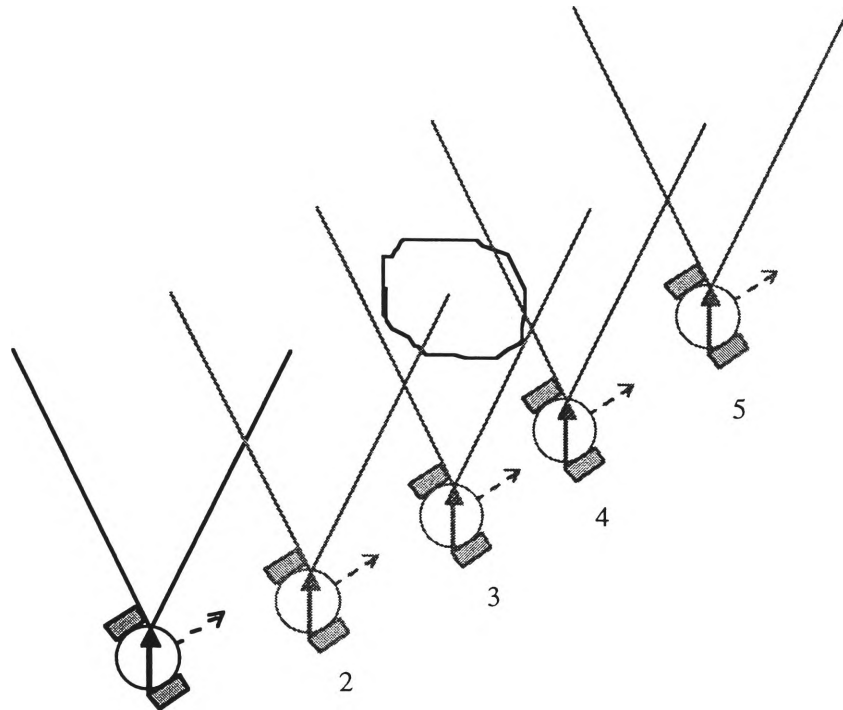


Figure 11.5 A robot sensing orthogonally to the direction in which is moving. The sensing positions are numbered

A similar, but different situation occurs when the robot is moving at some angle to the plant and this is shown in Figure 11.6. In this particular example, the plant is detected from sensing position 2 but is only partially in the field of audition. It becomes entirely within the width of the beam from position 3 before it moves out of the sensing beam. Partial detection of a plant may cause a problem as the section of the plant in the field of audition may not be representative of the whole plant.



Sensing position : 1

Figure 11.6 A robot sensing at an angle to the direction in which is moving. The sensing positions are numbered

The problem of partial detection is avoided by fusing the information from several scans. A simple scheme would be to take several scans of the plant and then chose the scan which has the most information, for example the largest acoustic area. This acoustic density profile can then be interpreted using the methods outlined in Chapter 9, or using plant recognition methods described in Chapter 10.

A landmark navigation system will pan the sensor to track the land mark as the robot moves past it (Figure 11.7). This will result in several acoustic density profiles from different angles, and from these recognise the plant and measure its exact position relative to the robot. Borenstein & Koren [1995] developed a sensing ring which detects most objects in the environment but it can have a problem with convex corners as outlined by McKerrow [1995]. He proposes an alternate system which uses several panning sensors in order to eliminate this problem.

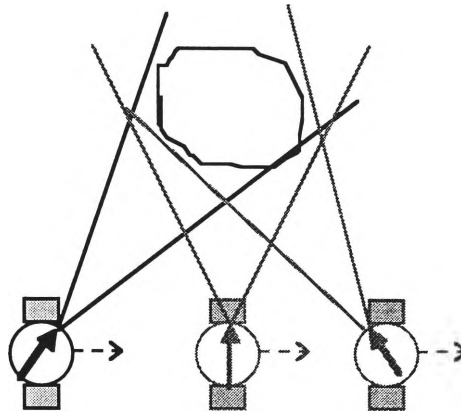


Figure 11.7 The sensor is panned to be oriented towards the plant as it moves past

The way that the sensor is used on a moving platform depends on the specific problem. Some different tasks are outlined in Table 11.3.

Table 11.3 Some sensing methods

Sensing task	Method
Landmark detection	The sensor is panned as the robot is moved past the plant, followed by a pan forward to detect the next plant.
Path following	The sensor is panned back and forward across the boundary between the path and the grass.
Collision avoidance	A forward pointing sensor detects objects in the path of the robot. Note that two sensors are required to capture all possible collision situations [McKerrow, 1995].
Wall following	A sensor points towards the wall and is used to adjust for changes in the position of the wall relative to the robot.

11.3 The effect of a moving sensor

A robot which needs to stop in order to sense its environment is of limited use. In this section, a system which senses on the move is discussed. Section 11.3.1 describes the effect of the change in transmit / receive point and how it affects the received signal, and Section 11.3.2 analyses the change in the signal which is caused by the effect of the waves being compressed in time due to the movement of the source and the receiver. This is known as the Doppler effect and it causes the greatest impact when sensing either directly ahead or behind the robot but if this feature is recognised by the system designer then the situation can be used to advantage.

11.3.1 Change in position of sense / receive point

The general case of a moving robot and a stationary plant is shown in Figure 11.8. The robot is moving forward at speed u_s and a signal is transmitted at time t_0 . The signal reflects from the plant and arrives at the receiver at time t_1 . Using the CTFM sensor, the maximum range at which a plant can be detected is 1.5 metres. For a plant at the maximum range, it will take $1.5 / 343.52$ seconds (at 20°C) or 0.0044 seconds for the sound to return (Equation 2.1). For a robot travelling at 0.5 ms^{-1} , the maximum total change in movement of the robot between sense and receive for any particular transmitted frequency will be 0.0022 m or 2.2 mm. That is, when travelling at say, 0.5 ms^{-1} (this is not top speed for a robot, but is a speed which will facilitate sensing more easily) the robot will travel 2.2 mm in 0.0044 seconds. This means that the plant (or any other object) will appear to be 1.1 mm closer than it is in the reflected signal. If however, the plant is not at the maximum range of the sensor, for example at a range of 1 m then the error in absolute range will be accordingly smaller (0.7 mm for a plant at a range of 1 m). Since most of the information used to identify species is in the relative range information (rather than the absolute range) this difference is very small for a robot travelling at this speed. The Doppler shift must be added to this (Section 11.3.2).

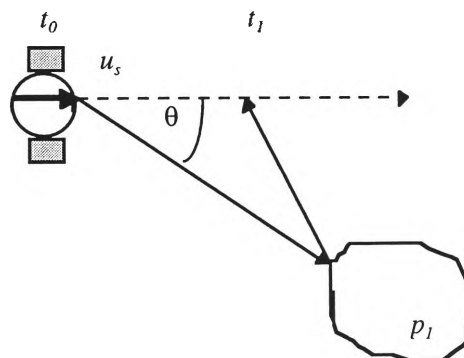


Figure 11.8 The robot is moving towards the right at speed u_s . Plant p_1 is at an angle of θ to the direction of travel

11.3.2 The effect of the change in wavelength with motion (Doppler shift)

When an ultrasonic wave source or receiver is moving, the frequency observed at the receiver is different to that transmitted by the source [Tipler, 1982] and is dependant

on which of the transmitter or receiver is moving. Figure 11.9 shows successive waves transmitted from point 1, while the source is moving at speed u_s towards the right. As shown, the waves are more compressed over time at a point directly in front of the moving source.

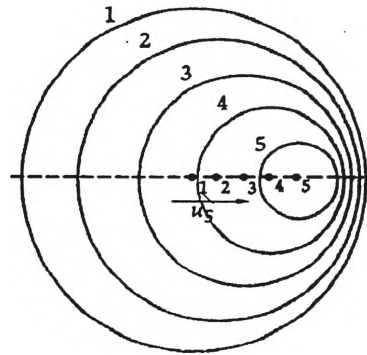


Figure 11.9 Wavefronts of signal emitted from a source moving as speed u_s to the right from Tipler [1982, pp 412]

Figure 11.8 (in Section 11.3.1) shows the general case, where a robot is moving towards the right, at speed u_s , and a plant is at angle θ from its direction of travel. The process of transmit / receive is modelled by two separate events. Initially, the transmitted signal can be thought of as a single frequency transmitted from the robot to the plant - in this case, the source is moving and the plant is stationary. The reflection from a surface of the plant, back to the receiver is then modelled as a stationary transmitter with an approaching receiver.

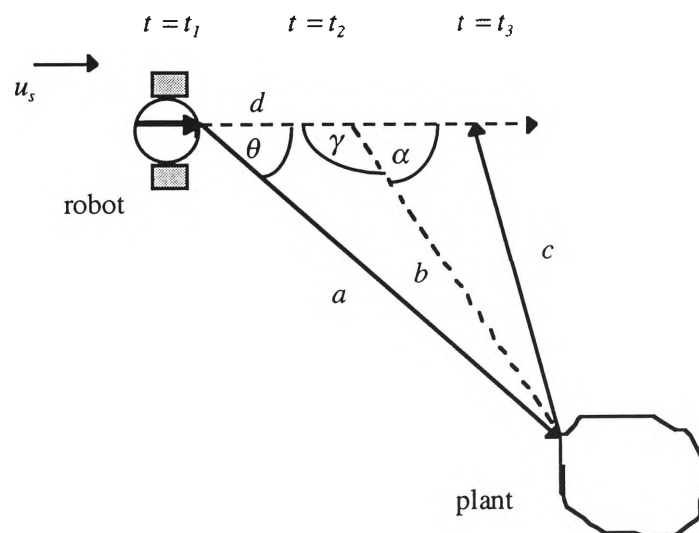


Figure 11.10 The model of the transmit / receive process

The model of the system is shown in Figure 11.10. Initially, the transmitter is moving at speed u_s in the direction given (or velocity $u_s \cos \theta$ relative to the plant) and an ultrasonic wave of speed c (the speed of sound in air is 343.52 ms^{-1} at 20° C) is transmitted at time t_1 at frequency f_t . The frequency observed at the receiver f_p (in this case, the plant) at time t_2 is given by Equation 11.1.

$$f_p = \frac{f_t}{1 - \frac{u_s \cos \theta}{c}} \quad 11.1$$

The wave then reflects from the plant (which is now modelled as a stationary transmitter), transmitting at frequency f_p . At this point in time (t_2), the robot has moved a distance of $d = a * u_s / c$ along its original path (where a is the range to the plant). The robot is moving at velocity $u_s \cos \alpha$ (where α is the angle between the path of the robot and the point of reflection on the plant) and the frequency detected at the receiver, f_r is given by Equation 11.2.

$$f_r = f_p \left(1 + \frac{u_s \cos \alpha}{c} \right) \quad 11.2$$

The angle α can be calculated as $180 - \gamma$, since the angles are on a straight line. γ is calculated using the cosine rule given a , b and d , and b is calculated using the cosine rule since we know d , θ and a . Hence γ is given by Equation 11.3. a is calculated as $180 - \gamma$ and is expanded in terms of all of the known quantities a , u_s , c and θ in Equation 11.4.

$$\gamma = \cos^{-1} \left(\frac{a^2 - d^2 - b^2}{-2db} \right) \quad 11.3$$

$$\text{where } b = \sqrt{a^2 + d^2 - 2ad \cos \theta}$$

$$\text{and } d = \frac{au_s}{c}$$

$$\alpha = 180^\circ - \cos^{-1} \left(\frac{a^2 - \left(\frac{au_s}{c} \right)^2 - \left(a^2 + \left(\frac{au_s}{c} \right)^2 - 2a \left(\frac{au_s}{c} \right) \cos \theta \right)}{-2 \left(\frac{au_s}{c} \right) \sqrt{a^2 + \left(\frac{au_s}{c} \right)^2 - 2a \left(\frac{au_s}{c} \right) \cos \theta}} \right) \quad 11.4$$

For example, a robot which is moving at speed $u_s = 0.5 \text{ ms}^{-1}$ transmits a single frequency of 100 kHz. There is a plant at an angle of 45° from the direction of travel at a range of 1.3 m. The speed of sound is 343.52 ms^{-1} at 20° C).

The frequency received at the plant f_p is given by Equation 11.1 and is 100103.03 Hz.

The frequency received at the receiver f_r is 100205.95 Hz.

In the case of a CTFM sensor, the signal is typically swept through frequencies from 100 kHz to 50 kHz. For the example given above, the difference frequencies and error in metres are shown in Table 11.4. This shows that the received signal is higher (up to 206 Hz for a signal transmitted at 100 kHz) than that transmitted so the object will appear to be further away than it actually is.

Table 11.4 The effect of Doppler shift for a plant at $\theta = 45^\circ$

Transmitted frequency (Hz)	Frequency at plant (Hz)	Frequency at receiver (Hz)	Difference Frequency (Hz)	Error (mm)
100000	100103	100206	206	6.18
95000	95098	95196	196	5.87
90000	90093	90185	185	5.56
85000	85088	85175	175	5.25
80000	80082	80165	165	4.94
75000	75077	75154	154	4.63
70000	70072	70144	144	4.32
65000	65067	65134	134	4.02
60000	60062	60124	124	3.71
55000	55057	55113	113	3.40
50000	50052	50103	103	3.09

As shown above, the results can be impacted by doppler shift in the signal (0.2 %). The amount of effect is dependent on the angle of the object relative to the angle of the sensor. The largest effect is for a plant which is either directly in front of or behind the sensor. The fact that the doppler shift is the same percentage at all frequencies means that there will be a change in the absolute range to the sensed object. This means that if the features are calculated from this acoustic density profile, there is still good information for plant recognition as the features rely on the relative range information which is preserved. Alternatively, the robot could use a measure of its velocity to calculate the doppler shift and modify the acoustic density profile.

11.4 Multiple objects in the field of audition

If there are surfaces other than those from the plant of interest in the field of insonification then there will be a significant impact on the resulting acoustic density profile. The methods proposed for dealing with these objects is discussed in this section

11.4.1 Separating man made indoor surfaces

In Chapter 3, it was shown that man made surfaces such as walls or table legs produce specular reflections with very high amplitudes compared to those that are reflected from plants. In fact, the amplitude of an echo from a wall is an order of

magnitude larger than that which reflects from a plant (even a plant with many large reflective surfaces).

Since these amplitudes are so high, they can be easily filtered from the resulting acoustic density profile based on amplitude alone. In the case where the surface is not at the same range as the plant surfaces it is simply removed. In the case where the significant amplitude is at the same range as surfaces within the plant then it is difficult to determine how much of the signal is a result of specular reflection from the man made surface and how much is a result of the plant surfaces. This situation of a specular surface appearing within the plant would often occur then the plant is near a piece of furniture, the end of a wall, or in a door frame. In this situation, the echo from the specular surface would be distinct from the rest of the acoustic density profile so only one range cell is corrupted. It can be set to a value which is the average of the range cells on each side of it in the acoustic density profile.

11.4.2 Distinguishing multiple plants

When there are two plants in the field of audition of the sensor, they are difficult to separate when they are at the same range unless they are tracked individually using the information from multiple sensing points. Two plants which are at distinct ranges will be separated by some distance in the acoustic density profile so can be resolved based on the presence of the “gap” in the profile. Depending on the position from which the plants are sensed, may appear as one. In order to resolve this situation, a model of the positions of the plants is required to be updated as the robot moves. This situation is shown in Figure 11.11 - from position *a*, the plants appear as distinctly different objects in the acoustic density profile but from position *b*, they appear as a single entity as they are at the same range. Note that when sensing from position *a*, the second plant may not be detected at all depending on the amount of acoustic shadowing.

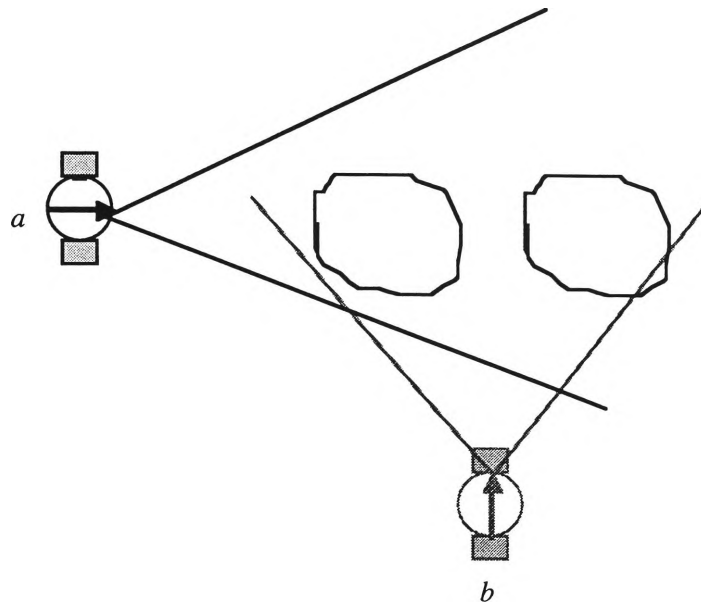


Figure 11.11 Plants are initially perceived as two plants from position *a*, but at position *b* both are at the same range so appear to be one plant

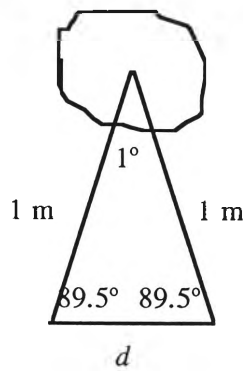
11.5 Some specific mobile sensing scenarios

In this section, some specific mobile robot sensing scenarios are outlined and a description of how this sensor can be implemented is provided.

11.5.1 Static environment, known path, robot senses regularly

In the situation where the environment is fixed, the path is known and the robot is able to sense regularly (that is, in the case where it is can sense at adjacent small displacements so is more than likely not moving at high speed) then the most efficient method of navigation using natural landmarks is to use local correlation of the raw acoustic density profile (Chapter 6).

If the robot is at a distance of say one metre, and it moves more than 17.5 mm (Figure 11.12) between sensing points, techniques such as those outlined in 11.5.3 should be used.



$$\frac{d}{\sin 1^\circ} = \frac{1}{\sin 89.5^\circ}$$

$$d = \frac{1 \sin 1^\circ}{\sin 89.5^\circ} \\ = 0.0175 \text{ metres}$$

Figure 11.12 The distance moved by the robot when the plant is at a range of one metre and the sensing points are separated by one degree

Predetermined paths are used extensively in guidance systems such as those which control the movement of automated vehicles around a steel plant or in assembly work in the car industry. Often these systems navigate with artificial beacons, such as lines painted on a factory floor, or following cables buried in the floor. Beacons are generally used to reduce any errors inherent in dead reckoning. The position of the beacon is known and any misalignment between the sensed position (relative to the beacon) and the currently estimated position on the internal map can be adjusted.

In an office or other indoor environment which remains static, the position of plants can be defined in set locations and these natural landmarks can be used as navigational cues or to re-align the map. Local correlation is extremely fast and is also robust as shown in Chapter 6. This allows the processor time to perform other tasks such as processing information from other sensors or performing high level reasoning. Echo tracking would also be of benefit as the robot moves around the plant and adjacent orientations of the plant are insonified. These techniques are outlined in Chapter 6. This method is fast as it requires very little processing.

Consider the path shown in Figure 11.13. The robot has a set path to follow to its goal and this path is indicated by the broken line in the figure. There are 2 plants shown in the immediate vicinity of the path and they can be used as natural landmarks by the robot. The region over which these plants will be observed by the robot is shown.

When a mobile robot is required to follow a path, there are several ways of giving the robot information about the environment in which it is working. One way is to drive

the robot along the required path and during this process, it senses freely and records information about the environment. As the robot is driven, the sensing system should determine the landmarks which are good as reference cues and the complexity of the resulting path is proportional to the density of the landmarks detected. This allows the robot to build knowledge of the positioning of the surfaces relative to its path in order to reach the goal. Another way is to provide it information about the specific course which it is following similar to the way that you might be given directions about how to find a building in a city.

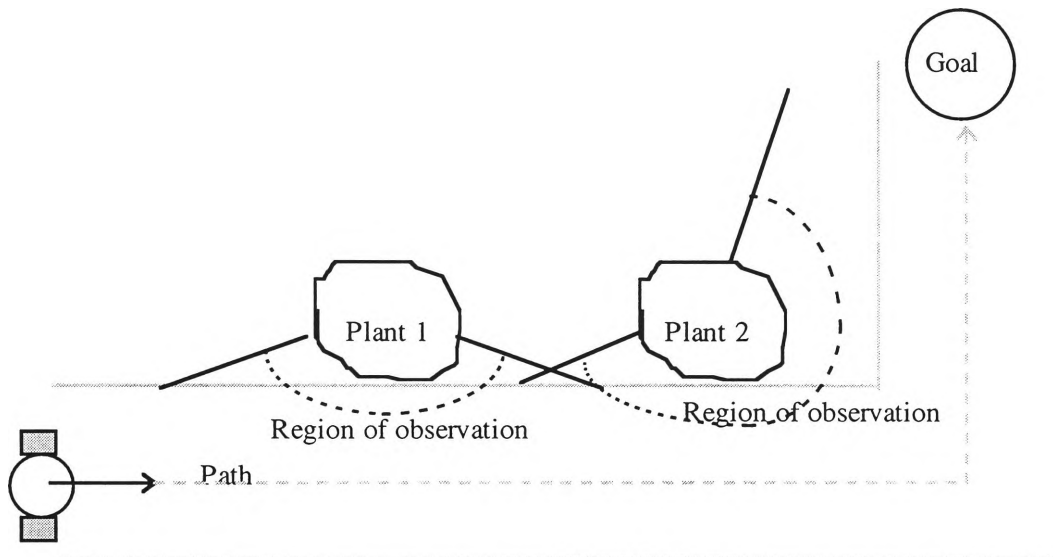


Figure 11.13 A simple path flanked by 2 plants

<p>Move forward. On the left there will be an acoustically symmetric plant This will be followed by another similar plant Turn left after you pass this second plant</p>

Figure 11.14 The high level description of the path

In this first example, the plants have good acoustic symmetry, so the acoustic density profile is relatively stable with change in viewing position of the sensor. The mobile robot is given information about the specific path as a high level description and this is shown in Figure 11.14.

This high level description is interpreted into a series of processing steps and a high level overview of this is shown in Figure 11.15.

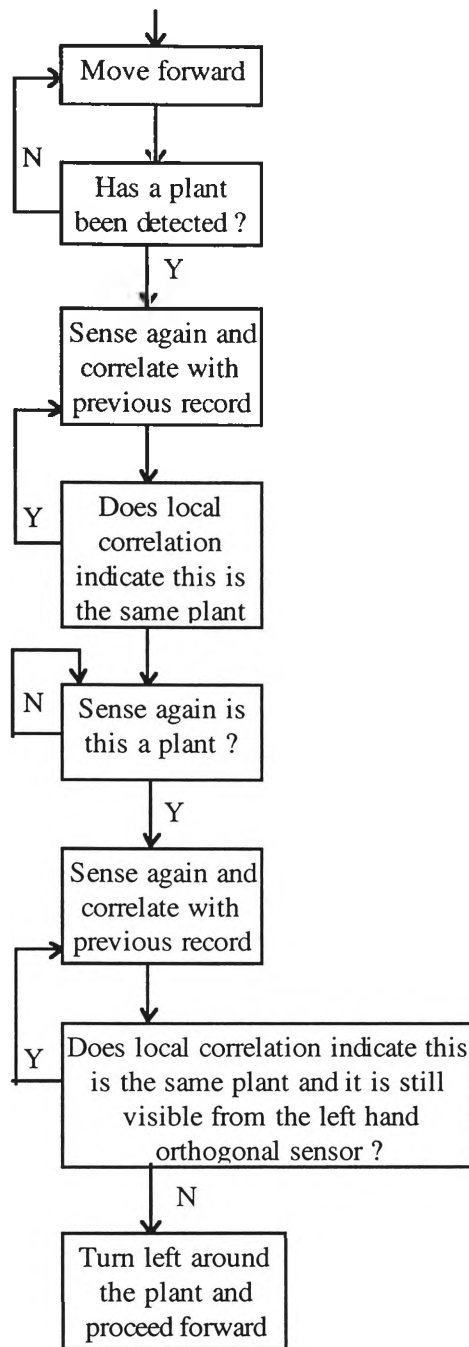


Figure 11.15 The processing chain for the path shown in Figure 11.13

11.5.2 Using the acoustic symmetry of plants for localisation

In Chapter 8, it was shown that some plants have a large variation of features with orientation. A practical system can utilise this property of plants in order to further localise its position (Figure 11.16). The plant shown has three sectors where the acoustic density profile is similar within the sectors but each of the sectors produce an acoustic density profile which is different. There are several ways to segment a plant. One technique is to establish a template when the plant is first sensed based on the features calculated from the

acoustic density profile. This template is used to correlate against adjacent orientation until the correlation drops below 0.7. At this point, a new template is established and associated with the known position of the robot. A similar process is repeated until the entire environment is mapped out and the plants are completely segmented. So, when the robot comes to following its path, it established a template and correlates adjacent orientations until the value drops below 0.7. It can now localise its position and orientation relative to the plant based on the map.

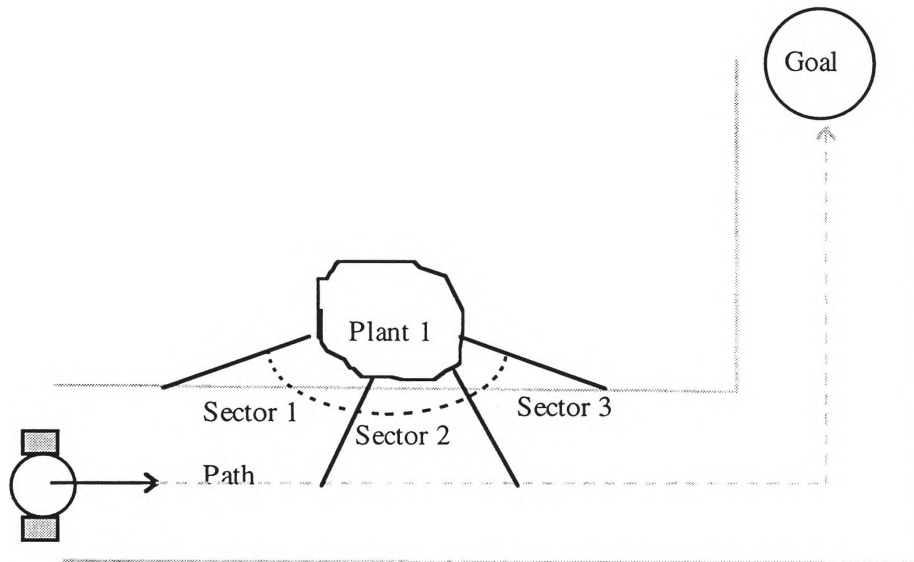


Figure 11.16 A plant which is acoustically different between sectors but similar within sectors

11.5.3 Static environment, known path, robot senses irregularly

When the robot is sensing irregularly, that is if it moves through an angle of more than one degree as is often the case when it is moving at high speed, two signals from completely different orientations may need to be compared. Local correlation is not sufficient for this (see Chapter 8), instead a more sophisticated method is required. Global correlation is not effective unless the relevant information in the acoustic density profile is compared, so features should be calculated from the raw acoustic density profile and these features correlated (see Chapter 9).

11.5.4 Non-static environment and possible unknown path

When the plants are not in set places in the environment, or in the case of an unknown path (or both), a single orientation of a plant is processed with a classifier in order to recognise the plant (see Chapter 10).

11.5.5 Classified as an unknown plant

In a case where a plant is classified as an unknown plant, the features can be interpreted directly to provide information about the physical structure of the plant (see Chapter 9). The plant can also be classified as one of a group of plants using cluster analysis in order to determine the plant type. The robot can also move and sense the plant again to get more information about the plant.

11.6 Improving sensor resolution

A single transmitter / receiver pair provides a sensing area which is conical in shape. The cone is elliptical (with the longest side horizontal) for the transducers used. The FFT effectively divides this cone into a sequence of spherical annuli in the direction of the beam axis, where each annuli is represented by a range cell in the signal. As the annuli have depth, each range cell includes information from all surfaces within the volume of each annulus. If the range cells can be reduced further in volume, the reflections from the individual surfaces can be localised further. This means that there is more information that can be reasoned about and could be the subject of further work.

The sensor described in this thesis produces good results because the signal from the sensor is a relatively coarse grained measure of the acoustic area. This means that it is possible to reason about the physical structure of the plant. However, a sensor which produces more fine grain results will provide more detail about the plant's physical structure. This can be done by either dividing the volume into voxels or by sensing multiple times with a steerable beam. From this fine grain information, the resolution can be reduced with a simple post-processing step to combine the information from adjacent range cells.

Improving this localisation can provide more detailed information about the positioning of the surfaces within the plant. A sensor has been specifically designed for landmark navigation by Ratner & McKerrow [1997] and consists of a 20 element phased array transmitter which is oriented horizontally. Four circular shaped receivers are used to detect the 3D echoes. Their sensor (Figure 11.7) has a horizontal beam width of 3° and a vertical beam angle of 30° . This results in the environment being insonified with a vertical sheet of ultrasonic energy that can be steered both electronically and mechanically.

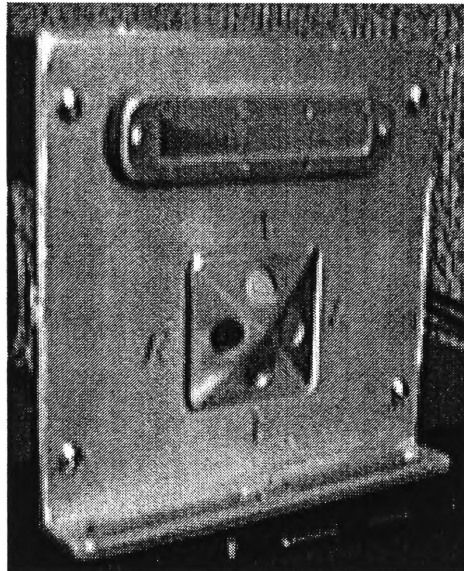


Figure 11.17 The sensor from Ratner & McKerrow [1997]

The sensor arrangement shown in Figure 11.7 results in range cells which are very narrow but tall. A sensor which will localise the surfaces within a plant more accurately will need to have a range cell which is small in both the vertical and horizontal direction and this is modelled in Figure 11.18. Figure 11.19 shows a steerable sensor set up which results in very small range cells. This sensor is designed for tracking and will transmit both a wide beam (central circular transducer) and a narrow beam (mills cross).

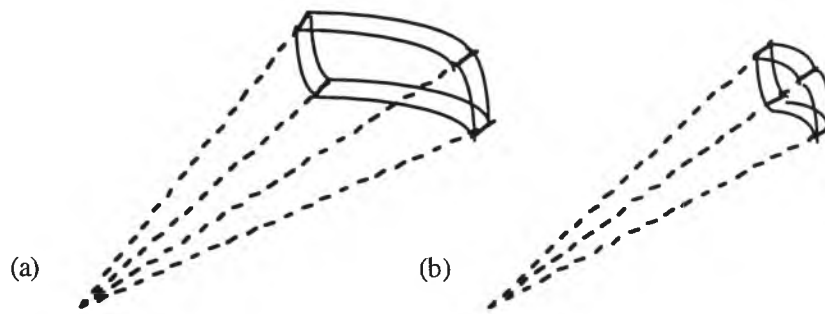


Figure 11.18 Model of a single range cell for (a) the binaural sensor used in this thesis and (b) a higher resolution sensor

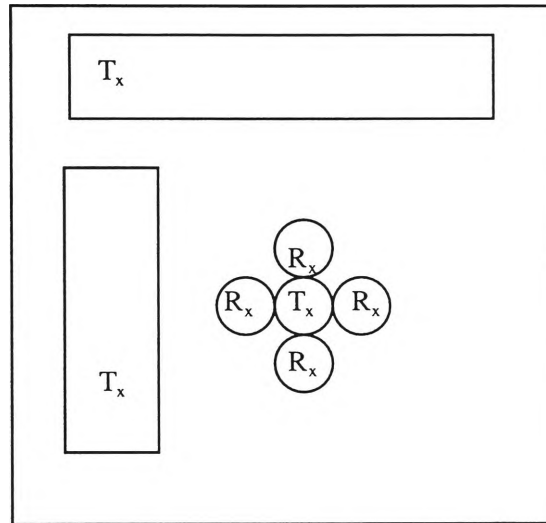


Figure 11.19 A sensing arrangement which produces a narrow beam. The large transmitters ensonify the environment and echoes are detected by the four circular receivers

11.7 Summary

1. The processing of data from the sensor is very fast compared to the time that it takes to acquire the data which leaves the processor available for other processing;
2. A system which uses multiple sensors around the robot is more practical than a system that uses a single sensor;
3. Plants should be tracked between one sense point and another;
4. When a robot is moving at high speed, the Doppler affect causes changes in the wave pattern particularly for sensors which point either directly in line with the direction of travel;
5. Reflections from objects other than plants can be removed from the acoustic density profile; and

6. Different sensing situations call for different approaches.

12. Conclusion

The key concept of this thesis is the notion that the frequency spectra can be modelled as an acoustic density profile. Each range line of the acoustic density profile represents the reflective properties of the surfaces at that particular range. The acoustic density profile can then be interpreted directly (Chapter 9) in order to determine the physical structure of the plant.

This results in a detailed analysis of the signal in the other chapters, including :

1. the physics of the system;
2. the output of the system for different types of objects;
3. a proof of concept that plants can be differentiated;
4. an analysis of how the signal changes depending on the orientation of the plant;
5. a set of measures (features) which characterise plants;
6. an inverse transformation between the signal and the physical structure of the plants;
7. a classifier which can accurately differentiate plant specimens; and
8. a set of implementation recommendations for a mobile robot.

This chapter contains a summary of all of the results of this thesis. This includes the theory of acoustic density profile information content (Section 12.1); a review of how that information can be used in a practical system (Section 12.4.8); recommendations for using this thesis as a basis for implementation and a discussion of further work arising from this thesis (Section 12.6).

12.1 A basis for the interpretation of CTFM sensor data

In this thesis, many facets of the data produced by a CTFM ultrasonic system have been investigated independently. This section consolidates these facets into one cohesive whole. The information available is recapped in point form and conclusions are drawn about the information content and its relationship to using plants as natural landmarks for

mobile robot navigation. This Chapter can also serve as a quick reference for a system designer.

12.2 Acoustic density profile

The principal of operation of the sensor system is, a FM signal is transmitted and the echoes are detected by a passive receiver. A typical system is swept from 100 down to 50 kHz. The received echo is then demodulated against a copy of the transmitted signal and filtered, resulting in a signal which is in the audible frequency range and is between 0 and 5 kHz. In this processed signal, the frequency (or pitch) is directly proportional to the range to the surface which is within the field of insonification of the sensor. The signal is then transformed into the frequency domain using an FFT and the individual frequency lines in the spectra then represent the reflective properties of the surfaces at different ranges. The amplitude at each individual frequency line represents the reflective properties of the surfaces which are at the range represented by the particular frequency. For the system described in this thesis, each frequency line represents a range difference of 3.44 mm.

Since each cell in the frequency spectra is a measure of the acoustic density of the surfaces at the particular range, the frequency spectra can be modelled as the acoustic density profile of the ensonified target. Each of the frequency lines is thus interpreted as a range cell, where the range cell represents the reflective properties of the surfaces within the range resolution of the sensor (in this case 3.44 mm). Each range cell is a measure of the acoustic area at that range and hence the entire acoustic density profile measures the acoustic area of the entire scene. The notion of the acoustic density profile is fundamental to the process of interpreting the signal in order to reason about the scene which is presented to the sensor (Chapter 3).

12.3 Sensor facilities

In this section, the sensor highlights and constraints are illustrated in point form.

Highlights

1. Range information can be extracted directly from the acoustic density profile. Both absolute and relative range information is available directly and can be decoupled from each other easily. The absolute range information can be extracted as a direct range to the plant. The relative range information is the key to the physical structure of the plant however, and can be referenced to a standard range and can be either interpreted directly or used as an input to a classifier;
2. Information in the acoustic density profile is less complex than with vision systems as it is a projection of a three dimensional scene onto a single dimension (instead of a projection onto two dimensions). The one dimensional nature of the data means that less processing is required as there is inherently less data;
3. The information can be processed rapidly. The speed of processing is limited by the speed of the FFT which itself is limited by the sweep time. This means that during each sweep, the processor is available to perform other processing tasks such as fusing information from multiple sensors, or performing high level reasoning tasks such as is required for mobile robot navigation;
4. This sensor has no need for special lighting conditions. Most successful vision systems need to control the light source in some way as small lighting differences affect the results considerably. These systems do this by either operating during certain parts of the day, or by having their own light source. The lack of lighting requirements of acoustic sensors means that they are suitable for not only working in areas of inconsistent light but areas of reduced visibility, poor weather conditions or in the complete absence of light;
5. Resistance to ultrasonic noise is provided by the fact that CTFM has a very specific frequency swept signature which does not commonly occur in nature or in background machine noise;
6. Low cost. The system is cheap to implement as high quality optical engineering and complex signal processing is not required;

7. Low power requirements mean that it can be easily mounted on a mobile robot; and
8. The sensor has reasonable range resolution (3.44 mm).

Constraints

1. Poor angular resolution from a single sensor. For a system which sweeps from 100 to 50 kHz, the average beam width is 55 degrees in the horizontal plane and 18.5 degrees in the vertical plane. Systems which require better directivity should use an alternate sensor arrangement in order to localise the position of surfaces more accurately (Chapter 11);
2. Signal content is not intuitively obvious because we do not see with sound;
3. Ultrasonic sensing suffers from the specularity problem where non normal surfaces will return limited signal;
4. The overall speed of capturing the signal is constrained by the speed of sound in air;
5. Air movement can cause amplitude variation in the received signal; and

12.4 Data interpretation

In this study, the following major aspects of research can be highlighted :

1. A theory of how plant foliage affects the acoustic density profile (Chapter 3 and Chapter 9);
2. A list of features which have been shown to discriminate plants (Chapter 8);
3. Information about how symmetric different plants are (Chapter 8);
4. A classifier which uses the features to identify individual plants (Chapter 10); and
5. Clustering of plants into similar groups and the characteristics of those groups (Chapter 10 and Appendix D).

A brief overview of each of the areas of study is presented in the following sections.

12.4.1 Effects of plant foliage

The most important information contained in the signal is the spatial position of surfaces within the plant. All of the following aspects are important influences on the acoustic density profile :

1. Size, orientation and number of leaves;
2. The spatial positioning of leaves within the plant;
3. The amount of shadowing caused by leaves and other plant structures; and
4. The absolute range to the plant.

12.4.1.1 Size, Orientation and number of leaves

The size and orientation of the leaves affect the amplitude of the range cell at a particular range. The following effects of the leaf size and orientations are defined :

1. Larger leaves will reflect more signal and produce a stronger return, hence a higher amplitude;
2. The signal is however, dependent on the orientation of the leaf surfaces. Those which have no parts of the leaf normal to the receiver will reflect the signal away from the receiver and it may not be detected at all (this is irrespective of the size of the leaf). Leaves are generally bent surfaces, so reflect acoustic energy over a wide solid angle and hence can be detected from several orientations. In general, a leaf with no part of its surface normal to the sensor will reflect most of the signal away from the receiver but there may still be some diffuse reflection. This is valid for three dimensions as the signal may be reflected not only to the left or right of the receiver but also below or over the top.
3. Multiple surfaces at a given range from the sensor will add to the return amplitude. Each range cell may consist of one or more specular surfaces; one or more diffuse

surfaces; or a combination of both and all will combine to produce an amplitude corresponding to their range.

4. The more leaves there are on a plant, the more signal will be returned (depending on their size and orientation).

12.4.1.2 Positioning of leaves within the specimen

1. Positioning of leaves determines the distribution of amplitudes throughout the acoustic density profile;
2. If there is no shadowing then leaves spread throughout the plant will reflect signal and the acoustic density profile will show the leaves spread throughout a width of range cells.
3. When leaves are gathered around the extremities of the plant, then the returns will be mainly concentrated around the front half of the plant. Signal will still be present through the first half of the range profile as the leaves at the side of the plant will return some signal.

12.4.1.3 Shadowing

1. Shadowing occurs when leaves are obscured by other leaves between them and the sensor. This prevents the signal reaching some (or all) of the leaves within the plant. The foliage may be hidden by the foliage nearer the sensor.
2. In the extreme case, the internal structure of the plant will be completely invisible to the sensor.

12.4.1.4 Absolute range to the plant

1. There is a known response based on the absolute range to the plant. Relative information is constant since the range resolution is constant. Individual acoustic density profiles can be referenced to a standard place on the calibration curve (Chapter 3). The calibration curve is specific to the sensor and is a measure of the

change in amplitude with range for some standard object. Hence the absolute range can be used independently and is completely decoupled from the relative range information which can be used for plant recognition.

12.4.1.5 Orientation of the plant

1. Small changes in orientation can result in a significant change in the acoustic density profile;
2. With sparse plants, this effect is more significant as leaves come in and out of view.

12.4.2 Correlation

1. Local correlation can be used to compare adjacent orientations of a plant to determine how much the acoustic density profile changes from one orientation to the next (Chapter 6).
2. Global correlation proves to be poor when used with the raw acoustic density profile (Chapter 7).
3. Features calculated from the raw spectra are well correlated using global correlation and this is improved by using template correlation (Chapter 8).
4. Plants which exhibit symmetry are easier to classify as each acoustic density profile from any particular orientation will be representative of the entire population;
5. This can be used to select the best plants which can be used in a practical application which requires identification of specific plants.

12.4.3 Features

A set of features which capture the information important for differentiating plants out of the population of 100 have been developed. Feature reduction pruned the set to 19 key

features listed below. The features are measures of the amplitude and spread of the acoustic density profile.

Feature	Description
no_above_threshold1 - 9	<p>Thresholds.</p> <p>These 10 features are the number of lines in the acoustic density profile above a set threshold t mV where $t = 59 * m / 10000, 78 * m / 10000, 98 * m / 10000, 117 * m / 10000, 156 * m / 10000, 195 * m / 10000, 295 * m / 10000, 300 * m / 10000, 490 * m / 10000$ and $580 * m / 10000$ mV where m is the calibration measure = 100 mV for the sensors used in this research. These thresholds were chosen based on approximately equal intervals. Full details of the function used to reference the acoustic density profile for range is given in Chapter 5.</p> <p>These features give an indication of the specularity of the surfaces, the number of surfaces, the orientation of the surfaces, the size of the individual surfaces and the depth of the plant. Different threshold levels serve to differentiate plants with different spreads of those properties.</p>
sum_of_density_profile	This is the sum of all of the range cells in the acoustic density profile and indicates the properties over the entire plant.
variance_range, stdev_range, mean_abs_dev_range, coeff_of_var_range	These features measure the variation of the detected reflections from the central point of the acoustic density profile. It is an indicator of the spread of ranges over which a signal is received.
front_to_peak_dist	This is the distance from the first detectable surface to the surface with the highest amplitude. This indicates the rate at which the foliage builds up over subsequent range cells
length_of_density_profile	This is a measure of the range over which reflections are detected. It gives the minimum depth of the plant.
range_50_acoustic_area	The range line from the first detected reflecting surface to the point where 75% of the sum of the acoustic area is accumulated
no_of_major_peaks1, no_of_major_peaks2	A range line is a major peak if its amplitude is greater than $195/m$ mV and 5 of the range lines (17.2 mm) on each side of it are less than it. It is a count of range cells which have reflections significantly stronger than those around it and is a measure of the grouping of leaves. Note that <code>no_of_major_peaks2</code> is the same except that the amplitude has to be greater than $156/m$ mV to be counted.

12.4.4 Mapping of features to plant structure

1. The features (and hence the acoustic density profile) can be mapped onto the physical structure of plants. This completes the inverse transformation from signal to plant physical structure.

2. `length_of_density_profile` is calculated as the distance between the first range line of the plant and the last range line of the plant. If there are surfaces at both extremities of the plant then it is a measure of how deep the plant is. In general however, it is a measure of the minimum depth of the plant.
3. Threshold features `no_above_threshold1` - 9 measure the number of range cells in the acoustic density profile which are above different threshold levels. They can be normalised by `length_of_density_profile` and directly provide a measure of both the density of the foliage and the size of the reflective surfaces within the plant. A set of rules has been developed which classify a set of features (and hence the acoustic density profile) as either dense or sparse and also, having either large reflecting surfaces or small reflecting surfaces.
4. `sum_of_density_profile` is the sum of all of the range lines between the start and the end of the plant. It is directly proportional to the sum of the surfaces within the region of insonification of the sensor so directly gives a measure of the total reflective surfaces in the form of the total acoustic area. In general, plants with more foliage produce a larger value for this feature so directly provides a measure of the size of the plant or when it is normalised by the depth of the plant (`length_of_density_profile`) is a measure of the size of the reflecting surfaces.

12.4.5 Classification

1. A classifier can differentiate a plant from a group of plants when the number of plants is small. Once the sample size becomes larger than 10 plants then there is more chance of two particular plants being too similar so are hard to differentiate.
2. Selection of the best features significantly enhances the ability of a classifier to classify plants correctly.
3. When the features are used as input to the classifier, better results are achieved than when using the acoustic density profile directly.

12.4.6 Clustering

1. Plants can be grouped into clusters which have similar acoustic reflections.
2. This can be used to determine the plants which are similar to each other in acoustically. Plants which cluster together are hard to separate with a classifier while those in separate clusters are much easier

12.4.7 Implementation issues

1. The time required to calculate features from the signal is very low compared to the time that it takes to sweep through a one octave range.
2. A moving platform will need to build a model of the position of a plant in order to track it as it moves past.
3. Doppler shift has some effect on the received signal. The effect can be minimised by avoiding the direct interpretation of the signal from plants which are either directly in front of behind the moving platform.

12.4.8 Summary

All of this information combined provides a comprehensive information base for interpreting acoustic density profiles. Given a particular plant specimen, a good model of its acoustic density profile can be developed. Particularly if the acoustic density profile from more than one orientation is available.

Plants can be differentiated using the range information from a CTFM ultrasonic sensing system. The range information not only provides the distance to the plant but also directly provides information about the positioning of surfaces within the plant and the depth of the plant. Other information is present in the signal such as the size of the surfaces, their orientation and their texture.

The acoustic density profile can vary significantly from one orientation of a plant to the next but contains the same basic information. A set of calculated features have been

optimised and they characterise the acoustic density profile more consistently through rotation than the basic range information.

A classifier can differentiate plants based on the feature data. It can do so with a high degree of accuracy (>95%) for up to 10 plants, provided that the plants are relatively consistent through rotation and are different in their acoustic density profile.

If a plant cannot be differentiated from a population of plants based on its acoustic density profile then some basic information about the plant can still be extracted from the acoustic density profile.

For a practical implementation, the plants (or similarly complex objects) can be chosen (or manufactured) so that their acoustic density profiles are different to each other and a very efficient and robust system can be developed.

Plant acoustic density profiles can be grouped into clusters of similar plants using statistical techniques. These clusters group plants which are similar in terms of their acoustic density profiles. These plants however may look different physically but reflect the signal in similar ways.

12.5 Fitness for purpose

The CTFM system with the associated software, is ideal for navigating a mobile robot platform. One of the goals of this thesis is to explore and define the limitations of the system. An application can then be designed to within these boundaries, and even exploit them in order to achieve a goal.

A navigation task may involve moving from start point *A*, to destination point *B* along a series of outdoor paths. As shown in Chapter 10, a highly accurate classifier can be developed that can distinguish a group of different plants independent of their orientation but is less accurate if the group becomes large. In order to classify a larger number of specimens, the environment is decomposed into smaller, more manageable segments. So even though a path may be long, it can be divided into smaller more manageable segments and hence a classifier is operating within a much smaller domain, that is, a segment of the path. Paths are also often bounded by groups of the same

species, so a function such as counting the number of a particular species can assist the navigation.

Navigation clues may also be gathered using additional sensors and fused with the information from a CTFM sensor in order to improve reliability. For example an inclinometer may measure a change in the slope of the path, so this section of path can be treated as a segment of the path with its own characteristics, for example it may have 2 occurrences of species x on the left of the platform and 1 occurrence of species y on the right hand side.

This thesis also shows that some plants are very difficult to classify and change significantly through rotation so this type of plant would be useless as a landmark, so can be simply ignored. For example, species z may be on segment of path but may be difficult to identify so it is ignored by the high level navigation module.

The CTFM sensor makes its best contribution in areas where the overall structure of the plant is required. For example, a robot that is working within an environment that is difficult to segment easily, such as a nursery, will have so many plant types that it is impossible to build a classifier to recognise them all to high accuracy. In this environment, the localisation is done using the overall geometric structure of the plants instead of isolating any particular species.

12.6 Future work

A more sophisticated system is required to differentiate plants more finely. A single sensing point has low angular resolution. A second sensing point increases the resolution of the system to some extent. A third sensing point would result in a highly localised sensing area and hence more can be deduced about the plant. This is a natural enhancement of the work

Techniques for implementing the system for different application areas were discussed in Chapter 11.

If the leaves are moving in response to vibrations or wind in the case of outdoors then echo tracking of multiple acoustic density profiles can be performed in order to correlate the acoustic density profiles temporally.

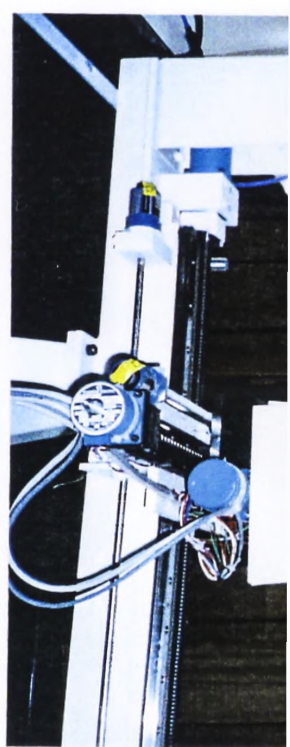
1. movement of leaves changes the acoustic density profile.
2. air motion changes time of flight depending on the direction of the wind.

12.7 Conclusion

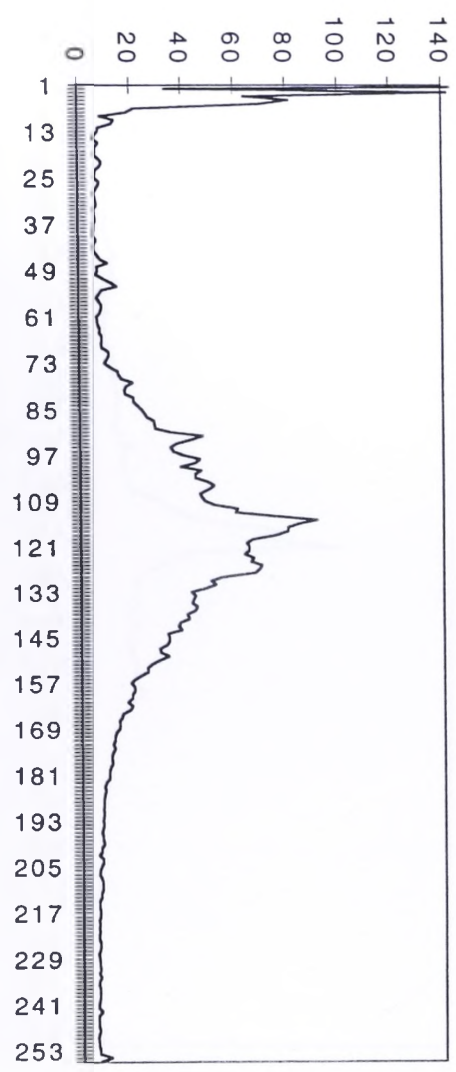
This thesis describes a sensing system which can be used for plant classification. The output of the sensor can be interpreted using the acoustic density profile model. The output has been studied in detail and the inverse transform from signal to plant physical structure has been defined.

A classifier can be trained to look at a set of plants and discriminate between them. For this particular problem, this technique is insufficient, that is, plants grow and there is also a large variety of possible plants to recognise. The techniques developed in this thesis overcome the problems by identifying the primary structural characteristics of the plant from the acoustic density profile.


 2cm x 0.9cm



Binoniaceae



A. Appendix Sample plant portfolios

Biagnoñaceae

Her - Feneis

23/7/196 14 00

T : 24.4°

H 33.5%

height : 31cm

width 40cm

any small opposite leaves



Sarcomelicope simplicifolia

Rutaceae

Sarco-simpli

17/96 13:30

T: 24.1°

H: 36.9%

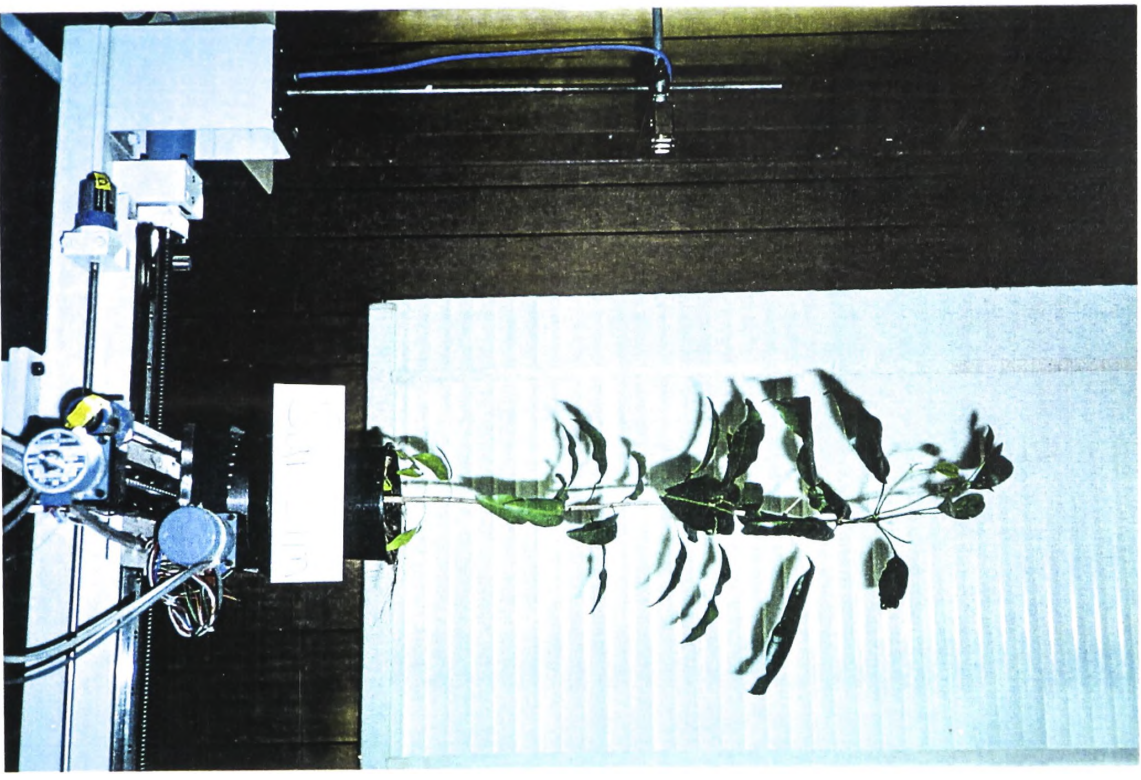
height 70cm

width 20cm

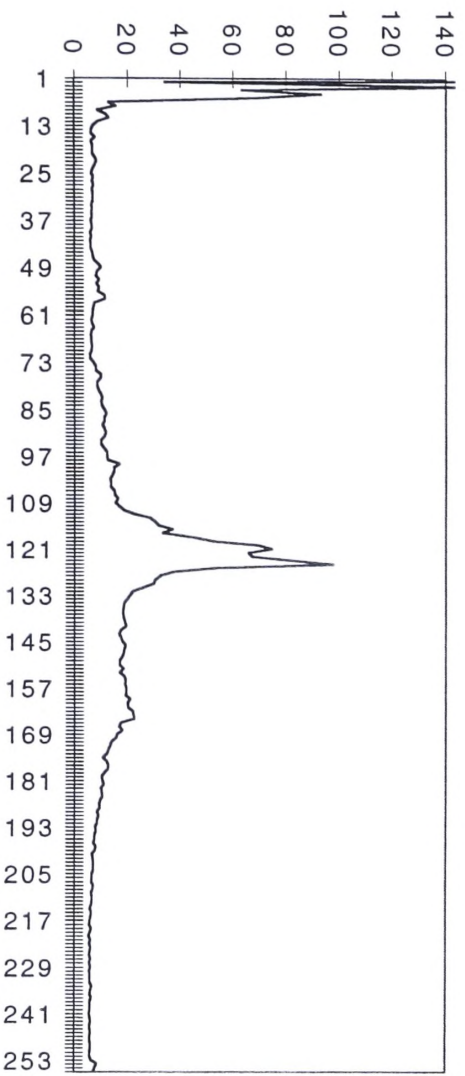
leaves opposite, simple
holate

re-elliptic or obovate

11cm x 5cm



Sarcomelicope simplicifolia - Rutace



Polyscias australiana

Araliaceae

Polyscias aust

12/7/96 15:07

T: 24.9°

H: 33-1%

height: 60 cm

width: 50 cm

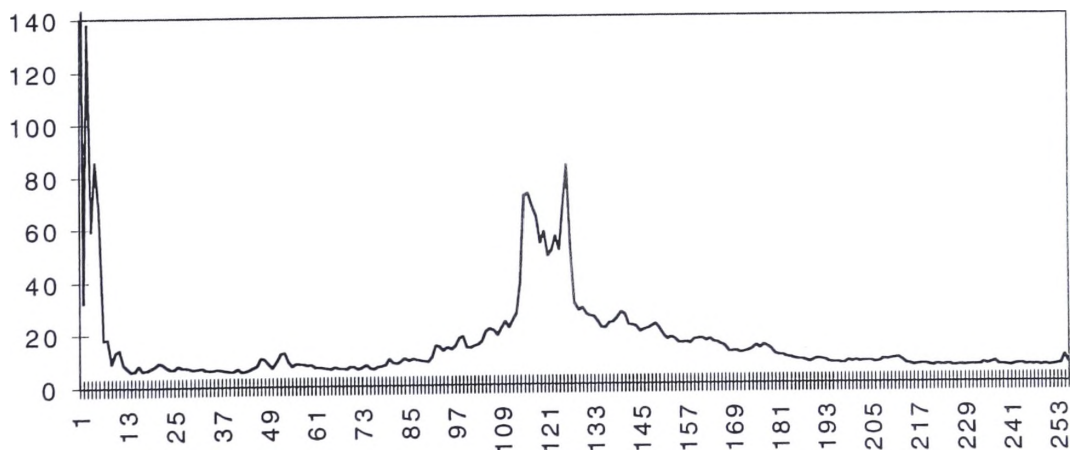
large horizontal leaves

opposite

upto 8 cm x 5 cm



***Polyscias australiana* - Araliaceae**



B. Appendix Echo tracking source code

B.1 Calculate echo range possibility

The function below is used to calculate the range over which surfaces may appear from adjacent orientations of the plant. It is discussed in detail in Chapter 6.

```
/*
 *      Calc_echo_range_possibility
 *
 * This function calculates the threshold for determining the range over which a
 * surface could be visible from one orientation to the next. The object is rotated
 * around its axis (or the sensing point is moved around the object). This function
 * is specific to the following two situations :
 *
 * 1. In the case of the object being rotated
 *      the range to the axis of rotation is fixed and the object is moved
 *      through a fixed angle
 * 2. In the case of the sensing point being moved
 *      the range to the axis of the object is held constant and moved through
 *      some angle
 *
 * The range spectrum is captured at a set orientation. The object is sensed
 * using a sensor with a fixed beam angle (passed to this function). The object
 * is then rotated by a certain angle (orientation_change - which is in degrees)
 * and a new spectrum is captured. The echoes present in the first spectrum may
 * be present in the second spectrum but may be offset within a certain threshold
 * which is calculated. The echo can be within a certain range of the original
 * echo given by the following equations :
 *      min_range = SQRT
 *      (
 *          2 * range_to_object_axis**2 * (1 - Cos (orientation change)) +
 *          range_to_the_sensed_surface**2 -
 *          (
 *              2 *
 *              SQRT
 *              (
 *                  2*range_to_object_axis**2 * (1-Cos(orientation change))*
 *                  range_to_the_sensed_surface *
 *                  Cos
 *                  (
 *                      (180 - orientation_change) / 2 -
 *                      beam_angle / 2
 *                  )
 *              )
 *          )
 *      )
 *      max_range = SQRT
 *      (
 *          2 * range_to_object_axis**2 * (1 - Cos (orientation change)) +
 *          range_to_the_sensed_surface**2 -
 *          (
 *              2 *
 *              SQRT
 *              (
 *                  2*range_to_object_axis**2 * (1-Cos(orientation change)) *
 *                  range_to_the_sensed_surface *
 *                  Cos
 *                  (
 *                      (180 - orientation_change) / 2 -
 *                      beam_angle / 2
 *                  )
 *              )
 *          )
 *      )
 *
 * The difference in this range (ie. max_range - min_range) gives the range over
 * which the echo in the first spectrum could be in the second spectrum centred at
 * the current point. This is a value in metres. The equations above were derived
 * using the geometry of the physical set up.
 *
 * Parameters:
```

```

*
* double const surface_range,          the range to the surface under consideration
* double const axis_range,            the range to the axis of rotation of the plant
* double const orientation_chang the change in orientation from the previous sample
*                                   to the next sample (in degrees)
* double const beam_angle             the beam angle of the sensor being used
*
* Returns :
*
* threshold this is the number of FFT lines each side of the passed surface range
*
*/
double Calc_echo_range_possibility
(
    double const surface_range, /* the range to the surface under consideration */
    double const axis_range, /* the range to the axis of rotation of the plant */
    double const orientation_change, /* the change in orientation from the
previous                                   * sample to the next sample (in degrees)
                                         */
    double const beam_angle /* The beam angle of the sensor being used */
)
{
    double const pi = 3.14159265;

    double r_min, /* the minimum possible range in metres
*/
    r_max, /* the maximum possible range in metres
*/
    cos_degrees, /* an intermediate calculation for the
cos                * of the orientation change
                  */
    rsq1_cos, /* an intermediate calculation for d**2
*/
    gamma_angle, /* intermediate calculation */
    range_possibility; /* the possible range over which the surface
                        * could be
                        */

    /*
    * calculate some intermediate values for performance reasons
    */
    cos_degrees = cos(orientation_change * pi / 180);
    rsq1_cos = 2 * pow(axis_range,2) * (1 - cos_degrees);
    gamma_angle = (180 - orientation_change) / 2.0;

    /*
    * calculate the min and max range
    */
    r_min = sqrt
    (
        rsq1_cos +
        pow(surface_range,2) -
        (
            2 *
            sqrt(rsq1_cos) *
            surface_range *
            cos((gamma_angle - (beam_angle / 2)) * pi / 180)
        )
    );
    r_max = sqrt
    (
        rsq1_cos +
        pow(surface_range,2) -
        (
            2 *
            sqrt(rsq1_cos) *
            surface_range *
            cos((gamma_angle + (beam_angle / 2)) * pi / 180)
        )
    );
    range_possibility = r_max - r_min;
    return range_possibility;
} /* Calc_echo_range_possibility */

```

B.2 Echo tracking

The function below is used for tracking echoes from surfaces over adjacent orientations of the plant.

```

/*
 * Echo_tracking
 *
 * This function tracks signal returns between one orientation and the next
 * by adjusting for the geometry. The sensor is fixed with the plant at a
 * certain distance. The spectrum is captured before the plant is rotated by
 * fixed angle. Once the plant is at the new orientation, the surfaces which
 * produced reflections at the previous orientation may still be present in
 * the spectrum but offset by 1 or a number of frequency lines. This amount
 * by which they are offset can be set by passing the movement threshold
 * parameter or calculated using function Calc_movement_threshold.
 *
 * Parameters:
 *
 * double const base_range      the range to the first fft line in the arrays
 * double const axis_range      the range to the axis of the plant
 * double const orientation_change  than angle in degrees through which the
plant has been rotated between array1 and array2
 * double const beam_angle      the beam angle of the sensor
 * double const fft_range_resolution the resolution of an individual fft line
 * double const *array1         the data from the first orientation.
 * double *array2               the data from the second orientation.
 * int const array_length        the length of the arrays of data.
 * int movement_threshold        the amount of FFT lines which the features can
move or 0 in which case function
Calc_movement_threshold will be called to
calculate the threshold.
 *
 * Updates :
 *
 * array2      this is modified so that it geometrically adjusts for the change in
orientation.
 */
void Echo_tracking
(
    double const base_range, /* the range to the first fft line in the arrays */
    double const axis_range, /* the range to the axis of the plant */
    double const orientation_change, /* the angle in degrees through which the
    * plant has been rotated between array1 and
    * array2 */
    double const beam_angle, /* the beam angle of the sensor */
    double const fft_range_resolution, /* the resolution of an individual fft
    * line */
    double const *array1, /* the data from the first orientation */
    double *array2, /* the data from the second orientation
 */
    int const array_length, /* the length of the arrays of data */
    int movement_threshold /* the amount of FFT lines which the
    * features can move or 0 to calculate */
)
{
    int i, j, /* loop counters */
    descending_indexes[kMaxDataItems], /* the indexes in descending order */
    max_pos, /* used for the sort */
    index, /* the index of the number we are
    * working with */
    length_value_array, /* the length of the value array which
    * is based on the movement threshold */
    calculate_movement_threshold; /* whether or not the movement
    * threshold needs to be calculated */
    double descending_array[kMaxDataItems], /* to hold the descending values */
    max_value, /* used for the sort */
    value_array[kMaxDataItems], /* holds values for feat swapping */
    possible_range; /* the range over which the surface
    * should be */

    /* check some of the parameters passed in */
    if(array_length <= 0)
        return;
    if((array1 == NULL) || (array2 == NULL))
        return;

    if(movement_threshold == 0)
        calculate_movement_threshold = true;
    else
        calculate_movement_threshold = false;

    /*
    * copy array1 into the descending array so that it can be sorted and also
    * initialise the array of indexes
    */
    Copy_array(array1, descending_array, array_length);
    for(i = 0; i < array_length; i++)
        descending_indexes[i] = i;

```

```

/*
 * now do a sort to get an array which has the indexes of the original
 * array1 in order of descending magnitude. (selection sort)
 */
for(i = 0; i < array_length; i++)
{
    max_value = descending_array[i];
    max_pos = i;

    for(j = i; j < array_length; j++)
    {
        if(descending_array[j] > max_value)
        {
            max_value = descending_array[j];
            max_pos = j;
        }
    }
    Swap_values(&descending_array[i], &descending_array[max_pos]);
    Swap_values_int(&descending_indexes[i], &descending_indexes[max_pos]);
}

/*
 * now, we can go through and massage the records so that some of the echoes
 * line up. This is based on the movement threshold which is calculated
 */

/* calculate the length of the difference array */
length_value_array = (movement_threshold * 2) + 1;

/*
 * go through array1 working from the highest amplitude first. Determine if
 * any of the data in array2 will be moved to line up with these amplitudes
 * in array1
 */
for(i = 0; i < array_length; i++)
{
    index = descending_indexes[i];
    /*
     * re-calc the movement threshold for the surface at this range
     * if required
     */
    if(calculate_movement_threshold)
    {
        possible_range = Calc_echo_range_possibility
            (
                base_range+((i-1)
fft_range_resolution),
                axis_range,
                orientation_change,
                beam_angle
            );
        movement_threshold=(possible_range/fft_range_resolution+0.5)/2;
        length_value_array = (movement_threshold * 2) + 1;
    }

    /* initialise the difference_array */
    Initialise_array(value_array, 0, array_length);
    /*
     * Calculate the difference between this element in array1 and the
     * movement_threshold elements each side of it.
     */
    for(j = 0; j < length_value_array; j++)
    {
        /*
         * are we within the bounds of array2
         * is it off the bottom or the top of array2
         */
        if
        (
            (j + index - movement_threshold) < 0 ||
            (j + index - movement_threshold) >= array_length
        )
            value_array[j] = kASmallValue;
        else
        {
            /*
             * Now we should check to see if this index is adjacent
             * to a higher value which has ALREADY been checked. We
             * cant take a value out from under the other one
             */
            if(array1[j+index-movement_threshold] > array1[index])
                value_array[j] = kASmallValue;
            else
                /* copy the value over into value_array */
                value_array[j]=array2[j+index - movement_threshold];
        }
    }
}

```



```

    }

    /*
    * now search the value array for the maximum value and swap the
    * element at that index in array2 with the element in the current
    * index.
    */
    max_pos = Position_maximum(value_array, length_value_array);

    /*
    * we have now calculated that the item with the largest value is in
    * position max_pos in the difference_array, or
    * index - movement_threshold - 1 + max_pos
    */

    /* check to see whether the item needs to be swapped */
    if
    (
        (index != (max_pos + (index - movement_threshold))) &&
        (value_array[max_pos] > kASmallValue)
    )
    {
        Swap_values
        (
            &array2[index],
            &array2[max_pos + (index - movement_threshold)]
        );
    }
}
} /* Echo_tracking */

```

C. Appendix - code segments

C.1 Background

The code in this section is based on 3 simple classes and is written in C++. The Array class is a class which is used to create array objects. It has code which performs various mathematical operations on the array. The CTFM_data class holds the raw acoustic density profile and the Feature_data class is the one which calculates the features. The header files are given below. In this Appendix, the header files for the classes is given along with some code segments which are referenced in the text.

C.2 Array class

The array class is a template class. It is passed the `element_type` when it is declared in a function. This allows arrays of any data type to be created. The format of the declaration is :

```
template <class element_type>
class Array
{
public:
    ..
    ..
private:
    ..
    ..
}
```

The class offers the following services :

```
//constructor initialise the length and allocate memory
Array(int len)

//constructor where an array is modelled on another
Array(const Array<element_type>& model)

// destructor
~Array()

// Zero the entire array
void Zero()

//return the length of the array
```

```

int Length() const

//display the entire contents of the array
void Display(ostream& os = cout) const

//read a record from a file into the array
int Read_record(istream &infile)

//write a record out to the file in text format. If the passed
//parameter for the end of record != 1 then dont write the endln
//character. An alternative write record function allows items_used to be
//passed and this contains an element for each item in the array and an
//indicator of true or false as to whether the element
//should be written to the file
int Write_record
(
    ostream &outfile,
    const int end_of_record = 1,
    const char delimiter = '\t'
) const
int Write_record
(
    ostream &outfile,
    int items_used[],
    const int end_of_record = 1 ,
    const char delimiter = '\t'
) const

//set a particular item to a value
void Set(const int element_no, const element_type value)

//get a particular item
element_type Get(const int element_no) const

// return the position of the maximum value
int Pos_max() const

// return the position of the maximum value
int Pos_max(int start, int end) const

// return the maximum value in the array. the position of the
// maximum value between 2 indexes can also be found
element_type Max_val() const
element_type Max_val(int start,int end) const

// return the position of the minimum value. the position of the
// minimum value between 2 indexes can also be found or the
//position of the minimum value from a certain offset
int Pos_min() const
int Pos_min(const int start) const
int Pos_min(const int start_index, const int end_index) const

// return the minimum value. the minimum value between 2
// indexes can also be found or minimum value from a certain offset
element_type Min_val() const
element_type Min_val(int start) const
element_type Min_val(int start, int end) const

// multiply all of the elements of the array together and return the result
element_type Mult_through() const

//selection sort the array and return the sorted array
void SelectionSort()

//Calculate the square root of every item in the array and do it in place
//in the array
void Sqrt()

```

```

//Calculate the square of every item in the array
void Sqr()

//Calculate the sum of all of the elements in the array - also starting from
//a set index OR from start to end indexes
element_type Sum() const
element_type Sum(const int start_index) const
element_type Sum(const int start_index, const int end_index) const

//Calculate the absolute value of every item in the array
void Abs()

// find the average of the array. or the average between start and end
float Average() const
float Average(const int start_index, const int end_index) const

// find the median of the array. or the median between start and end
element_type Median() const
element_type Median(const int start_index, const int end_index) const

// find the standard deviation of the array - or the standard deviation
// between start and end
float StandardDev() const
float StandardDev(const int start_index, const int end_index) const

//Calculate the coefficient of variation or the coefficient of variation
//between start and end
float CoeffVariation() const
float CoeffVariation(const int start_index, const int end_index) const

//Calculate the Mean Absolute Deviation. or the mean absolute deviation
//between the start and end indeces
float MeanAbsDeviation() const
float MeanAbsDeviation(const int start_index, const int end_index)

//calculate the skew of the elements in the array or the skew between the
//start and end indexes
float Skew() const
float Skew(const int start_index, const int end_index) const

//calc mean squared difference of 2 array objects. items used is an array of
//flags to indicate which of the array elements should be included in the
//calculation
int Calc_mean_squared_difference
(const Array& other, const int items_used[]) const

//calculate the poduct moment correlation between 2 arrays. items used
//is an array of flags to indicate which of the array elements should
//be included in the calculation
float Calc_product_moment_correlation
(
    const Array& other,
    const int items_used[]
) const

//calculate the special correlation as outlined in Chapter 6. items used
//is an array of flags to indicate which of the array elements should
//be included in the calculation
float Calc_special_correlation
(
    const Array& other,
    const int items_used[]
) const

//array operators
Array& operator=(const Array& other)
Array& operator=(const Array *other)
Array& operator=(const float value)

```

```

Array& operator+=(const Array& other)
Array& operator+=(const element_type& increment)
Array operator+(const Array& other)
Array operator+(const element_type& increment)

Array& operator-=(const Array& other)
Array& operator-=(const element_type& decrement)
Array operator-(const Array& other)
Array operator-(const element_type& decrement)

Array& operator/=(const Array& other)
Array& operator/=(const float scaler)
Array operator/(const Array& other)
Array operator/(const element_type scaler)

Array& operator*=(const Array& other)
Array& operator*=(const float scaler)
Array operator*(const Array& other)
Array operator*(const float scaler)

int operator==(const Array& other)

int operator!=(const Array& other)

```

C.3 CTFM class

```

#ifndef CTFMCLASS_H_
#define CTFMCLASS_H_
#include <fstream.h>
#include "Array.h"

const short kMaxInputs = 512;
const short kMaxOutputs = 4;
const short kNoFFTLines = 512;

class CTFM_data
{
public:

    // constructor
    CTFM_data(int no_inputs, int no_outputs);
    CTFM_data(CTFM_data *model);

    // destructor
    ~CTFM_data();

    // display a record
    void display() const;
    void display_object() const;

    // read a record from the file
    int read_record(ifstream& infile, int start_index = 0);

    // write the record out to the file
    int write_record(ofstream& outfile,
                    const int items[], char delimiter) const;
    int write_record(ofstream& outfile) const;

    // access an item from the sonar data
    float access_item(int item_no) const; // 0 to N-1
    int access_category() const;
    int access_no_outputs() const;

    // zero out the items in the object
    void reset();

    void remove_narrow_band(const int level); // remove narrow band

```

```

// feature calculating routines

int count_points_above_threshold(const float threshold);
int count_major_peaks(const int min_height, const int peak_width);

float sum_of_acoustic_density_profile();
float sum_complete_acoustic_density_profile_from_10() const;
float sum_complete_acoustic_density_profile() const;

float calc_perc_within_points(const int points);
float find_max_amplitude();
int calc_length_of_acoustic_density_profile();
int calc_front_to_peak();
int calc_thresh_value(int sum, float proportion);

float calc_average_amplitude();
float calc_median_amplitude();
float calc_stdev_of_amplitude();
float calc_coefficient_variation();
float calc_mean_abs_dev_amp();
float calc_skew_amplitude();

float calc_avg_posn_narrowband(const int level);

float calc_avg_range();
float calc_median_range();
float calc_stdev_range();
float calc_coeff_var_range();
float calc_abs_dev_range();
float calc_skew_range();
float count_frequencies_above(float level);

float calc_perc_slope_to_peak(const int percentage);
float calc_perc_slope_to_peakA(const int percentage);
float calc_freq_perc_power(const int percentage);

void draw_acoustic_density_profile(const float maximum);

int find_start_of_object();
int find_end_of_object();

void Feature_tracking
(
    double const *array1,
    double *array2,
    int const array_length,
    int movement_threshold
);

// operator functions
void operator=(const CTFM_data& other);
int operator==(const CTFM_data& other) const;
CTFM_data& operator/(const float scaler) const;
CTFM_data operator+(const CTFM_data object) const;
CTFM_data operator-(const CTFM_data object) const;
CTFM_data operator*(const CTFM_data object) const;
void sqrt();
void sqr();
void abs();

private:

int          fno_of_inputs,          // the number of data items
             fno_of_outputs;         // the number of actual outputs

Array<float> *finput_data;            // input data
Array<int>   *foutput_data;           // output data
int          fStartOfObject,         // stored so doesnt have to calculate

```

```

        fEndOfObject,          // over and over
        fcategory;             // category corresponding to output data

}; //end of class definition

#endif //CTFMCLASS_H_

```

C.4 Feature class

The feature class declaration below is the functionality calculating features from the acoustic density profile. Most of the calculation of features is done by calling functions in the CTFM class. The conditional compilation directive FEATS19 controls whether just the 19 or all of the features are included.

```

#ifndef FEATURECLASS_H_
#define FEATURECLASS_H_

#include <fstream.h>          // for reading files
#include <stddef.h>
#include <math.h>             // maths functions
#include "CTFMclass.h"       // CTFM data class

#define FEATS19

class Feature_data
{
public:

    // constructor
    Feature_data();

    // reading and writing data
    int write_record(ofstream &outfile, char delimiter) const;

    // calculate the features
    void calculate_features(const CTFM_data object);

    // set the category
    void set_category(const int category);

private:

    float
    /* 1 */ no_above_threshold1, /* 15 */
    /* 2 */ no_above_threshold2, /* 20 */
    /* 3 */ no_above_threshold3, /* 25 */
    /* 4 */ no_above_threshold4, /* 30 */
    /* 5 */ no_above_threshold5, /* 40 */
    /* 6 */ no_above_threshold6, /* 50 */
    /* 7 */ no_above_threshold7, /* 75 */
    /* 8 */ no_above_threshold8, /* 100 */
    /* 9 */ no_above_threshold9, /* 125 */
#ifdef FEATS19
    /* 10 */ no_above_threshold10, /* 150 */
#endif
    /*
     * The number of lines in the acoustic_density_profile that fall

```

```

* above the amplitude for that particular threshold
*
* why : this will give an indication of the size of the
*       reflective surfaces and the distribution of them
*/

/* 11 */
no_of_major_peaks1,
/*
* An amplitude is defined as a major peak if 5 of the points
* on each side of it are less than it.
*
* why : this will give an indication of the number of layers
*       of foliage
*/

/* 12 */
sum_of_density_profile,
/*
* Go through the acoustic density profile and add all of the
* amplitudes between the start and the end
*
* why : this feature will indicate the size of the "area under
*       the curve". The size of the area is an indication of
*       the height and length of the curve. This in turn relates
*       to the reflectivity (maybe orientation of the leaf as
*       well) and the depth of the plant.
*/

#ifdef FEATS19
/* 13 */
maximum_amplitude,
/*
* Find the maximum value in the acoustic density profile
*
* why : this will indicate amplitude of the greatest audible
*       surface. it is a function of the specularity of the
*       surface at that range, the size of the surface at that
*       range and the orientation of the surface at that range.
*/

/* 14 */
percentage_within_thresh_1, /* 10 */
/* 15 */
percentage_within_thresh_2, /* 15 */
/* 16 */
percentage_within_thresh_3, /* 20 */
/* 17 */
percentage_within_thresh_4, /* 25 */
/* 18 */
percentage_within_thresh_5, /* 30 */
/* 19 */
percentage_within_thresh_6, /* 35 */
/* 20 */
percentage_within_thresh_7, /* 40 */
/*
* Accumulate the amplitude values within n range points each
* side of the centre and calculate the result to be the
* percentage of this sum of the sum of the total acoustic
* density profile. This will show how energy is distributed.
*
* why : this will indicate how spread the signal is from the
*       centre. it will give an indication of the density of the
*       plant.
*/

#endif //FEATS19

/* 21 */
length_of_density_profile,
/*
* The length = end - start.
*
* why : this will give an indication of the depth of the plant
*       and can be used to standardise other features
*/

/* 22 */
front_to_peak_dist,
/*
* Find the peak of the acoustic density profile. subtract the
* position of the start from the position of the peak.
*
* why : this will give a measure of how compact the plant is
*/

```



```

#ifndef FEATS19

/* 23 */      repetition_of_layers,
/*
 * divide the length of the acoustic density profile by the
 * number of major peaks
 *
 * why : this will give a measure of the distance between
layers of
 *
 * foliage
 */

/* 24 */      threshold_data_mass1, /* 80 */
/* 25 */      threshold_data_mass2, /* 70 */
/* 26 */      threshold_data_mass3, /* 60 */
/* 27 */      threshold_data_mass4, /* 50 */
/* 28 */      threshold_data_mass5, /* 40 */
/* 29 */      threshold_data_mass6, /* 30 */
/*
 * Returns the height of the acoustic density profile which
 * contains this percentage of the data mass. eg.
 * threshold_data_mass1 will be the amplitude at which 80% of
 * the sum of the data falls below.
 */

/* 30 */      average_amplitude,
/* 31 */      median_amplitude,
/* 32 */      stdev_amplitude,
/* 33 */      variance_amplitude,
/* 34 */      coeff_of_var_amplitude,
/* 35 */      mean_abs_dev_amplitude,
/* 36 */      skew_amplitude,
/*
 * some statistics based on the amplitude of the acoustic
 * density profile between the start and end of the object of
 * interest
 */

/* 37 */      avg_posn_narrowband,
/*
 * The average position from the start of the plant
 * to the narrowband lines
 */

/* 38 */      average_range,
/* 39 */      median_range,

#endif // #ifndef FEATS19

/* 40 */      stdev_range,
/* 41 */      variance_range,
/* 42 */      coeff_of_var_range,
/* 43 */      mean_abs_dev_range,

#ifndef FEATS19

/* 44 */      skew_range,
/*
 * some simple stats on the distribution of the
 * acoustic density profile. This gives information about the
 * distribution of the power
 */

/* 45 */      count_quarter_height,
/* count the number of lines in the acoustic density profile
 * which are above one quarter of the height of the maximum
 * amplitude
 */
/* 46 */      count_half_height,
/* count the number of lines in the acoustic density profile
 * which are above half of the height of the maximum amplitude
 */

```

```

/* 47 */      count_3quarter_height,
/* count the number of lines in the acoustic density profile
 * which are above three quarters of the height of the maximum
 * amplitude
 */

/* 48 */      ratio_max_height_len,
/* 49 */      ratio_avg_height_len,
/* 50 */      ratio_max_amp_avg,

/* 51 */      ratio_max_height_sum_profile,
/* 52 */      ratio_avg_height_sum_profile,
/* 53 */      ratio_length_sum_profile,
/* 54 */      ratio_range_stdev_sum_profile,
/* 55 */      ratio_range_stdev_max_height,
/* 56 */      ratio_range_stdev_avg_height,
/* 57 */      ratio_range_stdev_length,
/*
 * some ratios between previously calculated features
 */

/* 58 */      slope_25_peak,
/* 59 */      slope_50_peak,
/* 60 */      slope_75_peak,
/* the rise slope between the range at 25% (50,75) of the
 * maximum and the maximum
 */

/* 61 */      slope_25_peakA,
/* 62 */      slope_50_peakA,
/* 63 */      slope_75_peakA,
/* the rise slope between the range at 25% (50,75) of the
 * maximum and the maximum (note that in this case the maximum
 * is actually the average of 5 points around the average
 */

/* 64 */      range_25_acoustic_area,
/* 65 */      range_50_acoustic_area,

#endif //ifndef FEATS19

/* 66 */      range_75_acoustic_area,
/* the range line from the start at which 25% (or 50,75)
 * of the total power is observed
 */

/* 67 */      no_of_major_peaks2;

      int      fStart,fEnd;

      int      fcategory;      // the category ie. 1 = plant1, 2 = plant2, etc.
}; //end of class definition

```

C.5 Reference the spectra to a standard range

The function below is used to reference the acoustic density profile of a plant to a standard range. This is discussed in Chapter 5.

```

/*
 * CTFM_data::reference_for_range
 *
 * This function is passed a standardised range to which the acoustic density profile
 * in this object is referenced to. A pointer to the referenced acoustic density
 * profile is returned. Note that this function will only standardise the plant so

```

```

* the rest of the acoustic density profile will contain 0.
*
* Parameters
*
*     the standardised range to scale to
*     the ctfm object which is used as input
*
* Returns
*
*     a pointer to the new object which is referenced to the standard range
*
* Note that this function assumes that the calibration_array is already
* established. It has the empirical measurements of the scaling for this
* particular sensor.
*/
CTFM_data *
CTFM_data::reference_for_range
(
    const int ref_to_range_mm      /* the range in mm to reference to to */
)
{
    int     element_no;
    int     ref_to_range_fftline, /* the equivalent fftline for the ref to range
*/
        start_plant_fftline, /* the fftline of the start of the plant */
        end_plant_fftline,   /* the fftline of the end of the plant */
        plant_length,        /* the number of fft lines this plant spans */
        element_no;          /* array looping variable */
    float   scale,            /* intermediate value to hold the scale */
        new_val;              /* intermediate value to hold the new value */

    /*
     * this is the storage to hold the new acoustic density profile referenced to
     * the range
     */
    CTFM_data *referenced_profile = new CTFM_data
(fno_of_inputs,fno_of_outputs);

    /*
     * find the start and end of the plant
     */
    start_plant_fftline = this->find_start_of_object();
    end_plant_fftline = this->find_end_of_object();
    plant_length = end_plant_fftline - start_plant_fftline;
    /*
     * calc the ref to range as a fftline
     */
    ref_to_range_fftline = int(ref_to_range_mm / 3.44);

    /*
     * loop through the plant referencing the items by scaling them and
     * moving them to the new range
     */
    for (element_no = 0; element_no < plant_length; element_no++)
    {
        scale = calibration_array[ref_to_range_fftline + element_no]
/
        calibration_array[start_plant_fftline + element_no];

        new_val = finput_data->Get(start_plant_fftline + element_no) * scale;
        finput_data->Set(ref_to_range_fftline + element_no, new_val);
        referenced_profile->finput_data-
>Set(ref_to_range_fftline+element_no,new_val);
    }

    return referenced_profile;
} // CTFM_data::reference_for_range

```

C.6 Calculate the number of range lines above threshold

The function below is used to calculate the threshold features. It is called with different threshold values for which it returns the count. It is discussed in Chapters 8 and 9.

```
int
CTFM_data::count_points_above_threshold
(
    const float threshold,
    const float calibration_measure
)
{
    int      element_no,           // loop counter
    no_above_threshold = 0,       // to hold the value to return to the
main function
    start,           // position of start of data
    end;             // position of the end of data

    start = this->find_start_of_object();
    end = this->find_end_of_object();

    for(element_no = start; element_no < end; element_no++)
    {
        if
        (
            finput_data->Get(element_no)
            >
            threshold / calibration_measure
        )
            no_above_threshold++;

    }

    return(no_above_threshold);
} // count_points_above_threshold
```

C.7 Calculate the number of major peaks

The function below is used to calculate the threshold features. It is called with different threshold values for which it returns the count. It is discussed in Chapters 8 and 9.

```
int
CTFM_data::count_major_peaks
(
    const int min_height,
    const int peak_width
)
{
    int element_no = 0,           // loop counter for peak searching
    peak_check = 0,              // for checking around a peak
    no_major_peaks = 0,          // to hold the value to return to the
main function
    major_peak = true,           // is this point a major peak
    start,           // position of start of data
    end;             // position of the end of data

    start = this->find_start_of_object();
    end = this->find_end_of_object();

    for(element_no = start; element_no < end; element_no++)
    {
```

```

        // just check that the item is above some reasonable figure
        if(fininput_data->Get(element_no) > min_height)
        {
            major_peak = true;

            // start peak_width bins left of the current element
            peak_check = element_no - peak_width;

            // while we havent checked all of the items each side
            // of the peak and while we havent proved that this is NOT a
            // major peak

            while(peak_check < (element_no + peak_width) && major_peak)
            {
                if(fininput_data->Get(peak_check)>fininput_data->Get(element_no))
                    major_peak = false;

                peak_check++;
            }
            if(major_peak)
                no_major_peaks++;
        }

        return(no_major_peaks);
    } // count_major_peaks

```

C.8 Calculate the sum of the acoustic density profile

The function below is used to calculate the sum of the acoustic density profile.

```

float
CTFM_data::sum_of_acoustic_density_profile()
{
    int    start,          // start of the plants acoustic density profile
           end;            // end of the plants acoustic density profile
    float  total = 0;      // to hold the value to return to the main function

    start = this->find_start_of_object();
    end = this->find_end_of_object();

    total = fininput_data->Sum(start,end);

    return(total);
} // sum_of_acoustic_density_profile

```

C.9 Calculate the front to peak distance

The function below is used to calculate distance (in fft lines) from the start of the plants acoustic density profile to the peak of the acoustic density profile.

```

int
CTFM_data::calc_front_to_peak()
{
    int start,              // position of start of the plant
       end,                // position of the end of the plant

```

```
        peak_index;  
  
        start = this->find_start_of_object();  
        end = this->find_end_of_object();  
  
        peak_index = finput_data->Pos_max(start,end);  
  
        return (peak_index - start);  
    } // calc_front_to_peak
```

D. Appendix Plant Grouping

This Appendix has information about clustering individual species with other plants whose features (and hence acoustic density profiles) are similar. A mapping of similar plants is established and is developed. The mapping is validated by running the data through a classifier which groups each record into one of the pre-defined groups.

The mapping of similar plants tabulated in Table D.8 gives a difference between the physical structure of any one group compared to other groups in the table. The differences between the groups were difficult to quantify and are somewhat subjective. This appendix does not provide any direct conclusions of the thesis but serves as a valuable resource for further work in the area.

D.1 Taxonomy

Taxonomy is the science of classification [Macquarie, 1991] and is a term often used to describe classification systems for organisms. Plant identification uses a formal taxonomy which have been developed over a long period of time. It is an orderly system resulting in the assignment of each individual plant to a descending series of groups of related plants [Benson, 1979].

Plant classification schemes are based on physical measurements of the plant, such as the number of petals in the flower, the leaf arrangement, subtle leaf shapes, or even the hair arrangement of the underside of the leaf. There is a universally accepted system of plant classification known as The International Code of Botanical Nomenclature [Stace, 1989] which is used widely by botanists to classify a large number of species.

The research described in this thesis is not attempting to classify plants to the level of a botanist. There is enough information in the signal however to differentiate plants based on their overall structure for the purpose of a system which can be used in robotics.

D.2 Introduction to cluster analysis

Cluster Analysis is the name of the various numerical methods which find similarity amongst objects in a given set. It is a standard statistical technique that is applied in many fields.

In general, Cluster Analysis attempts to identify groups, not to establish rules relating to the separation of data. The process of clustering, progressively groups objects according to their similarity. Individual elements of the group are more similar to other members of their group than to members of other groups. It is used as an exploratory technique and it can identify natural groups in the data. It is very different from the classification methods that were discussed in Chapter 10 which are based around a predefined number of known groups (or classes). Clustering makes no assumptions about the distribution of the data, the size of each group or the number of the groups.

In the case where there are only two features, clusters can be identified through visual inspection by looking for dense regions on a graph of the features as shown in Chapter 8. Often the classes are not separable using just two features and distinct classes may exist in high dimensional feature space. These classes are not usually apparent when viewing the data in lower dimensions so formal clustering techniques are required.

D.2.1 A Simple clustering example

The four plants shown in Figure D.1 will be used to illustrate cluster analysis techniques. The steps in cluster analysis are:

1. Create a similarity matrix;
2. Group the clusters and modify the similarity matrix step by step; and
3. Arrange the dendogram.

In this study, the input to the cluster analysis is the 19 features developed in Chapter 8 but since these four particular specimens are structurally quite different to each other, the first three features will provide enough information to illustrate how the plants cluster into

different groups. The input vector is the average of each of the features across the entire dataset for the particular plant.

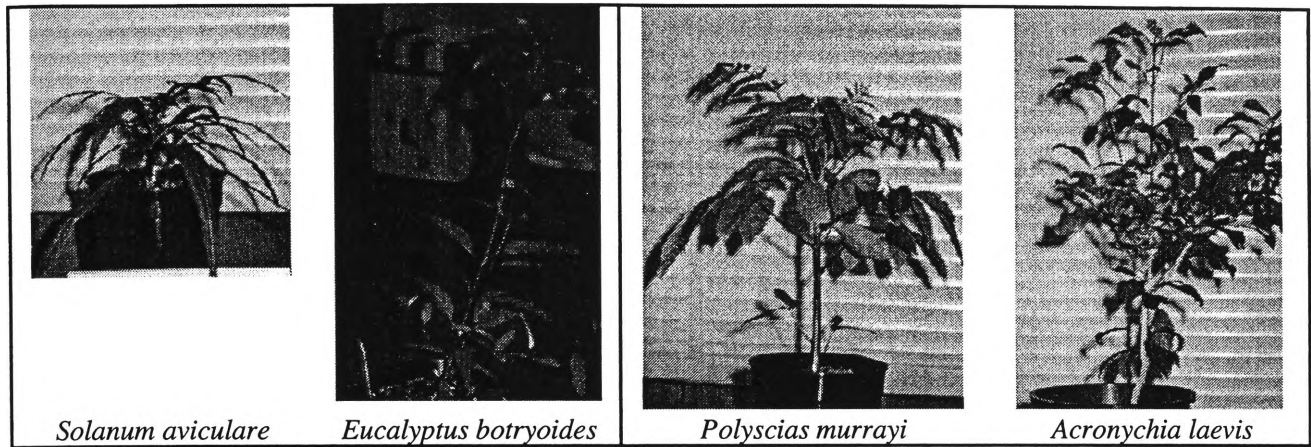


Figure D.1 Four plants in similar pairs

Details of the physical characteristics of the plants are given in Table D.1.

Table D.1 Physical characteristics of the four plants

Plant Name	Plant Hgt cm	Plant Wth cm	Leaf length	Leaf Width	No Leaves	Leaves density	Leaf orient.	Comments
<i>Solanum aviculare</i>	15	20	20	8	7	medium	down	large lobed leaves on a very small plant
<i>Polyscias murrayi</i>	30	30	7	2.5	54	high	horizontal	leaves on small branches symmetric
<i>Eucalyptus botryoides</i>	25	12	1	6	37	medium	horizontal	random leaves on many small stems from main trunk
<i>Acronychia laevis</i>	48	40	4	2	168	high	various	very specular medium sized waxy leaves

The input matrix for the cluster analysis is shown in Figure D.2. The first three features calculated from the acoustic density profile are shown in the matrix for each plant.

	no_above_threshold1	no_above_threshold2	no_above_threshold3
<i>Solanum aviculare</i>	38	32	26
<i>Polyscias murrayi</i>	91	88	84
<i>Eucalyptus botryoides</i>	33	27	22
<i>Acronychia laevis</i>	89	87	84

Figure D.2 The input matrix for the four plants

Once the input matrix is established, the next step is to use this matrix to calculate similarity (or distance) measures between individual items and the results are used as a similarity matrix. The similarity matrix for the four plants is shown in Figure D.3. The similarity values in this example are calculated using the Euclidean distance metric as outlined in Section D.3 - this distance measure is the straight line distance between the points in n dimensional space (where n is the number of input features which is three in this case).

	<i>Solanum aviculare</i>	<i>Polyscias murrayi</i>	<i>Eucalyptus botryoides</i>	<i>Acronychia laevis</i>
<i>Solanum aviculare</i>	0	96	8	94
<i>Polyscias murrayi</i>	96	0	104	2
<i>Eucalyptus botryoides</i>	8	104	0	103
<i>Acronychia laevis</i>	94	2	103	0

Figure D.3 Similarity matrix for the four plants

Several clustering algorithms are introduced in Section D.3. Agglomerative hierarchical clustering methods merge the two nearest groups at each step until there is only one single cluster (Algorithm D.1). From Figure D.3, the two most similar plants are *Polyscias murrayi* and *Acronychia laevis* with a Euclidean distance of 2. These two plants are now merged into a cluster (Cluster one). The rows and columns for these two plants

are removed and a new column is inserted which contains the distance between the new cluster and the remaining two plants (Figure D.4).

For this example (Figure D.4), Average linkage clustering has been used to determine the distance between the clusters. This is simply the average distance between both the plants in the cluster and the individual plants still remaining. So, to calculate the distance between this newly formed cluster (Cluster one) and *Solanum aviculare*, the average of the distance between the two pairs - *Polyscias murrayi* and *Solanum aviculare* (96), and *Acronychia laevis* and *Solanum aviculare* (94) is calculated (note that the same distance metric is used to calculate the distance which in this example is the euclidean distance). This comes to $(96+94)/2 = 95$. The resulting similarity matrix is shown in Figure D.4 (a).

Algorithm D.1 The algorithm for hierarchical agglomerative clustering

Start with n clusters each containing a single entity and a similarity matrix.

While there is more than one cluster in the set.

Search the similarity matrix for the two most similar clusters.

Merge the two clusters and update the similarity matrix by removing the columns and rows of the merged clusters and add a new row and column for the new cluster.

End

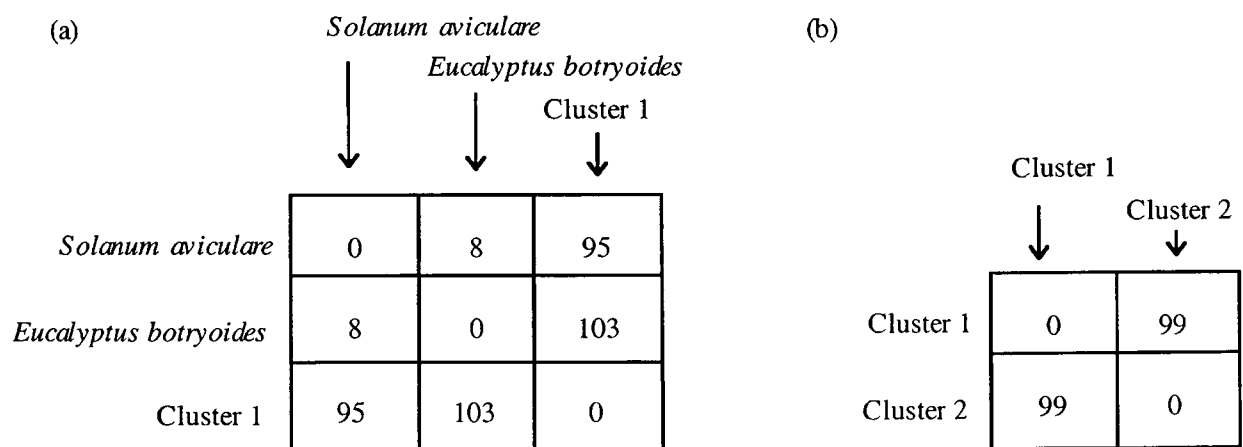


Figure D.4 The similarity matrix on completion of (a) the first merge and (b) the second merge

Solanum aviculare and *Eucalyptus botryoides* are now the two closest items (similarity = 8), so they are merged to give the matrix in Figure D.4(b). The final step involves merging cluster one and cluster 2 which are separated by a distance of 99.

Finally, the results of the clustering are reported to provide information about the relationships between the clusters. In general, results of hierarchical clustering methods are shown in the form of a tree diagram and this is illustrated in Figure D.5. This type of tree diagram is known as a dendrogram.

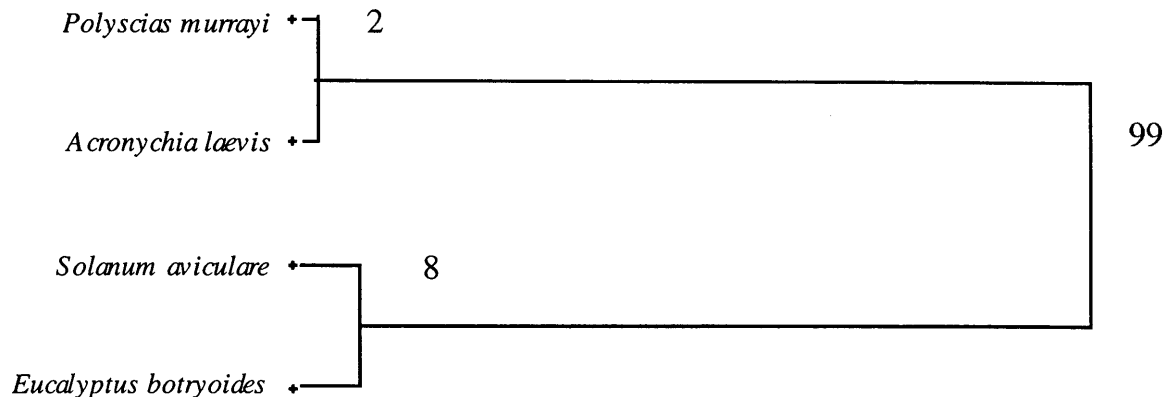


Figure D.5 The dendrogram for the four plants

The dendrogram shows how the individual objects are grouped according to their similarity measures. Starting from the left, the individual plants are in groups (or clusters) of their own moving to the right, clusters are grouped and a smaller number of clusters occur until there is only one cluster at the right hand side of the diagram.

The length of the branches on the dendrogram are a measure of similarity between the two clusters. The shorter the branch, the more similar the two (or more) clusters are. Some dendrograms also have a number on at each cluster join (as shown in Figure D.5). This number indicates the similarity measure between the two clusters. Clusters which join on the left hand side of the diagram are more similar to each other than the ones which join at the right of the diagram. The horizontal axis is a measure of the similarity between all of the clusters which have been joined at any particular point.

The plants with similar characteristics in terms of features have clustered together on the dendrogram. *Polyscias murrayi* and *Acronychia laevis* are both compact plants with a large number of leaves (reflectors) and are more similar to each other than the other two plants. You can see on the dendrogram that the cluster which joins them has very short branches. *Solanum aviculare* and *Eucalyptus botryoides* are also similar to one another but the slightly longer branches (length = 8) indicate that they are not quite as similar to each other as the other two plants are to each other in the diagram. The third cluster

groups both of the clusters but the distance measure of 99 indicates that the groups are relatively dissimilar. This shows the analyst that this third grouping may not be meaningful due to the large distances between the groups.

Thus, the four plants fall naturally into two easily separable clusters. The approach of repeatedly dividing clusters into sub clusters is a very powerful way of reducing the number of plants which match. Also, the dividing only needs to go to the level of discrimination required by the task.

The main two issues in cluster analysis algorithms involve the definition of the distance measure between each of the classes (or objects) and also the way that the clusters are actually formed. The example above used the Euclidean distance measure and a hierarchical agglomerative clustering method which used average linkage to calculate the distance between clusters. There are innumerable clustering methods which have their own distance measures and there is no general agreement of the best techniques [Velleman, 1988].

They are documented in many places and some can be found in [Romesburg, 1994]. Johnson & Wichern [1992] note that there is a great deal of subjectivity in the choice of similarity measures. Bouguettaya [1996] found that there is little difference between the different clustering approaches.

D.3 Common clustering techniques

Cluster analysis techniques are well documented, and detailed information can be found in Everitt [1980], Jain & Dubes [1988], Kaufman & Rousseeuw [1990], and Romesburg [1984].

The differences between classes (or objects) is measured using some type of distance measure. The most common distance measures are shown in Table D.2. Complete details can be found in the references mentioned above.

Table D.2 Common distance measures

Euclidean	$d(\mathbf{x}, \mathbf{y}) = \sqrt{(x_1 - y_1)^2 + (x_2 - y_2)^2 + \dots + (x_n - y_n)^2} = \sqrt{(\mathbf{x} - \mathbf{y})'(\mathbf{x} - \mathbf{y})}$
Statistical	$d(\mathbf{x}, \mathbf{y}) = \sqrt{(\mathbf{x} - \mathbf{y})' \mathbf{A} (\mathbf{x} - \mathbf{y})}$
Minkowski	$d(\mathbf{x}, \mathbf{y}) = \left[\sum_{i=1}^n x_i - y_i ^m \right]^{1/m}$ <p>where $\mathbf{A} = \mathbf{S}^{-1}$, where \mathbf{S}^{-1} contains the sample variances and covariances</p>
Mahalanhois	$\mathbf{D}^2 = (\mathbf{X}_i - \mathbf{X}_j)' \mathbf{S}^{-1} (\mathbf{X}_i - \mathbf{X}_j)$ <p>where \mathbf{S} is the pooled within group covariance matrix</p>

For any particular problem, the literature suggests testing out several different techniques in order to explore the data.

Clustering algorithms are generally divided into two major types :

1. Partitioning methods; and
2. Hierarchical methods.

Partitioning methods involve constructing k clusters, where k is provided by the researcher. The researcher is responsible for running the algorithm for several different values of k and identifying the value of which produces natural clusters. Partitioning involves the optimisation of a criterion which minimises the within class variation and maximises the between class variation.

Hierarchical methods construct a hierarchy of objects in one of two different ways.

Agglomerative methods start with all of the objects as individual clusters and at each step merge the two individual objects which are most similar (based on their similarity measures). The process is repeated until there is only one cluster left in the hierarchy.

Divisive methods start with all of the objects in one cluster and at each step, split the cluster until there are the same number of clusters as objects.

Much of the literature is focussed on hierarchical agglomerative methods as are many of the commercially available statistical packages. For these reasons, this study has used hierarchical agglomerative methods. The algorithm for this method was given in Algorithm D.1.

When analysing the results of hierarchical clustering, the interest lies in the intermediate steps when the population is divided into a reasonable number of groups. Distance measures are available at each step of the merging process and can be analysed in order to identify the appropriate number of groups to select. The distance measures are plotted at each merge and the point where the graph changes its slope indicates the point where the distances between groupings is becoming large. These larger distances indicate that the groups merged at this point were dissimilar so clustering should have been stopped at that point.

Merging of clusters is done using single linkage clustering, complete linkage clustering, or average linkage clustering or centroid clustering. Figure D.6 illustrates the criteria for merging the clusters.

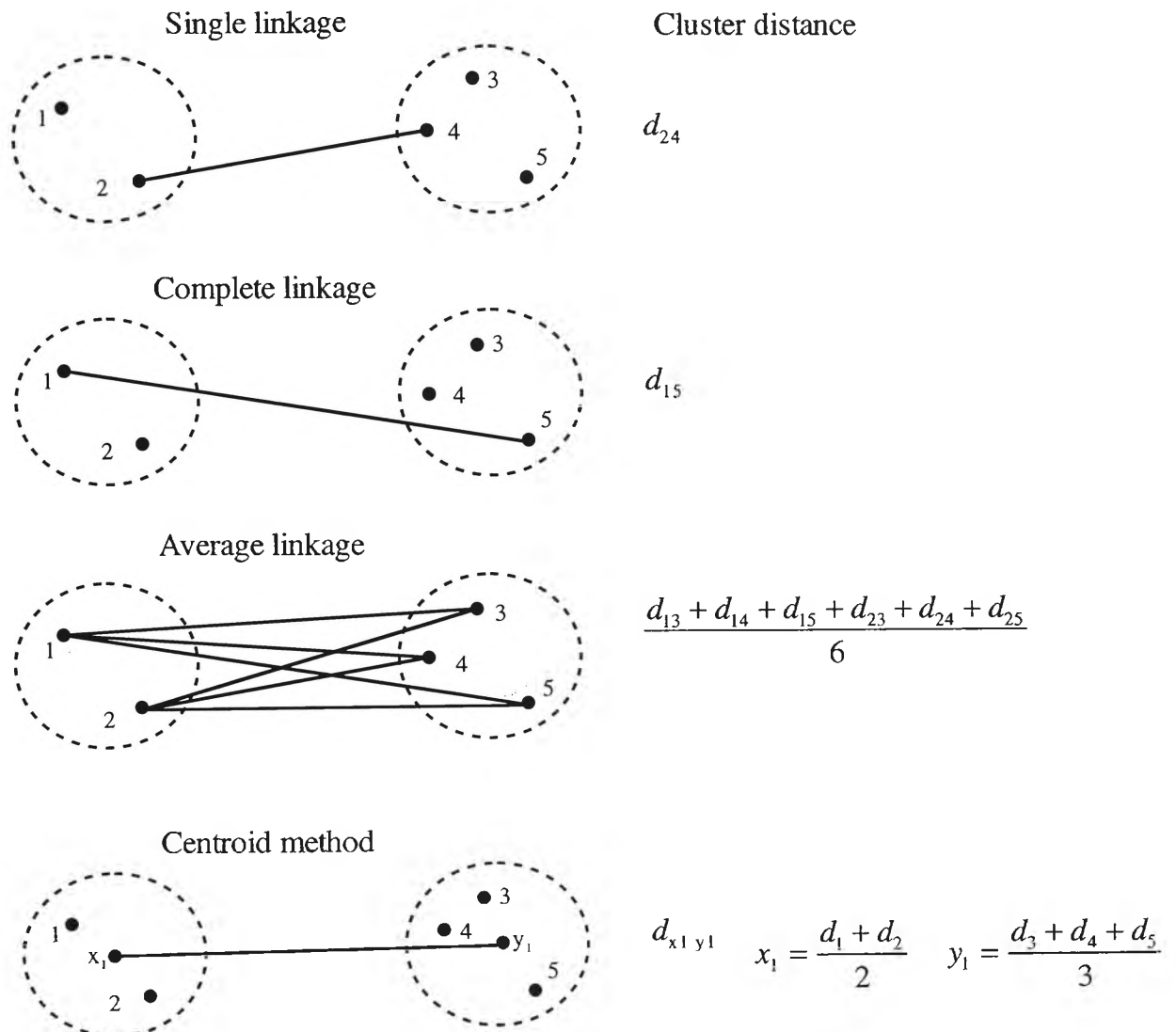


Figure D.6 Inter-cluster distance measures

In this study, several clustering methods have been used and are outlined in Table D.3. The results of the different techniques turned out to be relatively similar as was also reported by Dillon & Goldstein [1994].

Table D.3 Clustering Methods

Single linkage clustering	The distance is the minimum distance between an observation in one cluster and an observation in another cluster. This method is the only one which can pick out stringlike clusters but has drawbacks such as not being able to discern poorly separated clusters.
Complete linkage clustering	The distance is given by the maximum distance between an observation in one cluster and an observation in another cluster. This technique produces clusters with roughly equal diameters by ensuring that all items within a cluster are within some maximum distance.
Average linkage clustering	This is the average of the distance between all of the pairs of observations in each of the clusters. This method tends to join clusters with small variances.
Centroid method	This measures the squared difference between the centroids (or means) of the clusters. This technique is generally robust to outliers but in other respects may not perform as well [SAS, 1993].

D.4 Plant clustering using range data

In order to keep the problem bounded and to take advantage of available software, a fixed set of clustering algorithms were chosen. Single, Complete, Average and Centroid clustering methods were tested with euclidean distance measures using hierarchical agglomerative methods.

Each of the cluster merging algorithms produced similar (but not identical) grouping of plants. In general researchers study the groupings produced by the clustering to see which ones are most reasonable. This was found to be difficult (if not subjective) so a physically grounded method was needed.

An analytical measure was developed which produces the grouping which is the most consistent with the pairwise plant classification matrix (developed in Chapter 8). The goal of cluster analysis is to group similar plants together and similar plants are those which are hard to differentiate, that is, they have a low classification percentage. Similarly, plants which are easy to differentiate are not similar. A technique has been developed which is used to select the best clustering result based on this criterion.

At the left hand side of a dendogram is a list of plants, most of which are similar to those around them (the exception is where the adjacent plant is in a separate major branch of the dendogram). A reasonable approximation over the population is to say that any plant is similar to the adjacent plants and is more similar to the adjacent plant than the

plant two positions away on each side of it. Consider the portion of a larger dendrogram shown in Figure D.7. *Melaleuca erubescens* is adjacent to *Banksia ericifolia* so we would expect it to be more similar to that, than it is to *Melaleuca styphelioides*. Similarity can be measured by how difficult it is to separate the two samples with a classifier. From the pairwise classification table in Chapter 8, we see that the classification of *Melaleuca erubescens* and *Banksia ericifolia* is 66% and the classification of *Melaleuca erubescens* and *Melaleuca styphelioides* is 73% which supports the argument.

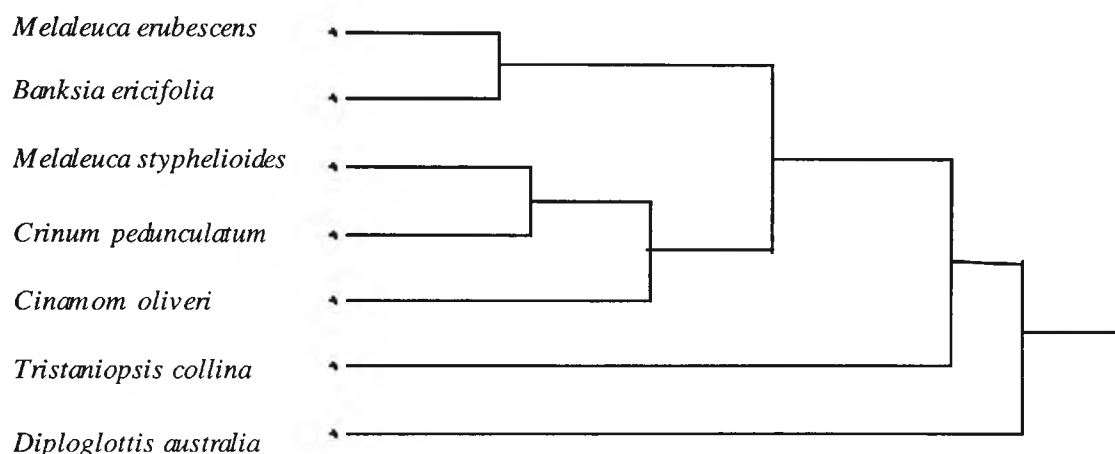


Figure D.7 A dendrogram for seven plants

The pairwise classification for these plants can be tabulated and this is shown in Table D.4. In review, the cells in the table contain the classification percentage on the test set when the statistical classifier is run.

Table D.4 Table of pairwise combinations

	<i>Melaleuca erubescens</i>	<i>Banksia ericifolia</i>	<i>Melaleuca styphelioides</i>	<i>Crinum pedunculatum</i>	<i>Cinnamom oliveri</i>	<i>Tristaniopsis collina</i>	<i>Diploglottis australis</i>
<i>Melaleuca erubescens</i>							
<i>Banksia ericifolia</i>	66						
<i>Melaleuca styphelioides</i>	73	69					
<i>Crinum pedunculatum</i>	75	76	69				
<i>Cinnamom oliveri</i>	75	84	70	76			
<i>Tristaniopsis collina</i>	81	86	81	90	70		
<i>Diploglottis australis</i>	83	100	100	100	99	99	

In general, plants which are adjacent on the dendrogram are similar to each other and hence have a lower recognition percentage with the test set. The table is formatted so that recognition percentages of “near” plants in the cluster will appear close to the diagonal line down the table. The plants adjacent to any plant will appear in the line either across (for plants before it in the list) or down (for plants after it in the list). Consider the cell for *Melaleuca styphelioides* in Table D.4 which is marked in with an asterisk. Plants preceding it in the list are in a line horizontally with plants further away from it being further away in the list. Plants after it appear in the vertical line from the square marked with the asterisk. As highlighted by the arrow, as you move successive cells away from the plant, the classification improves. This is due to the fact that the plants become less similar. This is a general rule which holds for almost the entire table. If it does not hold, then this plant may be in the wrong cluster.

If there is a cell with a low classification percentage, some distance away from the diagonal then this indicates that there are two similar plants which have been mapped into separate groups. These “outliers” can be used to determine how good the clustering is.

A count of these outliers can be used to indicate the number of pairs of plants which are similar but haven't been grouped together. The higher the count, the less suitable is the grouping which has been produced by the clustering method. Consider the dendrogram in Figure D.8, it is the result of a complete linkage cluster analysis of all 100 plants using the 19 features. The recognition percentages can be plotted as a table similar to that in Table D.4. It is shown in Table D.5 with recognition percentages less than or equal to 75 highlighted. Most of the low values are positioned around the diagonal where they are expected, with some outliers scattered around particularly in the lower half of the table. The separation between major clusters is also evident as sections of the diagonal where the classification percentages are high.

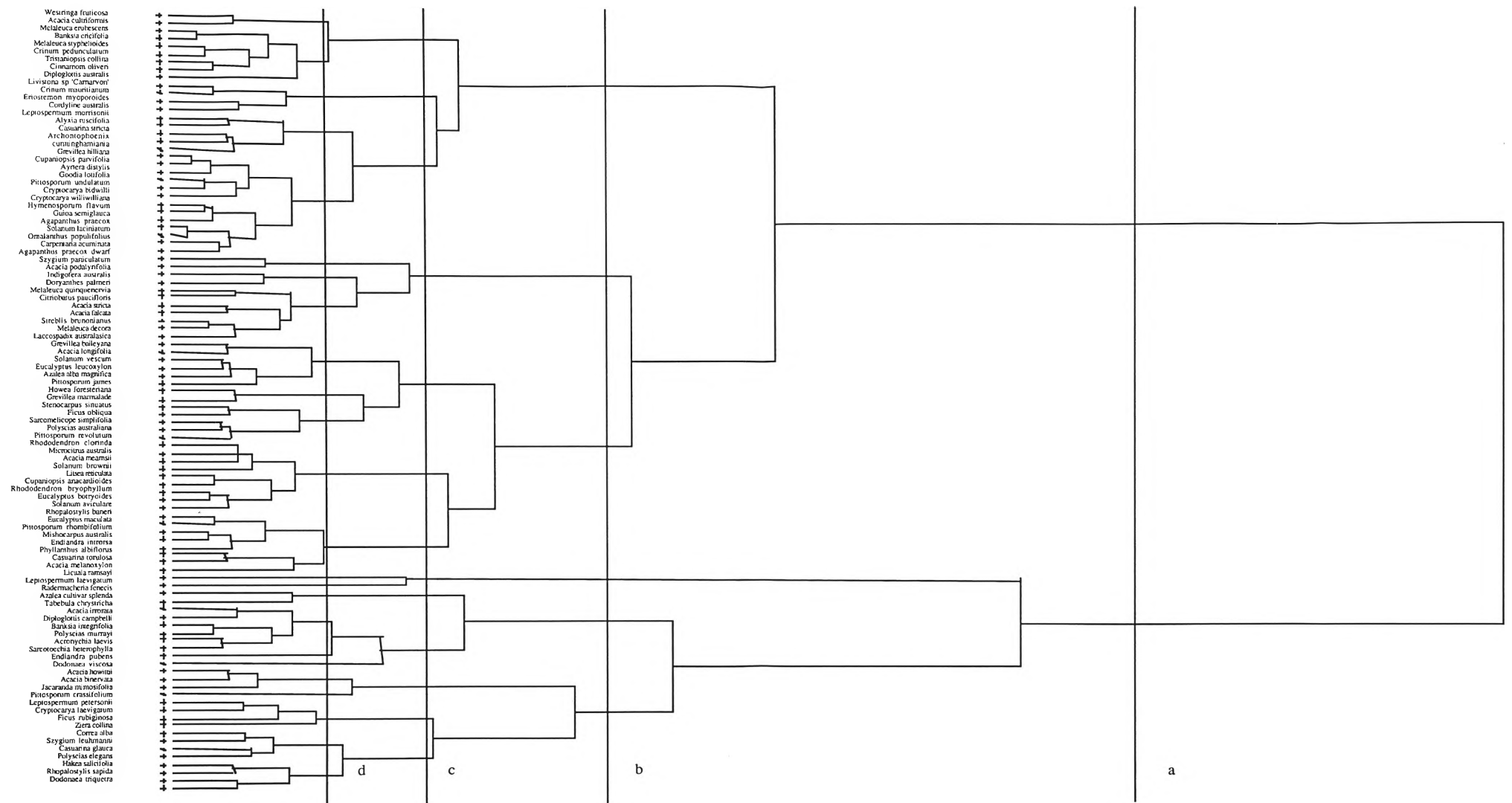


Figure D.8 The dendrogram for all 100 plants (Complete Linkage Cluster Analysis)

Table D.5 Table of pairwise combinations for all 100 plants

	1	2	3	4	5	6	7	8	9	10	11	12	13	14	15	16	17	18	19	20	21	22	23	24	25	26	27	28	29	30	31	32	33	34	35	36	37	38	39	40	41	42	43	44	45	46	47	48	49	50	51																																																																																									
80	81	82	83	84	85	86	87	88	89	90	91	92	93	94	95	96	97	98	99	100	101	102	103	104	105	106	107	108	109	110	111	112	113	114	115	116	117	118	119	120	121	122	123	124	125	126	127	128	129	130	131	132	133	134	135	136	137	138	139	140	141	142	143	144	145	146	147	148	149	150	151	152	153	154	155	156	157	158	159	160	161	162	163	164	165	166	167	168	169	170	171	172	173	174	175	176	177	178	179	180	181	182	183	184	185	186	187	188	189	190	191	192	193	194	195	196	197	198	199	200																				
160	161	162	163	164	165	166	167	168	169	170	171	172	173	174	175	176	177	178	179	180	181	182	183	184	185	186	187	188	189	190	191	192	193	194	195	196	197	198	199	200	201	202	203	204	205	206	207	208	209	210	211	212	213	214	215	216	217	218	219	220	221	222	223	224	225	226	227	228	229	230	231	232	233	234	235	236	237	238	239	240	241	242	243	244	245	246	247	248	249	250	251	252	253	254	255	256	257	258	259	260	261	262	263	264	265	266	267	268	269	270	271	272	273	274	275	276	277	278	279	280	281	282	283	284	285	286	287	288	289	290	291	292	293	294	295	296	297	298	299	300
280	281	282	283	284	285	286	287	288	289	290	291	292	293	294	295	296	297	298	299	300	301	302	303	304	305	306	307	308	309	310	311	312	313	314	315	316	317	318	319	320	321	322	323	324	325	326	327	328	329	330	331	332	333	334	335	336	337	338	339	340	341	342	343	344	345	346	347	348	349	350	351	352	353	354	355	356	357	358	359	360	361	362	363	364	365	366	367	368	369	370	371	372	373	374	375	376	377	378	379	380	381	382	383	384	385	386	387	388	389	390	391	392	393	394	395	396	397	398	399	400																				
400	401	402	403	404	405	406	407	408	409	410	411	412	413	414	415	416	417	418	419	420	421	422	423	424	425	426	427	428	429	430	431	432	433	434	435	436	437	438	439	440	441	442	443	444	445	446	447	448	449	450	451	452	453	454	455	456	457	458	459	460	461	462	463	464	465	466	467	468	469	470	471	472	473	474	475	476	477	478	479	480	481	482	483	484	485	486	487	488	489	490	491	492	493	494	495	496	497	498	499	500																																								
500	501	502	503	504	505	506	507	508	509	510	511	512	513	514	515	516	517	518	519	520	521	522	523	524	525	526	527	528	529	530	531	532	533	534	535	536	537	538	539	540	541	542	543	544	545	546	547	548	549	550	551	552	553	554	555	556	557	558	559	560	561	562	563	564	565	566	567	568	569	570	571	572	573	574	575	576	577	578	579	580	581	582	583	584	585	586	587	588	589	590	591	592	593	594	595	596	597	598	599	600																																								
600	601	602	603	604	605	606	607	608	609	610	611	612	613	614	615	616	617	618	619	620	621	622	623	624	625	626	627	628	629	630	631	632	633	634	635	636	637	638	639	640	641	642	643	644	645	646	647	648	649	650	651	652	653	654	655	656	657	658	659	660	661	662	663	664	665	666	667	668	669	670	671	672	673	674	675	676	677	678	679	680	681	682	683	684	685	686	687	688	689	690	691	692	693	694	695	696	697	698	699	700																																								
700	701	702	703	704	705	706	707	708	709	710	711	712	713	714	715	716	717	718	719	720	721	722	723	724	725	726	727	728	729	730	731	732	733	734	735	736	737	738	739	740	741	742	743	744	745	746	747	748	749	750	751	752	753	754	755	756	757	758	759	760	761	762	763	764	765	766	767	768	769	770	771	772	773	774	775	776	777	778	779	780	781	782	783	784	785	786	787	788	789	790	791	792	793	794	795	796	797	798	799	800																																								
800	801	802	803	804	805	806	807	808	809	810	811	812	813	814	815	816	817	818	819	820	821	822	823	824	825	826	827	828	829	830	831	832	833	834	835	836	837	838	839	840	841	842	843	844	845	846	847	848	849	850	851	852	853	854	855	856	857	858	859	860	861	862	863	864	865	866	867	868	869	870	871	872	873	874	875	876	877	878	879	880	881	882	883	884	885	886	887	888	889	890	891	892	893	894	895	896	897	898	899	900																																								
900	901	902	903	904	905	906	907	908	909	910	911	912	913	914	915	916	917	918	919	920	921	922	923	924	925	926	927	928	929	930	931	932	933	934	935	936	937	938	939	940	941	942	943	944	945	946	947	948	949	950	951	952	953	954	955	956	957	958	959	960	961	962	963	964	965	966	967	968	969	970	971	972	973	974	975	976	977	978	979	980	981	982	983	984	985	986	987	988	989	990	991	992	993	994	995	996	997	998	999	1000																																								

52 53 54 55 56 57 58 59 60 61 62 63 64 65 66 67 68 69 70 71 72 73 74 75 76 77 78 79 80 81 82 83 84 85 86 87 88 89 90 91 92 93 94 95 96 97 98 99 100

[illegible]

Table D.6 Plant information grouped by cluster

id	Plant	Family	Common name	Hgt cm	Wth cm	Leaf lgth	Leaf wth	Leaf l / w	Leaf area l*w*.75	No Leaves	LArea NoLeav	Leaves density	Orthog Angle	Plane Angle	Internal spread	curtain measure	Subjective Symmetry	Leaves orient.	Comments
99	Westringia fruticosa	Lamiaceae	Rosemary	15	6	1	0.2	5	0.15	60	9	low	0	30	2	30	6	45	rosemary - leaves from central stem
2	Acacia cultriformis	Mimosaceae	Knife-leaf wattle	40	4	2	1	2	1.5	52	78	low	0	10	1	1	9	horizontal	single central stem with small leaves
66	Melaleuca erubescens	Myrtaceae		15	4	1	0.1	10	0.08	170	14	low	0	75	2	5	8	various	tiny leaves along tiny branches and trunk
19	Banksia ericifolia	Proteaceae	Heath Banksia	40	4	1.5	0.3	5	0.34	67	23	low	0	10	1	5	5	horizontal	1 main stem with very small leaves around it
68	Melaleuca styphelioides	Myrtaceae	Prickly-leaved TeaT	40	5	3	0.5	6	1.13	64	72	low	0	10	1	10	7	horizontal	single central stem with small leaves
30	Crinum pedunculatum	Amarylilidaceae	Swamp Lily	30	15	50	3	16.67	112.5	6	675	low	0	85	1	40	8	vertical	short stem with long leaves radiating upwards
98	Tristanopsis collina	Myrtaceae	Mount. Water Gum	35	10	5	1.5	3.33	5.63	27	152	low	0	10	1	10	6	horizontal	leaves from central trunk
25	Cinnamom oliveri	Lauraceae	Olivers Sassatras	48	10	6	1.5	4	6.75	7	47	low	0	0	1	5	10	horizontal	a stick with about 6 leaves near the top
36	Diploglottis australis	Sapindaceae	Native Tamarind	15	20	12	6	2	54	5	270	low	0	5	1	10	8	horizontal	small plant with large leaves
64	Livistona sp 'Carnarvon'	Arecaceae	Cabbage Palm	35	15	20	5	4	75	5	375	low	0	45	2	5	10	vertical	a couple of very large leaves oriented vertically
29	Crinum mauritianum	Amarylilidaceae		60	30	60	2	30	90	6	540	medium	0	70	2	10	9	vertical	long leaves from base from each side of the plant
43	Eriostemon myoporoides	Rutaceae	Native Daphne	25	10	6	0.8	7.5	3.6	34	122	medium	0	50	1	30	6	vertical	single main stem slightly on and angle
27	Cordylone australis	Agavaceae		35	60	40	0.6	66.67	18	450	8100	medium	0	30	1	20	7	45	very long thin leaves from the base
60	Leptospermum morrisonii	Myrtaceae	Tea Tree	31	16	6	2	3	9	110	990	medium	0	45	2	20	8	45	symmetric plant with leaves on branches
14	Alyxia ruscifolia	Apocynaceae	Prickly Alyxia	55	6	2	0.8	2.5	1.2	77	92	low	0	10	2	0	10	horizontal	tail spindly plant with a single stem. very few leaves
23	Casuarina stricta	Casuarinaceae	Drooping Sheoak	60	50	15	0.1	150	1.13	160	181	medium	0	10	2	5	7	45	very long needles mainly off the central stem
15	Archontophoenix cunninghamiana	Arecaceae	Bangalow Palm	35	40	20	15	1.33	225	5	1125	medium	0	45	1	30	10	45	very large pinnately divided leaves. only about 6
50	Grevillea hilliana	Proteaceae	White Silky Oak	38	35	22	2	11	33	11	363	medium	0	10	1	10	8	horizontal	long thin alternate leaves with many thin lobes
35	Cupaniopsis parvifolia	Sapindaceae		30	12	6	2	3	9	17	153	low	0	10	2	10	9	horizontal	leaves on branches off main trunk sparse
16	Ayrtera distylis	?	Twin-leaf Cogera	40	18	6	2	3	9	28	252	medium	0	15	1	10	9	horizontal	wobbly edge leaves mostly oriented in one direction
48	Goodia lotifolia	Fabaceae		44	10	1	0.8	1.25	0.6	80	48	low	0	90	2	30	8	down	clover type leave stem forks about half way up
78	Pittosporum undulatum	Pittosporaceae		30	10	8	2	4	12	12	144	medium	0	30	1	20	7	45	medium size leaves on main stem
31	Cryptocarya bidwillii	Lauraceae	Yellow Laurel	25	12	6	2	3	9	15	135	low	0	10	1	20	6	horizontal	small plant with only a few leaves
33	Cryptocarya williwilliana	Lauraceae	Small-leaved Laurel	25	15	1.5	1	1.5	1.13	80	90	low	0	10	2	10	7	horizontal	small leaves many branches from trunk with leaves
55	Hymenosporum flavum	Pittosporaceae	Native Frangipani	22	8	4	1	4	3	10	30	low	0	20	1	20	6	horizontal	small plant with few leaves alternate folded
52	Guioa semiglauc	Sapindaceae		37	15	4	1.5	2.67	4.5	28	126	low	0	5	2	5	8	horizontal	leaves grouped on small stems from main trunk
13	Agapanthus praecox	Agavaceae	Agapanthus	33	44	32	3	10.67	72	12	864	medium	0	60	1	50	5	vertical	large leaves sprouting from the base
91	Solanum laciniatum	Solanaceae	Lrg Flower. Kang. Appl	40	12	10	1.5	6.67	11.25	6	68	low	0	0	1	10	8	horizontal	a few leaves on the end of main trunk
72	Omalanthus populifolius	Euphorbiaceae	Bleeding Heart	15	8	5	4	1.25	15	5	75	medium	0	80	1	50	8	down	tiny bleeding heart
21	Carpentaria acuminata	Arecaceae	Carpentaria Palm	50	30	20	10	2	150	4	600	low	0	10	1	10	10	various	large pinnately divided leaves but not many of them
12	Agapanthus praecox dwarf	Agavaceae	Dwarf Agapanthus	15	15	12	1	12	9	7	63	medium	0	45	1	40	4	vertical	leaves sprouting up from the base
96	Szygium paniculatum	Myrtaceae		45	12	5	2	2.5	7.5	94	705	medium	0	45	2	40	5	various	leaves off stem and also angled branch
9	Acacia podalyrifolia	Mimosaceae	Old Silver wattle	30	10	4	3	1.33	9	56	504	medium	0	45	2	40	7	horizontal	main stem with one side branch same as one out front
56	Indigofera australis	Fabaceae	Australian Indigo	29	13	12	3	4	27	11	297	medium	0	80	2	10	7	down	branches with many leaves grouped like wattle but bigger
40	Doryanthes palmeri	Agavaceae	Spear Lily	60	60	60	6	10	270	8	2160	medium	0	80	1	60	7	vertical	large sword shaped leaves radiating from base
67	Melaleuca quinquenervia	Myrtaceae	Broad-leaved Paper	53	15	5	0.8	6.25	3	184	552	medium	0	35	2	40	4	45	leaves along symmetrical branches upright plant
26	Citriobatus paucifloris	Pittosporaceae	Orange Thorn	15	15	0.5	0.5	1	0.19	300	57	high	0	45	2	50	6	various	a very compact plant with many small leaves
10	Acacia stricta	Mimosaceae		30	20	8	0.7	11.43	4.2	64	269	medium	0	20	2	30	4	vertical	symmetrical looking all leaves pointing up
3	Acacia falcata	Mimosaceae		60	25	8	3	2.67	18	31	558	low	0	10	2	20	6	horizontal	1 or 2 side branches
94	Strelbis brunonianus	Moraceae	Whalebone Tree	40	8	7	3	2.33	15.75	16	252	medium	0	90	1	55	5	down	leaves hanging down from small stalks from trunk
65	Melaleuca decora	Myrtaceae		50	16	1	0.2	5	0.15	280	42	medium	10	45	2	35	5	various	tiny leaves along trunk and several branches
58	Laccospadix australasica	Aracaceae	Atherton Palm	34	38	20	8	2.5	120	5	600	low	20	80	1	30	7	vertical	small spindly palm
49	Grevillea baileyana	Proteaceae		25	20	15	15	1	168.75	8	1350	medium	0	40	2	30	7	30	large leaves with lobes coming from central stem
6	Acacia longifolia	Mimosaceae	Syd Golden wattle	35	35	10	1	10	7.5	340	2550	high	10	60	2	60	4	various	many long thin leaves
92	Solanum vescum	Solanaceae		30	40	20	10	2	150	11	1650	medium	0	5	2	10	8	various	large lobed leaves in various orientations
45	Eucalyptus leucoxylon	Myrtaceae	Rosea	60	24	6	5	1.2	22.5	52	1170	low	0	5	1	20	7	30	large roundish leaves off a single main stem
17	Azalea alba magnifica	Ericaceae	Azalea	50	40	2	0.8	2.5	1.2	140	168	medium	10	0	2	15	10	45	spindly large azalea with several large sub-branches
75	Pittosporum james	Pittosporaceae		55	30	1.1	0.8	1.38	0.66	160	106	low	0	30	2	20	10	various	many long branches with small leaves scattered
54	Howea forsteriana	Arecaceae	Kentia Palm	50	50	30	30	1	675	4	2700	medium	0	30	1	30	9	45	spindly palm
51	Grevillea marmalade	Proteaceae	Orange Marmalade	40	40	10	1.5	6.67	11.25	36	405	medium	30	60	2	10	10	vertical	central stem with 1 large branch angled alternate leaves
93	Stenocarpus sinuatus	Proteaceae	Firewheel Tree	40	40	20	30	0.67	450	8	3600	medium	0	10	2	40	6	horizontal	huge lobed leaves on stalks from trunk
70	Ficus obliqua	Moraceae	Small-leaved Fig	50	20	6	2	3	9	29	261	medium	0	45	1	20	10	30	plant with 2 major stems but with a big lean on it
88	Sarcomelicope simplifolia	Rutaceae		70	20	11	5	2.2	41.25	22	908	medium	0	20	1	30	5	30	large leaves on stalks off main trunk
79	Polyscias australiana	Araliaceae		60	50	8	5	1.6	30	40	1200	medium	0	30	2	40	5	horizontal	fairly symmetric with 5 or 6 minor branches w/leaves
76	Pittosporum revolutum	Pittosporaceae	Brisbane Laurel	55	22	8	4	2	24	33	792	medium	0	10	2	30	8	down	groups of leaves on the end of 3 branches

ID	Plant	Family	Common name	Hgt cm	Wth cm	Leaf lgth	Leaf wth	Leaf l / w	Leaf area l * w * .75	No Leaves	LArea * NoLeav	Leaves density	Orthog Angle	Plane Angle	Internal spread	curtain measure	Subjective Symmetry	Leaves orient.	Comments
84	Rhododendron clorinda	Ericaceae		40	25	8	3	2.67	18	40	720	medium	20	20	2	40	10	30	large folded waxy leaves around end of trunk & main branch
69	Microcitrus australis	Rutaceae	Bush Lime	35	15	1	0.2	5	0.15	206	31	medium	30	0	2	20	10	horizontal	crazy plant with strange zig zag branches with leaves
7	Acacia mearnsii	Mimosaceae	Black wattle	38	25	10	6	1.67	45	9	405	low	30	10	2	30	10	horizontal	typical wattle leaves similar to irrorata smaller specimen
90	Solanum brownii	Solanaceae	Devil's Needles	60	35	15	8	1.88	90	15	1350	medium	0	20	1	30	10	30	large leaves with spikes on stalks from main trunk angled
63	Litsea reticulata	Lauraceae	Bolly Gum	60	10	6	1.5	4	6.75	16	108	low	0	10	2	20	10	horizontal	a few leaves on a stem and end of an angled branch
34	Cupaniopsis anacardioides	Sapindaceae	Tuckeroo	28	14	8	3	2.67	18	22	396	low	30	15	2	40	10	horizontal	leaves on branches off main trunk sparse
83	Rhododendron bryophyllum	Ericaceae		32	18	5	1	5	3.75	150	563	medium	0	35	2	50	9	horizontal	odd shaped rhodo one large off centre branch plus others
44	Eucalyptus botryoides	Myrtaceae	Southern Mahogany	25	12	1	6	0.17	4.5	37	167	medium	0	20	2	30	9	horizontal	random leaves on many small stems from main trunk
89	Solanum aviculare	Solanaceae	Kangaroo Apple	15	20	20	8	2.5	120	7	840	medium	0	0	1	30	7	down	large lobed leaves on a very small plant
85	Rhopalostylis baneri	Arecaceae	Norfolk Palm	25	25	20	10	2	150	4	600	medium	0	45	1	40	9	vertical	another palm
46	Eucalyptus maculata	Myrtaceae	Spotted Gum	48	32	20	4	5	60	18	1080	medium	0	30	1	30	7	30	very large leaves on small stalks from central stem
77	Pittosporum rhombifolium	Pittosporaceae		30	15	4	2	2	6	30	180	medium	0	20	2	30	8	horizontal	several minor branches from trunk with leaves on all
71	Mishocarpus australis	Sapindaceae		28	15	13	4	3.25	39	15	585	medium	0	0	1	30	5	horizontal	small plant with large leaves on stalks from trunk
41	Endiandra introrsa	Lauraceae	Dorrigo Plum	35	15	8	2	4	12	47	564	medium	0	15	2	40	7	30	many large leaves from stems
73	Phyllanthus albidiflorus	Euphorbiaceae		38	22	1.2	0.8	1.5	0.72	350	252	medium	10	40	2	30	8	30	leaves along stems opposite several minor stems
24	Casuarina torulosa	Casuarinaceae	Forest Sheoak	40	33	6	0.1	60	0.45	400	180	high	10	30	2	30	4	30	dense shapely kind of symmetrical
8	Acacia melanoxylon	Mimosaceae	Blackwood	43	12	8	1	8	6	20	120	low	10	60	1	30	10	various	2 different kinds of leaves long thin and wattle type
62	Licuala ramsayi	Arecaceae	Hessian Hair Fan Palm	46	48	20	20	1	300	5	1500	medium	0	30	1	50	7	vertical	large hand like leaves about 6
59	Leptospermum laevigatum	Myrtaceae	Coast Tea Tree	30	28	2	0.7	2.86	1.05	900	945	high	0	30	2	60	4	various	bushy plant with many branches covered in leaves
82	Radermachera fenecis	Bignoniaceae	China Doll	31	40	2	0.9	2.22	1.35	400	540	high	0	0	2	50	3	30	china doll, numerous leaves
18	Azalea cultivar splenda	Ericaceae	Azalea	44	40	3	1	3	2.25	250	563	medium	0	80	2	70	4	45	bushy but not symmetric about 9 minor vertical branches
97	Tabebuia chrystricha	Bignoniaceae		30	29	5	5	1	18.75	43	806	medium	0	5	2	40	7	horizontal	furry leaves in groups of 3 at end of stems. serrated
5	Acacia irrorata	Mimosaceae	Green wattle	35	38	10	5	2	37.5	18	675	medium	45	20	2	35	9	horizontal	typical wattle type leaves bipinnate
37	Diploglottis campbelli	Sapindaceae		60	28	6	1.5	4	6.75	77	520	high	0	20	2	55	4	horizontal	quite a few leaves spread well throughout the branches
20	Banksia integrifolia	Proteaceae	Coast Banksia	60	30	10	2	5	15	212	3180	high	0	10	2	40	8	various	bushy plant. most of the leaves on one angled branch
81	Polyscias murrayi	Araliaceae	Pencil Cedar	30	30	7	2.5	2.8	13.13	54	709	high	0	35	2	60	2	horizontal	leaves on small branches symmetric
11	Acronychia laevis	Rutaceae	Glossy Acronychia	48	40	4	2	2	6	168	1008	high	0	10	2	60	7	various	very specular medium sized waxy leaves
87	Sarcotoechia heterophylla	Sapindaceae		40	40	15	3	5	33.75	38	1283	medium	0	40	2	40	6	30	large leaves on branches off main trunk
42	Endiandra pubens	Lauraceae	Hairy Walnut	22	8	2.5	3.2	15	41	615	medium	0	0	2	50	3	30	small with large leaves compact and dense	
39	Dodonaea viscosa	Sapindaceae		39	23	10	1	10	7.5	140	1050	high	20	20	2	50	4	30	bushy plant with long leaves from several branches
4	Acacia howittii	Mimosaceae		40	30	1.2	0.4	3	0.36	450	162	high	30	5	2	40	7	various	small roundish leaves along branches, bent over
1	Acacia binervata	Mimosaceae	2-veined hickory	55	30	8	4	2	24	66	1584	high	10	45	2	60	3	45	medium size leaves prominent veins
57	Jacaranda mimosifolia	Bignoniaceae	Jacaranda	40	27	1.5	0.5	3	0.56	500	280	medium	45	10	2	50	3	horizontal	jacaranda
74	Pittosporum crassifolium	Pittosporaceae	Karo	38	30	5	4	1.25	15	100	1500	high	0	10	2	60	2	45	waxy leaves round numerous
61	Leptospermum petersonii	Myrtaceae	Lemon Sc. TeaT	50	15	0.7	0.1	7	0.05	520	26	high	0	45	2	50	3	various	lots of leaves and many small branches
32	Cryptocarya laevigatum	Lauraceae	Red-fruited Laurel	39	20	6	3	2	13.5	56	756	medium	0	45	2	40	6	30	glossy leaves. 2 minor branches leaves angled down
9	Port Jackson Fig	Moraceae	Port Jackson Fig	42	20	8	3	2.67	18	26	468	high	0	50	2	60	2	down	a "ball" of laves on a central stem
28	Correa collina	Rutaceae		50	25	1.5	0.2	7.5	0.23	146	34	medium	45	5	2	20	6	various	many small leaves along trunk and branches angled
28	Correa alba	Rutaceae	White Correa	30	20	3	2	1.5	4.5	88	396	medium	0	45	2	40	6	45	cupped leaves from 3 main branches. lop sided
95	Szygium leuhmanni	Myrtaceae	Riberry	40	25	2	1	2	1.5	208	312	high	0	10	2	50	6	various	a dense kind of plant kind of like a fig
22	Casuarina glauca	Casuarinaceae	Swamp Oak	65	35	8	0.1	80	0.6	300	180	medium	0	30	2	20	6	45	needle like leaved. relatively bushy for a casuarina
80	Polyscias elegans	Araliaceae	Celery Wood	50	25	7	3	2.33	15.75	40	630	medium	0	80	2	40	8	down	leaves on small branches. a bit lop sided
53	Hakea salicifolia	Proteaceae	Willow-leaf Hakea	46	34	6	2	3	9	48	432	medium	0	20	2	30	8	45	central stem with 1 large angled branch
86	Rhopalostylis sapida	Arecaceae	Nikau Palm	55	40	25	15	1.67	281.25	3	844	medium	0	45	1	40	9	vertical	scrappy palm with large leaves
38	Dodonaea triquetra	Sapindaceae	Hopbush	39	31	15	6	2.5	67.5	30	2025	high	0	10	2	30	5	horizontal	large leaves of main stem and 2 small branches

Low values away from the diagonal in Table D.5 are the ones which indicate inconsistent grouping, so a count of these “outliers” provide a measure to compare clustering methods. A threshold for tagging outliers is tested as 75, 85 and 95. If the tagged cell is more than 10 units from the diagonal then it is included in the count of outliers. Comparisons of the results for the different clustering methods is shown in Table D.7. The complete linkage clustering algorithm produced a lower count for all thresholds so it can be considered as the most natural grouping of the acoustic density profiles of this particular sample of 100 plants.

Table D.7 Outlier counts

Threshold Method	75	85	95
Single Linkage	138	669	1858
Complete Linkage	120	596	1812
Average Linkage	138	659	1859
Centroid Linkage	133	652	1872

D.5 Analysis of generated clusters

Visualisation of the clusters is carried out by carefully arranging photos of the plant specimens into their cluster groups. It is then a matter of determining the differences between the clusters at different levels of detail. Table D.6 shows all of the plants from the dendrogram in tabular form with some of their physical properties listed. The dendrogram in Figure D.8 has been divided at various levels (*a*, *b*, *c* and *d*) which represent large cluster groups on the right hand side, with the number of groups increasing as we move to the left. As we move to the left, the number of plants in each group reduces and the differences between plants within any group becomes smaller.

At level *a* there are two major groups and the differences between them are noted. At the next level (level *b*), the first cluster is split into two smaller groups with each of the groups having its own distinguishing characteristics. As the groups are broken down, a form of classification tree emerges. Table D.6 is formatted so that the information recorded about the plants can be cross-referenced against the dendrogram. Level *a* is two major clusters - the first cluster is shown on the first page of the table and the other is

shown on the second page of the table. Level *b*, *c*, and *d* are shown in the table with increasingly lighter shaded dividing lines.

Table D.8 preserves the format of the hierarchical classification tree. The broad clusters are at the top of the table, with the clusters being broken down step by step until a good description of the plant is available at the lower levels. As the clusters become smaller, it becomes more difficult to separate the plants.

Table D.8 The differences between classes as clusters become finer

Cluster level <i>a</i>	Cluster 1 (72 plants) These plants are relatively sparse in foliage. They are a mixture of large leaves, small leaves and needled plants but have the characteristics of either being small or spindly. They give the appearance that they are all relatively young plants and are “gangly” in appearance.												Cluster 2 (28 plants) These plants are compact and dense with most of the leaves on the end of the stems. These leaves shield most of the internal plant structure from the signal (there is a considerable amount of acoustic shadowing). Most of them have small leaves which are close together compared to Cluster 1 in which many of the plants have large leaves.								
Cluster level <i>b</i>	Cluster 1 (31 plants) These plants are basal or have a single central stem with very few leaves.					Cluster 2 (11 plants) Some basal plants but with more foliage than Cluster 1. Small leaves.			Cluster 3 (30 plants) These plants have larger leaves but still with central stems.				Cl 4 (2) 1 or 2 Large leaves or compact bushy plant?	Cluster 5 (10 plants) Large total leaf area (>500 cm ²) Leaf tips oriented either upward or down. Outer leaves shadow the internal structure and the rear of the plant			Cluster 6 (16 plants) Leaves are more spread throughout the plant				
Cluster level <i>c</i>	Cluster 1 (9 plants) Very compact plants with a single central stem and small leaves.		Cl 2 (4) Basal or protruding from a point in the stem similar to basal	Cluster 3 (18 plants) Generally larger leaves more spread throughout the plant		Cluster 4 (11 plants) as above			Cluster 5 (13 plants) Plants with a medium number of large leaves		Cluster 6 (9 plants) Very large leaves spread through the plant	Cluster 7 (8 plants) Medium size leaves with plenty of gaps in the foliage	Cl 8 (2) as above	Cl 9 (2) Large number of leaves (400, 200) minor branches, leaves on various angles	Cluster 10 (8 plants) Leaves on long stalks protruding from the central stem		Cl 11 (4) Large number of small leaves		Cl 12 (4) Relatively symmetric plants with drooping leaves	Cl 13 (8) Lopsided plants with small branches	
Cluster level <i>d</i>	Cl 1 (2) Single stem plants with tiny leaves	Cl 2 (7) Slightly larger plants	Cl 3 (4) as above	Cl 4 (5) Long thin leaves from the central stem	Cl 5 (13) More leaves than cluster 4	Cl 6 (2) Some side branches	Cl 7 (2) Protrude a bit more widely	Cl 8 (7) Symmetric plants with medium size leaves	Cl 9 (6) Branchy from the central stem	Cl 10 (7) More symmetric	Cl 11 (9 plants) as above	Cl 12 (8 plants) as above	Cl 13 (2) as above	Cl 14 (2) as above	Cl 15 (7) larger plants	Cl 16 (1) Smaller more compact plant	Cl 17 (3) Leaves oriented upright	Cl 18 (1) small leaves various angles	Cl 19 (4) as above	Cl 20 (4) similar sized leaves evenly distributed	Cl 21 (4) Fewer larger leaves spread more

D.6 A set of plant groupings

Now that we have a grouping of the plants based on their acoustic density profiles, we can run a classifier to see whether we can classify the individual plants as one of the major groups. In chapter 10, it was found that once the number of plants became large, the identification a particular species from the group of different plants using a single return from the plant was very difficult.

Instead of dividing the data set into individual plants, it can be divided into clusters as given by the clustering procedure. At cluster level a (on Figure D.8) the data is divided into two classes. All of the plants in cluster 1 are identified as class 1 and all of the plants in cluster two are identified as class 2. Of the 36000 records, approximately 18000 are used to build the templates, 9000 are used for the validation set, and 9000 are used as the new unseen test set. The records are allocated to each of the datasets randomly as described in chapter 10. The classifier is run and the classification matrix for the unseen test set for separating plants from these two clusters is shown in Table D.9.

Table D.9 Classification into one of two major groups

Classification Matrix		
Actual	Calculated Class1	Calculated Class2
Class1	5817	489
Class2	304	2223
Total number of records in the test set = 8833		
Number of records misclassified = 793		
Classification Error Rate = 8.98%		

Of the 8833 randomly selected test records, only 9% were allocated to the incorrect class which is a good result.

As the granularity is decreased and the data is attempted to be classified into finer classes then the error rate increases. This follows from the fact that it becomes increasingly hard to tell the difference between two similar groups of plants. A graph of the results using the cluster groupings established in Figure D.8 is shown in Figure D.9.

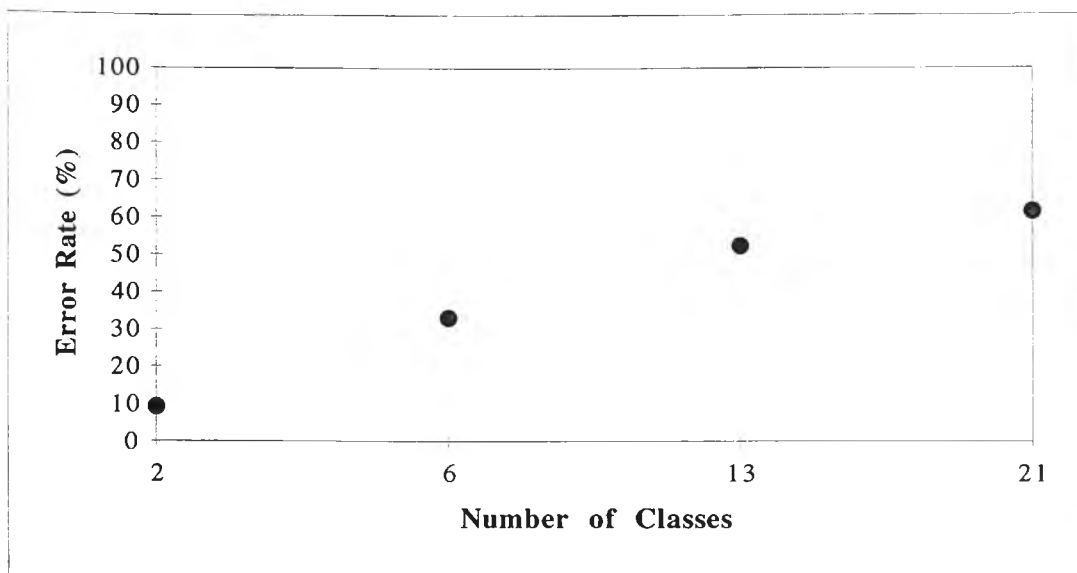


Figure D.9 The recognition percentage as a function of the number of classes being considered

Features can be used to differentiate between the major classes of plants to a much greater degree of accuracy than classifying plants as individual species. That is, if a plant needs to be recognised as belonging to one of two clusters, there is a 9% chance that it will be allocated to the incorrect cluster. If however, the plant has to be allocated as one of 100 plants, the error rate is much higher as shown in Chapter 10.

D.7 Conclusion

This chapter shows that plants can be grouped based on the features calculated from the acoustic density profile. Plants in similar groups can be differentiated from other groups using a classifier.

A table of the different clusters is shown in Table D.8. The table shows the clusters and the differences between the physical plants as the groups get smaller. The differences between groups is small once a larger number of clusters is formed and differences between the groups were difficult (if not impossible) to determine through visual inspection. The resulting table is not scientifically sound because the small differences between groups are quantified somewhat subjectively. A simple classifier can separate plants from different clusters with some degree of success.

E. Appendix - Sample plant returns

E.1 Background

The acoustic density profiles of plant specimens can change significantly depending on the orientation from which the plant is ensonified. This Appendix contains fifty acoustic density profiles for adjacent orientations of two different plants. *Eucalyptus maculata* has a relatively high correlation of the acoustic density profile, that is, the plant is relatively consistent, over adjacent orientations as shown in Chapter 6. Alternatively, *Leptospermum laevigatum* is a plant which has a large number of reflective surfaces and was shown to have a low correlation between adjacent orientations. The images of both of the plants are shown in Figure E.1. In Sections 2 and 3, the acoustic density profiles of the plants are shown with the orientation number in parenthesis following the name of the plant.

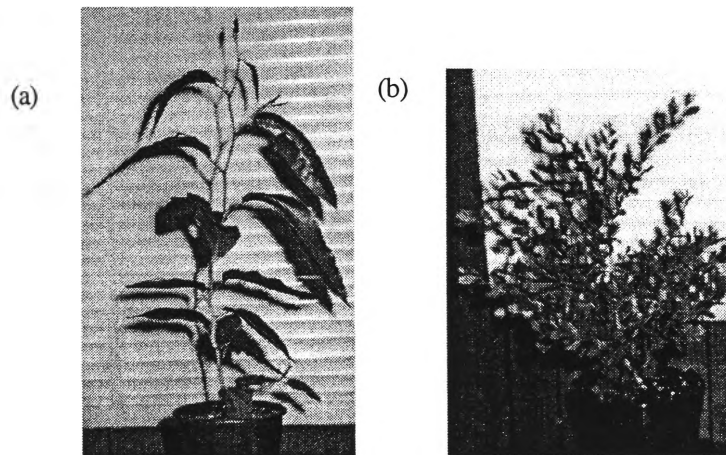
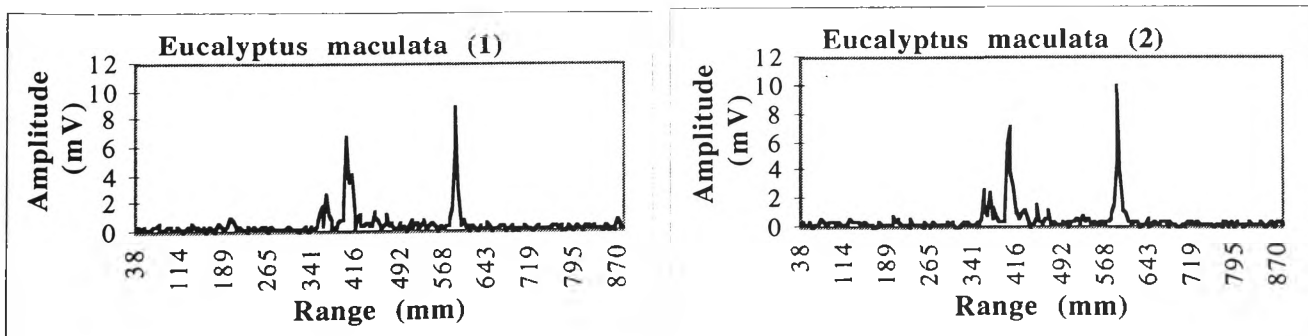
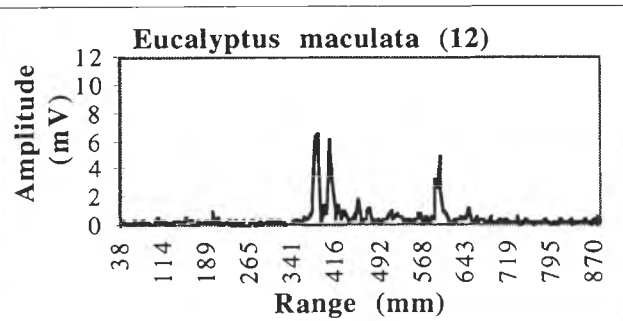
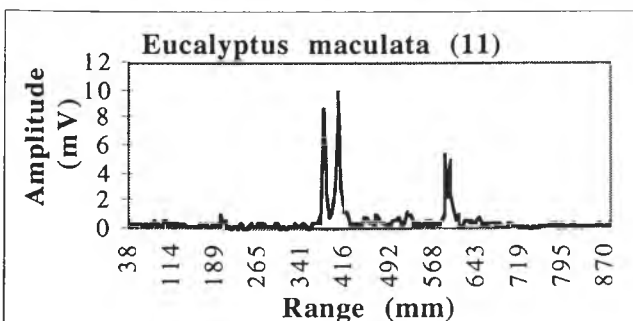
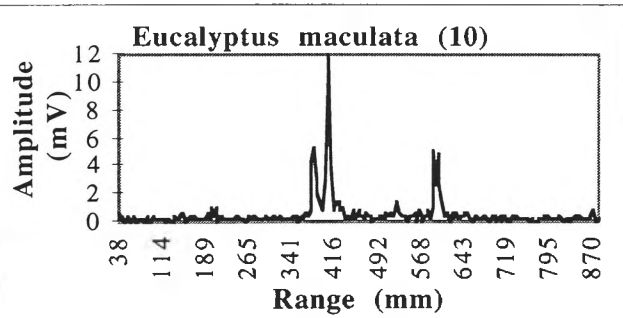
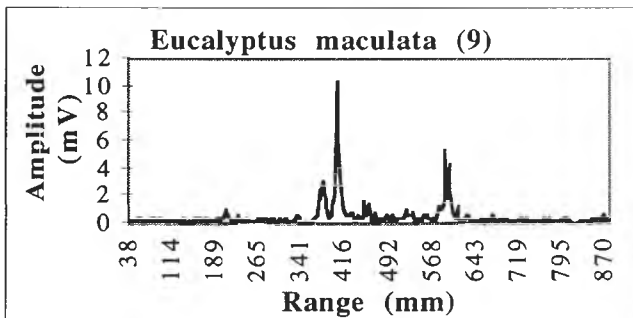
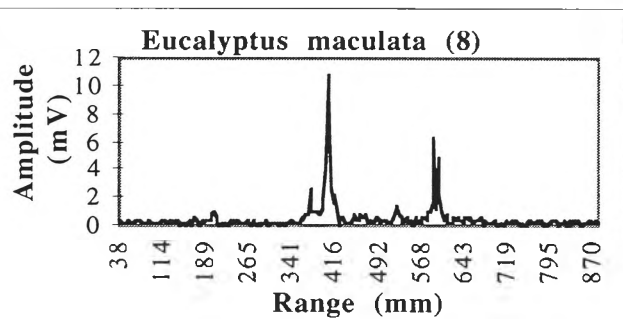
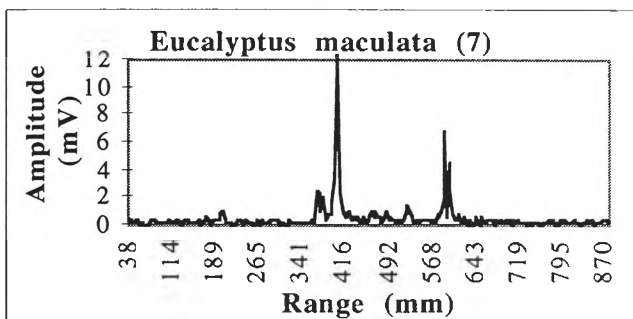
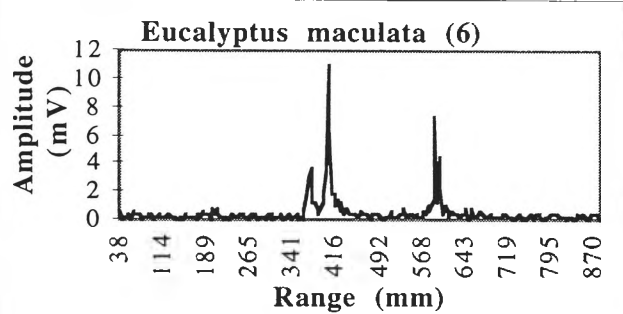
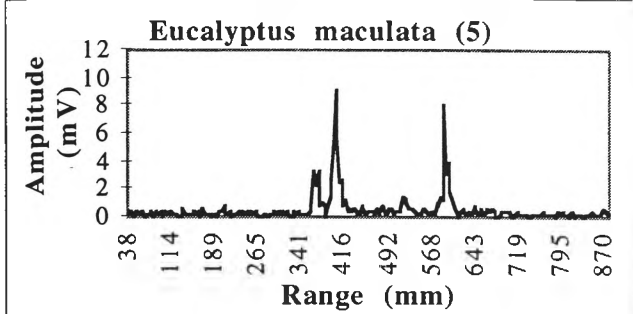
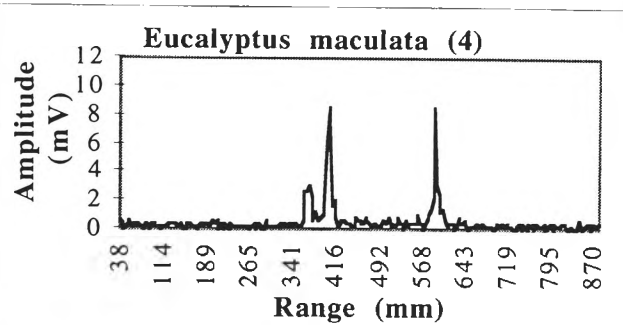
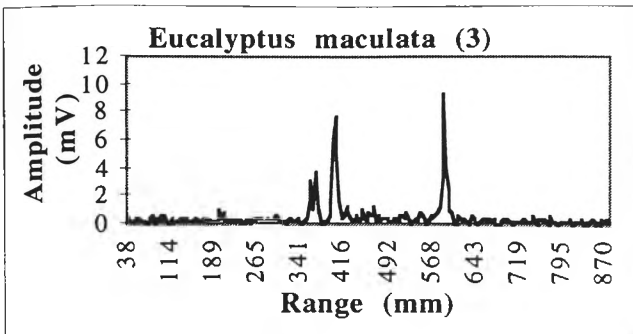
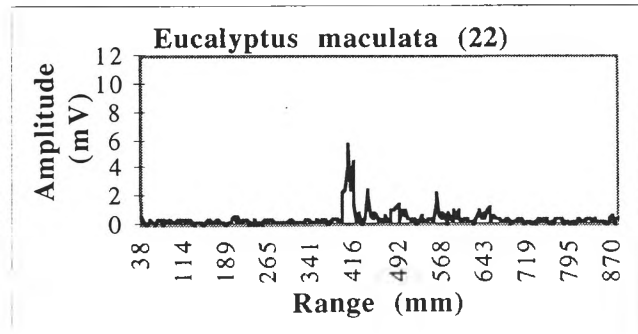
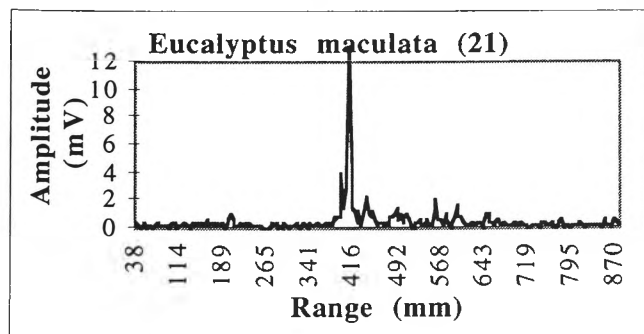
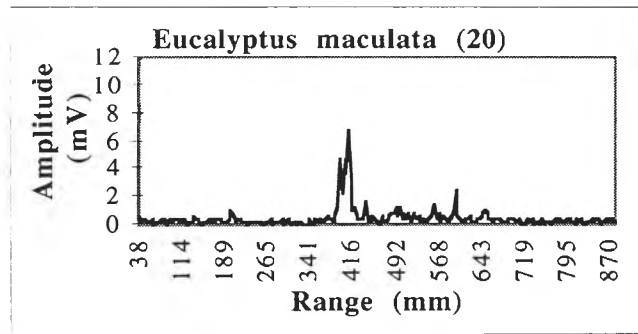
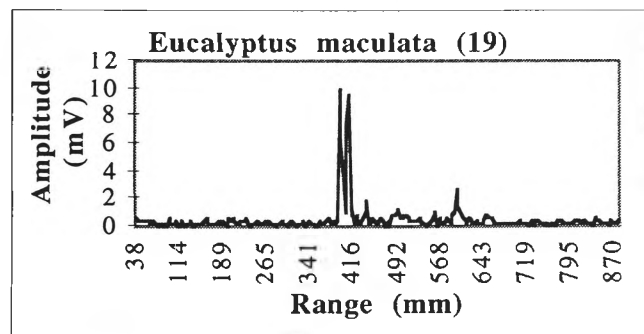
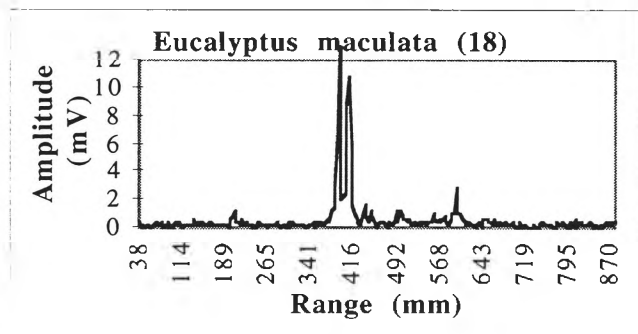
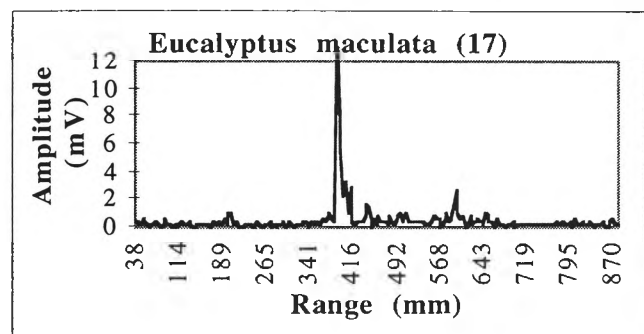
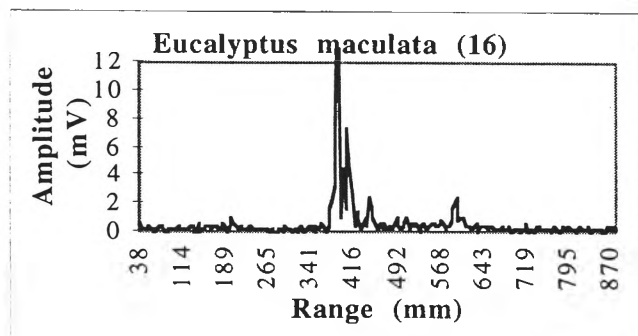
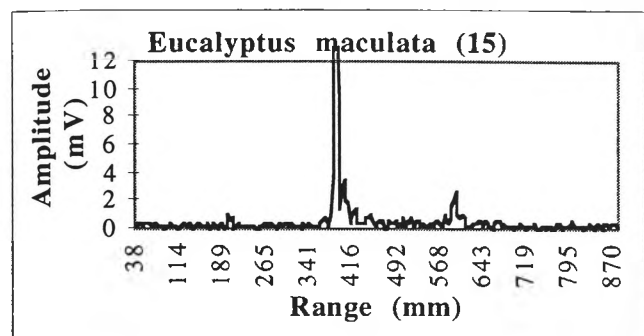
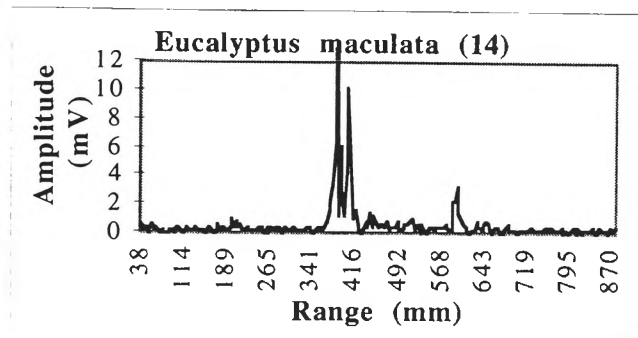
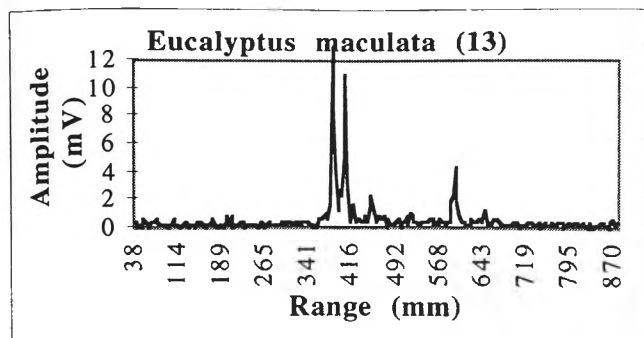


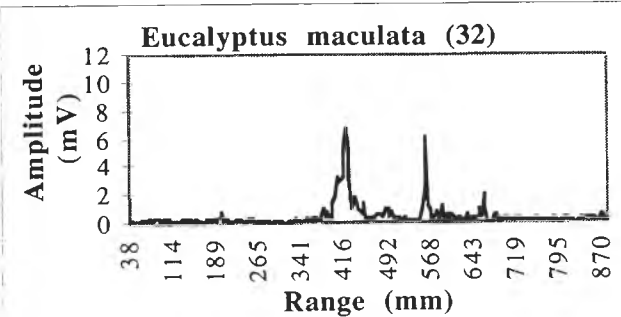
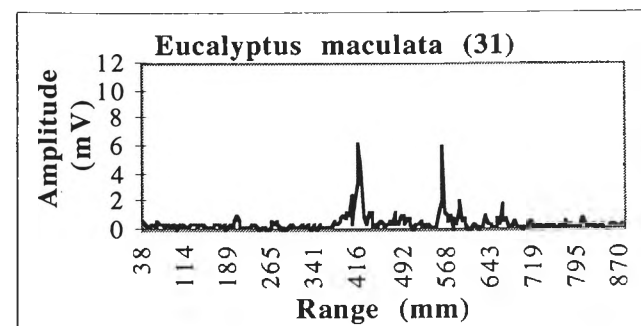
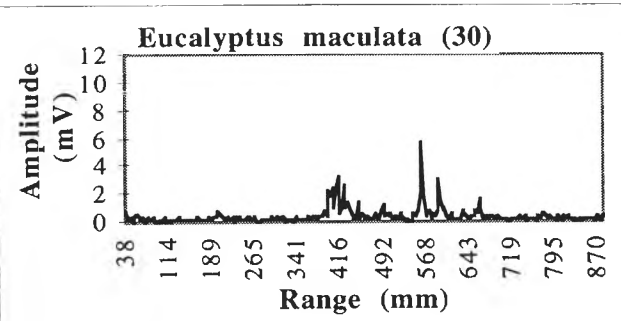
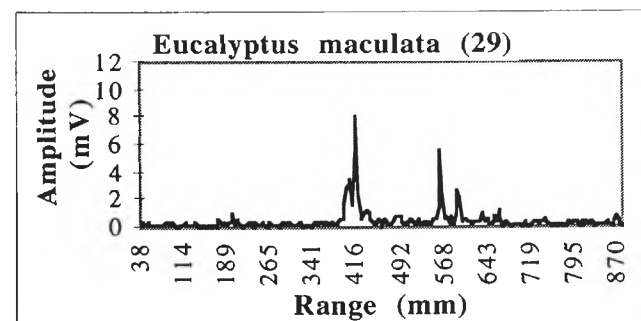
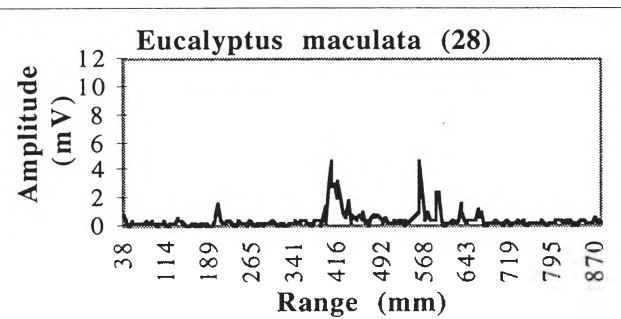
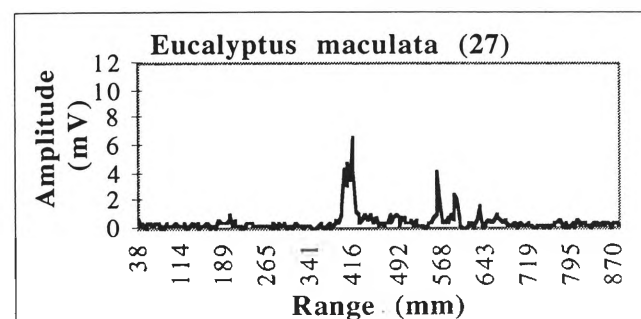
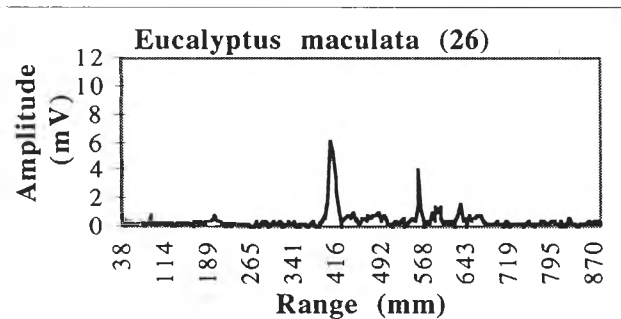
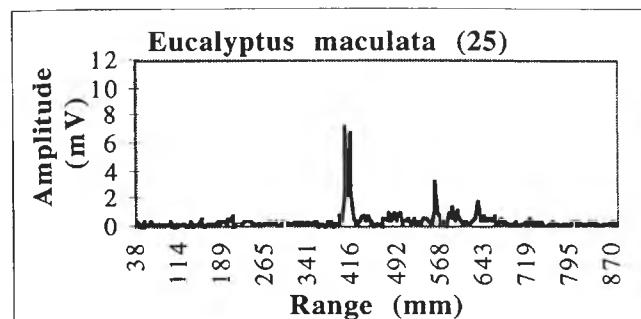
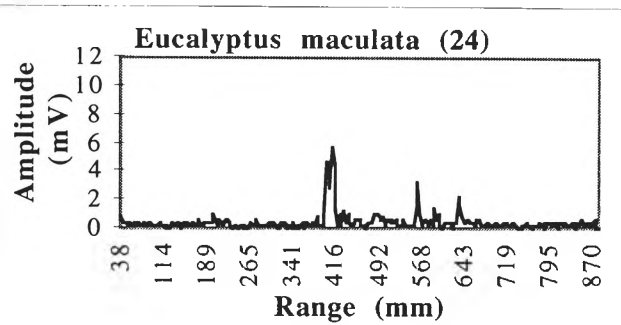
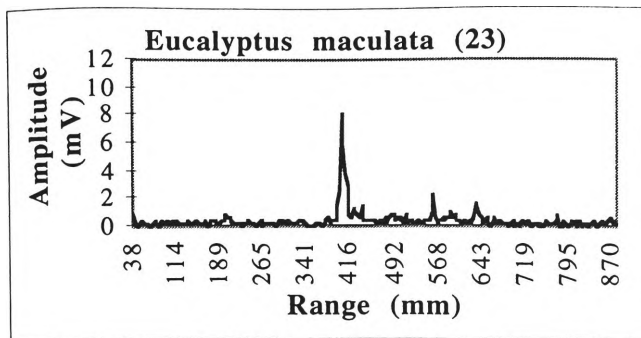
Figure E.1 Images of (a) *Eucalyptus maculata* and (b) *Leptospermum laevigatum*

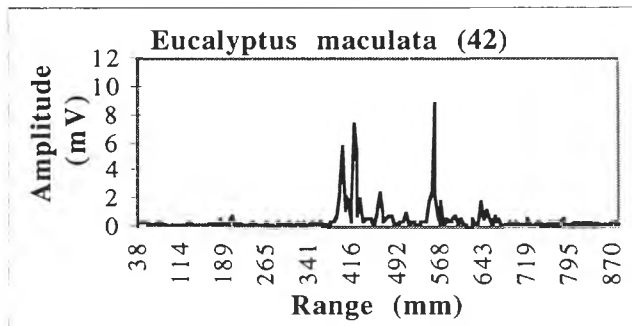
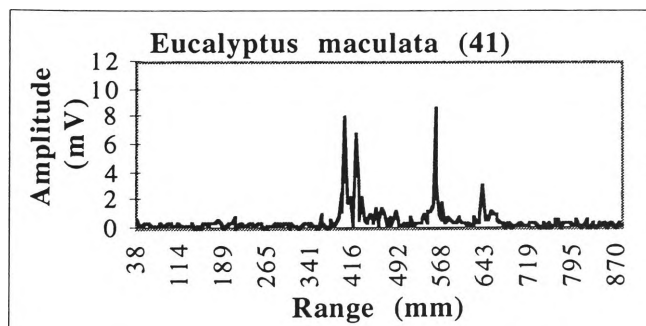
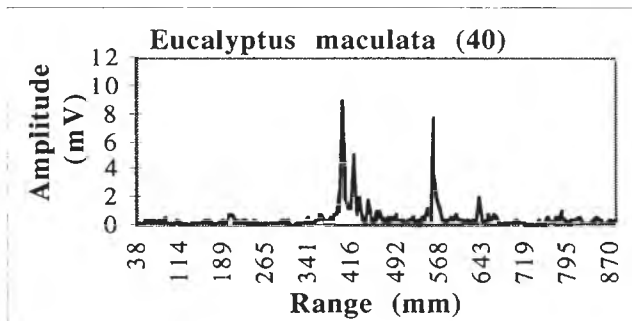
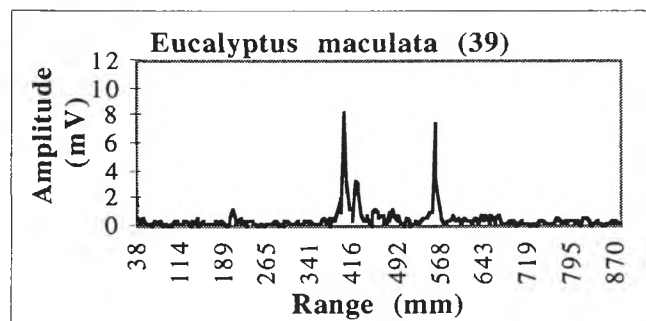
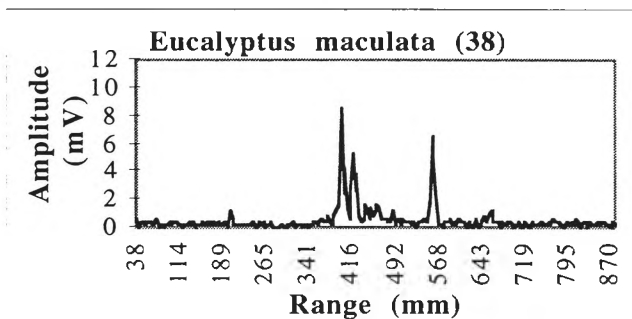
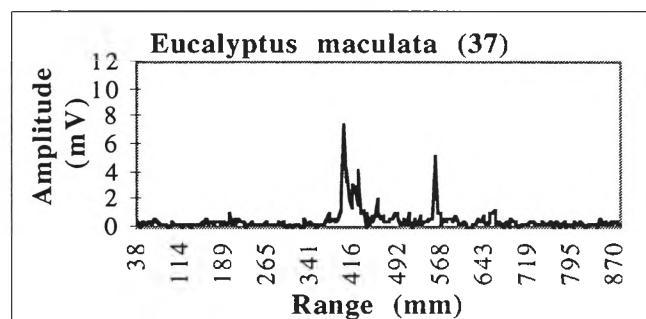
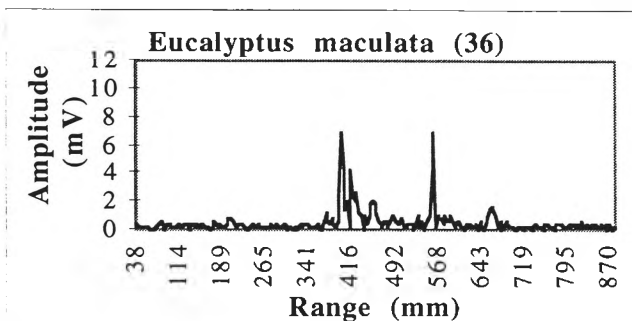
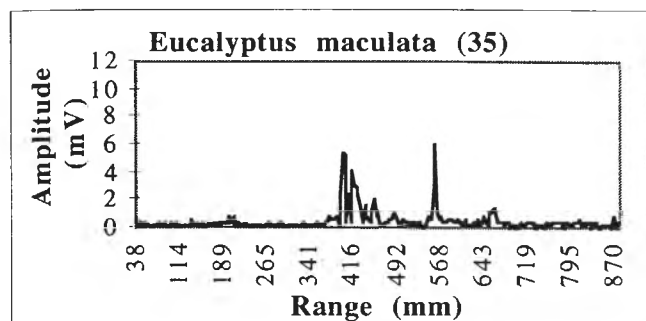
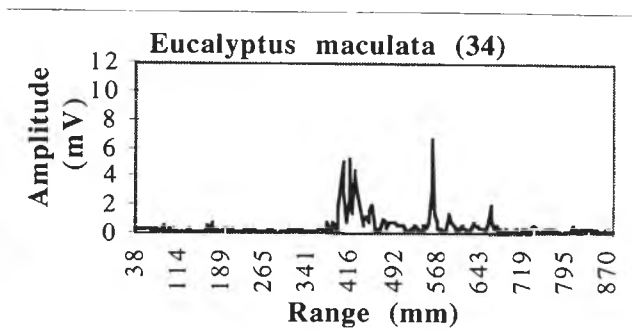
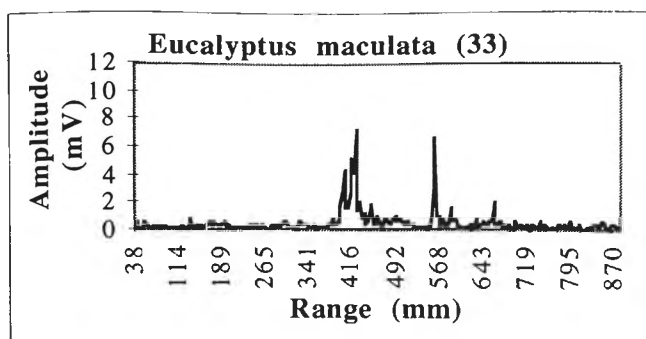
E.2 *Eucalyptus maculata*

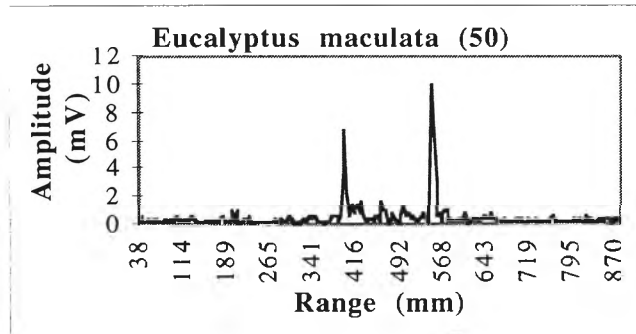
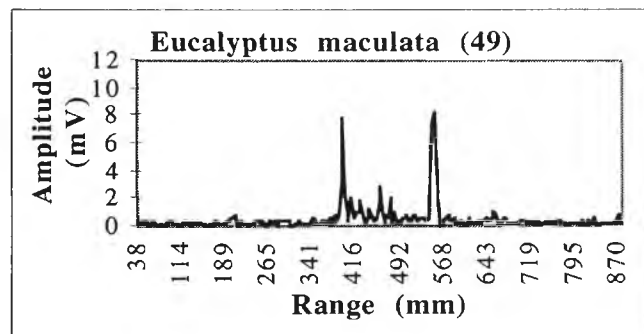
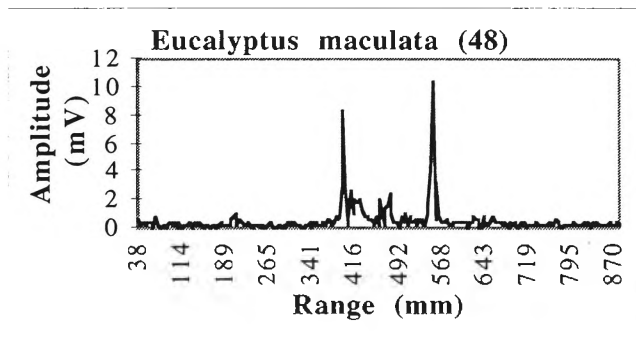
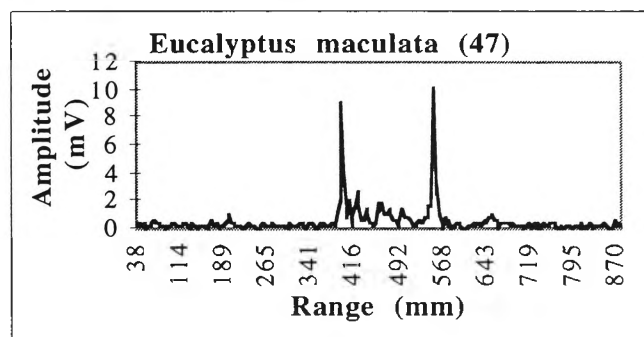
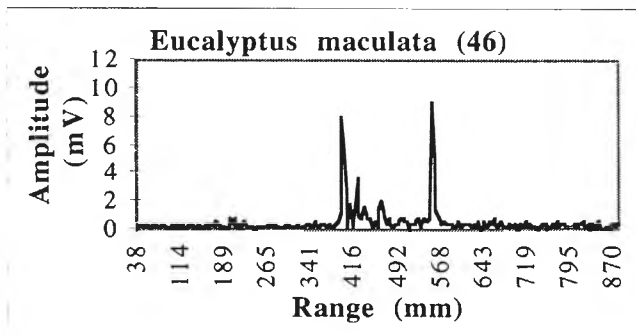
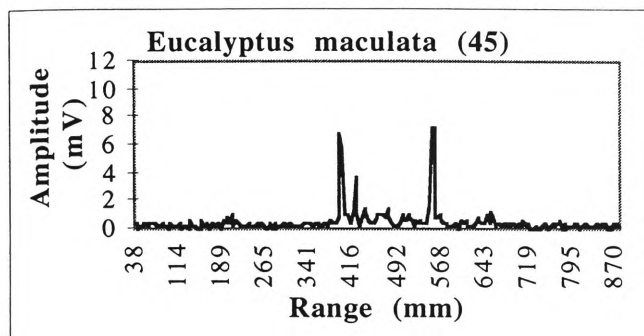
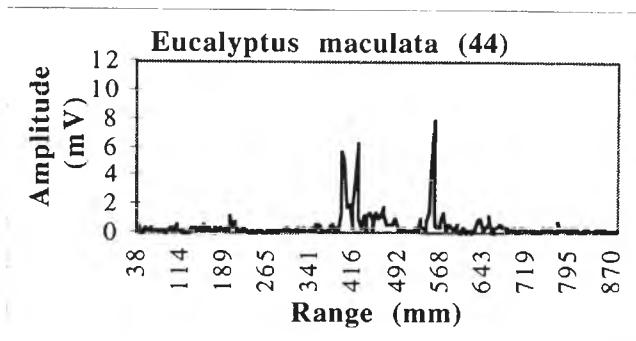
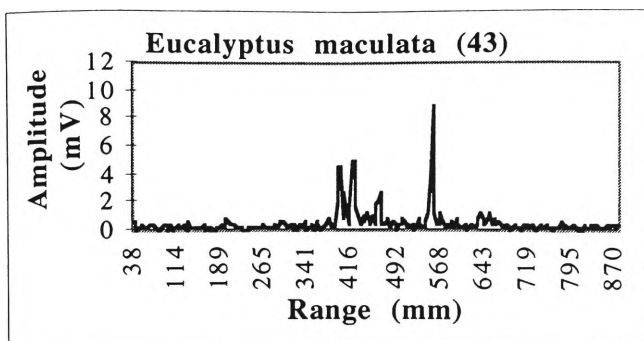




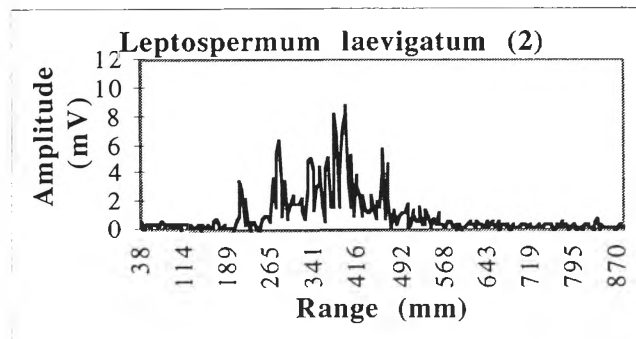
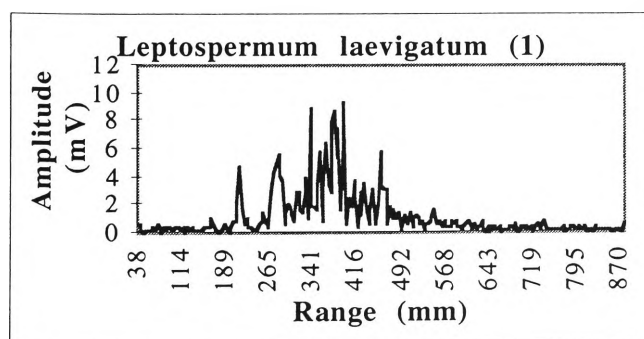


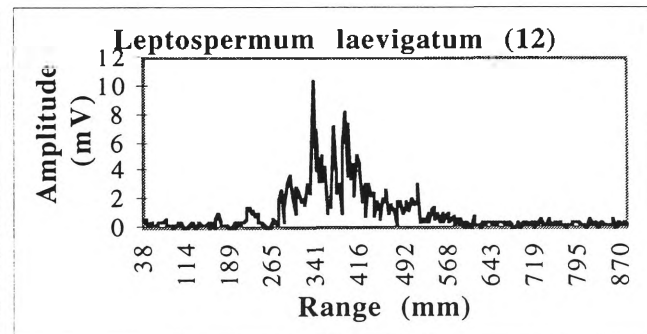
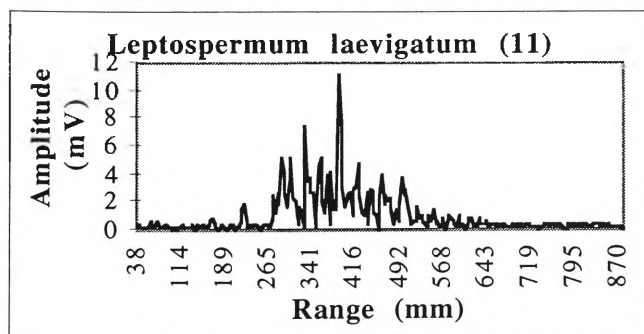
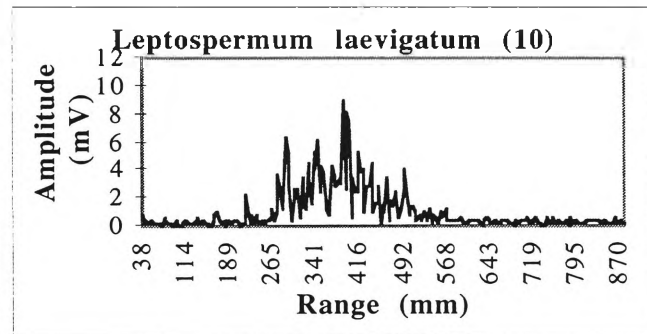
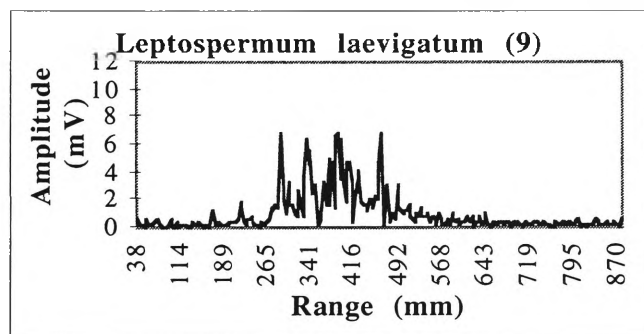
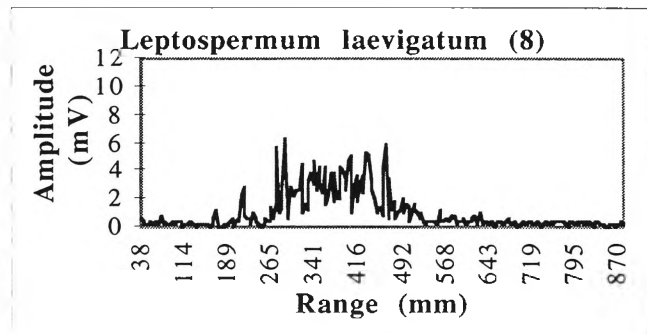
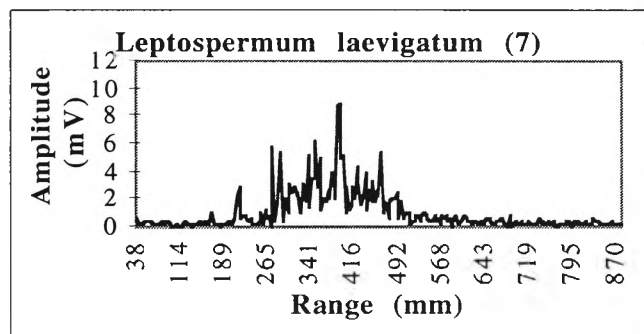
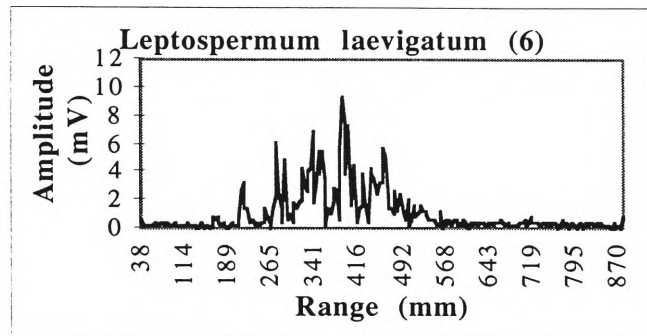
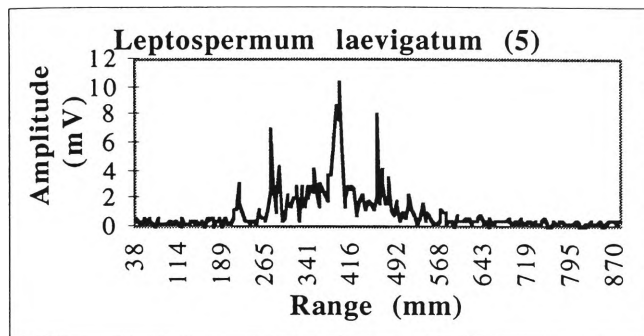
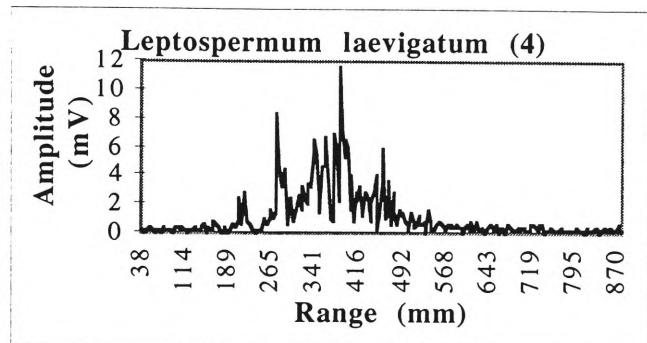
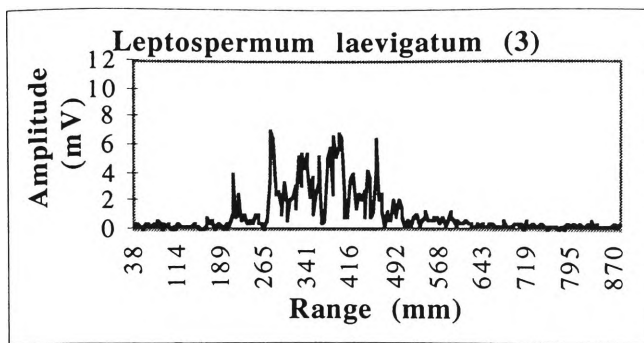


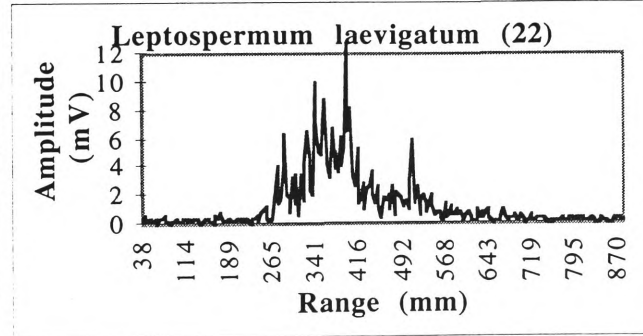
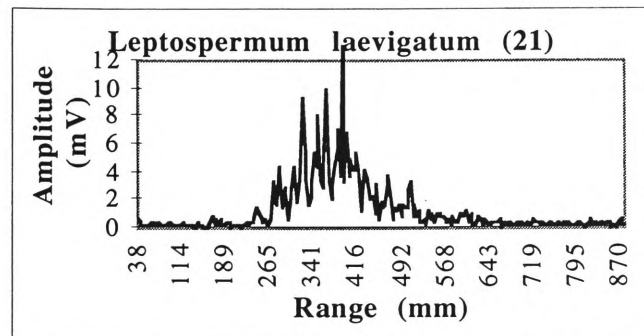
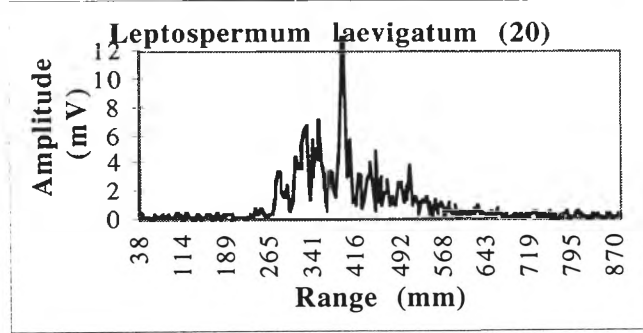
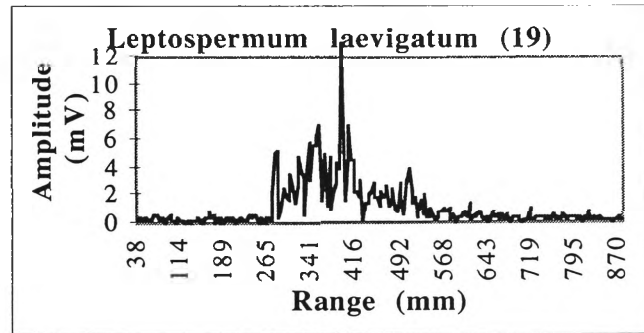
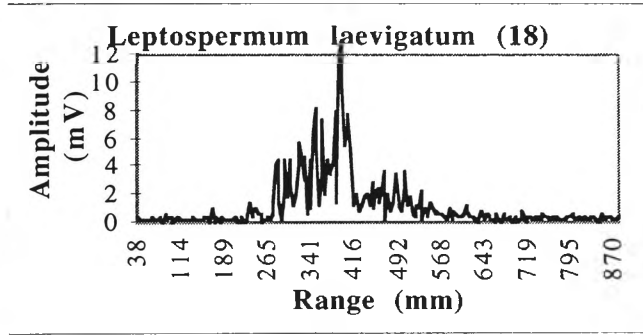
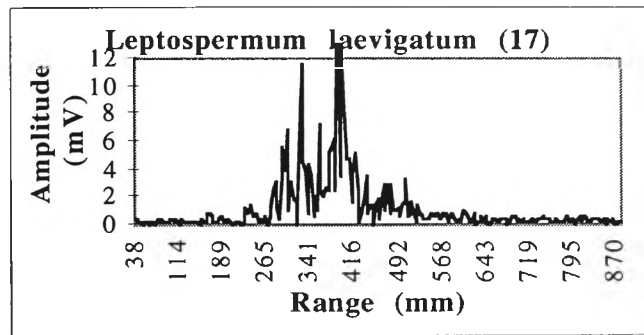
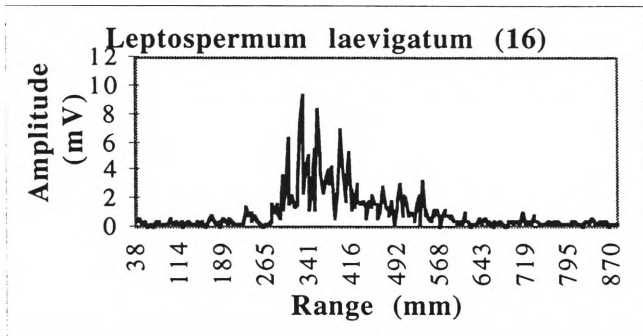
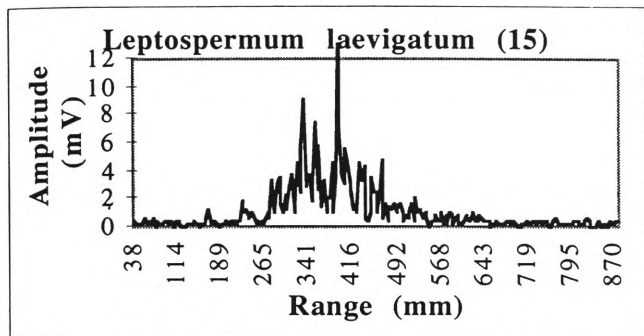
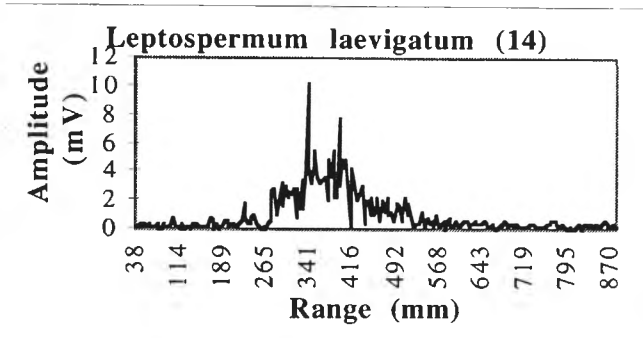
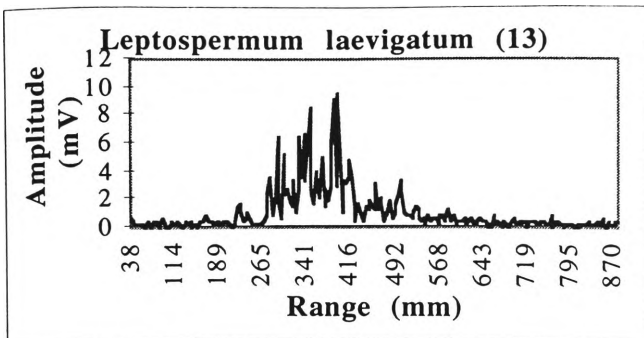


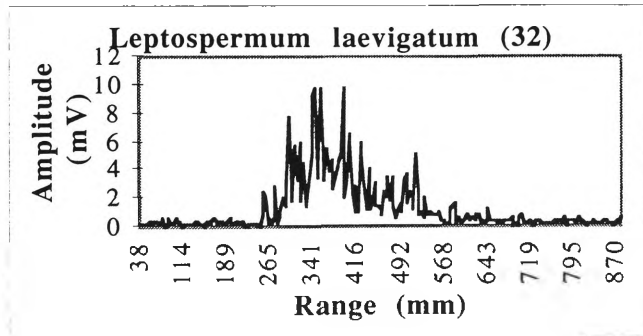
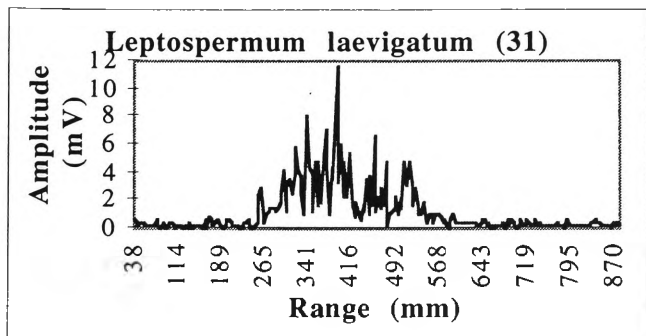
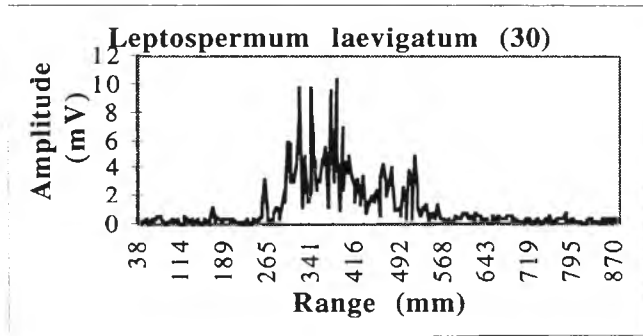
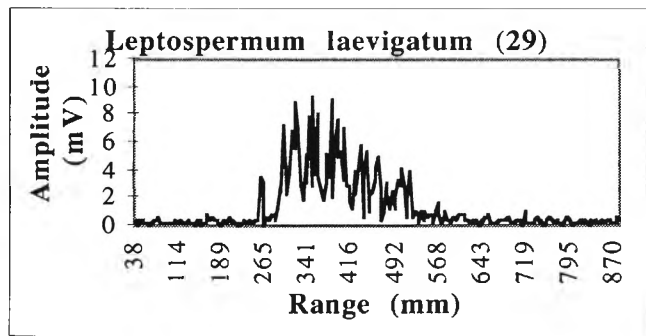
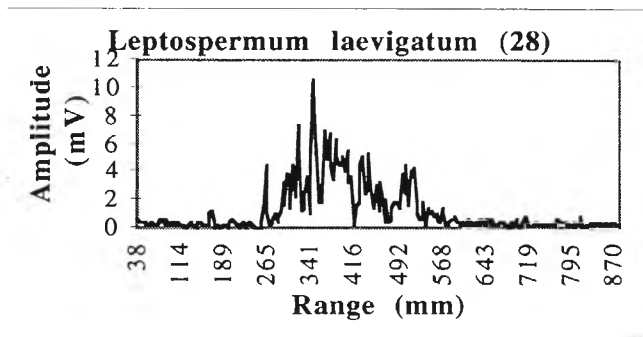
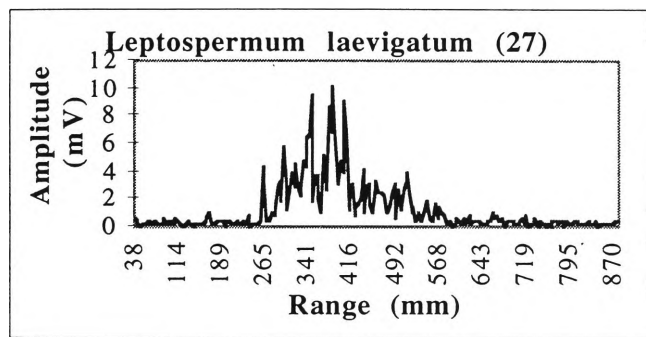
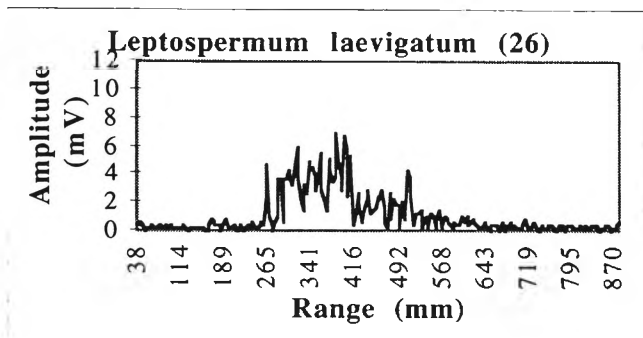
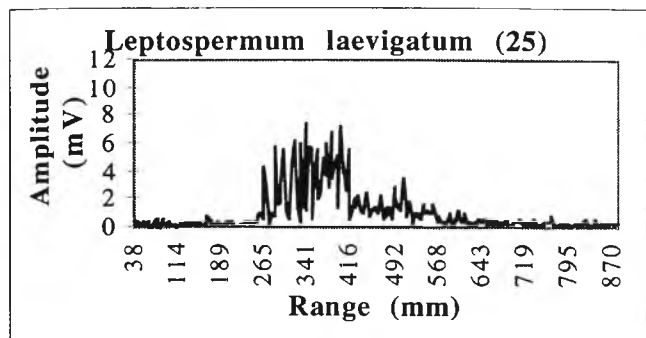
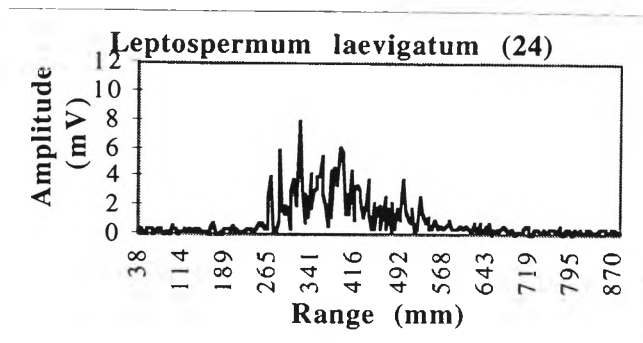
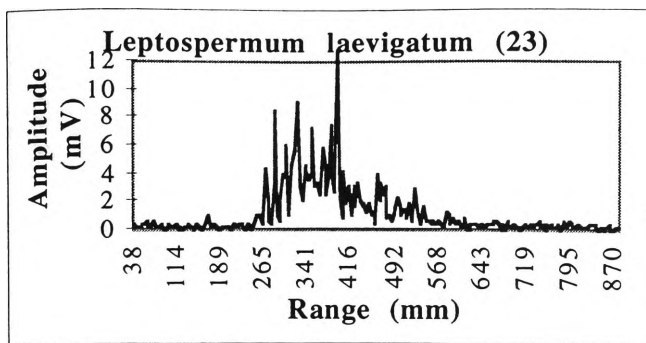


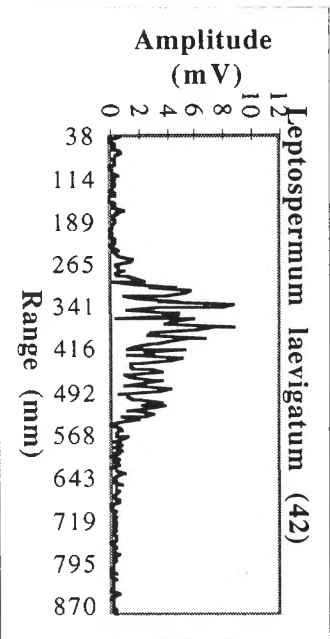
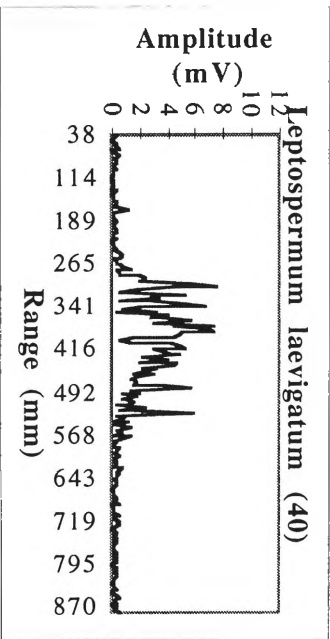
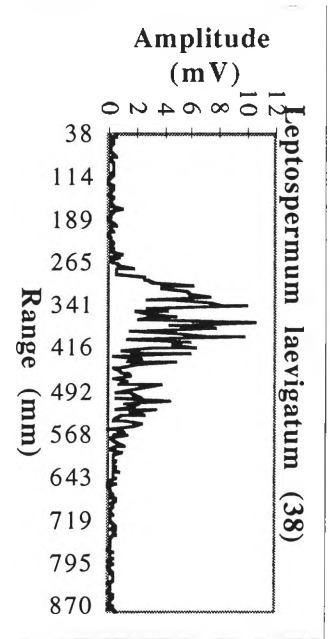
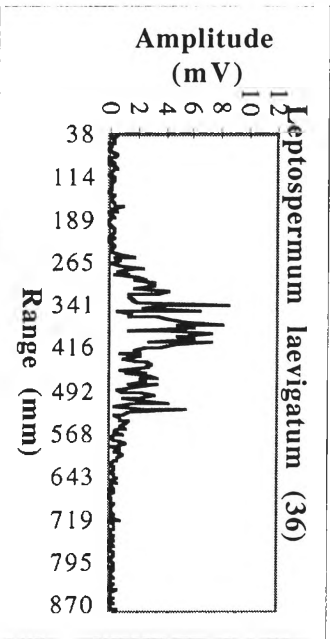
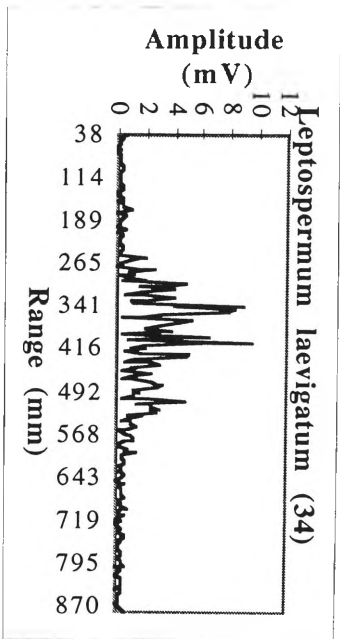
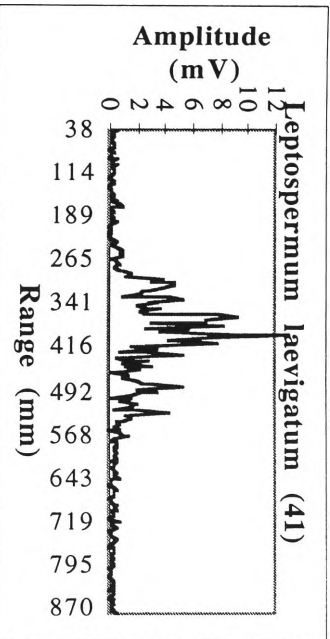
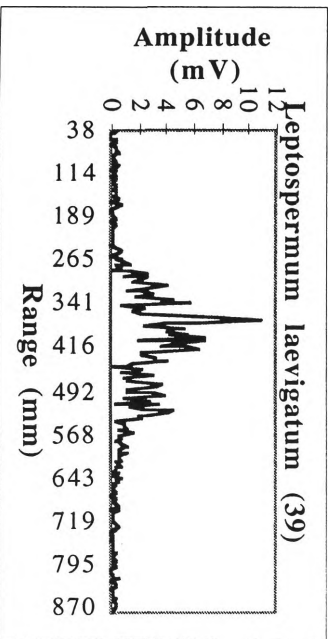
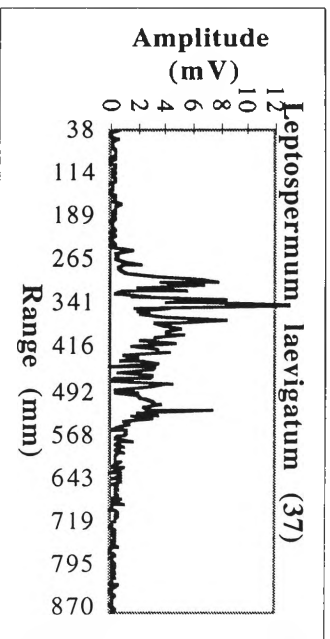
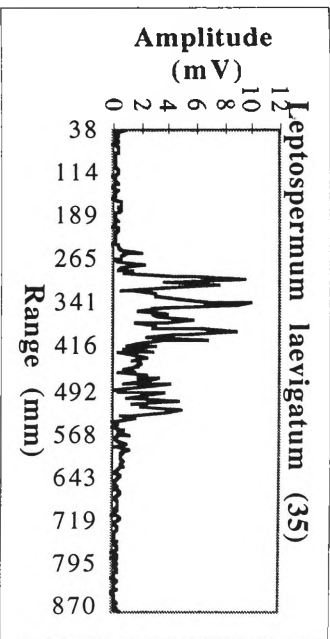
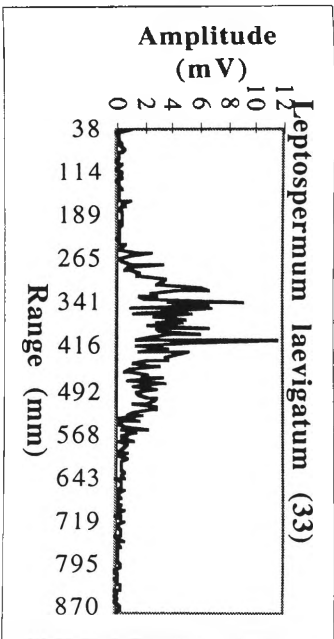
E.3 Leptospermum laevigatum

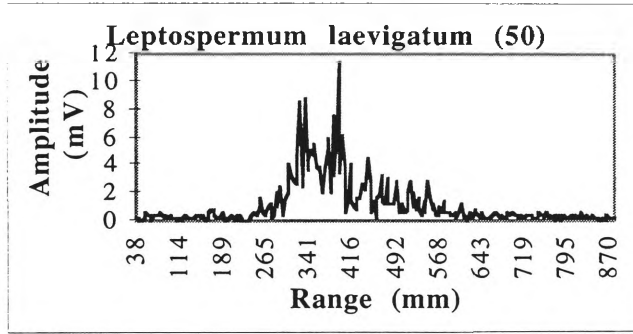
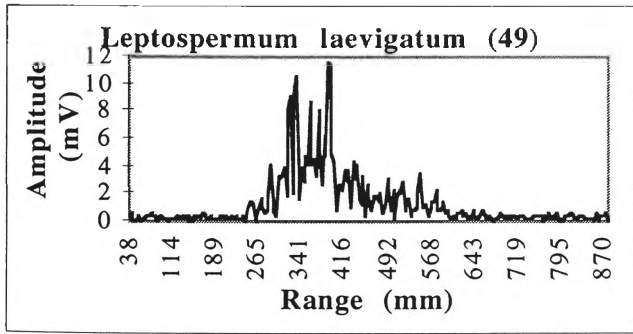
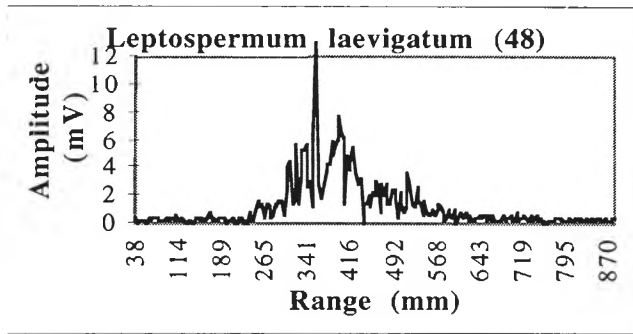
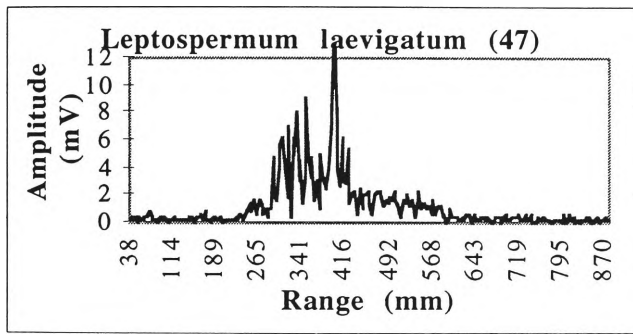
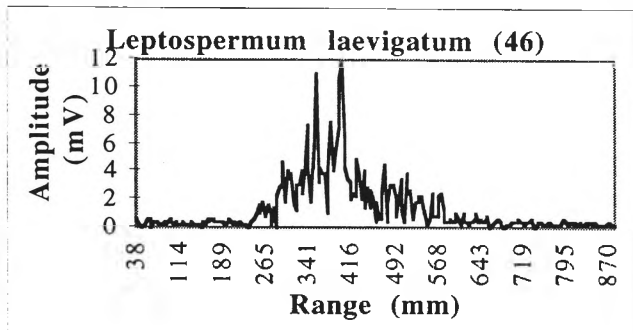
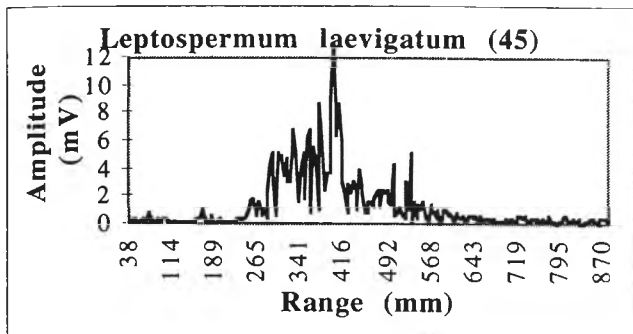
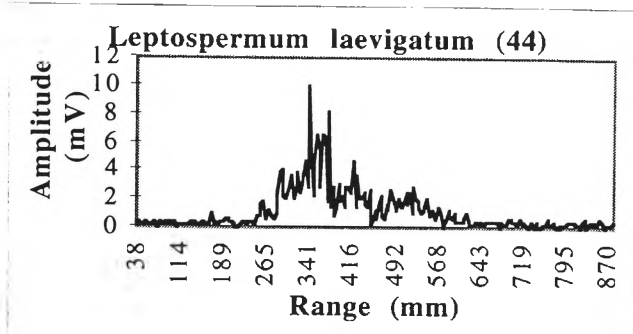
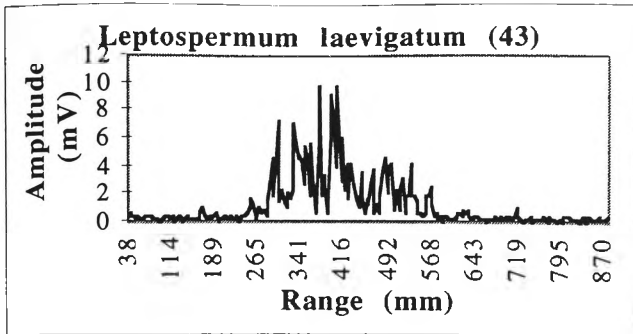












Appendix F Glossary and Acronyms

Acoustic area	This is the sum of all of the reflective surfaces within the field of the transmitter/receiver.
Acoustic Density Profile	When an object is insonified with CTFM, the resulting spectrum is a profile of the field of insonification. This profile contains information about all of the surfaces within the field of the sensor / transmitter and the ranges at which they occur.
Acoustic Depth	This is the depth over which echoes are received from an object. In the case of plants, the acoustic depth is the minimum depth of the plant ie. surfaces at the extremities of the plant may not produce an echo either due to the orientation of the surfaces or acoustic shadowing.
Acoustic shadowing	A surface is shadowed acoustically when sound energy is prevented from reaching the surface by other surfaces between it and the source.
Acoustic Symmetry	The dictionary definition [Macquarie, 82] of symmetry is being regular in form or arrangement of corresponding parts. An object displays acoustic symmetry when the reflected echo is similar from one orientation to another.
Acute	(leaf shape) Pointed, having a short, sharp apex, the converging edges forming an angle less than 90°.
Alternate	(leaves) inserted singly at different levels along the branches.
AM	Amplitude Modulated energy.
ANN	Artificial Neural Network.
Annular	(leaves) ring shaped.
Apex	(leaves) tip.
Audition	The act, sense, or power of hearing.
Backscatter	When an object is insonified, backscatter is the process of the signal being reflected back to the receiver.
Bandwidth	The frequency band of the transducer.
Beacon	An artificial object in the environment which can be placed strategically so that it can be used to localise the position of a mobile robot.
Beamwidth	The angle between the directions where the response is 3 dB less than at its maximum.
Bipinnate	(leaves) Of a compound leaf, with the lamina divided twice pinnately.
Blind Aid	See Ultrasonic Blind Mobility Aid
c	The speed of sound in air (342.52 ms ⁻¹ at 20° C)
Calibration curve	The calibration curve is used to adjust for the degradation of amplitude with range to the object. It is calculated by measuring and recording the amplitude for different ranges of a set object (for example, a flat wall). It is important that the sensor is orthogonal at all ranges which the value is noted.
Cluster Analysis	A statistical technique for grouping samples into similar groups.
Convolution	A weighted mean of two signals. Convolution is commutative, associative and distributive.
Correlation	Correlation is used to compare 2 signals. The result of a correlation is a measure of the similarity between them (see

Cross-validation	Chapter 6). is a technique where a certain amount of data is retained for testing the classifier once the model has been developed. Test data is used to help select the best features for a particular set of plants and on completion, the cross-validation set is used to provide a more accurate estimate of the predictive capability of the classifier.
CTFM	Continuous Transmission Frequency Modulation. The literature occasionally refers to CTFM as Continuous Tone Frequency Modulation.
DDA	Descriptive Discriminant Analysis.
Dead Reckoning	The process of estimating the current position of a robot based on the previous position and the current velocity information.
Diffuse Scatterer	A diffuse scatterer is one which spreads the reflected echo over a wide angle. This means that little (if any) signal will be reflected back to the receiver.
Discrete systems	A discrete system is one which samples data at set points in time.
Discriminant Analysis	Discriminant analysis is a tool which is used to classify an individual sample into one of a finite number of groups of classes.
Echo	An echo is sound energy which is reflected from a surface to the receiver.
Electrostatic transducer	
Feature	A measure of the input data calculated using Feature Extraction.
Feature extraction	s used to create new features which are calculated directly from the input pattern. The goal of the new features are to characterise the input pattern.
Feature selection	The process of selecting a subset of features in order to reduce the amount of data to be presented to a classifier. This is discussed in Chapter 210
FFT	Fast Fourier Transform. The FFT transforms the signal from the time domain to the frequency domain by identifying the component frequencies of any signal.
Field of audition	the acoustic equivalent of the optics term field of view.
FMCW	Frequency Modulated Continuous Wave sensing. Term used in Radar.
Foliage	The representation of leaves, branches and flowers.
Freedman's Model	[Freedman, 62] found that as the cross-section area of an ensonified object is increased, so is the amplitude of the returned signal.
Frequency Analysis	This involves analysing the signal in the frequency domain. The signal is converted from the time domain to a spectrum of individual frequencies which make up the signal. It is often done using a Fast Fourier Transform (FFT). This tells us which individual frequencies are present at a certain period in time.
Frequency spectrum	This is the reduction of a signal into its component frequency elements. The x-axis represents the frequency and the y-axis represents the amplitude at that frequency
Gaussian	
Global Correlation	This is when a signal is compared against another signal from a non-adjacent orientation.
Human hearing	2 Hz to 20 kHz.
Hydrophone	A receiver which converts acoustic pressure into an electrical signal.

Hz	Hertz. Cycles per second.
Insonify	To irradiate with sound energy.
KASPA	Kays' Advanced Spatial Perception Aid. A mobility aid which is used by blind people to perceive their environment.
Landmark	A natural object in the environment which can be used for localising the position of a mobile robot. An example may be a piece of office furniture, a door frame or a pot plant.
Leaf density	This is the number of leaves per unit area. A dense plant is one which has many leaves in a certain area. A sparse plant is one which has few leaves in the same size area.
Lidar	Light Direction and Ranging. Used to determine the range to objects by transmitting a signal in the light spectrum and detecting the echo.
Local Correlation	This is when signals from adjacent orientations of the plant are compared
<i>m</i>	Calibration measure. Some of the features calculated from the acoustic density profile are measured relative to the standard calibration measure, <i>m</i> , in order to make them independent of minor variations in the particular transducers that are being used for the experiments. The calibration measure, <i>m</i> , was selected as the amplitude detected at the transducer when a large specular surface is insonified at a range of 0.500 metres. This calibration value was established when the plant database was collected in Chapter 5 and was found to be 100 mV.
Mobility aid	see Ultrasonic Blind Mobility Aid
Multivariate Analysis	When analysing a dataset with more than 1 variable, it is useful to study all of the variables simultaneously. Methods used to conduct such analysis are known as multivariate methods.
Narrow Band	Signals whose spectra are concentrated in a small band relative to the mean frequency.
Neural Network	An implementation of a learning algorithm inspired by research about the brain. Often referred to as an Artificial Neural Network and typically contains layers of so called artificial neurons with nodes, connections and nodes.
Neuron	The basic building block of the brain, and is a stand-alone analogue logical processing unit.
NN	Neural Network.
Outlier	A data item which
PDA	Predictive Discriminant Analysis.
Perception	The reception, coding, transmission and processing of information.
Point Scatterer	A surface which acts as a point and reflects the signal over a wide angle.
Pulse Sonar	See TOF
Radar	Radio Direction and Ranging. Used to determine the range of objects by transmitting a signal in the radio spectrum and detecting the echo.
Range Cell	The result of CTFM processing is a FFT on which frequency is proportional to range and range can be calculated directly from frequency if you know the sweep time and the sweep range for the system. Each of the cells in the FFT represent an absolute range whose amplitude is related to the sum of the reflective surfaces at that range. These cells are known as range cells.
Receiver	A transducer which records sound energy
Region of insonification	the acoustic equivalent of the optics terms region of

R_x	illumination.
Sampling	Receiver.
Sensor	taking parts of a signal at set time intervals.
SNR	A transmitter/receiver pair.
Sonar	signal-to-noise ratio.
	Sound Direction and Ranging. Used to determine the range to objects by transmitting a signal in the ultrasonic spectrum and detecting the echo.
Sonicguide	The previous commercial name for KASPA.
Spectra	See Frequency Spectrum
Spectral Content	refers to when the signal is viewed in the frequency domain. The signal is made up of a series of frequencies and when represented as a series of frequencies, it is known as a frequency spectrum.
Specular	A specular surface is one which has the same properties that a mirror does in visible light. At ultrasonic wavelengths, all smooth surfaces are specular.
Stepwise backward feature selection	This feature selection technique starts with a complete set of features which are removed one at a time based on the removal of the feature which produces the best classification achieved. Feature removal continues until it reaches some set error rate or all of the features are removed.
Stepwise forward feature selection	This feature selection technique starts with the best single feature which classifies the data well and then continues to add the best single feature to the current feature set until it reaches some set error rate or all of the features are exhausted.
Template correlation	This is where a template is built of a plant which is the average of all of the features through a complete rotation. This template can be used to correlate with specific orientations of the plant.
The Filter method of feature selection	This is a method of reducing the number of features presented to the classifier by looking at the training data before any optimisations are performed. This is demonstrated in Chapter 8.
The Wrapper method of feature selection	This is a method of reducing the number of features where the classifier is run on the candidate features and the resulting classification error is used to select the best combination, that is the combination of candidate features which produce the lowest error.
Time Analysis	This involves looking at the signal in the time domain. The time domain is fundamental for any signal.
Time delay	The elapsed time between one action and the next.
Time Domain	A signal which is represented with amplitude on the y-axis and time on the x-axis is in the time domain.
Time of Flight	see TOF.
TOF	Time of Flight. This is used to describe a sensing system which transmits a signal and then records the amount of time that it takes for the signal to be detected at the receiver. This signal can be used to calculate the range of objects. Some examples of TOF systems are Sonar and Radar.
Transmitter	A transducer which transmits sound energy.
T_x	Transmitter.
Ultrasonic	An ultrasonic wave is a wave whose frequency is above the audible range of 20 kHz.
Undersampling	can cut off peaks by not taking enough points. Causes a high frequency problem called 'aliasing'.
US	Ultrasonic.

Vision	A sensor which collects the light reflected from a scene and forms it into an image.
Voxel	A unit of volume area.
Wide Band	Signals whose spectra is spread relative to the mean frequency.

Appendix G Bibliography

- [Aha & Bankert, 1994] Aha, D.W., Bankert, R.L.,1994,Feature selection for case-based classification of cloud types, Working Notes of the AAAI94 Workshop on Case-Based Reasoning pp 106-112. Seattle, WA : AAAI Press.
- [Ainsworth, 1998] Ainsworth, W.A.,1988, Speech Recognition by Machine, Peter Perigrinis
- [Airasian, 1973] Airasian, P.,1973, Evaluation of the binaural sensory aid for the blind, A.F.B. Res. Bull., 26, 51
- [Aitken & Bower, 1982] Aitken, S., Bower, T.G.R.,1982, Use of the Sonicguide in infancy, Journal of Visual Impairment and Blindness, 76, pp91-100
- [Akaho & Amari, 1990] Akaho, S., Amari, S.,1990,On the Capacity of 3-layer neural networks, Proceedings IJCNN-90 (San Diego), Vol III, June 1990., pp1-6
- [Aleksander, 1989] Aleksander, I. (Ed),1989, Neural Computing Architectures, MIT Press
- [Almuallim & Dietterich, 1992] Almuallim, H., Dietterich, T.G.,1992, Efficient Algorithms for Identifying Relevant Features, Proceedings of the Ninth Canadian Conference on Artificial Intelligence
- [Altes, 1980] Altes, R.A.,1980,Detection, Estimation and Classification with Spectrograms, Journal of the Acoustical Society of America, Vol. 67, No. 4, April, pp 1232-1246
- [Aluallim & Dietterich, 1994] Almuallim, H., Dietterich, T.G.,1994,Learning Boolean concepts in the presence of many irrelevant features, Artificial Intelligence, 69(1-2) : pp 279-305, November 1994
- [Andrews, 1972] Andrews, H.C.,1972, Mathematical Techniques in Pattern Recognition, Wiley-interscience
- [Arias & Curet, 1993] Arias, C., Curet, C.A.,1993, Echolocation : A study of Auditory Functioning in blind and Sighted subjects, Journal of Visual impairment and Blindness, March 01, v 87, n 3
- [Atlas *et al*, 1990] Atlas, L., Cole, R., Connor, J., El-Sharkawi, M., Marks II, R., Muthusamy, Y., Barmard, E.,1990, Performance Comparisons between backpropagation networks and classification trees on three real-world applications, In Advances in Neural Information Processing Systems (Vol 2), D. Touretzky (Ed.) San Mateo CA : Morgan Kauffmann
- [Auran & Malvig, 1996] Auran, P.G., Malvig, K.E.,1996,Clustering and Feature Extraction in a 3D Real-Time Echo Management Framework, Proceedings of the 1996 IEEE Symposium on Autonomous Underwater Vehicle Technology, pp.300-307
- [Barnard, 1992] Barnard, E.,1992,Optimization for training neural nets, IEEE Transactions on Neural Networks, vol 3, pp 232-240, March 1992
- [Barshan & Durrant-Whyte, Barshan, B., Durrant-Whyte, H.F., 1993, An

- 1993] Inertial Navigation System for a Mobile Robot, Proceedings of the 1st IAV, Southampton, England, pp. 54-59, April 18-21, 1993.
- [Barshan & Kuc, 1990] Barshan, B., Kuc, R., 1990, Differentiating Sonar Reflections from Corners and Planes by Employing an Intelligent Sensor, IEEE Transactions on Pattern Analysis and Machine Intelligence, June 1990, pp 560-569
- [Barshan & Kuc, 1992] Barshan, B., Kuc, R., 1992, A Bat-like Sonar system for Obstacle Localisation, IEEE Transactions on Systems, Man, and Cybernetics, Jul 01, v22, n4
- [Bass, 1966] Bass, J., 1966, Elements of Probability Theory , Academic Press
- [Bass, 1984] Bass, H.E., 1984, Physical acoustics volume XVII, Chapter 3, Absorption of Sound in Air, Edited by W. P. Mason and R.N. Thurston.
- [Baum, 1988] Baum, E.B., 1988, On the capabilities of multilayer perceptrons, J. Complexity, vol 4, pp. 193-215
- [Baum, 1989] Baum, E.B., 1989, What size net gives valid generalisation ?, In Neural Information Processing Systems 1, Ed. Touretzky, D., pp81-89, San Mateo, CA, Morgan Kaufman
- [Beale & Jackson, 1990] Beale, R., Jackson, T., 1990, Neural Computing : An Introduction, IOP Publishing Ltd.
- [Bedworth, 1996] Bedworth, M., 1996, Markov Chain Prediction Fusion for Automatic Target Recognition,
- [Belforte *et al*, 1979] Belforte, G., DeMori, R., Ferraris, F.A., 1979, A contribution to the automatic processing of electrocardiogram using syntactic methods, IEEE Transactions on Biomedical. Engineering, BME-26, 1979
- [Bendat & Piersol, 1971] Bendat, J.S., Piersol, A.G., 1971, Random Data : Analysis and Measurement Procedures, New York : John Wiley and Sons
- [Benson, 1979] Benson, L., 1979, Plant Classification, D.C. Heath and Company
- [Berenak, 1954] Berenak, L.L., 1954, Acoustics, McGraw-Hill, New York.
- [Beuter, 1985] Beuter, K., 1985, Sound Pattern Recognition Supports Automatic Inspection, Sensor Review, Jan, pp 13-17
- [Blum *et al*, 1991] Blum, Edward, Li, Leong, 1991, Approximation Theory and Feedforward Networks, Neural Networks 4:4, 511 - 515
- [Booth & Booth, 1993] Booth, I.J.; Booth, K.H.V., 1993, Using neural nets to identify marine mammals, OCEANS '93. Engineering in Harmony with Ocean Proceedings
- [Borenstein & Koren, 1995] Borenstein, J., Koren, Y., 1995, Error Eliminating Rapid Firing for Mobile Robot Obstacle Avoidance, IEEE Transactions on Robotics and Automation, February 1995, Vol. 11, No. 1, pp 132-138.
- [Borland *et al*, 1984] Borland, D.J., Brooker, M.I.H., Chippendale, G.M., Hall, N., Hyland, B.P.N., Johnstone, R.D., Kleinig, D.A., Turner, J.D., 1984, Forest Trees of Australia, Nelson-CSIRO
- [Bortolan *et al*, 1991] Bortolan, G.; Degani, R.; Willems, J.L., 1991, Neural networks for ECG classification,

- [Bouguettaya, 1996] Proceedings. Computers in Cardiology
Bouguettaya, A.,1996,On-line Clustering, IEEE Transactions on Knowledge and Data Engineering, vol 8, no 2, April 1996
- [Bower, 1977] Bower, T.,1977,Babies are more important than machines, New Scientist June 23, pp 712-715
- [Boye *et al*, 1978] Boys, J.T., Mason, J.L., Hodgson, R.M.,1978, Improved cwfm Sonar with Aural Displays, Ultrasonics 16(3), pp 123-126
- [Boys *et al*, 1979] Boys, J.T., Strelow, E.R., Clark, G.R.S.,1979, A prosthetic aid for a developing blind child, Ultrasonics, 17, pp 37-42
- [Bozma & Kuc, 1992] Bozma, O., Kuc, R.,1992,Characterising the Environment using Echo Energy, Duration and Range : The ENDURA method, IEEE/RSJ International conference on Intelligent Robots and Systems, 1993, pp813-820
- [Brabyn *et al*, 1978] Brabyn, J.A., Sirsena, H.R., Clarke, G.R.,1978, Instrumentation system for blind mobility aid simulation and evaluation, IEEE Transactions on Biomedical Engineering, 25, 556-559.
- [Brabyn, 1985] Brabyn, J.A.,1985, A review of mobility aids and means of assessment,D.H.Warren and E.R.Strelow (Eds), Electronic Spatial sensing for the blind, pp 13-27.Dordrecht, The Netherlands:Martinus Nijhoff
- [Brabyn, 1989] Brabyn, J.,1989, Some practical vocational aids for the blind, IEEE Engineering in Medicine and Biology Society, Annual Conference, Seattle, November.
- [Bracewell, 1965] Bracewell, R.N.,1965, The Fourier transform and its applications, New York : McGraw-Hill, [1965]
- [Bratko, 1992] Bratko, I.,1992, Applications of Machine Learning : Towards Knowledge Synthesis, Proceedings of the International Conference on Fifth Generation Computer Systems, 1992
- [Breeuwer, 1989] Breeuwer, R.,1989, Ultrasonic scanning, imaging and recognition of bottles, Proceedings, IEEE Ultrasonics Symposium, 1989, pp. 635-638
- [Bregman, 1990] Bregman, A.S.,1990, Auditory Scene Analysis, MIT Press
- [Brieman *et al*, 1984] Brieman, L., Friedman, R.A., Olshen, R.A., Stone, C.J.,1984,Classification and Regression Trees, Wedsworth International, Belmont, CA, 1984
- [Broadley & Smyth, 1997] Broadley, C.E., Smyth, P.,1997, Applying Classification Algorithms in Practice, Statistics and Computing (in press)
- [Brown, 1985] Brown, M.K.,1985,Feature Extraction Techniques for Recognising Solid Objects with an Ultrasonic Range Sensor, IEEE Journal of Robotics and Automation, Vol. RA-1, No. 4, December, pp 191-205
- [Bullock, 1977] Bullock, T.H.(Ed),1977,Recognition of Complex Acoustic Signals,Dohlem Konferenzen
- [Bunke & Sanfeliu, 1990] Bunke, H., Sanfeliu, A.,1990, Syntactic and structural pattern recognition : theory and applications, Singapore ; New Jersey : World

- [Cabell & Fuller, 1989] Scientific, c1990
Cabell, R.H., Fuller, C.R., 1989, A Smart Pattern Recognition System for the Automatic Identification of Aerospace Acoustic Sources, Journal of the American Institute of Aeronautics and Astronautics Paper 89-1114, April 1989
- [Cai *et al*, 1993] Cai, Canhui; Regtien, P. P. L., 1993, Smart sonar object recognition system for robots., Measurement Science & Technology v 4 n 1 Jan 1993 p 95-100
- [Carolin & Tindale, 1994] Carolin, R.C., Tindale, M.D., 1994, Flora of the Sydney Region, Reed
- [Case & Waag, 1996] Case, T.J., Waag, R.C., 1996, Flaw Identification from Time and Frequency Features of Ultrasonic Waveforms, IEEE Transactions on Ultrasonics, Ferroelectrics and Frequency Control, vol 43, no 4, July 1996
- [Chan & Hay, 1982] Chan, R.W.Y., Hay, R.D., 1982, A Case Study of Sensitivity of Some Pattern Classifiers Used in Sorting Acoustic Emission Signals, Review of Progress in Quantitative Nondestructive Evaluation, Vol.1 1982
- [Chandran & Elgar, 1991] Chandran, V., Elgar, S., 1991, Pattern Recognition using Invariants Defined from Higher Order Spectra-One-Dimensional Inputs, IEEE Transactions on Signal Processing, 40, 205-212, 1991
- [Chang *et al*, 1994] Chang, W., Bosworth, B., Clifford Carter, G., 1993, Results of using an artificial neural network to distinguish single echoes from multiple sonar echoes, Journal of the Acoustics Society of America, 1994 (3), Pt. 1, pp 1404-1408
- [Chapron *et al*, 1993] Chapron, M., Ivanov, N., Boissard, P., Valey, P., 1993, Visualisation of Corn Acquired from Stereovision, Conference Proceedings of the 1993 International Conference on Systems, Man and Cybernetics, pp384 - 338 vol 5.
- [Chatfield, 1983] Chatfield, C., 1983, Statistics for technology : a course in applied statistics, London ; New York : Chapman and Hall, 1983
- [Chatfield, 1989] Chatfield, C., 1989, The analysis of time series : an introduction, London ; New York : Chapman and Hall, c1989.
- [Chauvin *et al*, 1994] Chauvin, Y., Rumelhart, D.E., 1994, Back-propagation: Theory, Architectures and Applications, Lawrence Erlbaum Associates
- [Chauvin, 1989] Chauvin, Y., 1989, A back-propagation algorithm with optimal use of hidden units, Touretzky, D (Ed), Advances in Neural Information Processing systems, Morgan Kaufmann
- [Chen, 1976] Chen, C.H., 1976, Pattern Recognition and Artificial Intelligence, Academic Press
- [Chen, 1982] Chen, C.H., 1982, Digital Waveform Processing and Recognition, CRC Press
- [Chen, 1983] Chen, C.H., 1983, Pattern Recognition Processing in Underwater Acoustics, Pattern Recognition 16 (6), pp627-640
- [Chestnut & Floyd, 1981] Chestnut, P.C., Floyd, R.W., 1981, An Aspect Independent Sonar Recognition method, Journal of

- the Acoustical Society of America, Vol. 70, No. 3, September, pp 727-734
- [Chittajallu & Wong, 1995] Chittajallu, S.K., Wong, D., 1995, Connectionist Networks in auditory system modelling, Computational. Biol. Med. 24(6), pp 431-439
- [Chittajallu *et al*, 1995] Chittajallu, S.K., Palakal, M.T., Wong, D., 1995, Analysis and Classification of Delay-sensitive neurons based on response, Hearing Research
- [Choitiros *et al*, 1985] Chotiros, N.P., Boehme, T.P., Goldsberry, T.P., Pitt, S.P., Lamb, R.A., Garcia, A.L., Altenberg, R.A., 1985, Acoustic Backscatter at low grazing angles from the ocean bottom, Part II - Statistical characteristics of bottom backscatter at a shallow water site, Journal. Acoustical Society of America
- [Choo *et al*, 1990] Choo, T., Connors, R.W., Araman, P.A., 1990, A Computer Vision System for Automated Grading of Rough Hardwood Lumber Using a Knowledge-Based Approach, 1990 IEEE International Conference on Systems, Man, & Cybernetics, pp 345 - 350.
- [Churnside & Clifford, 1987] Churnside, J.H., Clifford, S.F., 1987, Log-normal Rician probability-density function of optical scintillations in the turbulent atmosphere, Journal Optical Society of America, 4(10): 1923-1930
- [Ciaccio *et al*, 1993] Ciaccio, E.J., Dunn, S.M., Akay, M., 1993, Biosignal Pattern Recognition and Interpretation Signals, IEEE Engineering in Medicine and Biology, December 1993, pp 106-113
- [Cohen, 1995] Cohen, L., 1995, Time-Frequency Analysis, Prentice Hall
- [Coifman & Wickerhauser, 1992] Coifman, R.R., Wickerhauser, M.V., 1992, Entropy-Based Algorithms for Best Basis Selection, IEEE Transactions on Information Theory, vol 38., no. 2, pp. 713-718, March, 1992
- [Coke *et al*, 1993] Coke, M.P., Beet, S., Crawford, M., 1993, Visual representations of speech signals, Chichester ; New York : J. Wiley & Sons, c1993
- [Committee, 1967] Committee on Prosthetics Research and Development, 1967, Sensory Aids for the Blind, Washington, DC: National Academy Press
- [Connell & Mahadevan, 1993] Connell, J.H., Mahadevan, S. (Eds), 1993, Robot learning, Boston : Kluwer Academic Publishers, c1993.
- [Cooke & Brown, 1992] Cooke, M.P., Brown, G.J., 1992, Computational Auditory Scene Analysis : grouping sound sources using common pitch contours, Proceedings Institute Acoustics, Windemere, November, pp 439-446
- [Cooke & Brown, 1993] Cooke, M.P., Brown, G.J., 1993, Computational auditory scene analysis : Exploiting principles of perceived continuity, Speech Communication, December, v13, pp 391-399
- [Cooke *et al*, 1990] Cooke, D., Craven, A.H., Clarke, G.M., 1990, Basic Statistical Computing, Edward Arnold
- [Cooke, 1993] Cooke, M.P., 1993, Modelling Auditory Processing and Organisation, book

- [Cooper & McGillem, 1967] Cooper, G.R., McGillem, C.D.,1967, Methods of Signal and Systems Analysis, Holt, Rinehart, Winston
- [Cooper, 50] Cooper, F.S.,1950,Guidance Devices for the Blind, Physics Today, pp6-14, July
- [Couvreur & Bresler, 1995] Couvreur, C., Bresler, Y,1995, A Statistical Framework for Automatic Classification of Acoustic Signatures, Submitted to Acustica
- [Crecraft & Kay, 1990] Crecraft, D.I.; Kay, L.,1990, Airborne ultrasonic inspection at 2 MHz; its application, IEE Colloquium on 'NDT Evaluation of Electronic Components and Assemblies'
- [Cronin, 1989] Cronin, L.,1989, Key Guide for Australian Palms, Reed
- [Cusdin & de Roos, 1984] Cusdin, M.J., de Roos, A.,1984,CTFM Sonar Enhances Diver's Eyes with Sound, Sea Technology, Vol. 25, No. 9, Sept., pp 44-46
- [Cusdin *et al*, 1984] Cusdin, M.J., de Roos, A., Gough, P.T., Sinton, J.J.,1984, A New Type of CTFM Sonar with no Blind Time and a One Octave Bandwidth, New Zealand National Electronics Conference Proceedings, Vol. 21, pp 59-64
- [Cytowic, 1989]] R.E.Cytowic, Synesthesia : a union of the senses, New York : Springer-Verlag, 1989
- [Cytowic, 1993] Cytowic, R.E.,1993, The man who tasted shapes : A Bizarre Medical Mystery offers Revolutionary Insight into Synesthesia, New York: Putnam
- [Davenport, 1987] Davenport, W.B,1987, An introduction to the theory of random signals and noise, New York : IEEE Press, c1987.
- [Davis, 1993] Davis, B.G.,1993, Tools for Teaching, San Francisco : Jossey-Bass Publishers, 1993
- [de Roos *et al*, 1981] de Roos, A., Kay, L., Cusdin, M.J., Vernon, A.N.,1981, A Sonar Aid for Divers using Binaural Displays, Ultrasonics International '81 Conference Proceedings (IPC Science and Technology, Brighton, U.K.), pp 171-175
- [de Roos *et al*, 1983] de Roos, D., Cusdin, M.J., Kay, L.,1983, A Diver's Sonar with Auditory Display, Transactions Institute Professional Engineers New Zealand 10, 55-58
- [de Roos *et al*, 1988] de Roos, A., Sinton, J.J., Gough, P.T., Kennedy, W.K., Cusdin, M.J.,1988, The detection and classification of objects lying on the seafloor, Journal of the Acoustical Society of America 84(4), pp 1456-1476
- [de Roos, 1986] de Roos, D.,1986, Spectral Analysis Classification Sonars, University of Canterbury
- [de Villiers & Barnard, 1993] de Villiers, J., Barnard, E.,1993,Backpropagation neural nets with one and two hidden layers, IEEE Transactions on Neural Networks Vol: 4 Iss: 1 p. 136-41 Date: Jan. 1993
- [Desai *et al*, 1995] Desai, M.N., Pien, H.H., Bello, M.G.,1995, Underwater image processing and Target classification, Proceedings of the Autonomous Vehicles in Mine Countermeasures Symposium, Naval Postgraduate School, USA, 1995
- [Devore & Peck, 1993] Devore, J., Peck, R.,1993, Statistics : The

- [Dietterich *et al*, 1990] Exploration and Analysis of Data, Duxbury Press
Dietterich, T.G., Hild, H., Bakiri, G.,1990, A comparative study of ID3 and backpropagation for English text-to-speech mapping, Proceedings of the Seventh international Conference on Machine Learning (pp24-31), Austin, TX : Morgan Kaufmann
- [Dow & Sietsma, 1993] Dow, R.J.F.; Sietsma, J.,1993, Using neural networks for underwater target ranging,1993 IEEE International Conference on Neural Networks
- [Downie & Heath, 1965] Downie, N.M., Heath, R.W.,1965, Basic Statistics, Harper & Row
- [Duda & Hart, 1973] Duda, R.O., Hart, P.E.,1973, Pattern Classification and Scene Analysis, John Wiley and sons
- [Edgerton, 1986] Edgerton, H.E.,1986, Sonar Images, Englewood Cliffs, N.J. : Prentice-Hall, c1986
- [Edmonds *et al*, 1996] Edmonds, E.A., Pan, L.Y., O'Brien, S.M.,1996, Automatic Feature Extraction from Spectrograms for Acoustic-Phonetic Analysis, Proceedings of the 11th International Conference on Pattern Recognition, Volume II, pp.701-704
- [Ehrich & Foith, 1976] Ehrich, R.W., Foith, J.P.,1976, Representation of random waveforms by relational trees, IEEE Transactions on Computing, C-25,726,1976
- [Embree, 1995] Embree, P.M., 1995, C Algorithms for real-time DSP, Prentice Hall
- [Erment *et al*, 1985] Erment, H., Schmolke, J., Weth, G.,1985, An adaptive ultrasonic sensor for object identification, Proceedings, IEEE Ultrasonics Symposium, 1985, pp. 457-462
- [Etemad & Chellappa, 1995] Etemad, K., Chellappa, R.,1995, Dimansinality Reduction of Multi-scale Feature spaces using a Separability Criterion, IEEE
- [Everett, 1995] Everett, H.R.,1995, Sensors for Mobile Robots, A K Peters, Ltd. Wellesley, Massachusetts
- [Everitt, 1980] Everitt, B.,1980, Cluster Analysis, London : Heinmann
- [Fahlman & Lebiere, 1990] Fahlman, S.E., Lebiere, C.,1990, The Cascade-Correlation Learning Architecture, Technical Report CMU-CS-90-100, School of Computer Science, Carnegie Mellon University, Pittsburgh, PA 15213, February 1990
- [Fahlman, 1988] Fahlman, S.E.,1988, An Empirical Study of Learning Speed in Back-Propagation Networks, Technical Report CMU-CS-88-162, School of Computer Science, Carnegie Mellon University, Pittsburgh, PA, 15213
- [Fahlman, 1991] Fahlman, S.,1991, The Recurrent Cascade-Correlation Architecture, Technical Report CMU-CS-91-100, School of Computer Science, Carnegie Mellon University, Pittsburgh, PA, 15213
- [Fan, 1990] Fan, T,1990, Describing and Recognising 3-D Objects Using Surface Properties, Springer-Verlag
- [Farmer, 1975] Farmer, L.W.,1975, Travel in adverse weather using electronic mobility guidance devices, New Outlook for the Blind, 1969, pp433-439, 451
- [Ferrel, 1980] Ferrell, K.A.,1980, Can infants use Sonicguide?

- [Fisher *et al*, 1989] Two years experience of project view, Journal of Visual Impairment and Blindness, 1974, 209-220
Fisher, D.H., McKusick, K.B., 1989, An empirical comparison of ID3 and backpropagation, Proceedings of the Eleventh Joint International Conference on Artificial Intelligence (pp 788-793), detroit : Morgan Kaufmann
- [Foulke, 1971] Foulke, E., 1971, Perceptual Basis for Mobility, American Foundation for the Blind Research Bulletin, No. 23, pp 1-8, June
- [Fox & Lang, 1990] Fox, J., Lang, J.S., 1990, Modern Methods of Data Analysis, SAGE Publications
- [Freedman, 1962a] Freedman, A., 1962, A Mechanism of Acoustic Echo Formation, Robotica, 12:10, pp 10 - 21.
- [Freedman, 1962b] Freedman, A., 1962, The High Frequency Echo Structure of Some Simple Body Shapes, Acustica, 12:2.
- [Fritsch *et al*, 1993] Fritsch, C., Anaya, J.J., Ruiz, A., 1993, A high-resolution object recognition ultrasonic system, Sensors and actuators. Part A, Physical JUN 01 1993 v 37 / 38, p644
- [Fu, 1968] Fu, K.S., 1968, Sequential Methods in Pattern Recognition and Machine Learning, Academic press
- [Fu, 1974] Fu, K.S., 1974, Syntactic methods in pattern recognition, New York : Academic Press, 1974
- [Fu, 1977] Fu, K.S., 1977, Syntactic Pattern Recognition, Applications, Springer-Verlag
- [Fukunaga, 1990] Fukunaga, K., 1990, Introduction to Statistical Pattern Recognition, Academic Press Ltd.
- [Fuller, 1976] Fuller, W.A., 1976, Introduction to Statistical Time Series, John Wiles & sons
- [George & Bahl, 1995] George, O., Bahl, R., 1995, Simulation of Backscattering of High Frequency Sound from Complex Objects and Sand Sea-bottom, IEEE Journal of Oceanic Engineering, vol 20, no. 2, April 1995
- [Getty & Howard, 1981] Getty, D.J., Howard, J.H. (Eds), 1981, Auditory and Visual Pattern Recognition,
- [Ghosh *et al*, 1992] Ghosh, J., Deuser, L.M., Beck, S.D., 1992, A Neural Network Based Hybrid System for Detection, Characterisation, and Classification of Short-Duration Oceanic Signals, IEEE Journal of Oceanic Engineering, vol 17, no 4, October, pp 351-363
- [Gillison & Anderson, 1978] Gillison, A.N., Anderson, D.J., 1978, Vegetation Classification in Australia, CSIRO
- [Ginsberg, 1993] Ginsberg, M.L., 1993, Essentials of Artificial Intelligence, Morgan Kaufmann
- [Gissoni, 1966] Gissoni, F., 1966, My Cane is Twenty Feet Long, The New Outlook for the Blind, February
- [Goldberg, 1989] Goldberg, D.E., 1989, Genetic Algorithms in Search, Optimisation, and Machine Learning, Addison-Wesley Publishing Company, inc
- [Gonzalez, 1978] Gonzalez, R.C., 1978, Syntactic pattern recognition : an introduction, Reading, Mass. : Addison-Wesley Publishing Company, Advanced Book Program

- [Gooberman, 1968] Gooberman, G.L.,1968, Ultrasonics Theory and Application, The English Universities Press Ltd.
- [Gorman & Sejnowski, 1988b] Gorman, R.P., Sejnowski, T.J.,1988, Learned Classification of Sonar Targets Using a Massively Parallel Network, IEEE Transactions on Acoustics, Speech, and Signal Processing, pp1135-1140
- [Gorman & Sejnowski, 1988] Gorman, R.P., Sejnowski, T.J.,1988, Analysis of hidden units in a layered network trained to classify sonar targets, Neural Networks 1, 1975-79
- [Gorman, 1991] Gorman, R.P.,1991, Neural networks and the classification of complex sonar, IEEE Conference on Neural Networks for Ocean Engineering
- [Gough *et al*, 1984a] Gough, P.T., Cusdin, M.J., de Roos, A., Sinton, J.J.,1984, A High Speed Side Scan Sonar based on Wide Band CTFM, Proceedings of the International Conference on Developments in Marine Acoustics, pp 225-230
- [Gough *et al*, 1984b] Gough, P.T., de Roos, A., Cusdin, M.J.,1984, A Continuous Transmission FM Sonar with one octave Bandwidth and no blind time, Proceedings Transactions of the IEEE part F, v131, June, p270-274
- [Gough, 1994] Gough, P.T.,1994, A fast spectral estimation algorithm based on the FFT, IEEE Transactions on Signal Processing Vol: 42 Iss: 6 p. 1317-22 Date: June 1994
- [Greenwell, 1988] Greenwell, M.,1988, Knowledge engineering for expert systems, Chichester : E. Horwood ; New York : Halsted Press
- [Griffin, 1958] Griffin, D.R.,1958, Listening in the Dark, Yale University Press
- [Griffin, 1959] Griffin, D.,1959, Echoes of Bats and Men, Anchor Books
- [Group, 1986] Working group on Mobility Aids for the Visually Impaired and Blind,1986, Electronic Travel Aids : New Directions for research, Washington, DC: National Academy Press
- [Gunawardera *et al*, 1991] Gunawardera, C.A., Dennis, T.J., Clark, L.J., 1991, Colour identification and quality inspection for agricultural produce, 33rd Midwest Symposium on Circuits & Systems p657-60 Vol 2, 1991.
- [Guyer *et al*, 1993] Guyer, D.E., Miles, G.E., Gaultney, L.D., Schreiber, M.M., 1993, Application of Machine Vision to Shape Analysis in Leaf and Plant Identification, Transactions of the American Society of Agricultural Engineers, Vol 36(1) January - February, 1993, pp163 - 171.
- [Haley, 1991] Haley, T.B.,1991, An assessment of the impact of Neural Network Technology on automatic active sonar classifier development, International Journal of Pattern Recognition and Artificial Intelligence, Vol 5., No. 4, pp143-151
- [Hallom *et al*, 1990] Hallom, N.J., Hopgood, A.A., Woodcock, N.,1990, Defect Classification in welds using a feedforward network with a blackboard system, International Neural Network Conference, Paris, 1990
- [Hammerstrom, 1993a] Hammerstrom, D.,1993, Neural Networks at

- [Hammerstrom, 1993b] Work, IEEE Spectrum, June, pp26-32
- [Hand, 1981] Hammerstrom, D.,1993, Working with neural networks, IEEE Spectrum, July, v30 n7 pp 46 - 53
- [Hand, 1982] Hand, D.J.,1981,Discrimination and Classification, Wiley, New York
- [Handel, 1989] Hand, D.J.,1982, Kernel Discriminant Analysis, New York : Research Studies Press
- [Hansch *et al*, 1994] Handel, S.,1989,Listening, The MIT Press
- [Harmon, 1983] Hansch, M.K.T., Rajana, K.M., Rose, J.L.,1994,Characterization of Aircraft Joints using Ultrasonic Guided Waves and physically based Feature Extraction,1994 Ultrasonics Symposium
- [Harper & McKerrow, 1994] Harmon, L.D., 1983, Tactile Sensing for Mobile Robots, Recent Advances in Robotics, Vol. 1, John Wiley and Sons, 1983.
- [Harper & McKerrow, 1995] Harper, N.L., McKerrow, P.J.,1994, Perception of Object Characteristics by the Interpretation of Ultrasonic Range Data, In Proceedings of the 7th Australian Joint Conference on Artificial Intelligence, 1994, pp418-426, World Scientific
- [Harper & McKerrow, 1995] N.L.Harper, P.J.McKerrow, Classification of Plant Species from CTFM Ultrasonic Range Data Using a Neural Network, Proceedings of the IEEE International Conference on Neural Networks, 1995, Causal Productions, pp V-2348-2353, 1995.
- [Harper & McKerrow, 1995] Harper, N., McKerrow, P.J., 1995, Discrimination Between Plants with CTFM Range Information Using a Backpropagation Learning Algorithm, The 1995 Australian Artificial Intelligence conference, World Scientific, pp 227-234.1
- [Harper & McKerrow, 1997] Harper, N., McKerrow, P.J., 1997, Recognition of Plants with CTFM Ultrasonic Range Data using a Neural Network., The 1997 IEEE International Conference on Robotics and Automation, Albuquerque
- [Harris & Ledwidge, 1974] Harris, R.W., Ledwidge, T.J.,1974, Introduction to Noise Analysis, Pion Limited
- [Hayes & Gough, 1992] Hayes, M.P.; Gough, P.T.,1992,Broad-band synthetic aperture sonar, IEEE Journal of Oceanic Engineering Vol: 17 Iss: 1 p. 80-94 Date: Jan. 1992 Country of Publication: USA
- [Hayes, 1985] Hayes, A.D.,1985, Microprocessor techniques applied to ultrasonic pulse/echo travel aids for the blind, Electronic spatial sensing for the blind : contributions from perception rehabilitation, and computer vision, NATO Advanced Research Workshop on Visual Spatial Prostheses for the Blind, Lake Arrowhead, California., David H. Warren, Edward R. Strelow, (Ed.) Boston pp 161-169
- [Hayes, 1989] Heyes, M.,1990, PhD Thesis : A CTFM Synthetic Aperture Sonar, University of Canterbury
- [Hecht-Nielson, 1990] Hecht-Nielson, R.,1990, Neurocomputing, Addison-Wesley Publishing Company Inc.
- [Hopgood *et al*, 1991] Hopgood, A.A., Hallam, N.J., Woodcock, N.,1991, Interpretation of Ultrasonic Images of Weld Defects using a hybrid system, Neural

- [Hopgood, 1989] Networks and their applications, Nimes, France
Hopgood, A.A., Hallam, N.J., Woodcock, N., 1989, On-line knowledge based interpretation of industrial ultrasonic images, POP-11 comes of age (Ed. J. Anderson, Ellis Horwood
- [Hopgood, 1993] Hopgood, A.A., 1993, Knowledge Based Systems for Engineers and Scientists, CRC Press
- [Horn, 1986] Horn, B.K.P., 1986, Robot Vision, MIT Press, Cambridge, Mass.
- [Hornik *et al*, 1989] Hornik, K.M., Slichcombe, M., White, H., 1989, Multilayer feedforward networks are universal approximators, Neural Networks, 2 : 359 - 366
- [Horvath & Cook, 1982] Horvath, P., Cook, F.J., 1982, Establishing Signal Processing and Pattern Recognition Techniques for Inflight Discrimination Between Crack-Growth Acoustic Emissions and Other Acoustic Waveforms, Review of Progress in Quantitative Nondestructive Evaluation, Vol. 1, 1982
- [Hu *et al*, 1995] Hu, B.G., Gosine, R.G., de Silva, C.W., 1995, Classifier Design for computer grading systems for food processing, 1995 IEEE International Conference on Systems, Man and Cybernetics, pp 730 - 5
- [Huang *et al*, 1992] Huang, Q., Jain, A.K., Stockman, G.C., 1992, Automatic Image Analysis of Plant Root Structures, Proceedings of the 11th International Conference on Pattern Recognition Vol 2, pp569 - 572.
- [Humphries & Simonton, 1993] Humphries, S., Simonton, W., 1993, Identification of Plant Parts Using Colour and Geometric Image Data, Transactions of the American Society of Agricultural Engineers, Vol 36(5) September-October, 1993, pp1493 - 1501.
- [Hunt, 1975] Hunt, E.B., 1975, Artificial intelligence, Academic Press series in cognition and perception
- [Ifukube *et al*, 1991] Ifukube, T., Tadayuki, S., Peng, C., 1991, A Blind Mobility Aid Modeled After Echolocation of Bats, IEEE Transactions on biomedical engineering, v38, n5, May, pp461-465
- [Jacobs, 1988] Jacobs, R.A., 1988, Increased Rates of convergence through learning rate adaption, Neural Networks, Vol 1, No. 1, pp 295-308, 1988
- [Jain & Dubes, 1988] Jain, A.K., Dubes, R.C., 1988, Algorithms for Clustering Data, Prentice Hall
- [Jain, 1987] Jain, A.K., 1987, Advances in Statistical Pattern Recognition, In Pattern Recognition Theory and Applications, Devijur, P.A. and Kittler, J. (Eds), Springer-Verlag, pp1-19
- [James, 1985] James, M., 1985, Classification Algorithms, New York : Wiley
- [Jamshidi *et al*, 1993] Jamshidi, M., Vadiiee, N., Ross, T.J., (Eds), 1993, Fuzzy Logic and Control : Software and Hardware applications, Prentice Hall
- [John *et al*, 1994] John, G.H., Kohavi, R., Pfleger, K., 1994, Irrelevant Feature and the subset selection problem, In Machine Learning : Proceedings of the Eleventh International Conference, pp121 - 129. Morgan Kaufmann
- [Johnson & Wichern, 1992] Johnson, R.W., Wichern, D.W., 1992, Applied

- [Jones & Flynn, 1993] Multivariate Statistical Analysis - Third Edition, Prentice-Hall.
- [Jordan & Rumelhart, 1992] Jones, J.L., Flynn, A.M., 1993, Mobile Robots Inspiration to Implementation, A K Peters, Ltd
- [Jurs & Isenhour, 1975] Jordan, M.I., Rumelhart, D.E., 1992, Forward Models : Supervised learning with a distal teacher, Cognitive Science, 16, 307-354
- [Kalman & Kwansky, 1992] Jurs, P.C., Isenhour, T.L., 1975, Chemical Applications of Pattern Recognition, Wiley-Interscience
- [Kamiyama *et al*, 1992] Kalman, B.L., Kwansky, S.C., 1992, Why Tanh : Choosing a sigmoidal Function, International Joint Conference on Neural Networks, Baltimore, MD
- [Kao *et al*, 1996] Kamiyama, N., Iijima, N., Taguchi, A., Mitsui, H., Yoshida, Y., Sone, M., 1992, Tuning of learning rate and momentum on back-propagation, Communications on the Move. Singapore. ICCS/ISITA '92
- [Kasabov, 1993] Kao, G., Probert P. and Lee, D., 1996, Object Recognition with FM Sonar: An Assistive Device for Blind and Visually-Impaired People, American Association for Artificial Intelligence Fall Symposium on Developing Assistive Technology for People with Disabilities, MIT, Cambridge, MA, 199-11 November 1996
- [Kasabov, 1994] Kasabov, N.K., 1993, Hybrid Connectionist Production Systems : An Approach to Realising Fuzzy Expert Systems, Journal of Systems Engineering
- [Kasabov, 1994] Kasabov, N.K., 1994, Hybrid Fuzzy Connectionist Rule-based Systems and the Role of Fuzzy Rules Extraction, University of Otago
- [Kaufman & Rousseeuw, 1990] Kaufman, L., Rousseeuw, P.J., 1990, Finding Groups in Data : An Introduction to Cluster Analysis, John Wiley and Sons
- [Kay & Bishop, 1965] Kay, L., Bishop, M.J., 1965, The Effect of a Linear Phase Taper on the Near Field of an Ultrasonic Multi-element Array, The Radio and Electronic Engineer, April
- [Kay & Strelow, 1977] Kay, L., Strelow, E.R., 1977, Blind Babies need Specially Designed Aids, New Scientist June 23, 19709-712
- [Kay *et al*, 1977a] Kay, L., Strelow, E.R., Kay, N., 1977, Electronic spatial sensors as training aids for blind children, Journal of Visual Impairment and Blindness, 1971, pp174-175
- [Kay *et al*, 1977b] L.Kay, J.Boys, G.Clark, The echocardiophone : a new means for observing spatial movement of the heart, Ultrasonics, pp136-141 May 1977.
- [Kay *et al*, 1977c] Kay, L., Bui, S.T., Brabyn, J.A., Strelow, E.R., 1977, Single Object Sensor : A Simplified Binaural Mobility Aid, Journal of Visual Impairment and Blindness, May
- [Kay *et al*, 1981] Kay, L., Kay, N., Sinton, J.J., de Roos, A., 1981, Characterization of Surface and Volume Structure using an Air Sonar with Auditory Display for the Blind, Ultrasonics International '81 Conference Proceedings (IPC Science and

- [Kay *et al*, 1984] Technology, Brighton, UK), pp38-42
Kay, L., Anderson, C.L., Cusdin, M.J., Sinton J.J.,1984, Ultrasonic Imaging in Air for Robots, Nelcon 1984
- [Kay, 1961a] L.Kay, Progress in Underwater Echo Ranging, British Communications and Electronics, October, pp 753-759, 1961.
- [Kay, 1961b] Kay, L.,1961,Orientation of Bats and Men by Ultrasonic Echo Location, Journal of British Communications and Electronics, August, pp582-586
- [Kay, 1962] Kay, L.,1962, Auditory Perception and its Relation to Ultrasonic Blind Guidance Aids, Journal Brit. I.R.E., October, pp309-317
- [Kay, 1963] Kay, L.,1963, Active Energy Radiating Systems : Ultrasonic guidance for the blind, In Clarke, L.L. (Ed), Proceedings of the International congress on Technology and Blindness, v1, American Foundation for the Blind, New York, pp137-156
- [Kay, 1964] Kay, L.,1964, An Ultrasonic Sensing Probe as a Mobility Aid for the Blind, Ultrasonics, v2 pp53-59
- [Kay, 1965] Kay, L.,1965, The Effect of a Linear Phase Taper on the Near Field of an Ultrasonic Multi-element array, The Radio and Electronic Engineer, April
- [Kay, 1966a] Kay, L.,1966, Ultrasonic Spectacles for the Blind, In Dufton, R. (Ed), Proceedings of International Conference on Sensory devices for the blind, St Dunstons, England p275
- [Kay, 1966b] Kay, L.,1966, Introduction to the Technology of Ultrasonics, Promotional Material
- [Kay, 1970] Kay, L.,1970, An Ultrasonic Sensor for Automatic Control, The Radio and Electronic Engineer
- [Kay, 1971] Kay, L.,1971, Ultrasonic Imaging in Solids, The Radio and Electronic Engineer, v41, n2, February
- [Kay, 1973a] Kay, L.,1973, Sonic glasses for the blind - Presentation of evaluation data, A.F.B. Res. Bull., 26, 35
- [Kay, 1973b] Kay, L.,1973, Ultrasonic Image Synthesis, Sharpe, R.S. (Ed), Research Techniques in Non-Destructive testing, v II
- [Kay, 1974] Kay, L.,1974, A sonar aid to enhance spatial perception of the blind : engineering design and evaluation, The Radio and Electronic Engineer, Vol. 44 No. 11, pp605-626
- [Kay, 1976] Kay, L.,1976, An Artificially Generated Multiple Object Auditory Space for use where Vision is impaired, Acustica 1976/77, 36, pp 1-9
- [Kay, 1977] L.Kay, An Artificially Generated Multiple Object Auditory Space for use where Vision is impaired, Acustica, 36, pp 1-9, 1976/77.
- [Kay, 1985] Kay, L.,1985, Airborne ultrasonic imaging of a robot work space, Sensor Review, January, pp 8-12
- [Kay, 59] Kay, L.,1959, A Comparison between Pulse and Frequency-Modulation Echo-Ranging Systems, Journal Brit.I.R.E.
- [Kellog, 1962] Kellog, W.N.,1962, Sonar Systems of the Blind,

- [Kelly & White, 1993] Science, 137, 399-404
Kelly, P.M., White, J.W., 1993, Preprocessing Remotely-Sensed Data for Efficient Analysis and Classification, Applications of Artificial Intelligence, Proceedings of the SPIE-The International Society for Optical Engineering-1993, Orlando, FL. (1993), Pp24-30
- [Kelly *et al*, 1992] Kelly, J.G., Carpenter, R.N., Tague, J.A., 1992, Object Classification and acoustic imaging with active sonar, Journal of the Acoustic Society of America 91 pp 2073-2081 (1992)
- [Kino, 1987] Kino, G.S., 1987, Acoustic waves : devices, imaging, and analog signal processing, Englewood Cliffs, N.J. : Prentice-Hall, c1987.
- [Kinsler *et al*, 1982] Kinsler, L.E., Frey, A.R., Coppens, A.B., Sanders, J.V., 1982, Fundamentals of Acoustics, Third Edition, John Wiley and Sons
- [Kirra & Rendell, 1992] Kirra, K., Rendell, L.A., 1992, The feature selection problem : Traditional Methods and a new algorithm, AAAI-92, Proceedings Ninth National Conference on Artificial Intelligence, pages 129-134. AAAI Press/ The MIT Press, 1992
- [Kittler, 1986] Kittler, T., 1986, Feature Selection and Extraction in Young, T.Y. and Fu, K-S, (Eds.); Handbook of Pattern Recognition and Image Processing, Academic Press, Orlando, pp59-83
- [Kleeman & Kuc, 1994] Kleeman, L., Kuc, R., 1994, An Optimal Sonar Array for Target Localisation and Classification, 1994 IEEE International Conference on Robotics and Automation, pp3130-3135
- [Kodratoff, 1988] Kodratoff, Y., 1988, Introduction to Machine Learning, Pitman
- [Kohonen, 1984] Kohonen, T., 1984, Self-Organising and Associative Memory, Springer - Verlag
- [Korona & Kokar, 1996] Korona, Z., Kokar, M.M., 1996, Model Theory Based Fusion Framework with Application to Multisensor Target Recognition, Proceedings of the 1996 IEEE/SICE/RSJ International Conference on Multisensor Fusion and Integration for Intelligent Systems
- [Korona, 1996] Korona, Z., 1996, Model Theory Based Feature Selection for Multisensor Recognition, PhD Dissertation, Northeastern University
- [Krishnapuvan & Keller, 1993] Krishnapuvam, R., Keller, J.M., 1993, A probabilistic Approach to Clustering, IEEE Transactions on Fuzzy Systems, Vol 1, No 2, pp98-160
- [Kuc & Barshan, 1989] Kuc, R., Barshan, B., 1989, Navigating Vehicles through an unstructured environment with sonar, 1989 IEEE International Conference on Robotics and Automation, p1422-6, vol 3, may 1989
- [Kuc & Barshan, 1992] Kuc, R., Barshan, B., 1992, Bat-like Sonar for Guiding Mobile Robots, IEEE Control Systems magazine
- [Kuc & Siegel, 1987] Kuc, R., Siegel, M.W., 1987, Physically Based Simulation Model for Acoustic Sensor Robot Navigation, IEEE Transactions on Pattern Analysis

- and Machine Intelligence, 199(6), 19766-778, 1987
- [Kuc, 1996] Kuc, R.,1996,Fusing binaural sonar information for object recognition, Proceedings of the 1996 IEEE/SICE/RSJ International Conference on Multisensor Fusion and Integration for Intelligent Systems
- [Kukunaga, 1972] Kukunaga, K.,1972, Introduction to Statistical Pattern Recognition, Academic Press
- [Kummert, 1993] Kummert, A.,1993,Fuzzy Technology implemented in Sonar Systems, IEEE Journal of Oceanic Engineering, Oct 01, v18, n4
- [Kuyel *et al*, 1996] Kuyel, T, Ghosh, J., Geisler, W,1996, A Nonparametric Statistical Analysis of Texture Segmentation Performance Using a Foveated Image Preprocessing Similar to the Human Retina, IEEE Southwest Symposium on Image Analysis and Interpretation, 1996, p207-212, IEEE
- [Lach & Ermert, 1991] Lach, M., Ermert, H.,1991, An acoustic sensor system for object recognition., Sensors and actuators. Part A, Physical, MAR 01 1991 v 26 n 1 / 3, pp 541
- [Lang *et al*, 1989] Lang, S., Korba, L., Wong, A.,1989,Characterising and Modelling a sonar ring, Proceedings SPIE Conference on Mobile Robots IV, pp 291-304, Philadelphia, PA
- [Langley & Simon, 1994] Langley, P., Simon, H.A.,1994, Applications of Machine Learning and Rule Induction, Draft (Seminar at UNSW)
- [Langley, 1994] Langley, P.,1994, Selection of Relevant Features in Machine Learning, Proceedings of the AAAI Fall Symposium on Relevance, New Orleans, LA : AAAI Press.
- [Le Chevalier *et al*, 1978] Le Chevalier, F., Bobillot, G., Fugier-Garrel, C,1978, Syntactic Signal Processing,1987 Int. Symposium on Information Theory, Ithaca, N.Y., October 10 to 14 1978
- [Le Cun *et al*, 1989] Le Cun, Y., Boser, B., Denker, J., Henderson, D., Howard, R., Hubbard, W., Jackel, L.,1989,Backpropagation applied to handwritten zip codes, Neural Computation, 1, 1-38
- [Le Cun *et al*, 1990] LeCun, Y., Boser, B., Decker, J.S., Henderson, D., Howard, R.E., Hubbard, W., Jackel, L.D.,1990, Handwritten digit recognition with a backpropagation network, in Advances in Neural Information Processing Systems 2, Ed. Touretzky, D., San Mateo, CA, Morgan Kaufman
- [Le Cun, 1989] LeCun, Y.,1989,Generalisation and Network Design Strategies, Pfeifer, R., Schreter, Z., Fogelman, F., Steels, L., (Eds), Connectionism in Perspective, Zurich, Switzerland. Elsevier
- [Lee *et al*, 1995] Lee, D. N., Simmons, J. A., Bouffard, F.,1995, Steering by echolocation: a paradigm of ecological acoustics, Journal of comparative physiology. A, Sensory 1995 v 176 n 3 p347
- [Leon-Garcia, 1994] Leon-Garcia, A.,1994, Probability and Random Processes for Electrical Engineering, Addison Wesley

- [Leonard & Carpenter, 1964] Leonard, J.A., Carpenter, A., 1964, Trial of an Acoustic Blind Aid, A.F.B.Res.Bull. No 4, pp 70-119, Jan
- [Leonard & Durrant-Whyte, 1992] Leonard, J.J., Durrant-Whyte, H.F., 1992, Directed Sonar Sensing for Mobile Robot Navigation Kluwer Academic Publishers
- [Li, 1989] Li, S.Z., 1989, 3D Object Recognition from Range Images : Computational Framework, Intelligent Autonomous Systems 2, Vol 1
- [Lindstrom *et al*, 1982] Lindstrom, K., Mauritzon, L., Benoni, G., Svedman, P., Willer, S., 1982, Application of Airborne Ultrasound to Biomedical Measurements, Medical and Biological Engineering and Computing, May, pp 393-400
- [Linggard *et al*, 1992] Linggard, R., Myers, D.J., Nightingale, C., 1992, Neural Networks for Vision, Speech and Natural Language, Chapman & Hall
- [Linnet *et al*, 1995] Linnett, L.M., Carmichael, D.R., Clarke, S.J., 1995, Texture Classification using a spatial-point process model, IEEE Proceedings on Vis Image Signal Processing, Vol 142, No. 1, Feb 1995
- [Lippman, 1987] Lippman, R.P., 1987, An introduction to computing with Neural Networks, IEEE ASSP Mag. April., pp4-22
- [Lippman, 1989] Lippman, S.B., 1989, A C++ Primer, AT&T Bell Laboratories
- [Long, 1975] Long, M.W., 1975, Radar Reflectivity of Land and Sea, D.C. Heath
- [Lui & Setiono, 1996] Lui, H., Setiono, R., 1996, Feature Selection and Classification - A Probabilistic Wrapper Approach, Proceedings of the 9th International Conference on Industrial and Engineering Applications of AI and ES
- [MacCormac, 1993] MacCormac, J.K.M., 1993, On-Line Image Processing for Tobacco Grading in Zimbabwe, IEEE International Symposium on Industrial Electronics 1993, pp327 - 331.
- [Macq, 1991] The Macquarie Dictionary, Macquarie Library, NSW Australia, 1991.
- [Maginness & Kay, 1968] Maginness, M.G., Kay, L., 1968, Signal Processing for Acoustic Imaging Systems, The 6th International Congress on Acoustics, Tokyo, Japan, August 21-28
- [Maginness & Kay, 1971] Maginness, M.G., Kay, L., 1971, Ultrasonic Imaging in Solids, The Radio and Electronic Engineer, vol 41, no 2, February
- [Mammone *et al*, 1996] Mammone, R.J., Zhang, X., Ramachandran, R.P., 1996, Robust Speaker Recognition, IEEE Signal Processing Magazine, September 1996
- [Mandalow *et al*, 1996] Mandalow, A., Gomez-de-Gabriel, J.M., Martinez, J.L., Munoz, V.F., Ollero, A., Garcia-Cerezo, A., 1996, The Autonomous Mobile Robot AURORA for Greenhouse Operation, IEEE Robotics and Automation Magazine, Vol. 3, No. 4, December 1996.
- [Mandelbaum & Mintz, 1994] Mandelbaum, R., Mintz, M., 1994, Sonar Signal Processing using Tangent Clusters, Proceedings of

- the IEEE Oceanic Engineering Society OCEANS 94 Conference
- [Mann, 1965] Mann, R.W.,1965, The evolution and simulation of Mobility Aids for the Blind, A.F.B.Res.Bull., No 11, pp 93-98, Oct.
- [Marchand *et al*, 1983] Marchand, A., Van Lente, F., Galen, R.,1983, The Assessment of Laboratory Tests in the Diagnosis of Acute Appendicitis, American Journal of Clinical Pathology 80:3 (1983), pp369-374
- [Maren *et al*, 1990] Maren, A.J., Horston, C.T., Pap, P.M.,1990, Handbook of Neural Computing Applications, Academic Press, Inc.
- [Marsh *et al*, 1984] Marsh, K.A., Richardson, J.M., Schoenwald, J.S., Martin, J.F.,1984, Acoustic Imaging in Robotics Using a Small Set of Transducers, Proceedings of the 4th International Conference on Robotic Vision and Sensory Controls, Oct, IFS Publications, pp 261-268
- [Martin, 1969] Martin, G.,1969, Electronics and Transducers for an Ultrasonic Blind Mobility Aid, M.E. Thesis, University of Canterbury, 1969
- [Masters, 1993] Masters, T.,1993, Practical Neural Network Recipes in C++, Academic Press, Inc.
- [McKerrow & Hallam, 1990] McKerrow, P.J., Hallam, J.C.T.,1990, An Introduction to the Physics of Echolocation, The Third Australian National Conference on Robotics, 1990, pp198-209.
- [McKerrow, 1991] McKerrow, P.J., 1991, Introduction to Robotics, Addison-Wesley Publishing Company.
- [McKerrow, 1993] McKerrow, P.J.,1993, Echolocation - From range to outline segments, Robotics and Autonomous Systems 11 (1993) 205-211, Elsevier.
- [McKerrow, 1995] McKerrow, P.J., 1995, Progress in Ultrasonic Sensing for Service Robots, Proceedings of the First International Workshop on Robotics for the Service Industries, Sydney, May, 1995, pp 44-52.
- [McLachlan, 1992] McLachlan, G.J.,1992,Discriminant Analysis and Statistical Pattern Recognition, Wiley.
- [Mehrots *et al*, 1991] Mehrota, K.G., Moham, C.K., Ranka, S.,1991,Bounds on the Number of Samples needed for neural learning, IEEE Transactions on Neural Networks, Vol 2, No 6, New York : IEEE.
- [Mendel, 1991] Mendel, J.M.,1991, Tutorial on Higher-Order Statistics (Spectra) in Signal Processing and System Theory : Theoretical Results and Some Applications, Proceedings of the IEEE, Vol. 79, pp 278-305
- [Michie & Johnson, 1985] Michie, D., Johnson, R.,1985, The creative computer : machine intelligence and human knowledge, Harmondsworth, Middlesex : Penguin Books, 1985
- [Michie *et al*, 1994] Michie, D., Spiegelhalter, D.J., and Taylor, C.C.(eds),1994, Machine Learning, Neural and Statistical Classification, London : Ellis Horwood
- [Michie, 1982] Michie, D.,1982, Machine Intelligence and Related Topics : an Information Scientists Weekend Book, Gordon and Breach
- [Michie, 1986] Michie, D,1986,On machine intelligence,

- [Michie, 1994b] Chichester : E. Horwood ; New York : Halsted Press, 1986
- [Michie, 1994] Michie, D.,1994, Working with Large Industrial Clients, UNSW seminar
- [Mins, 1973] Michie, D.,1994, Structured Induction in two large process plants
- [Minsky & Papert, 1988] Mims, F.M.,1973, Sensory aids for blind persons, New Outlook for the Blind, 1967, pp407-414
- [Mirchandani & Cao, 1989] Minsky, M.L., Papert, S.A.,1988, Perceptrons : An Introduction to Computational Geometry, The MIT Press
- [Mitchell & Thrun, 1993] Mirchandani, G., Cao, W.,1989,On hidden nodes for neural nets, IEEE Transactions on Circuits Systems. , Vol 36, pp 661-664, May 1989
- [Mohajeri & Fricke, 1996] Mitchell, T.M., Thrun, S.,1993, Explanation based neural network learning for Robot control, Advances on Neural Information Processing Systems (Vol 5), S.Hanson, J.Cowans, L.Giles (Eds.), San Mateo, CA : Morgan Kaufmann
- [Mohanty, 1986] Mohajeri, R., Fricke, F.R.,1996, Acoustical Feature Extraction from Aircraft and Traffic Noise, Acoustics Australia, Vol 24, No.1
- [Moore *et al*, 1991] Mohanty, N.,1986,Random signals, estimation, and identification : analysis and applications, New York : Van Nostrand Reinhold, c1986
- [Moukas *et al*, 1982] P.B.W.Moore, H.L.Roitblat, R.H.Penner, P.E.Nachtigall, Recognising Successive Dolphin Echoes With an Integrator Gateway Network, Neural Networks, v4, pp 701-709, 1991.
- [Muller & Reinhart, 1991] Moukas, P., Simson, J., Norton-Wayne, L.,1982, Automatic Identification of Noise Pollution Sources, IEEE Transactions on Systems, Man and Cybernetics, Vol. SMC-12, No. 5, Sept./Oct., 1982
- [Murch, 1973] Muller, B., Reinhardt, J.,1991, Neural Networks An Introduction, Springer - Verlag
- [Nabout *et al*, 1994] Murch, G.M.,1973,Visual and Auditory Perception,
- [Narayanan & Shankar, 1994] Nabout, A., Gerhards, R., Su, B., Nour Eldin, A., Kuhbauch, W., 1994, Plant Species Identification using Fuzzy Set Theory, Proceedings of the IEEE Southwest Symposium on Image Analysis and Interpretation, 1994, pp48 - 53.
- [Narendra & Fukunaga, 1977] Manoj Narayanan, V., Shankar, P.M.,1994, Non-rayleigh Statistics of Ultrasonic Backscattered Signals, IEEE Transactions on Ultrasonics, Ferroelectrics and Frequency Control, Vol 41, No 6, Nov. 1994, pp845-852
- [NATO, 1976] Narendra, P., Fukunaga, K.,1977, A branch and Bound Algorithm for Feature Subset Selection, IEEE Transactions on Computers C-26 (1977), pp 917-922
- NATO Advanced Study Institute on Aspects of Signal Processing with Emphasis on Underwater Acoustics (1976 : Portovenere, La Spezia, Italy),1976, Aspects of signal processing with emphasis on underwater acoustics : proceedings of the NATO Advanced Study Institute held at

- [Neuralware, 1990] NeuralWare Inc., Software Reference for NeuralWorks Professional II / PLUS.
- [Newcomer, 1977] Newcomer, J., 1977, Sonicguide : Its Use with Public School Blind Children, J Visual Impairment and Blindness 71, pp268-271
- [Ng, 1992] Ng, S.S., 1992, Sonic Electronic Guide for the Blind, Proceedings 13th IEEE Engineering in Medicine and Biology Society.
- [Nigrin, 1993] Nigrin, A., 1993, Neural Networks for Pattern Recognition, MIT Press
- [Nilsson, 1965] Nilsson, N.J., 1965, Learning Machines, New York : McGraw-Hill
- [Olshevski, 1978] Olshevski, V.V., 1978, Statistical methods in sonar, New York : Consultants Bureau, 1978
- [Oran, 1974] Oran Brigham, E., 1974, The Fast Fourier Transform, Prentice-Hall, Inc.
- [Parent & O'Brien, 1993] Parent, M.P., O'Brien, T.F., 1993, Linear Swept FM (chirp) Sonar Seafloor Imaging System, Sea Technology, Jun 01, v34, N6, P49
- [Parsons, 1987] Parsons, T.W., 1987, Voice and Speech Processing, McGraw-Hill Book Company
- [Patrick, 1972] Patrick, E.A., 1972, Fundamentals of Pattern Recognition, Prentice-Hall
- [Pavel, 1991] Pavel, M., 1991, Fundamentals of Pattern Recognition, Dekker
- [Pavlidis, 1976] Pavlidis, T., 1976, Syntactic Pattern recognition on the basis of functional approximation, Pattern Recognition and artificial intelligence edited by Chen, C.H.
- [Peale, 1992] Peale, S., Speed / Motion Sensing in Challenging Environments, Sensors, pp. 45-46, January, 1992.
- [Pednekar, 1993] Pednekar, S., 1993, Giving Vision to the Blind, Business in Thailand v24 n2
- [Peng & Harlow, 1996] Peng, S., Harlow, C.A., 1996, A System for Vehicle Classification from Range Imagery, 28th Southeastern Symposium on System Theory, 1996, pp327-31, IEEE
- [Petrov *et al*, 1998] Petrov, M., Talapov, A., Robertson, T., Lebedev, A., Zhilyaev, A., Polonskit, L., 1998, Optical 3D Digitisers : Bringing Life to the Virtual World, IEEE Computer Graphics and Applications, IEE Computer Society.
- [Piper, 1990] Piper, S.O., 1990, FMCW range resolution for MMW seeker applications, SOUTHEASTCON '90. Proceedings (Cat. No.90CH2883-7)
- [Piper, 1991] Piper, S.O., 1991, FMCW linearizer bandwidth requirements, Proceedings of the 1991 IEEE National Radar Conference
- [Pollack & Cassaday, 1989] Pollack, G.D., Cassaday, J.H., 1989, The Neural Basis of Echolocation in Bats, Springer-Verlag Berlin Heidelberg
- [Pomerleau *et al*, 1991] Pomerleau, D.A., Gowdy, J., Thorpe, E.E., 1991, Combining artificial neural networks and symbolic processing for autonomous robot guidance, Engineering Applications of Artificial Intelligence

- [Pomerleaux, 1993] Pomerleaux, D.A.,1993, Neural Network Perception for mobile robot Guidance, Kluwer Academic Publishers
- [Porges, 1977] Porges, G.,1977, Applied Acoustics,London : Edward Arnold, 1977.
- [Porter, 1993] Porter, M.B.,1993, Acoustic Models and Sensor Systems, IEEE Journal of Oceanic Engineering, Oct 01, v18, n4
- [Porto & Fogel, 1990] Porto, V.W., Fogel, D.B.,1990, Neural Network Techniques for Navigation of AUV's, Proceedings of the Symposium on Autonomous Underwater Vehicle Technology, 1990
- [Porto & Fogel, 1992] Porto, V.W., Fogel, D.B.,1992, Neural Networks for AUV guidance control, Sea Technology v33 (Feb 1992) p. 25+
- [Porto, 1989] Porto, V.W.,1989, Pattern recognition of undersea objects using neural networks,23rd Annual Asilomar Conference on Signals, Systems and Computers, pp 376-380, 1989.
- [Prance, 1988] Prance, G.T.,1988,Leaves, Thomas and Hudson
- [Prechelt, 1994a] Prechelt, L.,1994, A study of experimental evaluations of neural network learning algorithms : Current research practice, Technical Report 19/94, Fakultat fur Informatik, University of Karlsruhe, Karlsruhe, Germany
- [Prechelt, 1994b] Prechelt, L.,1994, PROBEN1 - A Set of Neural Network Benchmark Problems and Benchmarking Rules, Technical Report 21/94, University of Karlsruhe, Germany
- [Priestly, 1981] Priestly, M.B.,1981, Spectral Analysis and Time Series, Academic Press
- [Proakis, 1992] Proakis, J.G.,1992,Digital signal processing : principles, algorithms, and Applications, New York : Macmillan ; Toronto : Maxwell Macmillan Canada
- [Qiang & Wenxian, 1995] Qiang, F, Wenxian, Y.,1995, Automatic Target Recognition Based on Incoherent Radar Returns, IEEE
- [Quan & Sejnowski, 1988] Qian, N., Sejnowski, T.J.,1988, Predicting the Secondary Structure of globular proteins using Neural Network models, Journal of Molecular Biology, 202, pp865-884
- [Quinlan, 1986] Quinlan, J.R.,1986, Induction of Decision Trees, Machine Learning, 1, 1981-106
- [Quinlan, 1993] Quinlan, J. R.,1993,C4.5 : programs for machine learning, San Mateo, Calif. : Morgan Kaufmann Publishers, c1993.
- [Rabiner, 1993] Rabiner, L., Juang, B.,1993,Fundamentals of Speech Recognition, Prentice Hall
- [Ratner & McKerrow, 1997] Ratner, D., McKerrow, P.J., Recognising landmarks with ultrasonic sensing for autonomous mobile robot navigation, The 1997 International Conference on Field and Service Robotics, 1997.
- [Reece & Taylor, 1996] Reece, M., Taylor, J., 1996, High Speed Vision-based Quality Grading of Oranges, Proceedings of the International Conference on Neural Networks for Identification, Control, Robotics and Signal / Image Processing, Venice-Italy, pp136 - 144.

- [Rice, 1944] Rice, S.O.,1944, The Mathematical Analysis of Random Noise,Bell System Technical Journal, v23, p282-332,1944
- [Rice, 1945] Rice, S.O.,1945, The Mathematical Analysis of Random Noise Part II,Bell System Technical Journal, v24, pp46-156, 1945
- [Rice, 1954] Rice, S.O.,1954, Mathematical Analysis of Random Noise, In N.Wax (Ed), Selected papers on Noise and Stochastic processes, Dover Publications, New York
- [Riedmiller, 1994] Riedmiller, M,1994, Advanced Supervised Learning in Multi-Layer Perceptrons - from Backpropagation to Adaptive Learning Algorithms, International Journal of Computer Standards and Interfaces, Special Issue on Neural Networks
- [Ristic, 1983] Ristic, V.M.,1983, Principles of acoustic devices,
- [Roe & Robson, 1992] Roe, H., Robson, G.S.,1992,Classification of Road Vehicles from Microwave Profiles,6th International Conference on Road Traffic Monitoring and Control, pp 128-31,1992
- [Roitblat *et al*, 1989] Roitblat, H.L., Moore, P.W.B., Nachtigall, P.E., Penner, R.H., Au, W.W.L.,1989, Natural Echolocation with an Artificial Neural Network, International Journal of Neural Networks, 1, pp239-248.
- [Roitblat *et al*, 1990] Roitblat, H.L., Penner, R.H., Nachtigall, P.E.,1990, Matching-to-Sample by an Echolocating Dolphin, Journal of Experimental Psychology Animal Behaviour Proceedings, 16, pp85-95
- [Romesburg, 1984] Romesburg, H.C.,1984,Cluster Analysis for Researchers,London: Lifetime Learning Publications
- [Rose & Singh, 1979] Rose, J.L., Singh, G.P.,1979, A pattern recognition reflector classification study in the ultrasonic inspection of stainless steel pipe welds,British Journal of Non-destructive Testing, vol 21, no 6, pp308-311, Nov 1979
- [Rose *et al*, 1982] Rose, J.L., Jeong, Y.H., Avioli, M.J.,1982, Utility of a Probability-Density-Function Curve and F-Maps in Composite Material Inspection, Experimental Mechanics, April 1982, pp155-160
- [Rose *et al*, 1988] Rose, J.L., Nestelroth, J.B., Balasubramaniam, K., 1988, Utility of feature-mapping in ultrasonic non-destructive evaluation, Ultrasonics, 1988, Vol. 26, pp121-131
- [Rose *et al*, 1990] Rose, J.L., Balasubramaniam, K., Chen, G., 1990, Ultrasonic Feature Based Imaging for Post Factum Control, IEEE
- [Rose *et al*, 1982] Rose, J.L., Avioli, M.J., Lapidis, M.,1982, A physically modeled feature based ultrasonic system for IGSCC classification, Materials Evaluation, vol 40, no 13, pp1367-1383, December 1992
- [Rossing, 1982] Rossing, T.D.,1982, The Science of Sound, Addison-Wesley Publishing Company, Inc.
- [Rowell & Kay, 1968] Rowell, D., Kay, L.,1968, Auditory Perception and Blind Guidance, The 6th International Congress on Acoustics, Tokyo, Japan, August 21-

- [Rowell, 1970] Rowell, D., 1970, Auditory Display of Spatial Data, PhD Thesis, University of Canterbury
- [Rudgers, 1971] Rudgers, A.J., 1971, Separation and Analysis of the Acoustic Field Scattered by a Rigid Sphere, The Journal of the Acoustical Society of America, Volume 52, Number 1 (part 2) pp234-246
- [Rumelhart *et al*, 1986] Rumelhart, D.E., Hinton, G.E., Williams, R.J., 1986, Learning internal representations by error propagation, Parallel Distributed Processing : explorations in the microstructure of cognition, Vol 1 The MIT Press
- [Rummelhart & McClelland, 1986] D.E. Rumelhart, J.L. McClelland (Eds), Parallel Distributed Processing : explorations in the microstructure of cognition Vol 1 : Foundations, MIT Press, 1986.
- [Runtz, 1991] Runtz, K.J., 1991, IEEE Western Canada Conference on Computer, Power and Communication Systems, pp84 - 88.
- [Russell *et al*, 1996] Russell, G.T., Bell, J.T., Holt, P.O., Clarke, S.J., 1996, Sonar Image Interpretation and Modelling, Proceedings of the 1996 IEEE Symposium on Autonomous Underwater Vehicles
- [Rzevski, 1995] Rzevski, G., 1995, Designing Intelligent Machines Volume 1 : Perception, Cognition and Execution, Butterworth Heinmann
- [Sabatini, 1995] Sabatini, A.M., 1995, Adaptive target tracking algorithms for airborne ultrasonic rangefinders, IEEE proceedings. radar, sonar, and navigation. APR 01 1995 v 142 n 2
- [Saito, 1994] Saito, N., 1994, Local Feature Extraction and Its Applications Using a Library of Bases, PhD Dissertation, Yale University, December 1994
- [Samal *et al*, 1994] Samal, A., Peterson, B., Holliday, D.J., 1994, Recognising Plants using Stochastic L-Systems, Proceedings IEEE International Conference on Image Processing, pp183 - 187.
- [Sampaio, 1989] Sampaio, E., 1989, Is There a Critical Age for Using the Sonicguide with Blind Infants, Journal of Visual Impairment and Blindness, v83, n2, p 105
- [Saniie *et al*, 1992] Saniie, J., Unluturk, M., Chu, T., 1992, Frequency Discrimination Using Neural Networks with Applications in Ultrasonics Microstructure Characterisation, IEEE
- [Sarle, 1994] Sarle, W.S., 1994, Neural Networks and Statistical Models, Proceedings of the Nineteenth annual SAS Users Group International conference, April, 1994
- [Schouten *et al*, 1993] Schouten, Th.E.; Klein Gebbinck, M.; Thijssen, J.M.; mVerhoeven, J.T.M., 1993, Ultrasonic tissue characterisation using neural networks, Third International Conference on Artificial Neural Networks (Conference. Publication No.372) p. 110-2
- [Schwartz & Shaw, 1975] Schwartz, M., Shaw, L., 1975, Signal Processing : Discrete Spectral Analysis, Detection, and Estimation, McGraw-Hill
- [Scott *et al*, 1993] Scott, E.A., Fuller, C.R., O'Brien, W.F., Cabells,

- R.H.,1993, Sparse distributed associative memory for the identification of aerospace acoustic sources, AIAA Journal 31(9) pp1583-1589(American Institute of Aeronautics and Astronautics)
- [Seginer, *et al*, 1992] Seginer, I., Elseter, R.T., Goodrum, J.W., Rieger, M.W., 1992, Plant Wilt Detection by Computer-Vision Tracking of Leaf Tips, Transactions of the American Society of Agricultural Engineers, Vol 35(5) September - October, 1992, pp1563 - 1567.
- [Sekuler & Blake, 1994] Sekuler, R., Blake, R.,1994, Perception - 3rd Edition, McGraw-Hill
- [Shang & Brown, 1992] Shang, C., Brown, K.,1992,Feature based texture classification of side-scan sonar images using a neural network approach, Electronics letters November 5, v 28, n 23, pp2165-2167
- [Shao, 1985] Shao, S.,1985, Mobility aids for the blind, Electronics Devices for Rehabilitation. New York : Chapman and Hall, ch 3
- [Shavlik, 1992] Shavlik, J.W.,1992, A Framework for Combining Symbolic and Neural Learning, Technical Report 1123, Computer Sciences Department, University of Wisconsin - Madison, November 1992
- [Shenderov, 1998] Shenderov, 1998, Some physical models for estimating scattering of underwater sound by algae, Journal of the Acoustical Society of America, August 1998.
- [Shimizu *et al*, 1989] Shimizu, M., Hoh, K., Fujiwara, T.,1989, Swept Frequency Type of Ultrasonic Inspection Method for Liner-Propellant Separations of the H-1 Upper Stage Motors, Journal of Spacecraft and Rockets, September 01, v26, n5, p379
- [Shoval *et al*, 1994] Shoval, S., Borenstein, J., Koren, Y.,1994, Mobile robot obstacle avoidance in a computerized travel aid for the blind, Proceedings 1994 IEEE International Conference on Robotics and Automation (Cat. No.94CH3375-3) p. 2023-8 vol.3
- [Shrager & Susskind, 1964] Shrager, P.G., Susskind, C.,1964, Electronics and the Blind, Morton, L. (Ed), Advances in Electron Physics, v20
- [Siegal, 1988] Siegal, A.F.,1988, Statistics and Data Analysis, John Wiley and Sons
- [Simpson, 1990] Simpson, P.K.,1990, Artificial Neural Systems, Pergamon Press
- [Singh & Montemerlo, 1997] Singh, S., Montemerlo, M., 1997, Recent Results in the Grading of Vegetative Cuttings Using Computer Vision, Innovative Robotics for Real-World Applications (IROS-97). Grenoble, France, September, 1997.
- [Sinnot & Wilson, 1963] Sinnot, E.W., Wilson, K.S.,1963,Botany : Principles and Problems, International Student Edition, 196th Edition, McGraw Hill
- [Sistler, 1990] Sistler, F., 1990, Grading Agricultural Products with Machine Vision, IEEE International Workshop on Intelligent Robots and Systems, pp255 - 261
- [Sites & Delwiche, 1998] Sites, P.W., Delwiche, M.J., 1988, Computer Vision to Locate Fruit on a Tree, Transactions of

- the American Society of Agricultural Engineers, Vol 31(1) January - February, 1988, pp257 - 263 (and p272).
- [Siuru, 1994] Siuru, B.,1994, The Smart Vehicles are Here, Popular Electronics, Vol. 11, No. 1, pp41-45, January, 1994
- [Skinner *et al*, 1977] Skinner, D.P., Altes, R.A., Jones, J.D.,1977,Broadband Target Classification using a Bionic Sonar, Journal of the Acoustical Society of America, Vol 62, No. 5, Nov, pp 1239 - 1246
- [Skolnik, 1980] Skolnik, M.,1980, Introduction to RADAR systems, McGraw-Hill
- [Smith & Kay, 1970] Smith, R.P., Kay, L.,1970, A fishfinding sonar utilising an audio information display, Digest of Technical Papers, IEEE Ocean Conference, Panama City, Florida, 1970, p113.
- [Spatz, 1993] Spatz, C., 1993, Basic Statistics Tales of Distributions, Brooks / Cole Publishing Company.
- [Spiedel, 1992] Speidel, S.L.,1992, Neural Adaptive Sensory processing for undersea Sonar, IEEE Journal of Oceanic Engineering, October, v 17, n 4, p 341
- [Squires, 1985] Squires, G.L.,1985, Practical Physics,Cambridge University Press
- [Srikanth *et al*, 1996] Srikanth, T, Reddy, M.R.S., Prabhajar, D., Sridevi, M.R.,1996,Correlation of Autonomic Tesrs to the HRV Signal Analysed using Short Time Fourier Transform,15th Southern Biomedical Engineering Conference, pp274-277, 1996, IEEE
- [Stace, 1989] Stace, C.A.,1989, Plant Taxonomy and Biosystematics, Edward Arnold
- [Stanic & Kennedy, 1993] Stanic, S., Kennedy, E.,1993,Reverberation fluctuations from a smooth seafloor, IEEE Journal of Oceanic Engineering 18 (April 1993)
- [Stanley & McKerrow, 1997] Stanley, B.D., McKerrow, P.J. 1997. Measuring Range and Bearing with a Binaural Ultrasonic Sensor, IROS , IEEE/RSJ, September, Grenoble, pp 565-571.
- [Steinmetz *et al*, 1994] Steinmetz, V., Delwiche, M.J., Giles, D.K., Evans, R., 1994, Sorting Cut Roses using Computer Vision, Transactions of the ASAE, Vol. 37(4):1347:1353.
- [Stockman *et al*, 1976] Stockman, G., Kanel, L.N., Kyle, M.C.,1976, Structural Pattern Recognition of cartoid pulse waves using a general waveform parsing system,Communications of the ACM, 19(12), 19688, 1976
- [Strelow & Boys, 1979] Strelow, E.R., Boys, J.T.,1979, The Canterbury child's aid : A binaural spatial sensory for research with blind children, Journal of Visual Impairment and Blindness, 5, 179-184
- [Strelow & Hodgson, 1976] Strelow, E.R., Hodgson, R.M.,1976, The development of a spatial sensing system for blind children, The New Outlook for the Blind, 1, pp22-24
- [Strelow *et al*, 1975] E.R.Strelow, L.Kay, N.Kay, Binaural Sensory Aid : Case Studies of it's use by two children, Journal of Visual Impairment and Blindness, 1972(1), pp 1 - 9, 1978.

- [Strelow *et al*, 1978] Strelow, E.R., Kay, L., Kay, N., 1978, Binaural Sensory Aid : Case Studies of its use by two children, *J Visual Impairment and Blindness* 72 (1), pp 1 - 9
- [Strelow, 1981] Strelow, E.R., 1981, Visual prosthesis : Use by an infant macaque, *Society for Neuroscience Abstracts*, 197, 296
- [Strelow, 1983] Strelow, E.R., 1983, Use of the Binaural Sensory aid by young children, *Journal of Visual Impairment and Blindness*, 1977, 429-437
- [Strum & Kirk, 1989] Strum, R.D., Kirk, D.E., 1989, *Discrete Systems and Digital Signal Processing*, Addison-Wesley Publishing Company.
- [Suga & Kanwal, 1990] Suga, N., Kanwal, J.S., *Echolocation : Creating Computational Maps*, *Handbook of Brain Theory and Neural Networks* Ed. Arbib
- [Symposium, 1979] International Interdisciplinary Symposium on Animal Sonar Systems, 1979, *Animal Sonar Systems*,
- [Tacconi, 1976] Tacconi, G., 1976, Aspects of signal processing with emphasis on underwater, *NATO Advanced Study Institute on Aspects of Signal Processing*
- [Taylor, 1976] Taylor, F.J., 1976, *Digital signal processing in Fortran*, Lexington, Mass : Lexington Books, c1976
- [Tesauro & Sejnowski, 1989] Tesauro, G., Sejnowski, T.J., 1989, A parallel network that learns to play backgammon, *Artificial Intelligence*, 39, 357-309
- [Teti *et al*, 1996] Teti, J.G., Gorman, R.P., Berger, W.A., 1996, A Multifeature Decision Space Approach to Radar Target Identification, *IEEE Transactions on Aerospace and Electronic Systems*, vol 32, no 1, Jan 1996
- [Therrien, 1989] Therrien, C.W., 1989, *Decision, Estimation and Classification, An Introduction to pattern recognition and related topics*, John Wiley and Son, New-York
- [Thomas, 1962] Thomas, G.B., 1962, *Calculus and Analytic Geometry*, Addison-Wesley Publishing Company, Inc.
- [Thomas, 1978] Thomas, D. W., 1978, Vehicle Sounds and Recognition in *Pattern Recognition : Ideas in Practice*, Ed. Batchelor, B.G., 1978, pp333-361, Plenum Press
- [Thornton, 1969] W.Thornton, Four years' use of the binaural sensory aid, *New Outlook for the Blind*, 1969, pp7-10, 1975.
- [Thornton, 1975] Thornton, W., 1975, Four years' use of the binaural sensory aid, *New Outlook for the Blind*, 1969, pp7-10
- [Timmermans *et al*, 1996] Timmermans, A.J.M., Borm, T.J.A., Meinders, M.B.J., 1996, Colour vision for online sorting of begonias based on learning techniques, In *Proceedings SPIE East 96, Optics in Agriculture, Forestry, and Biological Processing II*, Boston, Nov 1996.
- [Trukhachev, 1990] Trukhachev, A.A., 1990, The Distribution Function and Probability Density Function for the Ratio of

- Correlated Rician Random Variables, Telecommunications and radio engineering, JUL 01 1990 v 45 n 7, p103
- [Tsakiris & McKerrow, 1998] Tsakiris, J., McKerrow, P.J., 1998, An analysis of Freedman's "Image pulse" model in air, submitted to The Journal of the Acoustical Society of America, June, 1998.
- [Turban, 1992] Turban, E., 1992, Expert Systems and Applied Artificial Intelligence, Maxwell Macmillan International
- [Tuthill, 1990] Tuthill, G.S., 1990, knowledge engineering : concepts and practices for knowledge-based systems, Blue Ridge Summit, PA
- [Tyron & Bailey, 1970] Tyron, R.C., Bailey, D.E., 1970, Cluster Analysis, McGraw-Hill
- [Vafaie & De Jong, 1993] Vafaie, H., De Jong, K., 1993, Robust Feature Selection Algorithms, Proceedings of the Fifth IEEE Conference on Tools for Artificial Intelligence. pp 356-363, Boston, MA : IEEE Press.
- [Van Trees, 1968] Van Trees, H.L., 1968, Detection, estimation, and modulation theory (vol 3), New York.
- [Veraart *et al*, 1992] Veraart, C., Cremieux, J., Wonet-Defalque, M., 1992, Use of an Ultrasonic Echolocation Prosthesis by Early Visually Deprived Cats, Behavioural Neuroscience
- [Veraart, 1989] Veraart, C., 1989, Neurophysiological approach to the design of visual prostheses : A theoretical discussion, Journal of Medical Engineering and Technology, 13, 57-62
- [Vermuri, 1992] Vermuri, V., 1992, Artificial Neural Networks : concepts and control applications,
- [Walter, 1987] Walter, S.A., 1987, The sonar ring : obstacle avoidance for an autonomous mobile robot, [Michigan] : General Motors Research Laboratories, 1987
- [Wang & Zhu, 1988] Wang, H., Zhu, J.X., 1988, On Performance Improvement of Tone Frequency Estimation in Active Radar/Sonar Systems with Nonfluctuation Targets, IEEE Trans. Acoustics, Speech, and Signal Processing, 1988, ASSP-36, n10 p 1582
- [Wasserman, 1989] Wasserman, P.D., 1989, Neural Computing : Theory and Practice, Van Nostrand Reinhold
- [Wasserman, 1993] Wasserman, P.D., 1993, Advanced Methods in Neural Computing, Van Nostrand Reinhold
- [Watanabe & Masahide, 1992] Watanabe, S., Masahide, Y., 1992, An ultrasonic visual sensor for three-dimensional object recognition using neural networks, IEEE Transactions on Robotics and Automation, Vol 8, pp 240-249, April, 1992
- [Watanabe, 1969] Watanabe, S., 1969, Methodologies of Pattern Recognition, Academic Press
- [Webster, 1966] Webster, 1966, Some Acoustical Differences between bats and men, Proceedings of the International Conference on Sensory Devices for the Blind, London : St. Dunstons, pp63-68
- [Weiss & Kulikowski, 1991] Weiss, S.M., Kulikowski, C.A., 1991, Computer systems that learn : classification and prediction

- methods from statistics, neural nets, machine learning, and expert systems, San Mateo, Calif. : M. Kaufmann Publishers, c1991
- [Welstead, 1994] Welstead, S.T.,1994, Neural Network and Fuzzy Logic Applications in C/C++, John Wiley and Sons, inc.
- [Whitlow, 1994] Whitlow, A.U.,1994,Comparison of sonar discrimination : Dolphin and an artificial neural network, Journal of the Acoustical Society of America, May 01, v95, n5, p2728-2735
- [Wilding, 1982] Wilding, J.M.,1982, Perception, from sense to object,London : Hutchinson, c1982
- [Williems & Lesaffre] Williems, J.L., Lesaffre, E.,1987,Comparison of multigroup logistic and linear discriminant ECG and VCG classifications, Journal of Electrocardiology, 20:83-92, 1987
- [Willis & Kay, 1970] Willis, W.P., Kay, L.,1970, An Ultrasonic Position Sensor for Automatic Control, The Radio and Electronic Engineer, vol 40, no 6, December
- [Wilson & Farwell, 1993] Wilson, M.A., Farwell, R.W., Stanic, S.,1993, Statistics of Shallow Water, High-Frequency Acoustic Scattering and Propagation, JASA
- [Winters, 1988] Winters, J.H.,1988, Superresolution for Ultrasonic Imaging in Air using Neural Networks, Proceedings of the IEEE International Conference on Neural Networks, 1988
- [Wood, 50] Wood, A.,1950, Acoustics,Blackie and Son Limited
- [Wooldridge, 1974] Wooldridge, S.,1974,Computer Input Design, Petrocelli books
- [Wormell, 1987] Wormell, I.,1987, Knowledge engineering : expert systems and information retrieval,London : Taylor Graham
- [Yannakoudakis & Hutton, 1987] Yannakoudakis, E.J., Hutton, P.J.,1987, Speech Synthesis and Recognition Systems, Ellis Horwood Limited
- [Young & Calvert, 1974] Young, T.Y., Calvert, T.W.,1974,Classification, estimation and pattern recognition, New York
- [Zahl, 1962] Zahl, P.A. (Ed),1962,Blindness Modern Approaches to the Unseen Environment,
- [Zelano & Hoydal, 1991] Zelano, J.A., Hoydal, T.O.,1991, An Alternative Mobility Aid for the Blind, Proceedings of the 1991 IEEE 17th Annual Northeast Bioengineering conference.
- [Zelinsky, 1991] Zelinsky, A., 1991, Environment Exploration and Path Planning Algorithms for Mobile Robot Navigation using Sonar, University of Wollongong.
- [Zheng, 1993] Zheng, Z,1993, A benchmark for classifier learning, Technical Report TR474, Basser Department of Computer Science, University of Sydney, NSW, Australia 2006, November 1993.
- [Zyweck & Bogner, 1996] Zyweck, A., Bogner, R.E.,1996,Radar Target Classification of Commercial Aircraft, IEEE Transactions on Aerospace and Electronic Systems, vol 32, no 2, April 1996.